

Dissertation zur Erlangung des Doktorgrades
der Fakultät für Chemie und Pharmazie
der Ludwig-Maximilians-Universität München



Reactions of Michael Acceptors with Carbanions
Novel References for the Construction of
Comprehensive Reactivity Scales

Dipl. Chem. Oliver Kaumanns

aus

Bremen

2008

Erklärung

Diese Dissertation wurde im Sinne von § 13 Abs. 3 der Promotionsordnung vom 29. Januar 1998 von Herrn Prof. Dr. Herbert Mayr betreut.

Ehrenwörtliche Versicherung

Diese Dissertation wurde selbstständig und ohne unerlaubte Hilfe erarbeitet.

München, 03.12.2008

.....
Oliver Kaumanns

Dissertation eingereicht am 04.11.2008

1. Gutachter Prof. Dr. Herbert Mayr
2. Gutachter Prof. Dr. Rudolf Knorr

Mündliche Prüfung am 02.12.2008

Für
Heike

Danksagung

Mein besonderer Dank gilt Herrn Prof. Dr. Herbert Mayr für die Überlassung der interessanten Themen, seiner Diskussionsbereitschaft und Unterstützung während der Anfertigung dieser Arbeit sowie für die Bereitstellung der hervorragenden experimentellen Bedingungen.

Mein besonderer Dank gilt aber auch meinen ehemaligen Laborkollegen Alexander Tishkov, Erik Bräuer, Florian Seeliger und Hans Laub, nicht nur für ihre Diskussionsbereitschaft, sondern auch für die tolle Atmosphäre in unserem Labor. Darüber hinaus möchte ich meinen erstklassigen Bachelor- und Fortgeschrittenenstudenten Markus Wolf und Veronika Zinth für ihre hervorragenden Arbeiten danken.

Allen weiteren aktuellen Mitgliedern des Arbeitskreises möchte ich für das ausgezeichnete Arbeitsklima und die tolle Zusammenarbeit danken.

Herrn Prof. Dr. Xiǎo-Qíng Zhū und Herrn Prof. Dr. Jīn-Péi Chéng danke ich für die Möglichkeit in ihrem Arbeitskreis an der Nankai Universität in Tianjin zwei Monate intensiv forschen zu können. Insbesondere danke ich meinen dortigen Laborkollegen des „Chemistry Buildings“ Wāng Chūn-Huá, Shěn Yàn, Wú Shuài, Chéng Chéng, Dài Zhì und Chén Xī, sowie dem Bayerischen Hochschulzentrum für China für die finanzielle Unterstützung in Form eines Stipendiums.

Für die schnelle und kritische Durchsicht dieser Arbeit sei Heike Schaller, Martin Breugst und Patrick Kaumanns herzlich gedankt.

Abschließend möchte ich mich noch einmal bei meiner Freundin Heike für ihre Unterstützung nicht nur während der Promotion bedanken.

Publikationen

Electrophilicity Parameters of 5-Benzylidene-2,2-dimethyl-[1,3]dioxane-4,6-diones (Benzylidene Meldrum's Acids)

O. Kaumanns, H. Mayr, *J. Org. Chem.* **2008**, *73*, 2738-2745.

Determination of the Electrophilicity Parameters of Diethyl Benzylidenemalonates in DMSO: Reference Electrophiles for Characterizing Strong Nucleophiles

O. Kaumanns, R. Lucius, and H. Mayr, *Chem. Eur. J.* **2008**, *14*, 9675-9682.

Nucleophilicities of the Anions of Arylacetonitriles and Arylpropionitriles in Dimethyl Sulfoxide

O. Kaumanns, R. Appel, T. Lemek, F. Seeliger, and H. Mayr, *J. Org. Chem.*, **2008**,
angenommen.

Konferenzbeitrag

Electrophilicity of Substituted Diethyl Benzylidenemalonates

Posterpräsentation auf dem European Symposium on Organic Reactivity XI, 2007

List of Abbreviations

abs.	absolute
aq.	aqueous
Bu	butyl
calc.	calculated
conc.	concentrated
d	doublet
DME	dimethoxyethane (glyme)
DMSO	dimethyl sulfoxide
<i>E</i>	electrophilicity parameter
EA	elementary analysis
Et	ethyl
EtOAc	ethyl acetate
eq.	equivalent(s)
exp.	experimental
h	hour(s)
i.e.	id est
ITC	Isothermal titration calorimetry
<i>k</i>	rate constant
lit.	literature
M	mol/L
Me	methyl
MeOH	methanol
min	minute(s)
mp	melting point
MS	mass spectrometry
<i>N</i>	nucleophilicity parameter
NMR	nuclear magnetic resonance
Ph	phenyl
q	quartet
<i>R_f</i>	retention factor
<i>s</i>	nucleophile specific slope parameter
s	singlet
t	triplet
UV	ultra violet
Vis	visible
vs.	versus

Table of Contents

0	Summary	1
1	Introduction	16
2	Electrophilicity Parameters of 5-Benzylidene-2,2-dimethyl-[1,3]dioxane-4,6-diones (Benzylidene Meldrum's Acids)	20
	Introduction	20
	Results and Discussion	23
	Conclusion	36
	General Remarks	37
	References	40
	Experimental Section	44
3	Reactivities of Benzylidene Meldrum's Acids in Methanol	70
	Introduction	70
	Results and Discussion	73
	Conclusion	91
	References	91
	Experimental Section	94
4	Determination of the Electrophilicity Parameters of Diethyl Benzylidene-malonates in DMSO: Reference Electrophiles for Characterizing Strong Nucleophiles	127
	Introduction	127
	Results and Discussion	129
	Conclusion	143
	General Remarks	144
	References	147
	Experimental Section	151
5	Nucleophilicities of the Anions of Arylacetonitriles and Arylpropionitriles in Dimethyl Sulfoxide	178
	Introduction	178
	Results and Discussion	181
	Conclusion	194
	General Remarks	195
	References	197
	Experimental Section	200
	Appendix	228

6	Electrophilicities of Acceptor-Substituted Dienes	230
	Introduction	230
	Results and Discussion	232
	Conclusion	249
	References	250
	Experimental Section	252
7	Hydride Affinities of Michael Acceptors in Acetonitrile	282
	Introduction	282
	Results and Discussion	286
	Conclusion	295
	References	296
	Experimental Section	298

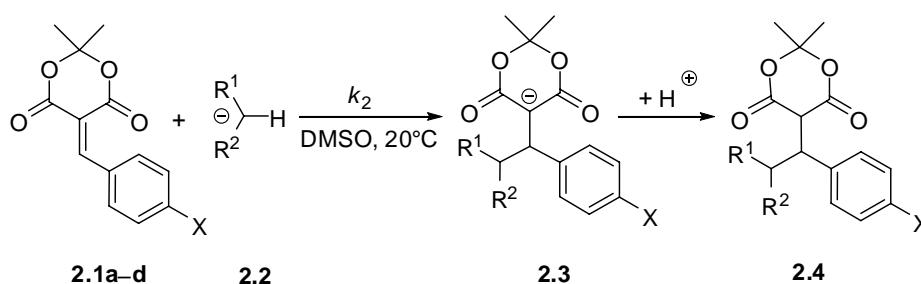
Chapter 0

Summary

Electrophilicity Parameters of 5-Benzylidene-2,2-dimethyl-[1,3]dioxane-4,6-diones (Benzylidene Meldrum's Acids)

Kinetics of the reactions of acceptor stabilized carbanions **2.2**, e.g., anions of nitro ethane, diethyl malonate, acetylacetone, dimedone or Meldrum's acid ($13.9 < N < 21.6$) with benzylidene Meldrum's acids **2.1a–d** have been investigated in dimethyl sulfoxide at 20 °C (Scheme 0.1). ^1H and ^{13}C NMR spectroscopy revealed the formation of the anionic products **2.3**, which gave the neutral compounds **2.4** after acidification with dilute acid, indicating that the nucleophilic attack of the carbon nucleophiles proceeds at the double bonds of the Michael acceptors **2.1a–d**.

Scheme 0.1. Reactions of Carbanions **2.2** with the Benzylidene Meldrum's Acids **2.1a–d** in DMSO.



The second-order rate constants k_2 for the reactions of the Michael acceptors **2.1a–d** and the carbanions **2.2** followed the linear free-energy relationship 0.1 (Figure 0.1), in which N and s are nucleophile-specific parameters and E is an electrophile-specific parameter.

$$\log k_2 (20 \text{ }^\circ\text{C}) = s(N + E) \quad (0.1)$$

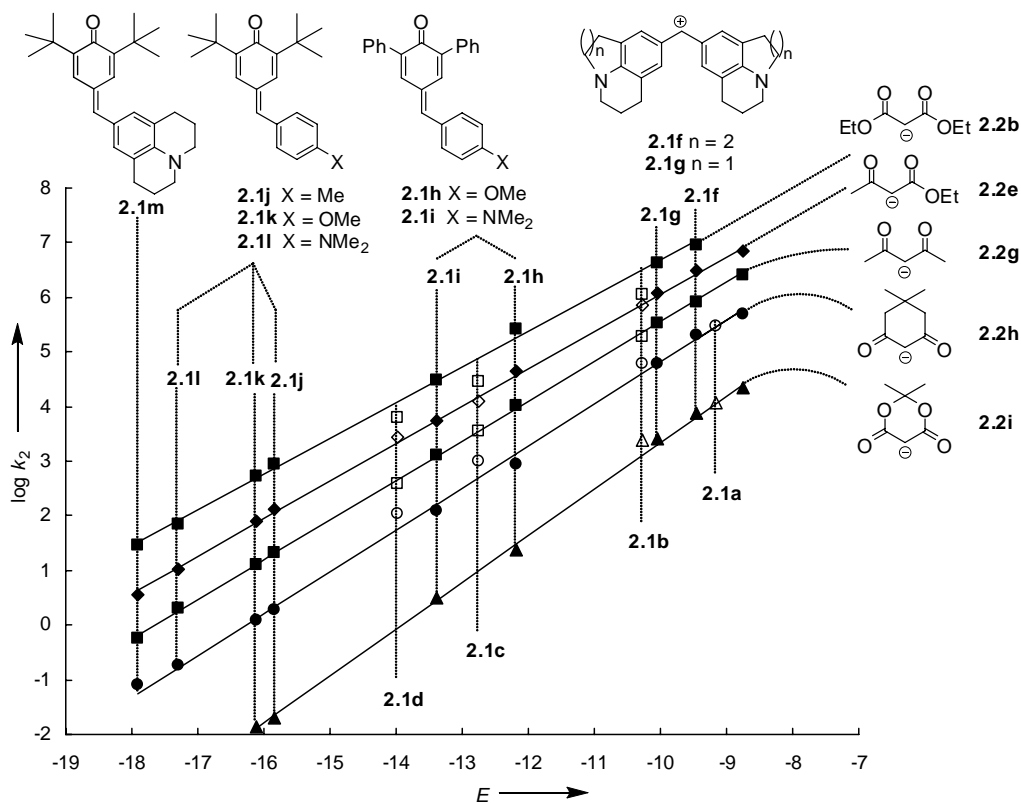


Figure 0.1. Logarithmic rate constants k_2 for the reactions of carbanions **2.2** with the benzylidene Meldrum's acids **2.1a-d** (open symbols) and with the reference electrophiles **2.1f-m** (filled symbols) in DMSO.

The second-order rate constants k_2 have been used to derive the electrophilicity parameters E for the Michael acceptors **2.1a-d** according to Equation (0.1). With $-14.0 < E < -9.2$, the electrophilicities of **2.1a-d** are comparable to the least reactive benzhydrylium ions and the most reactive quinone methides previously characterized by us (Figure 0.2).

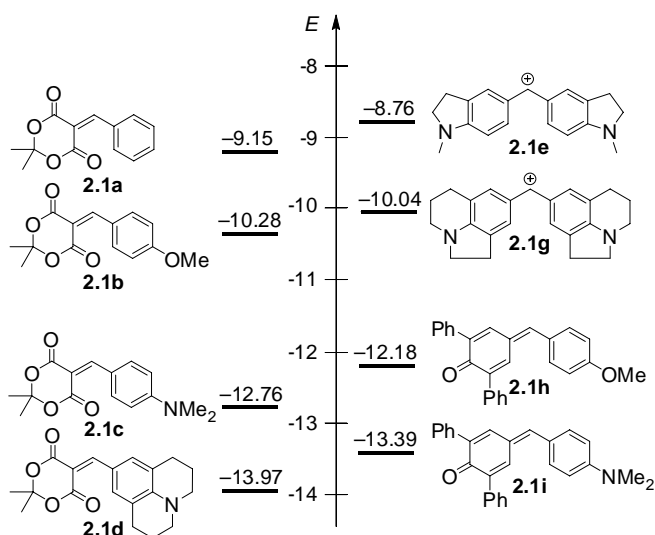
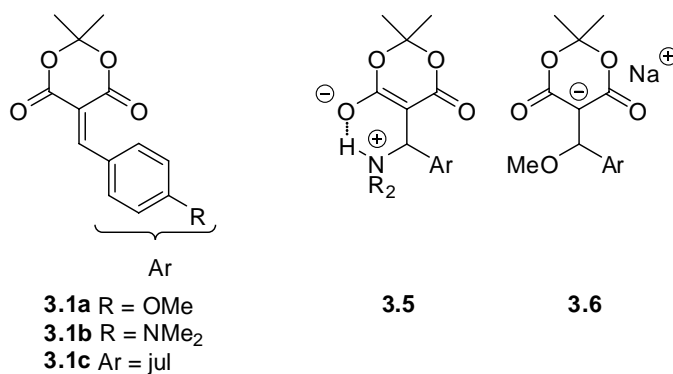


Figure 0.2. Comparison of the electrophilicity parameters E of the benzylidene Meldrum's acids **2.1a–d** (left), quinone methides, and benzhydrylium ions (right).

Reactivities of Benzylidene Meldrum's Acids in Methanol

The reactions of the Michael acceptors **3.1a–c** with carbanions, amines, and methoxide have been studied photometrically in methanol at 20 °C. The isolated products from the reactions of **3.1a–c** with the amines (**3.5**) and with methoxide (**3.6**) have been characterized by ^1H NMR spectroscopy (Scheme 0.2).

Scheme 0.2. Benzylidene Meldrum's acids **3.1a–c** and the Products of their Reactions with Amines (**3.5**) and Methoxide (**3.6**).



The second-order rate constants k_2 for the reactions of **3.1a–c** with the carbanions **3.2** have been used to derive the electrophilicity parameters E of the Michael acceptors **3.1a–c** in MeOH according to Equation (0.1). The electrophilicities E of **3.1a–c** are only slightly larger in MeOH than in DMSO, indicating that the influence of the solvent polarity on the electrophilicities of typical Michael acceptors is rather small (Figure 0.3).

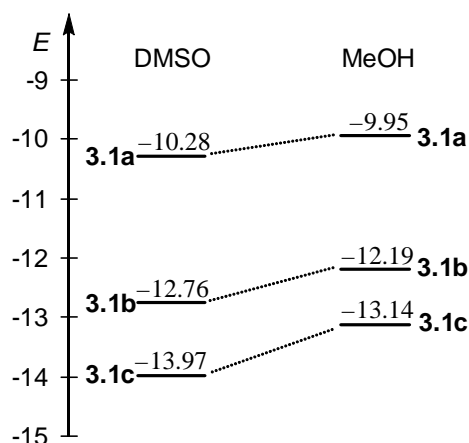


Figure 0.3. Comparison of the electrophilicity parameters E of the Michael acceptors **3.1a–c** in DMSO and MeOH.

The reactions of **3.1a–c** with amines proceed considerably faster than the analogous reactions of **3.1a–c** with carbanions of comparable nucleophilicity (Figure 0.4). The second-order rate constants k_2 for the reactions of **3.1a–c** with methoxide are located on the correlation lines for carbanions and not on those for amines.

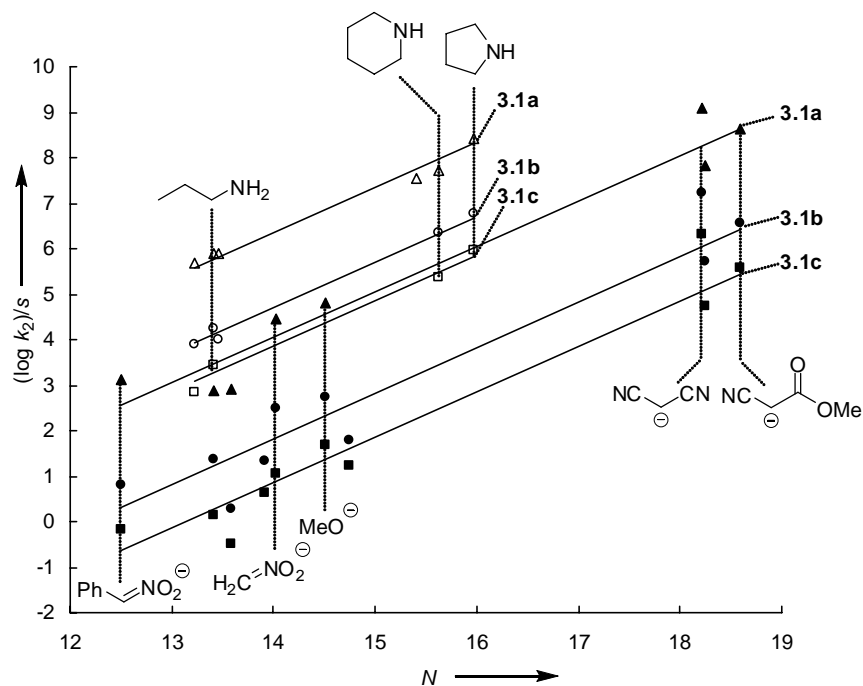


Figure 0.4. Correlation of $(\log k_2)/s$ for the reactions of carbanions (filled symbols), methoxide (filled symbols), and amines (open symbols) with benzylidene Meldrum's acids **3.1a–c** in MeOH versus the nucleophilicity parameter N of the nucleophiles.

Determination of the Electrophilicity Parameters of Diethyl Benzyldenemalonates in DMSO: Reference Electrophiles for Characterizing Strong Nucleophiles

The reactions of nine benzyldenemalonates **4.1a–i** (Figure 0.5) with acceptor stabilized carbanions **4.2** have been studied photometrically in DMSO at 20 °C. ^1H and ^{13}C NMR analysis of the addition products **4.4** and **4.5** confirmed the reaction course depicted in Figure 0.5.

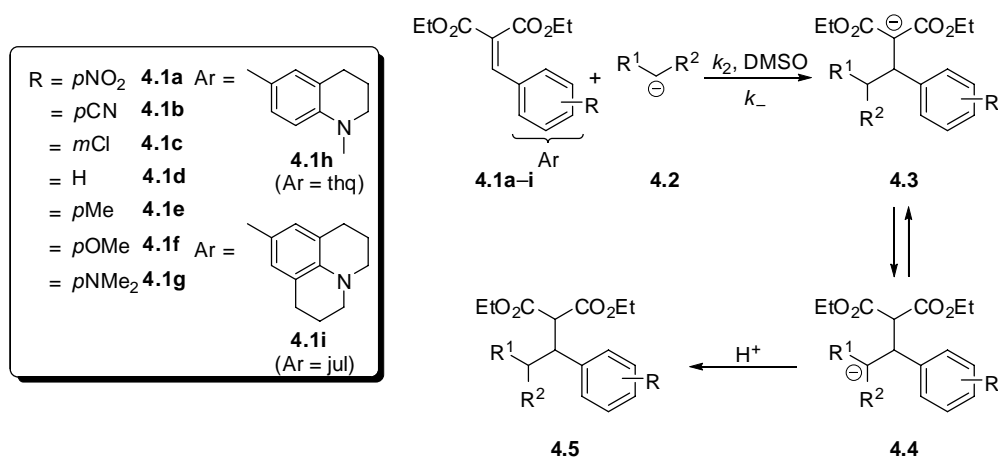


Figure 0.5. Addition of the carbanions **4.2a–f** to the benzyldenemalonates **4.1a–i** and possible subsequent protonation, elimination or cyclization paths.

Figure 0.6 reveals that the logarithmic second-order rate constants k_2 for the reactions of the carbanions **4.2** with **4.1a–i** follow Equation (0.1) and are on the same correlation line as the second-order rate constants for the reactions of **4.2** with the quinone methides **4.6a–f**.

The linear correlations of the second-order rate constants k_2 for the reactions of the carbanions **4.2** with the benzylidenemalonates **4.1a–i** and the analogous reactions of **4.2** with the quinone methides (Figure 0.6) allow us to determine the electrophilicity parameters E for compounds **4.1a–i** according to Equation 0.1 (Figure 0.7).

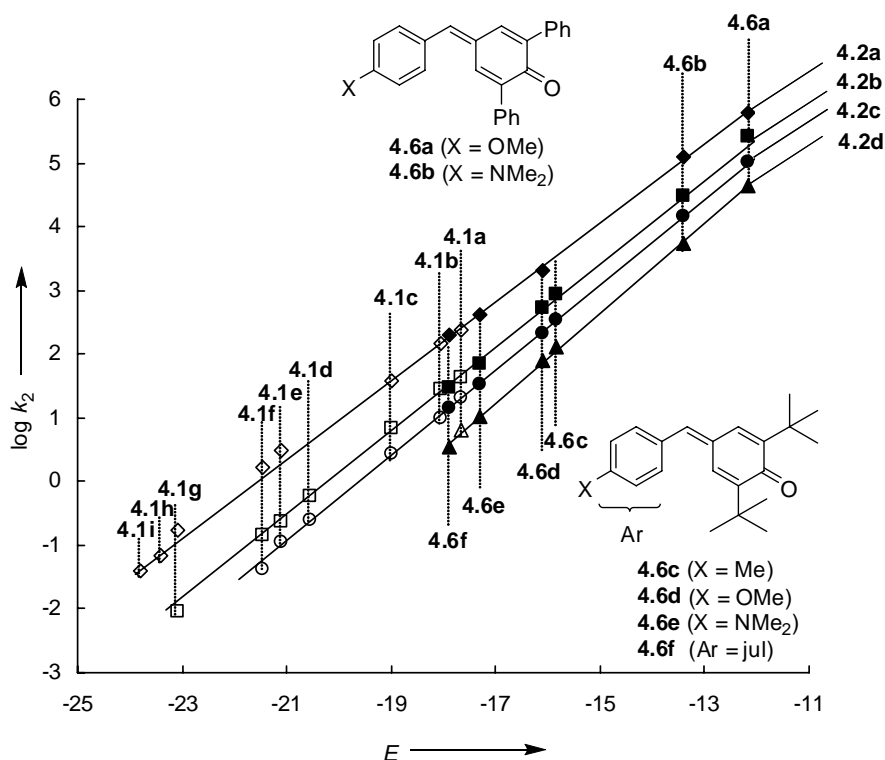


Figure 0.6. Logarithmic second-order rate constants for the reactions of the carbanions **4.2a–d** with the electrophiles **4.1a–i** (open symbols) compared with the reactivities of the reference electrophiles **4.6a–f** (filled symbols) in DMSO.

The benzylidenemalonates **4.1a–i** are more than 10^{10} times less reactive than the analogously substituted benzylidene Meldrum's acids **4.10a–d**, their cyclic counterparts. They extend the electrophilicity scale at the low-reactivity end by more than six orders of magnitude from $-17.7 > E > -23.8$ (Figure 0.7) and can, therefore, be used for determining nucleophilicities of highly reactive nucleophiles with N values of $16 < N < 30$.

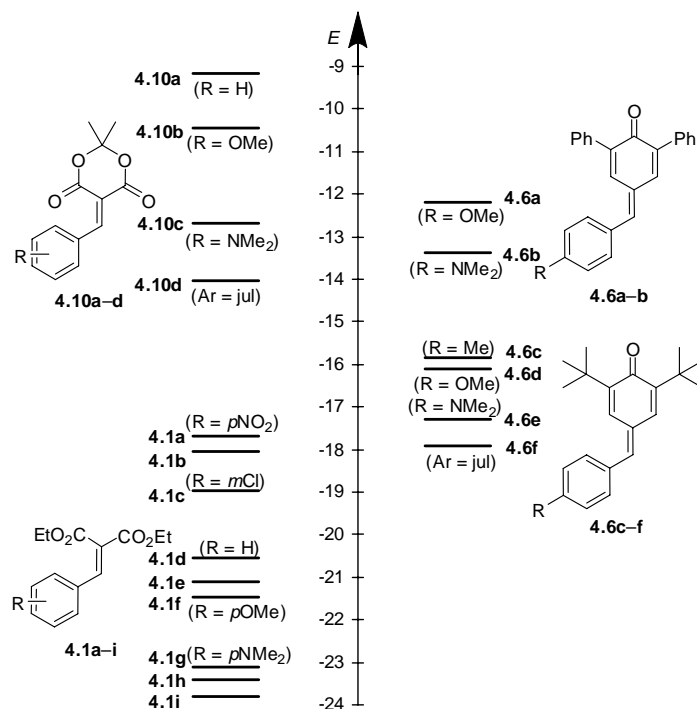


Figure 0.7. Comparison of the E parameters of the benzylidenemalonates **4.1a–i** with those of the reference electrophiles **4.6a–f** and analogously substituted benzylidene Meldrum's acids.

Nucleophilicities of the Anions of Arylacetonitriles and Arylpropionitriles in Dimethyl Sulfoxide

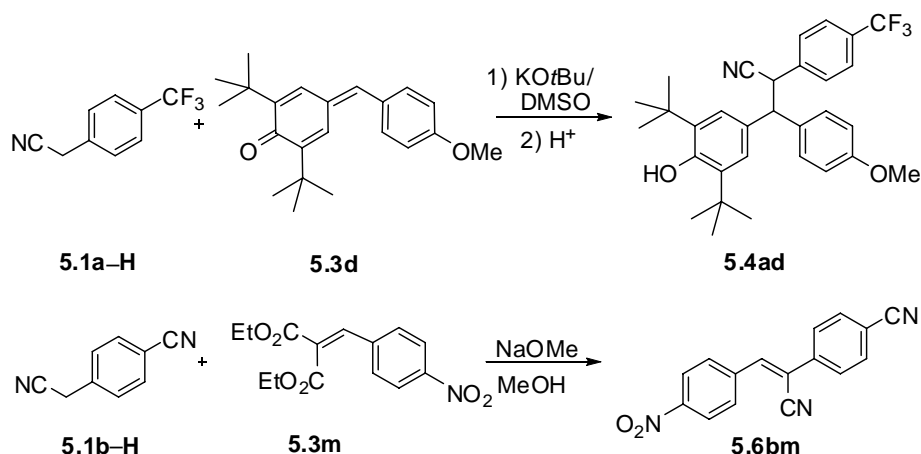
The kinetics of the reactions of the anions of the arylacetonitriles **5.1a–c** and the arylpropionitriles **5.2a–c** (Figure 0.8) with quinone methides and other classes of Michael acceptors have been studied in DMSO at 20 °C.

R	pK_{aH}	R	pK_{aH}
5.1a CF_3	18.1	5.2a H	23.0
5.1b CN	16.0	5.2b CN	–
5.1c NO_2	12.3	5.2c NO_2	–

Figure 0.8. Characterized anions of arylacetonitriles **5.1a–c** and arylpropionitriles **5.2a–c** and their pK_{aH} values in DMSO.

^1H and ^{13}C NMR analysis of the products from the reactions of **5.1a–c** and **5.2a–c** with Michael acceptors **5.3** showed the formation of the addition products as exemplarily depicted in Scheme 0.3 for the reaction of the anion **5.1a** with the methoxy substituted quinone methide (**5.3d**). From the reactions of the benzylidenemalonates **5.3m–u** with the arylacetonitrile **5.1b**, the substituted α -cyano stilbenes **5.6** were formed via retro-Michael addition as shown in Scheme 0.3 for the formation of compound **5.6bm**. Consecutive Michael additions, proton transfer and retro-Michael additions account for their formations.

Scheme 0.3. Reactions of Some Arylacetonitriles **5.1a–c** with the Quinone Methide **5.3d** and the Benzylidenemalonate **5.3m** with Formation of **5.4ad** and the Retro-Michael Product **5.6bm**.



The second-order rate constants k_2 for the reactions of **5.1a–c** and **5.2a–c** with the Michael acceptors **5.3** have been used to derive the nucleophilicity parameters N and s for compounds **5.1a–c** and **5.2a–c** using Equation (0.1) (Figure 0.9).

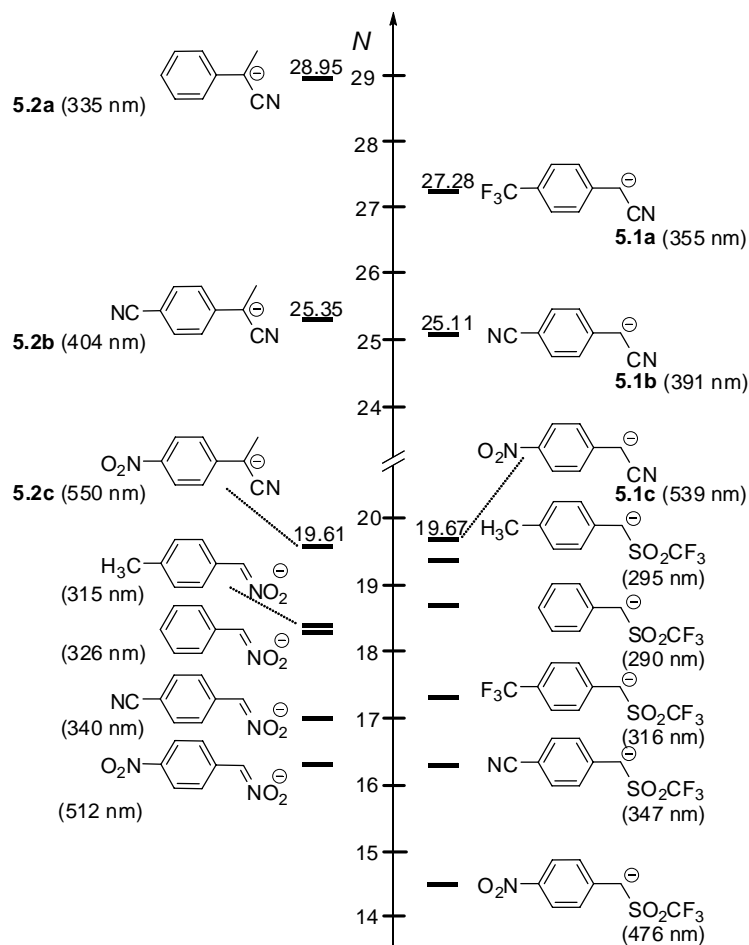


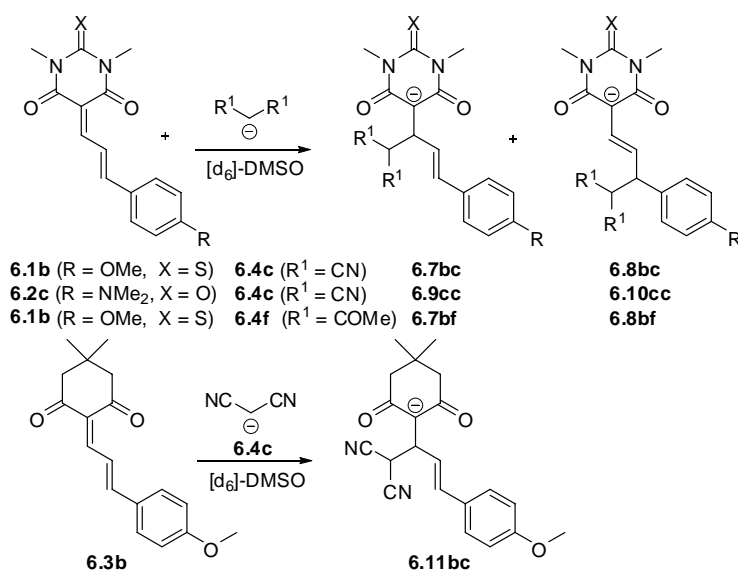
Figure 0.9. Comparison of the nucleophilicity parameters N of the arylacetone anions **5.1a–c** and the arylpropionitrile anions **5.2a–c** with those for α -nitro- and trifluoromethyl sulfonyl stabilized carbanions in DMSO.

The anions of the arylacetone nitriles **5.1a–c** and the arylpropionitriles **5.2a–c** are several orders of magnitude more nucleophilic than α -SO₂CF₃ and α -NO₂ substituted benzyl anions (Figure 0.9). As colored species of high nucleophilicity, these carbanions complement the series of reference nucleophiles, which can be employed for the photometric determination of the electrophilic reactivities of weak, colorless electrophiles.

Electrophilicities of Acceptor-Substituted Dienes

The reactions of nine acceptor substituted dienes **6.1–3** with carbanions and amines have been studied photometrically in DMSO at 20 °C. ^1H and ^{13}C NMR analysis of the products of the reactions of **6.1–3** with carbanions showed the formation of two regioisomers in varying ratios (Scheme 0.4.), indicating parallel 1,4- and 1,6-additions of the carbanions to the Michael acceptors.

Scheme 0.4. Reactions of the Dienes **6.1–3** with the Carbanions **6.4c** and **6.4f** in $[\text{d}_6]$ -DMSO under Formation of Isomeric Products.



For some reactions of the dienes **6.1–3** with carbanions **6.4**, Michael additions and subsequent formation of the retro-Michael adducts could be followed photometrically as exemplarily depicted in Figure 0.10 for the reaction of the amino substituted Michael acceptor **6.1c** with the anion of dimedone (**6.4g**).

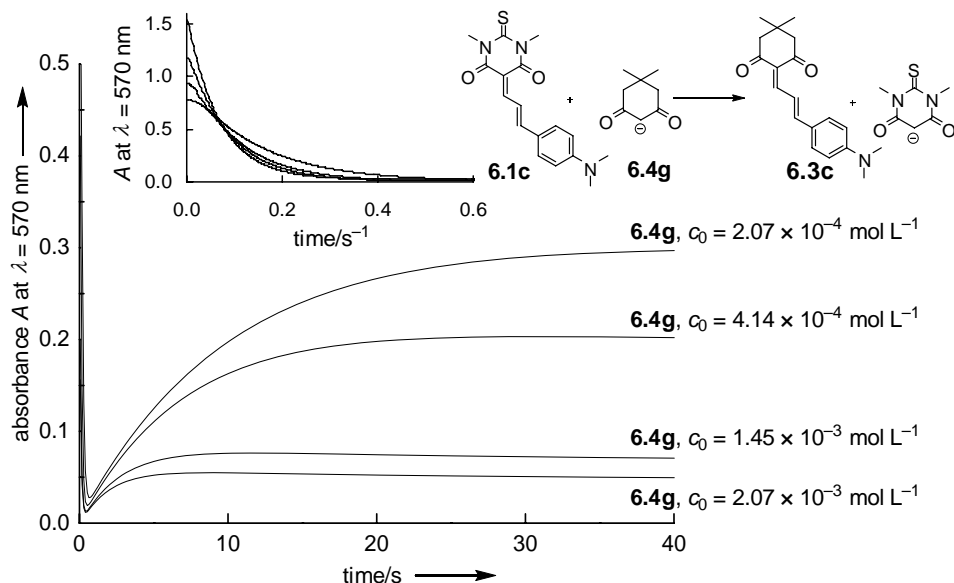
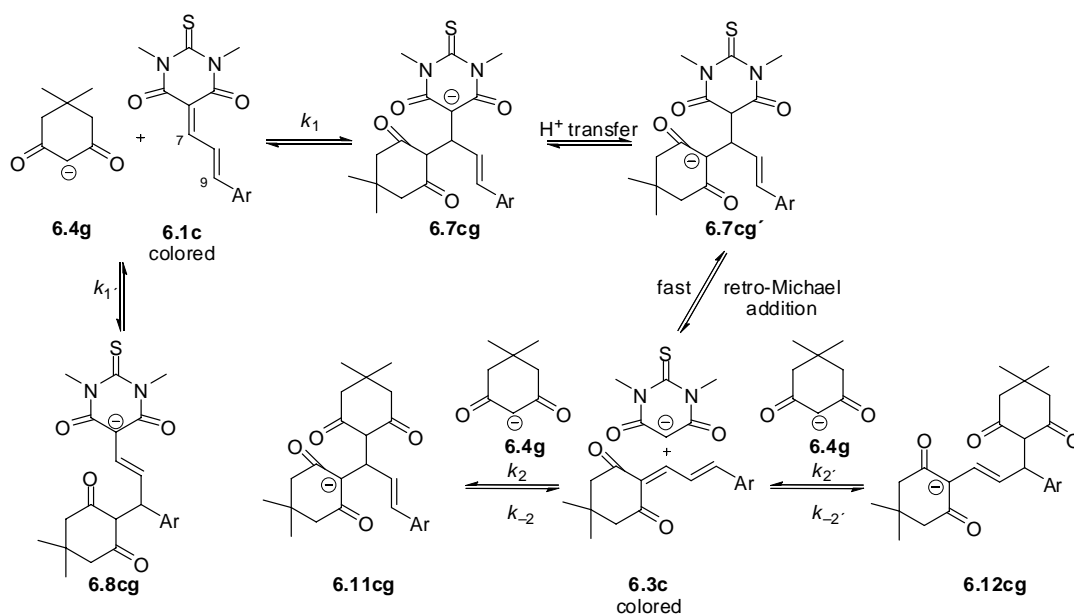


Figure 0.10. Reactions of **6.1c** ($c_0 = 1.89 \times 10^{-5}$ mol L $^{-1}$) with different amounts of the anion of dimedone (**6.4g**) in dimethyl sulfoxide at 20 °C.

The second-order rate constants k_1 for the reactions of the dienes **6.1–3** with the carbanions (Scheme 0.5.) can be estimated by Equation (0.1).

Scheme 0.5. Possible Reaction Pathways for the Addition of the Anion of Dimedone (**6.4g**) to the Michael Acceptor **6.1c** in Dimethyl Sulfoxide at 20 °C.



The rate constants have been employed to derive the electrophilicity parameters E for dienes **6.1–3**. With electrophilicities in a range of $-8.7 > E > -16.6$, their reactivities are comparable to their benzylidene (thio)barbituric acid analogs (Figure 0.11).

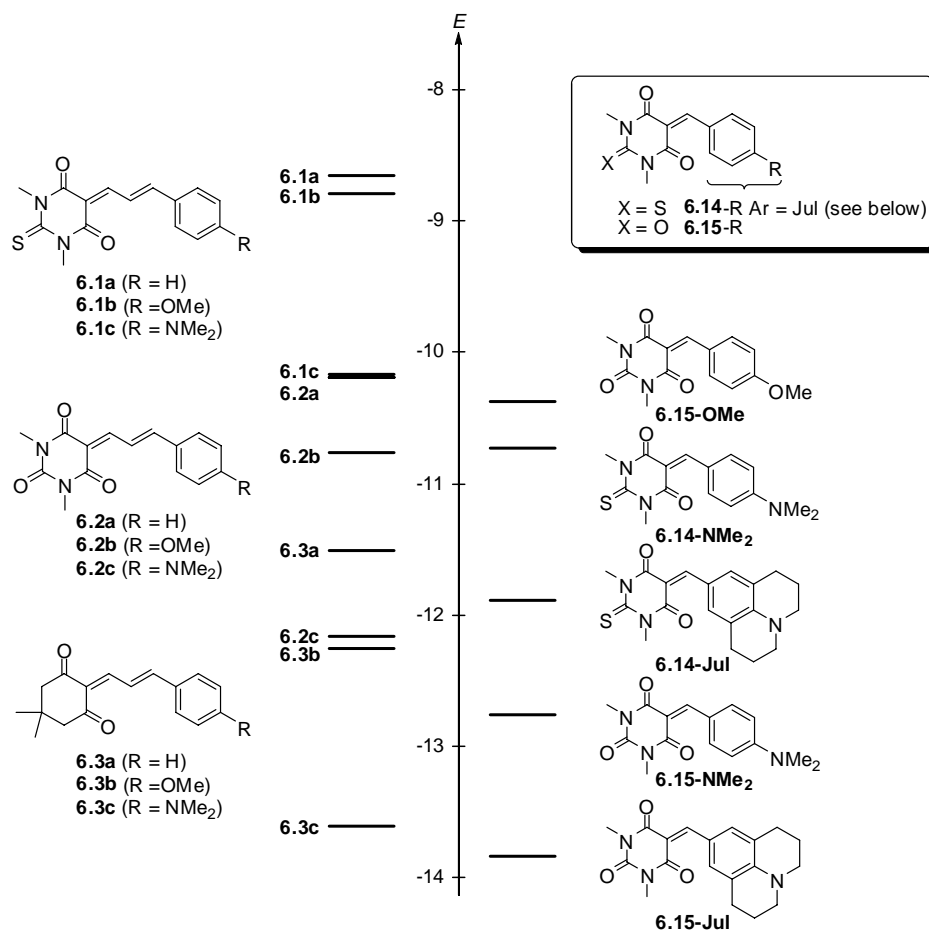


Figure 0.11. Comparison of the electrophilicity parameters E of the Michael acceptors **6.1–3** with those of some benzylidene(thio)barbituric acids **6.14** and **6.15**.

Hydride Affinities of Michael Acceptors in Acetonitrile

The hydride affinities ΔH_{H-A} (Figure 0.12) of several Michael acceptors (e.g., benzylidene Meldrum's acids, benzylidene barbituric acids, and quinone methides, **7.1g–q**) have been determined in acetonitrile using isothermal titration calorimetry.

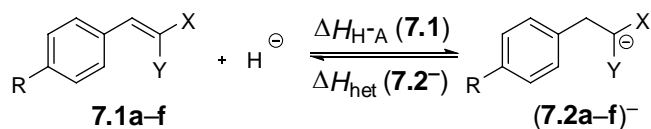


Figure 0.12 Hydride affinity $\Delta H_{\text{H-A}}$ for the reaction of an olefin **7.1** with a hydride ion under formation of the corresponding anion **7.2⁻**.

From the heats of reactions of the anions **7.2⁻** with the hydride acceptors (**7.3a-c⁺**), $\Delta H_{\text{H-A}}$ was calculated (determination of $\Delta H_{\text{H-A}}$ exemplarily depicted in Figure 0.13 for the reaction of carbanion **2⁻** with the *N*-methylacridinium ion **7.3a⁺**).

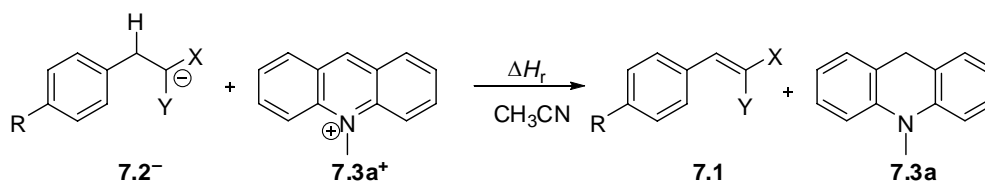
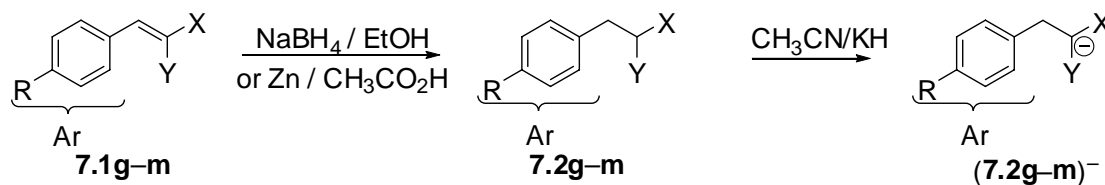


Figure 0.13. Reaction of a carbanion **7.2⁻** with the hydride acceptor **7.3a⁺** under formation of the olefin **7.1** and the reduced compound **7.3a**.

The anions (**7.2g-q⁻**) have been generated in situ by treating the reduced Michael acceptors **7.2g-q** with potassium hydride in acetonitrile as depicted exemplarily in Scheme 0.6 for the formation of the carbanions (**7.2g-m⁻**).

Scheme 0.6. Reduction of the Olefins **7.1g-m** and Subsequent Deprotonation of **7.2g-m** with KH under Formation of the Carbanions (**7.2g-m⁻**).



In contrast to the good agreement between E and $\Delta H_{\text{H-A}}$ for ten benzhydrylium ions **7.4**⁺, the electrophilicity parameters E of the Michael acceptors **7.1a–q** do not correlate well with their hydride affinities in acetonitrile (Figure 0.14).

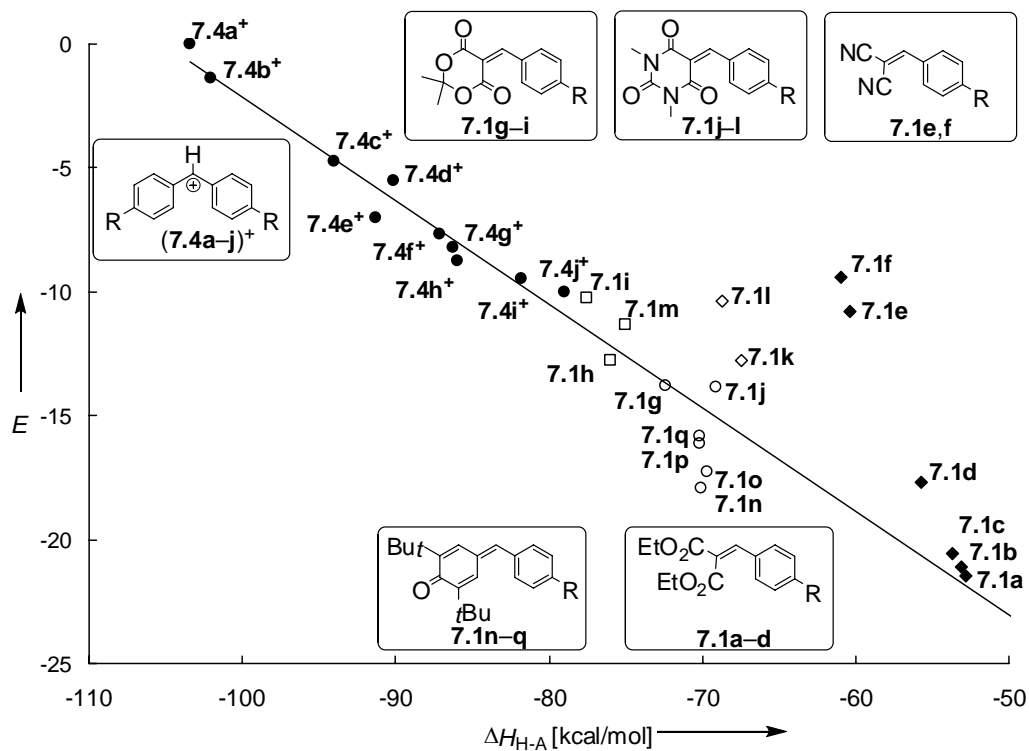


Figure 0.14. Plot of the electrophilicity parameter E of the benzhydrylium ions (**7.4a–j**)⁺ and the Michael acceptors **7.1a–q** versus their hydride affinities $\Delta H_{\text{H-A}}$ [kcal/mol] in acetonitrile at 25 °C.

Chapter 1

Introduction

Predicting whether a reaction between two compounds will take place under certain conditions is of fundamental importance for the planning of syntheses.

In the 1920s Ingold started to systemize organic reactivity and realized that most reactions in organic chemistry take place between electron-rich and electron-deficient compounds, which he named nucleophiles and electrophiles.¹ From that time on, many chemists tried to organize organic reactivity by studying the rates of reactions of nucleophiles with specific electrophiles. Swain and Scott reported on the rate constants of S_N2 reactions of methyl halides and derived the first nucleophilicity scale based on Equation (1.1), in which n characterizes the nucleophiles and the electrophiles are characterized by two parameters, s and $\log k_{\text{water}}$.²

$$\log (k/k_{\text{water}}) = sn \quad (1.1)$$

After several attempts to construct further nucleophilicity scales, Pearson claimed that general nucleophilicity scales cannot exist because he found that the relative nucleophilic reactivities towards methyl halides did not correlate with those towards Pt-complexes.³

Only four years later, Ritchie reported about a relationship of astonishing simplicity, which claims that the reactivities of a variety of carbenium ions and diazonium ions towards various nucleophiles can be described by a single, electrophile-independent nucleophilicity parameter N_+ and by only one parameter for the electrophiles ($\log k_0$).⁴

$$\log (k/k_0) = N_+ \quad (1.2)$$

Using this equation, it was for the first time possible to predict the rates of reactions, which covered more than 10 orders of magnitude.

The impact of this so-called constant selectivity relationship has significantly been extended by Kane-Maguire and Sweigart, who investigated the rates for the reactions of cationic π -complexes with different nucleophiles.^{5,6}

The most extensive nucleophilicity scale presently available has been derived from the rate constants of the reactions of benzhydrylium ions with alkenes, arenes, enol ethers, ketene acetals,⁷ enamines,⁸ transition-metal π -complexes,⁹ amines,¹⁰ alcohols,¹¹ alkoxides,¹² phosphanes,¹³ carbanions,¹⁴ and hydrides.¹⁵

So far, over 400 nucleophiles and 100 electrophiles have been characterized by the linear-free-energy relationship (1.3) introduced in 1994 by Mayr and Patz, in which the Ritchie correlation was extended by the nucleophile-specific slope parameter s .

$$\log k_2 (20 \text{ }^\circ\text{C}) = s(N + E) \quad (1.3)$$

This equation allows the prediction of the second-order rate constants k_2 at 20 °C for electrophile-nucleophile combinations from the nucleophile-specific N and s parameters and the nucleophile-independent, but electrophile-specific electrophilicity parameter E . Benzhydrylium ions and structurally related quinone methides, which have commonly been used as reference electrophiles cover only a limited range of reactivity. It was the goal of this work to characterize other types of Michael acceptors as novel reference electrophiles in order to extend the electrophilicity scale at the low-reactivity end and to add more electrophiles in the range of $-10 > E > -15$, where only few reference compounds had been available. On the

other side, highly reactive carbanions should be identified as new reference nucleophiles for the extension of the nucleophilicity scale at the high-reactivity end.

As some parts of this thesis have already been published or submitted for publication, individual introductions will be given separately for each topic at the beginning of each chapter. In order to identify my contributions to multi-author publications (Chapters 4 and 5), the Experimental Sections exclusively contain those experiments, which have been performed by me.

References

- (1) Ingold, C. K. *Chem. Rev.* **1934**, *15*, 225-274.
- (2) Swain, C. G.; Scott, C. B. *J. Am. Chem. Soc.* **1953**, *75*, 141-147.
- (3) Pearson, R. G.; Sobel, H. R.; Songstad, J. *J. Am. Chem. Soc.* **1968**, *90*, 319-326.
- (4) a) Ritchie, C. D. *Acc. Chem. Res.* **1972**, *5*, 348-354; b) Ritchie, C. D.; Virtanen, P. O. I. *J. Am. Chem. Soc.* **1972**, *94*, 4966-4971.
- (5) Kane-Maguire, L. A. P.; Honig, E. D.; Sweigart, D. A. *Chem. Rev.* **1984**, *84*, 525-543.
- (6) Pike, R. D.; Sweigart, D. A. *Coord. Chem. Rev.* **1999**, *187*, 183-222.
- (7) a) Tokuyasu, T.; Mayr, H. *Eur. J. Org. Chem.* **2004**, 2791-2796; b) Dilman, A. D.; Mayr, H. *Eur. J. Org. Chem.* **2005**, 1760-1764.
- (8) Kempf, B.; Hampel, N.; Ofial A., R.; Mayr, H. *Chem. Eur. J.* **2003**, *9*, 2209-2218.
- (9) Mayr, H.; Kuhn, O.; Schlierf, C.; Ofial, A. R. *Tetrahedron* **2000**, *56*, 4219-4229.
- (10) a) Minegishi, S.; Mayr, H. *J. Am. Chem. Soc.* **2003**, *125*, 286-295; b) Brotzel, F.; Kempf, B.; Singer, T.; Zipse, H.; Mayr, H. *Chem. Eur. J.* **2007**, *13*, 336-

- 345; c) Brotzel, F.; Chu, Y. C.; Mayr, H. *J. Org. Chem.* **2007**, *72*, 3679-3688;
- d) Brotzel, F.; Mayr, H. *Org. Biomol. Chem.* **2007**, *5*, 3814-3820; e) Baidya, M.; Kobayashi, S.; Brotzel, F.; Schmidhammer, U.; Riedle, E.; Mayr, H. *Angew. Chem.* **2007**, *119*, 6288-6292; *Angew. Chem. Int. Ed.* **2007**, *46*, 6176-6179.
- (11) Minegishi, S.; Kobayashi, S.; Mayr, H. *J. Am. Chem. Soc.* **2004**, *126*, 5174-5181.
- (12) Phan, T. B.; Mayr, H. *Can. J. Chem.* **2005**, *83*, 1554-1560.
- (13) Kempf, B.; Mayr, H. *Chem. Eur. J.* **2005**, *11*, 917-927.
- (14) a) Berger, S. T. A.; Ofial, A. R.; Mayr, H. *J. Am. Chem. Soc.* **2007**, *129*, 9753-9761; b) Lucius, R.; Loos, R.; Mayr, H. *Angew. Chem.* **2002**, *114*, 97-102; *Angew. Chem. Int. Ed.* **2002**, *41*, 91-95; c) Bug, T.; Lemek, T.; Mayr, H. *J. Org. Chem.* **2004**, *69*, 7565-7576; d) Phan, T. B.; Mayr, H. *Eur. J. Org. Chem.* **2006**, 2530-2537; e) Berger, S. T. A.; Lemek, T.; Mayr, H. *ARKIVOC* **2008**, (*x*), 37-53; f) Seeliger, F.; Mayr, H. *Org. Biomol. Chem.* **2008**, *6*, 3052-3058; g) Bug, T.; Mayr, H. *J. Am. Chem. Soc.* **2003**, *125*, 12980-12986.
- (15) a) Mayr, H.; Lang, G.; Ofial, A. R. *J. Am. Chem. Soc.* **2002**, *124*, 4076-4083; b) Funke, M.-A.; Mayr, H. *Chem. Eur. J.* **1997**, *3*, 1214-1222; c) Richter, D; Mayr, H.. *Angew. Chem.* **2008**, submitted.

Chapter 2

Electrophilicity Parameters of 5-Benzylidene-2,2-dimethyl-[1,3]dioxane-4,6-diones (Benzylidene Meldrum's Acids)

O. Kaumanns, H. Mayr, *J. Org. Chem.* **2008**, *73*, 2738-2745.

Introduction

Numerous kinetic investigations have shown that the rate constants for the reactions of carbocations with carbanions and neutral π -nucleophiles can be described by Equation (2.1), wherein s and N are nucleophile dependent parameters and E is an electrophile dependent parameter.^{1,2}

$$\log k_2(20\text{ }^\circ\text{C}) = s(N + E) \quad (2.1)$$

In order to assign nucleophilicity parameters for strong nucleophiles, such as carbanions,³⁻⁵ amines,⁶⁻⁸ enamines,⁹ silyl enol ethers,¹⁰ and ketene acetals¹¹ amino-substituted diarylcarbenium ions and structurally related quinone methides have been used as reference electrophiles. It has been shown that Equation (2.1) also holds for the reactions of ordinary Michael acceptors and electron deficient arenes with carbanions¹²⁻¹⁴ and other strong nucleophiles.^{15,16}

The nucleophilic attack at the electron deficient double bond of Michael acceptors has long been a field of great interest in physical organic chemistry. Bernasconi studied the kinetics of the reactions of numerous amines, carbanions, and alkoxides towards Michael acceptors, e.g.,

benzylidene indandiones and benzylidene Meldrum's acids in DMSO/H₂O mixtures.¹⁷⁻²¹ Rappoport investigated nucleophilic vinylic substitutions²² on chloro-substituted benzylidene Meldrum's acids which follow the addition-elimination mechanism.^{21,23} In recent years, Oh and Lee²⁴ reported mechanistic studies and rate constants of the reactions of benzylamines with benzylidene Meldrum's acids and other Michael acceptors in acetonitrile.

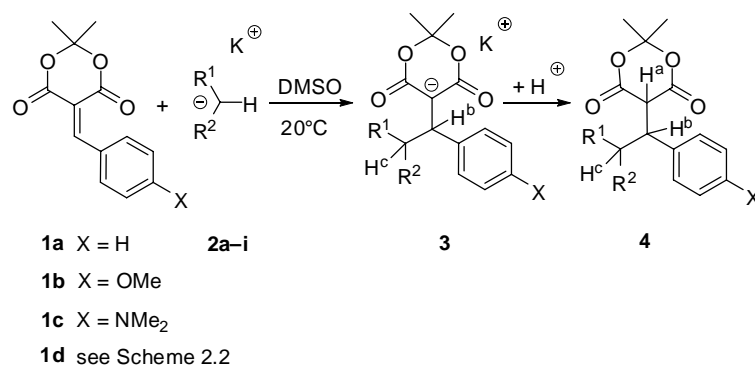
Benzylidene Meldrum's acids **1** are usually prepared by condensation of an aldehyde with Meldrum's acid in the presence of catalytic amounts of acid²⁵ or base in benzene or chloroform solutions,²⁶ but in some cases subsequent cyclizations occur.^{26c} Improved yields have been obtained under solvent-free conditions by grinding the reactants,²⁷ by DMAP-catalysis,²⁸ or by using water²⁹ or ionic liquids³⁰ as solvents. Compounds **1** are useful reactants for the synthesis of pharmacologically active heterocyclic compounds.³¹

In 1964, benzylidene Meldrum's acids have been termed "electronically neutral Lewis acids" by Swoboda and Wessely.²⁵ Schuster, Polansky and Wessely reported equilibrium constants for the addition of methoxide to a variety of neutral organic Lewis acids, including benzylidene Meldrum's acids.³² The formation of zwitterionic addition products from neutral organic Lewis acids and amines or phosphanes was reported by Margaretha.³³

Rate and equilibrium constants for the additions of amines to the electrophilic double-bond of these Michael acceptors were determined^{34a,b} and the kinetics of their hydrolytic cleavage was investigated in 10% aqueous methanol.^{34b} Regio- and stereoselective Cu-catalyzed additions of alkynes³⁵ and R₂Zn to benzylidene Meldrum's acids have recently been reported by Carreira³⁶ and Fillion.³⁷

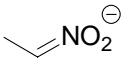
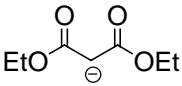
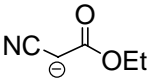
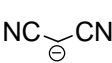
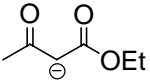
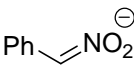
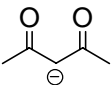
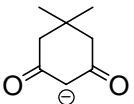
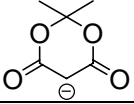
The higher electrophilic reactivity of benzylidene Meldrum's acids compared to benzylidene malonic esters, their open-chain analogs, is related to the unusually high acidity of the Meldrum's acid, which was attributed to the fixed bis-anti conformation of the ester groups.³⁸ Recently, Nakamura employed the "reactive hybrid orbital (RHO) theory" to rationalize the high acidity of Meldrum's acid.³⁹

Scheme 2.1. Reactions of the Carbanions **2a-i** (K^+ salts) with the Benzylidene Meldrum's Acids **1a-d**.



As part of our program of developing comprehensive nucleophilicity and electrophilicity scales, we have now studied the kinetics of the reactions of the carbanions **2a-i** (Table 2.1) with the benzylidene Meldrum's acids **1a-d** in DMSO (Scheme 2.1). We will show that Equation (2.1) can be used to describe the rates of these reactions and report on the determination of the electrophilicity parameters E for the Michael acceptors **1a-d**. We will furthermore present correlations between the E parameters of these and related electrophiles with Hammett's substituent constants σ_p and thus provide data to predict absolute rate constants for a manifold of Michael additions.

Table 2.1. *N* and *s* Parameters of the Carbanions **2a–i** in DMSO.

	Nucleophile	<i>N</i>	<i>s</i>
2a		21.54 ^a	0.62 ^a
2b		20.22 ^b	0.65 ^b
2c		19.62 ^b	0.67 ^b
2d		19.36 ^b	0.67 ^b
2e		18.82 ^b	0.69 ^b
2f		18.29 ^a	0.71 ^a
2g		17.64 ^b	0.73 ^b
2h		16.27 ^b	0.77 ^b
2i		13.91 ^b	0.86 ^b

^a From ref. 5. ^b From ref. 4.

Results and Discussion

Reaction Products. When equimolar amounts of **1** and **2-K⁺** were combined in DMSO, the potassium salts **3-K⁺** were formed and characterized by ¹H and ¹³C NMR spectroscopy without further workup (Scheme 2.1, Table 2.2). Compounds **4** were synthesized from equimolar amounts of **1** and **2-K⁺** in DMSO or 1,2-dimethoxyethane solution and subsequent treatment with hydrochloric acid. Since analogous products can be expected for different combinations of the electrophiles **1a–d** with the carbanions **2a–i**, product studies have not been performed for all combinations which were studied kinetically. In all cases quantitative product formation was indicated by the complete decolorization of the solutions and the fact

that the NMR spectra obtained after mixing **1** and **2-K⁺** showed the signals of **3-K⁺** exclusively. The differences in the isolated yields reported in Table 2.2 are due to non-optimized workup procedures.

Table 2.2. Characterized Michael Adducts and Some Characteristic ¹H NMR Chemical Shifts.^a

Electrophile	Nucleophile	Product (yield / %)	$\delta(\text{H}^a)$ / ppm	$\delta(\text{H}^b)$ / ppm	$\delta(\text{H}^c)$ / ppm	$J_{a,b}$ / Hz	$J_{b,c}$ / Hz
1a (X = H)	2h	3ah ^{b,c}	--	5.76 ^c	--	--	--
1b (X = OMe)	2b	3bb ^b	--	4.38	4.89	--	12.4
1b	2b	4bb (41)	4.43–4.47	4.43–4.47	4.78	--	12.4
1b	2d	4bd (48)	3.94	4.22	5.10	3.6	12.6
1b	2e	4be (66) ^d	--	4.96	--	--	--
1b	2g	4bg (85)	4.06	4.44	5.19	4.0	12.0
1b	2h	3bh (64) ^{c,ef}	--	5.68 ^c	--	--	--
1c (X = NMe ₂)	2b	3cb ^b	--	4.33	4.87	--	12.6
1c	2b	4cb	4.33–4.43	4.33–4.43	4.70	--	12.0
1c	2d	3cd (66) ^e	--	4.28	5.75	--	12.4
1c	2g	3cg ^b	--	4.46	5.24	--	12.4
1c	2h	3ch (46) ^{c,ef}	--	5.64 ^c	--	--	--
1d (X = jul)	2a	3da ^{b,g}	--	3.94/3.88 ^g	5.71/5.85 ^g	--	--
1d	2b	3db ^b	--	4.20	4.80	--	12.6
1d	2b	4db	4.26–4.30	4.26–4.20	4.65	--	12.0
1d	2d	3dd ^b	--	4.12	5.68	--	12.0
1d	2d	4dd ^e	4.01	4.18	5.12	3.3	12.5
1d	2g	3dg ^b	--	4.33	5.24	-	12.8

^a Anionic products **3** were characterized in *d*₆-DMSO, neutral products **4** were characterized in CDCl₃, for numbering see Scheme 2.1. ^b Analysis of the crude reaction mixture. ^c Enol form of the dimedone moiety. ^d Diastereomers in a ratio of 58:42. ^e The given yield refers to the reaction in 1,2-dimethoxyethane. ^f Thermally instable, NMR spectra were taken from the crude reaction mixture in DMSO. ^g Diastereomers in a ratio of 52:48.

Generally, the Michael adducts **3** and **4** show ^1H NMR spectra with resonances H^{a} , H^{b} and H^{c} in the range of $\delta = 3.8\text{--}5.9$ ppm with small coupling constants of 3.3–4.0 Hz between H^{a} and H^{b} , and large coupling constants of approximately 12.5 Hz between H^{b} and H^{c} . Only the dimedone adducts **3ah**, **3bh**, and **3ch** do not show the absorption of H^{c} around $\delta = 5$ ppm. Instead, a signal at $\delta = 13.5$ ppm was observed due to the enol form of the dimedone fragment.⁴⁰ As a consequence, H^{b} absorbs as a singlet at $\delta = 5.7$ ppm in the anions **3ah**, **3bh**, and **3ch**.

Kinetic Investigations with Carbanions. The kinetic investigations were performed at 20 °C in DMSO as solvent. Because the benzylidene Meldrum's acids **1a–d** show absorption bands at 325, 366, 460, and 484 nm, respectively, and neither the products **3** nor the carbanions **2a–i** absorb at these wavelengths, the progress of the reactions can be monitored photometrically at the absorption maxima of these electrophiles. Due to the high rates of these reactions, the stopped-flow technique was generally employed. All reactions described in this paper proceed quantitatively. The carbanions were either used as preformed potassium salts, or the corresponding CH acids were deprotonated with 1.05 equivalents of potassium *tert*-butoxide before use. UV-Vis spectroscopic monitoring of the titration showed that complete deprotonation of **2f-H** was obtained with 1.05 equivalents of KO*t*Bu. In order to confirm that the slight excess of KO*t*Bu did not affect the observed rate constants, we have also generated the carbanion **2f** by treating **2f-H** with 0.27 equivalents of KO*t*Bu. In this case, the concentration of the carbanion **2f** is given by the quantity of KO*t*Bu, and the second-order rate constant was found to be the same as that obtained with the slight excess of KO*t*Bu (Experimental Section, Tables S7a and S7b). In order to obtain pseudo-first order kinetics, the carbanions were used in large excess (10 to 100 equivalents) over the electrophiles. In all cases reported in Table 2.3, an exponential decay of the concentration of the electrophiles **1a–d** was observed (Equation (2.2)).

$$-d[\mathbf{1}]/dt = k_{1\psi}[\mathbf{1}] \quad (2.2)$$

The first-order rate constants $k_{1\psi}$ were obtained by least-squares fitting of the time-dependent absorbances A_t of the electrophiles to the exponential function $A_t = A_0 \exp(-k_{1\psi}t) + C$. Plots of $k_{1\psi}$ versus the carbanion concentration $[\mathbf{2}]$ resulted in linear correlations with almost zero intercepts, the slopes of which gave the second-order rate constants k_2 (Table 2.3).

Table 2.3. Second-Order Rate Constants k_2 for the Reactions of the Potassium Salts of Carbanions **2a–i** with the Electrophiles **1a–d** in DMSO at 20 °C.

Electrophile	E^a	Nucleophile	$k_2 / \text{L mol}^{-1} \text{s}^{-1}$
1a (X = H)	-9.15 ^b	2h	2.93×10^5
		2i	1.16×10^4
1b (X = OMe)	-10.28	2b	1.15×10^6
		2c	1.96×10^6
		2d	2.51×10^6
		2e	7.42×10^5
		2f	2.23×10^5
		2g	1.89×10^5
		2h	6.00×10^4
		2i	2.39×10^3
1c (X = NMe ₂)	-12.76	2b	2.89×10^4
		2c	4.76×10^4
		2d	7.21×10^4
		2e	1.27×10^4
		2f	3.87×10^3
		2g	3.50×10^3
		2h	9.82×10^2
		2i	2.12×10^4
1d (X = jul)	-13.97	2a ^c	2.12×10^4
		2b	6.08×10^3
		2c	7.98×10^3
		2d	1.48×10^4
		2e	2.83×10^3
		2f	4.93×10^2
		2g	3.84×10^2
		2h	1.08×10^2

^a The E parameters for **1a–d** result from a least-squares minimization of $\Delta^2 = \Sigma(\log k_2 - s(N + E))^2$ which uses the second-order rate constants k_2 (this Table) and the N and s parameters of the carbanions **2a–i** given in Table 2.1. Details of the calculation of E are discussed below.

^b A value of -9.5 is expected if the same set of reference nucleophiles would be employed as

for compounds **1b–d**. ^c The tetra-*n*-butyl ammonium salt of **2a** was used for the kinetic measurements.

Correlation analysis. If Equation (2.1) holds for the reactions of the benzylidene Meldrum's acids **1a–d** with carbanions, the plots of $(\log k_2)/s$ versus the nucleophilicity parameter N should have slopes of 1.0. Figure 2.1 shows that this is approximately the case. However, small systematic deviations of some of the nucleophiles are obvious. The dimedone anion (**2h**) and the malononitrile anion (**2d**) react two to four times faster with each of the electrophiles **1b–d** than expected from the correlations, whereas the nitroethyl anion (**2a**), the malonate anion (**2b**), and the phenyl nitronate (**2f**) are about two times less reactive than expected.

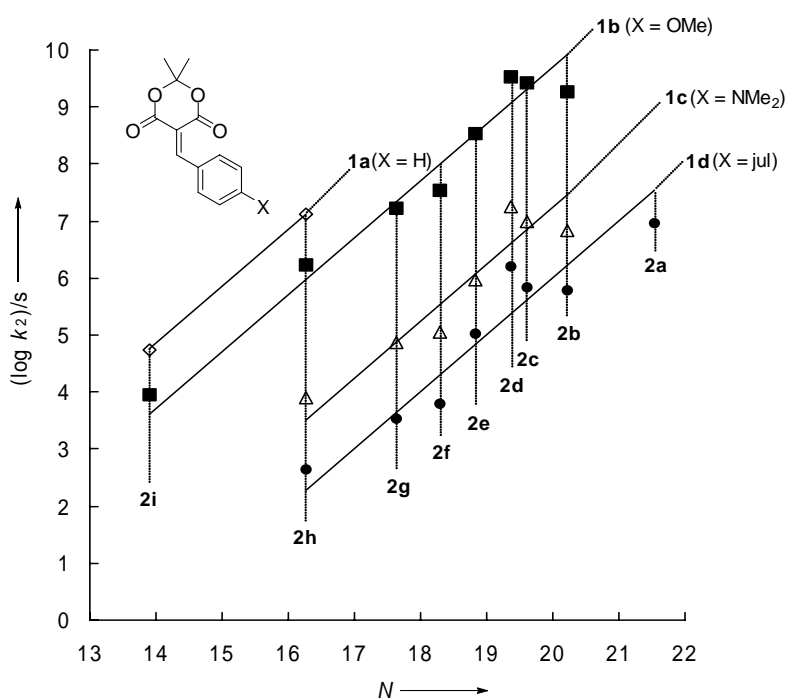


Figure 2.1. Correlation of $(\log k_2)/s$ versus the nucleophilicity parameters N of the carbanions **2a–i** for the reactions of the benzylidene Meldrum's acids **1a–d** with the carbanions **2a–i** in DMSO at 20 °C.

Though the correlations are only of moderate quality, one can conclude that the relative electrophilicities of the benzylidene Meldrum's acids **1a–d** are almost independent of the

nature of the carbanions. Therefore we have calculated the E parameters for **1a–d** by least-squares minimization of $\Delta^2 = \sum(\log k - s(N + E))^2$ using the second-order rate constants k_2 given in Table 2.3 and the N and s parameters of **2a–i** from Table 2.1. With the E parameters thus determined, a different illustration of the reactivities of the carbanions **2a–i** towards the electrophiles **1a–d** and the reference electrophiles **1e–m** becomes possible (Figure 2.2). The plots of $\log k_2$ against the electrophilicity parameters E show that in general, the reactivities of the carbanions **2a–i** toward **1a–d** correlate well with the electrophilicity parameter E , but the previously mentioned deviations are, again, evident. While, for the sake of clarity, the poorly correlating carbanions **2d** and **2f** are not included in Figure 2.2, one can see that the reactivities of **1b–d** with the anion of diethyl malonate (**2b**) are below the correlation line defined by the reference electrophiles **1e–m**. On the other hand the dimedone anion (**2h**) generally reacts faster with electrophiles **1b–d** than expected from the rates of its reactions with the reference electrophiles **1e–m**.

The different behavior of the dimedone anion (**2h**) towards the Michael acceptors **1a–d** and the reference electrophiles **1e–m** reminds of the previously reported behavior of **2h** towards electrophiles **5-X**,¹³ **6-X**,¹³ and **7-X**,¹⁴ but the reason for these deviations is presently not understood.

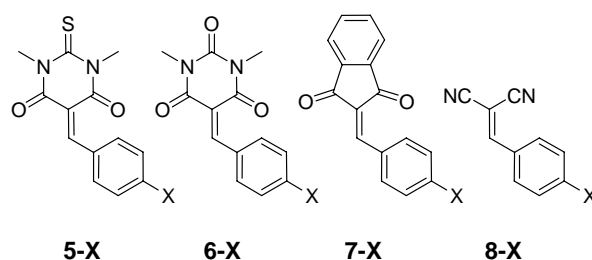


Figure 2.3 shows that there are clearly two distinct correlation lines for the different types of electrophiles, one for the reactions of **2h** with the quinone methides **1h–m** and the benzhydrylium ions **1e–g** and another one for the structurally related Michael acceptors **1-X**, **5-X**, **6-X**, and **7-X**. Despite this clear separation, one should note that all deviations from the lower (reference) line are much less than one order of magnitude. One can, therefore,

conclude that the reactivity order of the carbanions **2a–i** derived from the rates of the reactions with the reference electrophiles **1e–m** also holds roughly for the Michael acceptors **1a–d** and that the E parameters derived in Table 2.1 can be employed for the general prediction of rate constants for the reactions of **1a–d** with nucleophiles.

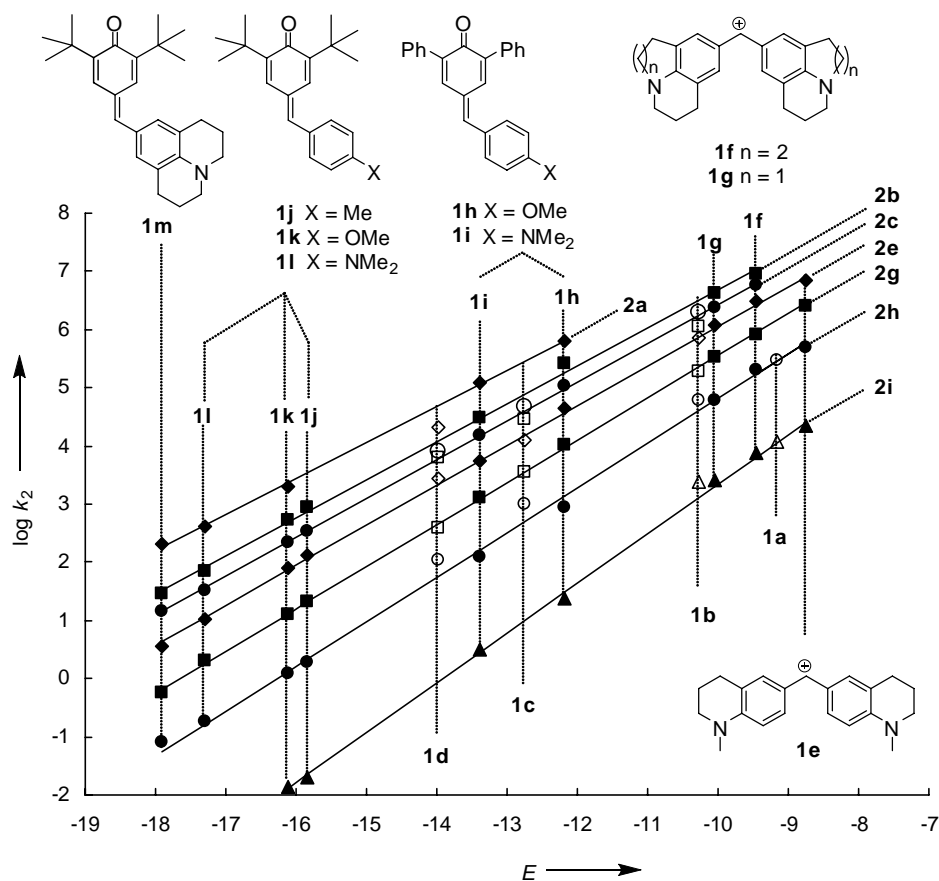


Figure 2.2. Rate constants for the reaction of the carbanions **2a–i** with the electrophiles **1a–d** (open symbols) and with the reference electrophiles **1e–m** (filled symbols) in DMSO.

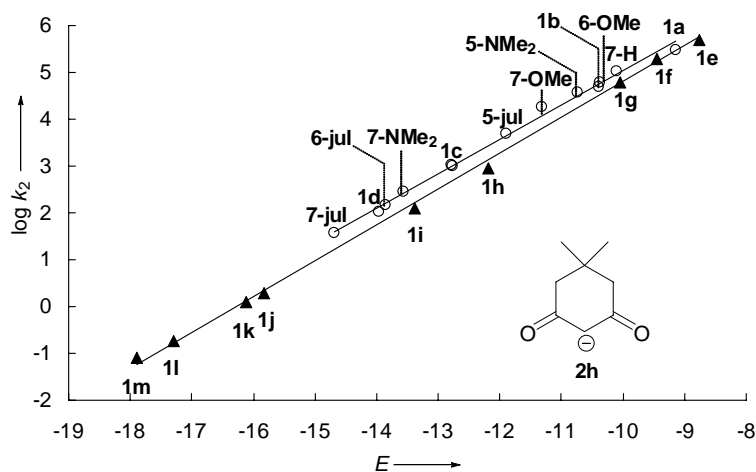


Figure 2.3. Rate constants for the reaction of the dimedone anion (**2h**) with the electrophiles **1a–d** and **5–7** (open symbols, $\log k_2 = 0.73E + 12.4$) and reference electrophiles **1e–m** (filled symbols, $\log k_2 = 0.77E + 12.5$) in DMSO.

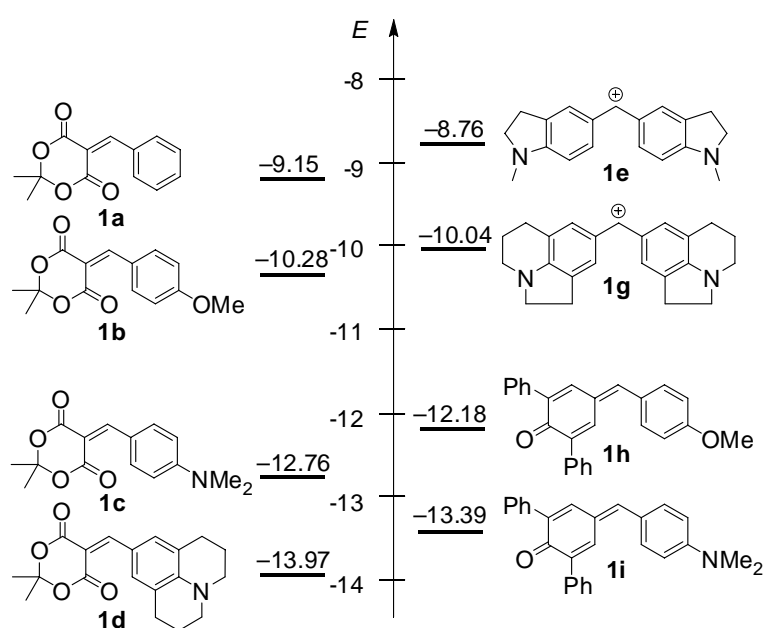
The positioning of the combination of dimedone **2h** with **1a** on the “wrong” correlation line of Figure 2.3 is due to the fact that the electrophilicity parameter of **1a** has been derived from the reactions of **1a** with **2i** and **2h** (Figure 2.1), i.e., two carbanions which react faster with **1b–c** than expected from their N parameters. If all carbanions **2a–i** had been used for the determination of $E(\mathbf{1a})$, and **1a** followed the same pattern as shown for compounds **1b–d** in Figure 2.1 one would expect the slightly smaller electrophilicity parameter $E(\mathbf{1a}) \approx -9.5$. An experimental test for this hypothesis was not possible because the reactions of **1a** with **2a–g** are too fast to be followed with conventional stopped-flow instruments.

Scheme 2.2 compares the electrophilicities of the benzylidene Meldrum's acids **1a–d** with those of some reference electrophiles and shows that their electrophilic reactivities cover a range of almost five orders of magnitude.

According to Figure 2.4, the electrophilicity parameters E of **1a–c**, **6-X**, **7-X**, and **8-X** correlate well with Hammett's σ_p -values for H, OMe, and NMe₂. The corresponding plots of E versus σ_p^+ show larger scatter. From the slopes of these correlations (5.20 – 5.74, Table 2.1) one can derive reaction constants of $\rho \approx 3.8 \pm 0.3$ for reactions with nucleophiles of $s = 0.7$

(Table 2.4), indicating that in all four reaction series electron-donating substituents in *p*-position exert comparable retarding effects.

Scheme 2.2. Comparison of the Electrophilicity Parameters E of Benzylidene Meldrum's Acids **1a–d** with Those of Some Reference Electrophiles. –^a E (**1a**) has been calculated from the rate constants of the reactions of **1a** with only two nucleophiles (see text). Depending on the choice of other reaction partners, the electrophilicity E may be lower by 0.3 to 0.4 units.



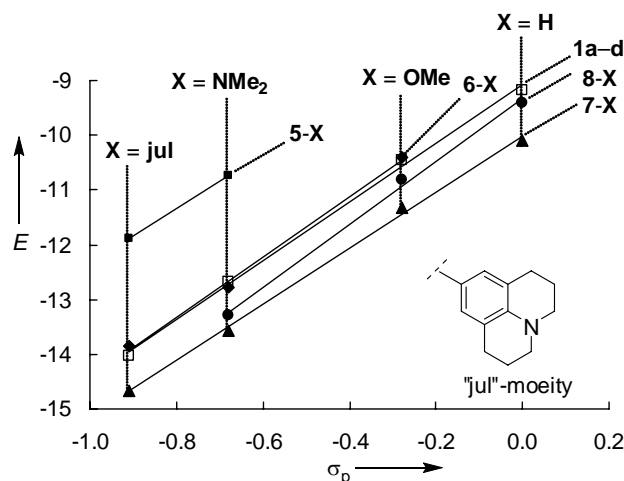


Figure 2.4. Correlation between the electrophilicity parameters E of the electrophiles **1a–d** (open symbols), and **5–8** (closed symbols) in DMSO with Hammett's σ_p -values⁴¹ – σ_p for “jul” calculated as described in the text.

Table 2.4. Correlation Between Electrophilicity Parameters E for Various Series of Electrophiles and Hammett's Substituent Constants σ_p .

Electrophile	Correlation	R^2
6-X	$E = 5.71\sigma - 8.83$	1.00
1a–c	$E = 5.37\sigma - 9.08$	0.99
8-X	$E = 5.74\sigma - 9.34$	0.99
7-X	$E = 5.20\sigma - 10.0$	0.99

Substitution of the E parameters for **1d**, **6-jul**, and **7-jul** into the correlation equations listed in Table 2.4 yields $\sigma_p(\text{jul}) = -0.91$, -0.86 , and -0.92 , respectively. When the average of these values, $\sigma_p(\text{jul}) = -0.89$, is used to locate **5-jul** in Figure 2.4, a correlation with a similar slope ($\rho = 3.5$) results for the reactions of compounds **5-X**. A considerably more negative value for $\sigma_p^+ = (-2.03)$ of the julolidyl substituent has recently been derived from the electrophilicities of benzhydrylium ions.⁴² From the similar slopes of the correlation lines for the different series of electrophiles in Figure 2.4 one can derive the general validity of the electrophilicity order **5-X** >> **6-X** \approx **1-X** > **8-X** > **7-X**.

Reactions with Other Nucleophiles. In order to check the applicability of the electrophilicity parameters E of the benzylidene Meldrum's acids **1a–d** (Scheme 2.2) for predicting the rates of reactions with other types of nucleophiles, we compared predicted and experimental rate constants for the addition reactions of amines to the electrophilic double bonds of **1a–d**.

Table 2.5. Comparison of Calculated and Experimental Second-Order Rate Constants for the Additions of Amines to Benzylidene Meldrum's Acids **1a–d** in Different Solvents (20 °C).

Entry	Nucleophile	<i>N</i> / <i>s</i> (solvent)	Electrophile	$k_2 / \text{L mol}^{-1} \text{s}^{-1}$			
				calcd ^a	experimental (solvent)		
1	piperidine	17.19/0.71 (DMSO)	1a	5.11×10^{5b}	2.09×10^6 (DMSO/H ₂ O = 90/10) ^c		
2					1.40×10^6 (DMSO/H ₂ O = 70/30) ^c		
3					6.69×10^5 (DMSO/H ₂ O = 50/50) ^c		
4					18.13/0.44 (H ₂ O)	8.94×10^3	1.70×10^5 (H ₂ O) ^c
5						2.70×10^5 (H ₂ O, 25 °C) ^c	
6						2.30×10^6 (CH ₃ CN, 25 °C) ^d	
7							1.20×10^6 (CHCl ₃ , 25 °C) ^d
8	17.19/0.71 (DMSO)	18.13/0.44 (H ₂ O)	1b	8.06×10^4	1.93×10^6 (DMSO) ^e		
9					2.89×10^5 (DMSO/H ₂ O = 50/50) ^e		
10					2.67×10^5 (DMSO/H ₂ O = 50/50) ^c		
11					18.13/0.44 (H ₂ O)	2.84×10^3	1.70×10^5 (H ₂ O, 25 °C) ^c
12							9.50×10^5 (CH ₃ CN, 25 °C) ^d
13					17.19/0.71 (DMSO)	18.13/0.44 (H ₂ O)	1c
14	3.76×10^4 (DMSO/H ₂ O = 50/50) ^e						
15	3.96×10^4 (DMSO/H ₂ O = 50/50) ^c						
16	18.13/0.44 (H ₂ O)	2.31×10^2	2.10×10^4 (H ₂ O, 25 °C) ^c				
17			1.10×10^5 (CH ₃ CN, 25 °C) ^d				
18	17.19/0.71 (DMSO)	18.13/0.44 (H ₂ O)	1d	1.93×10^2	1.80×10^4 (DMSO) ^e		
19					6.23×10^3 (DMSO/H ₂ O = 50/50) ^e		
20					morpholine	16.96/0.67 (DMSO)	1a
21	7.33×10^5 (DMSO/H ₂ O = 70/30) ^c						
22	3.19×10^5 (DMSO/H ₂ O = 50/50) ^c						
23	15.62/0.54 (H ₂ O)	3.12×10^3	1.47×10^5 (H ₂ O) ^c				
24			1.75×10^5 (H ₂ O, 25 °C) ^c				
25			4.0×10^5 (CH ₃ CN, 25 °C) ^d				
26			1.0×10^5 (CHCl ₃ , 25 °C) ^d				
27	16.96/0.67 (DMSO)	15.62/0.54 (H ₂ O)	1b	$(2.99 \times 10^4)^b$			
28					9.90×10^4 (H ₂ O, 25 °C) ^c		

Table 2.5. *Continued.*

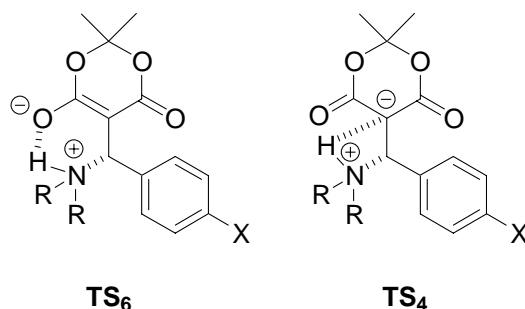
Entry	Nucleophile	<i>N</i> / <i>s</i> (solvent)	Electrophile	$k_2 / \text{L mol}^{-1} \text{s}^{-1}$	
				calcd ^a	experimental (solvent)
29		16.96/0.67 (DMSO)	1c	6.51×10^2	3.78×10^5 (DMSO) ^{e,f}
30					1.11×10^4 (DMSO/H ₂ O = 50/50) ^e
31					1.46×10^4 (DMSO/H ₂ O = 50/50) ^c
32		15.62/0.54 (H ₂ O)		3.50×10^1	1.00×10^4 (H ₂ O, 25 °C) ^c
33	glycinamide	12.29/0.58 (H ₂ O) ^g	1a	6.63×10^1	1.34×10^4 (H ₂ O) ^h
34	semicarbazid	11.05/0.52 (H ₂ O) ⁱ	1a	9.73	1.64×10^3 (H ₂ O) ^h

^a Calculated according to Equation (2.1) by using the *E* parameters for **1a–d** from Table 2.3 and the *N* and *s* parameters for amines from refs 7, 8, and 43. ^b For neat DMSO. ^c From ref. 17. ^d From ref. 34. ^e This work. ^f Fast kinetics, complete decay of the monitored absorbance within 6 ms. ^g From ref. 7. ^h From ref. 18. ⁱ From ref. 8.

Kinetics of the reactions of piperidine and morpholine with compounds **1b–d** have been determined in DMSO, using the same methodology as described above for the reactions with carbanions. The second-order rate constants for the reactions with piperidine in DMSO (Table 2.5, entries 8, 13, 18) were found to be 3–6 times greater than those in DMSO/H₂O (50/50) which have previously been determined by Bernasconi (entries 10, 15)¹⁷ and confirmed by us (entries 9, 14). The reactions are roughly one order of magnitude faster in neat DMSO than in water (cf entries 8/11 and 13/16). Solvent effects of similar magnitude have been observed for the corresponding additions of morpholine (Table 2.5, entries 20–32). Though variations of the solvent can be expected to affect nucleophilicities as well as electrophilicities, in the derivation of the parameters for Equation (2.1), solvent effects were exclusively considered in the nucleophile specific parameters *N* and *s*.⁴ Though this procedure was reported to cause some problems for the reactions with **7-X**,¹⁴ differential solvent effects on the electrophilicities of **1a–d** have not been considered.

Table 2.5 furthermore shows that the experimental rate constants are generally 20–120 times greater than the calculated values. The reaction of morpholine with **1c** in DMSO is even 580 times faster than calculated (entry 29). Though deviations from experimental values by two-orders of magnitude are still within the confidence limit of Equation (2.1),^{2,42} the

constantly higher experimental rate constants for the additions of secondary amines to **1a–d** may be indicative of a change of mechanism. Schuster,³⁴ Bernasconi,^{20,44} and Oh²⁴ presented evidence that the transition states of amine additions to **1** are stabilized by hydrogen bridging from NH to the carbonyl group (six-membered transition state **TS₆**) or from NH to the carbanionic center (four-membered ring **TS₄**). Analogous hydrogen bridging may account for the finding that glycynamide and semicarbazide react 200 times faster with **1a** than predicted by Equation (2.1) (Table 2.5, entries 33, 34).



This type of transition state stabilization by hydrogen bridging is not possible in additions of carbanions to **1a–d**, the rates of which have been used to derive the *E* parameters of these electrophiles (Table 2.3). A related study has recently shown that additions of secondary amines to benzylidene indandiones **7-X** are only three times faster than predicted by Equation (2.1).¹⁴ It has, therefore, been concluded that H-bridging as indicated in **TS₆** and **TS₄** cannot have a large effect on the transition states of the additions of secondary amines to **7-X**.

Conclusion

Benzylidene Meldrum's acids are another group of electrophiles, the reactivities of which can be described by the correlation equation (2.1). While the reactivities with carbanions can be reproduced with an accuracy of better than a factor of 5, primary and secondary amines react approximately 10^2 times faster than predicted by Equation (2.1). In line with previous work, these deviations are explained by additional stabilizing effect in the transition states (hydrogen bridging).

Accordingly, calculated and experimental rate constants for the reactions of **1** with tertiary amines, which cannot be accelerated by hydrogen bridging, differ by only one order of magnitude.⁴⁵ It is, therefore, concluded that the *E* parameters for **1a–d** in this work can be used to characterize the electrophilic potential of the title compounds.

General Remarks

Benzylidene Meldrum's Acids 1a–c. Benzylidene Meldrum's acids **1a–c** were prepared by following a procedure for the synthesis of structurally related benzylidene barbituric acids:⁴⁶ Equimolar amounts of *p*-substituted benzaldehyde and Meldrum's acid were stirred in EtOH under reflux for 2 h. The products precipitate immediately after cooling the reaction mixtures to room temperature. After filtration and recrystallization from EtOH, the electrophiles **1a–c** were obtained as colored crystals. ¹H and ¹³C NMR spectra for **1a–c** agreed with those described in the literature.^{26, 47} UV-Vis spectra of **1a–d** in DMSO are shown in Figure S2 of the Experimental Section.

2,2-Dimethyl-5-(julolidin-9-ylmethylene)-1,3-dioxane-4,6-dione (1d). Meldrum's acid (716 mg, 4.97 mmol) and 9-formyl-julolidine (1.00 g, 4.97 mmol) were added to EtOH (25 mL). The solution turned purple immediately. After 10 min under reflux, the solution was allowed to cool to room temperature. The product precipitated from the solution, was filtered and recrystallized from EtOH. The product **1d** (900 mg, 2.75 mmol, 55 %) was obtained as purple crystals; mp 138.0–138.4 °C. Further attempts to optimize the yield have not been made. ¹H NMR (300 MHz, CDCl₃): δ = 1.73 (s, 6 H, C(CH₃)₂), 1.96 (quint, *J* = 5.7 Hz, 4 H, 2 × CH₂), 2.74 (t, *J* = 5.7 Hz, 4 H, 2 × CH₂), 3.36 (t, *J* = 5.7 Hz, 4 H, 2 × CH₂), 7.85 (s, 2 H, ArH), 8.15 ppm (s, 1 H). ¹³C NMR (75.5 MHz, CDCl₃): δ = 21.0 (t, CH₂), 27.2 (q, CH₃), 27.5 (t, CH₂), 50.4 (t, CH₂), 102.6 (s), 103.0 (s), 119.4 (s), 120.5 (s), 136.6 (d, C_{ar}), 149.3 (s), 157.5 (d, =C-H), 161.8 (s), 165.6 ppm (s). Signal assignments are based on additional gHSQC

experiments. MS (ESI, positive): m/z (%): 328 (7) $[M + H]^+$, 270 (100). $C_{19}H_{21}NO_4$ (327.38): Calcd N 4.28, C 69.71, H 6.47. Found N 4.27, C 69.45, H 6.36.

5-[2-Acetyl-1-(4-methoxyphenyl)-3-oxo-butyl]-2,2-dimethyl-1,3-dioxane-4,6-dione (4bg).

A mixture of **1b** (365 mg, 1.39 mmol) and **2g-K⁺** (202 mg, 1.46 mmol) in dry DMSO (2 mL) was stirred until the color of the solution disappeared. Then the reaction mixture was poured on cold water (5 mL) and acidified with 2 M aq HCl. The precipitate was filtered and dissolved in CH_2Cl_2 . After removal of the traces of water by filtering the solution over a hot cotton batting, the solvent was evaporated and the residue was dried in vacuum: **4bg** (400 mg, 85 %), colorless solid; mp 116.6–116.9 °C. 1H NMR (300 MHz, $CDCl_3$): δ = 1.27, 1.62 (2 s, 2 \times 3 H, $C(CH_3)_2$), 1.95 (s, 3 H, $COCH_3$), 2.32 (s, $COCH_3$), 3.74 (s, 3 H, OMe), 4.06 (d, 3J = 4.0 Hz, 1 H, H^a), 4.44 (d, d, 3J = 4.0 Hz, 12.0 Hz, 1 H, H^b), 5.19 (d, 3J = 12 Hz, 1 H, H^c), 6.79 (d, 3J = 9.0 Hz, 2 H, ArH), 7.19 ppm (d, 3J = 9.0 Hz, 2 H, ArH). ^{13}C NMR (75.5 MHz, $CDCl_3$): δ = 28.3 (q, $C(CH_3)_2$), 28.5 (q, $C(CH_3)_2$), 29.9 (q, $COCH_3$), 30.6 (q, $COCH_3$), 43.2 (d, C^b), 48.2 (d, C^a), 55.4 (q, OCH_3), 71.0 (d, C^c), 105.8 (s, $C(CH_3)_2$), 114.7 (d, Ar), 128.5 (s), 130.8 (d, Ar), 159.7 (s), 165.0 (s, CO_2), 165.9 (s, CO_2), 202.4 (s, $COCH_3$), 203.5 ppm (s, $COCH_3$). Signal assignments are based on additional DEPT and gHSQC experiments. ESI-MS (negative): m/z (%): 361 (100) $[M - H]^+$. HR-MS: calcd 362.1366 ($C_{19}H_{22}O_7$), found 362.1327.

Reaction of 4-Dimethylaminobenzylidene Meldrum's Acid (1c) with Potassium Dicyanomethanide (2d-K⁺). A mixture of **1c** (71.5 mg, 0.260 mmol) and **2d-K⁺** (27.1 mg, 0.260 mol) was stirred in DME (2 mL) at room temperature. After decolorization of the solution, stirring was continued for 5 min. A yellow solid precipitated and hexane was added to support the precipitation. The precipitate was washed with diethyl ether/hexane: **3cd** (65 mg, 66 %), yellow solid; mp 129.1–129.5 °C. 1H NMR (400 MHz, d_6 -DMSO): δ = 1.46 (s, 6

H, C(CH₃)₂), 2.85 (s, 6 H, NMe₂), 4.28 (d, ³J = 12.4 Hz, 1 H, H^b), 5.75 (d, ³J = 12.0 Hz, 1 H, H^c), 6.61 (d, ³J = 8.8 Hz, 2 H, ArH), 7.29 ppm (d, ³J = 8.8 Hz, 2 H, ArH). ¹³C NMR (100.5 MHz, d₆-DMSO): δ = 25.7 (q, C(CH₃)₂), 26.6 (d, C^c), 40.1 (q, NMe₂), 43.2 (d, C^b), 73.2 (s, C^a), 99.7 (s, C(CH₃)₂), 111.8 (d, Ar), 115.1 (s, CN), 128.4 (d, Ar), 129.8 (s), 149.2 (s), 164.6 ppm (s, CO₂). Signal assignments are based on additional gHSQC experiments. ESI-MS (negative): m/z (%): 340 (100) [M – K⁺]⁻, 300 (63), 212 (23).

Kinetics. For the kinetic experiments, standard stopped-flow UV-Vis-spectrophotometer systems were used in their single mixing mode. Solutions of the electrophiles **1** in DMSO were mixed with solutions of the carbanions **2** in DMSO (either generated by deprotonation of **2**-H with 1.05 equiv. KO^tBu in DMSO or by dissolving **2**-K⁺ in DMSO). In order to obtain first-order kinetics, the carbanions were used in large excess (10 to 100 equivalents) over the electrophiles. The temperature of the solutions was kept constant (20 ± 0.1 °C) by using circulating bath thermostats.

Rate constants $k_{1\psi}$ (s⁻¹) were obtained by fitting the single exponential $A_t = A_0 \exp(-k_{1\psi}t) + C$ to the observed time-dependent electrophile absorbance (the monitored wavelengths are given in the Experimental Section). As depicted in the Experimental Section, the second-order rate constants k_2 (Table 2.3) were obtained from the slopes of the linear plots of $k_{1\psi}$ versus the carbanion concentrations [**2**].

References

- (1) (a) Mayr, H.; Ofial, A. R. *Pure Appl. Chem.* **2005**, *77*, 1807–1821. (b) Ofial, A. R.; Mayr, H. *Macromol. Symp.* **2004**, *215*, 353–367. (c) Mayr, H.; Ofial, A. R. In *Carbocation Chemistry*; Olah, G. A., Prakash, G. K. S., eds.; Wiley: Hoboken, NJ, 2004; pp. 331–358. (d) Mayr, H.; Kuhn, O.; Gotta, M. F.; Patz, M. *J. Phys. Org. Chem.* **1998**, *11*, 642–654. (e) Mayr, H.; Patz, M.; Gotta, M. F.; Ofial, A. R. *Pure Appl. Chem.* **1998**, *70*, 1993–2000. (f) Mayr, H.; Patz, M. *Angew. Chem.* **1994**, *106*, 990-1010; *Angew. Chem. Int. Ed.* **1994**, *33*, 938-957.
- (2) Mayr, H.; Kempf, B.; Ofial, A. R. *Acc. Chem. Res.* **2003**, *36*, 66–77.
- (3) (a) Phan, T. B.; Mayr, H. *Eur. J. Org. Chem.* **2006**, 2530–2537. (b) Lucius, R.; Mayr, H. *Angew. Chem.* **2000**, *112*, 2086-2089; *Angew. Chem., Int. Ed.* **2000**, *39*, 1995–1997.
- (4) Lucius, R.; Loos, R.; Mayr, H. *Angew. Chem.* **2002**, *114*, 97–102; *Angew. Chem., Int. Ed.* **2002**, *41*, 91–95.
- (5) Bug, T.; Lemek, T.; Mayr, H. *J. Org. Chem.* **2004**, *69*, 7565–7576.
- (6) (a) Brotzel, F.; Mayr, H. *Org. Biomol. Chem.* **2007**, *5*, 3814–3820. (b) Brotzel, F.; Kempf, B.; Singer, T.; Zipse, H.; Mayr, H. *Chem. Eur. J.* **2007**, *13*, 336–345.
- (7) Brotzel, F.; Chu, Y. C.; Mayr, H. *J. Org. Chem.* **2007**, *72*, 3679–3688.
- (8) Minegishi, S.; Mayr, H. *J. Am. Chem. Soc.* **2003**, *125*, 286–295.
- (9) Kempf, B.; Hampel, N.; Ofial, A. R.; Mayr, H. *Chem. Eur. J.* **2003**, *9*, 2209–2218.
- (10) (a) Dilman, A. D.; Mayr, H. *Eur. J. Org. Chem.* **2005**, 1760–1764. (b) Burfeindt, J.; Patz, M.; Müller, M.; Mayr, H. *J. Am. Chem. Soc.* **1998**, *120*, 3629–3634. (c) Patz, M.; Mayr, H. *Tetrahedron Lett.* **1993**, *34*, 3393–3396.
- (11) Tokuyasu, T.; Mayr, H. *Eur. J. Org. Chem.* **2004**, 2791–2796.

- (12) Lemek, T.; Mayr, H. *J. Org. Chem.* **2003**, *68*, 6880–6886.
- (13) Seeliger, F., Berger, S. T. A., Remennikov, G. Y., Polborn, K., Mayr, H. *J. Org. Chem.* **2007**, *72*, 9170–9180.
- (14) Berger, S. T. A.; Seeliger, F. H.; Hofbauer, F.; Mayr, H. *Org. Biomol. Chem.* **2007**, *5*, 3020–3026.
- (15) (a) Terrier, F.; Lakhdar, S.; Boubaker, T.; Goumont, R. *J. Org. Chem.* **2005**, *70*, 6242–6253. (b) Lakhdar, S.; Goumont, R.; Berionni, G.; Boubaker, T.; Kurbatov, S.; Terrier, F. *Chem. Eur. J.* **2007**, *13*, 8317–8324.
- (16) Remennikov, G. Y.; Kempf, B.; Ofial, A. R.; Polborn, K.; Mayr, H. *J. Phys. Org. Chem.* **2003**, *16*, 431–437.
- (17) Bernasconi, C. F.; Panda, M. *J. Org. Chem.* **1987**, *52*, 3042–3050.
- (18) Bernasconi, C. F. *Tetrahedron* **1989**, *45*, 4017–4090.
- (19) (a) Bernasconi, C. F.; Fornarini, S. *J. Am. Chem. Soc.* **1980**, *102*, 5329–5336. (b) Bernasconi, C. F.; Leonarduzzi, G. D. *J. Am. Chem. Soc.* **1980**, *102*, 1361–1366.
- (20) (a) Bernasconi, C. F.; Murray, C. J. *J. Am. Chem. Soc.* **1986**, *108*, 5251–5257. (b) Bernasconi, C. F.; Leonarduzzi, G. D. *J. Am. Chem. Soc.* **1982**, *104*, 5133–5142.
- (21) Bernasconi, C. F.; Ketner, R. J.; Chen, X.; Rappoport, Z. *J. Am. Chem. Soc.* **1998**, *120*, 7461–7468.
- (22) Rappoport, Z. *Acc. Chem. Res.* **1992**, *25*, 474–479.
- (23) Ali, M.; Biswas, S.; Rappoport, Z.; Bernasconi, C. F. *J. Phys. Org. Chem.* **2006**, *19*, 647–653.
- (24) (a) Oh, H. K.; Kim, T. S.; Lee, H. W.; Lee, I. *Bull. Korean Chem. Soc.* **2003**, *24*, 193–196. (b) Oh, H. K.; Lee, J. M. *Bull. Korean Chem. Soc.* **2002**, *23*, 1459–1462.

- (25) (a) Swoboda, G.; Swoboda, J.; Wessely, F. *Monatsh. Chem.* **1964**, *95*, 1283–1304. (b) Review: Kunz, J. F.; Margaretha, P.; Polansky, O. E. *Chimia* **1970**, *24*, 165–208.
- (26) (a) Schuster, P.; Polansky, O. E.; Wessely, F. *Monatsh. Chem.* **1964**, *95*, 53–58. (b) McNab, H. *Chem. Soc. Rev.* **1978**, *7*, 345–358. (c) Margaretha, P. *Tetrahedron Lett.* **1970**, *11*, 1449–1452. (d) Chen, B. C. *Heterocycles* **1991**, *32*, 529–597.
- (27) Kaupp, G.; Naimi-Jamal, M. R.; Schmeyers, J. *Tetrahedron* **2003**, *59*, 3753–3760.
- (28) Narsaiah, A. V.; Basak, A. K.; Visali, B.; Nagaiah, K. *Synth. Commun.* **2004**, *34*, 2893–2901.
- (29) Bigi, F.; Carloni, S.; Ferrari, L.; Maggi, R.; Mazzacani, A.; Sartori, G. *Tetrahedron Lett.* **2001**, *42*, 5203–5205.
- (30) Hu, Y.; Wei, P.; Huang, H.; Le, Z.-G.; Chen, Z.-C. *Synth. Commun.* **2005**, *35*, 2955–2960.
- (31) (a) Tu, S.; Zhu, X.; Zhang, J.; Xu, J.; Zhang, Y.; Wang, Q.; Jia, R.; Jiang, B.; Zhang, J.; Yao, C. *Bioorg. Med. Chem. Lett.* **2006**, *16*, 2925–2928. (b) Pita, B.; Sotelo, E.; Suarez, M.; Ravina, E.; Ochoa, E.; Verdecia, Y.; Novoa, H.; Blaton, N.; De Ranter, C.; Peeters, O. M. *Tetrahedron* **2000**, *56*, 2473–2479.
- (32) Schuster, P., Polansky, O. E., Wessely, F. *Tetrahedron* **1966**, *Suppl. 8 (II)*, 463–483.
- (33) Margaretha, P., Polansky, O. E. *Monatsh. Chem.* **1969**, *100*, 576–583.
- (34) (a) Schreiber, B.; Martinek, H.; Wolschann, P.; Schuster, P. *J. Am. Chem. Soc.* **1979**, *101*, 4708–4713. (b) Margaretha, P.; Leitlich, J.; Polansky, O. E. *Tetrahedron Lett.* **1969**, *11*, 4429–4432. (c) Margaretha, P.; Schuster, P.; Polansky, O. E. *Tetrahedron* **1971**, *27*, 71–79.

- (35) (a) Fujimori, S.; Carreira, E. M. *Angew. Chem., Int. Ed.* **2007**, *46*, 4964–4967.
(b) Knöpfel, T. F.; Zarotti, P.; Ichikawa, T.; Carreira, E. M. *J. Am. Chem. Soc.* **2005**, *127*, 9682–9683. (c) Knöpfel, T. F.; Carreira, E. M. *J. Am. Chem. Soc.* **2003**, *125*, 6054–6055.
- (36) Watanabe, T.; Knöpfel, T. F.; Carreira, E. M. *Org. Lett.* **2003**, *5*, 4557–4558.
- (37) Fillion, E.; Wilsily, A. *J. Am. Chem. Soc.* **2006**, *128*, 2774–2775.
- (38) (a) Arnett, E. M.; Harrelson, J. A., Jr. *J. Am. Chem. Soc.* **1987**, *109*, 809–812.
(b) Wang, X.; Houk, K. N. *J. Am. Chem. Soc.* **1988**, *110*, 1870–1872. (c) Wiberg, K. B.; Laidig, K. E. *J. Am. Chem. Soc.* **1988**, *110*, 1872–1874.
- (39) Nakamura, S.; Hirao, H.; Ohwada, T. *J. Org. Chem.* **2004**, *69*, 4309–4316.
- (40) (a) Shi, D. Q.; Chen, J.; Zhuang, Q. Y.; Wang, X. S.; Hu, H. W. *Chin. Chem. Lett.* **2003**, *14*, 1242–1245. (b) For analogous NMR spectra of related compounds see ref. 13.
- (41) Exner, O. *Correlation Analysis of Chemical Data*; Plenum: New York, 1988.
- (42) Mayr, H.; Bug, T.; Gotta, M. F.; Hering, N.; Irrgang, B.; Janker, B.; Kempf, B.; Loos, R.; Ofial, A. R.; Remennikov, G.; Schimmel, H. *J. Am. Chem. Soc.* **2001**, *123*, 9500–9512.
- (43) For a comprehensive database of reactivity parameters *E*, *N* and *s*:
www.cup.lmu.de/oc/mayr/DBintro.html.
- (44) Bernasconi, C. F.; Kanavarioti, A. *J. Am. Chem. Soc.* **1986**, *108*, 7744–7751.
- (45) Baidya, M., Mayr, H., unpublished.
- (46) Xu, Y.; Dolbier, W. R., Jr. *Tetrahedron* **1998**, *54*, 6319–6328.
- (47) (a) Schuster, I.; Schuster, P. *Tetrahedron* **1969**, *25*, 199–208; (b) Cornelis, A.; Lambert, S.; Laszlo, P.; Schaus, P. *J. Org. Chem.* **1981**, *46*, 2130–2134. (c) Fillion, E.; Dumas, A. M.; Hogg, S. A., *J. Org. Chem.* **2006**, *71*, 9899–9902.

Experimental Section

Electrophilicity Parameters of 5-Benzylidene-2,2-dimethyl-[1,3]dioxane-4,6-diones (Benzylidene Meldrum's Acids)

O. Kaumanns, H. Mayr, *J. Org. Chem.* **2008**, *73*, 2738-2745.

2.1. Materials

General. Commercially available DMSO (H₂O content < 50 ppm) was used without further purification. Stock solutions of KO^tBu in DMSO were prepared under a nitrogen atmosphere. *NMR spectroscopy.* In the ¹H and ¹³C NMR spectra chemical shifts are given in ppm and refer to *d*₆-DMSO ($\delta_{\text{H}} = 2.49$ ppm, $\delta_{\text{C}} = 39.7$ ppm) or to CDCl₃ ($\delta_{\text{H}} = 7.26$ ppm, $\delta_{\text{C}} = 77.00$ ppm) as internal standards. The coupling constants are given in Hz.

Potassium Salts of Carbanions 2. The potassium salts of **2b-i** were generated by mixing a solution of KO^tBu in dry EtOH with a solution of the corresponding CH acid in dry EtOH under nitrogen atmosphere. Because of the low solubility of (**2b-i**)-K⁺ in EtOH, the precipitates were filtered and dried to obtain (**2b-i**)-K⁺ as colorless solids.^{S1}

In some cases **2-K**⁺ was generated by mixing the corresponding CH acid **2-H** with 1.05 equiv. of KO^tBu in DMSO. For **2f-H** it was shown that the deprotonation by 1.05 equiv. KO^tBu (DMSO, 20 °C) is quantitative by following the increase of the absorption of **2f-K**⁺ at $\lambda = 365$ nm (Figure S1). The addition of a second equivalent of base does not result in a further increase of the absorption.

^{S1} R. Lucius, *Thesis*, Ludwig-Maximilians-Universität München, **2001**.

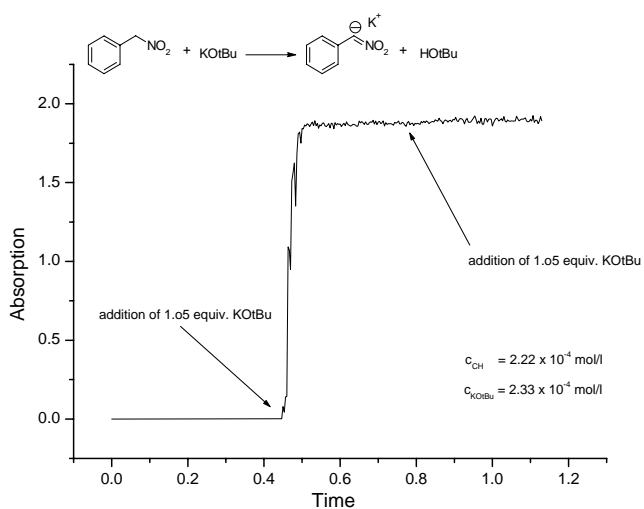


Figure S1. Titration of **2f-H** with KOtBu in DMSO.

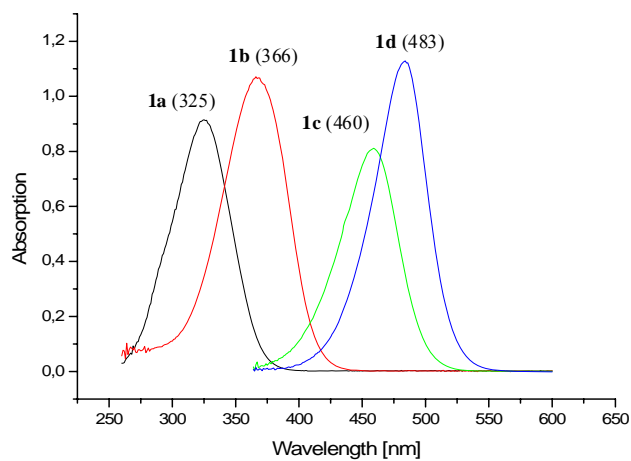
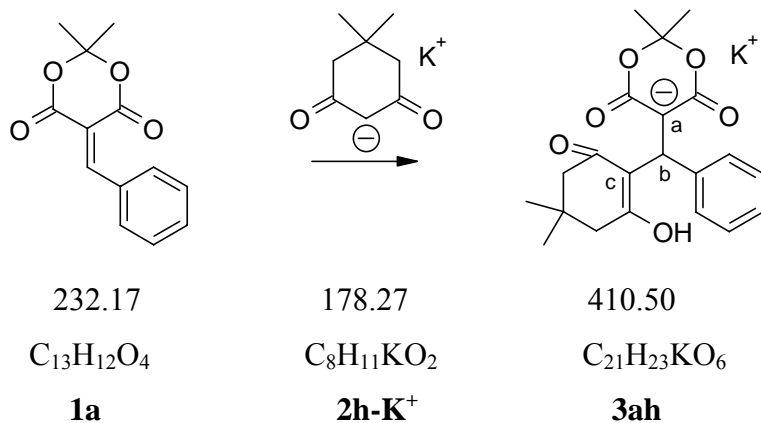


Figure S2. UV spectra of the benzylidene Meldrums' acids **1a–d** in DMSO (λ_{max} in nm).

2.2. Product Studies

Reactions of Electrophile **1a**

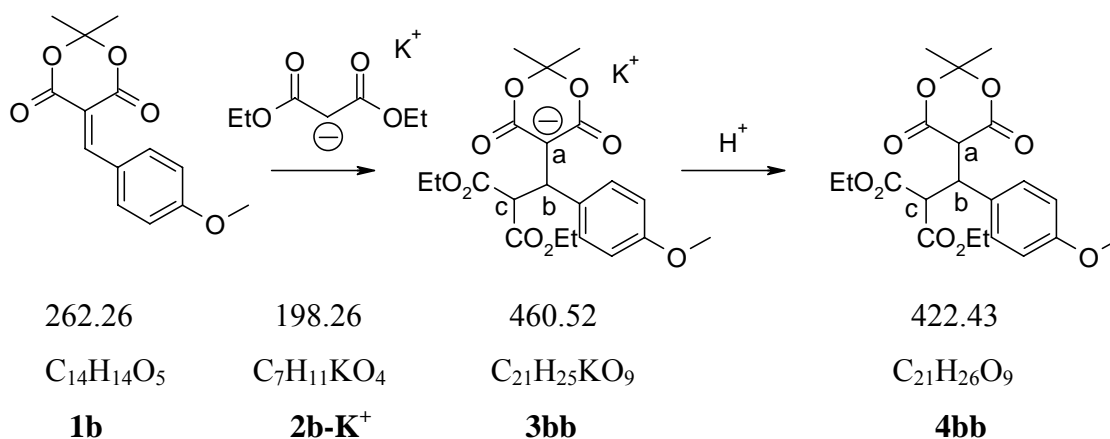
3ah: A mixture of benzylidene Meldrum's acid **1a** (64.5 mg, 0.278 mmol) and **2h-K⁺** (50.3 mg, 0.282 mmol) in dry *d*₆-DMSO (2 mL) was stirred for 5 min. Then a sample was transferred to an NMR tube and analyzed by NMR spectroscopy.



¹H-NMR (400 MHz, *d*₆-DMSO): δ = 1.03 (s, 6 H, dim-C(CH₃)₂), 1.52 (s, 6 H, C(CH₃)₂), 2.20-2.23 (m, 4 H, 2 × CH₂), 5.76 (s, 1 H, CH, H^b), 6.98-7.15 (m, 5 H, Ph), 13.49 ppm (s, br, 1 H, OH). ¹³C-NMR (100.5 MHz, CDCl₃): δ = 25.3 (q, dim-C(CH₃)₂), 27.2, 28.3 (2 q, C(CH₃)₂), 31.7 (d, CH), 44.1, 50.1 (2 × t, CH₂), 77.7 (s), 99.5 (s), 115.8 (s), 123.6 (d, Ph), 126.5 (d, Ph), 126.8 (d, Ph), 144.6 (s), 172.4 (s), 195.7 ppm (s). Signal assignments are based on additional gHSQC experiments.

Reactions of Electrophile 1b

3bb/4bb: A mixture of **1b** (195 mg, 0.743 mmol) and **2b-K⁺** (148 mg, 0.746 mmol) in dry DMSO (1 mL) was stirred until the solution was colorless (5 min). Then a sample was taken to analyze **3bb** by NMR spectroscopy. The remaining reaction mixture was poured on water (5 mL) and acidified with 2 M aq HCl (2 mL). The resulting precipitate was filtered and dried in vacuum (8×10^{-3} mbar) to yield **4bb** (130 mg, 0.308 mmol, 41 %).

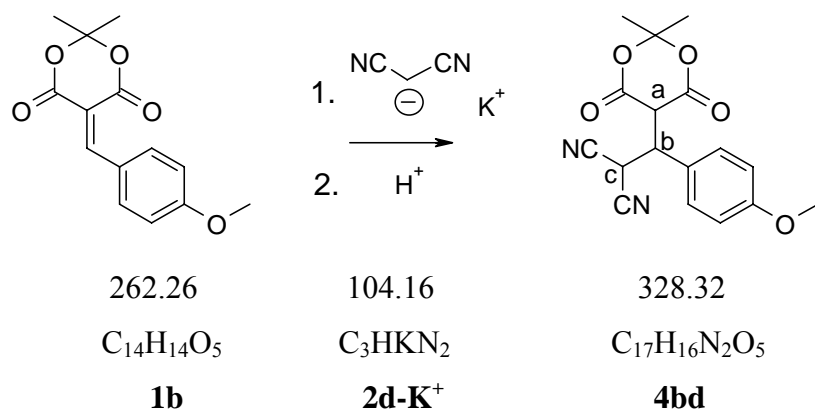


3bb: ¹H-NMR (400 MHz, *d*₆-DMSO): δ = 0.89 (t, ³*J* = 7.2 Hz, 3 H, CH₂CH₃), 1.13 (t, ³*J* = 7.2 Hz, 3 H, CH₂CH₃), 1.35 (s, 6 H, C(CH₃)₂), 3.66 (s, 3 H, OMe), 3.75-3.85 (m, 2 H, CH₂CH₃), 3.95-4.05 (m, 2 H, CH₂CH₃), 4.38 (d, ³*J* = 12.4 Hz, 1 H, H^b), 4.89 (d, ³*J* = 12.4 Hz, 1 H, H^c), 6.66 (d, ³*J* = 8.4 Hz, 2 H, ArH), 7.29 ppm (d, ³*J* = 8.4 Hz, 2 H, ArH). ¹³C-NMR (100.5 MHz, *d*₆-DMSO): δ = 13.6 (q, CH₂CH₃), 13.9 (q, CH₂CH₃), 25.6 (q, C(CH₃)₂), 40.5 (d, C^b), 54.2 (d, C^c), 54.8 (q, OCH₃), 59.8 (t, CH₂CH₃), 60.0 (t, CH₂CH₃), 74.6 (s, C^a), 98.8 (s, C(CH₃)₂), 112.3 (d, Ar), 128.9 (d, Ar), 137.5 (s), 156.7 (s), 164.4 (s), 168.4 (s, CO₂Et), 168.7 ppm (s, CO₂Et). Signal assignments are based on additional DEPT and gHSQC experiments. For the ESI-MS, a mixture of equimolar amounts of **1b** and **2b-K⁺** in dry EtOH was analyzed. MS: (ESI, negative) *m/z*: 421 (100) [M - K]⁻, (ESI, positive) *m/z*: 461 (100) [M + H]⁺, 423 (5) [M + 2H]⁺.

4bb: ¹H-NMR (400 MHz, CDCl₃): δ = 0.97 (t, ³*J* = 7.2 Hz, 3 H, CH₂CH₃), 1.27 (t, ³*J* = 7.2 Hz, 3 H, CH₂CH₃), 1.38, 1.66 (2 s, 2 × 3 H, C(CH₃)₂), 3.75 (s, 3 H, OMe), 3.88-3.96 (m, 2 H, CH₂CH₃), 4.17-4.27 (m, 2 H, CH₂CH₃), 4.43-4.47 (m, 2 H, H^a, H^b), 4.78 (d, ³*J* = 12.4 Hz, 1 H, H^c), 6.78 (d, ³*J* = 8.8 Hz, 2 H, ArH), 7.29 ppm (d, ³*J* = 8.8 Hz, 2 H, ArH). ¹³C-NMR (100.5 MHz, CDCl₃): δ = 13.7 (q, CH₂CH₃), 13.9 (q, CH₂CH₃), 27.7 (q, C(CH₃)₂), 28.2 (q,

$C(CH_3)_2$, 42.7 (d, C^b), 48.9 (d, C^a), 53.3 (d, C^c), 55.2 (q, OMe), 61.3 (t, CH_2CH_3), 62.0 (t, CH_2CH_3), 105.3 (s, $C(CH_3)_2$), 113.9 (d, Ar), 129.0 (s), 130.7 (d, Ar), 159.2 (s), 164.8 (s), 165.4 (s), 167.6 (s), 170.0 ppm (s). Signal assignments are based on additional DEPT, gHSQC, gHMBC and gDQCOSY experiments. MS: (ESI, negative) m/z : 421 (100) $[M - H]^-$, (ESI, positive) m/z : 440 (100), 423 (25) $[M + H]^+$. HR-MS: calcd 422.1577 ($C_{21}H_{26}O_9$), found 422.1535.

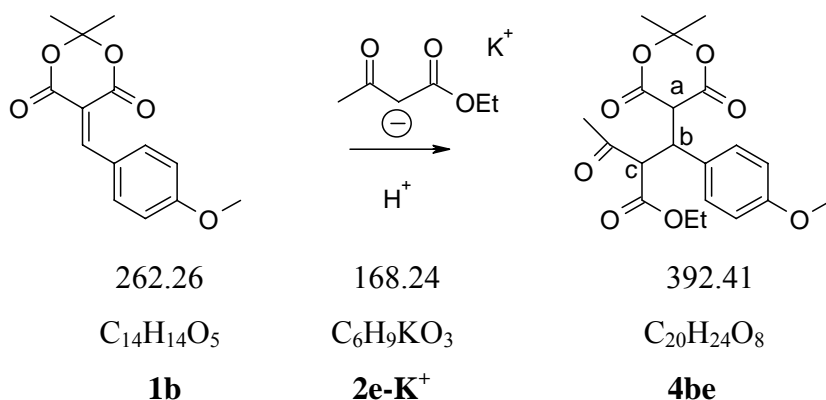
4bd: A mixture of **1b** (276 mg, 1.05 mmol) and **2d-K⁺** (117 mg, 1.12 mmol) in dry DMSO (5 mL) was stirred at room temperature until the color of the electrophile disappeared. The colorless solution was poured on cold water (5 mL) and acidified with 2 M aq HCl (2 mL). The colorless precipitate was filtered and dried to give **4bd** (160 mg, 0.487 mmol, 48 %) as a colorless solid which decomposed quickly at room temperature.



1H -NMR (600 MHz, $CDCl_3$): δ = 1.30, 1.62 (2 s, 2×3 H, $C(CH_3)_2$), 3.67 (s, 3 H, OMe), 3.94 (d, $^3J = 3.6$ Hz, 1 H, H^a), 4.22 (dd, $^3J = 3.6$ Hz, $^3J = 12.6$ Hz, 1 H, H^b), 5.10 (d, $^3J = 12.6$ Hz, 1 H, H^c), 6.76 (d, $^3J = 9.0$ Hz, 2 H, ArH), 7.13 ppm (d, $^3J = 9.0$ Hz, 2 H, ArH). ^{13}C -NMR (150 MHz, $CDCl_3$): δ = 27.3 (d, C^c), 27.9, 28.1 (2 q, $C(CH_3)_2$), 45.1 (d, C^b), 47.9 (d, C^a), 55.3 (q, OMe), 106.5 (s, $C(CH_3)_2$), 111.3 (s, CN), 112.1 (s, CN), 114.9 (d, Ar), 124.0 (s), 130.3 (d, Ar), 160.6 (s, C=O), 162.9 (s, C=O), 164.3 ppm (s). Signal assignments are based on additional gHSQC experiments.

4be: A mixture of **1b** (186 mg, 0.709 mmol) and **2e-K⁺** (143 mg, 0.850 mmol) in dry DMSO (2 mL) was stirred. After decolorization the solution was poured on cold water and acidified with 2 M aq HCl (2 mL). The colorless precipitate was filtered and dissolved in CH_2Cl_2 . After

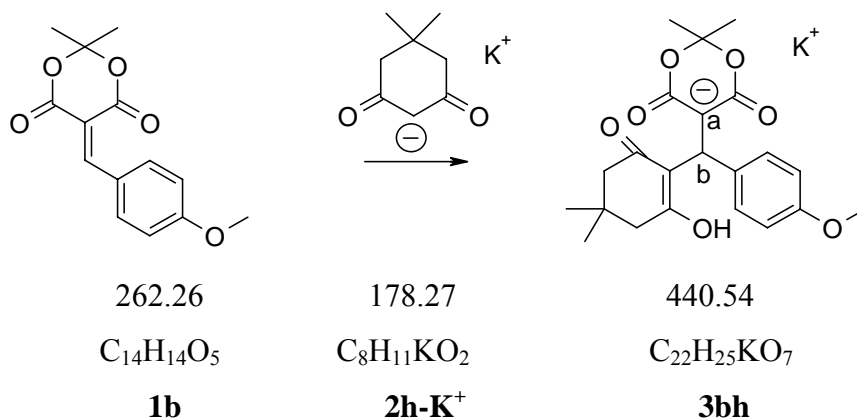
removal of water traces by filtering the solution over a hot cotton batting, the solvent was removed and the residue was dried in vacuum to yield **4be** (200 mg, 0.51 mmol, 72 %) as a 58/42 mixture of diastereomers.



¹H-NMR (300 MHz, CDCl₃): δ = 0.98 (t, ³J = 7.2 Hz, 3 H, CH₂CH₃ (A)), 1.26 (t, ³J = 7.2 Hz, 3 H, CH₂CH₃ (B)), 1.29 (s, 3 H, C(CH₃)₂ (A)), 1.37 (s, 3 H, C(CH₃)₂ (B)), 1.63 (s, 3 H, C(CH₃)₂ (A)), 1.66 (s, 3 H, C(CH₃)₂ (B)), 2.02 (s, 3 H, CH₃ (B)), 2.35 (s, 3 H, CH₃ (A)), 3.74 (s, 3 H, OCH₃ (A+B)), 3.88–3.92 (m, 1.5 H), 4.12–4.24 (m, 1.5 H), 4.38–4.48 (m, 2 H), 4.94 (m, 1 H, H^b), 6.77 (d, ³J = 9.1 Hz, 2 H, C-H_{ar}), 7.22 ppm (d, ³J = 9.1 Hz, 2 H, C-H_{ar}). (A) and (B) denote the major and the minor product, respectively. The assignment of the multiplets was not possible because of the overlapping proton signals of the ester groups with the methine protons. ¹³C-NMR (75.5 MHz, CDCl₃): δ = 13.7 (q), 13.9 (q), 27.7 (q), 28.0 (q), 28.1 (q), 29.6, (q), 31.3 (q), 40.9 (q), 42.2 (d), 42.3 (d), 47.9 (t), 48.7 (t), 55.1 (q, OMe), 59.8 (d), 61.6 (d), 61.8 (d), 62.0 (d), 105.2 (s), 105.4 (s), 113.9 (d, Ar), 114.2 (d, Ar), 129.1 (d, Ar), 130.5 (d, Ar), 159.2 (s), 164.7 (s), 165.6 (s), 165.8 (s), 167.3 (s), 168.7 (s), 201.8 (s), 202.9 ppm (s). Signal assignments are based on additional DEPT and gHSQC experiments.

3bh: A suspension of **1b** (285 mg, 1.09 mmol) and **2h-K⁺** (178 mg, 0.998 mmol) in DME (2 mL) was stirred at room temperature. After 2 min, the suspension became more viscous and a colorless solid precipitated. After filtering under nitrogen atmosphere and washing with benzene, **3bh** (280 mg, 0.636 mmol, 64 %) was obtained as a colorless solid; mp 219.3–219.6 °C.

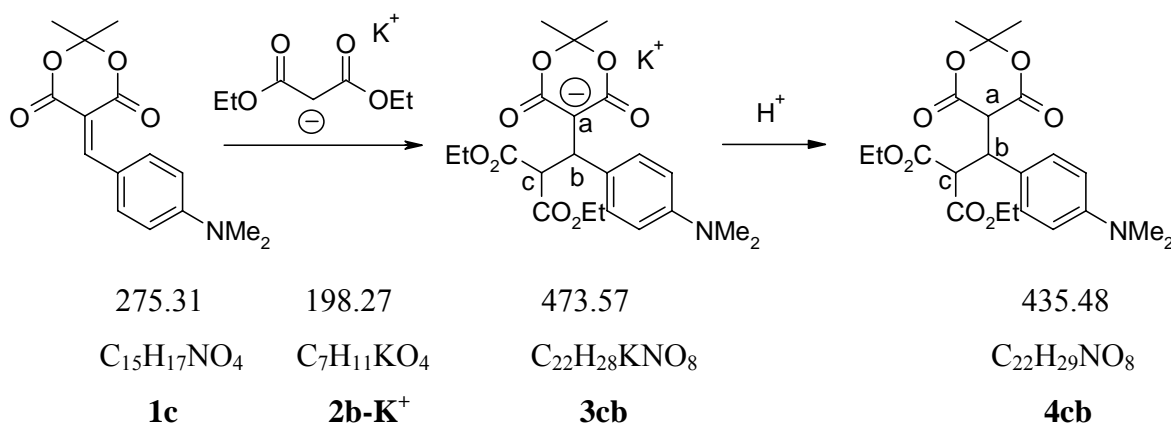
Due to fast decomposition of **3bh** at room temperature, **1b** (143 mg, 0.545 mmol) and **2h-K⁺** (89 mg, 0.499 mmol) were mixed in 2 mL dry *d*₆-DMSO and analyzed after complete conversion.



¹H-NMR (400 MHz, *d*₆-DMSO): δ = 1.00, 1.04 (2 s, 2 × 3 H, dim-C(CH₃)₂), 1.52 (s, 6 H, C(CH₃)₂), 2.09-2.28 (m, 4 H, 2 × CH₂), 3.68 (s, 3 H, OMe), 5.68 (s, 1 H, H^b), 6.71 (d, ³*J* = 8.8 Hz, 2 H, ArH), 6.96 (d, ³*J* = 8.8 Hz, 2 H, ArH), 13.50 ppm (s, 1 H, OH). ¹³C-NMR (100.5 MHz, *d*₆-DMSO): δ = 25.6 (q, C(CH₃)₂), 27.4 (q, dim-C(CH₃)₂), 28.7 (q, dim-C(CH₃)₂), 31.0 (d, C^b), 44.4 (t, CH₂), 50.4 (t, CH₂), 54.7 (q, OMe), 78.1 (s), 99.7 (s), 112.6 (d, Ar), 114.1 (s), 116.4 (s), 127.6 (d, Ar), 136.9 (s), 156.1 (s), 158.1 (s), 165.9 (s), 166.4 (s), 172.6 (s), 196.0 ppm (s). Signal assignments are based on additional gHSQC experiments. Due to the fast decomposition of **3bh** some signals in the ¹³C-NMR spectrum belong to decomposition products and cannot be assigned. MS (ESI, negative) *m/z*: 401 (100) [M - K]⁻, (ESI, positive) *m/z*: 441 (100) [M + H]⁺.

Reactions of Electrophile 1c

3cb/4cb: A mixture of equimolar amounts of **1c** and **2b-K⁺** were stirred in dry *d*₆-DMSO (5 mL) until the color disappeared. Then a sample was taken to analyze **3cb** by NMR spectroscopy. After pouring the remaining solution on cold water (5 mL) and addition of 2 M aq HCl (2 mL), a colorless solid precipitated which was filtered and dried under reduced pressure to give compound **4cb**.

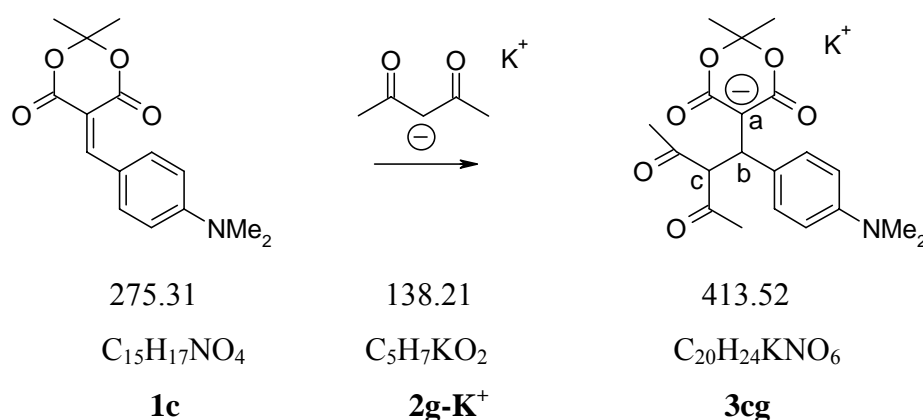


3cb: ¹H-NMR (600 MHz, *d*₆-DMSO): $\delta = 0.90$ (t, ³*J* = 6.6 Hz, 3 H, CH₂CH₃), 1.12 (t, ³*J* = 6.6 Hz, 3 H, CH₂CH₃), 1.34 (s, 6 H, C(CH₃)₂), 2.77 (s, 6 H, NMe₂), 3.76-3.82 (m, 2 H, CH₂CH₃), 3.94-4.04 (m, 2 H, CH₂CH₃), 4.33 (d, ³*J* = 12.6 Hz, 1 H, H^b), 4.87 (d, ³*J* = 12.6 Hz, 1 H, H^c), 6.49 (d, ³*J* = 9.0 Hz, 2 H, ArH), 7.20 ppm (d, ³*J* = 9.0 Hz, 2 H, ArH). ¹³C-NMR (100.5 MHz, *d*₆-DMSO): $\delta = 13.6$ (q, CH₂CH₃), 13.9 (q, CH₂CH₃), 25.7 (q, C(CH₃)₂), 39.4 (d, C^b), 40.5 (q, NMe₂), 54.4 (d, C^c), 59.7 (t, CH₂CH₃), 59.9 (t, CH₂CH₃), 74.8 (s, C^a), 98.6 (s, C(CH₃)₂), 111.7 (d, Ar), 128.4 (d, Ar), 133.8 (s), 148.2 (s), 164.4 (s, CO₂), 168.5 (s, CO₂Et), 168.8 ppm (s, CO₂Et). Signal assignments are based on additional DEPT, gHSQC, and gHMBC experiments. For the ESI-MS, a mixture of equimolar amounts of **1c** and **2b-K⁺** in dry EtOH was analyzed. MS: (ESI, negative) *m/z*: 434 (100) [M - K]⁻, (ESI, positive) *m/z*: 436 (100) [M - K + 2H]⁺.

4cb: ¹H NMR (300 MHz, CDCl₃): $\delta = 0.91$ (t, ³*J* = 7.2 Hz, 3 H, CH₂CH₃), 1.21 (t, ³*J* = 7.2 Hz, 3 H, CH₂CH₃), 1.30, 1.60 (2 s, 2 × 3 H, C(CH₃)₂), 2.85 (s, 6 H, NMe₂), 3.83-3.90 (m, 2 H, CH₂CH₃), 4.09-4.21 (m, 2 H, CH₂CH₃), 4.32-4.39 (m, 2 H, H^a and H^b), 4.70 (d, ³*J* = 12.0 Hz, 2 H, H^c), 6.65 (d, ³*J* = 8.7 Hz, 2 H, ArH), 7.17 ppm (d, ³*J* = 8.7 Hz, 2 H, ArH). ¹³C-NMR (75.5 MHz, CDCl₃): $\delta = 13.6$ (q, CH₂CH₃), 13.8 (q, CH₂CH₃), 27.6 (q, C(CH₃)₂), 28.0 (q,

$C(CH_3)_2$, 40.7 (q, NMe_2), 42.5 (d, C^b), 48.9 (d, C^a), 53.1 (d, C^c), 61.1 (t, CH_2CH_3), 61.7 (t, CH_2CH_3), 105.1 (s, $C(CH_3)_2$), 113.3 (d, Ar), 130.1 (d, Ar), 164.7 (s), 165.2 (s), 167.5 (s), 168.8 ppm (s). Signal assignments are based on additional DEPT, gHSQC, and gHMBC experiments. MS: (ESI, negative) m/z : 434 (100) $[M - H]^-$, (ESI, positive) m/z : 436 (100) $[M + H]^+$. HR-MS: calcd 435.1893 ($C_{22}H_{29}NO_8$), found 435.1859.

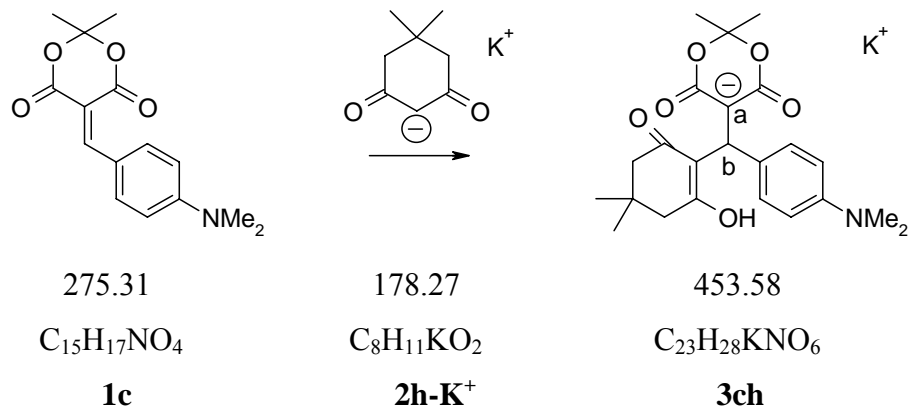
3cg: A mixture of **1c** (260 mg, 0.944 mmol) and **2g-K⁺** (179 mg, 1.30 mmol) was stirred in dry d_6 -DMSO (2 mL) at room temperature until decolorization was observed. Samples from this solution were analyzed by NMR and MS without further workup.



1H -NMR (400 MHz, d_6 -DMSO): δ = 1.32 (s, 6 H, $C(CH_3)_2$), 1.89 (s, 3 H, $COCH_3$), 2.11 (s, 3 H, $COCH_3$), 2.79 (s, 6 H, NMe_2), 4.46 (d, $^3J = 12.4$ Hz, 1 H, H^b), 5.24 (d, $^3J = 12.4$ Hz, 1 H, H^c), 6.52 (d, $^3J = 8.8$ Hz, 2 H, ArH), 7.20 ppm (d, $^3J = 8.8$ Hz, 2 H, ArH). ^{13}C -NMR (100 MHz, d_6 -DMSO): δ = 25.7 (q, $C(CH_3)_2$), 28.4 (q, $COCH_3$), 30.4 (q, $COCH_3$), 40.3 (q, NMe_2), 40.6 (d, C^b), 70.4 (d, C^c), 75.0 (s, C^a), 98.8 (s, $C(CH_3)_2$), 111.9 (d, Ar), 128.2 (d, Ar), 133.7 (s, Ar), 148.2 (s, Ar), 164.6 (s, CO_2), 204.0 (s, $COCH_3$), 204.8 ppm (s, $COCH_3$). Signal assignments are based on additional gHSQC experiments. MS (ESI, negative): m/z (%): 374 (100) $[M - K]^-$, (ESI, positive): m/z (%): 414 (46) $[M - K + H]^+$, 376 (55), 207 (63).

3ch: A mixture of **1c** (295 mg, 1.07 mmol) and **2h-K⁺** (177 mg, 0.993 mmol) was stirred in dry DME (2 mL) at room temperature until the color intensity of the solution remained constant. When the solvent was removed under reduced pressure, a solid precipitated. After washing the solid with a mixture of benzene/hexane it was dried to yield **3ch** (205 mg, 0.452 mmol, 46 %), orange solid; mp 193.3–193.6 °C.

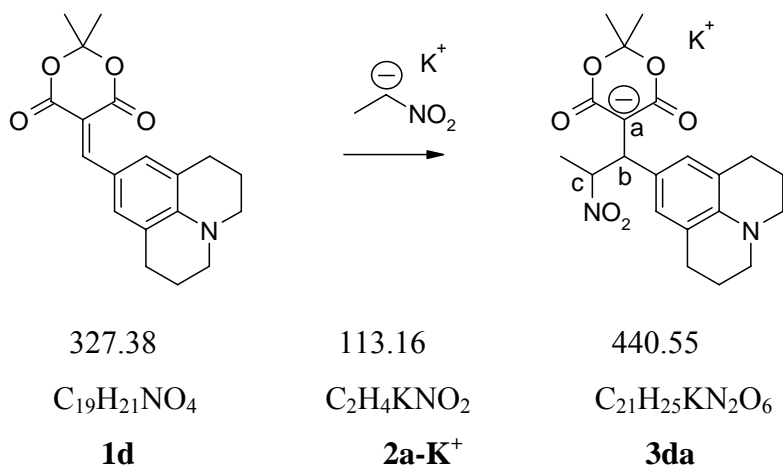
Because compound **3ch** decomposed slowly at room temperature, **1c** (95 mg, 0.35 mmol) was mixed with **2h-K⁺** (60 mg, 0.34 mmol) in *d*₆-DMSO until the solution was colorless. For the characterization by NMR spectroscopy samples from this solution were analyzed without further workup.



¹H-NMR (400 MHz, *d*₆-DMSO): δ = 1.01, 1.04 (2 s, 2 × 3 H, dim-C(CH₃)₂), 1.52 (s, 6 H, 2 × C(CH₃)₂), 2.09-2.28 (m, 4 H, 2 × CH₂), 2.80 (s, 6 H, NMe₂), 5.64 (s, 1 H, H^b), 6.56 (d, ³*J* = 8.8 Hz, 2 H, ArH), 6.89 (d, ³*J* = 8.8 Hz, 2 H, ArH), 13.53 ppm (s, 1 H, OH). ¹H- and ¹³C-NMR spectra taken after 1 h shows fast decomposition of **3ch**. Therefore an unambiguous assignment of the signals in the ¹³C NMR spectra was not possible.

Reactions of Electrophile **1d**

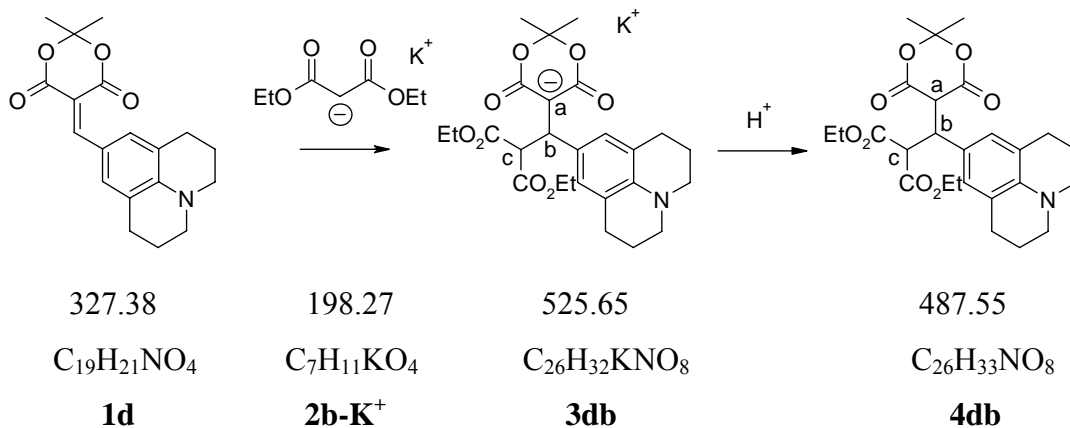
3da: A mixture of **1d** (61.4 mg, 0.188 mmol) and **2a-K⁺** (23.6 mg, 0.208 mmol) was stirred in dry *d*₆-DMSO (5 mL) until the color intensity of the solution remained constant. Samples from this solution were analyzed by NMR and MS without further workup and showed the formation of **3da**, mixture of diastereomers in a ratio of 52:48.



Major diastereomer: ¹H-NMR (600 MHz, *d*₆-DMSO): δ = 1.39 (s, 6 H, C(CH₃)₂), 1.40 (d, ³*J* = 6.6 Hz, 3 H, CH₃CH), 1.83 (m, 4 H, 2 × CH₂), 2.55 (t, ³*J* = 6.6 Hz, 4 H, 2 × CH₂), 3.00 (m, 4 H, 2 × CH₂), 3.94 (d, ³*J* = 12.0 Hz, 1 H, H^b), 5.71 (m, 1 H, H^c), 6.69 ppm (s, 2 H, ArH). ¹³C-NMR (75.5 MHz, *d*₆-DMSO): δ = 19.0 (q, CH₃CH), 21.8 (t, CH₂), 25.9 (q, C(CH₃)₂), 27.2 (t, CH₂), 45.5 (d, C^b), 49.4 (t, CH₂), 73.8 (s), 87.1 (d, C^c), 98.7 (s, C(CH₃)₂), 119.7 (s), 126.2 (d, Ar), 130.9 (s), 140.6 (s), 164.3 ppm (s, CO₂).

Minor diastereomer: ¹H-NMR (600 MHz, *d*₆-DMSO): δ = 1.19 (d, ³*J* = 6.6 Hz, 3 H, CH₃CH), 1.31 (s, 6 H, C(CH₃)₂), 1.83 (m, 4 H, 2 × CH₂), 2.60 (t, ³*J* = 6.6 Hz, 4 H, 2 × CH₂), 3.00 (m, 4 H, 2 × CH₂), 3.88 (d, ³*J* = 12.0 Hz, 1 H, H^b), 5.84-5.87 (m, 1 H, H^c), 6.83 ppm (s, 2 H, ArH). ¹³C-NMR (75.5 MHz, *d*₆-DMSO): δ = 19.4 (q, CH₃CH), 21.8 (t, CH₂), 25.6 (q, C(CH₃)₂), 27.2 (t, CH₂), 46.2 (d, C^b), 49.4 (t, CH₂), 73.9 (s), 84.3 (d, C^c), 99.0 (s, C(CH₃)₂), 119.7 (s), 127.1 (d, Ar), 131.4 (s), 131.7 (s), 140.6 (s), 164.3 ppm (s, CO₂). Signal assignments are based on additional DEPT, gHSQC, and gHMBC experiments.

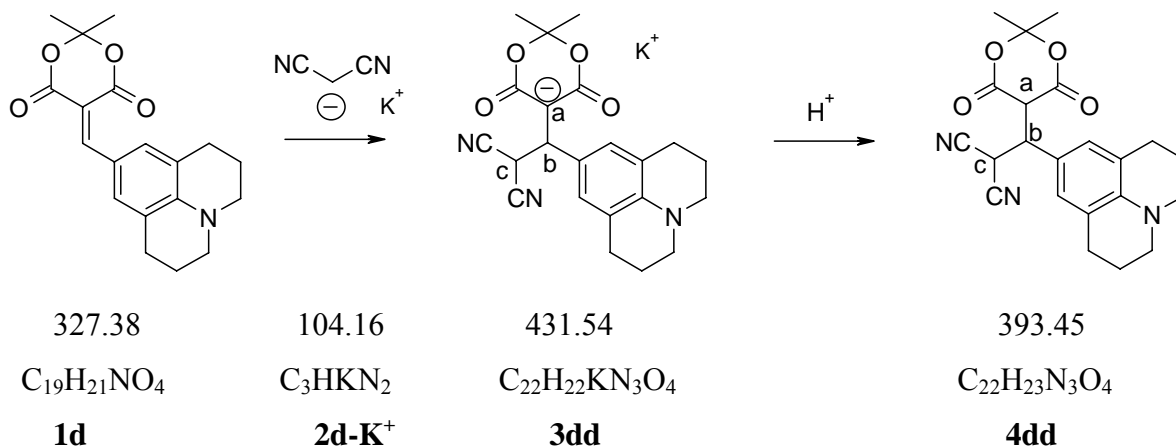
3db/4db: A mixture of equimolar amounts of **1d** and **2b-K⁺** in dry *d*₆-DMSO was stirred until decolorization was observed. Then a sample was taken to analyze **3db** by NMR spectroscopy. After acidifying the remaining solution with 2 M aq HCl, a solid (**4db**) precipitated which was filtered and dried.



3db: ¹H-NMR (600 MHz, *d*₆-DMSO): δ = 0.96 (t, ³*J* = 7.2 Hz, 3 H, CH₂CH₃), 1.11 (t, ³*J* = 7.2 Hz, 3 H, CH₂CH₃), 1.34 (s, 6 H, C(CH₃)₂), 1.83 (quint, t, ³*J* = 5.4 Hz, 4 H, 2 × CH₂), 2.56 (t, ³*J* = 5.4 Hz, 4 H, 2 × CH₂), 2.97 (t, ³*J* = 5.4 Hz, 4 H, 2 × CH₂), 3.80-3.88 (m, 2 H, CH₂CH₃), 3.92-4.00 (m, 2 H, CH₂CH₃), 4.20 (d, ³*J* = 12.6 Hz, 1 H, H^b), 4.80 (d, ³*J* = 12.6 Hz, 1 H, H^c), 6.70 ppm (s, 2 H, ArH). ¹³C-NMR (75.5 MHz, *d*₆-DMSO): δ = 13.7 (q, CH₂CH₃), 13.9 (q, CH₂CH₃), 22.0 (t, CH₂), 25.7 (q, C(CH₃)₂), 27.2 (t, CH₂), 40.3 (d, C^b), 49.5 (t, CH₂), 54.3 (d, C^c), 59.6 (t, CH₂CH₃), 59.8 (t, CH₂CH₃), 74.8 (s, C^a), 98.5 (s, C(CH₃)₂), 119.4 (s, Ar), 126.4 (d, Ar), 133.0 (s), 140.1 (s), 164.3 (s, CO₂), 168.5 (s, CO₂Et), 168.9 ppm (s, CO₂Et). Signal assignments are based on additional DEPT, gHSQC, and gHMBC experiments. For the ESI-MS, a mixture of equimolar amounts of **1d** and **2b-K⁺** in dry EtOH was analyzed. MS: (ESI, negative) *m/z*: 486 (100) [M – K][–].

4db: ¹H-NMR (300 MHz, CDCl₃): δ = 0.99 (t, ³*J* = 7.2 Hz, 3 H, CH₂CH₃), 1.24 (t, ³*J* = 7.2 Hz, 3 H, CH₂CH₃), 1.33, 1.63 (2 s, 2 × 3 H, C(CH₃)₂), 1.87 (quint, ³*J* = 5.7 Hz, 4 H, 2 × CH₂), 2.60 (t, ³*J* = 5.7 Hz, 4 H, 2 × CH₂), 3.04 (t, ³*J* = 5.7 Hz, 4 H, 2 × CH₂), 3.95 (q, ³*J* = 7.2 Hz, 2 H, CH₂CH₃), 4.13-4.22 (m, 2 H, CH₂CH₃), 4.26-4.30 (m, 2 H, H^a and H^b), 4.65 (d, ³*J* = 12.0 Hz, 1 H, H^c), 6.69 ppm (s, 2 H, ArH). ¹³C-NMR (75.5 MHz, CDCl₃): δ = 13.7 (q, CH₂CH₃), 21.9 (t, CH₂), 27.5 (t, CH₂), 28.8, 28.2 (2 q, C(CH₃)₂), 42.8 (d, C^b), 49.3 (d, C^a), 49.9 (t, CH₂), 53.3 (d, C^c), 61.0 (t, CH₂CH₃), 61.7 (t, CH₂CH₃), 105.2 (s, C(CH₃)₂), 121.4 (s), 127.6 (d, Ar), 142.3 (s), 164.9 (s), 165.5 (s), 167.7 (s, C=O), 169.1 ppm (s, C=O). Signal assignments are based on additional DEPT, gHSQC, and gHMBC experiments.

3dd/4dd: A mixture of equimolar amounts of **1d** and **2d-K⁺** in dry *d*₆-DMSO was stirred. The resulting solution of **3dd** was analyzed by NMR spectroscopy without further workup.

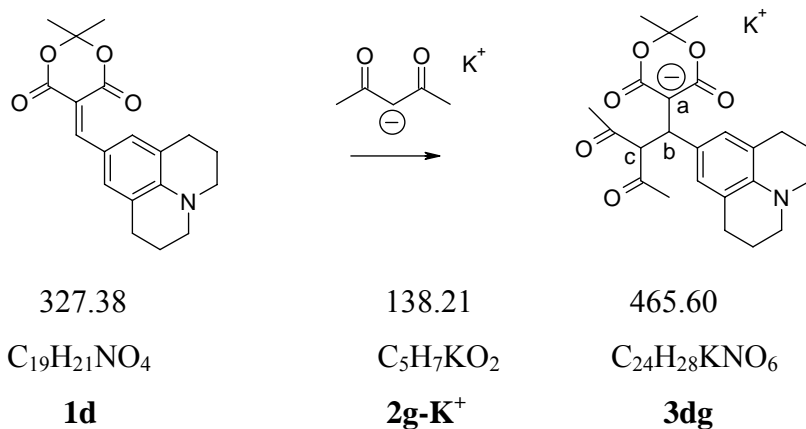


¹H-NMR (400 MHz, *d*₆-DMSO): δ = 1.46 (s, 6 H, C(CH₃)₂), 1.85 (quint, ³*J* = 5.6 Hz, 4 H, 2 × CH₂), 2.61 (t, ³*J* = 5.6 Hz, 4 H, 2 × CH₂), 3.04 (t, ³*J* = 5.6 Hz, 4 H, 2 × CH₂), 4.12 (d, ³*J* = 12.0 Hz, 1 H, H^b), 5.68 (d, ³*J* = 12.0 Hz, 1 H, H^c), 6.81 ppm (s, 2 H, ArH). ¹³C-NMR (100 MHz, *d*₆-DMSO): δ = 21.7 (t, CH₂), 25.8 (q, C(CH₃)₂), 26.6 (d, C^c), 27.2 (t, CH₂), 43.3 (d, C^b), 49.3 (d, CH₂), 73.2 (s, C^a), 99.7 (s, C(CH₃)₂), 115.2 (s, CN), 120.1 (d), 126.2 (s), 129.0 (s), 141.4 (s), 164.5 ppm (s, CO₂). Signal assignments are based on additional gHSQC experiments. MS (ESI, negative): *m/z* (%): 392 (100) [M - K]⁻, 212 (35), (ESI, positive): *m/z* (%): 394 (100) [M - K + 2H]⁺, 336 (17).

A mixture of **1d** (251 mg, 0.767 mmol) and **2d-K⁺** (88 mg, 0.85 mmol) in dry DME (2 mL) was stirred for 30 min at room temperature. A slight change of the color from purple to dark red indicated the beginning of the reaction. The reaction mixture was poured on cold water, acidified and after 10 min at 8 °C, a dark solid started to separate from the solution. Filtration and drying delivered **4dd** (175 mg), red solid; mp 124.7–124.9 °C (dec).

¹H-NMR (200 MHz, CDCl₃): δ = 1.40, 1.73 (2 s, 2 × 3 H, C(CH₃)₂), 1.96 (quint, ³*J* = 6 Hz, 4 H, 2 × CH₂), 2.69 (t, ³*J* = 6 Hz, 4 H, 2 × CH₂), 3.15 (t, ³*J* = 6 Hz, 4 H, 2 × CH₂), 4.01 (d, ³*J* = 3.3 Hz, 1 H, H^a), 4.21 (dd, ³*J* = 3.3 Hz, ³*J* = 12.5 Hz, 1 H, H^b), 5.12 (d, ³*J* = 12.5 Hz, 1 H, H^c), 6.68 ppm (s, 2 H, Ar-H). MS (ESI, negative): *m/z* (%): 392 (100) [M - H]⁻, (ESI, positive): *m/z* (%): 394 (100) [M + H]⁺. HR-MS: calcd. 393.1689 (C₂₂H₂₃N₃O₄), found 393.1657.

3dg: A mixture of equimolar amounts of **1d** (332 mg, 1.02 mmol) and **2g-K⁺** (138 mg, 0.998 mmol) in dry *d*₆-DMSO was stirred. The resulting solution of **3dg** was analyzed by NMR spectroscopy without further workup.



¹H-NMR (400 MHz, *d*₆-DMSO): δ = 1.32 (s, 6 H, C(CH₃)₂), 1.83 (quint, ³*J* = 5.2 Hz, 4 H, 2 × CH₂), 1.92 (s, 3 H, COCH₃), 2.08 (s, 3 H, COCH₃), 2.57 (t, ³*J* = 5.2 Hz, 4 H, 2 × CH₂), 2.98 (t, ³*J* = 5.2 Hz, 4 H, 2 × CH₂), 4.33 (d, ³*J* = 12.8 Hz, 1 H, H^b), 5.17 (d, ³*J* = 12.8 Hz, 1 H, H^c), 6.71 ppm (s, 2 H, ArH). ¹³C-NMR (75.5 MHz, *d*₆-DMSO): δ = 21.9 (t, CH₂), 25.6 (q, C(CH₃)₂), 27.2 (t, CH₂), 28.3 (q, COCH₃), 30.4 (q, COCH₃), 40.5 (d, C^b), 49.5 (t, CH₂), 70.2 (d, C^c), 75.0 (d, C^a), 98.7 (s, C(CH₃)₂), 119.7 (s), 126.1 (s), 132.9 (s), 140.2 (d, Ar), 164.6 (s, CO₂), 204.0 (s, COCH₃), 204.8 ppm (s, COCH₃). Signal assignments are based on additional DEPT and gHSQC experiments. MS (ESI, negative): *m/z* (%): 426 (100) [M - K]⁻, (ESI, positive): *m/z* (%): 466 (62) [M + H]⁺, 428 (60), 207 (35).

3.3. Reactivities of Benzylidene Meldrum's Acids 1a–d

3.1 Reactions of Electrophiles 1a–d with Carbanions 2

Reactions of Electrophile 1a

Table S1: Kinetics of the reaction of **1a** with the dimedone anion **2h** (K^+ salt) in DMSO at 20 °C (stopped-flow UV-Vis spectrometer, $\lambda = 322$ nm).

No.	$[E]_0 / M$	$[C^-]_0 / M$	k_{obs} / s^{-1}
F5-2	1.81×10^{-5}	1.77×10^{-4}	5.76×10^1
F5-3	1.81×10^{-5}	2.53×10^{-4}	7.31×10^1
F5-1	1.81×10^{-5}	3.65×10^{-4}	1.10×10^2
F5-4	1.81×10^{-5}	5.51×10^{-4}	1.67×10^2
F5-5	1.81×10^{-5}	7.38×10^{-4}	2.19×10^2

$k_2 = 2.93 \times 10^5 M^{-1} s^{-1}$

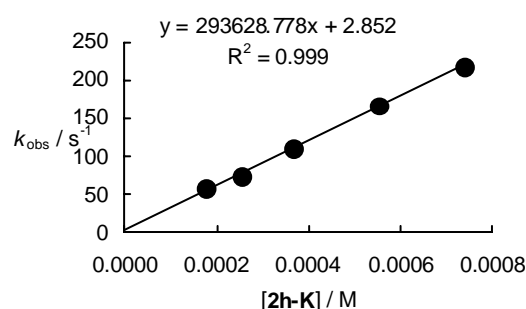
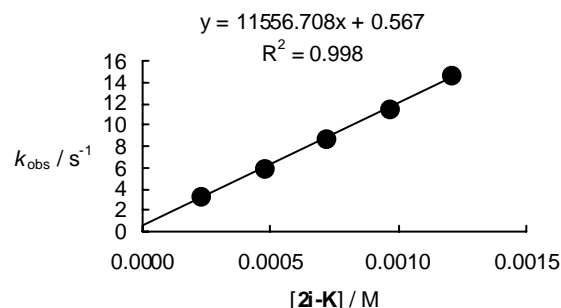


Table S2: Kinetics of the reaction of **1a** with the Meldrum's acid anion **2i** (K^+ salt) in DMSO at 20 °C (stopped-flow UV-Vis spectrometer, $\lambda = 322$ nm).

No.	$[E]_0 / M$	$[C^-]_0 / M$	k_{obs} / s^{-1}
F4-1	3.62×10^{-5}	2.27×10^{-4}	3.38
F4-2	3.62×10^{-5}	4.72×10^{-4}	5.89
F4-3	3.62×10^{-5}	7.17×10^{-4}	8.74
F4-4	3.62×10^{-5}	9.62×10^{-4}	1.16×10^1
F4-5	3.62×10^{-5}	1.21×10^{-3}	1.47×10^1

$k_2 = 1.16 \times 10^4 M^{-1} s^{-1}$



Reactions of Electrophile 1b

Table S3: Kinetics of the reaction of **1b** with the anion of diethyl malonate **2b** (K^+ salt) in DMSO at 20 °C (stopped-flow UV-Vis spectrometer, $\lambda = 369$ nm).

No.	$[E]_0 / M$	$[C^-]_0 / M$	k_{obs} / s^{-1}
331-1	1.06×10^{-5}	1.08×10^{-4}	1.08×10^2
331-2	1.06×10^{-5}	1.64×10^{-4}	1.71×10^2
331-3	1.06×10^{-5}	2.21×10^{-4}	2.41×10^2
331-5	1.06×10^{-5}	3.33×10^{-4}	3.65×10^2

$k_2 = 1.15 \times 10^6 M^{-1} s^{-1}$

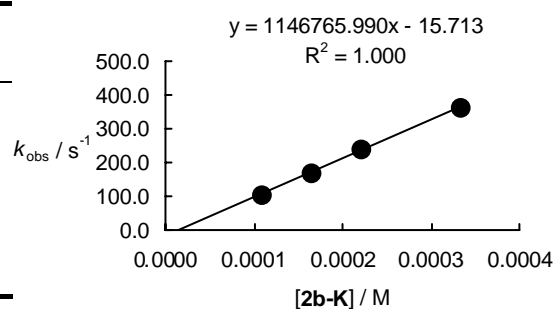
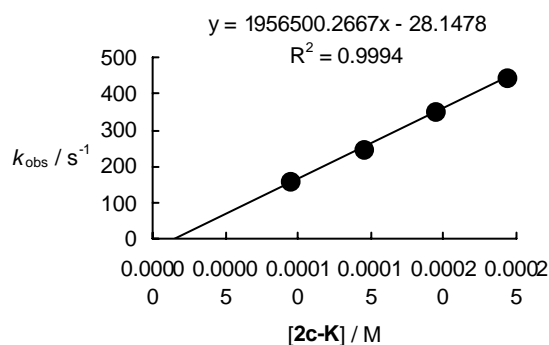


Table S4: Kinetics of the reaction of **1b** with the anion of ethyl cyano acetate **2c** (K^+ salt) in DMSO at 20 °C (stopped-flow UV-Vis spectrometer, $\lambda = 369$ nm).

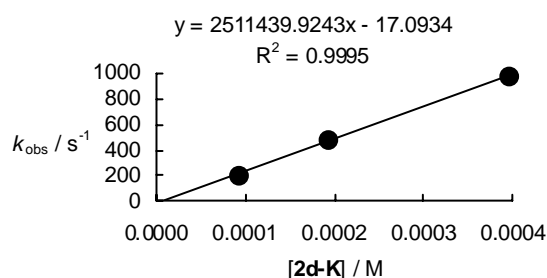
No.	$[E]_0 / M$	$[C^-]_0 / M$	k_{obs} / s^{-1}
288-1	9.15×10^{-6}	9.47×10^{-5}	1.59×10^2
288-5	9.15×10^{-6}	1.44×10^{-4}	2.51×10^2
288-2	9.15×10^{-6}	1.94×10^{-4}	3.54×10^2
288-4	9.15×10^{-6}	2.45×10^{-4}	4.48×10^2

$$k_2 = 1.96 \times 10^6 M^{-1} s^{-1}$$

**Table S5:** Kinetics of the reaction of **1b** with the anion of malononitrile **2d** (generated by deprotonation of **2d-H** with 1.05 equiv. $KOtBu$) in DMSO at 20 °C (stopped-flow UV-Vis spectrometer, $\lambda = 369$ nm).

No.	$[E]_0 / M$	$[C^-]_0 / M$	k_{obs} / s^{-1}
84-1	1.98×10^{-5}	9.16×10^{-5}	2.06×10^2
84-2	1.98×10^{-5}	1.93×10^{-4}	4.78×10^2
84-3	1.98×10^{-5}	3.96×10^{-4}	9.74×10^2

$$k_2 = 2.51 \times 10^6 M^{-1} s^{-1}$$

**Table S6:** Kinetics of the reaction of **1b** with ethyl acetoacetate **2e** (K^+ salt) in DMSO at 20 °C (stopped-flow UV-Vis spectrometer, $\lambda = 369$ nm).

No.	$[E]_0 / M$	$[C^-]_0 / M$	k_{obs} / s^{-1}
273-3	2.40×10^{-5}	1.02×10^{-4}	9.18×10^1
273-1	2.40×10^{-5}	2.16×10^{-4}	1.80×10^2
273-4	2.40×10^{-5}	3.30×10^{-4}	2.59×10^2
273-2	2.40×10^{-5}	4.44×10^{-4}	3.47×10^2

$$k_2 = 7.42 \times 10^5 M^{-1} s^{-1}$$

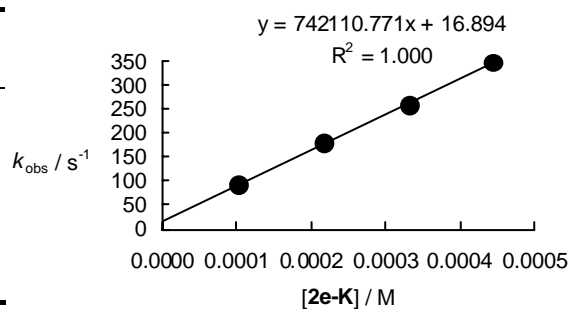
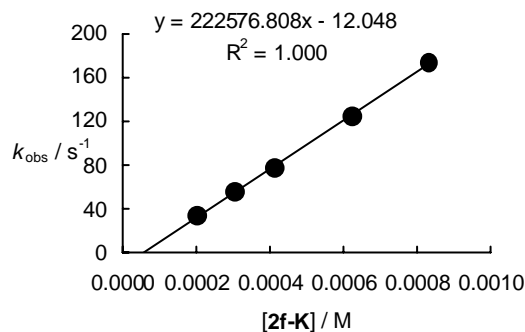


Table S7a: Kinetics of the reaction of **1b** with the phenyl nitromethyl anion **2f** (generated by deprotonation of **2f-H** with 1.05 equiv. KO t Bu) in DMSO at 20 °C (stopped-flow UV-Vis spectrometer, $\lambda = 400$ nm).

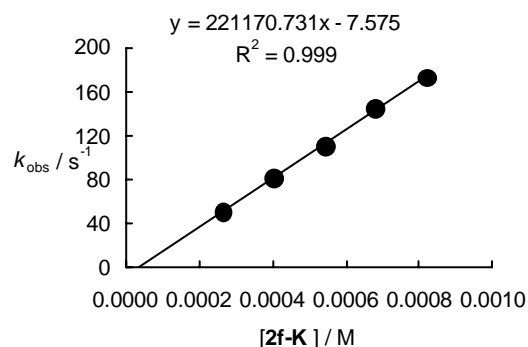
No.	[E] ₀ / M	[C ⁻] ₀ / M	$k_{\text{obs}} / \text{s}^{-1}$
348c-1	1.95×10^{-5}	2.00×10^{-4}	3.39×10^1
348c-4	1.95×10^{-5}	3.05×10^{-4}	5.54×10^1
348c-2	1.95×10^{-5}	4.09×10^{-4}	7.79×10^1
348c-5	1.95×10^{-5}	6.20×10^{-4}	1.25×10^2
348c-3	1.95×10^{-5}	8.29×10^{-4}	1.74×10^2

$$k_2 = 2.23 \times 10^5 \text{ M}^{-1} \text{ s}^{-1}$$

**Table S7b:** Kinetics of the reaction of **1b** with the phenyl nitromethyl anion **2f** (generated by deprotonation of **2f-H** with 0.27 equiv. KO t Bu) in DMSO at 20 °C (stopped-flow UV-Vis spectrometer, $\lambda = 400$ nm).

No.	[E] ₀ / M	[C ⁻] ₀ / M	$k_{\text{obs}} / \text{s}^{-1}$
348b-1	2.44×10^{-5}	2.65×10^{-4}	5.13×10^1
348b-4	2.44×10^{-5}	4.03×10^{-4}	8.21×10^1
348b-2	2.44×10^{-5}	5.42×10^{-4}	1.10×10^2
348b-5	2.44×10^{-5}	6.81×10^{-4}	1.45×10^2
348b-3	2.44×10^{-5}	8.20×10^{-4}	1.73×10^2

$$k_2 = 2.21 \times 10^5 \text{ M}^{-1} \text{ s}^{-1}$$

**Table S8:** Kinetics of the reaction of **1b** with the acetylacetonate anion **2g** (K⁺ salt) in DMSO at 20 °C (stopped-flow UV-Vis spectrometer, $\lambda = 369$ nm).

No.	[E] ₀ / M	[C ⁻] ₀ / M	$k_{\text{obs}} / \text{s}^{-1}$
80-1	1.98×10^{-5}	8.95×10^{-5}	1.49×10^1
80-2	1.98×10^{-5}	1.89×10^{-4}	3.27×10^1
80-3	1.98×10^{-5}	3.88×10^{-4}	6.95×10^1
80-4	1.98×10^{-5}	5.87×10^{-4}	1.07×10^2
80-5	1.98×10^{-5}	8.14×10^{-4}	1.52×10^2

$$k_2 = 1.89 \times 10^5 \text{ M}^{-1} \text{ s}^{-1}$$

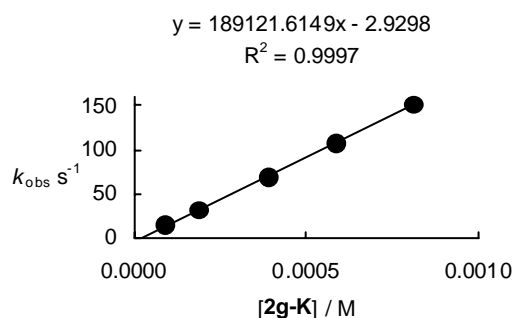
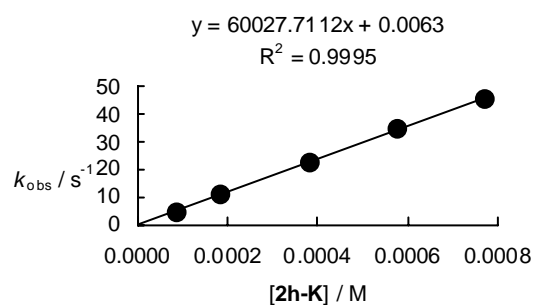


Table S9: Kinetics of the reaction of **1b** with the dimedone anion **2h** (K^+ salt) in DMSO at 20 °C (stopped-flow UV-Vis spectrometer, $\lambda = 369$ nm).

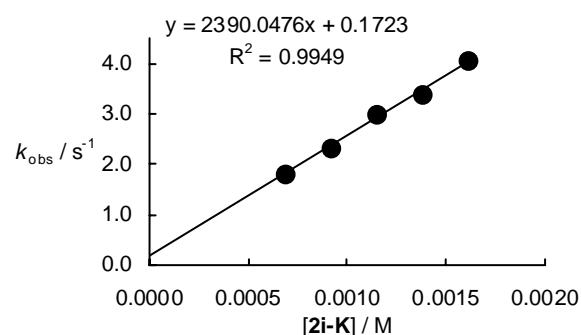
No.	$[E]_0 / M$	$[C^-]_0 / M$	k_{obs} / s^{-1}
82-1	1.98×10^{-5}	8.75×10^{-5}	5.11×10^0
82-2	1.98×10^{-5}	1.85×10^{-4}	1.11×10^1
82-3	1.98×10^{-5}	3.80×10^{-4}	2.28×10^1
82-4	1.98×10^{-5}	5.75×10^{-4}	3.51×10^1
82-5	1.98×10^{-5}	7.70×10^{-4}	4.58×10^1

$$k_2 = 6.00 \times 10^4 M^{-1} s^{-1}$$

**Table S10:** Kinetics of the reaction of **1b** with the Meldrum's acid anion **2i** (generated by deprotonation of **2i-H** with 1.05 equiv. $KOtBu$, 1 equiv. 18-crown-6) in DMSO at 20 °C (stopped-flow UV-Vis spectrometer, $\lambda = 369$ nm).

No.	$[E]_0 / M$	$[C^-]_0 / M$	k_{obs} / s^{-1}
328-3	2.35×10^{-5}	6.81×10^{-4}	1.81
328-4	2.35×10^{-5}	9.12×10^{-4}	2.32
328-7	2.35×10^{-5}	1.14×10^{-3}	2.98
328-2	2.35×10^{-5}	1.38×10^{-3}	3.37
328-1	2.35×10^{-5}	1.61×10^{-3}	4.05

$$k_2 = 2.39 \times 10^3 M^{-1} s^{-1}$$



Reactions of Electrophile **1c**

Table S11: Kinetics of the reaction of **1c** with the diethyl malonate anion **2b** (K^+ salt) in DMSO at 20 °C (stopped-flow UV-Vis spectrometer, $\lambda = 459$ nm).

No.	$[E]_0 / M$	$[C^-]_0 / M$	k_{obs} / s^{-1}
330-1	1.59×10^{-5}	5.56×10^{-4}	1.96×10^1
330-2	1.59×10^{-5}	1.12×10^{-3}	3.66×10^1
330-3	1.59×10^{-5}	1.68×10^{-3}	5.31×10^1
330-4	1.59×10^{-5}	2.25×10^{-3}	6.81×10^1
330-5	1.59×10^{-5}	2.81×10^{-3}	8.54×10^1

$$k_2 = 2.89 \times 10^4 M^{-1} s^{-1}$$

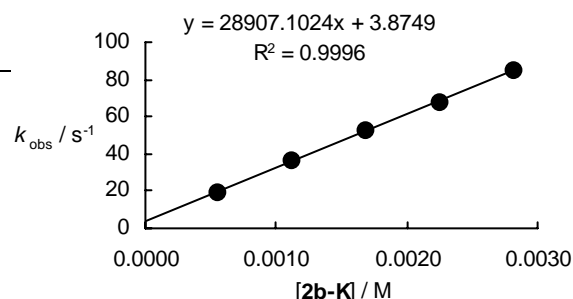
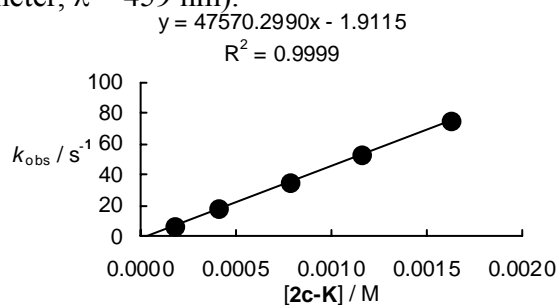


Table S12: Kinetics of the reaction of **1c** with the anion of ethyl cyano acetate **2c** (generated by deprotonation of **2c-H** with 1.05 equiv. KOtBu) in DMSO at 20 °C (stopped-flow UV-Vis spectrometer, $\lambda = 459$ nm).

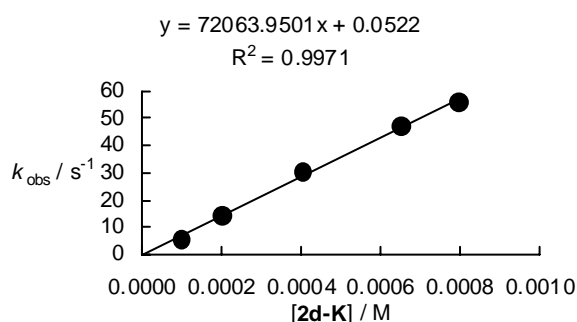
No.	$[\text{E}]_0 / \text{M}$	$[\text{C}^-]_0 / \text{M}$	$k_{\text{obs}} / \text{s}^{-1}$
73-1	2.00×10^{-5}	1.78×10^{-4}	6.24×10^0
73-2	2.00×10^{-5}	4.12×10^{-4}	1.81×10^1
73-3	2.00×10^{-5}	7.87×10^{-4}	3.55×10^1
73-4	2.00×10^{-5}	1.16×10^{-3}	5.33×10^1
73-5	2.00×10^{-5}	1.63×10^{-3}	7.57×10^1

$$k_2 = 4.76 \times 10^4 \text{ M}^{-1} \text{ s}^{-1}$$

**Table S13:** Kinetics of the reaction of **1c** with the anion of malonitrile **2d** (K^+ salt) in DMSO at 20 °C (stopped-flow UV-Vis spectrometer, $\lambda = 459$ nm).

No.	$[\text{E}]_0 / \text{M}$	$[\text{C}^-]_0 / \text{M}$	$k_{\text{obs}} / \text{s}^{-1}$
83-1	1.00×10^{-5}	9.65×10^{-5}	5.92×10^0
83-2	1.00×10^{-5}	1.98×10^{-4}	1.45×10^1
83-3	1.00×10^{-5}	4.01×10^{-4}	3.03×10^1
83-4	1.00×10^{-5}	6.47×10^{-4}	4.75×10^1
83-5	1.00×10^{-5}	7.92×10^{-4}	5.59×10^1

$$k_2 = 7.21 \times 10^4 \text{ M}^{-1} \text{ s}^{-1}$$

**Table S14:** Kinetics of the reaction of **1c** with the anion of ethyl acetoacetate **2e** (K^+ salt) in DMSO at 20 °C (stopped-flow UV-Vis spectrometer, $\lambda = 459$ nm).

No.	$[\text{E}]_0 / \text{M}$	$[\text{C}^-]_0 / \text{M}$	$k_{\text{obs}} / \text{s}^{-1}$
271-1	1.99×10^{-5}	4.46×10^{-4}	4.91×10^0
271-2	1.99×10^{-5}	9.02×10^{-4}	1.16×10^1
271-3	1.99×10^{-5}	1.36×10^{-3}	1.73×10^1
271-4	1.99×10^{-5}	1.82×10^{-3}	2.27×10^1
271-5	1.99×10^{-5}	2.27×10^{-3}	2.83×10^1

$$k_2 = 1.27 \times 10^4 \text{ M}^{-1} \text{ s}^{-1}$$

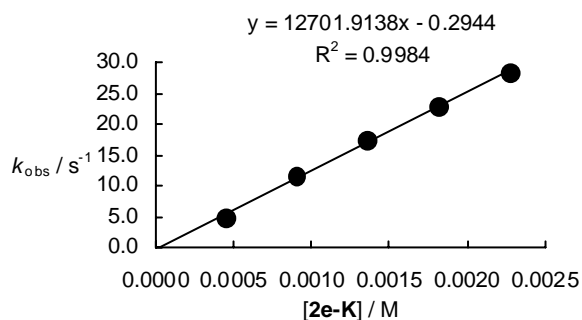
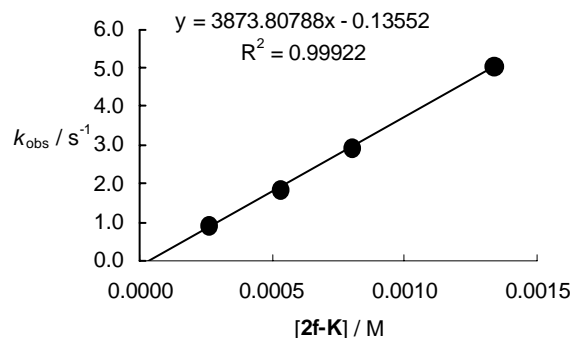


Table S15: Kinetics of the reaction of **1c** with the phenyl nitromethyl anion **2f** (K^+ salt) in DMSO at 20 °C (stopped-flow UV-Vis spectrometer, $\lambda = 460$ nm).

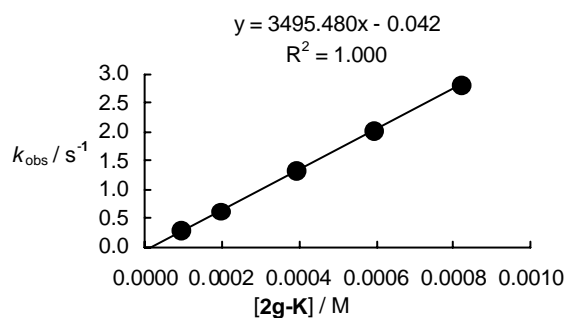
No.	$[E]_0 / M$	$[C^-]_0 / M$	k_{obs} / s^{-1}
a347-4	2.25×10^{-5}	2.59×10^{-4}	9.20×10^{-1}
a347-1	2.25×10^{-5}	5.28×10^{-4}	1.85
a347-2	2.25×10^{-5}	7.98×10^{-4}	2.94
a347-3	2.25×10^{-5}	1.33×10^{-3}	5.07

$$k_2 = 3.87 \times 10^3 M^{-1} s^{-1}$$

**Table S16:** Kinetics of the reaction of **1c** with the acetylacetonate anion **2g** (K^+ salt) in DMSO at 20 °C (stopped-flow UV-Vis spectrometer, $\lambda = 459$ nm).

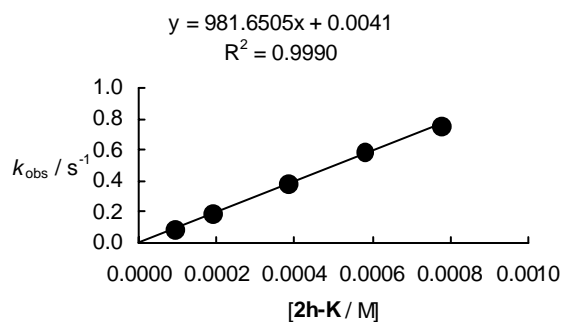
No.	$[E]_0 / M$	$[C^-]_0 / M$	k_{obs} / s^{-1}
79-1	1.00×10^{-5}	9.44×10^{-5}	2.96×10^{-1}
79-2	1.00×10^{-5}	1.94×10^{-4}	6.30×10^{-1}
79-3	1.00×10^{-5}	3.93×10^{-4}	1.32
79-4	1.00×10^{-5}	5.91×10^{-4}	2.03
79-5	1.00×10^{-5}	8.19×10^{-4}	2.82

$$k_2 = 3.50 \times 10^3 M^{-1} s^{-1}$$

**Table S17:** Kinetics of the reaction of **1c** with the dimedone anion **2h** (K^+ salt) in DMSO at 20 °C (stopped-flow UV-Vis spectrometer, $\lambda = 459$ nm).

No.	$[E]_0 / M$	$[C^-]_0 / M$	k_{obs} / s^{-1}
81-1	1.00×10^{-5}	9.25×10^{-5}	9.10×10^{-2}
81-2	1.00×10^{-5}	1.90×10^{-4}	1.91×10^{-1}
81-3	1.00×10^{-5}	3.85×10^{-4}	3.81×10^{-1}
81-4	1.00×10^{-5}	5.80×10^{-4}	5.87×10^{-1}
81-5	1.00×10^{-5}	7.75×10^{-4}	7.55×10^{-1}

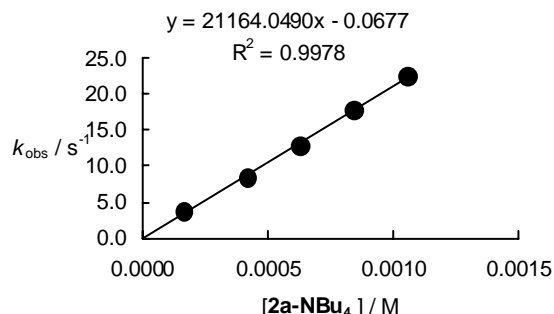
$$k_2 = 9.82 \times 10^2 M^{-1} s^{-1}$$



Reactions of Electrophile **1d****Table S18:** Kinetics of the reaction of **1d** with the nitroethyl anion **2a** ($n\text{Bu}_4\text{N}^+$ salt) in DMSO at 20 °C (stopped-flow UV-Vis spectrometer, $\lambda = 487$ nm).

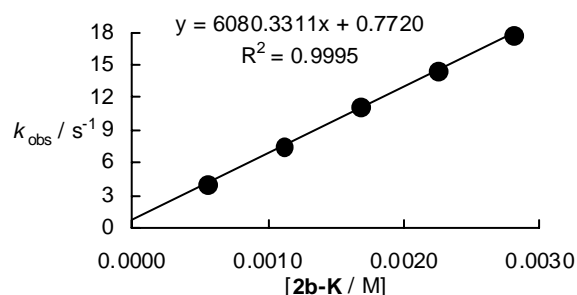
No.	$[\text{E}]_0 / \text{M}$	$[\text{C}^-]_0 / \text{M}$	$k_{\text{obs}} / \text{s}^{-1}$
275-1	1.33×10^{-5}	1.63×10^{-4}	3.79
275-2	1.33×10^{-5}	4.17×10^{-4}	8.32
275-3	1.33×10^{-5}	6.28×10^{-4}	1.30×10^1
275-4	1.33×10^{-5}	8.40×10^{-4}	1.78×10^1
275-5	1.33×10^{-5}	1.05×10^{-3}	2.24×10^1

$$k_2 = 2.12 \times 10^4 \text{ M}^{-1} \text{ s}^{-1}$$

**Table S19:** Kinetics of the reaction of **1d** with the diethyl malonate anion **2b** (K^+ salt) in DMSO at 20 °C (stopped-flow UV-Vis spectrometer, $\lambda = 483$ nm).

No.	$[\text{E}]_0 / \text{M}$	$[\text{C}^-]_0 / \text{M}$	$k_{\text{obs}} / \text{s}^{-1}$
329-1	2.41×10^{-5}	5.52×10^{-4}	4.04
329-2	2.41×10^{-5}	1.12×10^{-3}	7.55
329-3	2.41×10^{-5}	1.68×10^{-3}	1.12×10^1
329-4	2.41×10^{-5}	2.24×10^{-3}	1.44×10^1
329-5	2.41×10^{-5}	2.81×10^{-3}	1.78×10^1

$$k_2 = 6.08 \times 10^3 \text{ M}^{-1} \text{ s}^{-1}$$

**Table S20:** Kinetics of the reaction of **1d** with the ethyl cyano acetate anion **2c** (K^+ salt) in DMSO at 20 °C (stopped-flow UV-Vis spectrometer, $\lambda = 487$ nm).

No.	$[\text{E}]_0 / \text{M}$	$[\text{C}^-]_0 / \text{M}$	$k_{\text{obs}} / \text{s}^{-1}$
274-1	1.33×10^{-5}	3.65×10^{-4}	2.69
274-2	1.33×10^{-5}	7.36×10^{-4}	5.63
274-3	1.33×10^{-5}	1.11×10^{-3}	8.51
274-4	1.33×10^{-5}	1.48×10^{-3}	1.15×10^1
274-5	1.33×10^{-5}	1.85×10^{-3}	1.46×10^1

$$k_2 = 7.98 \times 10^3 \text{ M}^{-1} \text{ s}^{-1}$$

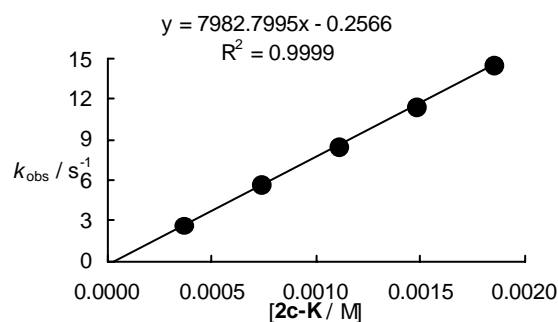
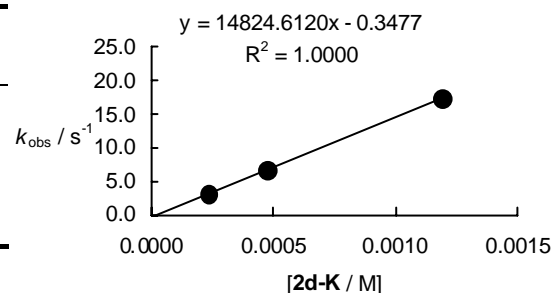


Table S21: Kinetics of the reaction of **1d** with the malonitrile anion **2d** (K^+ salt) in DMSO at 20 °C (stopped-flow UV-Vis spectrometer, $\lambda = 487$ nm).

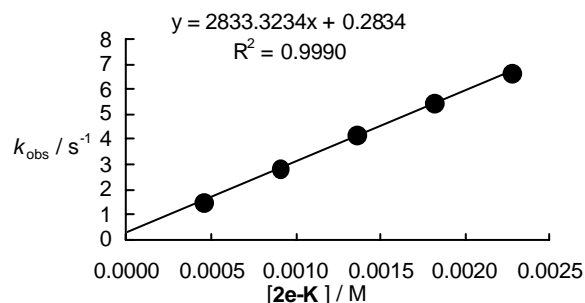
No.	$[E]_0 / M$	$[C^-]_0 / M$	k_{obs} / s^{-1}
276-1	1.33×10^{-5}	2.33×10^{-4}	3.13
276-2	1.33×10^{-5}	4.72×10^{-4}	6.66
276-5	1.33×10^{-5}	1.19×10^{-3}	1.73×10^1

$k_2 = 1.48 \times 10^4 M^{-1} s^{-1}$

**Table S22:** Kinetics of the reaction of **1d** with the ethyl acetoacetate anion **2e** (K^+ salt) in DMSO at 20 °C (stopped-flow UV-Vis spectrometer, $\lambda = 487$ nm).

No.	$[E]_0 / M$	$[C^-]_0 / M$	k_{obs} / s^{-1}
272-5	1.33×10^{-5}	4.50×10^{-4}	1.51
272-4	1.33×10^{-5}	9.06×10^{-4}	2.87
272-3	1.33×10^{-5}	1.36×10^{-3}	4.21
272-2	1.33×10^{-5}	1.82×10^{-3}	5.49
272-1	1.33×10^{-5}	2.27×10^{-3}	6.65

$k_2 = 2.83 \times 10^3 M^{-1} s^{-1}$

**Table S23:** Kinetics of the reaction of **1d** with the phenyl nitromethyl anion **2f** (generated by deprotonation of **2f-H** with 1.05 equiv. $KOtBu$) in DMSO at 20 °C (stopped-flow UV-Vis spectrometer, $\lambda = 480$ nm).

No.	$[E]_0 / M$	$[C^-]_0 / M$	k_{obs} / s^{-1}
f2-1	1.89×10^{-5}	4.12×10^{-4}	2.22×10^{-1}
f2-2	1.89×10^{-5}	8.47×10^{-4}	4.24×10^{-1}
f2-3	1.89×10^{-5}	1.28×10^{-3}	6.40×10^{-1}
f2-4	1.89×10^{-5}	1.70×10^{-3}	8.62×10^{-1}
f2-5	1.89×10^{-5}	2.13×10^{-3}	1.06

$k_2 = 4.93 \times 10^2 M^{-1} s^{-1}$

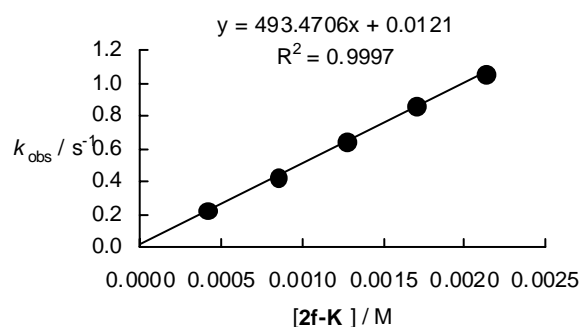
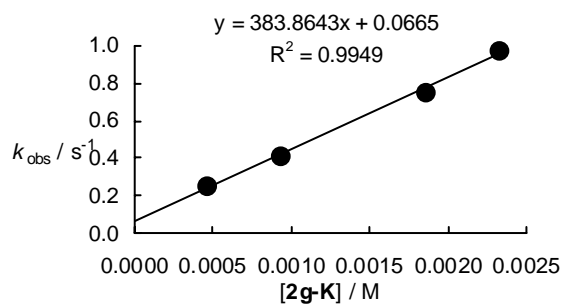


Table S24: Kinetics of the reaction of **1d** with the acetylacetonate anion **2g** (K^+ salt) in DMSO at 20 °C (stopped-flow UV-Vis spectrometer, $\lambda = 487$ nm).

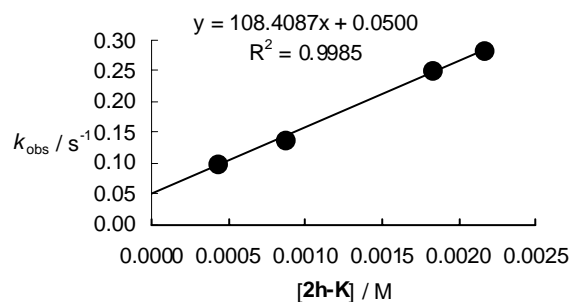
No.	$[E]_0 / M$	$[C^-]_0 / M$	k_{obs} / s^{-1}
SB38-1	1.53×10^{-5}	4.63×10^{-4}	2.63×10^{-1}
SB38-2	1.53×10^{-5}	9.26×10^{-4}	4.06×10^{-1}
SB38-3	1.53×10^{-5}	1.85×10^{-3}	7.51×10^{-1}
SB38-4	1.53×10^{-5}	2.32×10^{-3}	9.82×10^{-1}

$$k_2 = 3.84 \times 10^2 M^{-1} s^{-1}$$

**Table S25:** Kinetics of the reaction of **1d** with the dimedone anion **2h** (K^+ salt) in DMSO at 20 °C (stopped-flow UV-Vis spectrometer, $\lambda = 487$ nm).

No.	$[E]_0 / M$	$[C^-]_0 / M$	k_{obs} / s^{-1}
SB39-1	1.53×10^{-5}	4.32×10^{-4}	1.00×10^{-1}
SB39-2	1.53×10^{-5}	8.64×10^{-4}	1.39×10^{-1}
SB39-3	1.53×10^{-5}	1.83×10^{-3}	2.50×10^{-1}
SB39-4	1.53×10^{-5}	2.16×10^{-3}	2.84×10^{-1}

$$k_2 = 1.08 \times 10^2 M^{-1} s^{-1}$$

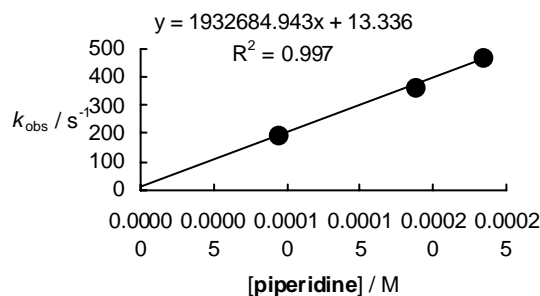


3.2 Reactions of Electrophiles 1b–d with Amines in Different Solvents

Table S26: Kinetics of the reaction of **1b** with piperidine in DMSO at 20 °C (stopped-flow UV-Vis spectrometer, $\lambda = 369$ nm).

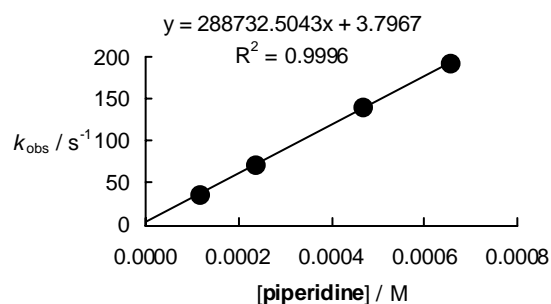
No.	$[E]_0 / M$	$[C^-]_0 / M$	k_{obs} / s^{-1}
283-1	1.14×10^{-5}	9.35×10^{-5}	1.97×10^2
283-3	1.14×10^{-5}	1.87×10^{-4}	3.65×10^2
283-2	1.14×10^{-5}	2.34×10^{-4}	4.71×10^2

$$k_2 = 1.93 \times 10^6 M^{-1} s^{-1}$$

**Table S27:** Kinetics of the reaction of **1b** with piperidine in DMSO/H₂O (50:50, v/v) at 20 °C (stopped-flow UV-Vis spectrometer, $\lambda = 369$ nm).

No.	$[E]_0 / M$	$[C^-]_0 / M$	k_{obs} / s^{-1}
282-1	9.15×10^{-6}	1.17×10^{-4}	3.63×10^1
282-2	9.15×10^{-6}	2.34×10^{-4}	7.23×10^1
282-3	9.15×10^{-6}	4.67×10^{-4}	1.40×10^2
282-4	9.15×10^{-6}	6.54×10^{-4}	1.92×10^2

$$k_2 = 2.89 \times 10^5 M^{-1} s^{-1}$$

**Table S28:** Kinetics of the reaction of **1c** with piperidine in DMSO at 20 °C (stopped-flow UV-Vis spectrometer, $\lambda = 459$ nm).

No.	$[E]_0 / M$	$[C^-]_0 / M$	k_{obs} / s^{-1}
278b-5	2.50×10^{-5}	3.21×10^{-4}	2.16×10^2
278b-3	2.50×10^{-5}	6.41×10^{-4}	2.70×10^2
278b-4	2.50×10^{-5}	1.03×10^{-3}	3.31×10^2
278b-1	2.50×10^{-5}	1.28×10^{-3}	3.82×10^2

$$k_2 = 1.71 \times 10^5 M^{-1} s^{-1}$$

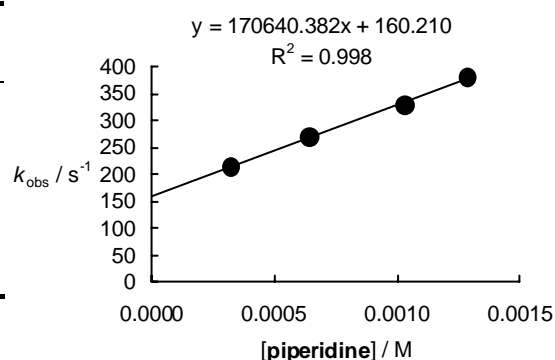
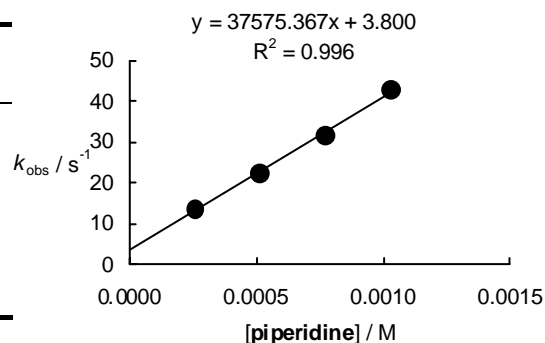


Table S29: Kinetics of the reaction of **1c** with piperidine in DMSO/H₂O (50:50, v/v) at 20 °C (stopped-flow UV-Vis spectrometer, $\lambda = 459$ nm).

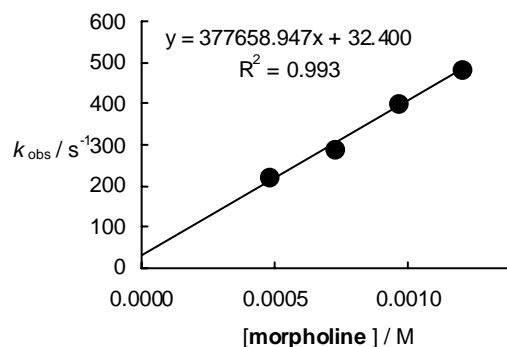
No.	[E] ₀ / M	[C ⁻] ₀ / M	$k_{\text{obs}} / \text{s}^{-1}$
279-2	1.25×10^{-5}	2.56×10^{-4}	1.39×10^1
279-3	1.25×10^{-5}	5.12×10^{-4}	2.28×10^1
279-4	1.25×10^{-5}	7.68×10^{-4}	3.17×10^1
279-5	1.25×10^{-5}	1.02×10^{-3}	4.30×10^1

$$k_2 = 3.76 \times 10^4 \text{ M}^{-1} \text{ s}^{-1}$$

**Table S30:** Kinetics of the reaction of **1c** with morpholine in DMSO at 20 °C (stopped-flow UV-Vis spectrometer, $\lambda = 459$ nm).

No.	[E] ₀ / M	[C ⁻] ₀ / M	$k_{\text{obs}} / \text{s}^{-1}$
284b-4	2.86×10^{-5}	4.80×10^{-4}	2.21×10^2
284b-1	2.86×10^{-5}	7.20×10^{-4}	2.90×10^2
284b-3	2.86×10^{-5}	9.60×10^{-4}	4.01×10^2
284b-2	2.86×10^{-5}	1.20×10^{-3}	4.86×10^2

$$k_2 = 3.78 \times 10^5 \text{ M}^{-1} \text{ s}^{-1}$$

**Table S31:** Kinetics of the reaction of **1c** with morpholine in DMSO/H₂O (50:50, v/v) at 20 °C (stopped-flow UV-Vis spectrometer, $\lambda = 459$ nm).

No.	[E] ₀ / M	[C ⁻] ₀ / M	$k_{\text{obs}} / \text{s}^{-1}$
287-1	1.99×10^{-5}	1.01×10^{-3}	7.37×10^1
287-2	1.99×10^{-5}	1.51×10^{-3}	7.73×10^1
287-3	1.99×10^{-5}	2.02×10^{-3}	8.41×10^1
287-4	1.99×10^{-5}	2.44×10^{-3}	8.77×10^1
287-5	1.99×10^{-5}	3.02×10^{-3}	9.60×10^1

$$k_2 = 1.11 \times 10^4 \text{ M}^{-1} \text{ s}^{-1}$$

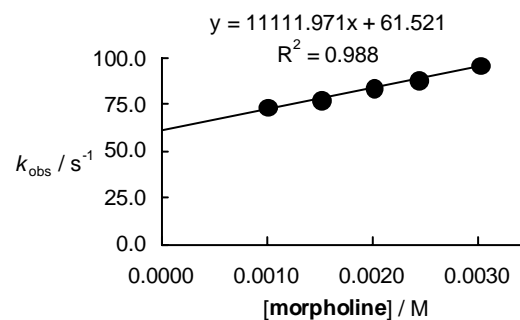
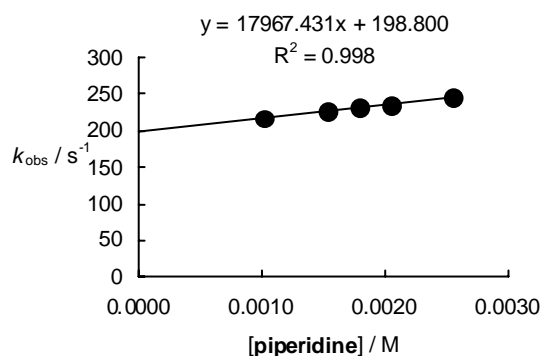


Table S32: Kinetics of the reaction of **1d** with piperidine in DMSO at 20 °C (stopped-flow UV-Vis spectrometer, $\lambda = 487$ nm).

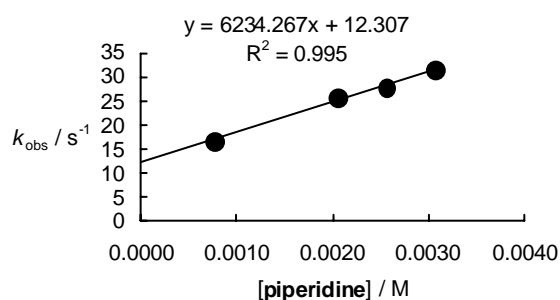
No.	$[E]_0 / M$	$[C^-]_0 / M$	k_{obs} / s^{-1}
280-3	1.05×10^{-5}	1.02×10^{-3}	2.17×10^2
280-2	1.05×10^{-5}	1.54×10^{-3}	2.27×10^2
280-5	1.05×10^{-5}	1.79×10^{-3}	2.31×10^2
280-4	1.05×10^{-5}	2.05×10^{-3}	2.35×10^2
280-1	1.05×10^{-5}	2.56×10^{-3}	2.45×10^2

$$k_2 = 1.80 \times 10^4 M^{-1} s^{-1}$$

**Table S33:** Kinetics of the reaction of **1d** with piperidine in DMSO/H₂O (50:50, v/v) at 20 °C (stopped-flow UV-Vis spectrometer, $\lambda = 487$ nm).

No.	$[E]_0 / M$	$[C^-]_0 / M$	k_{obs} / s^{-1}
281-1	1.05×10^{-5}	7.68×10^{-4}	1.69×10^1
281-2	1.05×10^{-5}	2.05×10^{-3}	2.57×10^1
281-4	1.05×10^{-5}	2.56×10^{-3}	2.79×10^1
281-3	1.05×10^{-5}	3.07×10^{-3}	3.14×10^1

$$k_2 = 6.23 \times 10^3 M^{-1} s^{-1}$$



Chapter 3

Reactivities of Benzylidene Meldrum's Acids in Methanol

Introduction

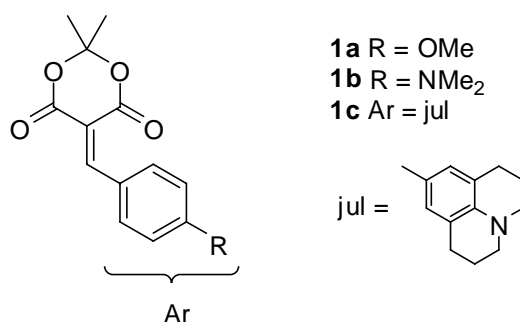
For our understanding of polar organic reactivity, the knowledge about the reactivities of nucleophiles is essential. Many kinetic investigations of the rates for nucleophile-electrophile combinations revealed that, in general, the nucleophilic reactivities of many classes of nucleophiles are highly solvent-dependent. The nucleophilicities of neutral molecules, such as primary and secondary amines^{1,2} or pyridines,³ have previously been reported to be considerably lower in water than in dimethyl sulfoxide (DMSO). Analogous behavior has also been found for various classes of carbanions.⁴⁻⁶ In contrast, triflate stabilized benzyl anions showed the opposite behavior and turned out to be more reactive in protic solvents than in DMSO.⁷ However, systematic investigations of the solvent-dependence of typically employed electrophiles (benzhydrylium ions and quinone methides) have not been carried out, as the solvent-dependence was reported to be small and negligible compared to those of most nucleophiles.⁸

Recent kinetic studies of the rates of reactions of benzhydrylium ions and benzylidene indandiones with carbanions and amines in DMSO and DMSO-water mixtures indicated that solvation affects the electrophilicities of benzylidene indandiones to a considerably larger degree than those of benzhydrylium ions.⁹ As a consequence, it has been recommended to use the electrophilicity parameters E of ordinary Michael acceptors exclusively for the prediction of rate constants for their reactions with nucleophiles in aprotic solvents like dimethyl sulfoxide. The recently reported nucleophilicities N of carbanions in MeOH⁴ allow us to

investigate these solvent effects in more detail and to quantify the electrophilicities E of Michael acceptors towards carbanions in MeOH by using Equation (3.1), in which s and N are nucleophile-specific parameters and E is an electrophile-specific parameter.

$$\log k_2 (20\text{ }^\circ\text{C}) = s(N + E) \quad (3.1)$$

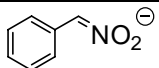
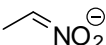
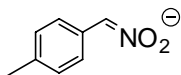
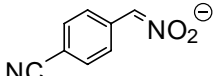
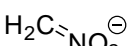
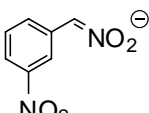
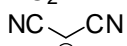
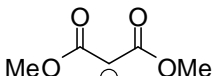
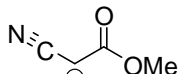
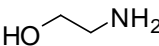
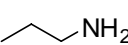
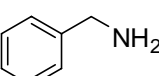
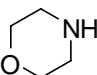
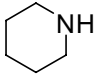
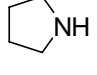
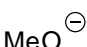
We chose benzylidene Meldrum's acids **1a–c** (Scheme 3.1), as model compounds to investigate their reactions with nucleophiles in MeOH and to derive their electrophilicities E .



Scheme 3.1. Employed benzylidene Meldrum's acids **1a–c**.

We now report on the rates of the addition reactions of the stabilized carbanions **2a–i**, amines **3a–c**, and methoxide (**4a**) (Table 3.1) to the benzylidene Meldrum's acids **1a–c** and show that the kinetics generally follow Equation (3.1). The second-order rate constants k_2 are subsequently employed to derive the electrophilicity parameters E for the Michael acceptors **1a–c** in MeOH and are compared with those for **1a–c** in DMSO.

Table 3.1. *N*- and *s* Parameters of the Carbanions **2a–i**, Amines **3a–f**, and Methoxide (**4a**) in 91%Methanol/9%Acetonitrile (v/v).

Nucleophile	<i>N</i>	<i>s</i>
2a 	12.51 ^a	0.66 ^a
2b 	13.41 ^a	0.67 ^a
2c 	13.58 ^a	0.63 ^a
2d 	13.92 ^a	0.73 ^a
2e 	14.02 ^a	0.60 ^a
2f 	14.75 ^a	0.71 ^a
2g 	18.21 ^a	0.68 ^a
2h 	18.24 ^a	0.64 ^a
2i 	18.59 ^a	0.65 ^a
3a 	13.23 ^b	0.65 ^b
3b 	13.41 ^b	0.66 ^b
3c 	13.46 ^b	0.62 ^b
3d 	15.40 ^b	0.64 ^b
3e 	15.63 ^b	0.64 ^b
3f 	15.97 ^b	0.62 ^b
4a 	14.51 ^c	0.68 ^c

^a From ref. 4, ^b from refs. 2, 10, ^c from ref. 11.

Results and Discussion

The Michael acceptors **1a–c** were synthesized by Knoevenagel condensation from the corresponding aldehydes and Meldrum's acid as described previously¹² and the covalent CH acids (**2a–i**)-H were commercial available or synthesized according to ref. 5.

Product Studies. General. As reported in Chapter 2, compounds **1a–c** react with the carbanions **2b** and **2g–i** under formation of the ordinary Michael addition products.¹²

Representative product studies for the reactions of **1a–c** with amines **3d–f** and methoxide **4a** show the formation of the corresponding adducts **5** and **6** (Figure 3.1).

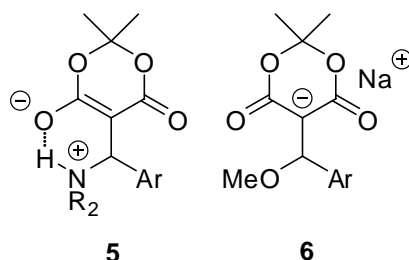


Figure 3.1. Products **5** and **6** from the reactions of amines **3d–f** and methoxide (**4a**) with the Michael acceptors **1a–c**.

Table 3.2. Characterized Products **5** and **6**.

Electrophile	Nucleophile	Product	Yield / [%]
1a	3d	5ad	77
1a	3e	5ae	72
1a	3f	5af	75
1b	3f	5bf	^a
1a	4a	6aa	^a
1b	4a	6ba	60
1c	4a	6ca	^a

^a Products identified by ¹H NMR experiments in the crude reaction mixtures.

Product Studies. Methoxide.

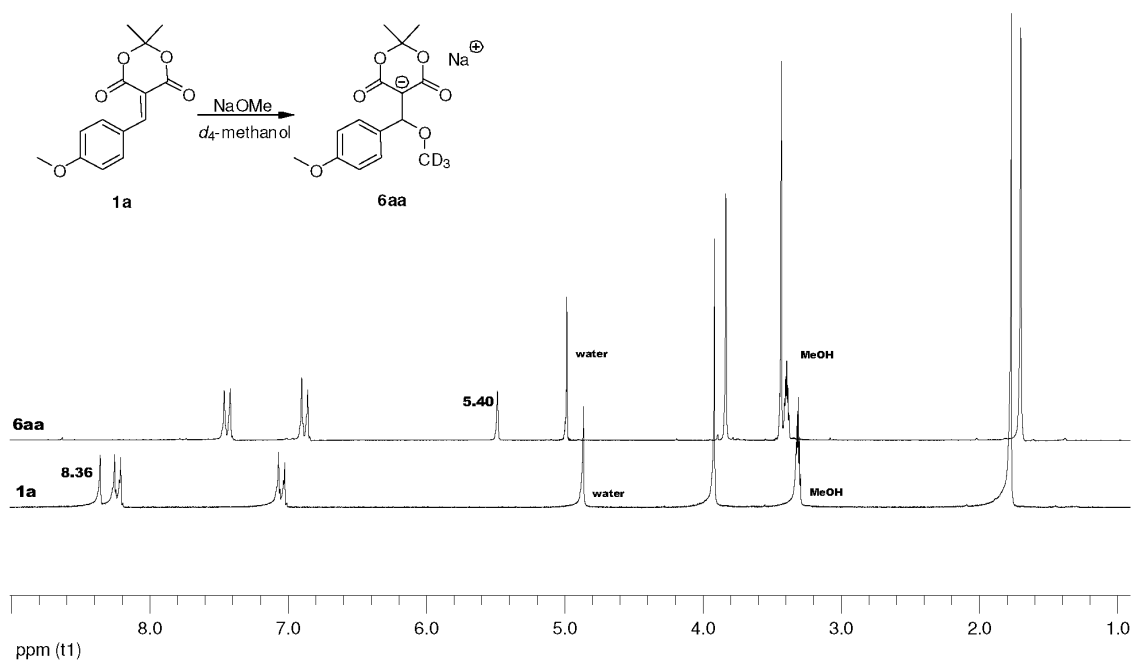
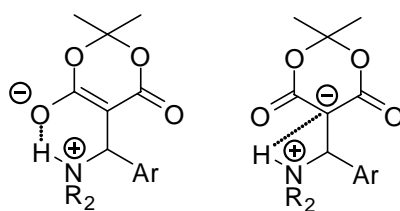


Figure 3.2. ^1H NMR spectra (200 MHz, $[\text{d}_4]$ -methanol) for the electrophile **1a** (below) and for the product **6aa** (above) from the reaction of electrophile **1a** with one equivalent of methoxide (**4a**) in $[\text{d}_4]$ -methanol.

The reactions of **1a–c** with methoxide (**4a**) were carried out in $[\text{d}_4]$ -methanol following a procedure described by Wessely et al.¹³ As depicted in Figure 3.2, the signal for the olefin proton of **1a** at $\delta = 8.36$ ppm disappeared completely when **1a** was combined with one equivalent of sodium methoxide (**4a**). In the spectrum of **6aa** a signal at $\delta = 5.40$ ppm indicates the formation of a sp^3 -hybridized carbon atom. Due to fast proton transfer between NaOCH_3 and DOCD_3 mainly OCD_3^- will react with **1a**, and hence no additional signals for the methoxy group are found within the spectrum. Analogously, the reactions of **1b,c** with sodium methoxide (**4a**) yielded the addition products **6ba** and **6ca**, from which compound **6ba** was isolated in substance (Table 3.2). After several hours, additional signals in the ^1H NMR spectrum of the crude reaction mixture of **6aa–6ca** in $[\text{d}_4]$ -methanol turned up, indicating slow decomposition of the addition products.

Product studies. Amines. Representative product studies for the reactions of the Michael acceptors **1a–c** with amines have mainly been carried out with electrophile **1a**, because of favorable equilibrium constants which account for almost quantitative conversion when **1a** was combined with equimolar amounts of the amines **3d–f**. The combinations of electrophile **1a** with the secondary amines **3d–f** were carried out in benzene due to the relatively low solubility of the benzyldiene Meldrum's acids in MeOH. The resulting pale yellow precipitates were isolated in good yields and identified as products **5ad–af** (Table 3.2). Typically, the zwitterionic adducts **5** do not dissolve readily in common solvents. Product **5ae** was insoluble in D₂O, CDCl₃, [d]₆-DMSO or [d]₄-methanol and CD₃CN. Its ¹H NMR spectra could only be obtained by dissolving **5ae** in warm [d]₆-DMSO resulting in a relatively poor quality of the obtained spectrum.

The ¹H NMR spectra of compounds **5** show broadened N-H signals and additionally, the ¹H NMR spectra of **5ad** and **5af** also reveal broadened signals for the aromatic ortho-protons. These broadened signals are indicative for intramolecular hydrogen bridging between the nitrogen atom of the amine moiety and the negatively charged oxygen or carbon atom of the Meldrum's acid. IR spectroscopy of the compounds **5ad–5af** showed signals around 3430 cm⁻¹ also indicating intramolecular hydrogen bridging as illustrated below.



Kinetics. Due to their extended conjugated π -system, electrophiles **1a–c** show absorption maxima in the visible part of the electromagnetic spectrum offering the possibility to follow their reactions with nucleophiles photometrically as exemplarily depicted in Figure 3.3 for the reaction of the benzyldiene Meldrum's acid **1a** with the anion of ethyl cyanoacetate **2i** in MeOH.

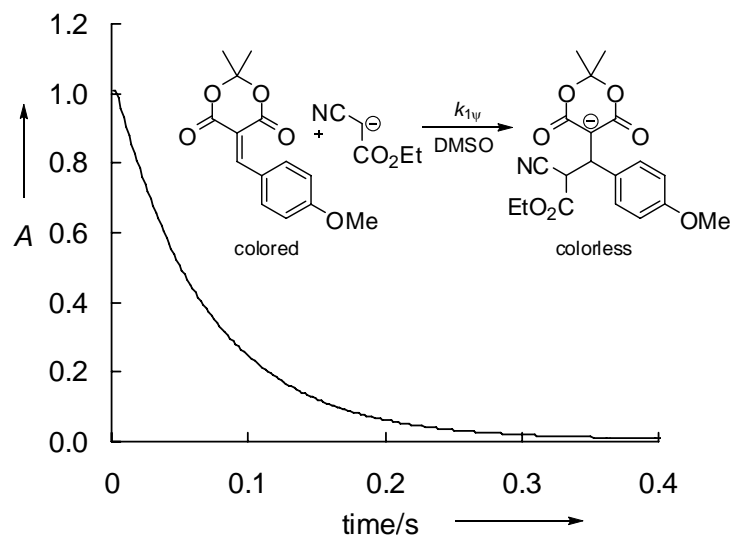
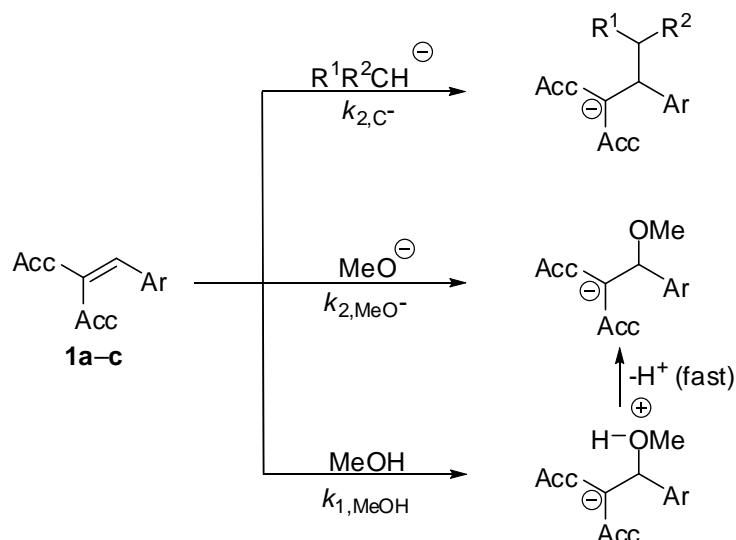


Figure 3.3. Reaction of the benzylidene Meldrum's acid **1a** ($c_0 = 1.68 \times 10^{-5} \text{ mol L}^{-1}$) with the anion of ethyl cyano acetate (**2i**, $c_0 = 8.50 \times 10^{-4} \text{ mol L}^{-1}$) in MeOH at $\lambda = 380 \text{ nm}$.

Determination of the second-order rate constants k_{2,C^-} for the reactions of **1a–c** with carbanions.

As illustrated in Scheme 3.2 and expressed by Equations (3.2) and (3.3), the pseudo first-order rate constants k_{obs} for the consumption of the electrophiles **1a–c** reflect the sum of the reactions of **1a–c** with the carbanions, methoxide, and methanol present in solution. The carbanions **2a–i** were freshly generated from the corresponding CH acidic compounds (**2a–i**)-H by treatment with sodium methoxide. The concentrations of the carbanion $[C^-]$ and of methoxide $[MeO^-]$ were almost constant because in all experiments a large excess of the carbanion over the electrophile was chosen (at least 10 equivalents).



Scheme 3.2. Competing reactions of the benzyldene Meldrum's acids **1a–c** with carbanions, methoxide, and methanol in MeOH.

$$\frac{dE}{dt} = -k_{obs}[E] \quad (3.2)$$

$$k_{obs} = k_{2,C^-}[C^-] + k_{2,MeO^-}[MeO^-] + k_{1,MeOH} \quad (3.3)$$

Knowledge of the previously reported equilibrium constants K_{CH} for the deprotonation reactions of the CH acids (**2a–i**)-H with methoxide⁴ and the total base concentrations makes it possible to calculate the equilibrium concentrations of the carbanion $[C^-]$ and of methoxide $[MeO^-]$ from Equations (3.4)–(3.7).



$$K_{CH} = [C^-] / [CH][MeO^-] \quad (3.5)$$

$$pK_{MeOH} = -\log ([MeO^-] [H^+]) = 16.92 \text{ (at } 20^\circ\text{C)} \quad (3.6)$$

$$pK_{aH} = -\log ([C^-][H^+]/[CH]) \quad (3.7)$$

In general, the competing reactions of methoxide **4a** with the electrophiles **1a–c** cannot be neglected. Therefore, $k_{2,MeO^-}[MeO^-]$ has to be subtracted from the observed rate constant k_{obs} ,

resulting in $k_{1\psi}$ (as will be discussed below k_{2,MeO^-} was obtained from independent kinetic experiments). Rearrangement of Equation (3.3) leads to Equation (3.8).

$$k_{1\psi} = k_{\text{obs}} - k_{2,\text{MeO}^-} [\text{MeO}^-] = k_{2,\text{C}^-} [\text{C}^-] + k_{1,\text{MeOH}} \quad (3.8)$$

The second-order rate constants k_{2,C^-} are obtained from plots of $k_{1\psi}$ versus the carbanion concentration $[\text{C}^-]$ as shown in Figure 3.4 for the reaction of electrophile **1a** with the anion of nitro methane (**2e**). The intercepts of these straight lines corresponds to the rates of the reactions of **1a–c** with the solvent ($k_{1\psi} = k_{1,\text{MeOH}}$ for $[\text{C}^-] = 0$). As they are much smaller than the corresponding reaction rates of **1a–c** with methoxide ($k_{1,\text{MeOH}} \ll k_{2,\text{MeO}^-}$) they can be neglected.

Figure 3.4 illustrates that the contribution of the reactions of **1a** with methoxide is rather small (8 %) in comparison to the one for the reactions of **1a** with the anion of nitro methane (**2e**). This is in line with the previously reported error limits for reactions of carbanions in MeOH.⁴

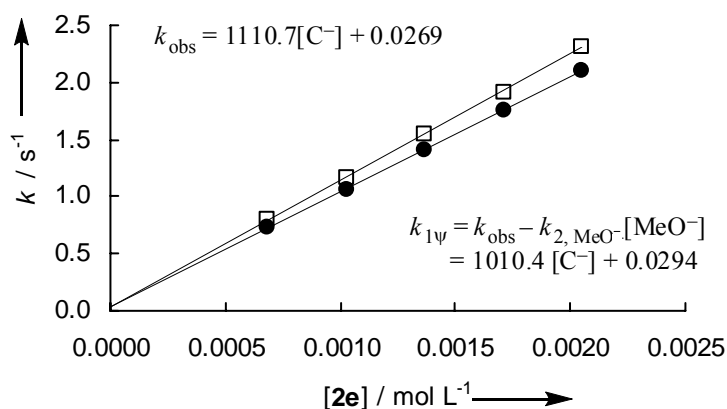


Figure 3.4. Determination of the second-order rate constant k_{2,C^-} ($1.01 \times 10^3 \text{ L mol}^{-1} \text{ s}^{-1}$) for the reaction of **1a** with the anion of nitro methane (**2e**) in MeOH at 20 °C (●). Observed first-order rate constant k_{obs} (□) and first-order rate constants $k_{1\psi}$ (●), for which the contribution of the reaction of **1a** with **4a** has been subtracted.

Determination of the second-order rate constants k_2 for the reactions of 1a–c with amines and methoxide. Plots of k_{obs} versus the concentrations of methoxide or the amines resulted in straight lines with the second-order rate constant k_2 as slopes. For those reactions which proceeded incompletely, the rates for the reverse reactions k_{-} could be derived from the intercepts.¹⁴

Table 3.3 and Table 3.4 summarize the second-order rate constants k_{2,C^-} and k_2 for the reactions of **1a–c** with the carbanions **2a–i**, and with methoxide (**4a**), and the amines **3a–f**, respectively. The rates of the reactions of electrophile **1a** with the carbanions **2d** and **2f** could not be determined due to overlapping absorption bands. Because of small equilibrium constants, the rates of the reaction between electrophile **1b** and morpholine (**3d**), as well as the reactions between electrophile **1c** and amines **3c,d** could not be determined.

Table 3.3. Second-Order Rate Constants k_{2,C^-} for the Reactions of the Electrophiles **1a–c** with the Carbanions **2a–i** in MeOH at 20 °C.

	E^a	Carbanion	$k_{2,C^-} / \text{L mol}^{-1}\text{s}^{-1}$		
1a	-10.28	2a	1.14×10^2		
		2b	8.52×10^1		
		2c	6.67×10^1		
		2e	4.74×10^2		
		2g	1.49×10^6		
		2h	1.02×10^5		
		2i	4.11×10^5		
		1b	-12.76	2a	3.44
				2b	8.24
2c	1.47				
2d	9.19				
2e	3.09×10^1				
2f	1.88×10^1				
2g	8.17×10^4				
2h	4.49×10^3				
2i	1.88×10^4				

Table 3.3. *Continued.*

	E^a	Carbanion	$k_{2, C^-} / \text{L mol}^{-1} \text{s}^{-1}$
1c	-13.97	2a	7.84×10^{-1}
		2b	1.24
		2c	4.88×10^{-1}
		2d	2.85
		2e	4.30
		2f	7.38
		2g	1.97×10^4
		2h	1.06×10^3
		2i	4.30×10^3

^a Electrophilicity parameters E for **1a–c** in DMSO as defined in ref. 12

Table 3.4. Second-Order Rate Constants k_2 for the Reactions of the Electrophiles **1a–c** with the Amines **3a–f** and with Methoxide (**4a**) in MeOH at 20 °C.

	E^a	Nucleophile	$k_2 / \text{L mol}^{-1} \text{s}^{-1}$
1a	-10.28	3a	4.30×10^3
		3b	6.73×10^3
		3c	4.60×10^3
		3d	6.90×10^4
		3e	8.93×10^4
		3f	1.64×10^5
1b	-12.76	4a	1.86×10^3
		3a	3.08×10^2
		3b	5.65×10^2
		3c	2.98×10^2
		3e	1.19×10^4
		3f	1.55×10^4
1c	-13.97	4a	7.38×10^1
		3a	6.72×10^1
		3b	1.68×10^2
		3e	2.69×10^3
		3f	5.08×10^3
		4a	1.42×10^1

^a Electrophilicity parameters E for **1a–c** in DMSO as defined in ref. 12

Correlation Analysis. In Figure 3.5, $(\log k_2)/s$ for the reactions of electrophiles **1a–c** with carbanions **2a–i** are plotted versus the corresponding nucleophilicity parameters N of the carbanions in MeOH. If Equation (3.1) holds for the reactions of benzylidene Meldrum's acids **1a–c** with carbanions in MeOH, the plot of $(\log k_2)/s$ versus N should result in linear correlations with slopes of 1.0. Figure 3.5 shows that some systematic deviations from linearity are obvious. On one hand, the rates of the reactions of the *p*-tolynitronate anion **2c** with the electrophiles **1a–c** are five times smaller than expected from Equation (3.1). On the other hand, the anion of malononitrile (**2g**) reacts approximately 4 times faster than predicted by Equation (3.1). Similar deviations of the overall correlations for the reactions of electrophiles **1a–c** with carbanions in DMSO have recently been reported.¹² It has to be noted, that the error limit for Equation (3.1) of 10 – 100 in a reactivity range of more than 30 orders of magnitude is never exceeded.

The electrophilicity parameters E for the benzylidene Meldrum's acids **1a–c** in MeOH have been calculated based on the second-order rate constants k_{2,C^-} given in Table 3.3 and the N and s parameters for the carbanions in MeOH as defined in Table 3.1 by least-squares minimization of $\Delta^2 = \sum(\log k - s(N + E))^2$.

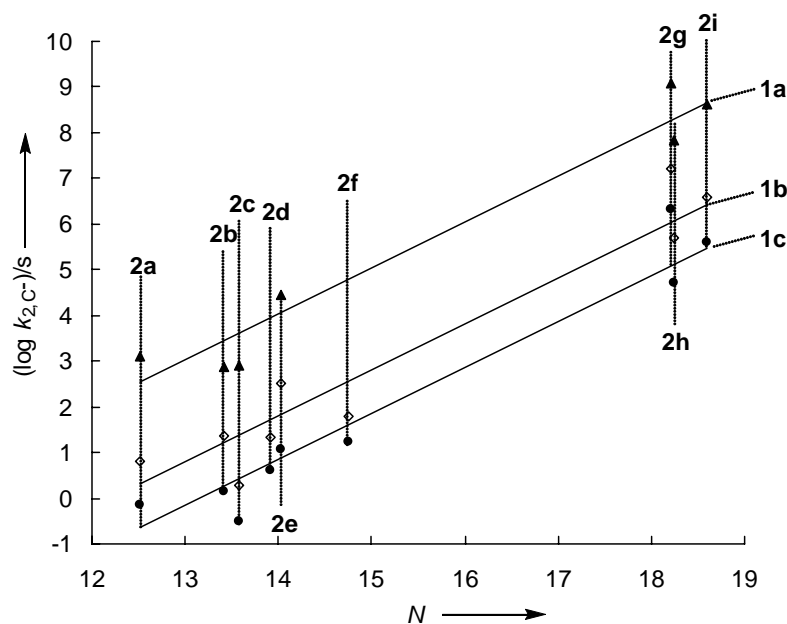


Figure 3.5. Plot of $(\log k_{2,C^-})/s$ for the reactions of carbanions **2a–i** with the benzyldene Meldrum's acids **1a–c** in MeOH versus the nucleophilicity parameter N of the employed carbanions.

Although the correlation lines are only of moderate quality, the derived electrophilicity parameters E can be used for a comparison with the E values for compounds **1a–c** in DMSO. As Figure 3.6 reveals, the electrophilicities E for the benzyldene Meldrum's acid **1a–c**, derived from their reactions with carbanions, are less than one order of magnitude larger in MeOH than in DMSO. Although the electrophilicity E has been regarded as almost solvent-independent, similar results have already been reported for the reactions of benzyldene indandiones with carbanions by changing the solvent from neat DMSO to DMSO/water mixtures (50/50 v/v).⁹ The results presented in this chapter sustain these findings by more detailed and systematic investigations.

Figure 3.6 indicates that the electrophilicities of benzyldene Meldrum's acids **1a–c** increase approximately by the same extent when going from DMSO to MeOH. The small differences may reflect the different solvation of **1a–c** in MeOH, i.e., electrophile **1a** is somewhat better solvated in MeOH than its less reactive analogs **1b** and **1c**. The relative

change of their electrophilicities E is therefore represented by the relative solvation of **1a–c** in MeOH.

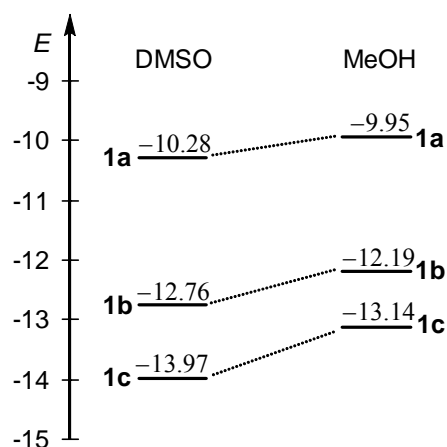


Figure 3.6. Comparison of the electrophilicity E of benzyldene Meldrum's acids **1a–c** in DMSO and MeOH.

The Hammett plot (Figure 3.7) emphasizes that the electrophilicities E of the benzyldene Meldrum's acids **1a–c** are larger in MeOH than in DMSO. For common nucleophiles with $s = 0.7$, a reaction constant of $\rho = 3.87$ results from the correlation equation for **1a–c** in MeOH given in Figure 3.7.

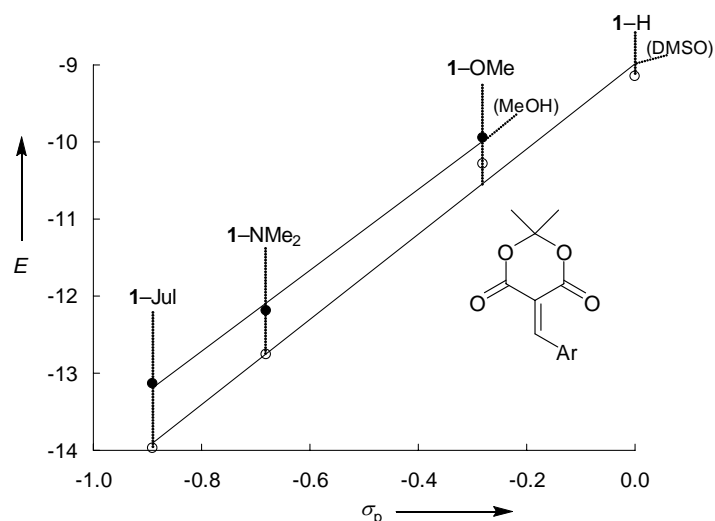


Figure 3.7. Plots of the electrophilicity parameters E of benzyldene Meldrum's acids **1a–c** in MeOH (\bullet $E = 5.26\sigma - 8.51$) and DMSO (\circ $E = 5.37\sigma - 9.08$) versus Hammett's σ_p values.¹⁵

The plots of $(\log k_2)/s$ for the reactions of electrophiles **1a–c** with the amines **3a–f** versus their nucleophilicity parameters N show linear correlations (Figure 3.8) of good qualities. Except for the reaction of electrophile **2b** with benzylamine (**3c**), which is faster than expected, only small deviations from linearity can be observed for the rates of the electrophile-nucleophile combinations.

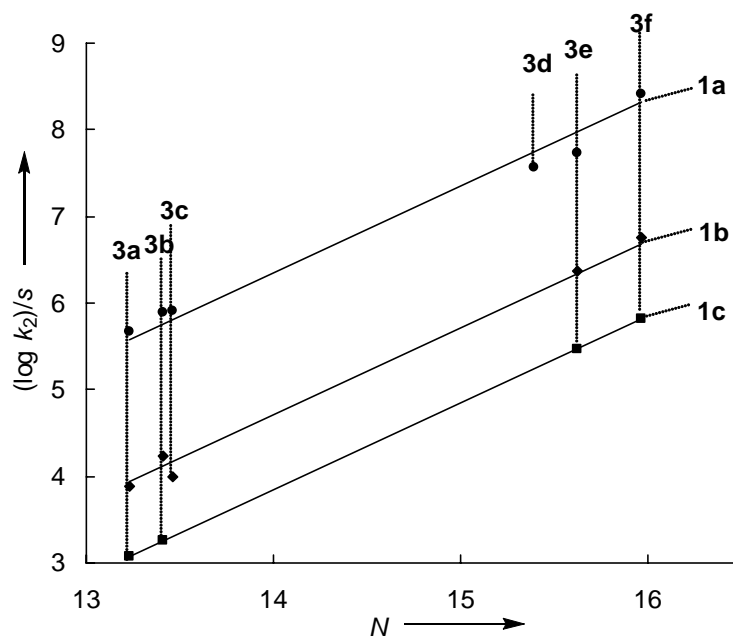


Figure 3.8. Plot of $(\log k_2)/s$ for the reactions of amines **3a–f** with benzyldene Meldrum's acids **1a–c** in MeOH versus the nucleophilicity parameters N of the amines **3a–f**.

When the rate constants for the reactions of **1a–c** with the carbanions (Figure 3.5) and with the amines (Figure 3.8) are summarized in one graph (Figure 3.9), one can see that the reactions of the electrophiles with amines are approximately 2 orders of magnitude faster than the corresponding reactions with the carbanions **2a–i**. These observations are in line with those previously reported for the analogous reactions of carbanions and amines with benzyldene Meldrum's acids in DMSO.¹²

The higher rates of additions of amines to benzyldene Meldrum's acids **1a–c** compared to the corresponding additions of carbanions have previously been attributed to the formation of

cyclic four- or six-membered structures, which profit from O–H interactions in the transition states.¹⁶

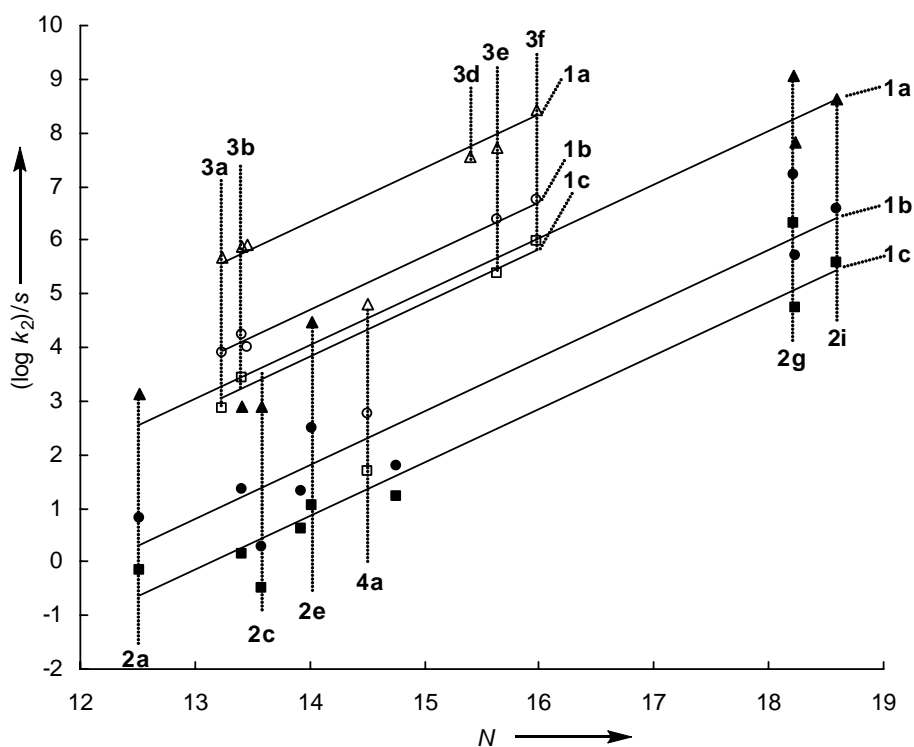


Figure 3.9. Correlation of $(\log k_2)/s$ for the reactions of carbanions **2a–i**, amines **3a–f**, and methoxide (**4a**) with benzylidene Meldrum's acids **1a–c** in MeOH versus the nucleophilicity parameter N of the employed nucleophiles. For the sake of clarity some nucleophile assignments have been omitted.

Figure 3.9 also indicates that the second-order rate constants k_2 for the reactions of MeO^- with the electrophiles **1a–c** fall on the correlation lines for carbanions and not on that for amines.

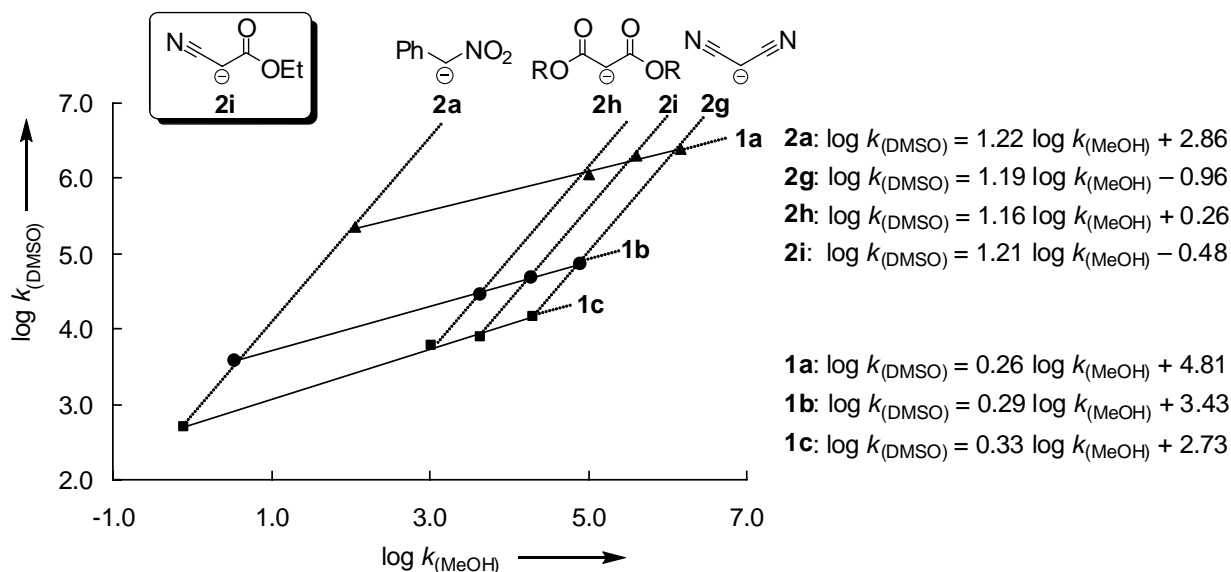


Figure 3.10. Plot of $\log k_{(\text{DMSO})}$ for the reactions of **1a-c** with the carbanions **2** versus $\log k_{(\text{MeOH})}$ for the corresponding reactions in methanol. (Please note that **2h** represents the reactions of **1a-c** with the anion of *dimethylmalonate* in MeOH and the reactions of **1a-c** with the anion of *diethylmalonate* in DMSO).

Figure 3.10 compares the logarithmic second-order rate constants k_2 for the reactions of the Michael acceptors **1a-c** with carbanions in dimethyl sulfoxide with the rates for the analogous reactions in methanol. It shows that the reactions of **1a-c** with the carbanions **2** are faster in DMSO than in MeOH. The linear correlations also reveal that systematic deviations of the rates, which were found for example for the reactions of the carbanion **2g** with **1a-c** in methanol (compare Figure 3.5), are comparable with the rates of the analogous reactions in DMSO. The slopes of the correlation lines, which vary from 0.26 to 0.33, reveal that variation of the carbanions affects the second-order rate constants k_2 of the reactions with the Michael acceptors **1a-c** in DMSO to a smaller extent than in MeOH. It has to be emphasized, however, that the linear correlations shown in Figure 3.10 must be accidental because other types of carbanions follow completely different orders of nucleophilicity in these two solvents.⁴ On the other hand, as discussed above, variation of **1a-c** has a slightly larger effect

in DMSO than in MeOH as indicated by the slopes of the correlation lines for **2a** and **2g–h** in Figure 3.10.

Equilibrium constants K in MeOH. While the Michael additions of the carbanions **2a–i** with the electrophiles **1a–c** (Table 3.3) proceed quantitatively in MeOH (indicated by negligible end absorptions of the solutions at the absorption maxima of the benzylidene Meldrum's acids **1a–c**), most of the reactions with the amines **2a–f** (Table 3.4) turned out to be highly reversible as illustrated in Figure 3.11 for the reactions of electrophile **1c** with *n*-propylamine (**3b**).

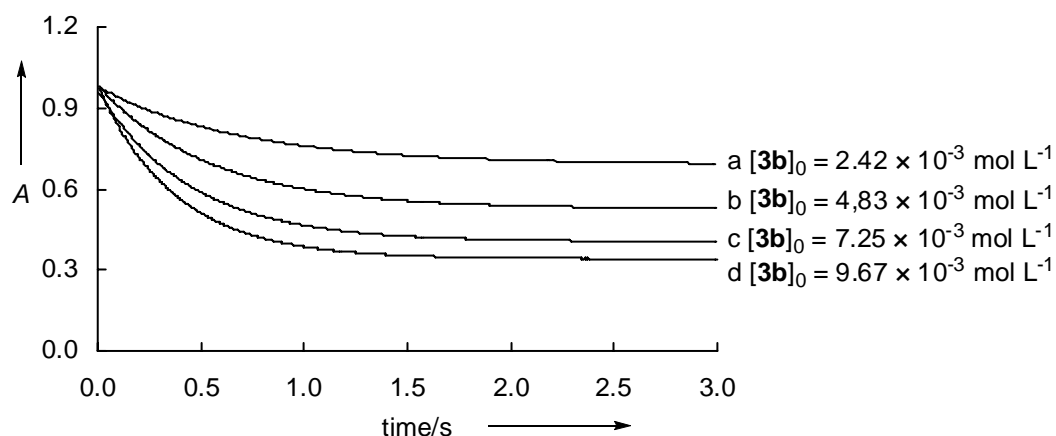


Figure 3.11. Plot of A versus time for the reversible reaction of electrophile **1c** ($c_0 = 2.02 \times 10^{-5}$ mol L⁻¹) with *n*-propylamine (**3b**) in MeOH at 20 °C ($\lambda = 480$ nm).

The equilibria observed in Figure 3.11 may reflect the reactions of the electrophiles **1a–c** with the amines or with MeOH as depicted in Figure 3.12.

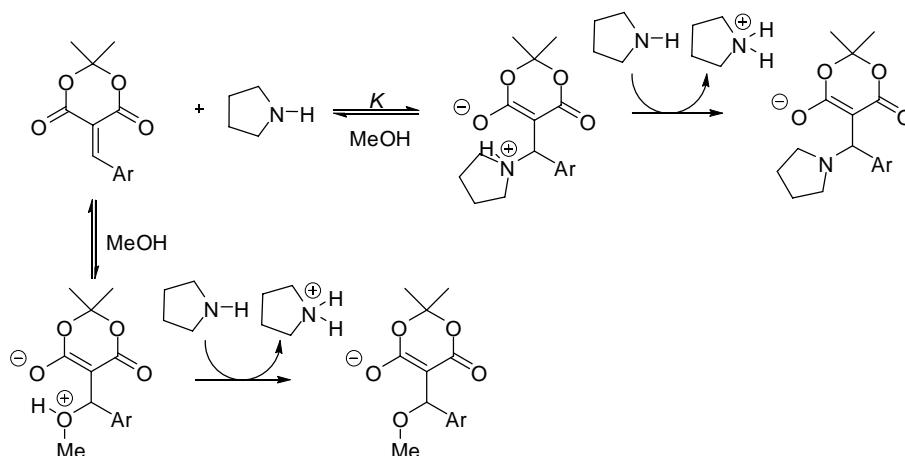


Figure 3.12. Determination of the equilibrium constant K for the reactions of the electrophiles **1a–c** with the amines in methanol, and possible side reactions.

The equilibrium constants K were determined directly from titration experiments using Equation (3.9), i.e., the nucleophiles were added stepwise to solutions of the electrophiles **1a–c** in MeOH, and from the decrease of the electrophile's absorptions, the equilibrium constant K could be calculated.

$$K = \frac{[\mathbf{1}]_0 - [\mathbf{1}]}{\{[Nu]_0 - ([\mathbf{1}]_0 - [\mathbf{1}])\}[\mathbf{1}]} \quad (3.9)$$

However, as shown in Tables S44–S54 in the Experimental Section, the derived equilibrium constants K show small systematic trends within a series of measurements. Usually, this effect is small (factor of 2), but becomes significant for the determination of the equilibrium constants K for the reactions of electrophile **1a** with morpholine (**3d**) and methoxide (**4a**), which show deviations by a factor of 7 between single measurements. The reasons for these observations are unknown and may be attributed to competing side reactions of the electrophiles **1a–c** with methanol, as depicted in Figure 3.12. The assumption of a reversible reaction of **1a–c** with methanol could explain the increasing equilibrium constants K within some series of measurements, because the observed absorbances A of **1a–c** after the reactions with the amines were lower than expected. On the other side, the reaction of methanol with **1a–c** cannot explain our findings that for some equilibrium situations, smaller K values than expected were found. Moreover, Equation (3.9) is only valid if the reactions of **1a–c** with the amines follow 1:1 equilibrium situations, i.e., one molecule of the amine reacts with one molecule of the electrophiles **1a–c**. We cannot exclude that a second amine molecule subsequently deprotonates the formed zwitterionic product as assumed in Figure 3.12, which would have an influence on the concentration of the amines used for the calculation of the equilibrium constants. The pK_{aH} values for pyrrolidine (11.3)¹⁷ and Me-pyrrolidine (10.5)¹⁸ in water indicate that pyrrolidine is the stronger base and can subsequently deprotonate the

zwitterionic adduct with formation of the conjugate acid and the anionic product as depicted in Figure 3.12.

This approach to determine the equilibrium constants K is therefore limited and contains some uncertainties. However, equilibrium constants have only been evaluated if the deviations within one series of measurements were smaller than a factor of 2 and consequently used to derive intrinsic barriers for their comparison with literature data.

As indicated by entries 3 and 5 in Table 3.5, the equilibrium constants K increase for reactions of a given amine with stronger electrophiles, e.g., the equilibrium constant K for the reaction of electrophile **1c** with pyrrolidine (**3f**) equals $K = 4.78 \times 10^2 \text{ L mol}^{-1}$ whereas the analogous reaction of **3f** with the stronger electrophile **1b** resulted in $K = 4.06 \times 10^3 \text{ L mol}^{-1}$. The analog result is also encountered for the reactions of electrophiles **1a–c** with methoxide (**4a**) (entries 6, 7).

From the equilibrium constants K based on titration experiments and the second-order rate constants k_2 (from Table 3.4) one can calculate (Equation 3.10) the rates for the reverse reactions k_- which are listed in the seventh column of Table 3.5.

If no side reactions affect the reaction of the amines and **1a–c**, it is possible to calculate the equilibrium constants K for these reactions as the ratio of the forward over the reverse reaction using Equation (3.10).

$$K = \frac{k_2}{k_-} \quad (3.10)$$

The values for the reverse reactions k_- derived from the titration experiments (column 7) are considered to be more accurate than those obtained from the intercepts (column 6), although some small systematic trends (factor of 2) were observed in some cases while determining the equilibrium constants K .

Table 3.5. Rate and Equilibrium Constants for the Reactions of the Electrophiles **1a–c** with the Amines **3** and Methoxide (**4a**) in MeOH at 20 °C.

Entry	Electro- phile	Nucleo- phile	$K /$ L mol^{-1a}	$k_2 /$ $\text{L mol}^{-1}\text{s}^{-1b}$	$k_{-} /$ s^{-1c}	$k_{-} /$ s^{-1d}	$\Delta G_0 /$ kJ mol^{-1}	$\Delta G^\ddagger /$ kJ mol^{-1}	$\Delta G_0^\ddagger /$ kJ mol^{-1e}
1	1b	3c	6.65×10^2	2.98×10^2	2.1	3.9×10^{-1}	-15.4	57.9	65.4
2		3e	1.63×10^3	1.19×10^4	3.9×10^1	7.3	-18.0	48.9	57.5
3		3e							59.8 ^f
4		3f	4.06×10^3	1.55×10^4	9.4	3.8	-20.3	48.2	57.9
5	1c	3b	2.83×10^2	1.68×10^2	1.0	5.9×10^{-1}	-13.8	59.3	66.0
6		3f	4.78×10^2	5.08×10^3	1.5×10^1	1.1×10^1	-15.0	51.0	58.3
7	1b	4a	2.47×10^4	7.38×10^1	–	3.0×10^{-3}	-24.7	61.3	73.1
8	1c	4a	2.93×10^3	1.42×10^1	4.0×10^{-3}	4.8×10^{-3}	-19.5	65.3	74.7

^a From individual titration measurements. ^b k_2 values from Table 3.4. ^c k_{-} estimated from the intercepts from plots of k_{obs} versus [Nu]. ^d Calculation based on Equation (3.10). ^e Based on the Marcus equation (3.11). ^f ΔG_0^\ddagger in H₂O from ref. 19

Insertion of ΔG^\ddagger and ΔG^0 calculated from the second-order rate constants k_2 and the equilibrium constants K for the reactions of **1a–c** with the amines **3** and methoxide (**4a**), in the Marcus equation (3.11), in which the work term has been omitted, yields intrinsic barriers ΔG_0^\ddagger varying from 57–75 kJ mol⁻¹ (Table 3.5).

$$\Delta G^\ddagger = \Delta G_0^\ddagger + 0.5\Delta G^0 + (\Delta G^0)^2 / 16 \Delta G_0^\ddagger \quad (3.11)$$

The intrinsic barriers for the reactions of **1b** with piperidine (**2e**) in MeOH were found to be comparable with those previously published for their analog reactions in water.¹⁹

Table 3.5 demonstrates that the intrinsic barriers ΔG_0^\ddagger for the reactions of electrophiles **1a–c** with secondary amines (**3d–f**) are approximately 6–8 kJ mol⁻¹ smaller than those for the analogous reactions with the primary amines (**3b,c**).

Table 3.5 reveals that the intrinsic barriers for the reactions of electrophiles **1b,c** with methoxide are significantly higher ($\Delta G_0^\ddagger \approx 74$ kJ mol⁻¹) than those of the reactions of **1a–c** with amines. The intrinsic barriers are therefore smaller than those found for the reactions of benzylidenemalonates with carbanions,²⁰ comparable with those reported for the additions of pyridines,³ but higher for the addition of tertiary amines²¹ to structurally related Michael acceptors.

Conclusion

The electrophilicities E of benzylidene Meldrum's acids in methanol are comparable to those in dimethyl sulfoxide and are, therefore, only slightly affected by the nature of the solvent. The increase of their electrophilicities E by less than one order of magnitude in MeOH can be attributed to the poor solvation of compounds **1a–c** in MeOH. The reactions of compounds **1a–c** with primary and secondary amines in MeOH are faster by approximately 2 orders of magnitude than the corresponding reactions of **1a–c** with carbanions of similar nucleophilicity. Intrinsic barriers were found to vary between 55.8–74.7 kJ mol⁻¹, indicating larger barriers for the reactions of **1a–c** with methoxide than with primary and secondary amines.

References

- (1) Brotzel, F.; Chu, Y. C.; Mayr, H. *J. Org. Chem.* **2007**, *72*, 3679-3688.
- (2) Phan, T. B.; Breugst, M.; Mayr, H. *Angew. Chem.* **2006**, *118*, 3954-3959; *Angew. Chem. Int. Ed.* **2006**, *45*, 3869-3874.

- (3) Brotzel, F.; Kempf, B.; Singer, T.; Zipse, H.; Mayr, H. *Chem. Eur. J.* **2007**, *13*, 336-345.
- (4) Phan, T. B.; Mayr, H. *Eur. J. Org. Chem.* **2006**, 2530-2537.
- (5) Bug, T.; Lemek, T.; Mayr, H. *J. Org. Chem.* **2004**, *69*, 7565-7576.
- (6) a) Bug, T.; Mayr, H. *J. Am. Chem. Soc.* **2003**, *125*, 12980-12986; b) Lucius, R.; Loos, R.; Mayr, H. *Angew. Chem.*, **2002**, *114*, 97-102; *Angew. Chem. Int. Ed.* **2002**, *41*, 91-95.
- (7) Berger, S. T. A.; Ofial, A. R.; Mayr, H. *J. Am. Chem. Soc.* **2007**, *129*, 9753-9761.
- (8) Mayr, H.; Bug, T.; Gotta, M. F.; Hering, N.; Irrgang, B.; Janker, B.; Kempf, B.; Loos, R.; Ofial, A. R.; Remennikov, G.; Schimmel, H. *J. Am. Chem. Soc.* **2001**, *123*, 9500-9512.
- (9) Berger, S. T. A.; Seeliger, F. H.; Hofbauer, F.; Mayr, H. *Org. Biomol. Chem.* **2007**, *5*, 3020-3026.
- (10) Phan, T. B.; Breugst, M.; Mayr, H. *Angew. Chem.* **2006**, *118*, 3954-3959; *Angew. Chem. Int. Ed.* **2006**, *45*, 3869-3874.
- (11) Phan, T. B.; Mayr, H. *Can. J. Chem.* **2005**, *83*, 1554-1560.
- (12) Kaumanns, O.; Mayr, H. *J. Org. Chem.* **2008**, *73*, 2738-2745.
- (13) Swoboda, G.; Swoboda, J.; Wessely, F. *Monatsh. Chem.* **1964**, *95*, 1283-1304.
- (14) Schmid, R.; Sapunov, V. N. *Non-Formal Kinetics*; VCH: Weinheim, 1982.
- (15) Exner, O. *Correlation Analysis of Chemical Data*; Plenum New York, 1988.
- (16) a) Bernasconi, C. F.; Murray, C. J. *J. Am. Chem. Soc.* **1986**, *108*, 5251-5257; b) Bernasconi, C. F.; Kanavarioti, A. *J. Am. Chem. Soc.* **1986**, *108*, 7744-7751; c) Schreiber, B.; Martinek, H.; Wolschann, P.; Schuster, P. *J. Am. Chem. Soc.* **1979**, *101*, 4708-4713; d) Oh, H. K.; Kim, T. S.; Lee, H. W.; Lee, I. *Bull.*

- Korean Chem. Soc.* **2003**, *24*, 193-196; e) Oh, H. K.; Lee, J. M. *Bull. Korean Chem. Soc.* **2002**, *23*, 1459-1462.
- (17) Searles, S.; Tamres, M.; Block, F.; Quarterman, L. A. *J. Am. Chem. Soc.* **1956**, *78*, 4917-4920.
- (18) Adams, R.; Carmack, M.; Mahan, J. E. *J. Am. Chem. Soc.* **1942**, *64*, 2593-2597.
- (19) Bernasconi, C. F.; Leonarduzzi, G. D. *J. Am. Chem. Soc.* **1982**, *104*, 5133-5142.
- (20) Kaumanns, O.; Lucius, R.; Mayr, H. *Chem. Eur. J.* **2008**, *14*, 9675-9682.
- (21) a) Baidya, M.; Mayr, H. *Chem. Commun.* **2008**, 1792-1794; b) Baidya, M.; Kobayashi, S.; Brotzel, F.; Schmidhammer, U.; Riedle, E.; Mayr, H. *Angew. Chem.* **2007**, *119*, 6288-6292; *Angew. Chem. Int. Ed.* **2007**, *46*, 6176-6179.

Experimental Section

Reactivities of Benzylidene Meldrum's Acids in Methanol

3.1. Materials

General. Commercially available MeOH (HPLC grade > 99.8 %) was used without further purification. Stock solutions of NaOMe in DMSO were prepared under nitrogen atmosphere. The employed carbanions **2a–i** were prepared directly before use by dissolving the corresponding CH acid (**2a–i**)-H in dry MeOH and subsequent addition of NaOMe solution. The amines **3a–f** have been distilled prior to use.

3.2. Instruments

¹H and ¹³C NMR spectra were recorded on Varian Inova 400 (400 MHz, 100.6 MHz), Bruker ARX 300 (300 MHz, 75.5 MHz), or Varian Mercury 200 (200 MHz) NMR spectrometers. Chemical shifts are expressed in ppm and refer to DMSO-*d*₆ (δ_{H} 2.49, δ_{C} 39.7), CDCl₃ (δ_{H} 7.26, δ_{H} 77.0), and MeOH-*d*₄ (δ_{H} 3.31, δ_{H} 49.05). The coupling constants are in Hz. Abbreviations used are s (singlet), d (doublet), t (triplet), q (quartet), quint (quintet), m (multiplet).

3.3. Determination of Rate Constants

The temperature of the solutions was kept constant (20 ± 0.1 °C) during all kinetic experiments by using a circulating bath thermostat.

For evaluation of fast kinetic experiments commercial stopped-flow UV-vis spectrometer systems were used (Hi-Tech SF-61 SX2). UV-Vis kinetics of slow reactions were determined by using a diode array spectrophotometer, which was connected to a quartz suprasil immersion probe (5 mm light path).

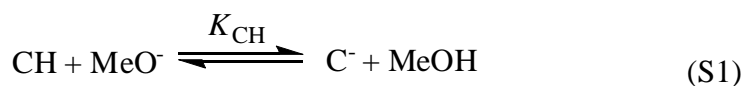
Rate constants k_{obs} (s^{-1}) were obtained by fitting the single exponential function $A_t = A_0 \exp(-k_{1\psi}t) + C$ to the observed time-dependent electrophile absorbance. Plotting k_{obs} for the reactions of electrophiles **1a–c** with amines **3a–f** or the $k_{1\psi}$ values for the reactions of

electrophiles **1a–c** with carbanions **2a–i**, respectively, against the concentrations of the corresponding nucleophiles resulted in linear correlations whose slopes correspond to the second-order rate constants k_2 ($\text{L mol}^{-1} \text{s}^{-1}$). In order to obtain pseudo-first order kinetics the nucleophile has always been used in large excess over the electrophile concentrations (> 10 equiv.). For those reactions which show significant end absorptions and thus reversible reactions, the rates of the backward reactions k_{-} can either be obtained by calculation using the equilibrium constant K and Equation (S2), or by using the value for the intercept of the slope k_2 for plots of k_{obs} versus the nucleophile concentration.

For kinetic experiments stock solutions were prepared as follows:

The carbanions were generated by deprotonation of the corresponding CH acid (**2a–i**)-H with NaOMe *in situ* directly before the kinetic experiments, whereas solutions of the electrophiles **1a–i**, the amines **3a–f**, and methoxide (**4a**) were obtained by dissolving the compounds in MeOH.

The equilibrium concentrations of the carbanions and of methoxide were calculated on the basis of the K_{CH} values of the CH acidic compounds **2–H**.



$$K_{\text{CH}} = K_{\text{aH}}/K_{\text{MeOH}} \quad (\text{S2})$$

$$K_{\text{CH}} = [\text{C}^-]/[\text{CH}][\text{MeO}^-] \quad (\text{S3})$$

When the initial concentrations of the CH acids and methoxide are known, their equilibrium concentrations are:

$$[\text{CH}] = [\text{CH}]_0 - [\text{C}^-] \text{ and } [\text{MeO}^-] = [\text{MeO}^-]_0 - [\text{C}^-] \quad (\text{S4})$$

With the known concentrations of CH acid and methoxide, based on Equations (S2–S4), one can calculate $[\text{C}^-]$ and $[\text{MeO}^-]$, which will be used for the determination of the rate constants for the reactions of the carbanions with the electrophiles **1a–c**.

$$[\text{C}^-]_{\text{eq}} = 0.5([\text{CH}]_0 + [\text{MeO}^-]_0 + \frac{1}{K_{\text{CH}}} - (([\text{CH}]_0 + [\text{MeO}^-]_0 + \frac{1}{K_{\text{CH}}})^2 - 4[\text{CH}]_0[\text{MeO}^-]_0)^{\frac{1}{2}}) \quad (\text{S5})$$

3.4. Determination of Equilibrium Constants in MeOH

The equilibrium constants K are based on the Equation (S6) by using the initial absorptions A from the electrophiles and the equilibrium absorptions after subsequent addition of nucleophile at 20 °C in MeOH. The titration experiments were carried out at least two times for every electrophile-nucleophile combination in order to reduce the error of measurement.

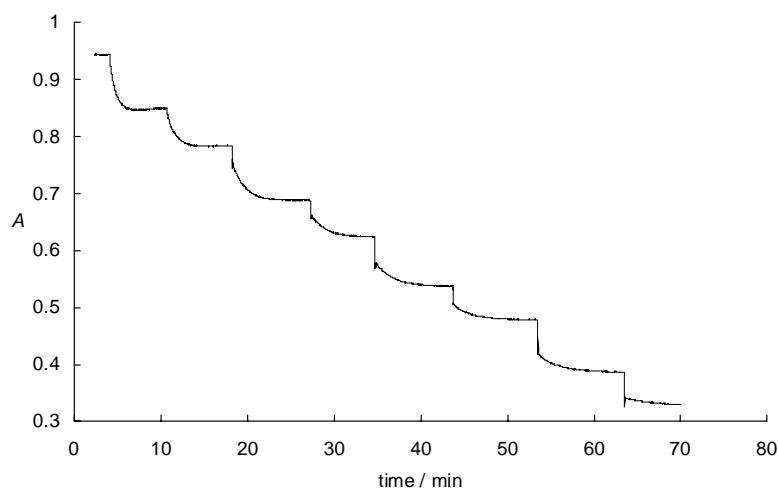


Figure S1: UV-Vis spectrum for the reaction of electrophile **1b** by subsequent addition of nucleophile **3a** in MeOH at 20 °C.

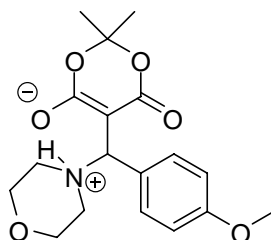
$$K = \frac{[S]_{eq}}{[E]_{eq}[Nu^-]_{eq}} = \frac{[E]_0 - [E]_{eq}}{[E]_{eq}([Nu^-]_0 - [E]_0 + [E]_{eq})} \quad (S6)$$

3.5. Product Studies

Product studies of electrophiles 1a–c with amines

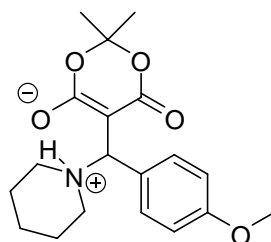
1a (96 mg, 3.7×10^{-4} mol) and morpholine (**3d**) (0.2 mL, 2.3×10^{-3} mol) were dissolved in dry benzene (3 mL). The solution turns colorless and the precipitating solid was filtered, washed with Et₂O and dried under reduced vacuum. **5ad** (100 mg, 2.9×10^{-4} mol, 77.4 %) was obtained as colorless solid, mp 145.6–146.0 °C.

5ad: ¹H-NMR (d₆-DMSO, 200 MHz): δ = 1.49 (s, C(CH₃)₂), 2.93 (br. s, 4 H, -NH⁺-CH₂CH₂), 3.77 (br. s, 7 H, -NH⁺-CH₂CH₂, -OCH₃), 5.13 (br. s, 1 H, CH), 6.93 (d, ³J = 8.4 Hz, 2 H, CH_{ar}), 7.64 (br. s, 2 H, CH_{ar}), 8.51 ppm (br. s, 1 H, NH⁺). IR (ATR, cm⁻¹): 3434 (-H bridging), 3040, 3005, 2853, 1653, 1598, 1515, 1407, 1258.



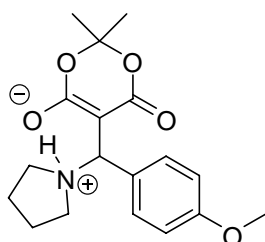
1a (100 mg, 3.8×10^{-4} mol) and **3e** (0.15 mL, 1.5×10^{-4} mol) were stirred in dry benzene (3 mL). The resulting precipitate was filtered, washed with Et₂O and dries under reduced pressure to yield product **5ae** (95 mg, 2.7×10^{-4} mol, 72.0 %) as colorless solid; mp 172.2–173.0 °C. **5ae** is not soluble in [d₆]-DMSO, CDCl₃, D₂O and [d₄]-MeOD at room temperature. The ¹H NMR spectrum could be obtained by gentle heating of the product **5ae** in d₆-DMSO with formation of a slightly yellow solution.

5ae: ¹H-NMR (d₆-DMSO, 200 Hz): δ = 1.29–1.82 (m, 12 H, C(CH₃)₂, -NH⁺-CH₂CH₂CH₂, -NH⁺-CH₂CH₂CH₂), 2.88 (br. m, 4 H, -NH⁺-CH₂CH₂CH₂), 3.75 (s, 3 H, OCH₃), 5.06 (br. s, 1 H, CH), 6.91 (d, ³J = 8.0 Hz, 2 H, CH_{ar}), 7.52 (br. s, 2 H, CH_{ar}), 8.66 ppm (br. s, 1 H, NH⁺). IR (ATR, cm⁻¹): 3434 (-H bridging), 3047, 2998, 2954, 2940, 2842, 1677, 1616, 1516, 1402, 1244, 1244, 780.



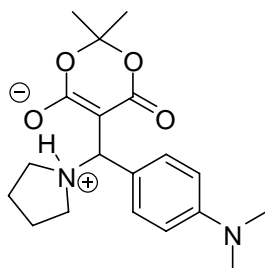
1a (95 mg, 3.6×10^{-4} mol) and pyrrolidine (**3f**) (0.15 mL, 1.8×10^{-3} mol) were stirred in benzene (3 mL) until the color of the electrophile disappeared and a solid started to separate from the solution. After filtration, the precipitate was washed with Et₂O and dried under reduced pressure to yield product **5af** (90 mg, 2.7×10^{-4} mol, 75.0 %) as colorless solid; mp 147.3–147.5 °C.

5af: ¹H-NMR (d₆-DMSO, 200 Hz): δ = 1.41 (s, 3 H, C(CH₃)₂), 1.91 (br. s, 2 × 2 H, -NCH₂CH₂), 3.08 (br. s, 4 H, N-CH₂), 3.74 (s, 3 H, -OCH₃), 4.98 (br. s, 1 H, CH), 6.88 (d, ³J = 8.8 Hz, 2 H, CH_{ar}), 7.51 (d, ³J = 8.2 Hz, 2 H, CH_{ar}), 9.32 ppm (br. s, 1 H, -NH⁺). IR (ATR, cm⁻¹): 3446 (-H bridging), 3056, 2989, 2879, 1680, 1601, 1517, 1404, 1242, 782.



1b (10 mg, 3.6×10^{-5} mol) was dissolved in d₆-DMSO (0.6 mL) when pyrrolidin dissolved in d₆-DMSO (100 μL, 0.37 M, 3.7×10^{-5} mol) was added.

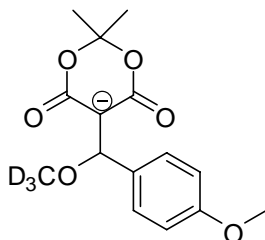
5bf: ¹H-NMR (d₆-DMSO, 200 MHz): δ = 1.43 (br. s, 6 H, C(CH₃)₂), 1.90 (br. s, 2 × 2 H, -NCH₂CH₂), 2.91 (s, 6 H, N(CH₃)₂), 3.06 (br. s, 2 × 2 H, -NCH₂CH₂), 4.91 (br. s, 1 H, CH), 6.67 (d, ³J = 8.4 Hz, 2 H, CH_{ar}), 7.43 (br. s, 2 H, CH_{ar}), 9.18 ppm (br. s, 1 H, -NH⁺).



Product studies of electrophiles 1a–c with methoxide

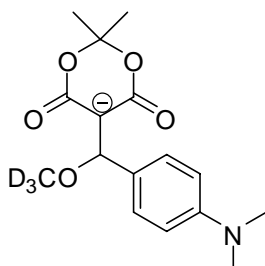
1a (13.8 mg, 5.26×10^{-5} mol) was suspended in d_4 -methanol (700 μ l) and a solution of NaOMe (107 μ l of a 0.49 M solution, 5.26×10^{-5} mol) was added in an NMR tube. After vigorous shaking, the color of the electrophile **1a** disappeared and the solution was homogenous.

6aa: $^1\text{H-NMR}$ (CD_3OD , 400 MHz): $\delta = 1.62$ (s, 6 H, $-\text{C}(\text{CH}_3)_2$), 3.75 (s, 3 H, $-\text{OCH}_3$ (ar)), 5.40 (s, 1 H, CH), 6.80 (d, $^3J = 8.8$ Hz, 2 H, CH_{ar}), 7.36 ppm (d, $^3J = 8.4$ Hz, 2 H, CH_{ar}). $^{13}\text{C-NMR}$ (CD_3OD , 100 MHz): $\delta = 26.2$ ($2 \times$ q, $\text{C}(\text{CH}_3)_2$), 55.7 (q, OCH_3 (ar)), 77.6 (s, C^-), 79.1 (d, CH), 102.7 (s, $-\text{C}(\text{CH}_3)_2$), 114.0 ($2 \times$ t, $-\text{CH}_{\text{ar}}$), 128.7 ($2 \times$ t, $-\text{CH}_{\text{ar}}$), 137.0 (s), 160.0 (s), 169.4 ppm (s).



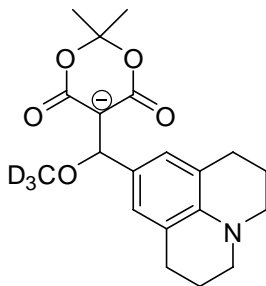
1b (86 mg, 3.12×10^{-4} mol) was dissolved in Et_2O (50 mL) and NaOMe (660 μ l of a 0.47 M solution, 3.12×10^{-4} mol) was added. Stirring was continued at room temperature until an orange solid precipitated from the solution, which was separated, washed with Et_2O and dried under reduced pressure to yield product **6ba** (61.7 mg, 1.87×10^{-4} mol, 60 %); orange solid.

6ba: $^1\text{H-NMR}$ (CD_3OD , 400 MHz): $\delta = 1.62$ (s, 6 H, $\text{C}(\text{CH}_3)_2$), 2.86 (s, 6 H, $-\text{N}(\text{CH}_3)_2$), 5.39 (s, 1 H, CH), 6.73 (d, $^3J = 8.8$ Hz, 2 H, CH_{ar}), 7.31 ppm (d, $^3J = 8.0$ Hz, 2 H, CH_{ar}).



1c (10 mg, 3.05×10^{-5} mol) was suspended in d_4 -methanol (700 μ l) and NaOMe (63 μ l, of a 0.49 M solution, 3.05×10^{-5} mol) were added. The color of the electrophile **1c** disappeared after vigorous shaking of the NMR tube. Due to the formation of small amounts of side-products, the assignment for the carbon spectrum is not complete.

6ca: $^1\text{H-NMR}$ (CD_3OD , 400 MHz): $\delta = 1.63$ (s, 6 H, $\text{C}(\text{CH}_3)_2$), 1.95 (quint., $^3J = 6.6$ Hz, 4 H, $-\text{NCH}_2\text{CH}_2\text{CH}_2$), 2.71 (t, $^3J = 6.6$ Hz, 4 H, $-\text{NCH}_2\text{CH}_2\text{CH}_2$), 3.04 (t, $^3J = 6.6$ Hz, 4 H, $-\text{NCH}_2\text{CH}_2\text{CH}_2$), 5.28 (s, 1 H, CH), 6.84 ppm (s, 2 H, CH_{ar}). $^{13}\text{C-NMR}$ (CD_3OD , 100 MHz): $\delta = 23.0$, 23.6 ($2 \times$ t, $-\text{NCH}_2\text{CH}_2\text{CH}_2$), 26.2 ($2 \times$ q, $\text{C}(\text{CH}_3)_2$), 28.8 ($2 \times$ t, $-\text{NCH}_2\text{CH}_2\text{CH}_2$), 51.6 ($2 \times$ t, $-\text{NCH}_2\text{CH}_2\text{CH}_2$), 77.5 (s, C^-), 79.4 (d, CH), 102.8 (s, $\text{C}(\text{CH}_3)_2$), 122.6 (s), 126.4 (d, CH_{ar}), 132.6 (s), 142.6 (s), 169.5 ppm (s).



3.6. Reactivities of electrophiles 1a–c

Kinetics for the reactions of the electrophiles 1a–c with carbanions

Kinetics of electrophile 1a

Table S1: Reaction of electrophile **1a** with the anion of (nitromethyl)benzene (**2a**) in MeOH at 20 °C, stopped flow, 380 nm.

concentrations ^[a] (mol L ⁻¹)				rate constants	
stock solution		cell			
[CH] ₀	[MeO ⁻] ₀	[C ⁻]	[MeO ⁻]	k _{obs} (s ⁻¹)	k _{1Ψ} (s ⁻¹)
8.54 × 10 ⁻³	3.47 × 10 ⁻⁴	3.44 × 10 ⁻⁴	2.10 × 10 ⁻⁵	1.29 × 10 ⁻¹	1.25 × 10 ⁻¹
8.54 × 10 ⁻³	6.93 × 10 ⁻⁴	6.89 × 10 ⁻⁴	4.39 × 10 ⁻⁵	1.70 × 10 ⁻¹	1.62 × 10 ⁻¹
8.54 × 10 ⁻³	1.04 × 10 ⁻³	1.03 × 10 ⁻³	6.88 × 10 ⁻⁵	2.13 × 10 ⁻¹	2.00 × 10 ⁻¹
8.54 × 10 ⁻³	1.39 × 10 ⁻³	1.38 × 10 ⁻³	9.61 × 10 ⁻⁵	2.58 × 10 ⁻¹	2.40 × 10 ⁻¹
8.54 × 10 ⁻³	1.73 × 10 ⁻³	1.72 × 10 ⁻³	1.26 × 10 ⁻⁵	3.06 × 10 ⁻¹	2.83 × 10 ⁻¹

^[a] [1a]_{cell} = 2.40 × 10⁻⁵ mol L⁻¹, the calculations of [C⁻] and [MeO⁻] based on K_{CH}(**2a**) = 2.00 × 10⁴ L mol⁻¹.

$$k_{2,C^-} = 1.14 \times 10^2 \text{ M}^{-1}\text{s}^{-1}.$$

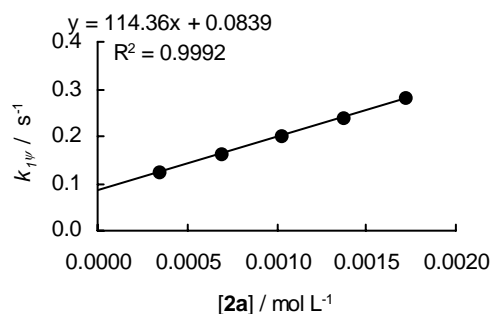


Table S2: Reaction of electrophile **1a** with the anion of nitroethane (**2b**) in MeOH at 20 °C, stopped flow, 380 nm.

concentrations ^[a] (mol L ⁻¹)				rate constants	
stock solution		cell			
[CH] ₀	[MeO ⁻] ₀	[C ⁻]	[MeO ⁻]	k _{obs} (s ⁻¹)	k _{1Ψ} (s ⁻¹)
2.91 × 10 ⁻²	4.82 × 10 ⁻⁴	4.51 × 10 ⁻⁴	3.15 × 10 ⁻⁵	1.43 × 10 ⁻¹	8.44 × 10 ⁻²
2.91 × 10 ⁻²	9.65 × 10 ⁻⁴	9.01 × 10 ⁻⁴	6.40 × 10 ⁻⁵	2.30 × 10 ⁻¹	1.11 × 10 ⁻¹
2.91 × 10 ⁻²	1.45 × 10 ⁻³	1.35 × 10 ⁻³	9.74 × 10 ⁻⁵	3.37 × 10 ⁻¹	1.56 × 10 ⁻¹
2.91 × 10 ⁻²	1.93 × 10 ⁻³	1.80 × 10 ⁻³	1.32 × 10 ⁻⁴	4.45 × 10 ⁻¹	2.00 × 10 ⁻¹
2.91 × 10 ⁻²	2.41 × 10 ⁻³	2.24 × 10 ⁻³	1.67 × 10 ⁻⁴	5.42 × 10 ⁻¹	2.31 × 10 ⁻¹

^[a] [1a]_{cell} = 3.66 × 10⁻⁵ mol L⁻¹, the calculations of [C⁻] and [MeO⁻] based on K_{CH}(**2b**) = 5.00 × 10² L mol⁻¹.

$$k_{2,C^-} = 8.52 \times 10^1 \text{ M}^{-1}\text{s}^{-1}$$

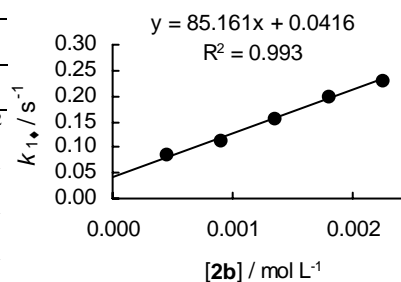
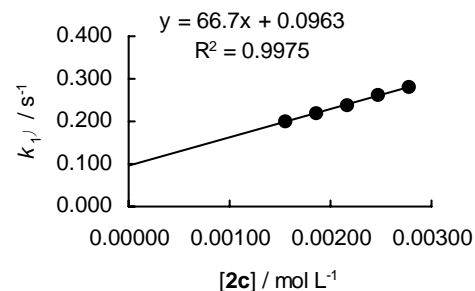


Table S3: Reaction of electrophile **1a** with the anion of 1-methyl-4-(nitromethyl)benzene (**2c**) in MeOH at 20 °C, stopped flow, 380 nm.

concentrations ^[a] (mol L ⁻¹)				rate constants	
stock solution		cell			
[CH] ₀	[MeO ⁻] ₀	[C ⁻]	[MeO ⁻]	k _{obs} (s ⁻¹)	k _{1Ψ} (s ⁻¹)
1.02 × 10 ⁻²	1.57 × 10 ⁻³	1.55 × 10 ⁻³	2.23 × 10 ⁻⁵	2.43 × 10 ⁻¹	2.02 × 10 ⁻¹
1.02 × 10 ⁻²	1.89 × 10 ⁻³	1.86 × 10 ⁻³	2.78 × 10 ⁻⁵	2.70 × 10 ⁻¹	2.18 × 10 ⁻¹
1.02 × 10 ⁻²	2.20 × 10 ⁻³	2.17 × 10 ⁻³	3.36 × 10 ⁻⁵	3.02 × 10 ⁻¹	2.40 × 10 ⁻¹
1.02 × 10 ⁻²	2.52 × 10 ⁻³	2.48 × 10 ⁻³	3.99 × 10 ⁻⁵	3.37 × 10 ⁻¹	2.63 × 10 ⁻¹
1.02 × 10 ⁻²	2.83 × 10 ⁻³	2.78 × 10 ⁻³	4.67 × 10 ⁻⁵	3.69 × 10 ⁻¹	2.82 × 10 ⁻¹

^[a] [1a]_{cell} = 2.40 × 10⁻⁵ mol L⁻¹, the calculations of [C⁻] and [MeO⁻] based on K_{CH}(**2c**) = 8.01 × 10³ L mol⁻¹.

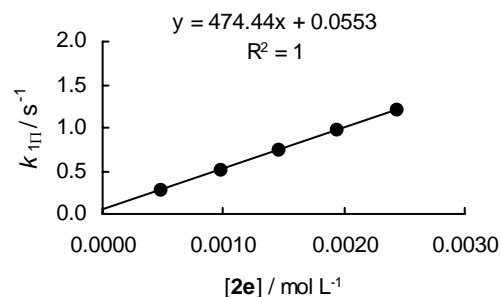
$$k_{2,C^-} = 6.67 \times 10^1 \text{ M}^{-1} \text{ s}^{-1}$$

**Table S4:** Reaction of electrophile **1a** with the anion of nitromethane (**2e**) in MeOH at 20 °C, stopped-flow, 380 nm.

concentrations ^[a] (mol L ⁻¹)				rate constants	
stock solution		cell			
[CH] ₀	[MeO ⁻] ₀	[C ⁻]	[MeO ⁻]	k _{obs} (s ⁻¹)	k _{1Ψ} (s ⁻¹)
3.74 × 10 ⁻¹	5.45 × 10 ⁻⁴	4.86 × 10 ⁻⁴	5.92 × 10 ⁻⁵	3.98 × 10 ⁻¹	2.88 × 10 ⁻¹
3.74 × 10 ⁻¹	1.09 × 10 ⁻³	9.72 × 10 ⁻⁴	1.18 × 10 ⁻⁴	7.34 × 10 ⁻¹	5.14 × 10 ⁻¹
3.74 × 10 ⁻¹	1.64 × 10 ⁻³	1.46 × 10 ⁻³	1.78 × 10 ⁻⁴	1.08	7.45 × 10 ⁻¹
3.74 × 10 ⁻¹	2.18 × 10 ⁻³	1.94 × 10 ⁻³	2.37 × 10 ⁻⁴	1.42	9.79 × 10 ⁻¹
3.74 × 10 ⁻¹	2.73 × 10 ⁻³	2.43 × 10 ⁻³	2.97 × 10 ⁻⁴	1.76	1.21

^[a] [1a]_{cell} = 3.32 × 10⁻⁵ mol L⁻¹, the calculations of [C⁻] and [MeO⁻] based on K_{CH}(**2e**) = 2.20 × 10⁴ L mol⁻¹.

$$k_{2,C^-} = 4.74 \times 10^2 \text{ M}^{-1} \text{ s}^{-1}$$

**Table S5:** Reaction of electrophile **1a** with the anion of malononitrile (**2g**) in MeOH at 20 °C, stopped-flow, 380 nm.

concentrations ^[a] (mol L ⁻¹)				rate constants	
stock solution		cell			
[CH] ₀	[MeO] ₀	[C ⁻]	[MeO]	k _{obs}	k _{1Ψ}
2.15 × 10 ⁻²	1.48 × 10 ⁻⁴	1.37 × 10 ⁻⁴	1.07 × 10 ⁻⁵	1.77 × 10 ²	1.62 × 10 ²
2.15 × 10 ⁻²	2.21 × 10 ⁻⁴	2.05 × 10 ⁻⁴	1.61 × 10 ⁻⁵	2.84 × 10 ²	2.84 × 10 ²
2.15 × 10 ⁻²	2.95 × 10 ⁻⁴	2.74 × 10 ⁻⁴	2.15 × 10 ⁻⁵	3.81 × 10 ²	3.81 × 10 ²

^[a] [1a]_{cell} = 1.46 × 10⁻⁵ mol L⁻¹, the calculations of [C⁻] and [MeO] based on K_{CH}(**2g**) = 6.00 × 10³ L mol⁻¹.

$$k_{2,C^-} = 1.49 \times 10^6 \text{ M}^{-1} \text{ s}^{-1}$$

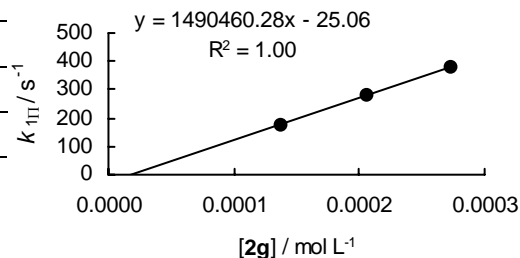
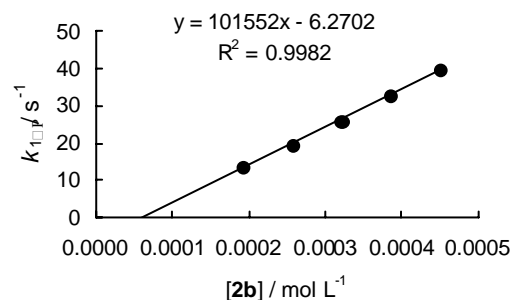


Table S6: Reaction of electrophile **1a** with the anion of dimethyl malonate (**2h**) in MeOH at 20 °C, stopped-flow, 380 nm.

concentrations ^[a] (mol L ⁻¹)				rate constants	
stock solution		cell			
[CH] ₀	[MeO ⁻] ₀	[C ⁻]	[MeO ⁻]	k _{obs} (s ⁻¹)	k _{1ψ} (s ⁻¹)
6.85 × 10 ⁻¹	8.18 × 10 ⁻⁴	1.93 × 10 ⁻⁴	6.25 × 10 ⁻⁴	1.49 × 10 ¹	1.38 × 10 ¹
6.85 × 10 ⁻¹	1.09 × 10 ⁻³	2.57 × 10 ⁻⁴	8.34 × 10 ⁻⁴	2.11 × 10 ¹	1.96 × 10 ¹
6.85 × 10 ⁻¹	1.36 × 10 ⁻³	3.21 × 10 ⁻⁴	1.04 × 10 ⁻³	2.77 × 10 ¹	2.58 × 10 ¹
6.85 × 10 ⁻¹	1.64 × 10 ⁻³	3.85 × 10 ⁻⁴	1.25 × 10 ⁻³	3.50 × 10 ¹	3.27 × 10 ¹
6.85 × 10 ⁻¹	1.91 × 10 ⁻³	4.49 × 10 ⁻⁴	1.46 × 10 ⁻³	4.25 × 10 ¹	3.98 × 10 ¹

^[a] [1a]_{cell} = 2.14 × 10⁻⁵ mol L⁻¹, the calculations of [C⁻] and [MeO⁻] based on K_{CH}(**2h**) = 4.50 × 10⁻¹ L mol⁻¹.

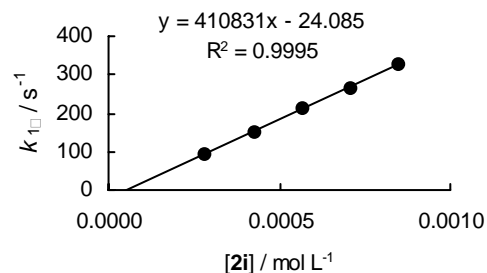
$$k_{2,C^-} = 1.02 \times 10^5 \text{ M}^{-1}\text{s}^{-1}$$

**Table S7:** Reaction of electrophile **1a** with the anion of ethyl 2-cyano acetate (**2i**) in MeOH at 20 °C, stopped-flow, 380 nm.

concentrations ^[a] (mol L ⁻¹)				rate constants	
stock solution		cell			
[CH] ₀	[MeO ⁻] ₀	[C ⁻]	[MeO ⁻]	k _{obs} (s ⁻¹)	k _{1ψ} (s ⁻¹)
3.08 × 10 ⁻¹	3.22 × 10 ⁻⁴	2.83 × 10 ⁻⁴	3.84 × 10 ⁻⁵	9.18 × 10 ¹	9.17 × 10 ¹
3.08 × 10 ⁻¹	4.82 × 10 ⁻⁴	4.25 × 10 ⁻⁴	5.76 × 10 ⁻⁵	1.50 × 10 ²	1.51 × 10 ²
3.08 × 10 ⁻¹	6.43 × 10 ⁻⁴	5.66 × 10 ⁻⁴	7.68 × 10 ⁻⁵	2.10 × 10 ²	2.11 × 10 ²
3.08 × 10 ⁻¹	8.04 × 10 ⁻⁴	7.08 × 10 ⁻⁴	9.60 × 10 ⁻⁵	2.64 × 10 ²	2.64 × 10 ²
3.08 × 10 ⁻¹	9.65 × 10 ⁻⁴	8.49 × 10 ⁻⁴	1.15 × 10 ⁻⁴	3.27 × 10 ²	3.26 × 10 ²

^[a] [1a]_{cell} = 2.56 × 10⁻⁵ mol L⁻¹, the calculations of [C⁻] and [MeO⁻] based on K_{CH}(**2i**) = 2.40 × 10¹ L mol⁻¹.

$$k_{2,C^-} = 4.11 \times 10^5 \text{ M}^{-1}\text{s}^{-1}$$



Kinetics of electrophile **1b****Table S8:** Reaction of electrophile **1b** with the anion of (nitromethyl)benzene (**2a**) in MeOH at 20 °C, J & M, 452 nm.

concentrations ^[a] (mol L ⁻¹)				rate constants	
stock solution		cell			
[CH] ₀	[MeO ⁻] ₀	[C ⁻]	[MeO ⁻]	k _{obs} (s ⁻¹)	k _{1Ψ} (s ⁻¹)
2.13 × 10 ⁻²	1.73 × 10 ⁻³	1.73 × 10 ⁻³	4.42 × 10 ⁻⁶	5.57 × 10 ⁻³	5.27 × 10 ⁻³
2.10 × 10 ⁻²	2.89 × 10 ⁻³	2.88 × 10 ⁻³	7.95 × 10 ⁻⁶	9.80 × 10 ⁻³	9.21 × 10 ⁻³
2.09 × 10 ⁻²	3.47 × 10 ⁻³	3.46 × 10 ⁻³	9.88 × 10 ⁻⁶	1.17 × 10 ⁻³	1.10 × 10 ⁻²
2.07 × 10 ⁻²	4.04 × 10 ⁻³	4.03 × 10 ⁻³	1.21 × 10 ⁻⁵	1.39 × 10 ⁻³	1.30 × 10 ⁻²
2.13 × 10 ⁻²	4.62 × 10 ⁻³	4.61 × 10 ⁻³	1.38 × 10 ⁻⁵	1.65 × 10 ⁻³	1.55 × 10 ⁻²

^[a][**1b**]_{cell} = 3.49 × 10⁻⁵ mol L⁻¹, the calculations of [C⁻] and [MeO⁻] based on K_{CH}(**2a**) = 2.00 × 10⁴ L mol⁻¹.

$$k_{2,C^-} = 3.44 \text{ M}^{-1} \text{ s}^{-1}$$

Table S9: Reaction of electrophile **1b** with the anion of nitroethane (**2b**) in MeOH at 20 °C, J & M, 452 nm.

concentrations ^[a] (mol L ⁻¹)				rate constants	
stock solution		cell			
[CH] ₀	[MeO ⁻] ₀	[C ⁻]	[MeO ⁻]	k _{obs} (s ⁻¹)	k _{1Ψ} (s ⁻¹)
6.22 × 10 ⁻²	8.36 × 10 ⁻⁴	8.10 × 10 ⁻⁴	2.64 × 10 ⁻⁵	9.96 × 10 ⁻³	8.01 × 10 ⁻³
6.32 × 10 ⁻²	1.42 × 10 ⁻³	1.37 × 10 ⁻³	4.44 × 10 ⁻⁵	1.58 × 10 ⁻²	1.25 × 10 ⁻²
5.88 × 10 ⁻²	1.58 × 10 ⁻³	1.53 × 10 ⁻³	5.34 × 10 ⁻⁵	1.79 × 10 ⁻²	1.40 × 10 ⁻²
5.52 × 10 ⁻²	1.73 × 10 ⁻³	1.67 × 10 ⁻³	6.24 × 10 ⁻⁵	1.97 × 10 ⁻²	1.51 × 10 ⁻²

^[a][**1b**]_{cell} = 3.21 × 10⁻⁵ mol L⁻¹, the calculations of [C⁻] and [MeO⁻] based on K_{CH}(**2b**) = 5.00 × 10² L mol⁻¹.

$$k_{2,C^-} = 8.24 \text{ M}^{-1} \text{ s}^{-1}$$

Table S10: Reaction of electrophile **1b** with the anion of 1-methyl-4-(nitromethyl)benzene (**2c**) in MeOH at 20 °C, J & M, 452 nm.

concentrations ^[a] (mol L ⁻¹)				rate constants	
stock solution		cell			
[CH] ₀	[MeO ⁻] ₀	[C ⁻]	[MeO ⁻]	k _{obs} (s ⁻¹)	k _{1Ψ} (s ⁻¹)
9.62 × 10 ⁻³	3.35 × 10 ⁻⁴	3.30 × 10 ⁻⁴	4.44 × 10 ⁻⁵	7.65 × 10 ⁻⁴	4.37 × 10 ⁻⁴
9.49 × 10 ⁻³	6.61 × 10 ⁻⁴	6.51 × 10 ⁻⁴	9.20 × 10 ⁻⁵	1.62 × 10 ⁻⁴	9.41 × 10 ⁻⁴
9.52 × 10 ⁻³	9.94 × 10 ⁻⁴	9.80 × 10 ⁻⁴	1.43 × 10 ⁻⁵	2.32 × 10 ⁻³	1.27 × 10 ⁻³
9.55 × 10 ⁻³	1.33 × 10 ⁻³	1.31 × 10 ⁻³	1.98 × 10 ⁻⁵	3.35 × 10 ⁻³	1.88 × 10 ⁻³
9.56 × 10 ⁻³	1.66 × 10 ⁻³	1.64 × 10 ⁻³	2.58 × 10 ⁻⁵	4.28 × 10 ⁻³	2.37 × 10 ⁻³

^[a][**1b**]_{cell} = 3.38 × 10⁻⁵ mol L⁻¹, the calculations of [C⁻] and [MeO⁻] based on K_{CH}(**2c**) = 8.01 × 10³ L mol⁻¹.

$$k_{2,C^-} = 1.47 \text{ M}^{-1} \text{ s}^{-1}$$

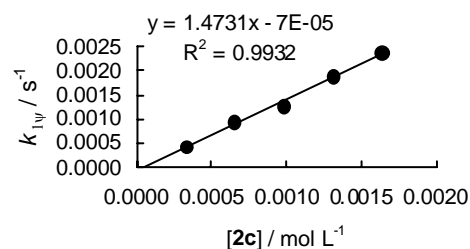
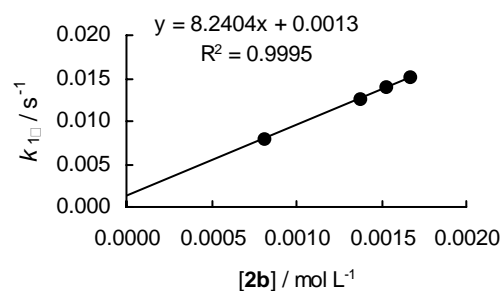
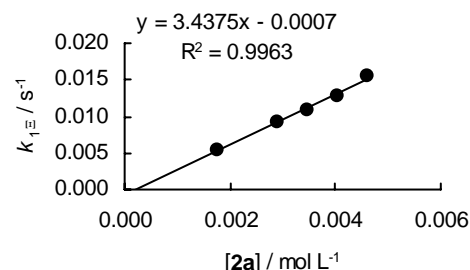


Table S11: Reaction of electrophile **1b** with the anion of 4-(nitromethyl)benzonitrile (**2d**) in MeOH at 20 °C, J & M, 452 nm.

concentrations ^[a] (mol L ⁻¹)				rate constants	
stock solution		cell			
[CH] ₀	[MeO ⁻] ₀	[C ⁻]	[MeO ⁻]	k _{obs} (s ⁻¹)	k _{1Ψ} (s ⁻¹)
5.69 × 10 ⁻³	2.12 × 10 ⁻⁴	2.12 × 10 ⁻⁴	4.48 × 10 ⁻⁷	2.09 × 10 ⁻³	2.06 × 10 ⁻³
5.59 × 10 ⁻³	4.17 × 10 ⁻⁴	4.16 × 10 ⁻⁴	9.34 × 10 ⁻⁷	3.93 × 10 ⁻³	3.86 × 10 ⁻³
5.59 × 10 ⁻³	6.25 × 10 ⁻⁴	6.24 × 10 ⁻⁴	1.46 × 10 ⁻⁶	5.84 × 10 ⁻³	5.73 × 10 ⁻³
5.59 × 10 ⁻³	8.33 × 10 ⁻⁴	8.31 × 10 ⁻⁴	2.03 × 10 ⁻⁶	7.78 × 10 ⁻³	7.63 × 10 ⁻³
5.59 × 10 ⁻³	1.04 × 10 ⁻³	1.04 × 10 ⁻³	2.65 × 10 ⁻⁶	9.87 × 10 ⁻³	9.67 × 10 ⁻³

^[a] [**1b**]_{cell} = 3.93 × 10⁻⁵ mol L⁻¹, the calculations of [C⁻] and [MeO⁻] based on K_{CH}(**2d**) = 8.61 × 10⁴ L mol⁻¹.

$$k_{2,C^-} = 9.18 \text{ M}^{-1}\text{s}^{-1}$$

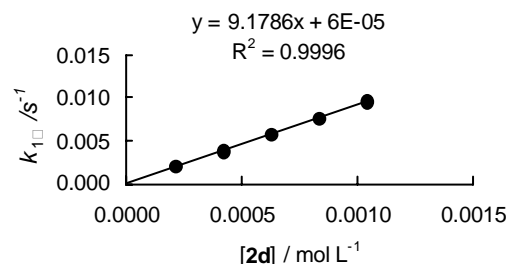


Table S12: Reaction of electrophile **1b** with the anion of nitromethane (**2e**) in MeOH at 20 °C, stopped-flow, 452 nm.

concentrations ^[a] (mol L ⁻¹)				rate constants	
stock solution		cell			
[CH] ₀	[MeO ⁻] ₀	[C ⁻]	[MeO ⁻]	k _{obs} (s ⁻¹)	k _{1Ψ} (s ⁻¹)
8.48 × 10 ⁻²	1.80 × 10 ⁻³	1.17 × 10 ⁻³	6.35 × 10 ⁻⁴	8.50 × 10 ⁻²	3.81 × 10 ⁻²
8.48 × 10 ⁻²	2.16 × 10 ⁻³	1.40 × 10 ⁻³	7.63 × 10 ⁻⁴	9.95 × 10 ⁻²	4.31 × 10 ⁻²
8.48 × 10 ⁻²	2.53 × 10 ⁻³	1.63 × 10 ⁻³	8.92 × 10 ⁻⁴	1.19 × 10 ⁻²	5.31 × 10 ⁻²
8.48 × 10 ⁻²	2.89 × 10 ⁻³	1.86 × 10 ⁻³	1.02 × 10 ⁻³	1.35 × 10 ⁻²	5.96 × 10 ⁻²
8.48 × 10 ⁻²	3.25 × 10 ⁻³	2.10 × 10 ⁻³	1.15 × 10 ⁻³	1.51 × 10 ⁻²	6.57 × 10 ⁻²

^[a] [**1b**]_{cell} = 2.40 × 10⁻⁵ mol L⁻¹, the calculations of [C⁻] and [MeO⁻] based on K_{CH}(**2e**) = 2.20 × 10⁴ L mol⁻¹.

$$k_{2,C^-} = 3.09 \times 10^1 \text{ M}^{-1}\text{s}^{-1}$$

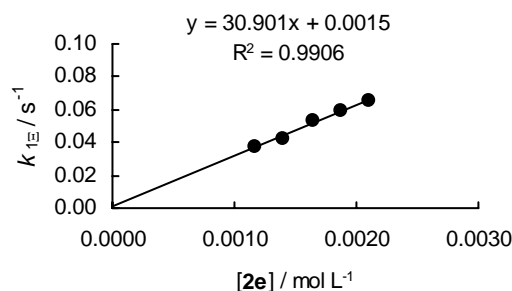


Table S13: Reaction of electrophile **1b** with the anion of 1-nitro-3-(nitromethyl)benzene (**2f**) in MeOH at 20 °C, J & M, 452 nm.

concentrations ^[a] (mol L ⁻¹)				rate constants	
stock solution		cell			
[CH] ₀	[MeO ⁻] ₀	[C ⁻]	[MeO ⁻]	k _{obs} (s ⁻¹)	k _{1Ψ} (s ⁻¹)
2.51 × 10 ⁻³	2.85 × 10 ⁻⁴	2.85 × 10 ⁻⁴	1.22 × 10 ⁻⁷	5.27 × 10 ⁻³	5.26 × 10 ⁻³
2.45 × 10 ⁻³	5.58 × 10 ⁻⁴	5.58 × 10 ⁻⁴	2.81 × 10 ⁻⁷	1.01 × 10 ⁻²	1.01 × 10 ⁻²
2.46 × 10 ⁻³	7.92 × 10 ⁻⁴	7.92 × 10 ⁻⁴	4.53 × 10 ⁻⁷	1.46 × 10 ⁻²	1.46 × 10 ⁻²
2.44 × 10 ⁻³	1.06 × 10 ⁻³	1.06 × 10 ⁻³	7.26 × 10 ⁻⁷	1.98 × 10 ⁻²	1.97 × 10 ⁻²

^[a] [**1b**]_{cell} = 5.23 × 10⁻⁵ mol L⁻¹, the calculations of [C⁻] and [MeO⁻] based on K_{CH}(**2f**) = 1.05 × 10⁶ L mol⁻¹.

$$k_{2,C^-} = 1.88 \times 10^1 \text{ M}^{-1}\text{s}^{-1}$$

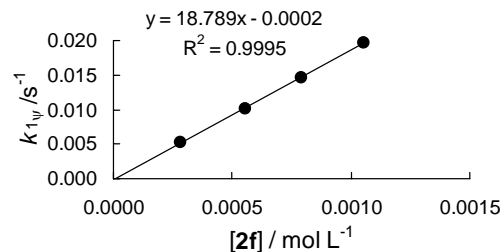


Table S14: Reaction of electrophile **1b** with the anion of malononitrile (**2g**) in MeOH at 20 °C, stopped-flow, 452 nm.

concentrations ^[a] (mol L ⁻¹)				rate constants	
stock solution		cell			
[CH] ₀	[MeO] ₀	[C ⁻]	[MeO ⁻]	k _{obs}	k _{1Ψ}
2.13 × 10 ⁻²	5.03 × 10 ⁻⁴	4.66 × 10 ⁻⁴	3.74 × 10 ⁻⁵	3.12 × 10 ¹	3.12 × 10 ¹
2.13 × 10 ⁻²	7.55 × 10 ⁻⁴	6.99 × 10 ⁻⁴	5.67 × 10 ⁻⁵	5.04 × 10 ¹	5.04 × 10 ¹
2.13 × 10 ⁻²	1.00 × 10 ⁻³	9.31 × 10 ⁻⁴	7.64 × 10 ⁻⁵	6.88 × 10 ¹	6.88 × 10 ¹
2.13 × 10 ⁻²	1.26 × 10 ⁻³	1.16 × 10 ⁻³	9.65 × 10 ⁻⁵	8.72 × 10 ¹	8.72 × 10 ¹
2.13 × 10 ⁻²	1.51 × 10 ⁻³	1.39 × 10 ⁻³	1.17 × 10 ⁻⁴	1.08 × 10 ²	1.08 × 10 ²

^[a] [1b]_{cell} = 2.10 × 10⁻⁵ mol L⁻¹, the calculations of [C⁻] and [MeO⁻] based on K_{CH}(**2g**) = 6.00 × 10² L mol⁻¹.

$$k_{2,C^-} = 8.17 \times 10^4 \text{ M}^{-1}\text{s}^{-1}$$

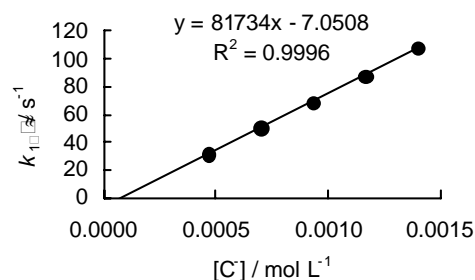


Table S15: Reaction of electrophile **1b** with the anion of dimethyl malonate (**2h**) in MeOH at 20 °C, stopped-flow, 452 nm.

concentrations ^[a] (mol L ⁻¹)				rate constants	
stock solution		cell			
[CH] ₀	[MeO ⁻] ₀	[C ⁻]	[MeO ⁻]	k _{obs} (s ⁻¹)	k _{1Ψ} (s ⁻¹)
6.85 × 10 ⁻¹	8.18 × 10 ⁻⁴	1.93 × 10 ⁻⁴	6.25 × 10 ⁻⁴	5.99 × 10 ⁻¹	5.53 × 10 ⁻¹
6.85 × 10 ⁻¹	1.09 × 10 ⁻³	2.57 × 10 ⁻⁴	8.34 × 10 ⁻⁴	8.50 × 10 ⁻¹	7.88 × 10 ⁻¹
6.85 × 10 ⁻¹	1.36 × 10 ⁻³	3.21 × 10 ⁻⁴	1.04 × 10 ⁻³	1.15	1.07
6.85 × 10 ⁻¹	1.64 × 10 ⁻³	3.85 × 10 ⁻⁴	1.25 × 10 ⁻³	1.49	1.40
6.85 × 10 ⁻¹	1.91 × 10 ⁻³	4.49 × 10 ⁻⁴	1.46 × 10 ⁻³	1.80	1.69

^[a] [1b]_{cell} = 1.61 × 10⁻⁵ mol L⁻¹, the calculations of [C⁻] and [MeO⁻] based on K_{CH}(**2h**) = 4.50 × 10¹ L mol⁻¹.

$$k_{2,C^-} = 4.49 \times 10^3 \text{ M}^{-1}\text{s}^{-1}$$

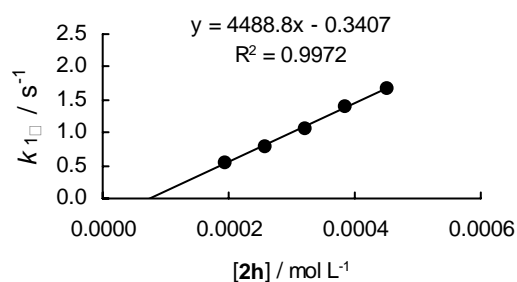
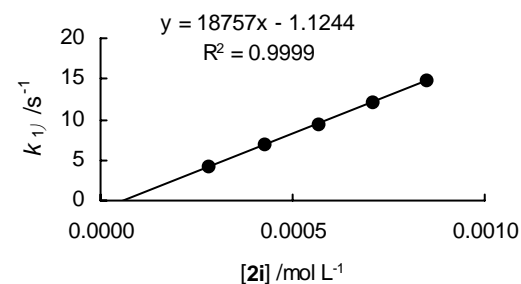


Table S16: Reaction of electrophile **1b** with the anion of ethyl 2-cyano acetate (**2i**) in MeOH at 20 °C, stopped-flow, 452 nm.

concentrations ^[a] (mol L ⁻¹)				rate constants	
stock solution		cell			
[CH] ₀	[MeO ⁻] ₀	[C ⁻]	[MeO ⁻]	k _{obs} (s ⁻¹)	k _{1Ψ} (s ⁻¹)
3.08 × 10 ⁻¹	3.22 × 10 ⁻⁴	2.83 × 10 ⁻⁴	3.84 × 10 ⁻⁵	4.19	4.20
3.08 × 10 ⁻¹	4.82 × 10 ⁻⁴	4.25 × 10 ⁻⁴	5.76 × 10 ⁻⁵	6.88	6.88
3.08 × 10 ⁻¹	6.43 × 10 ⁻⁴	5.66 × 10 ⁻⁴	7.68 × 10 ⁻⁵	9.43	9.43
3.08 × 10 ⁻¹	8.04 × 10 ⁻⁴	7.08 × 10 ⁻⁴	9.60 × 10 ⁻⁵	1.22 × 10 ¹	1.22 × 10 ¹
3.08 × 10 ⁻¹	9.65 × 10 ⁻⁴	8.49 × 10 ⁻⁴	1.15 × 10 ⁻⁴	1.48 × 10 ¹	1.48 × 10 ¹

^[a] [1b]_{cell} = 1.68 × 10⁻⁵ mol L⁻¹, the calculations of [C⁻] and [MeO⁻] based on K_{CH}(**2i**) = 2.40 × 10¹ L mol⁻¹.

$$k_{2,C^-} = 1.88 \times 10^4 \text{ M}^{-1}\text{s}^{-1}$$



Kinetics of electrophile **1c**

Table S17: Reaction of electrophile **1c** with the anion of (nitromethyl)benzene (**2a**) in MeOH at 20 °C, J & M, 480 nm.

concentrations ^[a] (mol L ⁻¹)				rate constants	
stock solution		cell			
[CH] ₀	[MeO ⁻] ₀	[C ⁻]	[MeO ⁻]	k _{obs} (s ⁻¹)	k _{1Ψ} (s ⁻¹)
1.82 × 10 ⁻²	2.27 × 10 ⁻³	2.27 × 10 ⁻³	7.11 × 10 ⁻⁶	2.8 × 10 ⁻³	2.08 × 10 ⁻³
1.63 × 10 ⁻²	2.54 × 10 ⁻³	2.53 × 10 ⁻³	9.21 × 10 ⁻⁶	2.38 × 10 ⁻³	2.25 × 10 ⁻³
1.78 × 10 ⁻²	3.33 × 10 ⁻³	3.32 × 10 ⁻³	1.15 × 10 ⁻⁵	3.10 × 10 ⁻³	2.93 × 10 ⁻³
1.79 × 10 ⁻²	4.46 × 10 ⁻³	4.45 × 10 ⁻³	1.66 × 10 ⁻⁵	4.00 × 10 ⁻³	3.76 × 10 ⁻³

^[a] [1c]_{cell} = 2.61 × 10⁻⁵ mol L⁻¹, the calculations of [C⁻] and [MeO⁻] based on K_{CH}(**2a**) = 2.00 × 10⁴ L mol⁻¹.

$$k_{2,C^-} = 7.84 \times 10^{-1} \text{ M}^{-1} \text{ s}^{-1}$$

Table S18: Reaction of electrophile **1c** with the anion of nitroethane (**2b**) in MeOH at 20 °C, J & M, 480 nm.

concentrations ^[a] (mol L ⁻¹)				rate constants	
stock solution		cell			
[CH] ₀	[MeO ⁻] ₀	[C ⁻]	[MeO ⁻]	k _{obs} (s ⁻¹)	k _{1Ψ} (s ⁻¹)
8.69 × 10 ⁻²	2.29 × 10 ⁻³	2.24 × 10 ⁻³	5.30 × 10 ⁻⁵	2.87 × 10 ⁻³	2.12 × 10 ⁻³
8.30 × 10 ⁻²	2.74 × 10 ⁻³	2.67 × 10 ⁻³	6.65 × 10 ⁻⁵	3.50 × 10 ⁻³	2.55 × 10 ⁻³
8.56 × 10 ⁻²	3.39 × 10 ⁻³	3.31 × 10 ⁻³	8.04 × 10 ⁻⁵	4.64 × 10 ⁻³	3.50 × 10 ⁻³
8.51 × 10 ⁻²	3.93 × 10 ⁻³	3.84 × 10 ⁻³	9.44 × 10 ⁻⁵	5.44 × 10 ⁻³	4.10 × 10 ⁻³
8.69 × 10 ⁻²	4.59 × 10 ⁻³	4.48 × 10 ⁻³	1.09 × 10 ⁻⁴	6.39 × 10 ⁻³	4.84 × 10 ⁻³

^[a] [1c]_{cell} = 2.29 × 10⁻⁵ mol L⁻¹, the calculations of [C⁻] and [MeO⁻] based on K_{CH}(**2b**) = 5.00 × 10² L mol⁻¹.

$$k_{2,C^-} = 1.24 \text{ M}^{-1} \text{ s}^{-1}$$

Table S19: Reaction of electrophile **1c** with the anion of 1-methyl-4-(nitromethyl)benzene (**2c**) in MeOH at 20 °C, J & M, 480 nm.

concentrations ^[a] (mol L ⁻¹)				rate constants	
stock solution		cell			
[CH] ₀	[MeO ⁻] ₀	[C ⁻]	[MeO ⁻]	k _{obs} (s ⁻¹)	k _{1Ψ} (s ⁻¹)
8.72 × 10 ⁻³	1.33 × 10 ⁻³	1.31 × 10 ⁻³	2.21 × 10 ⁻⁵	1.07 × 10 ⁻³	7.56 × 10 ⁻⁴
8.82 × 10 ⁻³	1.67 × 10 ⁻³	1.66 × 10 ⁻³	2.89 × 10 ⁻⁵	1.35 × 10 ⁻³	9.39 × 10 ⁻⁴
8.64 × 10 ⁻³	1.95 × 10 ⁻³	1.93 × 10 ⁻³	3.58 × 10 ⁻⁵	1.55 × 10 ⁻³	1.04 × 10 ⁻³
8.70 × 10 ⁻³	2.20 × 10 ⁻³	2.16 × 10 ⁻³	4.12 × 10 ⁻⁵	1.78 × 10 ⁻³	1.19 × 10 ⁻³
8.79 × 10 ⁻³	2.70 × 10 ⁻³	2.64 × 10 ⁻³	5.34 × 10 ⁻⁵	2.16 × 10 ⁻³	1.40 × 10 ⁻³

^[a] [1c]_{cell} = 2.34 × 10⁻⁵ mol L⁻¹, the calculations of [C⁻] and [MeO⁻] based on K_{CH}(**2c**) = 8.01 × 10³ L mol⁻¹.

$$k_{2,C^-} = 4.88 \times 10^{-1} \text{ M}^{-1} \text{ s}^{-1}$$

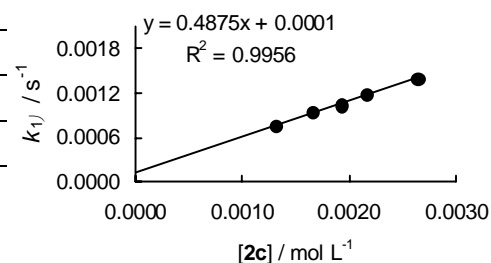
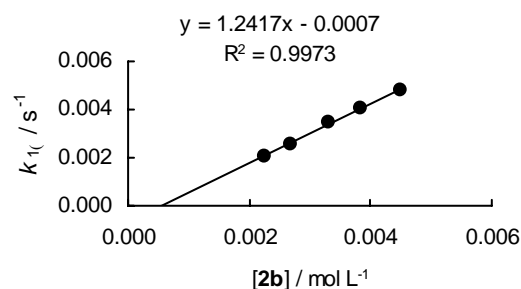
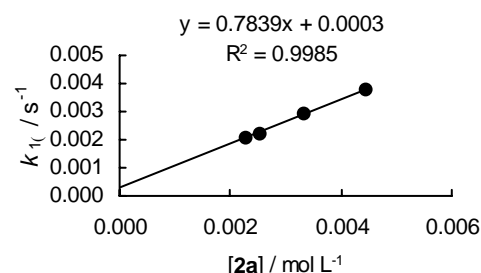


Table S20: Reaction of electrophile **1c** with the anion of 4-(nitromethyl)benzotrile (**2d**) in MeOH at 20 °C, J & M, 480 nm.

concentrations ^[a] (mol L ⁻¹)				rate constants	
stock solution		cell			
[CH] ₀	[MeO ⁻] ₀	[C ⁻]	[MeO ⁻]	k _{obs} (s ⁻¹)	k _{1Ψ} (s ⁻¹)
1.14 × 10 ⁻²	2.38 × 10 ⁻⁴	2.37 × 10 ⁻⁴	2.48 × 10 ⁻⁷	8.37 × 10 ⁻⁴	8.33 × 10 ⁻⁴
1.14 × 10 ⁻²	5.94 × 10 ⁻⁴	5.94 × 10 ⁻⁴	6.39 × 10 ⁻⁷	1.79 × 10 ⁻³	1.78 × 10 ⁻³
1.14 × 10 ⁻²	9.51 × 10 ⁻⁴	9.50 × 10 ⁻⁴	1.06 × 10 ⁻⁶	2.85 × 10 ⁻³	2.84 × 10 ⁻³
1.14 × 10 ⁻²	1.31 × 10 ⁻³	1.31 × 10 ⁻³	1.51 × 10 ⁻⁶	3.90 × 10 ⁻³	3.87 × 10 ⁻³
1.14 × 10 ⁻²	1.66 × 10 ⁻³	1.66 × 10 ⁻³	1.99 × 10 ⁻⁶	4.89 × 10 ⁻³	4.86 × 10 ⁻³

^[a] [1c]_{cell} = 1.13 × 10⁻⁵ mol L⁻¹, the calculations of [C⁻] and [MeO⁻] based on K_{CH}(**2d**) = 8.61 × 10⁴ L mol⁻¹.

$$k_{2,C^-} = 2.85 \text{ M}^{-1}\text{s}^{-1}$$

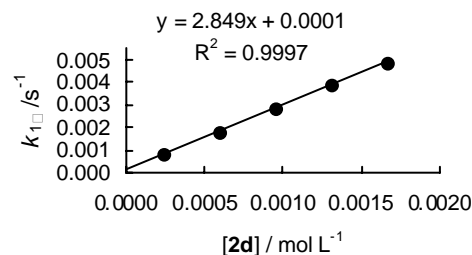


Table S21: Reaction of electrophile **1c** with the anion of nitromethane (**2e**) in MeOH at 20 °C, J & M, 480 nm.

concentrations ^[a] (mol L ⁻¹)				rate constants	
stock solution		cell			
[CH] ₀	[MeO ⁻] ₀	[C ⁻]	[MeO ⁻]	k _{obs} (s ⁻¹)	k _{1Ψ} (s ⁻¹)
2.93 × 10 ⁻¹	4.87 × 10 ⁻⁴	4.22 × 10 ⁻⁴	6.55 × 10 ⁻⁵	3.30 × 10 ⁻³	2.37 × 10 ⁻³
2.93 × 10 ⁻¹	9.74 × 10 ⁻⁴	8.43 × 10 ⁻⁴	1.31 × 10 ⁻⁴	4.81 × 10 ⁻³	3.40 × 10 ⁻³
2.93 × 10 ⁻¹	1.22 × 10 ⁻³	1.05 × 10 ⁻³	1.64 × 10 ⁻⁴	7.54 × 10 ⁻³	5.20 × 10 ⁻³
2.93 × 10 ⁻¹	1.70 × 10 ⁻³	1.47 × 10 ⁻³	2.30 × 10 ⁻⁴	1.03 × 10 ⁻²	6.93 × 10 ⁻³

^[a] [1c]_{cell} = 2.61 × 10⁻⁵ mol L⁻¹, the calculations of [C⁻] and [MeO⁻] based on K_{CH}(**2e**) = 2.20 × 10⁴ L mol⁻¹.

$$k_{2,C^-} = 4.30 \text{ M}^{-1}\text{s}^{-1}$$

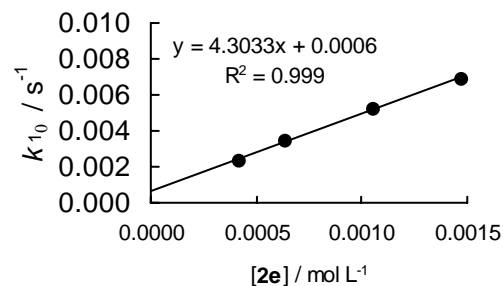


Table S22: Reaction of electrophile **1c** with the anion of 1-nitro-3-(nitromethyl)benzene (**2f**) in MeOH at 20 °C, J & M, 480 nm.

concentrations ^[a] (mol L ⁻¹)				rate constants	
stock solution		cell			
[CH] ₀	[MeO ⁻] ₀	[C ⁻]	[MeO ⁻]	k _{obs} (s ⁻¹)	k _{1Ψ} (s ⁻¹)
3.19 × 10 ⁻³	3.51 × 10 ⁻⁴	3.51 × 10 ⁻⁴	1.18 × 10 ⁻⁷	2.85 × 10 ⁻³	2.84 × 10 ⁻³
2.71 × 10 ⁻³	5.96 × 10 ⁻⁴	5.96 × 10 ⁻⁴	2.68 × 10 ⁻⁷	4.45 × 10 ⁻³	4.47 × 10 ⁻³
2.80 × 10 ⁻³	9.22 × 10 ⁻⁴	9.22 × 10 ⁻⁴	4.68 × 10 ⁻⁷	6.88 × 10 ⁻³	6.87 × 10 ⁻³
2.75 × 10 ⁻³	1.21 × 10 ⁻³	1.21 × 10 ⁻³	7.47 × 10 ⁻⁷	8.85 × 10 ⁻³	8.84 × 10 ⁻³
2.91 × 10 ⁻³	1.60 × 10 ⁻³	1.60 × 10 ⁻³	1.16 × 10 ⁻⁶	1.21 × 10 ⁻³	1.21 × 10 ⁻²

^[a] [1c]_{cell} = 2.26 × 10⁻⁵ mol L⁻¹, the calculations of [C⁻] and [MeO⁻] based on K_{CH}(**2f**) = 1.05 × 10⁶ L mol⁻¹.

$$k_{2,C^-} = 7.38 \text{ M}^{-1}\text{s}^{-1}$$

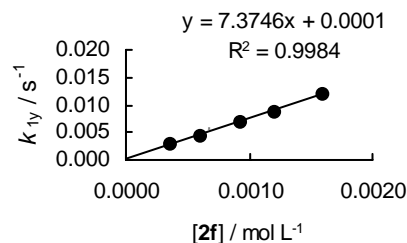


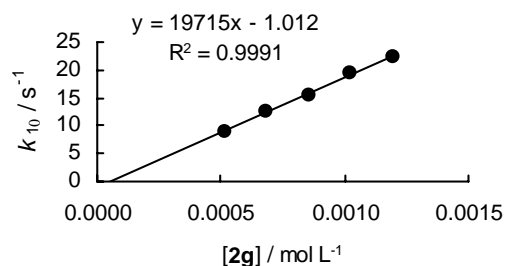
Table S23: Reaction of electrophile **1c** with the anion of malononitrile (**2g**) in MeOH

at 20 °C, stopped-flow, 480 nm.

concentrations ^[a] (mol L ⁻¹)				rate constants	
stock solution		cell			
[CH] ₀	[MeO] ₀	[C ⁻]	[MeO ⁻]	k _{obs}	k _{1Ψ}
2.15 × 10 ⁻²	5.53 × 10 ⁻⁴	5.12 × 10 ⁻⁴	4.08 × 10 ⁻⁵	9.01	9.00
2.15 × 10 ⁻²	7.38 × 10 ⁻⁴	6.83 × 10 ⁻⁴	5.48 × 10 ⁻⁵	1.25 × 10 ¹	1.25 × 10 ¹
2.15 × 10 ⁻²	9.22 × 10 ⁻⁴	8.53 × 10 ⁻⁴	6.90 × 10 ⁻⁵	1.58 × 10 ¹	1.58 × 10 ¹
2.15 × 10 ⁻²	1.11 × 10 ⁻³	1.02 × 10 ⁻³	8.34 × 10 ⁻⁵	1.94 × 10 ¹	1.94 × 10 ¹
2.15 × 10 ⁻²	1.29 × 10 ⁻³	1.19 × 10 ⁻³	9.81 × 10 ⁻⁵	2.23 × 10 ¹	2.23 × 10 ¹

^[a] [1c]_{cell} = 1.76 × 10⁻⁵ mol L⁻¹, the calculations of [C⁻] and [MeO⁻] based on K_{CH}(**2g**) = 6.00 × 10² L mol⁻¹.

$$k_{2,C^-} = 1.97 \times 10^4 \text{ M}^{-1}\text{s}^{-1}$$

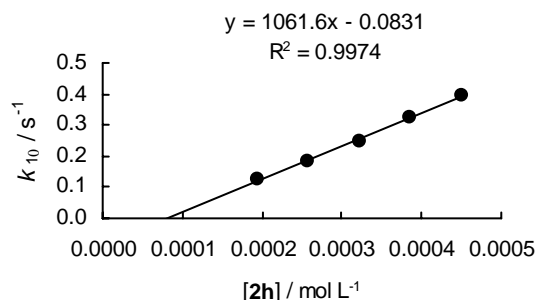
**Table S24:** Reaction of electrophile **1c** with the anion of dimethyl malonate (**2h**) in MeOH at

20 °C, stopped-flow, 480 nm.

concentrations ^[a] (mol L ⁻¹)				rate constants	
stock solution		cell			
[CH] ₀	[MeO ⁻] ₀	[C ⁻]	[MeO ⁻]	k _{obs} (s ⁻¹)	k _{1Ψ} (s ⁻¹)
6.85 × 10 ⁻¹	8.18 × 10 ⁻⁴	1.93 × 10 ⁻⁴	6.25 × 10 ⁻⁴	0.136	1.27 × 10 ⁻¹
6.85 × 10 ⁻¹	1.09 × 10 ⁻³	2.57 × 10 ⁻⁴	8.34 × 10 ⁻⁴	0.1974	1.86 × 10 ⁻¹
6.85 × 10 ⁻¹	1.36 × 10 ⁻³	3.21 × 10 ⁻⁴	1.04 × 10 ⁻³	0.265	2.50 × 10 ⁻¹
6.85 × 10 ⁻¹	1.64 × 10 ⁻³	3.85 × 10 ⁻⁴	1.25 × 10 ⁻³	0.345	3.27 × 10 ⁻¹
6.85 × 10 ⁻¹	1.91 × 10 ⁻³	4.49 × 10 ⁻⁴	1.46 × 10 ⁻³	0.418	3.97 × 10 ⁻¹

^[a] [1c]_{cell} = 2.14 × 10⁻⁵ mol L⁻¹, the calculations of [C⁻] and [MeO⁻] based on K_{CH}(**2h**) = 4.50 × 10¹ L mol⁻¹.

$$k_{2,C^-} = 1.06 \times 10^3 \text{ M}^{-1}\text{s}^{-1}$$

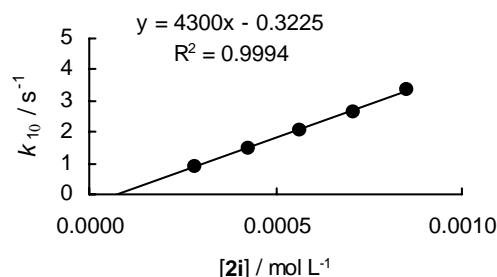
**Table S25:** Reaction of electrophile **1c** with the anion of ethyl 2-cyano acetate (**2i**) in MeOH

at 20 °C, stopped-flow, 480 nm.

concentrations ^[a] (mol L ⁻¹)				rate constants	
stock solution		cell			
[CH] ₀	[MeO ⁻] ₀	[C ⁻]	[MeO ⁻]	k _{obs} (s ⁻¹)	k _{1Ψ} (s ⁻¹)
3.08 × 10 ⁻¹	3.22 × 10 ⁻⁴	2.83 × 10 ⁻⁴	3.84 × 10 ⁻⁵	9.08 × 10 ⁻¹	9.09 × 10 ⁻¹
3.08 × 10 ⁻¹	4.82 × 10 ⁻⁴	4.25 × 10 ⁻⁴	5.76 × 10 ⁻⁵	1.51	1.50
3.08 × 10 ⁻¹	6.43 × 10 ⁻⁴	5.66 × 10 ⁻⁴	7.68 × 10 ⁻⁵	2.11	2.10
3.08 × 10 ⁻¹	8.04 × 10 ⁻⁴	7.08 × 10 ⁻⁴	9.60 × 10 ⁻⁵	2.69	2.69
3.08 × 10 ⁻¹	9.65 × 10 ⁻⁴	8.49 × 10 ⁻⁴	1.15 × 10 ⁻⁴	3.36	3.36

^[a] [1c]_{cell} = 1.41 × 10⁻⁵ mol L⁻¹, the calculations of [C⁻] and [MeO⁻] based on K_{CH}(**2i**) = 2.40 × 10¹ L mol⁻¹.

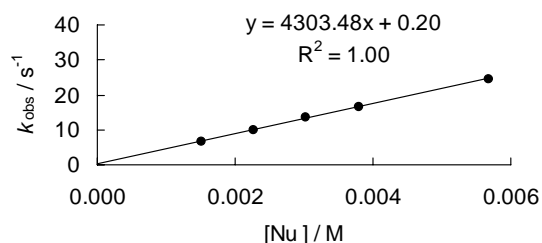
$$k_{2,C^-} = 4.30 \times 10^3 \text{ M}^{-1}\text{s}^{-1}$$



Kinetics of the reactions of the electrophiles **1a–c** with aminesKinetics of electrophile **1a****Table S26:** Reaction of electrophile **1a** with ethanolamine (**3a**) in MeOH at 20 °C, stopped-flow, 380 nm.

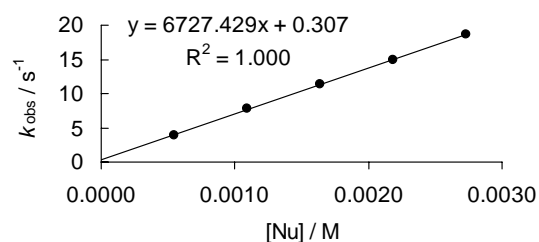
concentration (mol L ⁻¹)		rate constant
[1a]	[Nu] ₀	<i>k</i> _{obs} (s ⁻¹)
3.20 × 10 ⁻⁵	1.52 × 10 ⁻³	6.58
3.20 × 10 ⁻⁵	2.27 × 10 ⁻³	9.97
3.20 × 10 ⁻⁵	3.03 × 10 ⁻³	1.35 × 10 ¹
3.20 × 10 ⁻⁵	3.79 × 10 ⁻³	1.65 × 10 ¹
3.20 × 10 ⁻⁵	5.69 × 10 ⁻³	2.46 × 10 ¹

$$k_2 = 4.30 \times 10^3 \text{ M}^{-1} \text{ s}^{-1}$$

**Table S27:** Reaction of electrophile **1a** with *n*-propylamine (**3b**) in MeOH at 20 °C, stopped-flow, 380 nm.

concentration (mol L ⁻¹)		rate constant
[1a]	[Nu] ₀	<i>k</i> _{obs} (s ⁻¹)
2.52 × 10 ⁻⁵	5.45 × 10 ⁻⁴	3.92
2.52 × 10 ⁻⁵	1.09 × 10 ⁻³	7.76
2.52 × 10 ⁻⁵	1.64 × 10 ⁻³	1.13 × 10 ¹
2.52 × 10 ⁻⁵	2.18 × 10 ⁻³	1.50 × 10 ¹
2.52 × 10 ⁻⁵	2.73 × 10 ⁻³	1.87 × 10 ¹

$$k_2 = 6.73 \times 10^3 \text{ M}^{-1} \text{ s}^{-1}$$

**Table S28:** Reaction of electrophile **1a** with benzylamine (**3c**) in MeOH at 20 °C, stopped-flow, 380 nm.

concentration (mol L ⁻¹)		rate constant
[1a]	[Nu] ₀	<i>k</i> _{obs} (s ⁻¹)
3.66 × 10 ⁻⁵	9.00 × 10 ⁻⁴	4.18
3.66 × 10 ⁻⁵	1.80 × 10 ⁻³	8.27
3.66 × 10 ⁻⁵	2.70 × 10 ⁻³	1.24 × 10 ¹
3.66 × 10 ⁻⁵	3.60 × 10 ⁻³	1.64 × 10 ¹
3.66 × 10 ⁻⁵	4.50 × 10 ⁻³	2.08 × 10 ¹

$$k_2 = 4.60 \times 10^3 \text{ M}^{-1} \text{ s}^{-1}$$

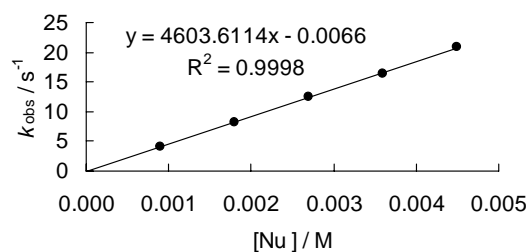
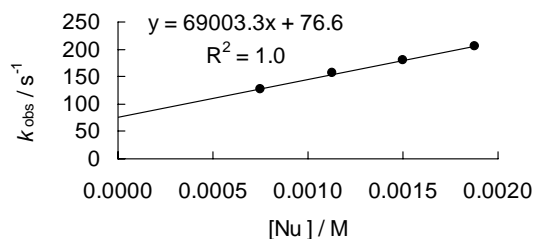


Table S29: Reaction of electrophile **1a** with morpholine (**3d**) in MeOH at 20 °C,

stopped-flow, 380 nm.

concentration (mol L ⁻¹)		rate constant
[1b]	[Nu] ₀	k _{obs} (s ⁻¹)
4.50 × 10 ⁻⁵	7.51 × 10 ⁻⁴	1.27 × 10 ²
4.50 × 10 ⁻⁵	1.13 × 10 ⁻³	1.56 × 10 ²
4.50 × 10 ⁻⁵	1.50 × 10 ⁻³	1.81 × 10 ²
4.50 × 10 ⁻⁵	1.88 × 10 ⁻³	2.05 × 10 ²

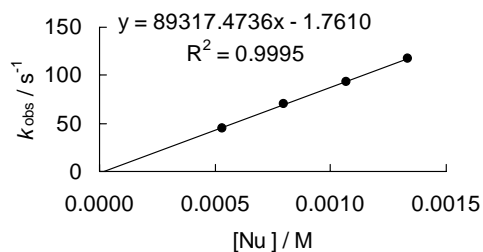
$$k_2 = 6.90 \times 10^4 \text{ M}^{-1} \text{ s}^{-1}$$

**Table S30:** Reaction of electrophile **1a** with piperidine (**3e**) in MeOH at 20 °C,

stopped-flow, 380 nm.

concentration (mol L ⁻¹)		rate constant
[1a]	[Nu] ₀	k _{obs} (s ⁻¹)
5.26 × 10 ⁻⁵	5.33 × 10 ⁻⁴	4.52 × 10 ¹
5.26 × 10 ⁻⁵	8.00 × 10 ⁻⁴	7.06 × 10 ¹
5.26 × 10 ⁻⁵	1.07 × 10 ⁻³	9.36 × 10 ¹
5.26 × 10 ⁻⁵	1.33 × 10 ⁻³	1.17 × 10 ²

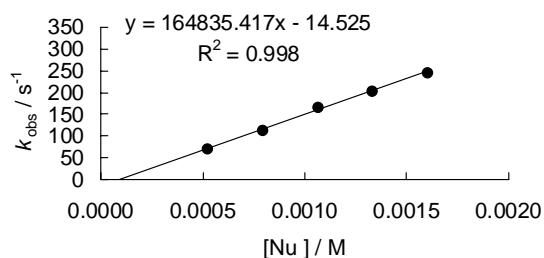
$$k_2 = 8.93 \times 10^4 \text{ M}^{-1} \text{ s}^{-1}$$

**Table S31:** Reaction of electrophile **1a** with pyrrolidine (**3f**) in MeOH at 20 °C,

stopped-flow, 380 nm.

concentration (mol L ⁻¹)		rate constant
[1a]	[Nu] ₀	k _{obs} (s ⁻¹)
3.66 × 10 ⁻⁵	5.40 × 10 ⁻⁴	7.06 × 10 ¹
3.66 × 10 ⁻⁵	8.10 × 10 ⁻⁴	1.13 × 10 ²
3.66 × 10 ⁻⁵	1.08 × 10 ⁻³	1.66 × 10 ²
3.66 × 10 ⁻⁵	1.35 × 10 ⁻³	2.05 × 10 ²
3.66 × 10 ⁻⁵	1.62 × 10 ⁻³	2.47 × 10 ²

$$k_2 = 1.64 \times 10^5 \text{ M}^{-1} \text{ s}^{-1}$$



Kinetics of electrophile **1b**

Table S32: Reaction of electrophile **1b** with ethanolamine (**3a**) in MeOH at 20 °C, stopped-flow, 452 nm.

concentration (mol L ⁻¹)		rate constant
[1b]	[Nu] ₀	k _{obs} (s ⁻¹)
3.05 × 10 ⁻⁵	1.52 × 10 ⁻³	2.14
3.05 × 10 ⁻⁵	2.27 × 10 ⁻³	2.38
3.05 × 10 ⁻⁵	3.03 × 10 ⁻³	2.63
3.05 × 10 ⁻⁵	3.79 × 10 ⁻³	2.83
3.05 × 10 ⁻⁵	5.69 × 10 ⁻³	3.43

$$k_2 = 3.08 \times 10^2 \text{ M}^{-1} \text{ s}^{-1}$$

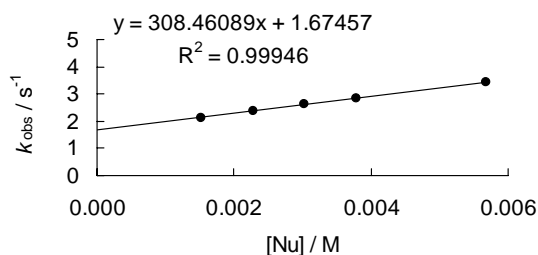


Table S33: Reaction of electrophile **1b** with *n*-propylamine (**3b**) in MeOH at 20 °C, stopped-flow, 452 nm.

concentration (mol L ⁻¹)		rate constant
[1b]	[Nu] ₀	k _{obs} (s ⁻¹)
2.40 × 10 ⁻⁵	1.09 × 10 ⁻³	1.07
2.40 × 10 ⁻⁵	2.18 × 10 ⁻³	1.68
2.40 × 10 ⁻⁵	2.73 × 10 ⁻³	1.99
2.40 × 10 ⁻⁵	4.09 × 10 ⁻³	2.77
2.40 × 10 ⁻⁵	5.45 × 10 ⁻³	3.56

$$k_2 = 5.69 \times 10^2 \text{ M}^{-1} \text{ s}^{-1}$$

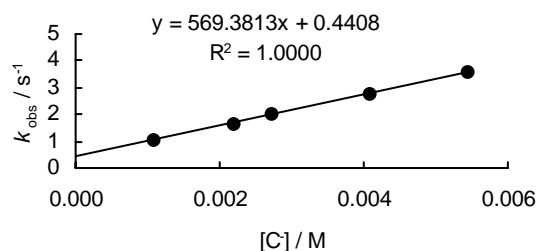


Table S34: Reaction of electrophile **1b** with benzylamine (**3c**) in MeOH at 20 °C, stopped-flow, 452 nm.

concentration (mol L ⁻¹)		rate constant
[1b]	[Nu] ₀	k _{obs} (s ⁻¹)
2.40 × 10 ⁻⁵	1.80 × 10 ⁻³	2.67
2.40 × 10 ⁻⁵	2.70 × 10 ⁻³	2.90
2.40 × 10 ⁻⁵	3.60 × 10 ⁻³	3.16
2.40 × 10 ⁻⁵	4.50 × 10 ⁻³	3.43
2.40 × 10 ⁻⁵	5.40 × 10 ⁻³	3.74

$$k_2 = 2.98 \times 10^2 \text{ M}^{-1} \text{ s}^{-1}$$

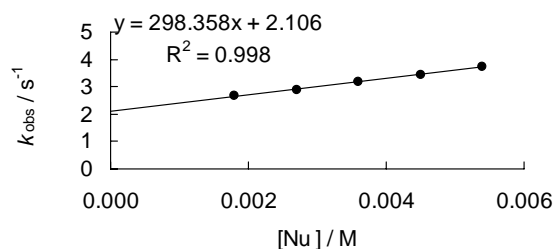


Table S35: Reaction of electrophile **1b** with piperidine (**3e**) in MeOH at 20 °C, stopped-flow, 452 nm.

concentration (mol L ⁻¹)		rate constant
[1b]	[Nu] ₀	k _{obs} (s ⁻¹)
3.76 × 10 ⁻⁵	1.33 × 10 ⁻³	5.59 × 10 ¹
3.76 × 10 ⁻⁵	2.67 × 10 ⁻³	6.75 × 10 ¹
3.76 × 10 ⁻⁵	4.00 × 10 ⁻³	8.91 × 10 ¹
3.76 × 10 ⁻⁵	5.33 × 10 ⁻³	1.05 × 10 ²
3.76 × 10 ⁻⁵	6.66 × 10 ⁻³	1.16 × 10 ²

$$k_2 = 1.19 \times 10^4 \text{ M}^{-1}\text{s}^{-1}$$

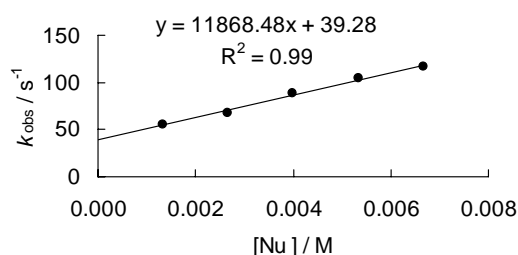
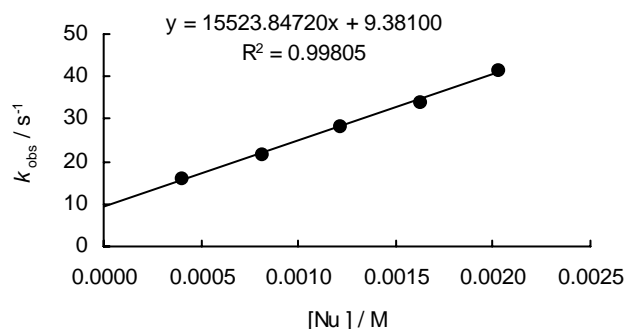


Table S36: Reaction of electrophile **1b** with pyrrolidine (**3f**) in MeOH at 20 °C, stopped-flow, 452 nm.

concentration (mol L ⁻¹)		rate constant
[1b]	[Nu] ₀	k _{obs} (s ⁻¹)
3.76 × 10 ⁻⁵	4.06 × 10 ⁻⁴	1.59 × 10 ¹
3.76 × 10 ⁻⁵	8.13 × 10 ⁻⁴	2.19 × 10 ¹
3.76 × 10 ⁻⁵	1.22 × 10 ⁻³	2.83 × 10 ¹
3.76 × 10 ⁻⁵	1.63 × 10 ⁻³	3.40 × 10 ¹
3.76 × 10 ⁻⁵	2.03 × 10 ⁻³	4.15 × 10 ¹

$$k_2 = 1.55 \times 10^4 \text{ M}^{-1}\text{s}^{-1}$$



Kinetics of electrophile **1c**

Table S37: Reaction of electrophile **1c** with ethanolamine (**3a**) in MeOH at 20 °C, stopped-flow, 480 nm.

concentration (mol L ⁻¹)		rate constant
[1c]	[Nu] ₀	k _{obs} (s ⁻¹)
2.20 × 10 ⁻⁵	2.62 × 10 ⁻³	3.66
2.20 × 10 ⁻⁵	5.24 × 10 ⁻³	3.86
2.20 × 10 ⁻⁵	7.86 × 10 ⁻³	3.96
2.20 × 10 ⁻⁵	1.05 × 10 ⁻²	4.21
2.20 × 10 ⁻⁵	1.31 × 10 ⁻²	4.37

$$k_2 = 6.72 \times 10^1 \text{ M}^{-1}\text{s}^{-1}$$

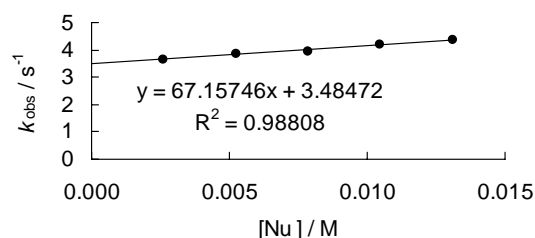


Table S38: Reaction of electrophile **1c** with *n*-propylamine (**3b**) in MeOH at 20 °C, stopped-flow, 480 nm.

concentration (mol L ⁻¹)		rate constant
[1c]	[Nu] ₀	<i>k</i> _{obs} (s ⁻¹)
2.02 × 10 ⁻⁵	2.42 × 10 ⁻³	1.43
2.02 × 10 ⁻⁵	4.83 × 10 ⁻³	1.84
2.02 × 10 ⁻⁵	7.25 × 10 ⁻³	2.23
2.02 × 10 ⁻⁵	9.67 × 10 ⁻³	2.66
2.02 × 10 ⁻⁵	1.21 × 10 ⁻²	3.05

$$k_2 = 1.68 \times 10^2 \text{ M}^{-1} \text{ s}^{-1}$$

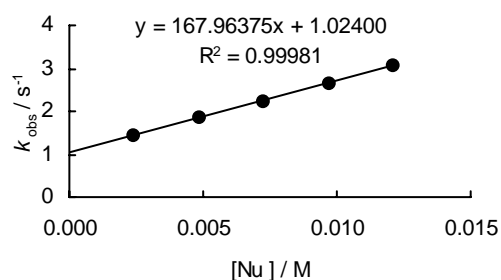


Table S39: Reaction of electrophile **1c** with piperidine (**3e**) in MeOH at 20 °C, stopped-flow, 480 nm.

concentration (mol L ⁻¹)		rate constant
[1c]	[Nu] ₀	<i>k</i> _{obs} (s ⁻¹)
2.20 × 10 ⁻⁵	3.52 × 10 ⁻³	9.38 × 10 ¹
2.20 × 10 ⁻⁵	4.69 × 10 ⁻³	9.45 × 10 ¹
2.20 × 10 ⁻⁵	5.86 × 10 ⁻³	9.86 × 10 ¹
2.20 × 10 ⁻⁵	8.79 × 10 ⁻³	1.07 × 10 ²

$$k_2 = 2.69 \times 10^3 \text{ M}^{-1} \text{ s}^{-1}$$

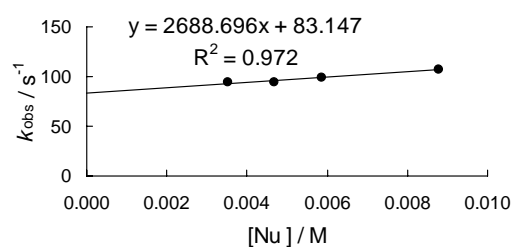
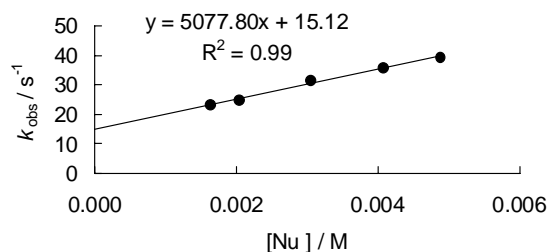


Table S40: Reaction of electrophile **1c** with pyrrolidine (**3f**) in MeOH at 20 °C, stopped-flow, 480 nm.

concentration (mol L ⁻¹)		rate constant
[1c]	[Nu] ₀	<i>k</i> _{obs} (s ⁻¹)
3.16 × 10 ⁻⁵	1.63 × 10 ⁻³	2.33 × 10 ¹
3.16 × 10 ⁻⁵	2.03 × 10 ⁻³	2.50 × 10 ¹
3.16 × 10 ⁻⁵	3.05 × 10 ⁻³	3.15 × 10 ¹
3.16 × 10 ⁻⁵	4.06 × 10 ⁻³	3.58 × 10 ¹
3.16 × 10 ⁻⁵	4.88 × 10 ⁻³	3.95 × 10 ¹

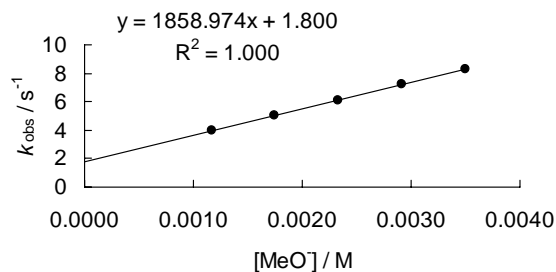
$$k_2 = 5.08 \times 10^3 \text{ M}^{-1} \text{ s}^{-1}$$



Kinetics for the reactions of the electrophiles **1a–c** with sodium methoxide**Table S41:** Reaction of electrophile **1a** with methoxide (**4a**) in MeOH at 20 °C, stopped-flow, 380 nm.

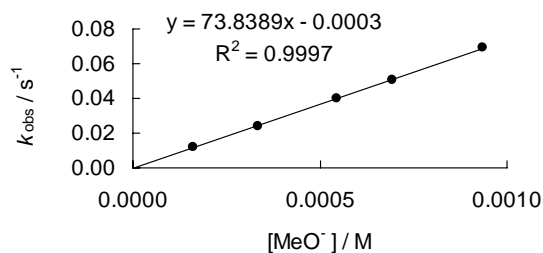
concentration (mol L ⁻¹)		rate constant
[1c]	[4a] ₀	<i>k</i> _{obs} (s ⁻¹)
1.91 × 10 ⁻⁵	1.17 × 10 ⁻³	3.97
1.91 × 10 ⁻⁵	1.75 × 10 ⁻³	5.07
1.91 × 10 ⁻⁵	2.33 × 10 ⁻³	6.11
1.91 × 10 ⁻⁵	2.92 × 10 ⁻³	7.21
1.91 × 10 ⁻⁵	3.50 × 10 ⁻³	8.32

$$k_2 = 1.86 \times 10^3 \text{ M}^{-1} \text{ s}^{-1}$$

**Table S42:** Reaction of electrophile **1b** with methoxide (**4a**) in MeOH at 20 °C, stopped-flow, 452 nm.

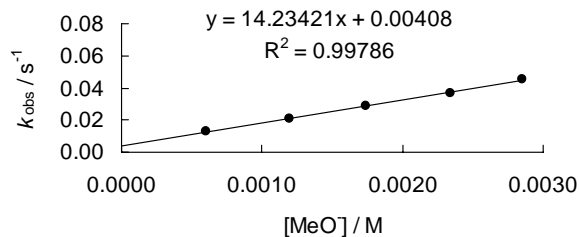
concentration (mol L ⁻¹)		rate constant
[1b]	[4a] ₀	<i>k</i> _{obs} (s ⁻¹)
1.86 × 10 ⁻⁵	1.59 × 10 ⁻⁴	1.19 × 10 ⁻²
1.86 × 10 ⁻⁵	3.18 × 10 ⁻⁴	2.40 × 10 ⁻²
1.86 × 10 ⁻⁵	5.30 × 10 ⁻⁴	4.01 × 10 ⁻²
1.86 × 10 ⁻⁵	6.36 × 10 ⁻⁴	5.04 × 10 ⁻²
1.86 × 10 ⁻⁵	9.01 × 10 ⁻⁴	6.91 × 10 ⁻²

$$k_2 = 7.38 \times 10^1 \text{ M}^{-1} \text{ s}^{-1}$$

**Table S43:** Reaction of electrophile **1c** with methoxide (**4a**) in MeOH at 20 °C, stopped-flow, 480 nm.

concentration (mol L ⁻¹)		rate constant
[1c]	[4a] ₀	<i>k</i> _{obs} (s ⁻¹)
2.02 × 10 ⁻⁵	5.30 × 10 ⁻⁴	1.32 × 10 ⁻²
2.02 × 10 ⁻⁵	1.06 × 10 ⁻³	2.06 × 10 ⁻²
2.02 × 10 ⁻⁵	1.59 × 10 ⁻³	2.87 × 10 ⁻²
2.02 × 10 ⁻⁵	2.12 × 10 ⁻³	3.68 × 10 ⁻²

$$k_2 = 1.42 \times 10^1 \text{ M}^{-1} \text{ s}^{-1}$$



3.7. Determination of Equilibrium Constants

All equilibrium measurements have been performed at 20 °C in MeOH using J&M instruments with $d = 0.5$ cm.

Table S44: Equilibrium constant for the reaction of electrophile **1a** with benzylamine (**3c**) at 380 nm.

Measurement 1				Measurement 2			
[1a] ₀	[1a] _{eq}	[3c] ₀	<i>K</i>	[1a] ₀	[1a] _{eq}	[3c] ₀	<i>K</i>
1.531×10^{-4}	8.290×10^{-5}	1.872×10^{-4}	7.24×10^3	1.554×10^{-4}	1.257×10^{-4}	9.381×10^{-5}	3.69×10^3
1.530×10^{-4}	4.052×10^{-5}	3.742×10^{-4}	1.06×10^4	1.553×10^{-4}	8.773×10^{-5}	1.876×10^{-4}	6.42×10^3
1.529×10^{-4}	2.379×10^{-5}	5.610×10^{-4}	1.26×10^4	1.553×10^{-4}	6.152×10^{-5}	2.813×10^{-4}	8.13×10^3
1.529×10^{-4}	1.599×10^{-5}	7.477×10^{-4}	1.40×10^4	1.552×10^{-4}	3.178×10^{-5}	4.686×10^{-4}	1.12×10^4
1.527×10^{-4}	8.550×10^{-6}	1.213×10^{-3}	1.58×10^4	1.551×10^{-4}	1.989×10^{-5}	6.557×10^{-4}	1.31×10^4
				1.549×10^{-4}	8.922×10^{-6}	1.216×10^{-3}	1.53×10^4

Measurement 3			
[1a] ₀	[1a] _{eq}	[3c] ₀	<i>K</i>
1.560×10^{-4}	1.217×10^{-4}	9.419×10^{-5}	4.69×10^3
1.559×10^{-4}	9.424×10^{-5}	1.883×10^{-4}	5.17×10^3
1.559×10^{-4}	6.970×10^{-5}	2.824×10^{-4}	6.30×10^3
1.558×10^{-4}	3.494×10^{-5}	4.705×10^{-4}	9.89×10^3
1.557×10^{-4}	2.082×10^{-5}	6.583×10^{-4}	1.24×10^4
1.555×10^{-4}	8.550×10^{-6}	1.221×10^{-3}	1.60×10^4

Table S45: Equilibrium constant for the reaction of electrophile **1a** with morpholine (**3d**) at 380 nm.

Measurement 1				Measurement 2			
[1a] ₀	[1a] _{eq}	[3d] ₀	<i>K</i>	[1a] ₀	[1a] _{eq}	[3d] ₀	<i>K</i>
1.298×10^{-4}	1.070×10^{-4}	2.835×10^{-5}	3.84×10^4	1.632×10^{-4}	1.393×10^{-4}	2.738×10^{-5}	4.88×10^4
1.297×10^{-4}	9.191×10^{-5}	5.666×10^{-5}	2.18×10^4	1.631×10^{-4}	1.204×10^{-4}	5.474×10^{-5}	2.97×10^4
1.296×10^{-4}	7.247×10^{-5}	1.132×10^{-4}	1.41×10^4	1.630×10^{-4}	9.642×10^{-5}	1.094×10^{-4}	1.61×10^4
1.295×10^{-4}	6.019×10^{-5}	1.696×10^{-4}	1.15×10^4	1.628×10^{-4}	8.040×10^{-5}	1.639×10^{-4}	1.26×10^4
1.292×10^{-4}	4.541×10^{-5}	2.822×10^{-4}	9.30×10^3	1.625×10^{-4}	6.159×10^{-5}	2.726×10^{-4}	9.54×10^3
1.287×10^{-4}	3.126×10^{-5}	5.059×10^{-4}	7.63×10^3	1.619×10^{-4}	4.215×10^{-5}	4.888×10^{-4}	7.70×10^3
1.280×10^{-4}	2.286×10^{-5}	7.830×10^{-4}	6.79×10^3	1.611×10^{-4}	3.064×10^{-6}	7.567×10^{-4}	6.80×10^3
				1.599×10^{-4}	2.193×10^{-5}	1.154×10^{-3}	6.20×10^3

Table S46: Equilibrium constant for the reaction of electrophile **1b** with ethanolamine (**3a**) at 452 nm.

Measurement 1				Measurement 2			
[1b] ₀	[1b] _{eq}	[3a] ₀	<i>K</i>	[1b] ₀	[1b] _{eq}	[3a] ₀	<i>K</i>
3.739×10^{-5}	3.364×10^{-5}	1.087×10^{-4}	1.06×10^3	3.121×10^{-5}	2.742×10^{-5}	1.033×10^{-4}	1.36×10^3
3.737×10^{-5}	3.103×10^{-5}	2.173×10^{-4}	9.69×10^2	3.120×10^{-5}	2.504×10^{-5}	2.065×10^{-4}	1.23×10^3
3.733×10^{-5}	2.730×10^{-5}	4.341×10^{-4}	8.66×10^2	3.117×10^{-5}	2.187×10^{-5}	4.127×10^{-4}	1.05×10^3
3.729×10^{-5}	2.477×10^{-5}	6.505×10^{-4}	7.93×10^2	3.113×10^{-5}	1.966×10^{-5}	6.184×10^{-4}	9.62×10^2
3.722×10^{-5}	2.132×10^{-5}	1.082×10^{-3}	6.99×10^2	3.107×10^{-5}	1.660×10^{-5}	1.029×10^{-3}	8.59×10^2
3.714×10^{-5}	1.894×10^{-5}	1.512×10^{-3}	6.43×10^2	3.101×10^{-5}	1.458×10^{-5}	1.437×10^{-3}	7.93×10^2
3.695×10^{-5}	1.530×10^{-5}	2.578×10^{-3}	5.54×10^2	3.086×10^{-5}	1.117×10^{-5}	2.452×10^{-3}	7.24×10^2
3.676×10^{-5}	1.308×10^{-5}	3.634×10^{-3}	5.02×10^2	3.071×10^{-5}	8.506×10^{-5}	3.457×10^{-3}	7.54×10^2
				3.049×10^{-5}	7.093×10^{-5}	4.946×10^{-3}	6.70×10^2

Table S47: Equilibrium constant for the reaction of electrophile **1b** with benzylamine (**3c**) at 452 nm.

Measurement 1				Measurement 2			
[1b] ₀	[1b] _{eq}	[3c] ₀	<i>K</i>	[1b] ₀	[1b] _{eq}	[3c] ₀	<i>K</i>
3.382×10^{-5}	2.932×10^{-5}	1.902×10^{-4}	8.26×10^2	3.497×10^{-5}	2.825×10^{-5}	1.822×10^{-4}	1.36×10^3
3.381×10^{-5}	2.671×10^{-5}	3.802×10^{-4}	7.12×10^2	3.496×10^{-5}	2.572×10^{-5}	3.642×10^{-4}	1.01×10^3
3.377×10^{-5}	2.255×10^{-5}	7.596×10^{-4}	6.65×10^2	3.492×10^{-5}	2.191×10^{-5}	7.277×10^{-4}	8.31×10^2
3.372×10^{-5}	1.857×10^{-5}	1.327×10^{-3}	6.22×10^2	3.487×10^{-5}	1.807×10^{-5}	1.272×10^{-3}	7.41×10^2
3.364×10^{-5}	1.438×10^{-5}	2.270×10^{-3}	5.95×10^2	3.479×10^{-5}	1.399×10^{-5}	2.175×10^{-3}	6.90×10^2
3.352×10^{-5}	1.058×10^{-5}	3.581×10^{-3}	6.09×10^2	3.467×10^{-5}	1.026×10^{-5}	3.431×10^{-3}	6.98×10^2
3.335×10^{-5}	7.608×10^{-6}	4.438×10^{-3}	6.25×10^2	3.450×10^{-5}	6.776×10^{-6}	4.212×10^{-3}	7.89×10^2

$$K_1 = 6.65 (\pm 0.75) \times 10^2 \text{ L mol}^{-1}$$

Table S48: Equilibrium constant for the reaction of electrophile **1b** with piperidine (**3e**) at 452 nm.

Measurement 1				Measurement 2			
[1b] ₀	[1b] _{eq}	[3e] ₀	<i>K</i>	[1b] ₀	[1b] _{eq}	[3e] ₀	<i>K</i>
3.719×10^{-4}	3.380×10^{-5}	5.075×10^{-5}	2.12×10^3	3.026×10^{-5}	2.738×10^{-5}	4.992×10^{-5}	2.23×10^3
3.717×10^{-4}	3.111×10^{-5}	1.015×10^{-4}	2.04×10^3	3.024×10^{-5}	2.497×10^{-5}	9.978×10^{-5}	2.24×10^3
3.711×10^{-4}	2.524×10^{-5}	2.532×10^{-4}	1.95×10^3	3.021×10^{-5}	2.199×10^{-5}	1.994×10^{-4}	1.96×10^3
3.705×10^{-4}	2.183×10^{-5}	4.046×10^{-4}	1.79×10^3	3.017×10^{-5}	1.914×10^{-5}	3.483×10^{-4}	1.71×10^3
3.696×10^{-4}	1.819×10^{-5}	6.557×10^{-4}	1.62×10^3	3.007×10^{-5}	1.573×10^{-5}	6.449×10^{-4}	1.45×10^3
3.680×10^{-4}	1.470×10^{-5}	1.055×10^{-3}	1.46×10^3	2.998×10^{-5}	1.371×10^{-5}	9.396×10^{-4}	1.29×10^3
3.661×10^{-4}	1.209×10^{-5}	1.549×10^{-3}	1.33×10^3	2.983×10^{-5}	1.141×10^{-5}	1.427×10^{-3}	1.15×10^3
3.633×10^{-4}	9.748×10^{-6}	2.281×10^{-3}	1.21×10^3	2.968×10^{-5}	9.947×10^{-6}	1.909×10^{-3}	1.05×10^3
3.587×10^{-4}	7.450×10^{-6}	3.476×10^{-3}	1.21×10^3				

$$K_1 = 1.62 (\pm 0.35) \times 10^3 \text{ L mol}^{-1}$$

$$K_2 = 1.63 (\pm 0.44) \times 10^3 \text{ L mol}^{-1}$$

$$K_{\emptyset} = 1.63 (\pm 0.00) \times 10^3 \text{ L mol}^{-1}$$

Table S49: Equilibrium constant for the reaction of electrophile **1b** with pyrrolidine (**3f**) at 452 nm.

Measurement 1				Measurement 2			
[1b] ₀	[1b] _{eq}	[3f] ₀	<i>K</i>	[1b] ₀	[1b] _{eq}	[3f] ₀	<i>K</i>
3.382×10^{-5}	2.774×10^{-5}	5.975×10^{-5}	4.09×10^3	3.326×10^{-5}	2.786×10^{-5}	5.939×10^{-5}	3.59×10^3
3.381×10^{-5}	2.294×10^{-5}	1.194×10^{-4}	4.36×10^3	3.325×10^{-5}	2.294×10^{-5}	1.187×10^{-4}	4.14×10^3
3.377×10^{-5}	1.700×10^{-5}	2.387×10^{-4}	4.45×10^3	3.321×10^{-5}	1.744×10^{-5}	2.372×10^{-4}	4.09×10^3
3.374×10^{-5}	1.375×10^{-5}	3.576×10^{-4}	4.31×10^3	3.318×10^{-5}	1.403×10^{-5}	3.554×10^{-4}	4.06×10^3
3.367×10^{-5}	1.003×10^{-5}	5.948×10^{-4}	4.13×10^3	3.311×10^{-5}	1.014×10^{-5}	5.912×10^{-4}	3.98×10^3
3.360×10^{-5}	7.886×10^{-6}	8.310×10^{-4}	4.05×10^3	3.305×10^{-5}	7.846×10^{-6}	8.260×10^{-4}	4.01×10^3
3.353×10^{-5}	6.539×10^{-6}	1.066×10^{-3}	3.97×10^3	3.298×10^{-5}	6.261×10^{-6}	1.060×10^{-3}	4.13×10^3
3.346×10^{-5}	5.429×10^{-6}	1.301×10^{-3}	4.06×10^3	3.285×10^{-5}	5.706×10^{-6}	1.525×10^{-3}	3.18×10^3
3.333×10^{-5}	4.082×10^{-6}	1.766×10^{-3}	4.13×10^3	3.268×10^{-5}	3.249×10^{-6}	2.101×10^{-3}	4.37×10^3

$$K_1 = 4.17 (\pm 0.15) \times 10^3 \text{ L mol}^{-1}$$

$$K_2 = 3.95 (\pm 0.33) \times 10^3 \text{ L mol}^{-1}$$

$$K_{\emptyset} = 4.06 (\pm 0.11) \times 10^3 \text{ L mol}^{-1}$$

Table S50: Equilibrium constant for the reaction of electrophile **1c** with propylamine (**3b**) at 480 nm.

Measurement 1				Measurement 2			
[1c] ₀	[1c] _{eq}	[3b] ₀	<i>K</i>	[1c] ₀	[1c] _{eq}	[3b] ₀	<i>K</i>
3.812×10^{-5}	3.691×10^{-5}	1.263×10^{-4}	2.61×10^2	3.922×10^{-5}	3.030×10^{-5}	6.485×10^{-4}	4.60×10^2
3.810×10^{-5}	3.538×10^{-5}	2.525×10^{-4}	3.08×10^2	3.912×10^{-5}	2.767×10^{-5}	1.294×10^{-3}	3.23×10^2
3.795×10^{-5}	2.758×10^{-5}	1.195×10^{-3}	3.17×10^2	3.897×10^{-5}	2.417×10^{-5}	2.256×10^{-3}	2.73×10^2
3.781×10^{-5}	2.677×10^{-5}	2.130×10^{-3}	2.79×10^2	3.882×10^{-5}	2.172×10^{-5}	3.210×10^{-3}	2.47×10^2
3.758×10^{-5}	1.940×10^{-5}	3.674×10^{-3}	2.56×10^2	3.863×10^{-5}	1.835×10^{-5}	4.471×10^{-3}	2.48×10^2
3.730×10^{-5}	1.581×10^{-5}	5.501×10^{-3}	2.48×10^2	3.838×10^{-5}	1.611×10^{-5}	6.030×10^{-3}	2.30×10^2
3.698×10^{-5}	1.287×10^{-5}	7.599×10^{-3}	2.47×10^2	3.810×10^{-5}	1.235×10^{-5}	7.876×10^{-3}	2.66×10^2
				3.772×10^{-5}	9.457×10^{-6}	1.029×10^{-2}	2.99×10^2

$K_1 = 2.74 (\pm 0.26) \times 10^2 \text{ L mol}^{-1}$
 $K_2 = 2.92 (\pm 0.70) \times 10^2 \text{ L mol}^{-1}$

$K_{\emptyset} = 2.83 (\pm 0.09) \times 10^2 \text{ L mol}^{-1}$

Table S51: Equilibrium constant for the reaction of electrophile **1c** with pyrrolidine (**3f**) at 480 nm.

Measurement 1				Measurement 2			
[1c] ₀	[1c] _{eq}	[3f] ₀	<i>K</i>	[1c] ₀	[1c] _{eq}	[3f] ₀	<i>K</i>
2.375×10^{-5}	2.211×10^{-5}	1.143×10^{-4}	6.59×10^2	4.661×10^{-5}	4.413×10^{-5}	1.209×10^{-5}	4.73×10^2
2.368×10^{-5}	1.874×10^{-5}	4.559×10^{-4}	5.85×10^2	4.651×10^{-5}	3.634×10^{-5}	6.034×10^{-4}	4.72×10^2
2.354×10^{-5}	1.480×10^{-5}	1.161×10^{-3}	5.12×10^2	4.642×10^{-5}	3.130×10^{-5}	1.084×10^{-4}	4.52×10^2
2.344×10^{-5}	1.151×10^{-5}	2.134×10^{-3}	4.84×10^2	4.628×10^{-5}	2.601×10^{-5}	1.801×10^{-4}	4.38×10^2
2.306×10^{-5}	8.713×10^{-6}	3.496×10^{-3}	4.73×10^2	4.614×10^{-5}	2.224×10^{-5}	2.514×10^{-4}	4.31×10^2
2.279×10^{-5}	7.093×10^{-6}	4.826×10^{-3}	4.60×10^2	4.596×10^{-5}	1.870×10^{-5}	3.458×10^{-4}	4.25×10^2
2.253×10^{-5}	5.954×10^{-6}	6.125×10^{-3}	4.56×10^2	4.573×10^{-5}	1.541×10^{-5}	4.628×10^{-4}	4.28×10^2
				4.540×10^{-5}	1.243×10^{-5}	6.360×10^{-3}	4.19×10^2
				4.485×10^{-5}	9.326×10^{-6}	9.192×10^{-3}	4.16×10^2
				4.431×10^{-5}	7.356×10^{-6}	1.196×10^{-2}	4.21×10^2

$K_1 = 5.18 (\pm 0.70) \times 10^2 \text{ L mol}^{-1}$
 $K_2 = 4.37 (\pm 0.20) \times 10^2 \text{ L mol}^{-1}$

$K_{\emptyset} = 4.78 (\pm 0.40) \times 10^2 \text{ L mol}^{-1}$

Table S52: Equilibrium constant for the reaction of electrophile **1a** with methoxide (**4a**) at 380 nm.

Measurement 1				Measurement 2			
[1a] ₀	[1a] _{eq}	[4a] ₀	<i>K</i>	[1a] ₀	[1a] _{eq}	[4a] ₀	<i>K</i>
2.389 × 10 ⁻⁵	2.212 × 10 ⁻⁵	5.201 × 10 ⁻⁶	2.32 × 10 ⁴	2.466 × 10 ⁻⁵	2.183 × 10 ⁻⁵	7.814 × 10 ⁻⁶	2.61 × 10 ⁴
2.387 × 10 ⁻⁵	2.022 × 10 ⁻⁵	1.040 × 10 ⁻⁶	2.68 × 10 ⁴	2.465 × 10 ⁻⁵	1.894 × 10 ⁻⁵	1.562 × 10 ⁻⁵	3.04 × 10 ⁴
2.385 × 10 ⁻⁵	1.650 × 10 ⁻⁵	2.077 × 10 ⁻⁵	3.32 × 10 ⁴	2.462 × 10 ⁻⁵	1.493 × 10 ⁻⁵	2.600 × 10 ⁻⁵	3.98 × 10 ⁴
2.381 × 10 ⁻⁵	1.091 × 10 ⁻⁵	3.630 × 10 ⁻⁵	5.05 × 10 ⁴	2.460 × 10 ⁻⁵	1.112 × 10 ⁻⁵	3.637 × 10 ⁻⁵	5.29 × 10 ⁴
2.378 × 10 ⁻⁵	6.078 × 10 ⁻⁶	5.178 × 10 ⁻⁵	8.55 × 10 ⁴	2.456 × 10 ⁻⁵	6.160 × 10 ⁻⁶	5.188 × 10 ⁻⁵	8.92 × 10 ⁴
2.374 × 10 ⁻⁵	2.729 × 10 ⁻⁶	6.721 × 10 ⁻⁵	1.67 × 10 ⁵	2.452 × 10 ⁻⁵	2.729 × 10 ⁻⁶	6.734 × 10 ⁻⁵	1.75 × 10 ⁵

Table S53: Equilibrium constant for the reaction of electrophile **1b** with methoxide (**4a**) at 452 nm.

Measurement 1				Measurement 2			
[1b] ₀	[1b] _{eq}	[4a] ₀	<i>K</i>	[1b] ₀	[1b] _{eq}	[4a] ₀	<i>K</i>
2.937 × 10 ⁻⁵	1.934 × 10 ⁻⁵	4.531 × 10 ⁻⁵	1.47 × 10 ⁴	3.056 × 10 ⁻⁵	2.088 × 10 ⁻⁵	4.463 × 10 ⁻⁵	1.33 × 10 ⁴
2.934 × 10 ⁻⁵	1.117 × 10 ⁻⁵	9.052 × 10 ⁻⁵	2.25 × 10 ⁴	3.053 × 10 ⁻⁵	1.228 × 10 ⁻⁵	8.917 × 10 ⁻⁵	2.09 × 10 ⁴
2.931 × 10 ⁻⁵	7.490 × 10 ⁻⁵	1.356 × 10 ⁻⁴	2.56 × 10 ⁴	3.050 × 10 ⁻⁵	8.005 × 10 ⁻⁶	1.336 × 10 ⁻⁴	2.53 × 10 ⁴
2.928 × 10 ⁻⁵	5.548 × 10 ⁻⁵	1.806 × 10 ⁻⁴	2.73 × 10 ⁴	3.046 × 10 ⁻⁵	5.984 × 10 ⁻⁶	1.780 × 10 ⁻⁴	2.67 × 10 ⁴
2.920 × 10 ⁻⁵	3.368 × 10 ⁻⁵	2.928 × 10 ⁻⁴	2.87 × 10 ⁴	3.038 × 10 ⁻⁵	3.487 × 10 ⁻⁶	2.884 × 10 ⁻⁴	2.95 × 10 ⁴
2.912 × 10 ⁻⁵	2.417 × 10 ⁻⁶	4.043 × 10 ⁻⁴	2.93 × 10 ⁴	3.030 × 10 ⁻⁵	2.497 × 10 ⁻⁶	3.983 × 10 ⁻⁴	3.01 × 10 ⁴
				3.022 × 10 ⁻⁵	2.021 × 10 ⁻⁶	5.076 × 10 ⁻⁴	2.91 × 10 ⁴

$$K_1 = 2.47 (\pm 0.49) \times 10^4 \text{ L mol}^{-1}$$

$$K_2 = 2.50 (\pm 0.56) \times 10^4 \text{ L mol}^{-1}$$

Measurement 3

[1b] ₀	[1b] _{eq}	[4a] ₀	<i>K</i>
3.199 × 10 ⁻⁵	2.144 × 10 ⁻⁵	4.672 × 10 ⁻⁵	1.36 × 10 ⁴
3.195 × 10 ⁻⁵	1.236 × 10 ⁻⁵	9.333 × 10 ⁻⁵	2.15 × 10 ⁴
3.192 × 10 ⁻⁵	8.243 × 10 ⁻⁶	1.398 × 10 ⁻⁴	2.47 × 10 ⁴
3.188 × 10 ⁻⁵	6.063 × 10 ⁻⁶	1.863 × 10 ⁻⁴	2.65 × 10 ⁴
3.179 × 10 ⁻⁵	3.685 × 10 ⁻⁶	3.018 × 10 ⁻⁴	2.79 × 10 ⁴
3.171 × 10 ⁻⁵	2.615 × 10 ⁻⁶	4.168 × 10 ⁻⁴	2.87 × 10 ⁴
3.162 × 10 ⁻⁵	2.061 × 10 ⁻⁶	5.311 × 10 ⁻⁴	2.86 × 10 ⁴

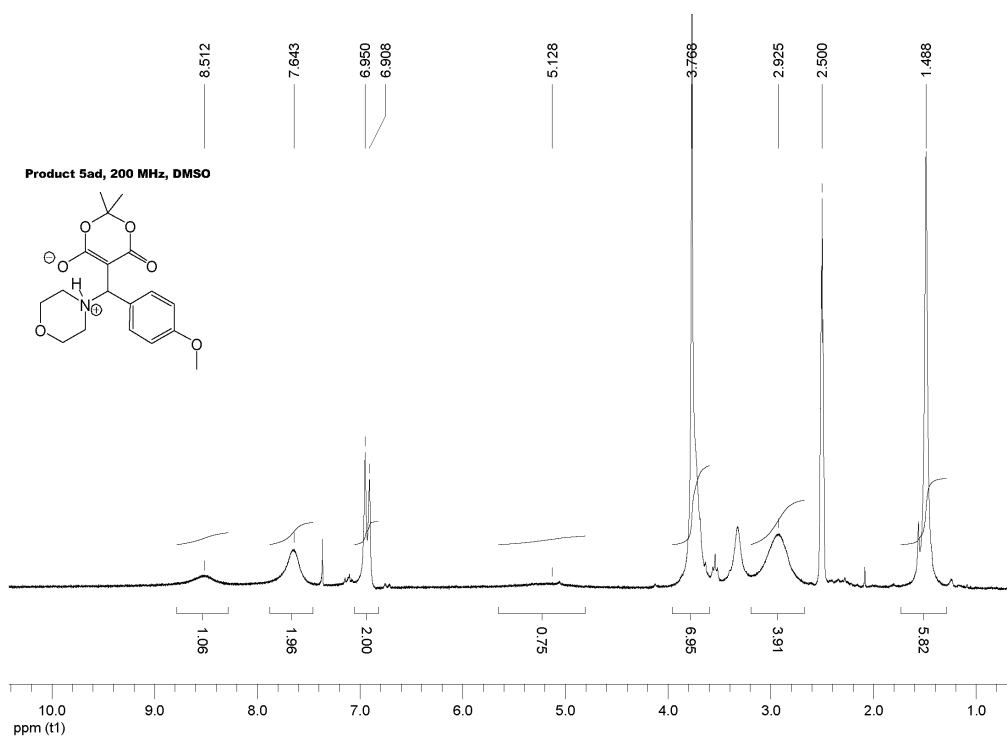
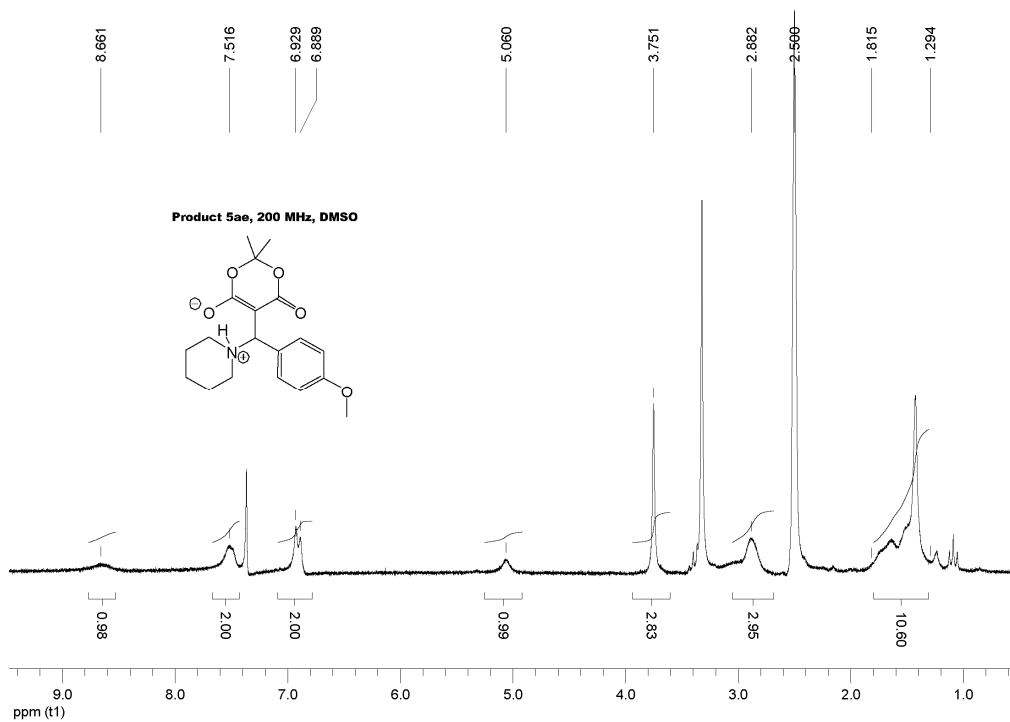
$$K_3 = 2.45 (\pm 0.50) \times 10^4 \text{ L mol}^{-1}$$

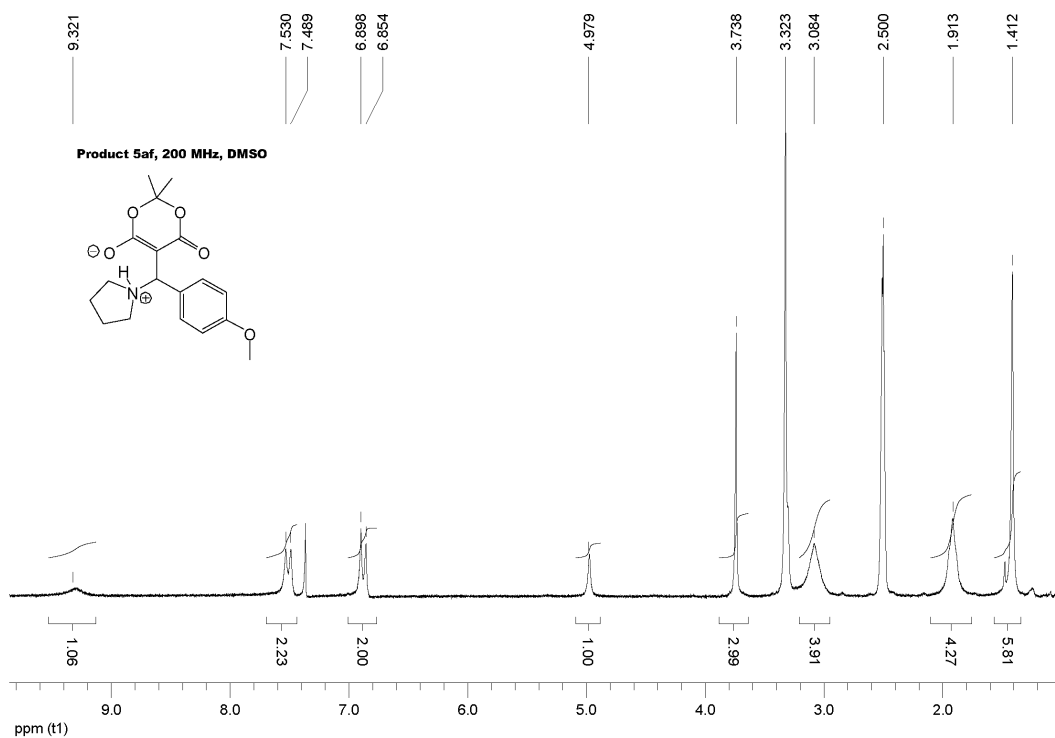
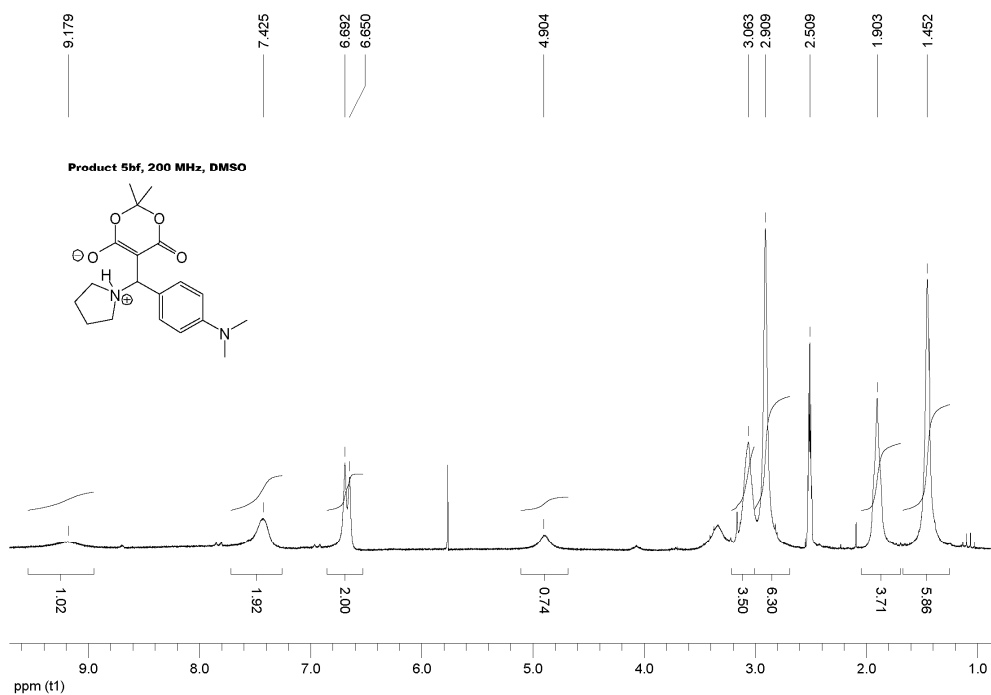
$$K_{\emptyset} = 2.47 (\pm 0.02) \times 10^4 \text{ L mol}^{-1}$$

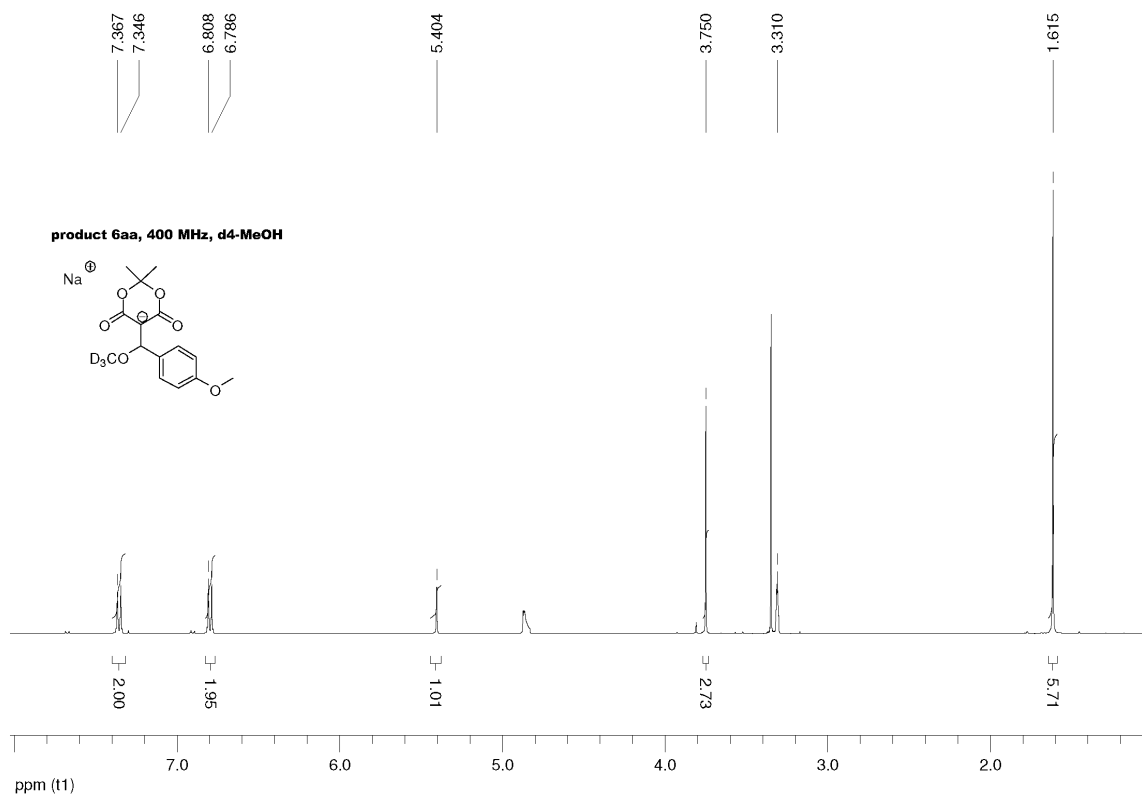
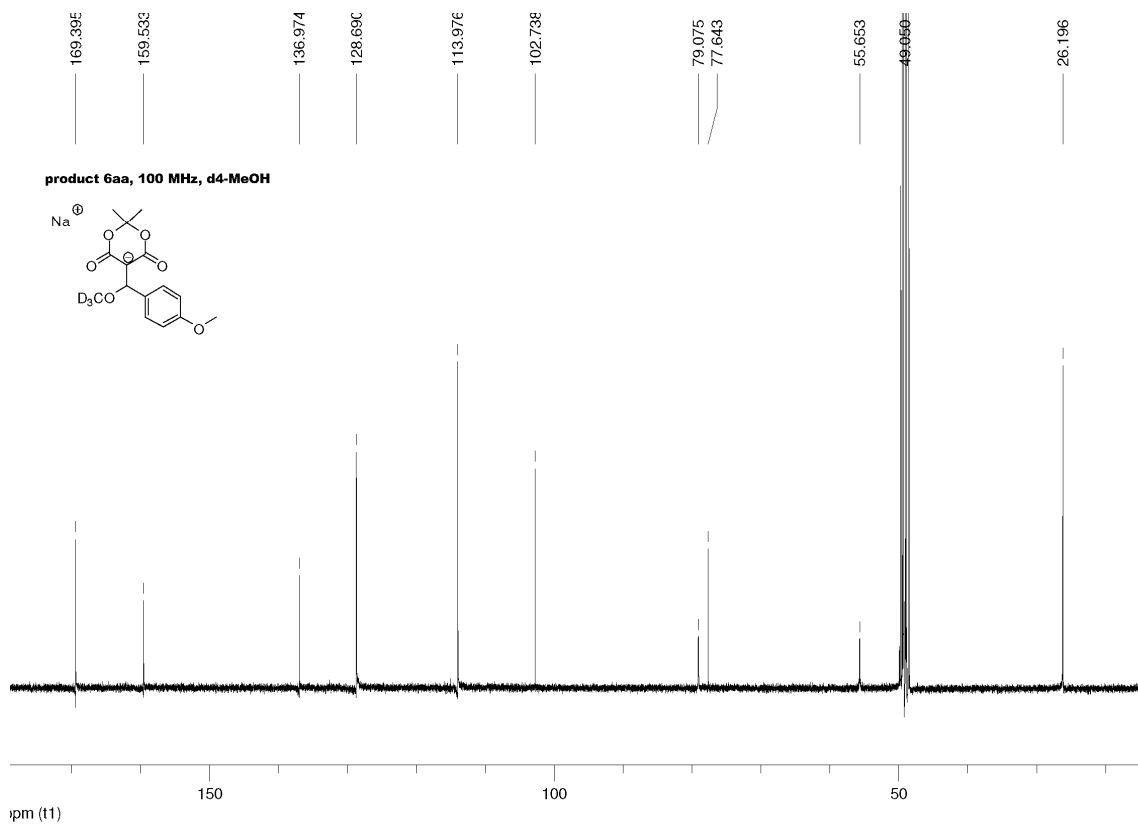
Table S54: Equilibrium constant for the reaction of electrophile **1c** with methoxide (**4a**) at 480 nm.

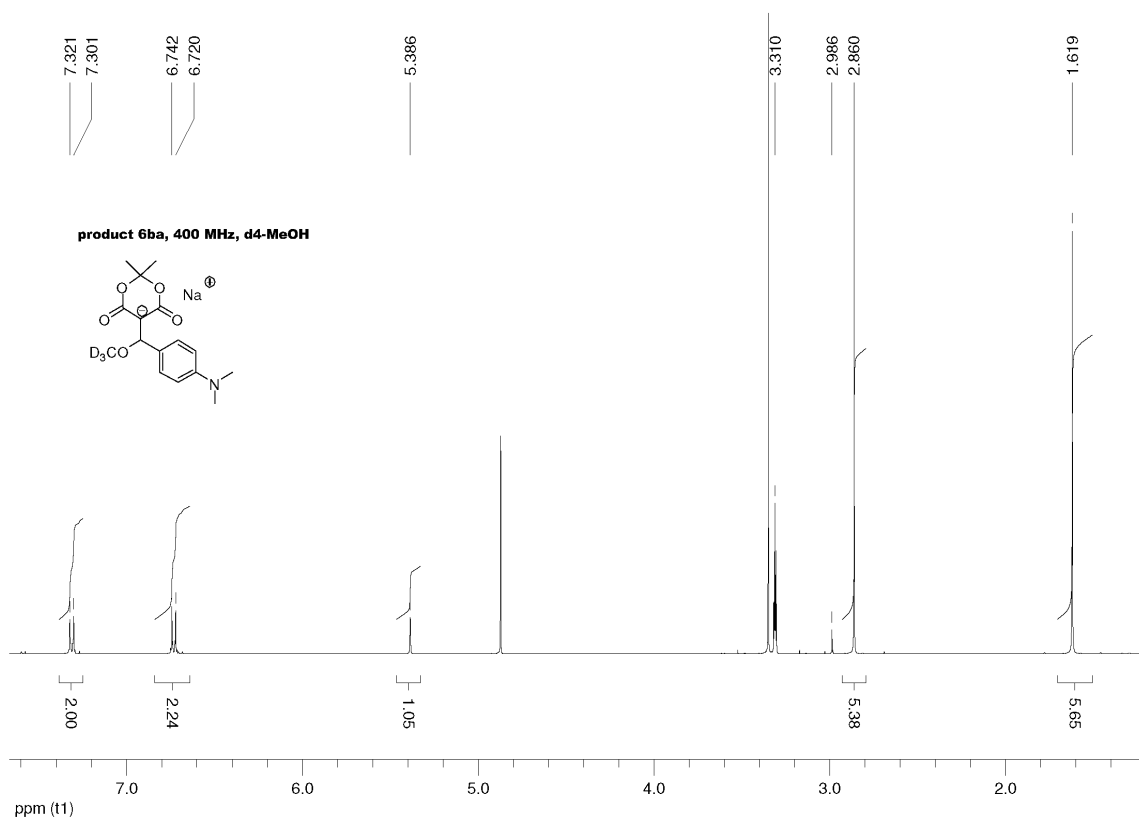
Measurement 1				Measurement 2			
[1c]₀	[1c]_{eq}	[4a]₀	<i>K</i>	[1c]₀	[1c]_{eq}	[4a]₀	<i>K</i>
3.898×10^{-5}	3.468×10^{-5}	8.325×10^{-5}	1.57×10^3	4.090×10^{-5}	3.551×10^{-5}	8.325×10^{-5}	1.95×10^3
3.894×10^{-5}	2.636×10^{-5}	1.663×10^{-4}	3.10×10^3	4.084×10^{-5}	2.693×10^{-5}	2.078×10^{-4}	2.66×10^3
3.888×10^{-5}	2.119×10^{-5}	2.907×10^{-4}	3.06×10^3	4.078×10^{-5}	2.141×10^{-5}	3.320×10^{-4}	2.89×10^3
3.882×10^{-5}	1.738×10^{-5}	4.146×10^{-4}	3.14×10^3	4.071×10^{-5}	1.756×10^{-5}	4.558×10^{-4}	3.05×10^3
3.873×10^{-5}	1.331×10^{-5}	6.204×10^{-4}	3.21×10^3	4.061×10^{-5}	1.344×10^{-5}	6.614×10^{-4}	3.19×10^3
3.863×10^{-5}	1.099×10^{-5}	8.251×10^{-4}	3.15×10^3	4.051×10^{-5}	1.060×10^{-5}	8.660×10^{-4}	3.38×10^3
3.844×10^{-5}	7.750×10^{-6}	1.232×10^{-3}	3.30×10^3	4.032×10^{-5}	7.531×10^{-6}	1.272×10^{-3}	3.51×10^3
				4.012×10^{-5}	5.648×10^{-6}	1.674×10^{-3}	3.72×10^3

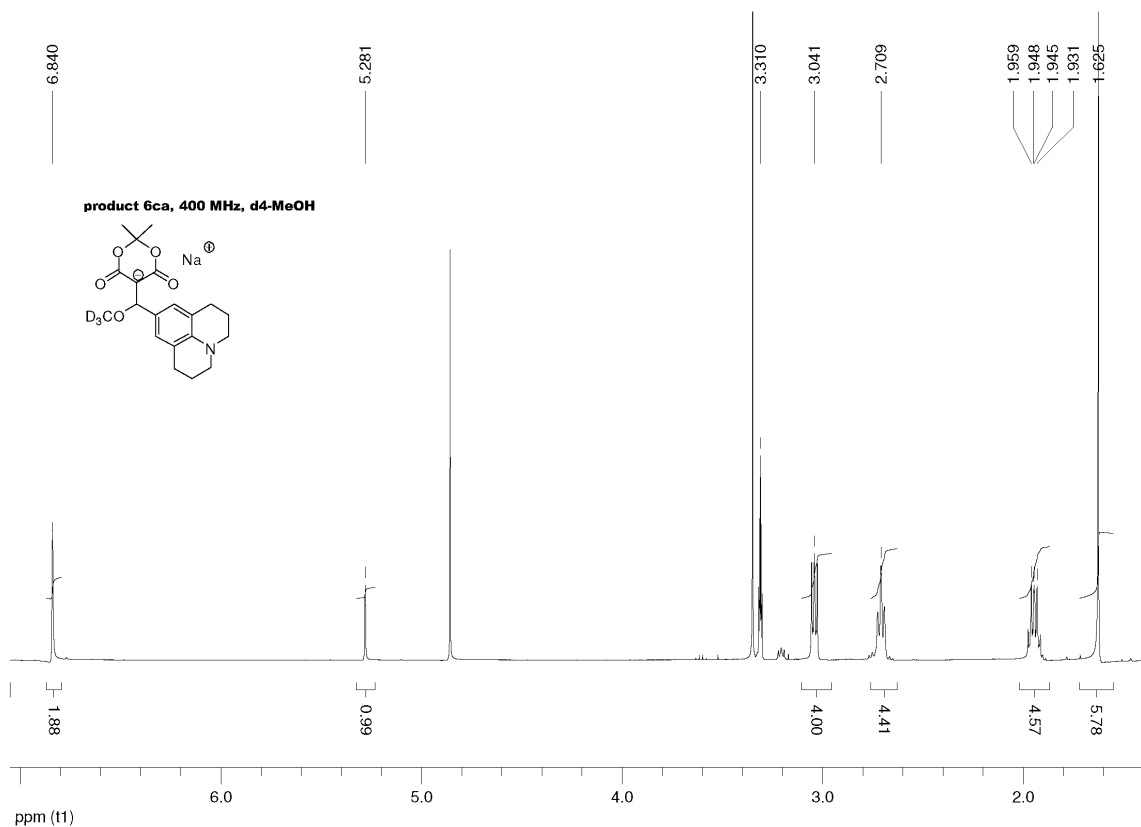
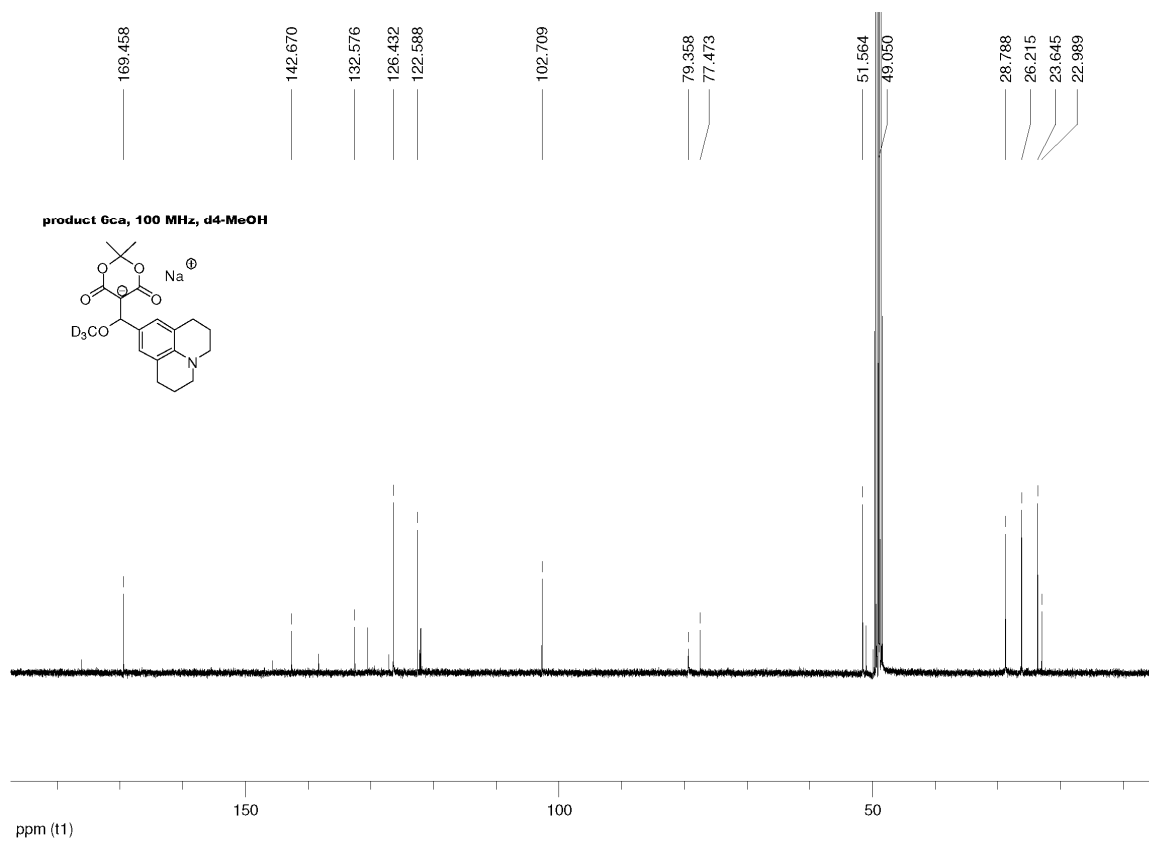
$$K_1 = 2.93 (\pm 0.56) \times 10^3 \text{ L mol}^{-1}$$

3.8. Copies of NMR spectra, Product 5ad, ^1H NMR:Product 5ae, ^1H NMR:

Product 5af, ^1H NMR:**Product 5bf, ^1H NMR:**

Product 6aa, ^1H NMR: **^{13}C NMR:**

Product 6ba, ^1H NMR:

Product 6ca, ^1H NMR: **^{13}C NMR:**

Chapter 4

Determination of the Electrophilicity Parameters of Diethyl Benzylidenemalonates in DMSO: Reference Electrophiles for Characterizing Strong Nucleophiles

O. Kaumanns, R. Lucius, and H. Mayr, *Chem. Eur. J.* **2008**, *14*, 9675-9682.

Introduction

In recent years, large efforts were made to develop nucleophilicity scales for comparing the reactivities of structurally different nucleophiles, such as alkenes and arenes,¹⁻³ alcohols and amines,⁴⁻⁶ carbanions^{7,8} and organometallics^{1,9} or hydride donors.^{1,10} In order to characterize the nucleophilicities of these compounds, kinetics of their reactions with benzhydrylium ions (Ar_2CH^+) and structurally related quinone methides have been investigated and evaluated by using the linear free-energy relationship (4.1),

$$\log k (20\text{ }^\circ\text{C}) = s(N + E) \quad (4.1)$$

where N and s are nucleophile-dependent parameters and E is an electrophile-dependent parameter. With the set of colored reference electrophiles defined in refs. 1, 2, and 8 it became possible to determine the reactivity parameters N for nucleophiles up to $N \approx 22$.

The characterization of more reactive nucleophiles has been problematic so far, because the least reactive electrophile, parametrized until now, had an electrophilicity parameter of $E = -17.9$, i.e., its reactions with nucleophiles of $N > 22$ are very fast and cannot easily be determined.

Recently we demonstrated that Equation (4.1) also holds for the reactions of carbanions with ordinary Michael acceptors, such as benzyldene malononitriles,¹¹ benzyldene indandiones,¹² benzyldene barbituric acids,¹³ and benzyldene Meldrum's acids.¹⁴ We now report on the reactivities of diethyl benzyldenemalonates, which are less electrophilic than benzyldene Meldrum's acids, their cyclic analogues, and therefore may be suitable for extending the scale of reference electrophiles on the low-reactivity end.

Oh and Lee showed that the reactions of substituted benzyl amines with 2-benzyldene-1,3-diketones,¹⁵ and diethyl benzyldenemalonates¹⁶ are much slower than the analogous reactions with benzyldene malononitriles,¹⁷ benzyldene Meldrum's acids,¹⁸ and benzyldene indandiones.¹⁹ The unusual high CH-acidity of Meldrum's acid compared to that of acyclic esters, such as dimethyl malonate, has been ascribed to the fixed (*E*)-conformation of the ester linkage in the bislactone structure of Meldrum's acid.²⁰ This rationalization has been supported by quantum chemical calculations by Houk and Wiberg, who showed that the deprotonation of methyl acetate requires approximately 20 kJ mol⁻¹ less energy than deprotonation of the (*Z*)-conformer.²¹

Benzyldenemalonates **1** have found synthetic applications as Michael acceptors in the reactions with propargyl alkoxides to create a variety of heterocycles such as highly substituted tetrahydrofurans under mild reaction conditions,²² and in diastereoselective oxy-Michael additions of 6-methyl δ lactol to yield protected β -hydroxy ester derivatives.²³ Organocatalytic enantioselective additions of ketones to benzyldenemalonates²⁴ and copper-catalyzed nucleophilic additions of indoles with formation of enantiomerically enriched 3-substituted indoles were reported.²⁵

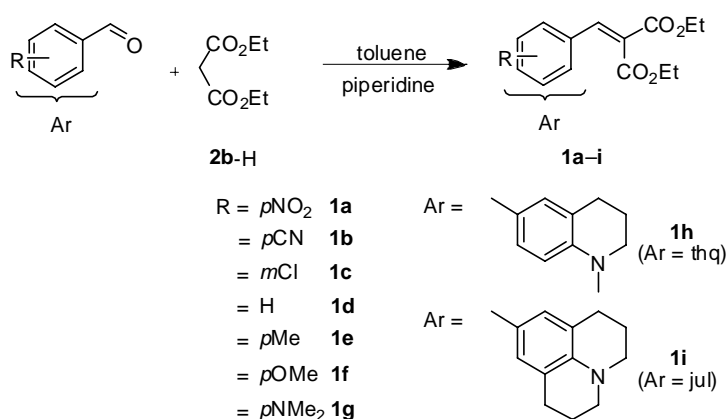
Benzylidene dimalonates, which have been claimed to serve as bone affinity agents have previously been synthesized by tandem-Michael additions of aryl sulfonimines with diethyl malonate.²⁶

We now report on the kinetics of the additions of carbanions towards electrophiles **1a–i** in DMSO and show that the second-order rate constants of these reactions can be described by Equation (4.1).

Results and Discussion

The previously reported compounds **1a–g** and the novel substrates **1h–i** (Scheme 4.1) were prepared by Knoevenagel condensation from diethyl malonate (**2b-H**) and the corresponding aldehyde in boiling toluene following a modified protocol of Zabicky.²⁷

Scheme 4.1. Synthesis of Diethyl Benzylidenemalonates **1a–i** via Knoevenagel Condensation.



The electrophiles **1a–f** are colorless compounds with absorption maxima between 277 and 316 nm, while their amino-substituted analogues **1g–i** are yellow with absorption maxima between 383 and 407 nm (Figure 4.1). The molar decadic absorption coefficients ϵ in DMSO

were found to be similar to those previously reported for some of these compounds in dioxane.²⁸

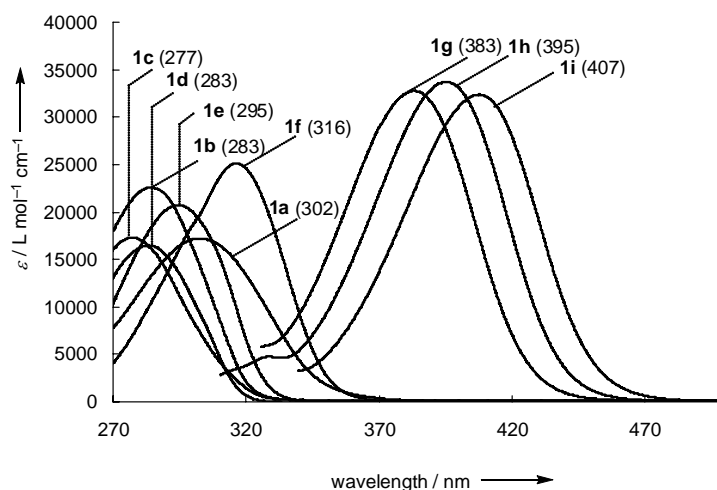


Figure 4.1. UV-Vis spectra of the electrophiles **1a–i** in DMSO, λ_{\max} in parentheses. Molar decadic absorption coefficient ϵ for **1a**: 17200, **1b**: 22500, **1c**: 17300, **1d**: 16500, **1e**: 20700, **1f**: 25100, **1g**: 32800, **1h**: 33700, and **1i**: 32400 L mol⁻¹ cm⁻¹ (for ϵ values for **1a**, **1d**, **1f**, and **1g** in dioxane see ref. 28).

In order to characterize the electrophilic reactivities of compounds **1a–i**, the kinetics of their reactions with the carbanions **2a–e** (Table 4.1) have been investigated.

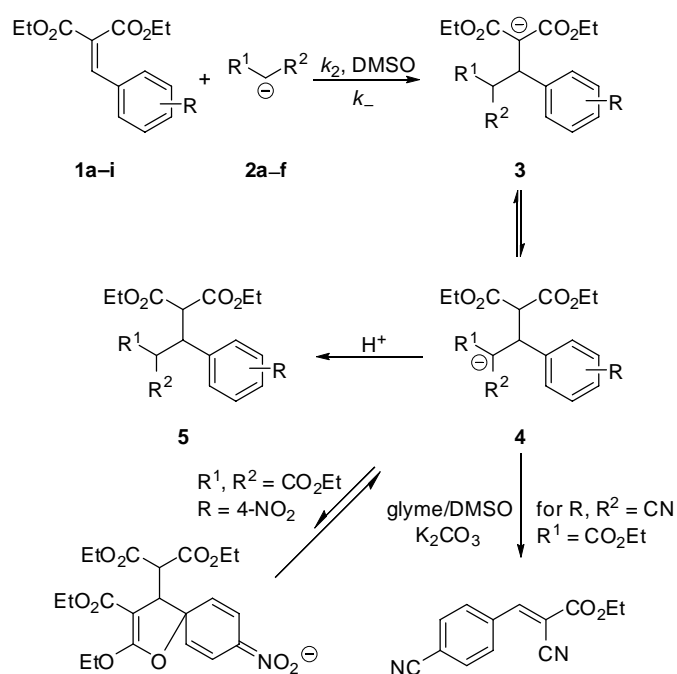
Table 4.1. Nucleophilicity Parameters of the Carbanions **2a–f** in DMSO.

	Nucleophile	N^a	s^a
2a		21.54	0.62
2b		20.22	0.65
2c		19.62	0.67
2d		18.82	0.69
2e		19.92	0.67
2f		19.36	0.67

^a For N and s parameters of **2a** see ref. 11, for **2b–d,f** see ref. 8, for **2e** see ref. 29.

Product studies. In order to confirm the course of the investigated Michael additions (Scheme 4.2), the products of representative combinations of the arylidene malonates **1a–i** with the carbanions **2a–f** have been studied by NMR spectroscopy (Table 4.2).

Scheme 4.2. Addition of the Carbanions **2a–f** to the Benzylidenemalonates **1a–i** and Possible Subsequent Protonation, Elimination or Cyclization Paths.



As depicted in Scheme 4.2, the nucleophilic additions of the carbanions **2a–f** to the diethyl benzylidenemalonates **1a–i** initially yield the anionic adducts **3**, which may undergo a proton transfer with formation of the isomeric carbanions **4**. Acidic workup of **4** then yields compounds **5**.

Thus, mixing the Michael acceptors **1c–f** with two equivalents of **2b–K⁺** in dry DMSO, subsequent workup with aqueous HCl solution and distillation gave products **5cb–5fb** in moderate to good yields (Table 4.2, entries 1–4). The NMR spectra of **5db–5fb**

(Experimental Section) agree with those previously described in ref. 26. The reactions of **1a–f** with the anion of ethyl cyanoacetate **2c**, which were studied in NMR experiments, showed the predominant formation of anions **4ac–4fc** (Table 4.2, entries 5, 6, and 8–11), in accordance with the higher acidity of ethyl cyanoacetate ($pK_a(\text{DMSO}) = 13.1$)³⁰ compared to diethyl malonate ($pK_a(\text{DMSO}) = 16.4$).³¹ Additional signals (< 10 %) indicate the presence of a second compound, potentially the corresponding anions **3**. Electrophile **1b** and ethyl cyanoacetate **2c**-H reacted in the presence of K_2CO_3 in a dimethoxyethane/DMSO mixture to yield the retro-Michael product shown at the bottom of Scheme 4.2 (Table 4.2, entry 7). The reaction of **1a** with **2d** and subsequent acidic workup as described for entries 1–4 in Table 4.2 yielded the product **5ad** as a mixture of diastereoisomers in a ratio of 2:1 in good quantity. The malononitrile anion **2f** reacted with electrophile **1a** to yield **4af**, which was converted into **5af** during acidic workup (Table 4.2, entries 13 and 14). Michael additions of the nitroethyl anion **2a**^{13,14} and the dinitrobenzhydryl anion **2e**²⁹ to similar electrophiles have recently been shown to proceed analogously, and the corresponding adducts to the benzyldienemalonates **1a–i** have not been identified.

Table 4.2. Characterized Michael Adducts **4** and **5**.

Entry	Electrophil	Nucleophil	Product	Yield [%]
1	1c	2b	5cb	47
2	1d	2b	5db	83
3	1e	2b	5eb	47
4	1f	2b	5fb	78
5	1a	2c	4ac	^a
6	1b	2c	4bc	^a
7	1b	2c	^b	25
8	1c	2c	4cc	^a
9	1d	2c	4dc	^a
10	1e	2c	4ec	^a

Table 4.2. *Continued.*

Entry	Electrophil	Nucleophil	Product	Yield [%]
11	1f	2c	4fc	^a
12	1a	2d	5ad	71 ^c
13	1a	2f	4af	^a
14	1a	2f	5af	35

^a Adducts **4** were not isolated, but identified in the crude reaction mixture by ¹H and ¹³C NMR spectroscopy. ^b Retro-Michael adduct (Scheme 4.2 bottom, see text and Experimental Section). ^c The yield of the isolated major diastereomer is 47 %.

Kinetic Measurements. In order to obtain pseudo-first order kinetics, solutions of the electrophiles **1a–i** ($1.0 \times 10^{-5} - 1.0 \times 10^{-3}$ mol L⁻¹) were mixed with more than ten equivalents of the compounds **2a–d**. The decay of the absorptions of the electrophiles was then followed spectrophotometrically[†] either with stopped-flow instruments or, for reactions with half-lives of more than ≈ 15 s, with conventional UV-Vis diode-array spectrometers equipped with fiber optics and a submersible probe. From the fit of the absorbance A_t to the exponential function $A_t = A_0 \exp(-k_{\text{obs}}t) + C$, the first-order rate constants k_{obs} were derived. Since the UV-absorption maxima of the electrophiles **1a–f** are close to those of the carbanions **2a–d**, the combinations of these substrates were not followed at the absorption maxima of the electrophiles, but at shoulders of the absorption bands of the electrophiles at which neither the carbanions **2** nor the resulting products showed significant absorptions.

Figure S1 (Experimental Section) furthermore shows the development of a weak absorption band at $\lambda_{\text{max}} \approx 360$ nm during the reaction of **1b** with **2c**, which may be specific for this electrophile because a comparable weak band ($\lambda_{\text{max}} \approx 350$ nm) was formed during the reaction of the *p*-cyano substituted benzyldenemalonate **1b** with **2a**.

[†] For the reactions of **1a–c** with the green dinitrobenzhydryl anion **2e** the first-order rate constants k_{obs} were determined with **2e** as the minor component.

Similar observations were made, when the *p*-nitro substituted benzyldenemalonate **1a** was combined with the nucleophiles **2a–d**. Orange products with weak absorptions at $\lambda_{\text{max}} = 455$ to 470 nm were formed, and for the reaction of **1a** with the anion of diethyl malonate the rate of the formation of the 455 nm band was found to equal the rate of the decay of the absorption band of **1a** at $\lambda = 325$ nm. Though the nature of these colored side products is not clear, it is conceivable that in the presence of *p*-NO₂ or *p*-CN groups (i.e. in the reactions with **1a** and **1b**) the initially formed adducts **4** undergo cyclization with formation of intra-molecular Meisenheimer-Jackson complexes³² as shown for the adduct of **2b** and **1a** on bottom left of Scheme 4.2.

Generally, plots of the first-order rate constants (k_{obs}) against the concentrations of the carbanions were linear with the slopes k_2 and negligible intercepts (Figure 4.2, Table 4.3).

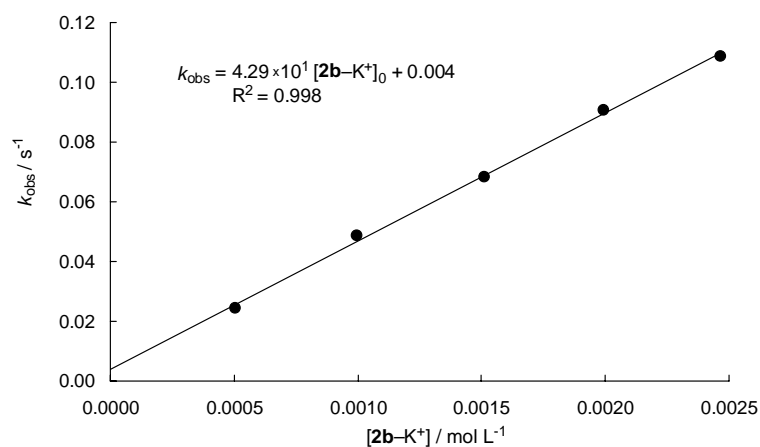


Figure 4.2. Determination of the second-order rate constant for the reaction of **1a** with **2b-K** in DMSO at 20 °C ($k_2 = 43.0 \text{ L mol}^{-1} \text{ s}^{-1}$).

Table 4.3. Second-Order Rate Constants k_2 for the Reactions of the Electrophiles **1a–i** with the Nucleophiles **2a–e** in DMSO at 20 °C.

Electrophil	E	Nucleophil	$k_2 / \text{L mol}^{-1} \text{s}^{-1}$
1a	-17.67	2a	2.41×10^2
		2b ^a	4.29×10^1
		2c	2.12×10^1
		2c ^b	2.24×10^1
		2d ^b	6.58
		2e	1.09×10^1
1b	-18.06	2a	1.45×10^2
		2b ^b	2.86×10^1
		2c	9.77
		2e	5.94
		2e ^b	6.03
1c	-18.98	2a	3.71×10^1
		2b ^b	6.81
		2c	2.68
		2c ^b	2.51
		2e	1.67
1d	-20.55	2b ^b	5.93×10^{-1}
		2c	2.43×10^{-1}
1e	-21.11	2a	2.99
		2b ^b	2.37×10^{-1}
		2b ^c	2.33×10^{-1}
		2c	1.11×10^{-1}
1f	-21.47	2a	1.70
		2b ^b	1.41×10^{-1}
		2c	4.27×10^{-2}
1g	-23.1	2a	1.68×10^{-1}
		2b ^c	8.85×10^{-3}
1h	-23.4	2a	6.96×10^{-2}
1i	-23.8	2a	3.94×10^{-2}

^a From the increase of the absorbance at $\lambda = 425 \text{ nm}$ one derives $k_2 = 42.6 \text{ L mol}^{-1} \text{ s}^{-1}$.
^b In presence of 18-crown-6. ^c Reaction in the presence of the conjugate CH acid **2b**-H.

Equilibrium Constants. While most of the Michael additions listed in Table 4.3 proceeded quantitatively as indicated by negligible end absorptions of the solutions at the absorption maxima of the benzyldenemalonates **1**, several reactions of the malonate anion **2b** turned out to be reversible.

Thus, the *p*-dimethylamino substituted benzyldenemalonate **1g** did not react at all when combined with the carbanion **2b-K⁺**. In the presence of 3–5 equivalents of the conjugate acid **2b-H** ($c_0 \approx 2 \times 10^{-2} \text{ mol L}^{-1}$) almost quantitative conversion of **1g** was achieved, however, and the k_2 value listed in Table 4.3 refers to these conditions. A similar behaviour was expected for other additions of the carbanions **2b–f** to the amino substituted benzyldenemalonates **1g–i**. Because of the expected low reaction rates, these additions have not been investigated, however.

The reactions of **2b-K⁺** with **1e,f** also proceeded incompletely as indicated by significant end absorptions of the mixtures at the absorption maxima of the electrophiles. In line with the assumption of a reversible Michael addition, the linear plot of k_{obs} vs. [**2b**] had a positive intercept (Figure 4.3, upper graph) which equals the rate constant of the reverse reaction.³³ Complete consumption of **1e** was achieved when the reaction of **1e** with **2b-K⁺** was performed in the presence of two equivalents of the conjugate CH acid **2b-H**. The linear plot of k_{obs} vs. [**2b**] obtained under these conditions had almost the same slope (Figure 4.3, lower graph) as the one obtained in the absence of **2b-H**, indicating that the rate-determining step is the same in both cases, i.e., the proton transfer from **2b-H** to **3** (= **4** for $R^1, R^2 = \text{CO}_2\text{Et}$) is a fast subsequent reaction. Analogously, the linear plot of k_{obs} vs. [**2b**] for the reaction of **2b** with **1f** showed a positive intercept.

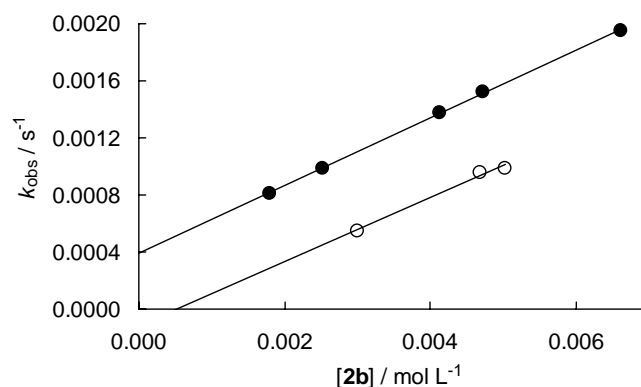


Figure 4.3. Reaction of the electrophile **1e** with the carbanion **2b** without addition of **2b-H** (●, $k_{\text{obs}} = 0.237 [\mathbf{2b}] + 0.0004$) and in the presence of 2 equivalents of **2b-H** (○, $k_{\text{obs}} = 0.233 [\mathbf{2b}] - 0.0001$) in DMSO at 20 °C.

By theory,³³ it is now possible to calculate the equilibrium constants K for the reactions of **2b** with **1e** and **1f** as the ratio of the forward (k_2 , slope of k_{obs} vs. $[\mathbf{2b}]$ plot) over backward (k_- , intercept of k_{obs} vs. $[\mathbf{2b}]$ plot) rate constants [eq. (4.2)]. However, because of the uncertainty in the determination of k_- as the intercept, the equilibrium constants K have directly been determined from the absorbances of **1e** and **2f** in the presence of variable concentrations of **2b** using Equation (4.3).

$$K = \frac{k_2}{k_-} \quad (4.2)$$

$$K = \frac{[\mathbf{3}]_{\text{eq}}}{[\mathbf{1}]_{\text{eq}}[\mathbf{2b}]_{\text{eq}}} = \frac{[\mathbf{1}]_0 - [\mathbf{1}]_{\text{eq}}}{[\mathbf{1}]_{\text{eq}}([\mathbf{2b}]_0 - [\mathbf{1}]_0 + [\mathbf{1}]_{\text{eq}})} \quad (4.3)$$

The equilibrium constants K derived from Equation (4.3) which are listed in Table 4.4 can then be combined with the rate constants k_2 from Table 4.3 to give the values of k_- which are listed in the fourth line of Table 4.4. The values for the reverse reactions derived in the two different ways differ by factors of 1.1 and 1.7, and we consider the values in the fourth line of Table 4.4 to be more reliable.

Table 4.4. Equilibrium and Rate Constants for the Reactions of Carbanion **2b** with the Electrophiles **1e,f** in DMSO at 20 °C.

	1e	1f
k_- / s^{-1}	$4 \times 10^{-4}{}^a$	$1 \times 10^{-3}{}^a$
$K / \text{L mol}^{-1}$	$5.3 \times 10^2{}^b$	$2.3 \times 10^2{}^b$
k_+ / s^{-1}	$4.5 \times 10^{-4}{}^c$	$6.0 \times 10^{-4}{}^c$
$\Delta G^0 / \text{kJ mol}^{-1}$	$-15.3{}^d$	$-13.3{}^d$
$\Delta G^\ddagger / \text{kJ mol}^{-1}$	$75.3{}^e$	$76.5{}^e$
$\Delta G_0^\ddagger / \text{kJ mol}^{-1}$	$82.7{}^f$	$83.0{}^f$

^a Intercept on the Y-axis for the plot of k_{obs} vs [**2b**] (as shown in Tables S20 and S23, Experimental Section). ^b From Equation (4.3) using the initial absorptions of the electrophiles **1e** and **1f** and the equilibrium absorptions after addition of carbanion **2b** (see Tables S1 and S2, Experimental Section). ^c Calculated on the basis of Equation (4.2) and the second-order rate constants listed in Table 4.3. ^d Calculated from the equilibrium constants K . ^e Forward reaction; from second-order rate constants k_2 in Table 4.3. ^f Calculated on the basis of Equation (4.4) and ΔG^0 and ΔG^\ddagger from this Table.

Substitution of ΔG^\ddagger and ΔG^0 for these reactions into the Marcus Equation³⁴ (4.4) where the work term has been neglected, yields intrinsic barriers of $\Delta G_0^\ddagger = 83 \text{ kJ mol}^{-1}$.

$$\Delta G^\ddagger = \Delta G_0^\ddagger + 0.5 \Delta G^0 + (\Delta G^0)^2 / (16\Delta G_0^\ddagger) \quad (4.4)$$

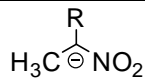
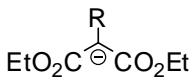
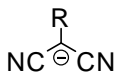
This value is considerably higher than those previously reported for the additions of pyridines⁵ and tertiary alkyl amines⁶ to structurally related Michael acceptors.

Interestingly, the addition reactions of the carbanion **2c** to the electrophiles **1e,f** proceed quantitatively, although **2c** reacts more slowly ($N = 19.62$) than the reversibly reacting carbanion **2b** ($N = 20.22$). How can this behavior be explained?

Scheme 4.2 shows that ΔG^0 for the reaction of **1** with **2** to give **4** includes the difference in “carbanion stabilization” of anions **2** and **4**. Because $\text{p}K_{\text{a}}$ values for the Michael adducts **5**, the conjugate acids of **4**, are not available, we have estimated the influence of alkyl groups on the

CH acidities of these compounds from a comparison of carbanions **2** with their methyl analogues as illustrated in Table 4.5.

Table 4.5. Influence of Methyl Groups on the Basicities of Carbanions (DMSO).

Carbanion	pK_{aH} (R = H)	pK_{aH} (R = CH ₃)
	16.7 ^a (2a)	16.8 ^a
	16.4 ^b (2b)	18.7 ^c
	11.1 ^d (2f)	12.4 ^d

^a From ref. 35. ^b From ref. 31. ^c From ref. 36. ^d From ref. 37

Though pK_{aH} values are not available for all methyl analogues of carbanions **2a–f**, the examples shown in Table 4.5 indicate that introduction of a methyl group leads to a particularly large decrease in carbanion stabilization in the case of malonate **2b**. This effect may account for the observation that the Michael additions of **2b** are less exergonic than the analogous reactions of the other carbanions of Table 4.1.

Correlation analysis. In Figure 4.4, the logarithmic second-order rate constants ($\log k_2$) for the reactions of the carbanions **2a–d** with the aryldiene malonates **1a–i** and the reference electrophiles **6a–f** (quinone methides) are plotted against the corresponding electrophilicity parameters E . The E parameters of **6a–f** were taken from ref. 8, and those for **1a–i** were calculated from the rate constants for their reactions with the carbanions **2a–d** (reference nucleophiles). For that purpose, the nonlinear solver “What’s Best!” was used to minimize the square of the deviations (Δ^2) between calculated and experimental rate constants $\Delta^2 = \sum(\log k_2 - s(N+E))^2$. Because N and s of the carbanions are given in Table 4.1 and the corresponding

rate constants k_2 are listed in Table 4.3, the electrophilicity parameters E for **1a–i** could thus be obtained.

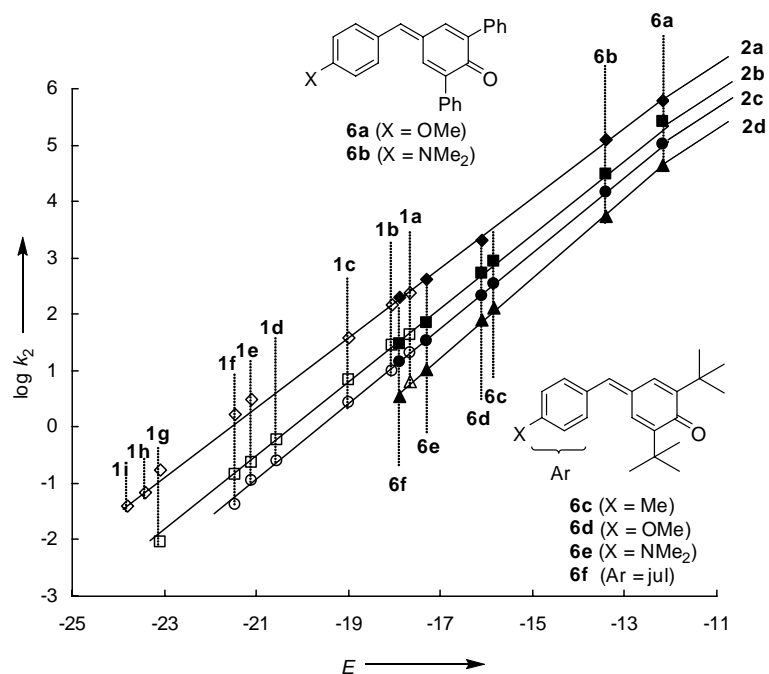
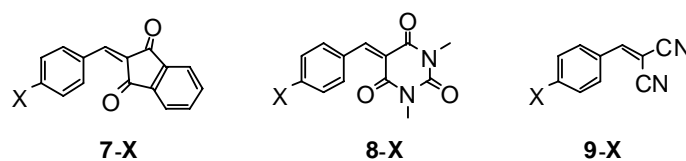


Figure 4.4. Plot of $\log k_2$ for the reactions of carbanions **2a–d** with electrophiles **1a–i** (open symbols) and with reference electrophiles **6a–f** (filled symbols) in DMSO versus the electrophilicity parameter E of the employed electrophiles.

Figure 4.5 illustrates that the rate constants of the reactions of the dinitrobenzhydryl anion **2e** with various classes of electrophiles follow separate $\log k$ vs. E correlations. The upper correlation line for the reactions of **2e** with the quinone methides **6a–e** was used for the calculation of the N and s parameters of **2e**.²⁹ The benzyldenemalonates **1a–c** are on the same, somewhat lower correlation line as the indandiones **7-X** and the barbiturates **8-X** (for structures see Scheme 4.3).

Scheme 4.3. Michael Acceptors (7–9)-X.



As a consequence, the $\log k_2$ values for the reactions of **2e** with **1a–c**, **7-X**, and **8-X** which are calculated by Equation (4.1) are 2–4 times higher than the experimental values for their reactions with **2e**. The benzylidene malononitriles **9-X** (Scheme 4.3) deviate even more, and the observed rate constants are approximately one order of magnitude smaller than calculated by Equation (4.1). Though a similar split up of the correlation lines for different classes of electrophiles has been reported earlier,¹⁴ we resist the temptation to improve the reliability of the correlations by the addition of correction terms. We rather keep the correlation simple and unambiguous and emphasize that the use of Equation (4.1) implies errors up to a factor of 10–100, which we consider acceptable in a reactivity range of more than thirty orders of magnitude.

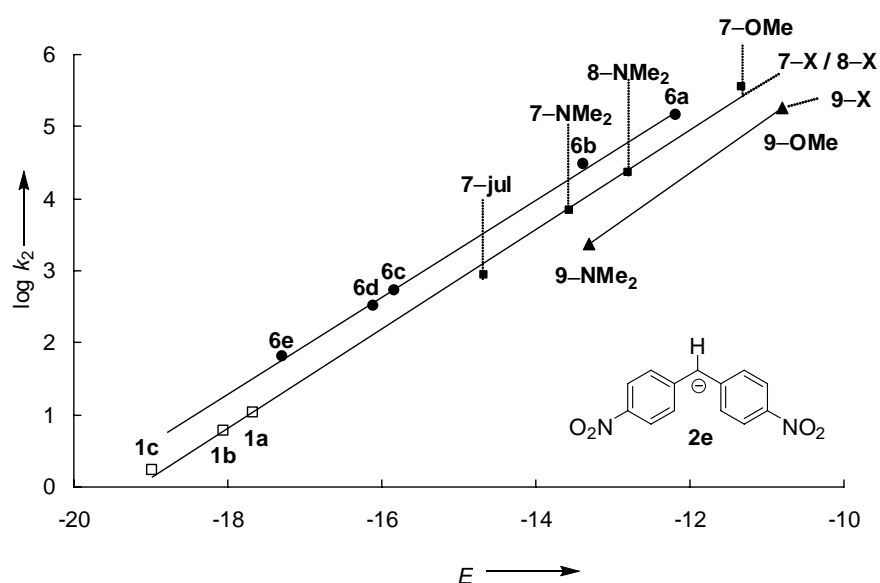


Figure 4.5. Correlation of $\log k_2$ versus E for the reactions of carbanion **2e** with different Michael acceptors in DMSO – Structures of **1a–c** in Scheme 4.1; structures of **6a–e** in Figure 4.4; structures of (7–9)-X in Scheme 4.3; for “jul”-substituent see **1i** in Scheme 4.1.

Figure 4.6 shows that the electrophilicities of the benzyldenemalonates **1a–i** cover a range of more than six orders of magnitude from $-17.7 > E > -23.8$ and are roughly ten to eleven orders of magnitude less reactive than their cyclic analogues **10a–d**. Thus, fixation of the two ester groups of **1** in a six-membered ring formation has an enormous effect on the reactivity of these Michael acceptors.

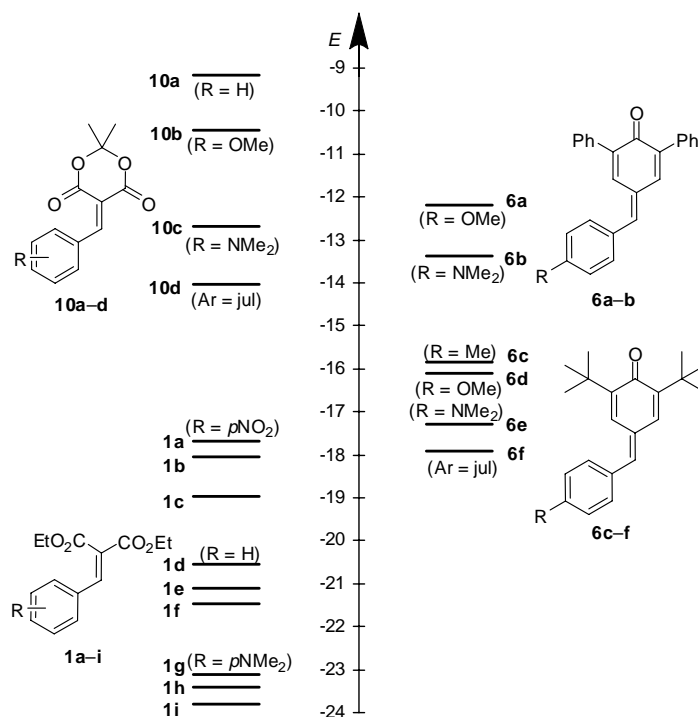


Figure 4.6. Comparison of the electrophilicity parameters E of diethyl benzyldenemalonates **1a–i** with those of some reference electrophiles **6a–f** and benzylidene Meldrum's acids **10a–d**. For “jul”-substituent see **1i** in Scheme 4.1.

According to Figure 4.7, the electrophilicity parameters E for the benzyldenemalonates **1a–i** correlate excellently with Hammett's σ_p -values.³⁸ Comparison with the corresponding Hammett plot for benzylidene Meldrum's acids shows that the electrophilicities of the acyclic Michael acceptors **1a–i** are less affected by substituent variation than the electrophilicities of their cyclic analogues **10a–d**. For reactions with typical amines and carbanions ($s \approx 0.65$, Table 4.1) the slopes given in Figure 4.7 correspond to Hammett reaction constants of $\rho \approx 2.4$ (for **1**) and $\rho \approx 3.5$ (for **10**).

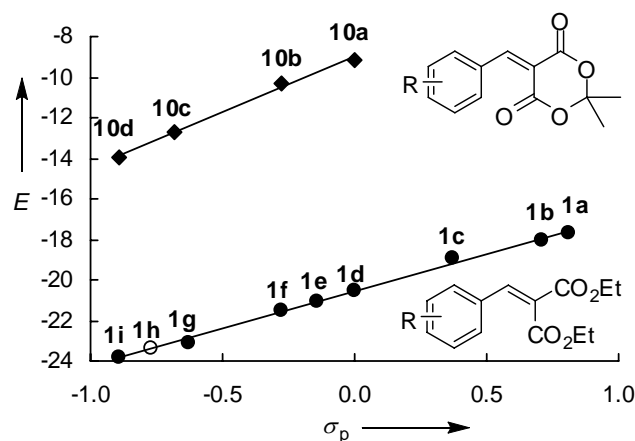


Figure 4.7. Correlation between the electrophilicity parameters E of electrophiles **1a–i** and **10a–d** in DMSO with Hammett's σ_p -values (for **1a–i**: $E = 3.68\sigma_p - 20.57$; for **10a–d**: $E = 5.37\sigma_p - 9.08$). σ_p for “thq” in **1h** has not been reported but is derived from this correlation.

The fact that compound **1i** with the “julolidyl” substituent (definition see Scheme 4.1) fits nicely on this correlation line confirms the validity of the Hammett substituent constant $\sigma_p(\text{jul}) = -0.89$, which has recently been derived from related experiments.¹⁴ Analogously, $\sigma_p(\text{thq}) = -0.77$ can be derived by substituting the E parameter for **1h** into the correlation equation given in Figure 4.7.

Conclusion

Diethyl benzyldenemalonates **1a–i** are more than 10^{10} times less reactive than benzyldene Meldrum's acids **10**, their cyclic counterparts. They extend our electrophilicity scale on the low-reactivity end by more than six orders of magnitude from $-17.7 > E > -23.8$ and are, therefore, recommended as reference electrophiles for determining nucleophilicities of highly reactive nucleophiles with N values of $16 < N < 30$. A report on the use of **1a–i** for the characterization of the anions of arylacetonitriles and arylpropionitriles is in preparation.

General Remarks

Diethyl benzyldenemalonates **1a–i**. Diethyl benzyldenemalonates **1a–i** were prepared following a modified method of Zabicky.²⁷ Diethyl malonate and the corresponding benzaldehyde (1 equiv.) were stirred under reflux in toluene for 3–4 h using piperidine (≈ 10 mol %) as a catalyst. The product formation was followed by TLC. The reaction mixture was consecutively washed with aqueous HCl, aqueous NaHCO₃ solution, and water. After drying the solution, the solvent was evaporated. The residue was either distilled or recrystallized from ethanol to obtain the diethyl benzyldenemalonates. ¹H NMR spectra and melting points for the thus obtained compounds **1a–g** were in agreement with literature reports (see Experimental Section).

Diethyl 2-(1-methyl-1,2,3,4-tetrahydroquinoline-6-ylmethylene)malonate (1h). Diethyl malonate (1.15 g, 7.18 mmol), 6-formyl-1-methyl-1,2,3,4-tetrahydroquinoline (1.26 g, 7.19 mmol) and piperidine (300 μ L) gave a crude product which was washed as described in the general procedure (Experimental Section) and further purified via MPLC (SiO₂, dichloromethane/*isohexane* = 1/1). The fractions were combined, the solvents evaporated in vacuum, and the residue was crystallized from ethanol/*isohexane* at -5 °C: **1h** (1.50 g, 4.7 mmol, 65 %), yellow solid; mp 56.2–56.7 °C. ¹H NMR (DMSO-*d*₆, 400 MHz): δ = 1.22 (t, J = 7.1 Hz, 3 H, CH₃), 1.26 (t, J = 7.1 Hz, 3 H, CH₃), 1.85 (quint, J = 6.3 Hz, 2 H, CH₂), 2.64 (t, J = 6.3 Hz, 2 H, CH₂), 2.92 (s, 3 H, NMe), 3.31 (t, J = 6.3 Hz, 2 H, NCH₂), 4.17 (q, J = 7.1 Hz, 2 H, OCH₂), 4.27 (q, J = 7.1 Hz, 2 H, OCH₂), 6.57 (d, J = 8.7 Hz, 1 H, ArH), 7.02 (s, 1 H, ArH), 7.18 (dd, J = 8.8 Hz, 2.3 Hz, 1 H, ArH), 7.45 ppm (s, 1 H, C=CH). ¹³C NMR (DMSO-*d*₆, 100.6 MHz): δ = 13.7 (q), 14.0 (q), 21.1 (t), 27.0 (t), 38.2 (q, NCH₃), 50.2 (t, NCH₂), 60.5 (t, OCH₂), 60.9 (t, OCH₂), 110.0 (d), 118.1 (s), 118.5 (s), 121.7 (s), 130.1 (d), 130.5 (d), 141.7 (d, =CH), 148.6 (s), 164.2 (s), 167.1 ppm (s). HR-MS: Calcd for C₁₈H₂₃O₄N: 317.1627;

Found 317.1610. Elemental analysis (C₁₈H₂₃O₄N): Calcd: C 68.12 %; H 7.30 %; N 4.41 %. Found C 67.96 %; H 7.28 %; N 4.38 %.

Diethyl 2-((1,2,3,5,6,7-hexahydropyrido[3,2,1-*ij*]quinolin-9-yl)methylene)malonate (1i).

A mixture of 1,2,3,5,6,7-hexahydropyrido[3.2.1-*ij*]quinoline-9-carbaldehyde (1.00 g, 4.98 mmol), diethyl malonate (0.79 g, 4.93 mmol) and piperidine (350 μ L) was stirred in toluene under reflux until TLC indicated full conversion (3 h). After washing the crude reaction mixture as described in the general procedure (Experimental Section), the resulting oily residue was crystallized from EtOAc/*iso*hexane (1:3). The solid was filtered and washed with *iso*hexane: **1i** (1.1 g, 65 %), yellow solid; mp 83.2–83.4 °C. ¹H NMR (CDCl₃, 600 MHz): δ = 1.30 (t, J = 6.2 Hz, 3 H, CH₃), 1.35 (t, J = 6.2 Hz, 3 H, CH₃), 1.93 (quint, J = 6.2 Hz, 2 \times 2 H, CH₂), 2.69 (t, ³ J = 5.6 Hz, 2 \times 2 H, CH₂), 3.23 (t, J = 5.6 Hz, 2 \times 2 H, NCH₂), 4.25 (q, J = 7.2 Hz, 2 H, OCH₂), 4.35 (q, J = 7.2 Hz, 2 H, OCH₂), 6.91 (s, 2 H, ArH), 7.52 ppm (s, 1 H, 1 H, C=CH). ¹³C NMR (CDCl₃, 150 MHz): δ = 14.0 (q), 14.2 (q), 21.4 (t), 27.6 (t), 49.9 (t, NCH₂), 60.9 (t, OCH₂), 61.2 (t, OCH₂), 118.5 (s), 119.0 (s), 120.6 (s), 129.7 (d), 143.0 (d, =CH), 145.2 (s), 165.3 (s), 168.2 ppm (s). HR-MS: Calcd for C₂₀H₂₅O₄N: 343.1784; Found 343.1775. Elemental analysis (C₂₀H₂₅O₄N): Calcd: C 69.95 %; H 7.34 %; N 4.08 %. Found C 69.66 %; H 7.35 %; N 4.09 %.

Procedure for the reactions of electrophiles 1 with nucleophile 2b. **2b-K⁺** (4.0–7.5 mmol) was dissolved in dry DMSO (20 mL), and a solution of **1a–f** (2.0–2.5 mmol) in dry DMSO was added under nitrogen atmosphere. Stirring was continued for 5 h at room temperature, and the solution was diluted with diethyl ether (25 mL). The reaction mixture was then poured on water (50 mL), cooled with ice, and acidified with acetic acid. After extraction with diethyl ether, the combined organic fractions were washed with water and dried over Na₂SO₄. After removal of the solvent under reduced pressure, the crude product was purified by distillation.

Tetraethyl 2-(4-methoxyphenyl)propane-1,1,3,3-tetracarboxylate (5fb). From **1f** (0.56 g, 2.0 mmol) and **2b-K** (0.79 g, 4.0 mmol): **5fb** (0.68 g, 78%), colorless oil; bp 210–220 °C (1.3×10^{-2} bar). ^1H NMR (300 MHz, CDCl_3): $\delta = 1.04$ (t, $J = 7.1$ Hz, 2×3 H, CH_3), 1.23 (t, $J = 7.1$ Hz, 2×3 H, CH_3), 3.75 (s, 3 H, OCH_3), 3.95 (q, $J = 7.1$ Hz, 2×2 H, OCH_2), 4.04–4.18 (m, 7 H), 6.76–6.79 ppm (m, 2 H, ArH), 7.24–7.27 (m, 2 H, ArH). ^{13}C NMR (75.5 MHz, CDCl_3): $\delta = 13.6$ (q), 13.8 (q), 43.0 (d, C^b), 54.9 (q, OCH_3), 55.1 (d, C^a), 61.1 (t), 61.4 (t), 113.1 (d), 129.0 (s), 130.4 (d), 158.7 (s), 167.4 (s), 167.9 ppm (s); the NMR chemical shifts are in agreement with the data reported in ref. 26

Kinetics. For fast kinetic experiments ($\tau_{1/2} < 15$ s), standard stopped-flow UV-Vis-spectrophotometer systems were used in their single mixing mode. Solutions of the electrophiles **1** in DMSO were mixed with solutions of the carbanions **2** in DMSO (either generated by deprotonation of **2-H** with 1.05 equiv. $\text{KO}t\text{Bu}$ in DMSO or by dissolving **2-K⁺** in DMSO). **CAUTION: Because of explosion hazards, the isolation of 2a-K⁺ should be avoided.**³⁹ We therefore recommend generating **2a** in situ from the corresponding CH acid **2a-H**. Kinetics of slow reactions ($\tau_{1/2} > 15$ s) were determined by UV-Vis spectrometry using a J&M TIDAS diode array spectrophotometer. In order to obtain pseudo-first order kinetics, the carbanions **2** were used in large excess (10 to 100 equivalents) over the electrophiles (except for kinetics with nucleophile **2e**, which was used as minor component, see footnote on page 3). The temperature of the solutions was kept constant (20 ± 0.1 °C) by using circulating bath thermostats. Rate constants k_{obs} (s^{-1}) were obtained by fitting the single exponential $A_t = A_0 \exp(-k_{\text{obs}}t) + C$ to the observed time-dependent electrophile absorbance (the evaluated wavelengths are given in the Experimental Section). As depicted in the Experimental Section, the second-order rate constants k_2 (Table 4.3) were obtained from the slopes of the linear plots of k_{obs} versus the carbanion concentrations [2].

References

- (1) Mayr, H.; Bug, T.; Gotta, M. F.; Hering, N.; Irrgang, B.; Janker, B.; Kempf, B.; Loos, R.; Ofial, A. R.; Remennikov, G.; Schimmel, H. *J. Am. Chem. Soc.* **2001**, *123*, 9500-9512.
- (2) Mayr, H.; Kempf, B.; Ofial, A. R. *Acc. Chem. Res.* **2003**, *36*, 66-77.
- (3) a) Mayr, H.; Ofial, A. R. *Pure Appl. Chem.* **2005**, *77*, 1807-1821; b) Dilman, A. D.; Mayr, H. *Eur. J. Org. Chem.* **2005**, 1760-1764; c) Lakhdar, S.; Westermaier, M.; Terrier, F.; Goumont, R.; Boubaker, T.; Ofial, A. R.; Mayr, H. *J. Org. Chem.* **2006**, *71*, 9088-9095; d) Nigst, T. A.; Westermaier, M.; Ofial, A. R.; Mayr, H. *Eur. J. Org. Chem.* **2008**, 2369-2374.
- (4) a) Phan, T. B.; Mayr, H. *Can. J. Chem.* **2005**, *83*, 1554-1560; b) Minegishi, S.; Mayr, H. *J. Am. Chem. Soc.* **2003**, *125*, 286-295; c) Brotzel, F.; Chu, Y. C.; Mayr, H. *J. Org. Chem.* **2007**, *72*, 3679-3688; d) Brotzel, F.; Kempf, B.; Singer, T.; Zipse, H.; Mayr, H. *Chem. Eur. J.* **2007**, *13*, 336-345; e) Brotzel, F.; Mayr, H. *Org. Biomol. Chem.* **2007**, *5*, 3814-3820; f) Minegishi, S.; Kobayashi, S.; Mayr, H. *J. Am. Chem. Soc.* **2004**, *126*, 5174-5181.
- (5) Baidya, M.; Mayr, H. *Chem. Commun.* **2008**, 1792-1794.
- (6) Baidya, M.; Kobayashi, S.; Brotzel, F.; Schmidhammer, U.; Riedle, E.; Mayr, H. *Angew. Chem.* **2007**, *119*, 6288-6292; *Angew. Chem. Int. Ed.* **2007**, *46*, 6176-6179.
- (7) a) Lucius, R.; Mayr, H. *Angew. Chem.* **2000**, *112*, 2086-2089; *Angew. Chem., Int. Ed.* **2000**, *39*, 1995-1997; b) Bug, T.; Mayr, H. *J. Am. Chem. Soc.* **2003**, *125*, 12980-12986; c) Bug, T.; Lemek, T.; Mayr, H. *J. Org. Chem.* **2004**, *69*, 7565-7576; d) Phan, T. B.; Mayr, H. *Eur. J. Org. Chem.* **2006**, 2530-2537; e) Berger, S. T. A.; Ofial, A. R.; Mayr, H. *J. Am. Chem. Soc.* **2007**, *129*, 9753-9761; f) Seeliger, F.; Mayr, H. *Org. Biomol. Chem.* **2008**, *6*, 3052-3058; g)

- Seeliger, F.; Blazej, S.; Bernhardt, S.; Makosza, M.; Mayr, H. *Chem. Eur. J.* **2008**, *14*, 6108-6118.
- (8) Lucius, R.; Loos, R.; Mayr, H. *Angew. Chem.* **2002**, *114*, 97–102; *Angew. Chem., Int. Ed.* **2002**, *41*, 91–95.
- (9) Dulich, F.; Müller, K.-H.; Ofial, A. R.; Mayr, H. *Helv. Chim. Acta* **2005**, *88*, 1754-1768.
- (10) a) Mayr, H.; Lang, G.; Ofial, A. R. *J. Am. Chem. Soc.* **2002**, *124*, 4076-4083; b) Funke, M.-A.; Mayr, H. *Chem. Eur. J.* **1997**, *3*, 1214-1222.
- (11) Lemek, T.; Mayr, H. *J. Org. Chem.* **2003**, *68*, 6880-6886.
- (12) Berger, S. T. A.; Seeliger, F. H.; Hofbauer, F.; Mayr, H. *Org. Biomol. Chem.* **2007**, *5*, 3020-3026.
- (13) Seeliger, F.; Berger, S. T. A.; Remennikov, G. Y.; Polborn, K.; Mayr, H. *J. Org. Chem.* **2007**, *72*, 9170-9180.
- (14) Kaumanns, O.; Mayr, H. *J. Org. Chem.* **2008**, *73*, 2738-2745.
- (15) a) Oh, H. K.; Lee, J. M.; Sung, D. D.; Lee, I. *J. Org. Chem.* **2005**, *70*, 3089-3093; b) Oh, H. K.; Lee, J. M. *Bull. Korean Chem. Soc.* **2002**, *23*, 1459-1462.
- (16) Oh, H. K.; Kim, I. K.; Lee, H. W.; Lee, I. *J. Org. Chem.* **2004**, *69*, 3806-3810.
- (17) Oh, H. K.; Yang, J. H.; Lee, H. W.; Lee, I. *J. Org. Chem.* **2000**, *65*, 2188-2191.
- (18) Oh, H. K.; Kim, T. S.; Lee, H. W.; Lee, I. *Bull. Korean Chem. Soc.* **2003**, *24*, 193-196.
- (19) Oh, H. K.; Yang, J. H.; Lee, H. W.; Lee, I. *J. Org. Chem.* **2000**, *65*, 5391-5395.
- (20) Arnett, E. M.; Harrelson, J. A., Jr. *J. Am. Chem. Soc.* **1987**, *109*, 809-812.
- (21) a) Wang, X.; Houk, K. N. *J. Am. Chem. Soc.* **1988**, *110*, 1870-1872; b) Wiberg, K. B.; Laidig, K. E. *J. Am. Chem. Soc.* **1988**, *110*, 1872-1874.
- (22) Cavicchioli, M.; Marat, X.; Monteiro, N.; Hartmann, B.; Balme, G. *Tetrahedron Lett.* **2002**, *43*, 2609-2611.

- (23) Buchanan, D. J.; Dixon, D. J.; Hernandez-Juan, F. A. *Org. Lett.* **2004**, *6*, 1357-1360.
- (24) a) Betancort, J. M.; Sakthivel, K.; Thayumanavan, R.; Barbas III, C. F. *Tetrahedron Lett.* **2001**, *42*, 4441-4444; b) Cao, C.-L.; Sun, X.-L.; Zhou, J.-L.; Tang, Y. *J. Org. Chem.* **2007**, *72*, 4073-4076.
- (25) a) Zhou, J.; Tang, Y. *J. Am. Chem. Soc.* **2002**, *124*, 9030-9031; b) Zhuang, W.; Hansen, T.; Jørgensen, K. A. *Chem. Commun.* **2001**, 347-348; c) Zhou, J.; Ye, M.-C.; Huang, Z.-Z.; Tang, Y. *J. Org. Chem.* **2004**, *69*, 1309-1320.
- (26) Fan, R.; Wang, W.; Pu, D.; Wu, J. *J. Org. Chem.* **2007**, *72*, 5905-5907.
- (27) Zabicky, J. *J. Chem. Soc.* **1961**, 683-687.
- (28) a) Moskvina, A. V.; Korsakov, M. V.; Smorygo, N. A.; Ivin, B. A. *Zh. Obshch. Khim.* **1984**, *54*, 2223-2237; b) Moskvina, A. V.; Korsakov, M. V.; Smorygo, N. A.; Ivin, B. A. *Russ. J. Gen. Chem.* **1985**, 1987-2000.
- (29) Berger, S. T. A.; Lemek, T.; Mayr, H. *ARKIVOC* **2008**, (x), 37-53.
- (30) Bordwell, F. G.; Fried, H. E. *J. Org. Chem.* **1981**, *46*, 4327-4331.
- (31) Olmstead, W. N.; Bordwell, F. G. *J. Org. Chem.* **1980**, *45*, 3299-3305.
- (32) a) Lakhdar, S.; Goumont, R.; Berionni, G.; Boubaker, T.; Kurbatov, S.; Terrier, F. *Chem. Eur. J.* **2007**, *13*, 8317-8324; b) Crampton, M. R. *J. Chem. Soc. Perkin Trans. 2* **1973**, 2157-2162; c) Bernasconi, C. F.; DeRossi, R. H. *J. Org. Chem.* **1973**, *38*, 500-507; d) Bernasconi, C. F.; Cross, H. S. *J. Org. Chem.* **1974**, *39*, 1054-1058; e) Bernasconi, C. F.; Terrier, F. *J. Am. Chem. Soc.* **1975**, *97*, 7458-7466.
- (33) Schmid, R.; Sapunov, V. N. *Non-Formal Kinetics*; Verlag Chemie: Weinheim, 1982.
- (34) a) Marcus, R. A. *J. Phys. Chem.* **1968**, *72*, 891-899; b) Albery, W. J. *Annu. Rev. Phys. Chem.* **1980**, *31*, 227-263.

- (35) Bordwell, F. G.; Satish, A. V. *J. Am. Chem. Soc.* **1994**, *116*, 8885-8889.
- (36) Bordwell, F. G. *Acc. Chem. Res.* **1988**, *21*, 456-463.
- (37) Matthews, W. S.; Bares, J. E.; Bartmess, J. E.; Bordwell, F. G.; Cornforth, F. J.; Drucker, G. E.; Margolin, Z.; McCallum, R. J.; McCollum, G. J.; Vanier, N. *R. J. Am. Chem. Soc.* **1975**, *97*, 7006-7014.
- (38) Exner, O. *Correlation Analysis of Chemical Data*; Plenum New York, 1988.
- (39) Bretherick, L. *Bretherick's Handbook of Reactive Chemical Hazards. 4th Ed*; Urban, P., 1990.

Experimental Section

Determination of the Electrophilicity Parameters of Diethyl Benzylidenemalonates in DMSO: Reference Electrophiles for Characterizing Strong Nucleophiles

O. Kaumanns, R. Lucius, and H. Mayr, *Chem. Eur. J.* **2008**, *14*, 9675-9682.

4.1. Materials

General. Commercially available DMSO (content of H₂O < 50 ppm) was used without further purification. Stock solutions of KO^tBu in DMSO were prepared under nitrogen atmosphere. The employed potassium salts **2a–d** and **2f** were prepared by dissolving the corresponding CH-acid in dry ethanol and subsequent addition of 0.9 equiv. of potassium KO^tBu dissolved in dry ethanol. The potassium salts **2a–d** and **2f** precipitated from the reaction mixture. After filtration, they were dried under reduced pressure. The anion of *bis*(*p*-nitrophenyl)methane (**2e**) was prepared following the procedure described in Ref. 29

CAUTION: Because of explosion hazards the isolation of 2a–K should be avoided!

4.2. Instruments

¹H and ¹³C NMR spectra were recorded on Varian Inova 400 (400 MHz, 100.6 MHz), Bruker ARX 300 (300 MHz, 75.5 MHz), or Varian Mercury 200 (200 MHz) NMR spectrometers. Chemical shifts are expressed in ppm and refer to DMSO-*d*₆ (δ_{H} 2.49, δ_{C} 39.7) or to CDCl₃ (δ_{H} 7.26, δ_{C} 77.0). The coupling constants are in Hz. Abbreviations used are s (singlet), d (doublet), t (triplet), q (quartet), quint (quintet), m (multiplet).

4.3. Determination of Rate Constants

The general method for the determination of the rate constants is described in the experimental part of the paper.

The temperature of the solutions was kept constant (20 ± 0.1 °C) during all kinetic experiments by using a circulating bath thermostat.

For evaluation of fast kinetic experiments commercial stopped-flow UV-Vis spectrometer systems were used. UV-Vis kinetics of slow reactions were determined by using a diode array spectrophotometer, which was connected to a quartz suprasil immersion probe (5 mm light path). Rate constants k_{obs} (s^{-1}) were obtained by fitting the single exponential function $A_t = A_0 \exp(-k_{\text{obs}} t) + C$ to the observed time-dependent electrophile absorbance. (For the reactions of **1a–c** with the green dinitrobenzhydryl anion **2e-K⁺** the first-order rate constants k_{obs} were determined with **2e-K⁺** as the minor component). Plotting the k_{obs} against the concentrations of the nucleophiles resulted in linear correlations whose slopes correspond to the second-order rate constants k_2 ($\text{L mol}^{-1} \text{s}^{-1}$). For stopped-flow experiments two stock solutions were used: A solution of electrophiles **1a–i** in DMSO and a solution of the carbanion **2**, which was either generated by deprotonation of the corresponding parent compound **2–H** with 1.05 equiv. KO^tBu in DMSO *in situ* directly before use, or by using the preformed carbanion **2** (potassium salt) in DMSO.

As the kinetic measurements performed by Dr. Roland Lucius are of significant importance for the understanding of the main text, his contributions are stated in *italics*.

Figure S1 shows that the reaction of electrophile **1b** with the carbanion **2c** was followed at $\lambda = 290$ nm. The decay of the absorption of **1b** was accompanied by a development of an absorption band at $\lambda \approx 360$ nm.

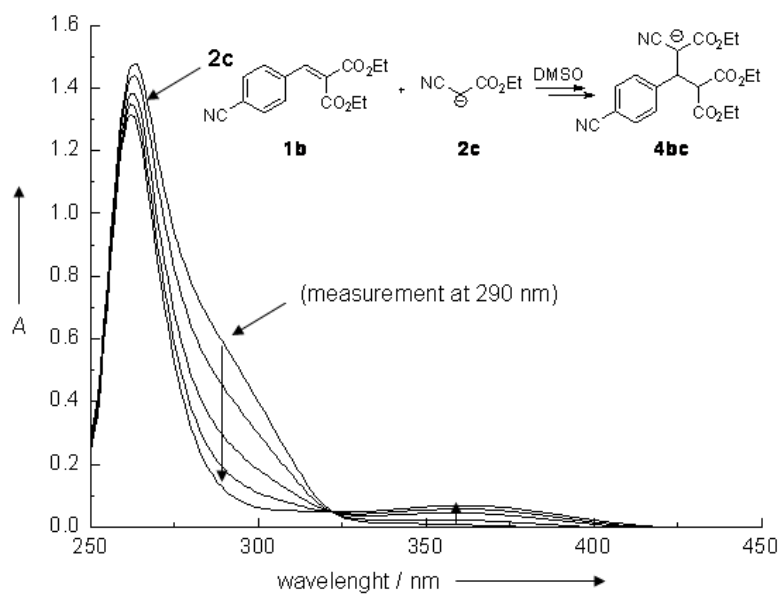


Figure S1: UV-Vis spectra during the reaction of electrophile **1b** ($c_0 = 4.12 \times 10^{-5} \text{ mol L}^{-1}$) with the carbanion **2c** ($c_0 = 3.57 \times 10^{-5} \text{ mol L}^{-1}$) in DMSO at 20 °C from an individual measurement.

4.4.1 Determination of Equilibrium Constants

The equilibrium constants K are based on the Equation (S1) by using the initial absorptions A from the electrophiles **1e** and **1f** and the equilibrium absorptions after addition of carbanion **2b** at 20 °C in DMSO. It has to be mentioned that the employed values are derived from the kinetic measurements and are not the result from individual titration experiments.

From the initial concentrations, $[E]_0$ and $[C^-]_0$, and the absorbance of the electrophile ($A = \varepsilon[E]d$), the equilibrium concentrations $[E]_{eq}$, and $[C^-]_{eq}$ were calculated. Substitution into Equation (S1) yielded the equilibrium constants K listed in Table S1 and S2. The equilibrium constants K presented herein are based only on the kinetic measurements and have not been repeated.

$$K = \frac{[adduct]_{eq}}{[E]_{eq}[Nu^-]_{eq}} = \frac{[E]_0 - [E]_{eq}}{[E]_{eq}([Nu^-]_0 - [E]_0 + [E]_{eq})} \quad (S1)$$

Table S1: Equilibrium constant for the reaction of **1e** with **2b** (DMSO, 20 °C)

No.	$[1e]_0 / M$	$[2b-K]_0 / M$	A_0	A_{eq}	$[1e]_{eq} / M$	$[2b-K]_{eq} / M$	K / M^{-1}
1	9.98×10^{-5}	1.79×10^{-3}	0.788	0.377	4.78×10^{-5}	1.74×10^{-3}	6.26×10^2
2	9.71×10^{-5}	2.52×10^{-3}	0.768	0.309	3.99×10^{-5}	2.46×10^{-3}	5.83×10^2
3	1.06×10^{-4}	4.13×10^{-3}	0.851	0.268	3.42×10^{-5}	4.06×10^{-3}	5.15×10^2
4	1.06×10^{-4}	4.72×10^{-3}	0.857	0.250	3.19×10^{-5}	4.65×10^{-3}	4.98×10^2
5	1.12×10^{-4}	6.61×10^{-3}	0.902	0.227	2.95×10^{-5}	6.52×10^{-3}	4.31×10^2

$$K = 5.31 \times 10^2 M^{-1}$$

$$\log K = (2.72 \pm 0.09)$$

Table S2: Equilibrium constant for the reaction of **1f** with **2b** (DMSO, 20 °C)

No.	$[1f]_0 / M$	$[2b-K]_0 / M$	A_0	A_{eq}	$[1f]_{eq} / M$	$[2b-K]_{eq} / M$	K / M^{-1}
1	7.95×10^{-5}	1.53×10^{-3}	0.95	0.67	5.60×10^{-5}	1.51×10^{-3}	2.77×10^2
2	9.64×10^{-5}	3.98×10^{-3}	1.14	0.59	4.98×10^{-5}	3.93×10^{-3}	2.38×10^2
3	9.52×10^{-5}	5.51×10^{-3}	1.13	0.50	4.21×10^{-5}	5.46×10^{-3}	2.31×10^2
4	9.20×10^{-5}	7.42×10^{-3}	1.13	0.43	3.47×10^{-5}	7.36×10^{-3}	2.25×10^2
5	9.04×10^{-5}	9.23×10^{-3}	1.07	0.38	3.20×10^{-5}	9.17×10^{-3}	1.99×10^2

$$K = 2.34 \times 10^2 M^{-1}$$

$$\log K = (2.37 \pm 0.08)$$

4.4.2 Determination of the Molar Decadic Absorption Coefficients ϵ in DMSO

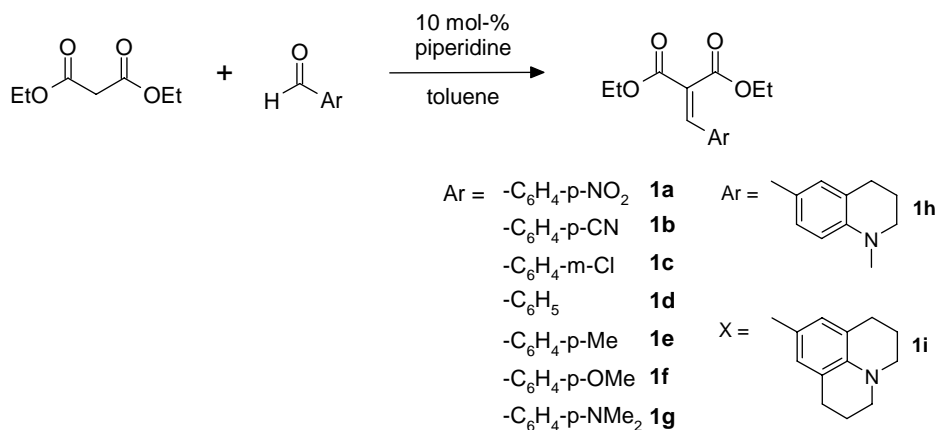
In order to determine the molar decadic absorption coefficients ϵ of electrophiles **1a–i** in DMSO, the absorption coefficients ϵ of the electrophiles **1a–i** were calculated at the absorption maximum on the basis of the Lambert–Beer law $A_{\max} = \epsilon c d$ (Table S3). UV–Vis spectra were recorded on a JASCO V–630 spectrometer using a cell of $d = 1$ cm.

Table S3: Molar decadic absorption coefficients ϵ ($\text{L mol}^{-1} \text{cm}^{-1}$) of **1a–i** (DMSO, 20 °C).

electrophile	[1] / mol L^{-1}	A_{\max} (λ_{\max} / nm)	ϵ_{\max} [$\text{L mol}^{-1} \text{cm}^{-1}$]
1a	3.66×10^{-5}	0.63 (302)	1.72×10^4
1b	5.98×10^{-5}	1.35 (283)	2.25×10^4
1c	2.93×10^{-5}	0.51 (277)	1.73×10^4
1d	5.65×10^{-5}	0.93 (283)	1.65×10^4
1e	4.52×10^{-5}	0.94 (295)	2.07×10^4
1f	4.53×10^{-5}	1.14 (316)	2.51×10^4
1g	3.05×10^{-5}	1.05 (383)	3.28×10^4
1h	3.64×10^{-5}	1.23 (395)	3.37×10^4
1i	2.93×10^{-5}	0.95 (407)	3.24×10^4

4.5. Synthesis of Diethyl Benzylidenemalonates

Diethyl benzylidenemalonates **1a–i** were prepared according to the protocol by Zabicky (Scheme S1, ref. S6).



Scheme S1: Synthesis of electrophiles **1a–i** from diethyl malonate and the corresponding aldehyde via Knoevenagel condensation in toluene.

General Procedure. Diethyl malonate and the corresponding arylaldehyde (1 equiv.) were stirred under reflux in toluene for several hours using piperidine (≈ 10 mol-%) as catalyst. The product formation was followed by TLC. The reaction mixture was consecutively washed with aqueous HCl, aqueous NaHCO_3 solution, and water. After drying the solution, the solvent was evaporated. The residue was either distilled (when liquid) or recrystallized from ethanol (when solid) to obtain the purified diethyl benzylidenemalonates. NMR spectra and melting points for the thus obtained compounds **1a–g** were in agreement with literature values.

Diethyl 2-(4-nitro-benzylidene)malonate (1a). From diethyl malonate (16 mmol) and 4-nitrobenzaldehyde: **1a** (3.61 g, 77 %), colorless needles; mp 89.3–89.8 °C (88 °C, ref. S1) ^1H NMR (CDCl_3 , 200 MHz): $\delta = 1.28$ (t, $J = 7.1$ Hz, 3 H, CH_3), 1.35 (t, $J = 7.1$ Hz, 3 H, CH_3), 4.33 (q, $J = 7.1$ Hz, 4 H, OCH_2), 7.60 (d, $J = 8.4$ Hz, 2 H, ArH), 7.75 ppm (s, 1 H, =CH), 8.23 (d, $J = 8.4$ Hz, 2 H, ArH); in agreement with ref. S1.

^{S1} F. Delgado, J. Tamariz, G. Zepeda, M. Landa, R. Miranda, J. Garcia, *Synth. Commun.* **1995**, *25*, 753–759.

Diethyl 2-(4-cyano-benzylidene)malonate (1b). From diethyl malonate (39 mmol) and 4-cyanobenzaldehyde: **1b** (6.82 g, 64 %), yellow needles; mp 72-73 °C (73°C, ref. S2). ¹H NMR (CDCl₃, 200 MHz): δ = 1.27 (t, J = 7.1 Hz, 3 H, CH₃), 1.33 (t, J = 7.1 Hz, 3 H, CH₃), 4.31 (q, J = 7.1 Hz, 4 H, OCH₂), 7.53 (d, J = 8.2 Hz, 2 H, ArH), 7.66 (d, J = 8.2 Hz, 2 H, ArH), 7.70 ppm (s, 1 H, =CH).

Diethyl 2-(3-chloro-benzylidene)malonate (1c). From diethyl malonate (39 mmol) and 3-chlorobenzaldehyde: **1c** (5.42 g, 50 %), colorless oil; bp 130–134 °C, (8×10^{-3} mbar). ¹H NMR (CDCl₃, 200 MHz): δ = 1.26 (t, J = 7.0 Hz, 3 H, CH₃), 1.33 (t, J = 7.0 Hz, 3 H, CH₃), 4.30 (q, J = 7.0 Hz, 2 H, OCH₂), 4.34 (q, J = 7.0 Hz, 2 H, OCH₂), 7.30–7.65 (m, 4 H, ArH), 7.65 ppm (s, 1 H, =CH); in agreement with ref. S3.

Diethyl 2-benzylidenemalonate (1d). From diethyl malonate (58 mmol) and benzaldehyde: **1d** (11.2 g, 78 %), colorless oil which crystallized slowly; mp: 31.0-31.2 °C; ¹H-NMR (CDCl₃, 200 MHz): δ = 1.26 (t, J = 7.2 Hz, 3 H, CH₃), 1.31 (t, J = 7.2 Hz, 3 H, CH₃), 4.26 (q, J = 7.2 Hz, 2 H, OCH₂), 4.32 (q, J = 7.2 Hz, 2 H, OCH₂), 7.26–7.46 (m, 5 H, ArH), 7.72 ppm (s, 1 H, =CH), in agreement with ref. S1.

Diethyl 2-(4-methyl-benzylidene)malonate (1e). From diethyl malonate (68 mmol) and 4-methylbenzaldehyde after crystallization of the crude product from ethyl acetate/petrol ether (2/8) at –32 °C: **1e** (6.91 g, 39 %), colorless solid; mp 47 °C (49–50°C, ref.^[S2]). ¹H NMR (CDCl₃, 200 MHz): δ = 1.29 (t, J = 7.1 Hz, 3 H, CH₃), 1.34 (t, J = 7.1 Hz, 3 H, CH₃), 2.36 (s, 3 H, 4-CH₃), 4.29, 4.34 (2q, J = 7.1 Hz, 2 \times 2 H, OCH₂CH₃), 7.17 (d, J = 7.9 Hz, 2 H, ArH), 7.35 (d, J = 7.9 Hz, 2 H, ArH), 7.70 ppm (s, 1 H, =CH); in agreement with ref. S4.

Diethyl 2-(4-methoxybenzylidene)malonate (1f). Diethyl malonate (84 mmol) and 4-methoxybenzaldehyde produced a crude product which after distillation (130 °C / 4×10^{-3} mbar) slowly crystallized: **1f** (12.5 g, 53%), solid; mp 38-39 °C (38-40°C, ref S5). ¹H NMR (CDCl₃, 200 MHz): δ = 1.29–1.36 (m, 6 H, 2 \times CH₃), 3.84 (s, OCH₃), 4.27, 4.38 (2q, J = 7.2 Hz, 2 \times 2 H, OCH₂CH₃), 6.89 (d, J = 8.8 Hz, 2 H, ArH), 7.42 (d, J = 8.8 Hz, 2 H, ArCH), 7.67 ppm (s, 1 H, =CH); in agreement with ref. S1.

^{S2} G. Deng, J. Yu, X. Yang, H. Xu, *Tetrahedron*, **1990**, *46*, 5967-5974.

^{S3} W. M. Phillips, D. J. Currie, *Can. J. Chem.*, **1969**, *47*, 3137-3146.

^{S4} J. K. Kim, P. S. Kwon, T. W. Kwon, S. K. Chung, J. W. Lee, *Synth. Commun.*, **1996**, *26*, 535-542.

^{S5} P. E. Papadakis, L. M. Hall, R. L. Augustine, *J. Org. Chem.*, **1958**, *23*, 123.

Diethyl 2-(4-dimethylamino-benzylidene)malonate (1g). From diethyl malonate (34 mmol) and 4-(dimethylamino)benzaldehyde: **1g** (3.90 g, 39 %), yellow plates; mp 112.1-112.5 °C (from EtOH), in agreement with ref. S6. ¹H NMR (CDCl₃, 200 MHz): δ = 1.30 (t, J = 7.0 Hz, 3 H, CH₃), 1.34 (t, J = 7.0 Hz, 3 H, CH₃), 3.01 (s, 6 H, NMe₂), 4.26 (q, J = 7.0 Hz, 2 H, OCH₂), 4.37 (q, J = 7.0 Hz, 2 H, OCH₂), 6.62 (d, J = 9.0 Hz, 2 H, ArH), 7.48 (d, J = 9.0 Hz, 2 H, ArH), 7.62 ppm (s, 1 H, =CH); in agreement with ref. S1

Diethyl 2-(1-methyl-1,2,3,4-tetrahydroquinoline-6-ylmethylene)malonate (1h). Diethyl malonate (1.15 g, 7.18 mmol), 6-formyl-1-methyl-1,2,3,4-tetrahydroquinoline (1.26 g, 7.19 mmol) and piperidine (300 μ L) gave a crude product which was washed as described in the general procedure (Experimental Section) and further purified via MPLC (silica gel, dichloromethane/*isohexane* = 1/1). The fractions were combined, the solvents evaporated in vacuum, and the residue was crystallized from ethanol/*isohexane* at -5°C: **1h** (1.50 g, 4.7 mmol, 65 %), yellow solid; mp 56.2-56.7 °C. ¹H NMR (DMSO-*d*₆, 400 MHz): δ = 1.22 (t, J = 7.1 Hz, 3 H, CH₃), 1.26 (t, J = 7.1 Hz, 3 H, CH₃), 1.85 (quint, J = 6.3 Hz, 2 H, CH₂), 2.64 (t, J = 6.3 Hz, 2 H, CH₂), 2.92 (s, 3 H, NMe), 3.31 (t, J = 6.3 Hz, 2 H, NCH₂), 4.17 (q, J = 7.1 Hz, 2 H, OCH₂), 4.27 (q, J = 7.1 Hz, 2 H, OCH₂), 6.57 (d, J = 8.7 Hz, 1 H, ArH), 7.02 (s, 1 H, ArH), 7.18 (dd, J = 8.8 Hz, 2.3 Hz, 1 H, ArH), 7.45 ppm (s, 1 H, C=CH). ¹³C NMR (DMSO-*d*₆, 100.6 MHz): δ = 13.7 (q), 14.0 (q), 21.1 (t), 27.0 (t), 38.2 (q, NCH₃), 50.2 (t, NCH₂), 60.5 (t, OCH₂), 60.9 (t, OCH₂), 110.0 (d), 118.1 (s), 118.5 (s), 121.7 (s), 130.1 (d), 130.5 (d), 141.7 (d, =CH), 148.6 (s), 164.2 (s), 167.1 ppm (s). HR-MS: Calcd for C₁₈H₂₃O₄N: 317.1627; Found 317.1610. Elemental analysis (C₁₈H₂₃O₄N): Calcd: C 68.12 %; H 7.30 %; N 4.41 %. Found C 67.96 %; H 7.28 %; N 4.38 %.

Diethyl 2-((1,2,3,5,6,7-hexahydropyrido[3,2,1-*ij*]quinolin-9-yl)methylene)malonate (1i). A mixture of 1,2,3,5,6,7-hexahydropyrido[3.2.1-*ij*]quinoline-9-carbaldehyde (1.00 g, 4.98 mmol), diethyl malonate (0.79 g, 4.93 mmol) and piperidine (350 μ L) was stirred in toluene under reflux until TLC indicated full conversion (3 h). After washing the crude reaction mixture as described in the general procedure (Experimental Section), the resulting oily residue was crystallized from EtOAc/*isohexane* (1:3). The solid was filtered and washed with *isohexane*: **1i** (1.1 g, 65 %), yellow solid; mp 83.2-83.4 °C. ¹H NMR (CDCl₃, 600 MHz): δ = 1.30 (t, J = 6.2 Hz, 3 H, CH₃), 1.35 (t, J = 6.2 Hz, 3 H, CH₃), 1.93 (quint, J = 6.2 Hz, 2 \times 2 H,

^{S6} J. Zabicky, *J. Chem. Soc.* **1961**, 683-687.

CH₂), 2.69 (t, ³J = 5.6 Hz, 2 × 2 H, CH₂), 3.23 (t, J = 5.6 Hz, 2 × 2 H, NCH₂), 4.25 (q, J = 7.2 Hz, 2 H, OCH₂), 4.35 (q, J = 7.2 Hz, 2 H, OCH₂), 6.91 (s, 2 H, ArH), 7.52 ppm (s, 1 H, 1 H, C=CH). ¹³C NMR (CDCl₃, 150 MHz): δ = 14.0 (q), 14.2 (q), 21.4 (t), 27.6 (t), 49.9 (t, NCH₂), 60.9 (t, OCH₂), 61.2 (t, OCH₂), 118.5 (s), 119.0 (s), 120.6 (s), 129.7 (d), 143.0 (d, =CH), 145.2 (s), 165.3 (s), 168.2 ppm (s). HR-MS: Calcd for C₂₀H₂₅O₄N: 343.1784; Found 343.1775. Elemental analysis (C₂₀H₂₅O₄N): Calcd: C 69.95 %; H 7.34 %; N 4.08 %. Found C 69.66 %; H 7.35 %; N 4.09 %.

4.6. Product Studies

Reactions of **2c-K** with Diethyl Benzylidenemalonates **1**

General Procedure. Equimolar amounts of **2c-K** and an electrophile **1** were mixed and stirred in dry DMSO-*d*₆ (3–5 mL). After 5 min samples were taken and analyzed by NMR spectroscopy. Samples for MS were obtained by mixing equimolar amounts (0.2–0.5 mmol) of **2c-K** and **1** in dry EtOH (2 mL).

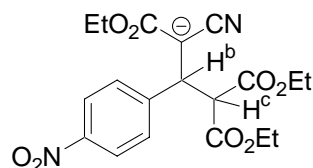
2-Cyano-1,5-diethoxy-4-(ethoxycarbonyl)-3-(4-nitrophenyl)-1,5-dioxopentan-2-yl) potassium (**4ac**).

Mixture of two tautomers (3:1)

Major tautomer

¹H NMR (DMSO-*d*₆, 400 MHz): δ = 0.87 (t, *J* = 7.1 Hz, 3 H, CH₃), 0.99 (t, *J* = 7.1 Hz, 3 H, CH₃), 1.16 (t, *J* = 7.1 Hz, 3 H, CH₃), 3.67–3.87 (m, 2 × 2 H, OCH₂), 4.05 (d, *J* = 12.3 Hz, 1 H, CH^b), 4.12–4.24 (m, 2 H, OCH₂), 4.22 (d, *J* = 12.4 Hz, 1 H, CH), 7.40 (d, *J* = 8.8 Hz, 2 H, ArH), 8.08 ppm (d, *J* = 8.8 Hz, 2 H, ArH). ¹³C NMR (DMSO-*d*₆, 100 MHz): δ = 13.5 (q), 13.7 (q), 15.3 (q), 42.6 (d, C^b), 47.4 (s, C⁻), 55.4 (d, C^c), 55.7 (t), 60.3 (t), 60.4 (t), 122.9 (d), 127.5 (d), 128.6 (s), 145.0 (s), 153.6 (s), 167.1 (s), 167.7 (s), 168.5 (s). MS (ESI, negative) *m/z* (%): 406.13 (15), 405.13 (100), 191.12 (7), 257.08 ppm (10).

Peak assignment in analogy to the neutral compound **4ac-H** from ref. S7



2-Cyano-3-(4-cyanophenyl)-1,5-diethoxy-4-(ethoxycarbonyl)-1,5-dioxopentan-2-yl) potassium (**4bc**).

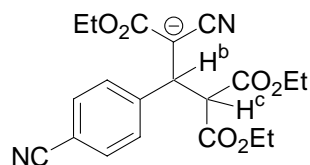
Mixture of two tautomers (3:1)

NMR spectra refer to the major tautomer

¹H NMR (DMSO-*d*₆, 400 MHz): δ = 0.86–0.89 (m, 3 H, CH₃), 0.98–1.01 (m, 3 H, CH₃), 1.15–1.18 (m, 3 H, CH₃), 3.72–3.82 (m, 2 × 2 H, OCH₂), 4.02–4.18 (m, 4 H), 7.35 (d, *J* = 8.0 Hz, 2 H, ArH), 7.63–7.65 ppm (m, 2 H, ArH). ¹³C NMR (DMSO-*d*₆, 100 MHz): δ = 13.3 (q), 13.5 (q), 15.1 (q), 42.6 (d, C^b), 47.2 (s, C⁻), 55.4 (d, C^c), 55.5 (t), 60.1 (t), 60.2 (t), 107.4 (s,

^{S7} G. Manickam, G. Sundararajan, *Tetrahedron*, **1999**, *55*, 2721–2736.

Ar-CN), 118.9 (s), 127.4 (d), 128.6 (s, C^a-CN), 131.3 (d), 151.1 (s), 166.9 (s), 167.5 (s), 168.3 ppm (s). MS (ESI, negative) *m/z* (%): 385.14 (100, C₂₀H₂₁O₆N₂).

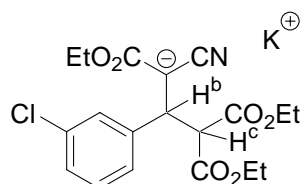


3-(3-Chlorophenyl)-2-cyano-1,5-diethoxy-4-(ethoxycarbonyl)-1,5-dioxopentan-2-yl) potassium (4cc).

Mixture of two tautomers

NMR spectra refer to the major tautomer

¹H NMR (DMSO-*d*₆, 400 MHz): δ = 0.87 (t, *J* = 7.1 Hz, 3 H, CH₃), 1.01 (t, *J* = 7.1 Hz, 3 H, CH₃), 1.15 (t, *J* = 7.1 Hz, 3 H, CH₃), 3.69–3.85 (m, 2 × 2 H, OCH₂), 3.96 (d, *J* = 12.3 Hz, 1 H, CH^c), 4.04–4.12 (m, 3 H, OCH₂ and CH^b), 7.10–7.22 ppm (m, 2 × 2 H, ArH). ¹³C NMR (DMSO-*d*₆, 100 MHz): δ = 13.2 (q), 13.5 (q), 15.1 (q), 42.2 (d, C^b), 47.3 (s, C⁻), 55.4 (t), 55.9 (d, C^c), 59.9 (t), 60.1 (t), 124.7 (d), 125.2 (d), 126.5 (d), 129.0 (d), 131.7 (s), 147.9 (s), 166.9 (s), 167.5 (s), 168.3 ppm (s). MS (ESI, negative) *m/z* (%): 394.11 (100).

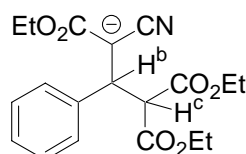


2-Cyano-1,5-diethoxy-4-(ethoxycarbonyl)-1,5-dioxo-3-phenylpentan-2-yl) potassium (4dc).

Mixture of two tautomers

NMR spectra refer to the major tautomer

¹H NMR (DMSO-*d*₆, 400 MHz): δ = 0.83 (t, *J* = 7.1 Hz, 3 H, CH₃), 0.99 (t, *J* = 7.1 Hz, 3 H, CH₃), 1.15 (t, *J* = 7.1 Hz, 3 H, CH₃), 3.70–3.78 (m, 2 × 2 H, OCH₂), 3.95 (d, *J* = 12.4 Hz, 1 H, CH^c), 4.05–4.13 (m, 3 H, OCH₂ and CH^b), 7.03–7.19 ppm (m, 5 H, ArH). ¹³C NMR (DMSO-*d*₆, 100 MHz): δ = 13.4 (q), 13.8 (q), 15.4 (q), 42.5 (d, C^b), 47.8 (s, C⁻), 55.5 (t), 56.6 (d, C^c), 59.9 (t), 60.1 (t), 125.0 (d), 126.9 (d), 127.2 (d), 129.5 (s), 145.7 (s), 167.4 (s), 167.9 (s), 168.5 ppm (s). MS (ESI, negative) *m/z* (%): 360.15 (100, C₁₉H₂₂NO₆).

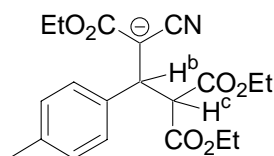


2-Cyano-1,5-diethoxy-4-(ethoxycarbonyl)-1,5-dioxo-3-*p*-tolylpentan-2-yl) potassium (4ec).

Mixture of two tautomers

NMR spectra refer to the major tautomer

^1H NMR (DMSO- d_6 , 400 MHz): δ = 0.86 (t, J = 7.1 Hz, 3 H, CH₃), 0.99 (t, J = 7.1 Hz, 3 H, CH₃), 1.15 (t, J = 7.1 Hz, 3 H, CH₃), 2.21 (s, CH₃), 3.67–3.80 (m, 2×2 H, OCH₂), 3.91 (d, J = 12.3 Hz, 1 H, CH^c), 4.04–4.09 (m, 3 H, OCH₂ and CH^b), 6.95 (d, J = 8.0 Hz, ArH), 7.06 ppm (d, J = 8.0 Hz, ArH). ^{13}C NMR (DMSO- d_6 , 100 MHz): δ = 13.5 (q), 13.8 (q), 15.4 (q), 20.5 (q), 42.1 (d, C^b), 47.9 (s, C⁻), 55.4 (t), 56.7 (d, C^c), 59.9 (t), 60.1 (t), 126.8 (d), 127.8 (d), 129.6 (s), 133.7 (s), 142.7 (s), 167.5 (s), 167.9 (s), 168.5 ppm (s). MS (ESI, positive) m/z (%): 414.13 (100, C₂₀H₂₅O₆N³⁹K), 461.16 (80). MS (ESI, negative) m/z (%): 241.09 (100), 374.16 (8), 386.14 (20).

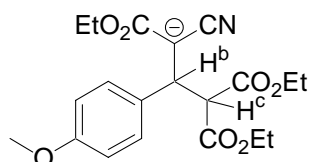


2-Cyano-1,5-diethoxy-4-(ethoxycarbonyl)-3-(4-methoxyphenyl)-1,5-dioxopentan-2-yl) potassium (4fc)

Mixture of two tautomers

NMR spectra refer to the major tautomer

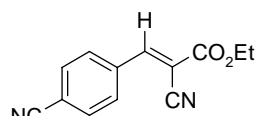
^1H NMR (DMSO- d_6 , 400 MHz): δ = 0.86 (t, J = 7.1 Hz, 3 H, CH₃), 0.99 (t, J = 7.1 Hz, 3 H, CH₃), 1.14 (t, J = 7.1 Hz, 3 H, CH₃), 3.67 (s, OCH₃), 3.70–3.78 (m, 2×2 H, OCH₂), 3.90 (d, J = 12.3 Hz, 1 H, CH^c), 4.02–4.07 (m, 3 H, OCH₂ and CH^b), 6.71 (d, J = 8.6 Hz, 2 H, ArH), 7.10 ppm (d, J = 8.6 Hz, 2 H, ArH). ^{13}C NMR (DMSO- d_6 , 100 MHz): δ = 13.5 (q), 13.8 (q), 15.4 (q), 41.8 (d, C^b), 48.0 (s, C⁻), 54.8 (q, OCH₃), 55.4 (t), 57.0 (d, C^c), 59.9 (t), 60.1 (t), 112.7 (d), 127.7 (s, CN) 127.9 (d), 129.7 (s), 137.9 (s), 156.9 (s), 167.4 (s), 167.9 (s), 168.5 ppm (s). MS (ESI, negative) m/z (%): 390.16 (15), 257.09 (100).



Ethyl-(*E*)-2-cyano-3-(4-cyanophenyl)acrylic acid ethyl ester (retro-Michael product).

After addition of **1b** (302 mg, 1.11 mmol) to a mixture of **2c-H** (510 μl , 4 mmol) and K₂CO₃ (1.2 g, 19 mmol) in DME/DMSO as solvent mixture the solution was stirred for 1 h at room

temperature. The solution turned yellow and after the excess K_2CO_3 was filtered off, and the solution was concentrated under reduced pressure. After extraction with ethyl acetate the solution was washed with sat. aqueous NaCl solution and dried over $MgSO_4$. After evaporation of the solvent, the crude product was crystallized from ethanol: **retro-Michael product** (60 mg, 24 %), yellow needles; mp 172.0–172.5 °C (from EtOH), (168.5–169.0 °C, ref. S8).



retro-Michael product

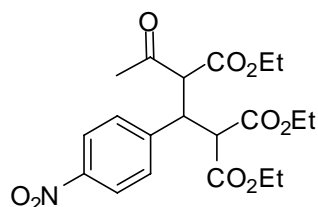
1H NMR ($CDCl_3$, 300 MHz): δ = 1.41 (t, J = 7.1 Hz, 3 H, CH_3), 4.41 (q, J = 7.1 Hz, 2 H, OCH_2), 7.79 (d, J = 8.3 Hz, 2 H, ArH), 8.06 (d, J = 8.3 Hz, 2 H, ArH), 8.24 ppm (s, 1 H, =CH), in agreement with ref. S9. ^{13}C NMR ($CDCl_3$, 75 MHz): δ = 14.1 (q), 63.3 (t), 106.8 (s), 114.6 (s), 116.0 (s), 117.7 (s), 131.0 (d), 132.8 (d), 135.3 (s), 152.2 (d, =CH), 161.5 ppm (s). HR-MS: Calcd. for $(C_{13}H_{10}N_2O_2)$ 226.0742; Found 226.0424

^{S8} D. T. Mowry, *J. Am. Chem. Soc.* **1949**, 65, 992.

^{S9} C. N. Robinson, C. D. Slater, J. S. Covington, C. R. Chang *et. al*, *J. Magn. Reson.* **1980**, 41, 293-301.

Reaction of 2d with Diethyl Benzylidenemalonate 1a**2-Acetyl-4-ethoxycarbonyl-3-(4-nitrophenyl)-pentanedioic acid diethyl ester (5ad).**

Potassium carbonate (1.38 g, 10 mmol) was added to a mixture of **1a** (293 mg, 1.00 mmol) and **2d-H** (510 μ l, 4 mmol) in DMSO (4 mL) at room temperature. After stirring for 2 h, the reaction mixture was diluted with ethyl acetate (40 mL) and poured into 5 % of hydrochloric acid with ice. After extraction with ethyl acetate, the combined organic layers were washed with water and brine and dried (Na_2SO_4). Removal of the solvents in the vacuum gave a residue, which was purified by column chromatography (SiO_2 , hexane/ethyl acetate). The crude product (420 mg, 2:1-mixture of diastereomers) was crystallized to yield the major diastereomer: **5ad** (200 mg, 47 %); mp 72 °C (from EtOH).

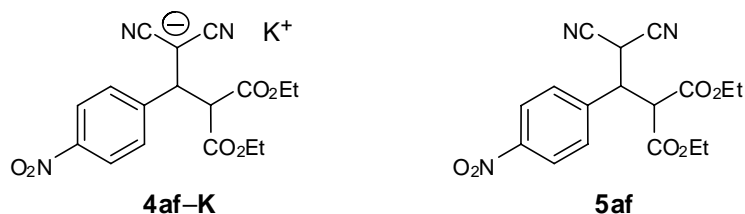
**5ad**

^1H NMR (CDCl_3 , 300 MHz): δ = 1.00 (t, J = 7.2, 3 H), 1.08, (t, J = 7.2 Hz, 3 H), 1.21 (t, J = 7.2 Hz, 3 H), 2.27 (s, 3 H), 3.88 (m, 1 H), 3.91 (q, J = 7.2 Hz, 2 H), 4.00 (q, J = 7.2 Hz, 2 H), 4.11 (q, J = 7.2 Hz, 2 H), 4.39 (m, 2 H), 7.51 (d, J = 8.8 Hz, 2 H), 8.11 ppm (d, J = 8.8 Hz, 2 H). ^{13}C NMR (CDCl_3 , 75 MHz): δ = 13.7, 13.8, 13.9, 29.7, 42.6, 54.5, 61.7, 61.8, 61.9, 62.3, 123.1, 130.5, 145.6, 147.2, 167.1, 167.3, 167.6, 200.6 ppm. MS (EI, 70 eV) m/z (%): 423 (M^+ , < 1), 380 (2), 377 (5), 364 (12), 334 (14), 304 (8), 288 (21), 248 (90), 218 (30), 203 (20), 176 (50), 160 (58), 133 (33), 115 (54), 102 (21), 43 (100). Elemental analysis ($\text{C}_{20}\text{H}_{25}\text{NO}_9$) Calcd. C 56.73 H 5.95 N 3.31. Found: C 56.68 H 5.84 N 3.26.

Reactions of 2f–K with Diethyl Benzylidenemalonates 1a

Diethyl 2-(2,2-dicyano-1-(4-nitrophenyl)ethyl)malonate (5af).

After addition of **1a** (283 mg, 0.965 mmol) to the potassium salt of malononitrile **2f-K** (103 mg, 0.983 mmol) dissolved in dry DMSO- d_6 (5 mL) the solution turned from pale yellow to orange-red. Stirring was continued for 5 min at room temperature. For the NMR spectroscopic characterization of **4af**, a sample of the crude reaction mixture was used. The reaction mixture was poured on cold water and acidified with conc. hydrochloric acid (2 mL). The solution turned yellow and a fine solid precipitated. Since the formed precipitate was too fine to be filtered, it was dissolved in CH_2Cl_2 , filtered over a warm cotton batting and evaporated under reduced pressure: **5af** (120 mg, 35 %), pale yellow oil.



4af-K: ^1H NMR (DMSO- d_6 , 400 MHz): δ = 0.87 (t, J = 7.1 Hz, 3 H, CH_3), 1.25 (t, J = 7.1 Hz, 3 H, CH_3), 3.66 (d, J = 12.0 Hz, 1 H, CH), 3.78–3.85 (m, 3 H, OCH_2 and CH), 4.19 (q, J = 7.1 Hz, 4 H, OCH_2), 7.39 (d, J = 8.1 Hz, 2 H, ArH), 8.13 ppm (d, J = 8.1 Hz, 2 H, ArH).

^{13}C NMR (DMSO- d_6 , 100 MHz): δ = 13.4 (q), 13.9 (q), 17.2 (s, C^-), 44.1 (d), 56.7 (d), 60.7 (t), 60.9 (t), 123.3 (d), 127.5 (d), 129.3 (s, CN), 145.5 (s), 152.3 (s), 166.8 (s), 167.0 ppm (s).

5af: ^1H -NMR (CDCl_3 , 300 MHz): δ = 0.97 (t, J = 7.1 Hz, 3 H, CH_3), 1.26 (t, J = 7.1 Hz, 3 H, CH_3), 3.90–3.96 (m, 2 H, OCH_2), 4.07 (m, 2 H, 2 \times CH), 4.24–4.27 (m, 2 H, OCH_2), 4.95–4.97 (m, 1 H, H^b), 7.60 (d, J = 8.8 Hz, 2 H, ArH), 8.24 ppm (d, J = 8.8 Hz, 2 H, ArH). ^{13}C NMR (CDCl_3 , 75.5 MHz): δ = 13.7 (q), 27.1 (d), 44.2 (d), 52.9 (d), 62.3 (t), 63.1 (t), 110.7 (s), 110.8 (s), 124.1 (d), 129.7 (d), 140.5 (s), 148.4 (s), 165.3 (s), 166.7 ppm (s).

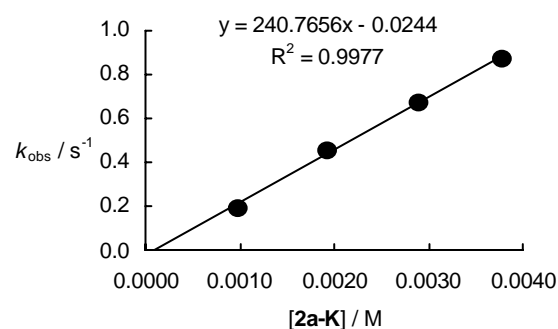
4.7. Reactivities of Diethyl Benzylidenemalonates 1a-i

Reactions of electrophile 1a

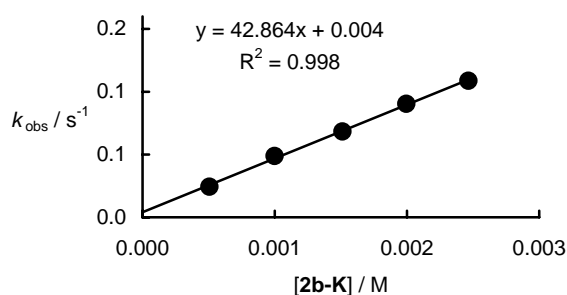
Table S1: Kinetics of the reaction of 1a with the nitro ethyl anion 2a (K⁺ salt, DMSO, 20 °C, stopped-flow UV-Vis spectrometer, decrease at $\lambda = 305$ nm).

No.	[E] ₀ / M	[Nu ⁻] ₀ / M	$k_{\text{obs}} / \text{s}^{-1}$
a370-1	2.83×10^{-5}	9.61×10^{-4}	1.94×10^{-1}
a370-2	2.83×10^{-5}	1.92×10^{-3}	4.56×10^{-1}
a370-3	2.83×10^{-5}	2.88×10^{-3}	6.74×10^{-1}
a370-4	2.83×10^{-5}	3.77×10^{-3}	8.74×10^{-1}

$$k_2 = 2.41 \times 10^2 \text{ L mol}^{-1} \text{ s}^{-1}$$

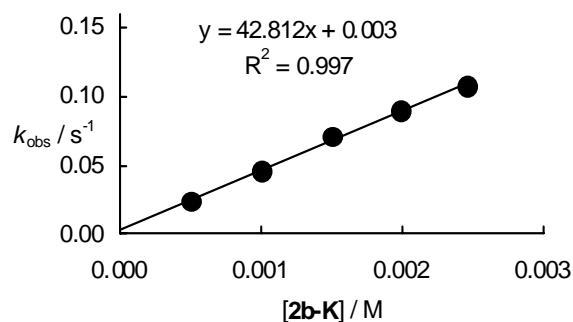
**Table S2:** Kinetics of the reaction of 1a with the diethyl malonate anion 2b (K⁺ salt, DMSO, 20 °C, diode array UV-Vis spectrometer)

No.	[E] ₀ / M	[Nu ⁻] ₀ / M	$k_{\text{obs}} / \text{s}^{-1}$ (decrease at $\lambda = 325$ nm)	$k_{\text{obs}} / \text{s}^{-1}$ (increase at $\lambda = 425$ nm)
a338-6	4.09×10^{-5}	5.06×10^{-4}	2.38×10^{-2}	2.43×10^{-2}
a338-2	4.09×10^{-5}	9.99×10^{-4}	4.55×10^{-2}	4.88×10^{-2}
a338-3	4.09×10^{-5}	1.51×10^{-3}	7.10×10^{-2}	6.83×10^{-2}
a338-4	4.09×10^{-5}	2.00×10^{-3}	9.02×10^{-2}	9.04×10^{-2}
a338-5	4.09×10^{-5}	2.47×10^{-3}	1.07×10^{-1}	1.09×10^{-1}



$$k_2 = 4.29 \times 10^1 \text{ L mol}^{-1} \text{ s}^{-1}$$

(from decrease at $\lambda = 325$ nm)



$$k_2 = 4.28 \times 10^1 \text{ L mol}^{-1} \text{ s}^{-1}$$

(from increase at $\lambda = 425$ nm)

Table S3: Kinetics of the reaction of **1a** with the anion of ethyl cyano acetate **2c** (K^+ salt, DMSO, 20 °C, diode array UV-Vis spectrometer, decrease at $\lambda = 310$ nm).

No.	$[E]_0 / M$	$[Nu^-]_0 / M$	k_{obs} / s^{-1}
a320-6	4.94×10^{-5}	1.14×10^{-3}	2.62×10^{-2}
a320-1 ^a	4.94×10^{-5}	1.14×10^{-3}	2.58×10^{-2}
a320-3	4.94×10^{-5}	1.70×10^{-3}	3.70×10^{-2}
a320-5	4.94×10^{-5}	2.13×10^{-3}	4.72×10^{-2}

^a in the presence of 1 equiv. 18-crown-6.

$$k_2 = 2.12 \times 10^1 \text{ L mol}^{-1} \text{ s}^{-1}$$

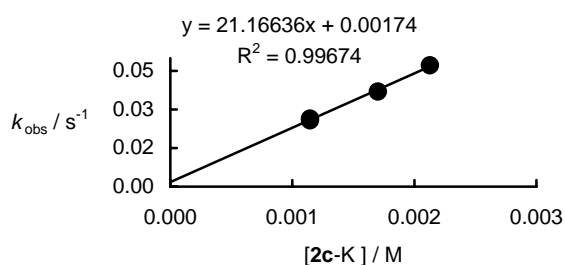


Table S4: Kinetics of the reaction of **1a** with the anion of ethyl cyano acetate **2c** (K^+ salt, in the presence of 1 equiv. of 18-crown-6, DMSO, 20 °C, diode array UV-Vis spectrometer, decrease at $\lambda = 302$ nm).

No.	$[E]_0 / M$	$[Nu^-]_0 / M$	k_{obs} / s^{-1}
72-1	1.29×10^{-4}	9.92×10^{-4}	1.64×10^{-2}
72-2	1.38×10^{-4}	1.97×10^{-3}	3.94×10^{-2}
72-3	1.38×10^{-4}	3.07×10^{-3}	6.52×10^{-2}
72-4	1.37×10^{-4}	4.05×10^{-3}	8.62×10^{-2}
72-5	1.36×10^{-4}	5.05×10^{-3}	1.07×10^{-1}

$$k_2 = 2.22 \times 10^1 \text{ L mol}^{-1} \text{ s}^{-1}$$

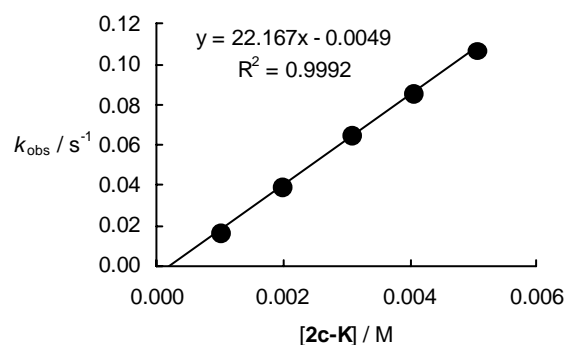


Table S5: Kinetics of the reaction of **1a** with the anion of ethyl aceto acetate **2d** (K^+ salt) in presence of 18-crown-6 (1 equiv.) and the corresponding CH acid **2d-H** (DMSO, 20 °C, diode array UV-Vis spectrometer, decrease at $\lambda = 310$ nm).

No.	$[E]_0 / M$	$[Nu^-]_0 / M$	$[2b-H]_0 / M$	k_{obs} / s^{-1}
102-1	7.03×10^{-5}	5.30×10^{-4}	7.03×10^{-5}	4.27×10^{-3}
102-2	6.93×10^{-5}	1.04×10^{-3}	6.93×10^{-5}	7.26×10^{-3}
102-3	6.91×10^{-5}	1.56×10^{-3}	6.91×10^{-5}	1.10×10^{-2}
102-4	6.86×10^{-5}	2.07×10^{-3}	6.86×10^{-5}	1.42×10^{-2}
102-5	6.85×10^{-5}	2.58×10^{-3}	6.85×10^{-5}	1.77×10^{-2}

$$k_2 = 6.58 \text{ L mol}^{-1} \text{ s}^{-1}$$

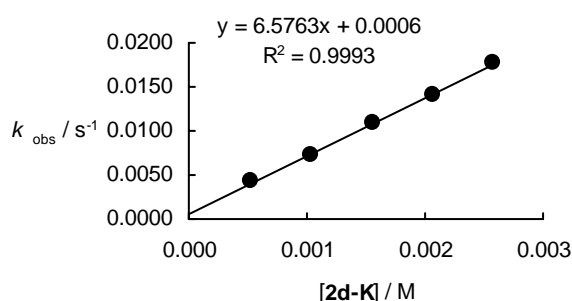
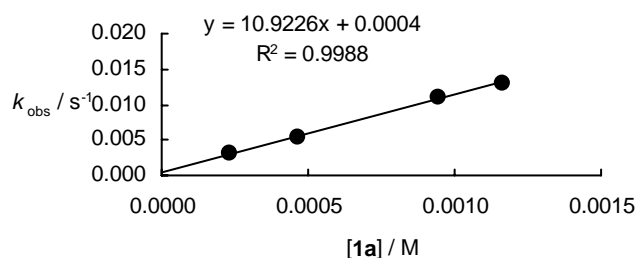


Table S6: Kinetics of the reaction of **1a** with the bis(4-nitrophenyl)methyl anion **2** (K^+ salt), DMSO, 20 °C, diode array UV-Vis spectrometer, decrease at $\lambda = 700$ nm).

No.	$[Nu^-]_0 / M$	$[E]_0 / M$	k_{obs} / s^{-1}
a294b-1	2.31×10^{-5}	2.31×10^{-4}	3.02×10^{-3}
a294b-2	2.31×10^{-5}	4.63×10^{-4}	5.34×10^{-3}
a294b-3b	2.31×10^{-5}	9.43×10^{-4}	1.09×10^{-2}
a294b-5	2.31×10^{-5}	1.16×10^{-3}	1.30×10^{-2}

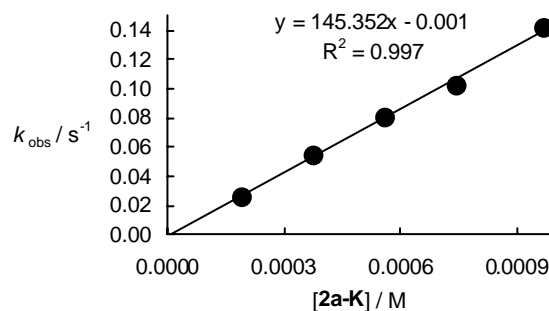
$$k_2 = 1.09 \times 10^1 \text{ L mol}^{-1} \text{ s}^{-1}$$



Reactions of electrophile **1b****Table S7:** Kinetics of the reaction **1b** with the nitroethyl anion **2a** (K^+ salt, DMSO, 20 °C, diode array UV-Vis spectrometer, decrease at $\lambda = 305$ nm).

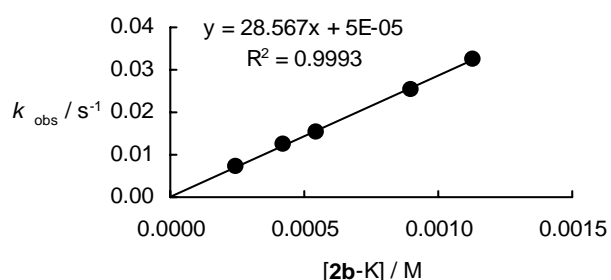
No.	$[E]_0 / M$	$[Nu^-]_0 / M$	k_{obs} / s^{-1}
a342b	1.55×10^{-5}	1.88×10^{-4}	2.64×10^{-2}
a342b-2	1.55×10^{-5}	3.74×10^{-4}	5.49×10^{-2}
a342b-3	1.55×10^{-5}	5.59×10^{-4}	8.15×10^{-2}
a342b-4	1.55×10^{-5}	7.41×10^{-4}	1.03×10^{-1}
a342b-5	1.55×10^{-5}	9.67×10^{-4}	1.42×10^{-1}

$$k_2 = 1.45 \times 10^2 \text{ L mol}^{-1} \text{ s}^{-1}$$

**Table S8:** Kinetics of the reaction of **1b** with the diethyl malonate anion **2b** (K^+ salt) in the presence of 1.5 to 2.0 equiv. 18-crown-6 (DMSO, 20 °C, diode array UV-Vis spectrometer, decrease at $\lambda = 300$ nm).

No.	$[E]_0 / M$	$[Nu^-]_0 / M$	k_{obs} / s^{-1}
40-5	6.01×10^{-5}	2.44×10^{-4}	7.01×10^{-3}
40-4	6.00×10^{-5}	4.25×10^{-4}	1.25×10^{-2}
49-3	5.98×10^{-5}	5.43×10^{-4}	1.54×10^{-2}
49-2	6.02×10^{-5}	9.00×10^{-4}	2.54×10^{-2}
49-1	6.04×10^{-5}	1.13×10^{-3}	3.26×10^{-2}

$$k_2 = 2.86 \times 10^1 \text{ L mol}^{-1} \text{ s}^{-1}$$

**Table S9:** Kinetics of the reaction of **1b** with the anion of ethyl cyano acetate **2c** (K^+ salt, DMSO, 20 °C, diode array UV-Vis spectrometer, decrease at $\lambda = 290$ nm).

No.	$[E]_0 / M$	$[Nu^-]_0 / M$	k_{obs} / s^{-1}
a291b-1	4.32×10^{-5}	1.86×10^{-4}	1.73×10^{-3}
a291b-2	4.32×10^{-5}	3.72×10^{-4}	3.64×10^{-3}
a291b-3	4.32×10^{-5}	5.54×10^{-4}	5.38×10^{-3}
a291b-4	4.32×10^{-5}	7.56×10^{-4}	7.41×10^{-3}
a291b-5	4.32×10^{-5}	9.45×10^{-4}	9.14×10^{-3}

$$k_2 = 9.78 \text{ L mol}^{-1} \text{ s}^{-1}$$

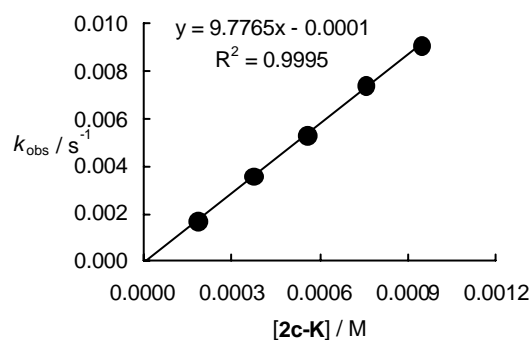


Table S10: Kinetics of the reaction of **1b** with the bis(4-nitrophenyl)methyl anion **2e** (K^+ salt, (DMSO, 20 °C, diode array UV-Vis spectrometer, decrease at $\lambda = 620$ nm).

No.	$[Nu^-]_0 / M$	$[E]_0 / M$	k_{obs} / s^{-1}
a295-1	2.30×10^{-5}	2.28×10^{-4}	1.75×10^{-3}
a295-2	2.30×10^{-5}	4.56×10^{-4}	2.89×10^{-3}
a295-3	2.30×10^{-5}	7.02×10^{-4}	4.81×10^{-3}
a295-4	2.30×10^{-5}	8.96×10^{-4}	5.69×10^{-3}
a295-5	2.30×10^{-5}	1.08×10^{-3}	6.70×10^{-3}

$$k_2 = 5.94 \text{ L mol}^{-1} \text{ s}^{-1}$$

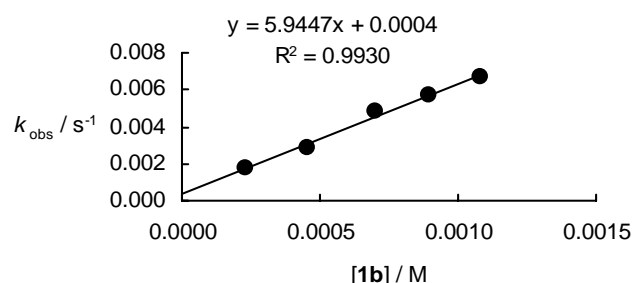
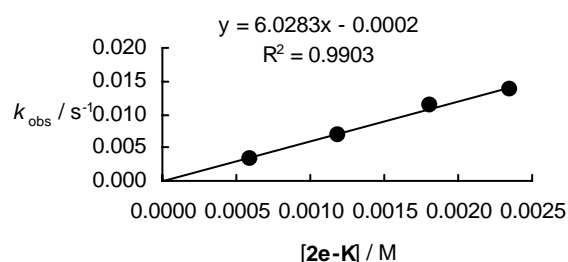


Table S11: Kinetics of the reaction of **1b** with the bis(4-nitrophenyl)methyl anion **2e** (K^+ salt) in the presence of 1 equiv. 18-crown-6 (DMSO, 20 °C, diode array UV-Vis spectrometer, decrease at $\lambda = 620$ nm).

No.	$[Nu^-]_0 / M$	$[E]_0 / M$	k_{obs} / s^{-1}
a323-1	4.98×10^{-5}	5.97×10^{-4}	3.38×10^{-3}
a323-2	4.98×10^{-5}	1.18×10^{-3}	6.77×10^{-3}
a323-3	4.98×10^{-5}	1.81×10^{-3}	1.15×10^{-2}
a323-4	4.98×10^{-5}	2.35×10^{-3}	1.36×10^{-2}

$$k_2 = 6.03 \text{ L mol}^{-1} \text{ s}^{-1}$$



Reactions of electrophile **1c**

Table S12: Kinetics of the reaction of **1c** with the nitro ethyl anion **2a** (K^+ salt, DMSO, 20 °C, diode array UV-Vis spectrometer, decrease at $\lambda = 305$ nm).

No.	$[E]_0 / M$	$[Nu^-]_0 / M$	k_{obs} / s^{-1}
a343-1	3.76×10^{-5}	2.89×10^{-4}	1.70×10^{-2}
a343-4	3.76×10^{-5}	4.19×10^{-4}	2.14×10^{-2}
a343-2	3.76×10^{-5}	5.71×10^{-4}	2.70×10^{-2}
a343-6	3.76×10^{-5}	7.18×10^{-4}	3.35×10^{-2}
a343-5	3.76×10^{-5}	8.49×10^{-4}	3.72×10^{-2}

$$k_2 = 3.71 \times 10^1 \text{ L mol}^{-1} \text{ s}^{-1}$$

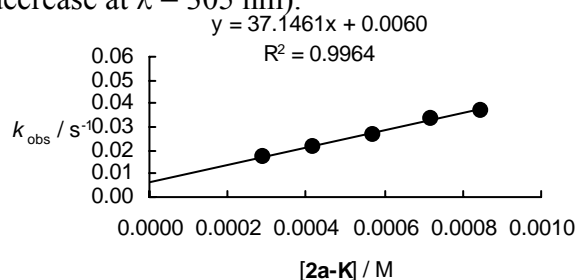


Table S13: Kinetics of the reaction of **1c** with the diethyl malonate anion **2b** (K^+ salt) in the presence of 1.5 equiv. 18-crown-6 (DMSO, 20 °C, diode array UV-Vis spectrometer, decrease at $\lambda = 303$ nm).

No.	$[E]_0 / M$	$[Nu^-]_0 / M$	k_{obs} / s^{-1}
56-1	2.26×10^{-4}	1.47×10^{-3}	1.02×10^{-2}
56-2	2.26×10^{-4}	1.95×10^{-3}	1.29×10^{-2}
56-3	2.40×10^{-4}	3.06×10^{-3}	2.14×10^{-2}
56-4	2.53×10^{-4}	5.60×10^{-3}	3.81×10^{-2}

$$k_2 = 6.81 \text{ L mol}^{-1} \text{ s}^{-1}$$

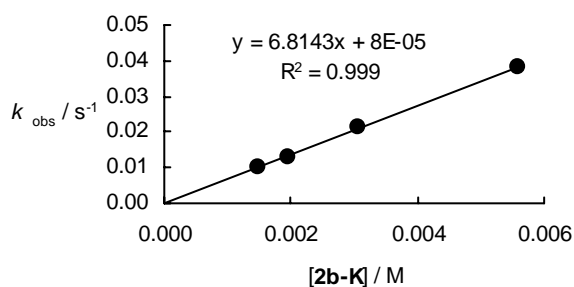


Table S14: Kinetics of the reaction of **1c** with the anion of ethyl cyano acetate **2c** (K^+ salt, DMSO, 20 °C, diode array UV-Vis spectrometer, decrease at $\lambda = 305$ nm).

No.	$[E]_0 / M$	$[Nu^-]_0 / M$	k_{obs} / s^{-1}
a292-1	3.85×10^{-5}	4.69×10^{-4}	1.46×10^{-3}
a292-2	3.85×10^{-5}	7.85×10^{-4}	2.11×10^{-3}
a292-3	3.85×10^{-5}	1.16×10^{-3}	3.21×10^{-3}
a292-4	3.85×10^{-5}	1.56×10^{-3}	4.16×10^{-3}
a292-5	3.85×10^{-5}	2.27×10^{-3}	6.26×10^{-3}

$$k_2 = 2.68 \text{ L mol}^{-1} \text{ s}^{-1}$$

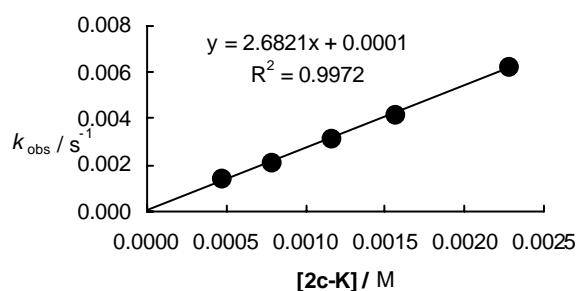


Table S15: Kinetics of the reaction of **1c** with the anion of ethyl cyano acetate **2c** (K^+ salt) in the presence of 1 equiv. 18-crown-6 (DMSO, 20 °C, diode array UV-Vis spectrometer, decrease at $\lambda = 290$ nm).

No.	$[E]_0 / M$	$[Nu^-]_0 / M$	k_{obs} / s^{-1}
a318b-2	3.89×10^{-5}	1.22×10^{-3}	3.31×10^{-3}
a318b-3	3.89×10^{-5}	1.84×10^{-3}	4.80×10^{-3}
a318b-4	3.89×10^{-5}	2.44×10^{-3}	6.26×10^{-3}
a318b-5	3.89×10^{-5}	3.15×10^{-3}	8.16×10^{-3}

$$k_2 = 2.51 \text{ L mol}^{-1} \text{ s}^{-1}$$

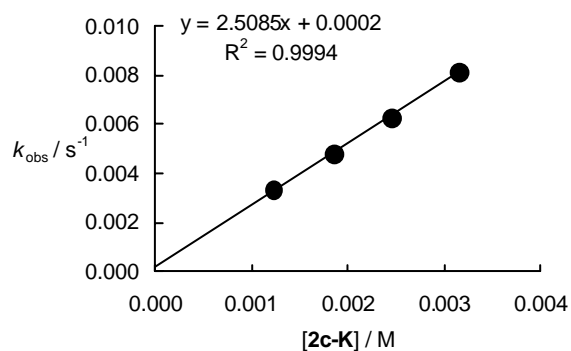
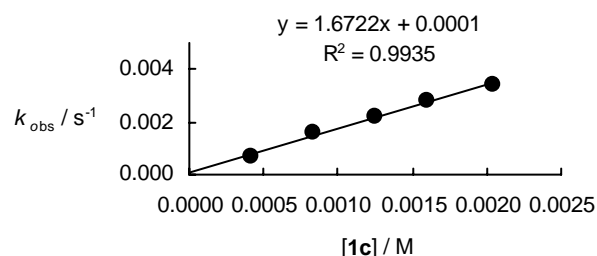


Table S16: Kinetics of the reaction of **1c** with the bis(4-nitrophenyl)methyl anion **2e** (K^+ salt, DMSO, 20 °C, diode array UV-Vis spectrometer, decrease at $\lambda = 785$ nm).

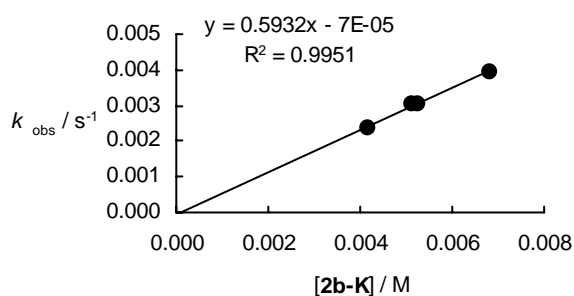
No.	$[\text{Nu}^-]_0 / \text{M}$	$[\text{E}]_0 / \text{M}$	$k_{\text{obs}} / \text{s}^{-1}$
a297b-1	3.56×10^{-5}	4.12×10^{-4}	6.72×10^{-4}
a297b-2	3.56×10^{-5}	8.33×10^{-4}	1.58×10^{-3}
a297b-3	3.56×10^{-5}	1.24×10^{-3}	2.23×10^{-3}
a297b-4	3.56×10^{-5}	1.60×10^{-3}	2.79×10^{-3}
a297b-5	3.56×10^{-5}	2.04×10^{-3}	3.43×10^{-3}

$$k_2 = 1.67 \text{ L mol}^{-1} \text{ s}^{-1}$$

**Reactions of electrophile 1d****Table S17:** Kinetics of the reaction of **1d** with the diethyl malonate anion **2b** (K^+ salt) in the presence of 1.6 equiv. 18-crown-6 (DMSO, 20 °C, diode array UV-Vis spectrometer, decrease at $\lambda = 303$ nm).

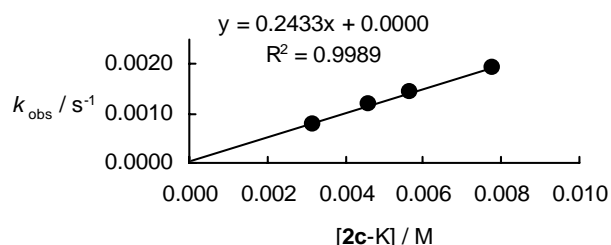
No.	$[\text{E}]_0 / \text{M}$	$[\text{Nu}^-]_0 / \text{M}$	$k_{\text{obs}} / \text{s}^{-1}$
41-1	2.04×10^{-4}	4.18×10^{-3}	2.36×10^{-3}
40-3	1.97×10^{-4}	5.15×10^{-3}	3.04×10^{-3}
40-2	3.00×10^{-4}	5.24×10^{-3}	3.05×10^{-3}
40-4	1.98×10^{-4}	6.83×10^{-3}	3.95×10^{-3}

$$k_2 = 5.93 \times 10^{-1} \text{ L mol}^{-1} \text{ s}^{-1}$$

**Table S18:** Kinetics of the reaction of **1d** with the ethyl cyano acetate anion **2c** (K^+ salt, DMSO, 20 °C, diode array UV-Vis spectrometer, decrease at $\lambda = 303$ nm).

No.	$[\text{E}]_0 / \text{M}$	$[\text{Nu}^-]_0 / \text{M}$	$k_{\text{obs}} / \text{s}^{-1}$
a304c-1	4.80×10^{-5}	3.17×10^{-3}	7.87×10^{-4}
a304c-2	4.80×10^{-5}	4.62×10^{-3}	1.17×10^{-3}
a304c-3	4.80×10^{-5}	5.64×10^{-3}	1.42×10^{-3}
a304c-4	4.80×10^{-5}	7.77×10^{-3}	1.91×10^{-3}

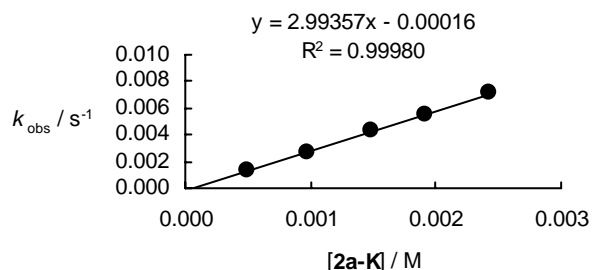
$$k_2 = 2.43 \times 10^{-1} \text{ L mol}^{-1} \text{ s}^{-1}$$



Reactions of electrophile **1e****Table S19:** Kinetics of the reaction of **1e** with the nitro ethyl anion **2a** (K^+ salt, DMSO, 20 °C, diode array UV-Vis spectrometer, decrease at $\lambda = 316$ nm).

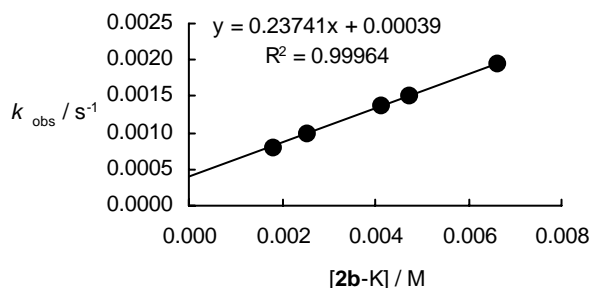
No.	$[E]_0 / M$	$[Nu^-]_0 / M$	k_{obs} / s^{-1}
a339-1	4.79×10^{-5}	4.91×10^{-4}	1.34×10^{-3}
a339-2	4.79×10^{-5}	9.71×10^{-4}	2.74×10^{-3}
a339-3	4.79×10^{-5}	1.49×10^{-3}	4.27×10^{-3}
a339-4	4.79×10^{-5}	1.92×10^{-3}	5.56×10^{-3}
a339-5	4.79×10^{-5}	2.42×10^{-3}	7.12×10^{-3}

$$k_2 = 2.99 \text{ L mol}^{-1} \text{ s}^{-1}$$

**Table S20:** Kinetics of the reaction of **1e** with the diethyl malonate anion **2b** (K^+ salt) in the presence of 1.6 equiv. 18-crown-6 (DMSO, 20 °C, diode array UV-Vis spectrometer, decrease at $\lambda = 310$ nm).

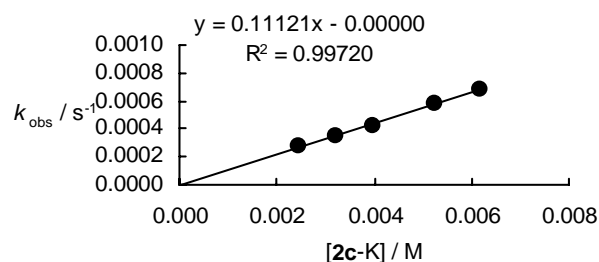
No.	$[E]_0 / M$	$[Nu^-]_0 / M$	k_{obs} / s^{-1}
50-1	9.98×10^{-5}	1.79×10^{-3}	8.06×10^{-4}
50-2	9.71×10^{-5}	2.52×10^{-3}	9.90×10^{-4}
50-3	1.06×10^{-4}	4.13×10^{-3}	1.38×10^{-3}
50-4	1.06×10^{-4}	4.72×10^{-3}	1.52×10^{-3}
50-5	1.12×10^{-4}	6.61×10^{-3}	1.95×10^{-3}

$$k_2 = 2.37 \times 10^{-1} \text{ L mol}^{-1} \text{ s}^{-1}; k_3 = 4 \times 10^{-4} \text{ s}^{-1}$$

**Table S21:** Kinetics of the reaction of **1e** with the ethyl cyano acetate anion **2c** (K^+ salt, DMSO, 20 °C, diode array UV-Vis spectrometer, decrease at $\lambda = 305$ nm).

No.	$[E]_0 / M$	$[Nu^-]_0 / M$	k_{obs} / s^{-1}
a315-4	2.91×10^{-5}	2.47×10^{-3}	2.82×10^{-4}
a315-5	2.91×10^{-5}	3.23×10^{-3}	3.51×10^{-4}
a315-3	2.91×10^{-5}	3.98×10^{-3}	4.29×10^{-4}
a315-2	2.91×10^{-5}	5.25×10^{-3}	5.82×10^{-4}
a315-1	2.91×10^{-5}	6.17×10^{-3}	6.87×10^{-4}

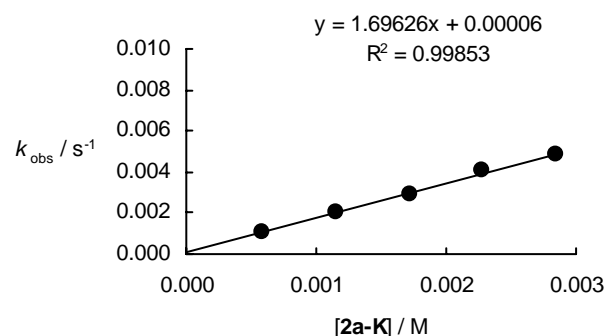
$$k_2 = 1.11 \times 10^{-1} \text{ L mol}^{-1} \text{ s}^{-1}$$



Reactions of electrophile **1f****Table S22:** Kinetics of the reaction of **1f** with the nitro ethyl anion **2a** (K^+ salt, DMSO, 20 °C, diode array UV-Vis spectrometer, decrease at $\lambda = 316$ nm).

No.	$[E]_0 / M$	$[Nu^-]_0 / M$	k_{obs} / s^{-1}
a336-1	2.60×10^{-5}	5.84×10^{-4}	1.04×10^{-3}
a336-2	2.60×10^{-5}	1.16×10^{-3}	2.02×10^{-3}
a336-3	2.60×10^{-5}	1.72×10^{-3}	2.95×10^{-3}
a336-4	2.60×10^{-5}	2.28×10^{-3}	4.03×10^{-3}
a336-5	2.60×10^{-5}	2.85×10^{-3}	4.83×10^{-3}

$k_2 = 1.70 \text{ L mol}^{-1} \text{ s}^{-1}$

**Table S23:** Kinetics of the reaction of **1f** with the diethyl malonate anion **2b** (K^+ salt) in the presence of 1.5 equiv. 18-crown-6 (DMSO, 20 °C, diode array UV-Vis spectrometer, decrease at $\lambda = 316$ nm).

No.	$[E]_0 / M$	$[Nu^-]_0 / M$	k_{obs} / s^{-1}
45-1	7.95×10^{-5}	1.53×10^{-3}	1.23×10^{-3}
45-2	9.64×10^{-5}	3.98×10^{-3}	1.58×10^{-3}
45-3	9.52×10^{-5}	5.51×10^{-3}	1.82×10^{-3}
45-4	9.20×10^{-5}	7.42×10^{-3}	2.08×10^{-3}
45-5	9.04×10^{-5}	9.23×10^{-3}	2.31×10^{-3}

$k_2 = 1.41 \times 10^{-1} \text{ L mol}^{-1} \text{ s}^{-1}$
 $k_{-1} = 1 \times 10^{-3} \text{ s}^{-1}$

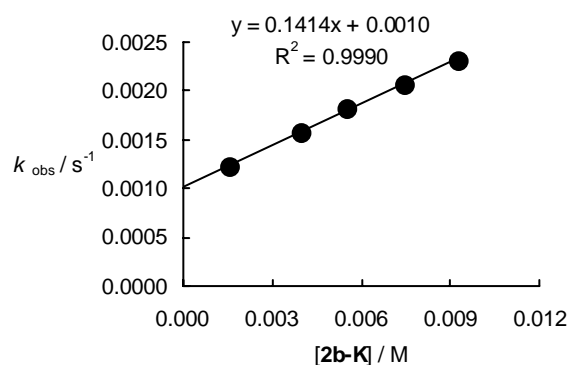
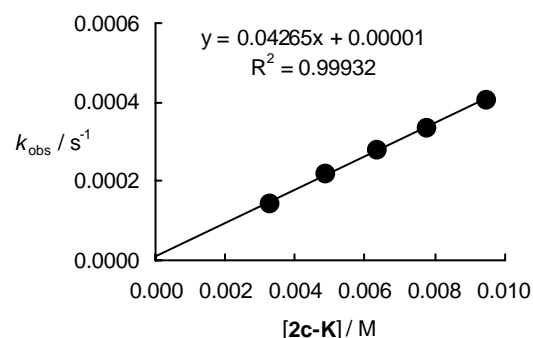


Tabelle S24: Kinetics of the reaction of **1f** with the ethyl cyano acetate anion **2c** (K^+ salt, DMSO, 20 °C, diode array UV-Vis spectrometer, decrease at $\lambda = 315$ nm).

No.	$[E]_0 / M$	$[Nu^-]_0 / M$	k_{obs} / s^{-1}
a316-1	3.98×10^{-5}	3.24×10^{-3}	1.44×10^{-4}
a316-2	3.98×10^{-5}	4.85×10^{-3}	2.20×10^{-4}
a316-3	3.98×10^{-5}	6.33×10^{-3}	2.81×10^{-4}
a316-4	3.98×10^{-5}	7.77×10^{-3}	3.39×10^{-4}
a316-5	3.98×10^{-5}	9.44×10^{-3}	4.11×10^{-4}

$k_2 = 4.27 \times 10^{-2} \text{ L mol}^{-1} \text{ s}^{-1}$



Reactions of electrophile **1g**

Table S25: Kinetics for the reaction of **1g** with the nitro ethyl anion **2a** (K^+ salt, DMSO, 20 °C, diode array UV-Vis spectrometer, decrease at $\lambda = 383$ nm).

No.	$[E]_0 / M$	$[Nu^-]_0 / M$	k_{obs} / s^{-1}
a333-1	4.20×10^{-5}	1.39×10^{-3}	2.62×10^{-4}
a333-2	4.20×10^{-5}	2.56×10^{-3}	4.60×10^{-4}
a333-3	4.20×10^{-5}	3.43×10^{-3}	6.13×10^{-4}
a333-4	4.20×10^{-5}	4.21×10^{-3}	7.49×10^{-4}
a333-5	4.20×10^{-5}	4.73×10^{-3}	8.13×10^{-4}

$k_2 = 1.68 \times 10^{-1} \text{ L mol}^{-1} \text{ s}^{-1}$

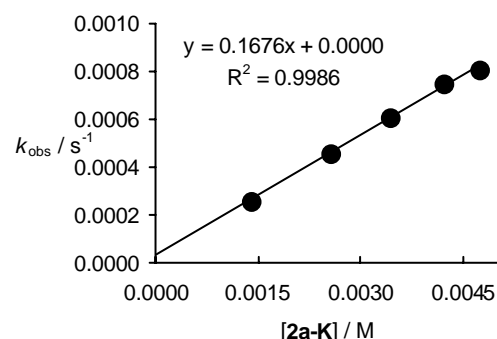
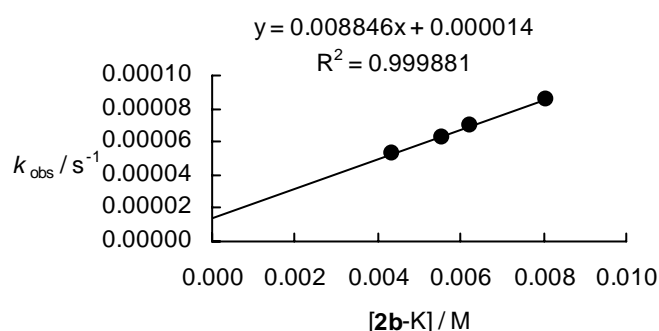


Table S26: Kinetics for the reaction of **1g** with the diethyl malonate anion **2b** (K^+ salt, DMSO, 20 °C, diode array UV-Vis spectrometer, decrease at $\lambda = 380$ nm).

No.	$[E]_0 / M$	$[Nu^-]_0 / M$	$[2b-H] / M$	k_{obs} / s^{-1}
a371b-1	4.41×10^{-5}	4.35×10^{-3}	2.13×10^{-2}	5.29×10^{-5}
a371b-2	4.41×10^{-5}	5.55×10^{-3}	1.77×10^{-2}	6.33×10^{-5}
a371b-3	4.41×10^{-5}	6.22×10^{-3}	1.82×10^{-2}	6.96×10^{-5}
a371b-4	4.41×10^{-5}	8.07×10^{-3}	2.23×10^{-2}	8.58×10^{-5}

$k_2 = 8.85 \times 10^{-3} \text{ L mol}^{-1} \text{ s}^{-1}$



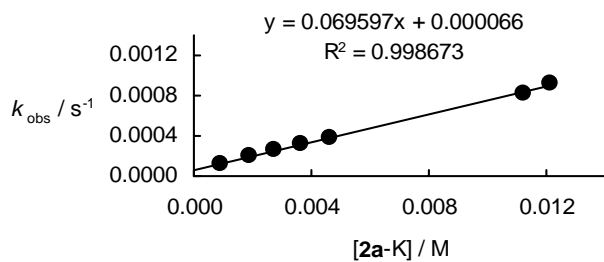
Reactions of electrophile **1h**

Table S27: Kinetics for the reaction of **1h** with the nitro ethyl anion **2a** (K^+ salt, DMSO, 20 °C, diode array UV-Vis spectrometer, decrease at $\lambda = 395$ nm).

No.	$[E]_0 / M$	$[Nu^-]_0 / M$	k_{obs} / s^{-1}
a348-1	3.59×10^{-5}	9.18×10^{-4}	1.25×10^{-4}
a348-2	3.59×10^{-5}	1.89×10^{-3}	2.03×10^{-4}
a348-3	3.59×10^{-5}	2.72×10^{-3}	2.58×10^{-4}
a348-4	3.59×10^{-5}	3.65×10^{-3}	3.15×10^{-4}
a348-5	3.59×10^{-5}	4.60×10^{-3}	3.91×10^{-4}
a348b*	4.00×10^{-5}	1.12×10^{-2}	8.24×10^{-4}
a348b-8**	4.00×10^{-5}	1.21×10^{-2}	9.27×10^{-4}

$k_2 = 6.96 \times 10^{-2} \text{ L mol}^{-1} \text{ s}^{-1}$

** Addition of 1.00 equiv. CH-acid, * 0.05 equiv. CH-acid

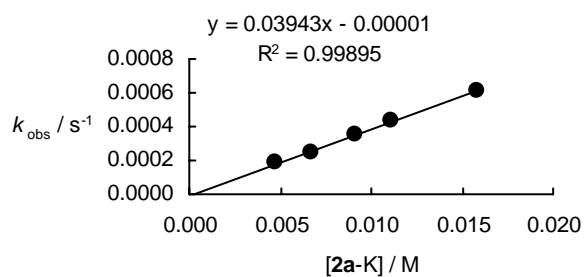


Reactions of electrophile **1i**

Table S28: Kinetics for the reaction of **1i** with the nitro ethyl anion **2a** (K^+ salt, DMSO, 20 °C, diode array UV-Vis spectrometer, decrease at $\lambda = 409 \text{ nm}$).

No.	$[\text{E}]_0 / \text{M}$	$[\text{Nu}^-]_0 / \text{M}$	$k_{\text{obs}} / \text{s}^{-1}$
a340-1	2.33×10^{-5}	4.77×10^{-3}	1.84×10^{-4}
a340-2	2.33×10^{-5}	6.66×10^{-3}	2.51×10^{-4}
a340-3	2.33×10^{-5}	9.13×10^{-3}	3.51×10^{-4}
a340-5	2.33×10^{-5}	1.11×10^{-2}	4.39×10^{-4}
a340-5	2.33×10^{-5}	1.58×10^{-2}	6.13×10^{-4}

$k_2 = 3.94 \times 10^{-2} \text{ L mol}^{-1} \text{ s}^{-1}$



Chapter 5

Nucleophilicities of the Anions of Arylacetonitriles and Arylpropionitriles in Dimethyl Sulfoxide

O. Kaumanns, R. Appel, T. Lemek, F. Seeliger, and H. Mayr, *J. Org. Chem.* **2008**, accepted.

Introduction

The comparison of the nucleophilicities of different classes of compounds is of considerable importance for our understanding of organic reactivity. The most comprehensive nucleophilicity scale presently available is based on the reactions of benzhydrylium ions and structurally related quinone methides with different nucleophiles.¹ With this method, we have been able to directly compare n -nucleophiles (amines, alcohols, phosphanes), π -nucleophiles (alkenes, arenes, organometallics), and σ -nucleophiles (hydride donors) with each other.¹⁻⁴ Recently, we investigated the reactivities of different carbanions⁵⁻¹⁰ including trifluoromethylsulfonyl stabilized carbanions,⁶ phenylsulfonyl stabilized carbanions,⁷ nitronates,^{8,9} as well as the bis(4-nitrophenyl)methyl anion¹⁰ and demonstrated that their additions to benzhydryl cations and structurally related quinone methides can be described by Equation (5.1), where E is an electrophile-specific parameter, and N and s are nucleophile-specific parameters.

$$\log k_2(20\text{ }^\circ\text{C}) = s(N + E) \quad (5.1)$$

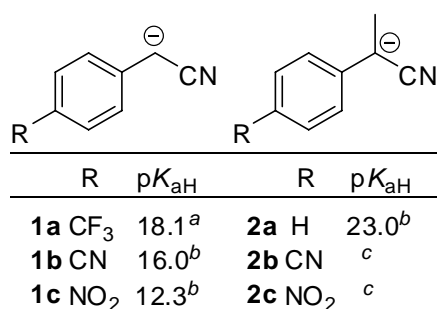
Vice versa, the second-order rate constants k_2 for the reactions of carbanions with Michael acceptors¹¹⁻¹³ have been used to determine the electrophilicities of these electron-deficient π -systems.

Because UV-Vis spectroscopy is an efficient method to determine reaction rates, we have selected a set of colored benzhydrylium ions,² quinone methides,⁴ and benzylidenemalonates¹⁴ as reference electrophiles for characterizing the reactivities of a large variety of nucleophiles. On the other hand, we do presently not yet have a comprehensive set of colored nucleophiles, which might be employed for the systematic investigation of the reactivities of electrophiles. So far, only colored carbanions of relatively low nucleophilicity ($N < 20$) have been characterized.^{6,8,10}

In view of the frequent use of cyano substituted carbanions in organic synthesis, we have selected the carbanions **1a–c** and **2a–c** for systematic studies of the relationship between structure and nucleophilic reactivity of highly reactive carbanions.¹⁵

Although the correlations between nucleophilicity (N) and basicity (pK_{aH}) of carbanions are not of high quality,⁶ the pK_{aH} values of the phenylacetonitrile anions (**1a–c**) and that of the phenylpropionitrile anion **2a** (Scheme 5.1) suggested that these carbanions have considerably higher reactivities than α -nitro- and α -trifluoromethylsulfonyl-stabilized benzyl anions.

Scheme 5.1. Phenylacetonitrile Anions **1a–c**, Phenylpropionitrile Anions **2a–c**, and their pK_{aH} Values in DMSO.



^a From ref. 16a, ^b from ref. 16b, ^c p*K*_{aH} values in DMSO not available.

Relative nucleophilicities of carbanions derived from α -substituted phenylacetonitriles **2** towards methyl iodide and other alkyl halides in liquid ammonia have previously been investigated by competition experiments.¹⁷ Recent studies of the oxidative nucleophilic substitution of hydrogen revealed that the phenylpropionitrile anion **2a** and its derivatives add to nitrobenzene and some nitrobenzene derivatives in liquid ammonia to form persistent σ^H -adducts, from which hydride was abstracted when treated subsequently with KMnO₄.¹⁸ When these σ^H -adducts were combined with dimethyldioxirane, replacement of the nitro group by hydroxyl took place prior to rearomatization, and the corresponding phenols were isolated as major products.¹⁹

We will now report on the kinetics of the reactions of the phenylacetonitrile anions **1a–c** and the phenylpropionitrile anions **2a–c** with the electrophiles **3a–u** (Table 5.1) in DMSO at 20 °C. The second-order rate constants *k*₂ will subsequently be used to derive the nucleophile-specific parameters *N* and *s* of the carbanions **1a–c** and **2a–c**.

Table 5.1. Michael Acceptors **3a–u** and their Electrophilicity Parameters *E*.

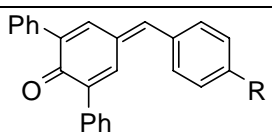
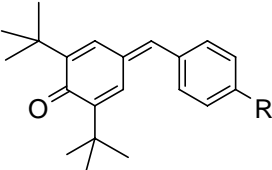
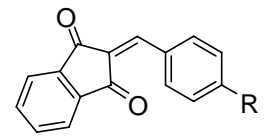
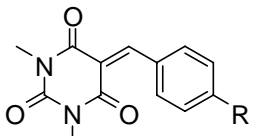
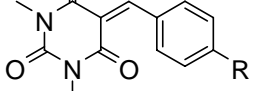
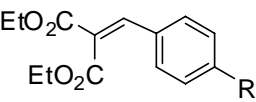
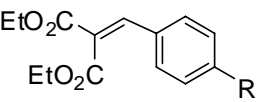
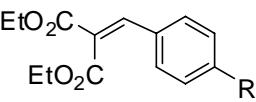
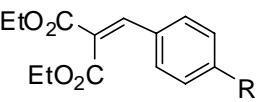
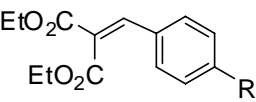
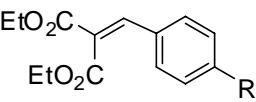
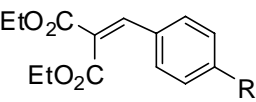
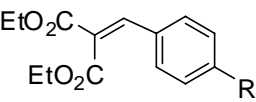
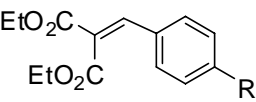
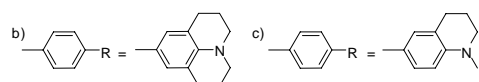
Electrophile	R	<i>E</i> ^a
	3a OMe	-12.18
	3b NMe ₂	-13.39
	3c Me	-15.83
	3d OMe	-16.11
	3e NMe ₂	-17.29
	3f jul ^b	-17.90
	3g H	-10.11
	3h OMe	-11.32
	3i NMe ₂	-13.56
	3j jul ^b	-14.68

Table 5.1. *Continued.*

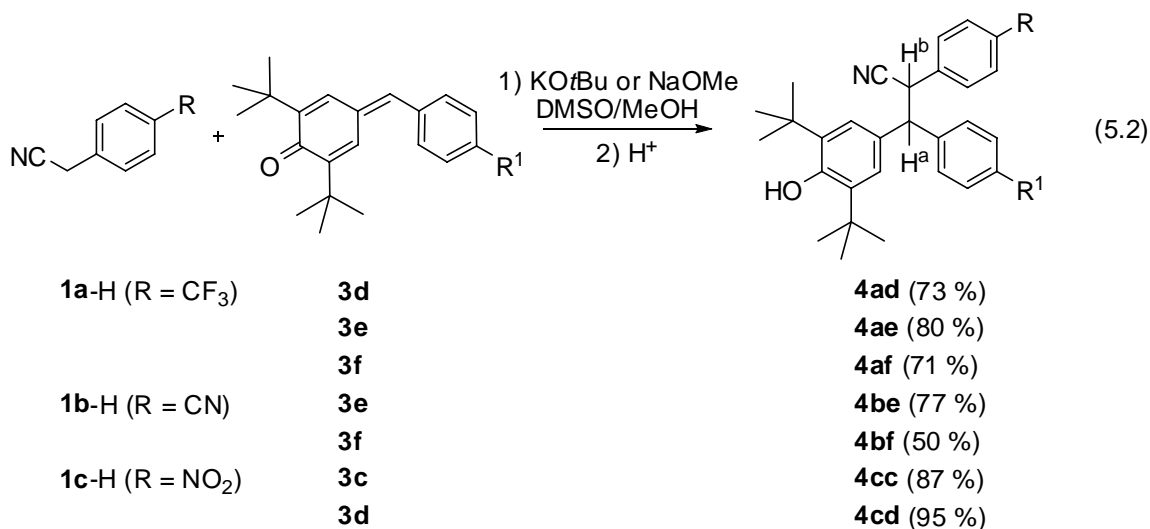
Electrophile	R	E^a
	3k OMe	-10.37
	3l NMe ₂	-12.76
	3m NO ₂	-17.67
	3n CN	-18.06
	3o <i>m</i> Cl	-18.98
	3p H	-20.55
	3q Me	-21.11
	3r OMe	-21.47
	3s NMe ₂	-23.1
	3t thq ^c	-23.4
	3u jul ^b	-23.8

^a Electrophilicity parameters E of **3a–f** were taken from ref. 4, of **3g–j** from ref. 13, of **3k,l** from ref. 12, and of **3m–u** from ref. 14

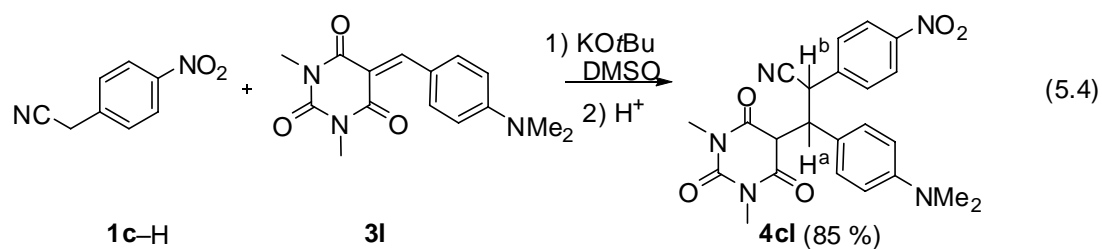
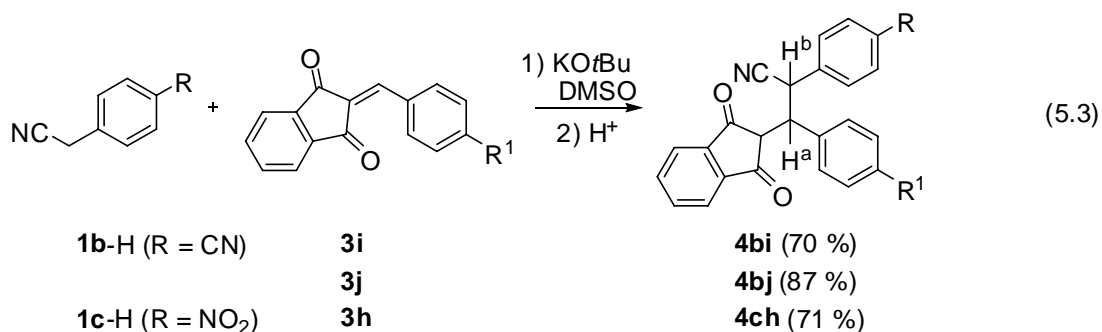


Results and Discussion

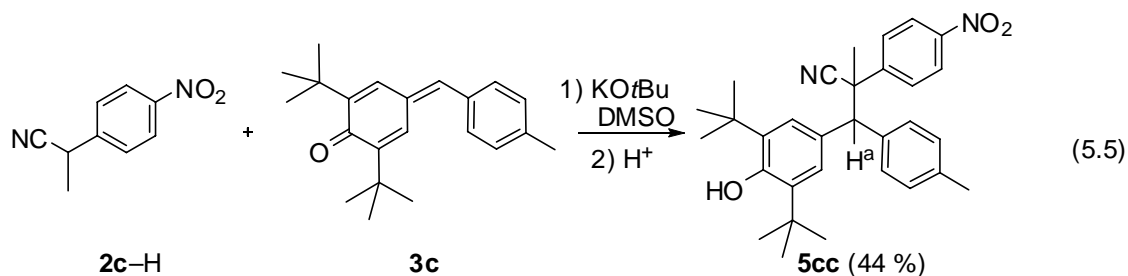
Product studies. Products of representative combinations of nucleophiles with electrophiles have been characterized. The phenylacetonitrile anions **1a–c**, which were generated from (**1a–c**)-H with KO^tBu in DMSO or DMSO/MeOH mixtures, reacted with the quinone methides **3c–f** to give the addition products **4ad–4cd** (Equation 5.2) in good yields. Their ¹H NMR spectra showed doublets for H^a and H^b at $\delta = 4.11$ – 4.54 ppm and a signal for the hydroxy group. Generally, two sets of signals in the ¹H NMR spectra of the products **4** indicated the formation of almost equal amounts of two diastereomers.



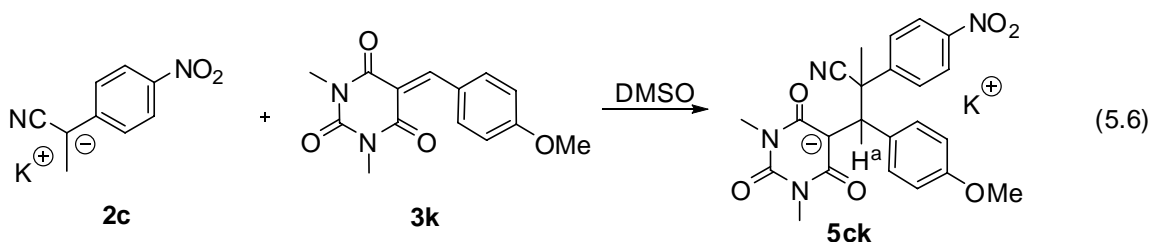
The reactions of carbanions **1b,c** with the benzylidene indandiones **3h–j** and of **1c** with the benzylidene barbituric acid **3l** showed the analogous formation of the addition products as a mixture of two diastereomers ($\approx 1:1$, Equations (5.3) and (5.4)).



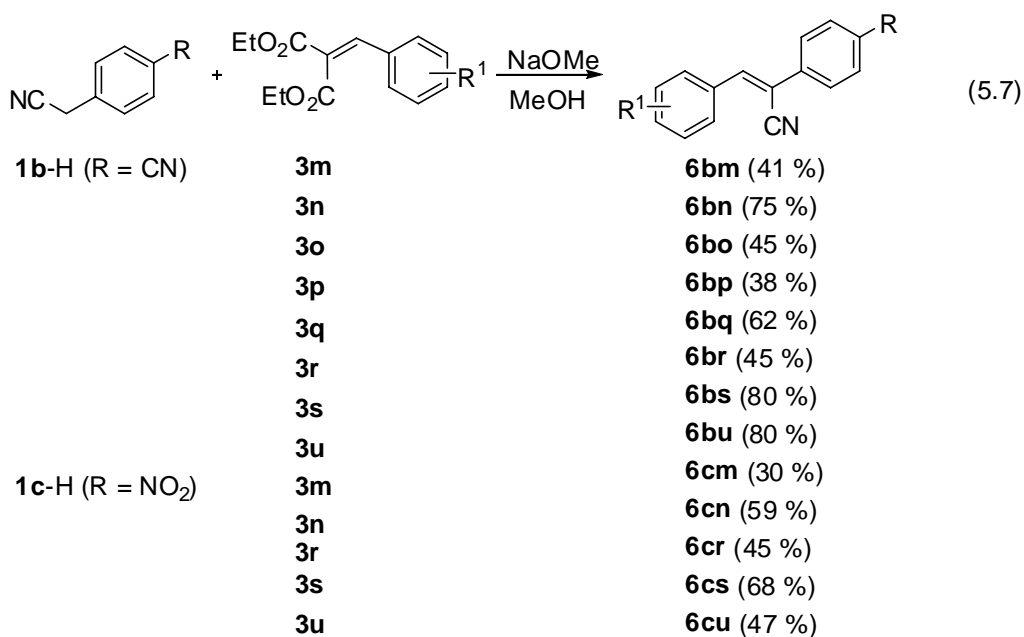
The reaction of the phenylpropionitrile anion **2c** with the quinone methide **3c** yielded **5cc** as a 1:1 pair of diastereomers, indicated by two singlets for H^a at $\delta = 3.95$ and 4.04 ppm, and for the hydroxy group at $\delta = 5.04$ and 5.20 ppm (Equation (5.5)).



The reaction of carbanion **2c** with **3k** was investigated by ^1H NMR spectroscopy, which shows the formation of equal amounts of diastereomers of the anionic adduct **5ck** (Equation (5.6)).



In contrast, the reactions of the benzylidenemalonates **3m–u** with the carbanions **1b,c** in methanol resulted in the formation of α -cyano stilbenes **6bm–6cu** via Michael addition, proton shift, and retro-Michael addition (Equation (5.7)). Compounds **6** were previously employed for the determination of H_R -acidity scales.²⁰



Kinetics. The rates of the reactions of the carbanions **1a–c** and **2b–c** with the electrophiles **3a–u** were determined photometrically under first-order conditions by using either the nucleophile or the electrophile in high excess as specified in Table 5.2.

Because of the large pK_a value of *t*BuOH in DMSO (29.4²¹ or 32.2²²), all carbanions listed in Scheme 5.1 ($pK_a < 23.0$) should be generated quantitatively when the corresponding CH acids were treated with one equivalent of KO*t*Bu. Analogously, the deprotonation of (**1a–c**)-H and (**2a–c**)-H should also be quantitative with one equivalent of the phosphazene base P₄-*t*Bu ($pK_{BH^+} = 30.2$).²³ In order to verify the complete deprotonation of the CH acids (**1a–c**)-H, KO*t*Bu was added stepwise to solutions of (**1a–c**)-H and **2a**-H in DMSO. UV-Vis spectroscopy showed that in all cases, the limiting absorbances of the corresponding carbanions were achieved after the addition of one equivalent of KO*t*Bu, indicating quantitative deprotonation of these CH acids. While the absorbance of **1c** was persistent under these conditions, the absorbances of the carbanions **1a** and **1b** decreased slowly, when only one equivalent of KO*t*Bu was added (Fig. S1–S3; Experimental Section). Persistent absorbances of the carbanions **1a,b** could be observed, when they were generated from their conjugate acids (**1a,b**)-H with 2 equivalents of KO*t*Bu. The unsubstituted phenylpropionitrile anion **2a**, which was also formed quantitatively with 1 equivalent of KO*t*Bu or P₄-*t*Bu was not even persistent when generated with an excess (2–3 equivalents) of base (Fig. S4, Experimental Section).

The kinetic experiments with the nitro-substituted carbanions **1c** and **2c** were unproblematic: Because of their stability, stock solutions of **1c**-K and **2c**-K have been employed. On the other hand, solutions of the reactive carbanions **1a,b** and **2a,b** were generated immediately before the kinetic experiments, and the kinetic investigations were restricted to reactions with active electrophiles, which proceeded faster than the decomposition of the carbanions.

For all reactions described in Table 5.2, first-order rate constants k_{obs} (s^{-1}) were obtained by least-squares fittings of the mono-exponential function $A_t = A_0 \exp(-k_{\text{obs}}t) + C$ to the time-dependent absorbances A of the minor components. Plots of k_{obs} versus the concentrations of the compounds used in excess were generally linear with negligible intercepts and the second-order rate constants k_2 ($\text{L mol}^{-1} \text{s}^{-1}$) as slopes (Figure 5.1, Table 5.2). Some exceptions are discussed below.

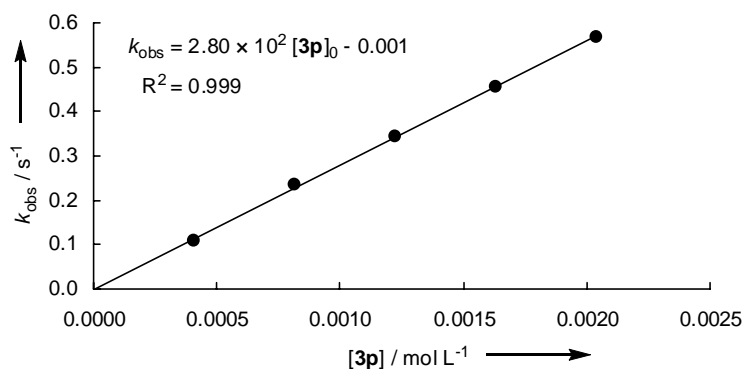


Figure 5.1. Determination of the second-order rate constant $k_2 = 2.80 \times 10^2 \text{ L mol}^{-1} \text{ s}^{-1}$ for the reaction of the *p*-cyanophenylacetonitrile anion (**1b**) with the Michael acceptor **3p** in DMSO at 20 °C.

As mentioned above, we were not able to obtain persistent solutions of the carbanion **2a**. When its reactions with **3s** (used as the minor component) were followed photometrically, exponential decays of the electrophile (**3s**) absorbance were observed. Plots of k_{obs} vs. the concentration of **2a** (calculated from $[\mathbf{2a-H}]$ assuming complete deprotonation) were linear, and the slopes, which equal the second-order rate constants k_2 were almost identical (Table 5.2) independent of the quantity of the base (1.05 equivalents of $\text{P}_4\text{-}t\text{Bu}$ or 1, 2, or 3 equivalents of $\text{KO}t\text{Bu}$) used for the deprotonation of **2a**. However, significant negative intercepts of variable magnitude were observed in all cases (Tables S15-20, Experimental Section), indicating fast and irreversible consumption of certain fractions of the carbanion **2a**. Similar observations, i.e., negative intercepts of variable magnitude and slopes, corresponding to second-order rate constants, which are almost independent of the nature and quantity of

base used for the deprotonation of **2a–H**, were made for the analogous reactions of the carbanion **2a** with the electrophiles **3t,u** (see Tables S21–S26).

Table 5.2. Second-Order Rate Constants k_2 for the Reactions of the Phenylacetonitrile Anions **1a–c** and the Phenylpropionitrile Anions **2a–c** with the Michael Acceptors **3a–u** in DMSO at 20 °C.

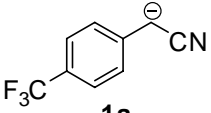
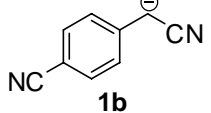
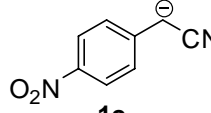
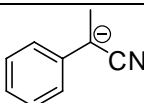
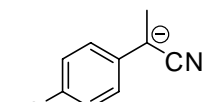
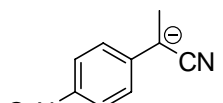
Nucleophile	Electrophile	λ / nm^a	$k_2 / \text{M}^{-1} \text{s}^{-1b}$
 1a $N = 27.28; s = 0.50$	3d	3d / 440	4.04×10^5
	3e	3e / 486	8.24×10^4
	3f	3f / 521	5.45×10^4
 1b $N = 25.11; s = 0.54$	3e	3e / 486	1.10×10^4
	3f	3f / 521	6.59×10^3
	3i	3i / 490	1.61×10^6
	3j	3j / 523	3.94×10^5
	3j	3j / 523	$4.09 \times 10^5^c$
	3m	1b / 394	1.70×10^4
	3m	1b / 398	$1.64 \times 10^4^c$
	3m	1b / 398	$1.60 \times 10^4^{c,d}$
	3m	1b / 398	$1.86 \times 10^4^{c,e}$
	3n	1b / 394	8.87×10^3
	3o	1b / 397	2.81×10^3
	3p	1b / 397	2.80×10^2
	3q	1b / 394	1.54×10^2
3r	1b / 394	6.50×10^1	
 1c $N = 19.67; s = 0.68$	3a	3a / 400	$1.29 \times 10^5^c$
	3c	3c / 380	4.19×10^2
	3c	3c / 400	$4.43 \times 10^2^c$
	3d	3d / 400	3.43×10^2
	3d	3d / 400	$3.26 \times 10^2^c$
	3h	3h / 388	5.23×10^5
	3l	3l / 560	4.17×10^4
	3m	1c / 537	$2.51 \times 10^1^f$
3n	1c / 537	9.98^g	

Table 5.2. Continued.

Nucleophile	Electrophile	λ / nm^a	$k_2 / \text{M}^{-1} \text{s}^{-1}^b$
 2a $N = 28.95; s = 0.58$	3f	3f / 524	$2.50 \times 10^6{}^g$
	3s	3s / 405	$3.05 \times 10^3{}^g$
	3s	3s / 410	$2.87 \times 10^3{}^g$
	3s	3s / 400	3.12×10^3
	3s	3s / 400	$3.09 \times 10^3{}^h$
	3s	3s / 400	$3.15 \times 10^3{}^i$
	3t	3t / 405	$1.86 \times 10^3{}^g$
	3t	3t / 405	$1.69 \times 10^3{}^h$
	3t	3t / 405	1.50×10^3
	3u	3u / 405	$9.90 \times 10^2{}^g$
	3u	3u / 405	8.54×10^2
	3u	3u / 405	$9.82 \times 10^2{}^h$
 2b $N = 25.35; s = 0.56$	3b	3b / 533	$7.73 \times 10^6{}^j$
	3e	3e / 488	$4.54 \times 10^4{}^j$
	3e	3e / 488	3.20×10^4
	3f	3f / 524	$2.51 \times 10^4{}^j$
	3m	2b / 403	1.08×10^4
	3m	2b / 403	1.15×10^4
	3n	2b / 403	5.68×10^3
	3o	2b / 403	2.44×10^3
	3p	2b / 403	1.19×10^3
 2c $N = 19.61; s = 0.60$	3a	3a / 410	$7.95 \times 10^4{}^k$
	3c	3c / 375	$2.04 \times 10^2{}^k$
	3d	2c / 590	$9.61 \times 10^1{}^k$
	3g	2c / 590	5.22×10^5
	3h	2c / 590	1.15×10^5
	3k	2c / 590	1.88×10^5
	3l	2c / 590	9.12×10^3

^a Minor component in the pseudo-first order kinetics and monitored wavelength. ^b In the presence of 1 equiv. KO t Bu. ^c In the presence of 18-crown-6. ^d In the presence of 3 equiv. of **1b**-H. ^e Measurement at 25 °C. ^f Reversible reactions, see text and Experimental Section. ^g Deprotonation of **2a**-H acid with P₄- t Bu phosphazene base. ^h In the presence of 2 equiv. of KO t Bu. ⁱ In the presence of 3 equiv. of KO t Bu. ^j Deprotonation of **2b**-H with P₂- t Bu phosphazene base. ^k In the presence of **2c**-H.

On the other hand, significant positive intercepts in plots of the first-order rate constants (k_{obs}) against the concentrations of the major component were observed for the reactions of the p-nitrophenylacetonitrile anion (**1c**) with the benzyldenemalonates **3m** and **3n**. Positive

intercepts are indicative of reversible reactions, and by theory, reflect the rate constants of the reverse reactions.²⁴ However, as discussed above, the intercepts are also affected by side reactions that we refrain to employ the intercepts of these plots for calculating the rates of the reverse reactions and the equilibrium constants K .

As shown in Table 5.2, the addition of 18-crown-6 caused only insignificant changes of the second-order rate constants k_2 for the reactions of **1b** with **3j** and **3m** and of **1c** with **3c** and **3d**. These results confirm that ion-pairing is negligible in dilute DMSO solution, in accordance with literature reports²⁵ and earlier findings of our group.^{6,8,26}

Nucleophilicity of *tert.*-Butoxide. As discussed above, persistent solutions of the more basic carbanions have only been obtained when more than one equivalent of KO t Bu was used for the deprotonation of the corresponding CH acids. In order to elucidate the influence of excess KO t Bu on the kinetics, we have studied the reaction of **2b** with the quinone methide **3e** in the presence of variable excess of KO t Bu. As shown in Figure 5.2, the slope of the plot of k_{obs} vs. [KO t Bu] was higher when [KO t Bu] > [**2b**-H] and from the different slopes in the range of [KO t Bu] < [**2b**-H] and [KO t Bu] > [**2b**-H] one can derive that KO t Bu is approximately two times more nucleophilic than **2b**. As a consequence, KO t Bu cannot be used in excess when nucleophiles with $N \leq 27$ are investigated. On the other hand, an excess of KO t Bu used for the deprotonation of **2a**-H will hardly affect the first order rate constant because **2a** reacts considerably faster than KO t Bu (Figure S6, Experimental Section).

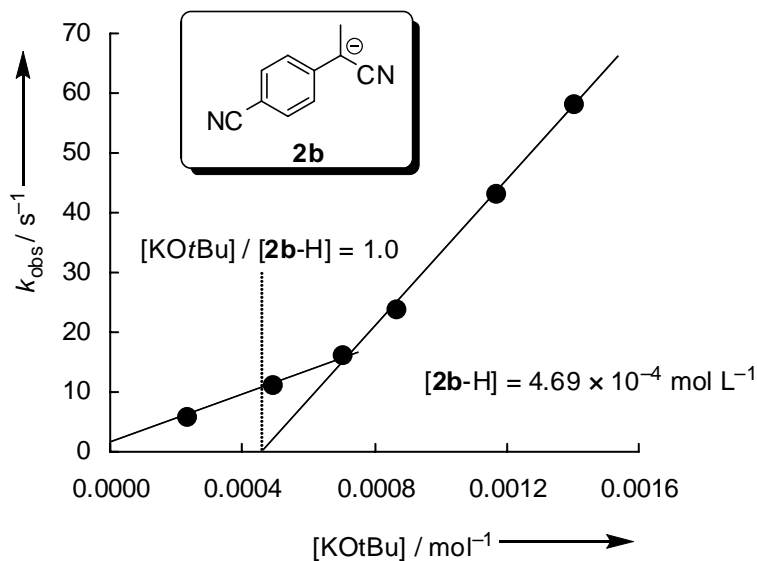


Figure 5.2. Plot of the observed first-order rate constants k_{obs} for the reactions of electrophile **3e** ($c_0 = 2.00 \times 10^{-5} \text{ mol L}^{-1}$) with the nucleophile **2b** against the concentration of KOtBu used for the deprotonation of **2b-H** ($c_0 = 4.69 \times 10^{-4} \text{ mol L}^{-1}$) in DMSO at 20 °C.

Correlation Analysis. In order to determine the nucleophile-specific parameters N and s for the phenylacetonitrile anions **1a-c** (Figure 5.3) and the phenylpropionitrile anions **2a-c** (Figure 5.4), the logarithmic second-order rate constants $\log k_2$ of their reactions with electrophiles **3a-u** were plotted against the electrophilicity parameters E of **3a-u**.

The linear correlations for the reactions of the phenylacetonitrile anions **1a-c** ($R^2 > 0.98$, Figure 5.3) allow us to determine the nucleophile-specific parameters N and s for these carbanions.

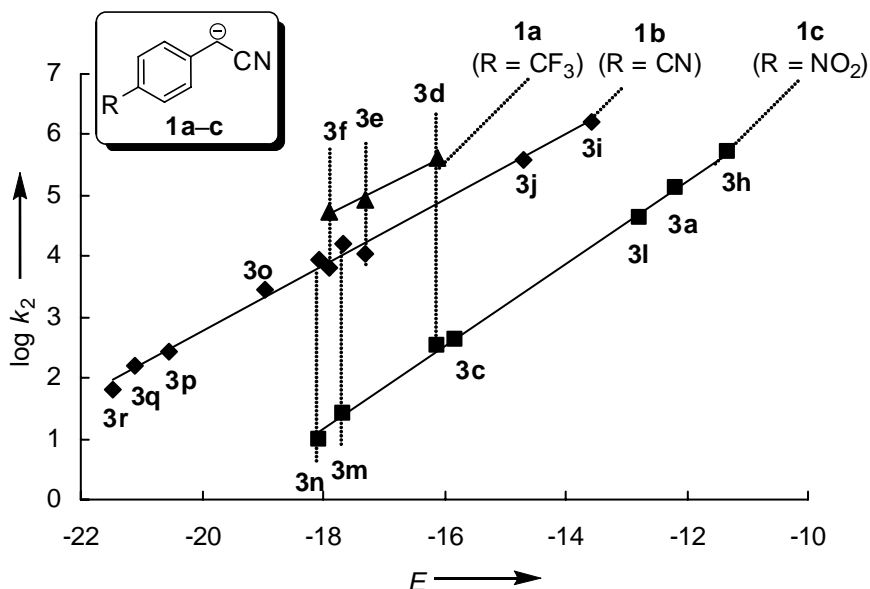


Figure 5.3. Plot of $\log k_2$ for the reactions of the nucleophiles **1a–c** with the electrophiles **3** in DMSO versus their electrophilicity parameters E .

The correlations for the reactions of the phenylpropionitrile anions **2a–c** ($R^2 \geq 0.95$, Figure 5.4) show larger deviations from linearity than those of the phenylacetonitrile anions **1a–c**. In particular, the reactions of the carbanion **2b** with benzylidenemalonate **3p**, as well as the reaction of carbanion **2c** with quinone methide **3a** are two times faster than expected. On the other hand, the reactions of **2b** with the benzylidenemalonates **3m,n** are approximately two times slower than expected. Taking into account that many different classes of Michael acceptors have been used as electrophiles, these deviations can be considered as rather small, and the correlation lines in Figure 5.6 were employed to determine the nucleophile-specific parameters N and s for the phenylpropionitriles **2a–c**.

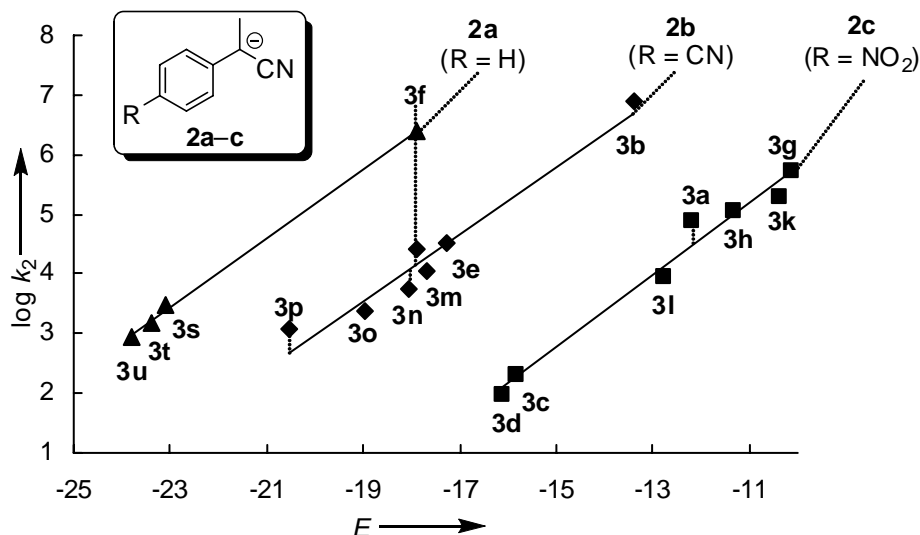


Figure 5.4. Plot of $\log k_2$ for the reactions of the nucleophiles **2a–c** with the electrophiles **3** in DMSO versus their electrophilicity parameters E .

As expected, electron-withdrawing groups at the *p*-position of the aromatic ring decrease the nucleophilicities N of the carbanions **1a–c** and **2a–c**. A comparison between the reactivities of the phenylacetonitrile anions **1a–c** and the phenylpropionitrile anions **2a–c** (Table 5.2 and Figure 5.5) shows that replacement of one hydrogen by a methyl group at the α -carbon of phenylacetonitrile anions does not significantly affect the nucleophilicities. The inductive effect of the methyl group and its steric demand obviously compensate each other resulting in similar reactivities of the analogously substituted carbanions **1b/2b** and **1c/2c**.

In order to determine reliable nucleophilicity or electrophilicity parameters, reaction partners should be employed, which differ by several orders of magnitude. The correlation lines for compounds **2a–c** fulfill this condition. However, it should be noted that the slopes of the correlation lines for compounds **2a** and **2b** are largely controlled by the reactions with the electrophiles **3f** and **3b**, respectively. The situation for compounds **1b,c** is much better, because their N and s parameters can be derived from a balanced series of rate constants (Figure 5.3). Because the parameters N and s for carbanion **1a** have only been derived from three rate constants, which differ by less than one order of magnitude, the nucleophilicity parameters N and s for **1a** should be regarded with caution.

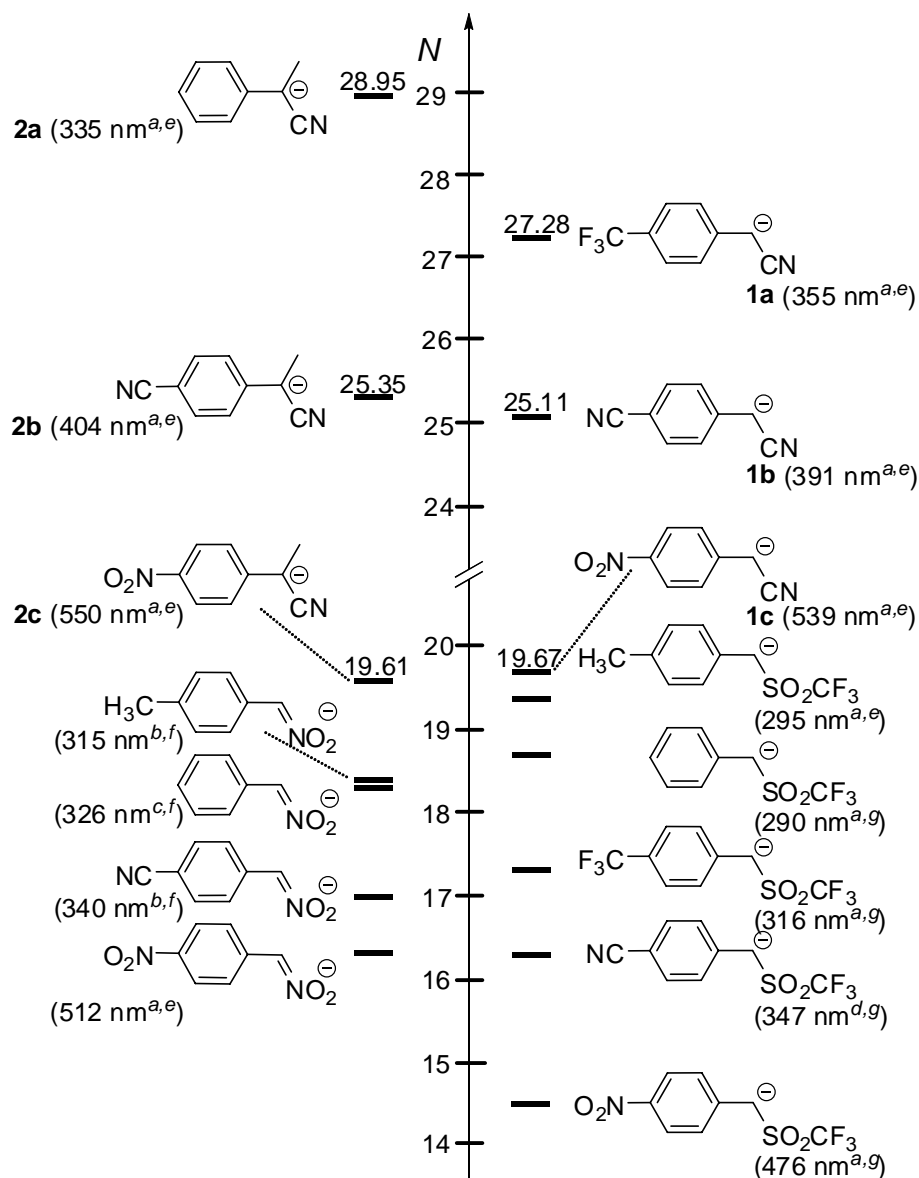


Figure 5.5. Comparison of the nucleophilicity parameters N of the phenylacetone anions **1a–c** and the phenylpropionitrile anions **2a–c** with those for α -nitro- and trifluoromethyl sulfonyl stabilized carbanions in DMSO. ^a λ_{\max} in DMSO, ^b λ_{\max} in MeOH, ^c λ_{\max} in DMSO/H₂O 10:90 (v/v), ^d λ_{\max} in DMSO/H₂O 30:70 (v/v), ^e this work, ^f see ref. 9, ^g see ref. 27

Figure 5.5 compares the colored α -acceptor substituted benzyl anions whose nucleophilicity parameters N have so far been determined. They cover a reactivity range of almost 15 orders of magnitude. It is obvious that the phenylacetone anions **1a–c** are much stronger nucleophiles than the analogously substituted α -triflate and α -nitro substituted

benzyl anions, whose reactivities have recently been determined.^{6,8} Because of the paucity of available data, Hammett-plots for the differently substituted phenylacetonitrile anions **1a–c** and phenylpropionitrile anions **2a–c** are not informative. Figure 5.5 reveals, however, that variation of the *p*-substituents in both series **1a–c** and **2a–c** have considerably larger effects on the nucleophilic reactivities than in the series of α -triflinate and much more than in the series of α -nitro substituted carbanions. Obviously more negative charge is localized in the aromatic rings of carbanions **1a–c** and **2a–c** than in the corresponding α -triflinate and nitro substituted benzyl anions.

pK_a values are generally considered to be a useful tool for estimating the nucleophilic reactivities of many compounds. We have already shown that this assumption only holds within groups of structurally closely related nucleophiles.^{6,28} For example, the correlation between nucleophilicities of primary and secondary amines versus their pK_{aH} values in water is very poor.^{28c} Figure 5.6 shows a moderate correlation between the nucleophilicity parameters *N* of carbanions and the pK_a values of their conjugate CH acids (cf. Scheme 5.1) in DMSO. It is obvious that the phenylacetonitrile anions **1a–c** and carbanion **2a** are considerably more nucleophilic than expected from the pK_a values of the corresponding CH acids,²⁹ indicating the limitation of pK_a for predicting nucleophilic reactivities. In accordance with earlier reports,^{5,8,30} the positive deviations of the cyano substituted carbanions are indicative of lower intrinsic barriers of their reactions.

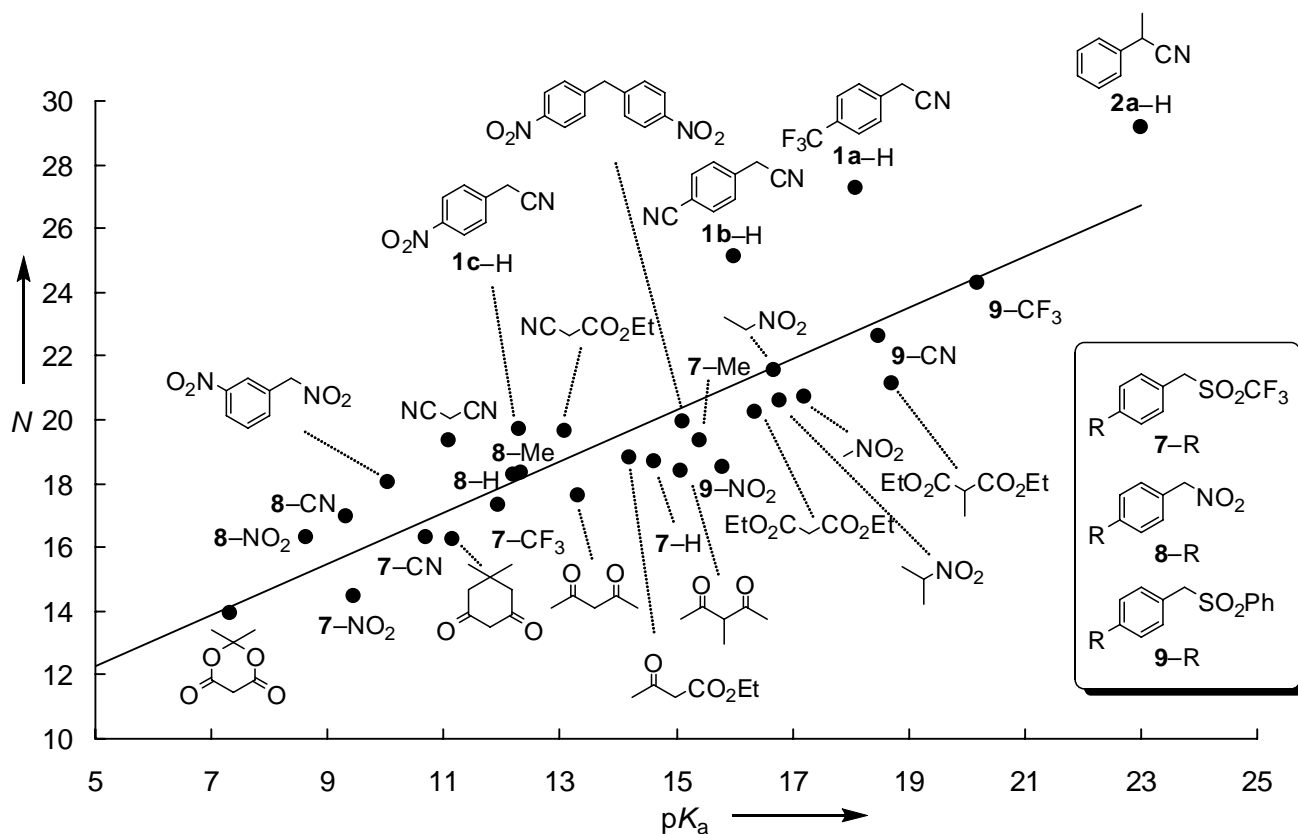


Figure 5.6. Correlation of the nucleophilicity parameters N of different carbanions versus the pK_a values of their corresponding CH acids in DMSO. Overall correlation equation: $N = 0.802pK_{aH} + 8.278$, $R^2 = 0.750$. (Nucleophilicity parameters N and pK_{aH} values used for this diagram are compiled in the Experimental Section).

Conclusions

α -Cyano substituted benzyl anions are several orders of magnitude more nucleophilic than α - SO_2CF_3 and α - NO_2 substituted benzyl anions. The high reactivities of the cyano substituted species **1a–c** and **2a–c** are only partially caused by their higher basicities (pK_{aH}). Lower intrinsic barriers for the reactions of these carbanions are indicated by positive deviations from the Brønsted plots and also contribute to their high nucleophilicities. Variation of the p -substituent in the aromatic ring has a considerably larger effect on the nucleophilicities of **1a–c** and **2a–c** than in the corresponding α - SO_2CF_3 and α - NO_2 substituted counterparts,

indicating a larger delocalization of the negative charge in the aromatic ring of carbanions **1a–c** and **2a–c**. As colored species of high nucleophilicities, these carbanions complement our series of reference nucleophiles, which can be employed for the photometric determination of electrophilic reactivities.

General Remarks

Phenylacetonitriles (**1a–c**)–H and Phenylpropionitriles (**2a–c**)–H. Phenylacetonitriles **1** are commercially available compounds and have been recrystallized from *n*-pentane/MeOH prior to use. Compounds (**2a–c**)–H have been prepared by methylation of the corresponding phenylacetonitriles by using methyl iodide as described in the literature.³¹

3-(3,5-Di-*tert*-butyl-4-hydroxyphenyl)-3-(4-methoxyphenyl)-2-(4-nitrophenyl)-propanenitrile (4cd). A mixture of **1c**–H (25.0 mg, 154 μ mol), NaOMe (8.30 mg, 170 μ mol) and **3d** (50.0 mg, 154 μ mol) was stirred in MeOH (10 mL) for 1 h under N₂ atmosphere. After work-up with diluted acetic acid and chromatography on silica gel (*i*hex/EtOAc 4:1, R_f = 0.38), the product was obtained as a yellow foam (71.0 mg, 146 μ mol, 95 % as a mixture of diastereomers in a ratio of 1:1.2). ¹H-NMR (CDCl₃, 300 MHz): δ = 1.32, 1.38 (2s, 18 H, CH₃ (*t*Bu)), 3.76, 3.80 (2s, 3 H, OCH₃), 4.19-4.24 (m, 1 H, CH), 4.51 (d, ³*J* = 8.4 Hz, 0.50 H, CH), 4.57 (d, ³*J* = 8.1 Hz, 0.47 H, CH), 5.13, 5.17 (2s, 1 H, OH), 6.78-6.81 (m, 1 H, CH_{ar}), 6.85-6.89 (m, 2.20 H, CH_{ar}), 6.97 (s, 1 H, CH_{ar}), 7.10-7.13 (m, 1 H, CH_{ar}), 7.19-7.27 (m, 3 H, CH_{ar}) 8.07-8.11 ppm (m, 2 H, CH_{ar}). ¹³C-NMR (CDCl₃, 75.5 MHz): δ = 30.15, 30.23 (2q, CH₃), 34.32, 34.35 (2s), 43.64, 43.73 (2d, CH), 55.22, 55.23 (2q, CH₃), 55.82, 56.07 (2d, CH), 114.07, 114.12 (2d, CH_{ar}), 119.13, 119.20 (2s, CN), 123.61, 123.66 (2d, CH_{ar}), 124.55, 125.10 (2d, CH_{ar}), 128.95, 129.32, 129.43 (3d, CH_{ar}, peak for the other diastereomer superimposed), 129.35, 130.08 (s), 131.30, 132.00 (2s), 135.93, 136.12 (2s), 142.44, 142.47

(2s), 147.48, 147.50 (2s), 152.96, 153.26 (2s), 158.69, 158.99 ppm (2d). HR-MS (ESI) [M-H]⁻: calcd 485.2446; found 485.2440.

4,4'-(Cyanoethene-1,2-diyl)-dibenzonitrile (6bn). Equimolar amounts of **1b**-H (81 mg, 0.57 mmol) and NaOMe were stirred in MeOH, when electrophile **3n** was added subsequently. The resulting precipitate was filtered, washed and dried to yield the pure product **6bn** as colorless solid (109 mg, 0.43 mmol, 75 %). ¹H-NMR (d₆-DMSO, 400 MHz): δ = 7.98-8.06 (m, 6 H, CH_{ar}), 8.09-8.12 (m, 2 H, CH_{ar}), 8.34 ppm (s, 1 H, C=CH). ¹³C-NMR (d₆-DMSO, 100 MHz): δ = 111.9 (s), 112.8 (s), 116.6 (s), 118.2 (s), 126.8 (d, CH_{ar}), 129.8 (d, CH_{ar}), 132.7 (d, CH_{ar}), 133.0 (d, CH_{ar}), 137.5 (s), 143.8 ppm (d, C=CH). MS (EI) *m/z* (%) = 256 (33) [M + H⁺], 255 (100) [M], 254 (82), 228 (39), 215 (63), 200 (14). HR-MS: calcd 255.0796, found 255.0786 (C₁₇H₉N₃), mp 303–304 °C (dec., ref.³² 302–303 °C).

Kinetics. The reactions of carbanions **1a–c** and **2a–c** were studied in DMSO at 20 °C. The rates of the reactions of carbanions **1a–c** and **2a–c** with the Michael acceptors **3a–u** were determined photometrically under first-order conditions using either a large excess of the electrophiles **3a–u** or of the carbanions **1a–c** and **2a–c** (for details see text and Experimental Section), which were generated by deprotonation of the corresponding CH acid (**1a–c**)-H and (**2a–c**)-H by using potassium *tert.*-butoxide or Schwesinger's phosphazene bases P₂-*t*Bu and P₄-*t*Bu.

The reactions were studied with conventional stopped-flow instruments as described earlier. The experiments were initiated by mixing equal volumes of solutions of the base and the CH acidic compounds (**1a–c**)-H and (**2a–c**)-H to generate the corresponding carbanions. After a delay time of *t* = 1 s the resulting solutions of the carbanions were mixed with equal volumes of solutions of the electrophiles. From the exponential decay of the absorptions of the minor components, first-order rate constants were obtained by least-squares fittings of the mono-exponential function $A_t = A_0 \exp(-k_{\text{obs}}t) + C$ to the absorbance data.

References

- (1) a) Mayr, H.; Kempf, B.; Ofial, A. R. *Acc. Chem. Res.* **2003**, *36*, 66-77; b) Mayr, H.; Ofial, A. R. in *Carbocation Chemistry*; Olah, H. A., Prakash, G. K. S., eds.; Wiley: Hoboken, (N. J.); **2004**, pp, 331-358; c) Ofial, A. R.; Mayr, H. *Macromol. Symp.* **2004**, *215*, 353-367; d) Mayr, H.; Ofial, A. R. *Pure Appl. Chem.* **2005**, *77*, 1807-1821; e) Mayr, H.; Ofial, A. R. *J. Phys. Org. Chem.* **2008**, *21*, 584-595.
- (2) Mayr, H.; Bug, T.; Gotta, M. F.; Hering, N.; Irrgang, B.; Janker, B.; Kempf, B.; Loos, R.; Ofial, A. R.; Remennikov, G.; Schimmel, H. *J. Am. Chem. Soc.* **2001**, *123*, 9500-9512.
- (3) Mayr, H.; Patz, M. *Angew. Chem.* **1994**, *106*, 990-1010; *Angew. Chem. Int. Ed.* **1994**, *33*, 938-955.
- (4) Lucius, R.; Loos, R.; Mayr, H. *Angew. Chem.* **2002**, *114*, 97-102; *Angew. Chem. Int. Ed.* **2002**, *41*, 91-95.
- (5) Bug, T.; Mayr, H. *J. Am. Chem. Soc.* **2003**, *125*, 12980-12986.
- (6) Berger, S. T. A.; Ofial, A. R.; Mayr, H. *J. Am. Chem. Soc.* **2007**, *129*, 9753-9761.
- (7) Seeliger, F.; Mayr, H. *Org. Biomol. Chem.* **2008**, *6*, 3052-3058.
- (8) Bug, T.; Lemek, T.; Mayr, H. *J. Org. Chem.* **2004**, *69*, 7565-7576.
- (9) Phan, T. B.; Mayr, H. *Eur. J. Org. Chem.* **2006**, 2530-2537.
- (10) Berger, S. T. A.; Lemek, T.; Mayr, H. *ARKIVOC* **2008**, (x), 37-53.
- (11) a) Lemek, T.; Mayr, H. *J. Org. Chem.* **2003**, *68*, 6880-6886; b) Kaumanns, O.; Mayr, H. *J. Org. Chem.* **2008**, *73*, 2738-2745.
- (12) Seeliger, F.; Berger, S. T. A.; Remennikov, G. Y.; Polborn, K.; Mayr, H. *J. Org. Chem.* **2007**, *72*, 9170-9180.

- (13) Berger, S. T. A.; Seeliger, F. H.; Hofbauer, F.; Mayr, H. *Org. Biomol. Chem.* **2007**, *5*, 3020-3026.
- (14) Kaumanns, O.; Lucius, R.; Mayr, H. *Chem. Eur. J.* **2008**, *14*, 9675-9682.
- (15) a) Collier, S. J.; Langer, P. In *Science of Synthesis*; Murahashi, S.-I., ed.; Thieme: Stuttgart, 2004; Vol. 19, Chapt. 19.5.15, pp 403-425. (b) Murahashi, S. I. In *Science of Synthesis*; Murahashi, S.-I., ed.; Thieme: Stuttgart, 2004; Vol. 19, Chapt. 19.5.14, pp 345-402. c) Fleming, F. F.; Zhang, Z. *Tetrahedron* **2005**, *61*, 747-789; d) Fleming, F. F.; Wang, Q. *Chem. Rev.* **2003**, *103*, 2035-2077.
- (16) a) Bordwell, F. G.; Bausch, M. J. *J. Am. Chem. Soc.* **1986**, *108*, 1979-1985; b) Bordwell, F. G.; Cheng, J.-P.; Bausch, M. J.; Bares, J. E. *J. Phys. Org. Chem.* **1988**, *1*, 209-223.
- (17) Smith, H. A.; Bissell, R. L.; Kenyon, W. G.; MacClarence, J. W.; Hauser, C. *R. J. Org. Chem.* **1971**, *36*, 2132-2137.
- (18) a) Makosza, M.; Stalinski, K.; Klepka, C. *Chem. Commun.* **1996**, 837-838; b) Makosza, M.; Stalinski, K. *Chem. Eur. J.* **1997**, *3*, 2025-2031; c) Makosza, M.; Stalinski, K. *Tetrahedron* **1998**, *54*, 8797-8810; d) Makosza, M.; Stalinski, K. *Synthesis* **1998**, 1631-1634.
- (19) a) Adam, W.; Makosza, M.; Zhao, C.-G.; Surowiec, M. *J. Org. Chem.* **2000**, *65*, 1099-1101; b) Adam, W.; Makosza, M.; Stalinski, K.; Zhao, C.-G. *J. Org. Chem.* **1998**, *63*, 4390-4391.
- (20) Kroeger, D. J.; Stewart, R. *Can. J. Chem.* **1967**, *45*, 2163-2171.
- (21) Arnett, E. M.; Small, L. E. *J. Am. Chem. Soc.* **1977**, *99*, 808-816.
- (22) Olmstead, W. N.; Margolin, Z.; Bordwell, F. G. *J. Org. Chem.* **1980**, *45*, 3295-3299.

- (23) Schwesinger, R.; Schlemper, H.; Hasenfratz, C.; Willaredt, J.; Dambacher, T.; Breuer, T.; Ottaway, C.; Fletschinger, M.; Boele, J.; Fritz, H.; Putzas, D.; Rotter, H. W.; Bordwell, F. G.; Satish, A. V.; Ji, G. Z.; Peters, E. M.; Peters, K.; v. Schnering, H. G.; Walz, L. *Liebigs Ann.* **1996**, 1055-1081.
- (24) a) Maskill, H.; Editor *The Investigation of Organic Reactions and Their Mechanisms*; Blackwell Publishing: Oxford, 2006; b) Schmid, R.; Sapunov, V. N. *Non-Formal Kinetics*; VCH: Weinheim, 1982.
- (25) Binev, I. G.; Tsenov, J. A.; Velcheva, E. A.; Juchnovski, I. N. *J. Mol. Struct.* **1995**, 344, 205-215.
- (26) Lucius, R.; Mayr, H. *Angew. Chem.* **2000**, 112, 2086-2089; *Angew. Chem., Int. Ed.* **2000**, 39, 1995-1997.
- (27) Goumont, R.; Kizilian, E.; Buncel, E.; Terrier, F. *Org. Biomol. Chem.* **2003**, 1, 1741-1748.
- (28) a) Nigst, T. A.; Westermaier, M.; Ofial, A. R.; Mayr, H. *Eur. J. Org. Chem.* **2008**, 2369-2374; b) Brotzel, F.; Kempf, B.; Singer, T.; Zipse, H.; Mayr, H. *Chem. Eur. J.* **2007**, 13, 336-345; c) Brotzel, F.; Chu, Y. C.; Mayr, H. *J. Org. Chem.* **2007**, 72, 3679-3688.
- (29) pK_a values for **2b** and **2c** have not been reported.
- (30) a) Bernasconi, C. F.; Zitomer, J. L.; Fox, J. P.; Howard, K. A. *J. Org. Chem.* **1984**, 49, 482-486; b) Bernasconi, C. F. *Acc. Chem. Res.* **1987**, 20, 301-308; c) Bernasconi, C. F.; Wenzel, P. J. *J. Org. Chem.* **2003**, 68, 6870-6879.
- (31) Bailey, W. F.; Jiang, X.-L.; McLeod, C. E. *J. Org. Chem.* **1995**, 60, 7791-7795.
- (32) Bell, F.; Waring, D. H. *J. Chem. Soc.* **1948**, 1024-1026.

Experimental Section

Nucleophilicities of the Anions of Arylacetonitriles and Arylpropionitriles in Dimethyl Sulfoxide

O. Kaumanns, R. Appel, T. Lemek, F. Seeliger, and H. Mayr, *J. Org. Chem.* **2008**, accepted.

5.1. General

Materials. Commercially available DMSO (content of H₂O < 50 ppm) was used without further purification. Stock solutions of KO^tBu in DMSO were prepared under nitrogen atmosphere. Phenylacetonitriles are commercially available compounds and have been used without further purification. Compounds **2a–c** were prepared by methylation of the corresponding phenylacetonitriles by using methyl iodide as described in ref. S1

NMR spectroscopy. In the ¹H and ¹³C NMR spectra chemical shifts are expressed in ppm and refer to DMSO-*d*₆ (δ_{H} 2.50, δ_{C} 39.4) or to CDCl₃ (δ_{H} 7.26, δ_{C} 77.0) as internal standard. The coupling constants are in Hz. Abbreviations used are s (singlet), d (doublet), t (triplet), q (quartet), quint (quintet), m (multiplet).

5.2. Determination of Rate Constants

The general method for the determination of the rate constants is described in the experimental part of the paper. The temperature of the solutions was kept constant (20 ± 0.1 °C) during all kinetic experiments by using a circulating bath thermostat.

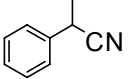
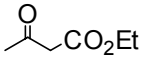
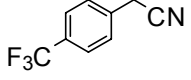
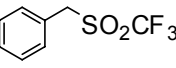
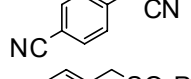
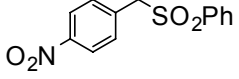
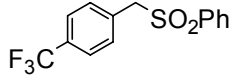
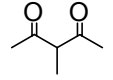
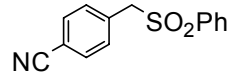
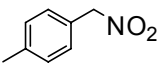
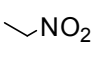
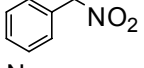
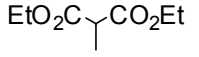
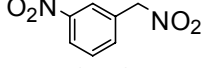
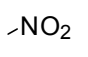
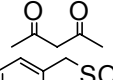
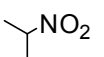
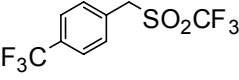
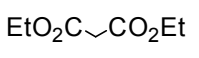
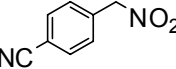
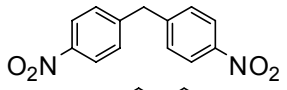
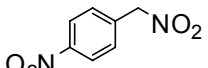
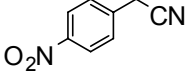
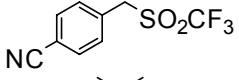
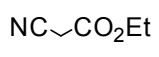
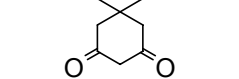
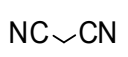
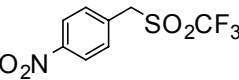
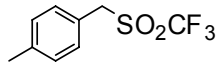
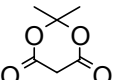
^{S1} Bailey, W. F.; Jiang, X.-L.; McLeod, C. E. *J. Org. Chem.* **1995**, *60*, 7791-7795.

For fast kinetic experiments ($\tau_{1/2} < 15$ s), standard stopped-flow UV-vis-spectrophotometer systems were used in their double mixing mode. Kinetics of slow reactions ($\tau_{1/2} > 15$ s) were determined by UV-Vis spectrometry using a diode array spectrophotometer which was connected to an insertion probe via fibre optic cables.

Rate constants k_{obs} (s^{-1}) were obtained by fitting the single exponential function $A_t = A_0 \exp(-k_{\text{obs}}t) + C$ to the observed time-dependent absorbance of the minor component. Plotting k_{obs} against the concentrations of the nucleophiles resulted in linear correlations whose slopes correspond to the second-order rate constants k_2 ($\text{L mol}^{-1} \text{s}^{-1}$). For stopped-flow experiments with **1c** and **2c** two stock solutions were used: A solution of electrophiles **3a–u** in DMSO and a solution of the carbanions **1c** and **2c** in DMSO generated by deprotonation of the corresponding CH acid with KO*t*Bu, P₂-*t*Bu, or P₄-*t*Bu or, in case of **2c**, by dissolving the corresponding preformed potassium salt (**2c-K**). Due to their high reactivities and slow decomposition in DMSO solution, the carbanions **1a,b** and **2a,b** were generated by using a double-mixing mode of conventional stopped-flow instruments. In the first step, the CH acids (**1a,b**)-H and (**2a,b**)-H were mixed with the base to generate the corresponding carbanions directly in the sample cell. After a short remaining time of the carbanion solution in the mixing cell (age time), the electrophile solutions were added in a second step. Conditions different from those mentioned here, will be described explicitly in the corresponding tables.

5.3. Nucleophilicities for Different Carbanions and The Acidities of Their Conjugate CH Acids in DMSO

Table S1: Nucleophilicities N for Different Types of Carbanions and the Acidity Constants pK_a of their Conjugate CH Acids in DMSO.

Compound	N	pK_a	Compound	N	pK_a
	29.14	23.00 ^[Bor88]		18.82	14.20 ^[Bor81]
	27.29	18.10 ^[Bor86]		18.67	14.62 ^[Gou03]
	25.11	16.00 ^[Bor88]		18.50	15.80 ^[Bor88a]
	24.30	20.20 ^[Bor88a]		18.38	15.07 ^[Olm80]
	22.60	18.50 ^[Bor88a]		18.31	12.33 ^[Kee79]
	21.54	16.70 ^[Bor94]		18.29	12.20 ^[Bor94]
	21.13	18.70 ^[Bor88d]		18.06	10.04 ^[Kee79]
	20.71	17.20 ^[Olm80]		17.64	13.33 ^[Olm80]
	20.61	16.80 ^[Bor94]		17.33	11.95 ^[Gou03]
	20.22	16.37 ^[Olm80]		16.96	9.31 ^[Kee79]
	19.92	15.10 ^[Bor88b]		16.29	8.62 ^[Kee79]
	19.68	12.30 ^[Bor88]		16.28	10.70 ^[Bor88]
	19.62	13.10 ^[Bor88c]		16.27	11.16 ^[Olm80]
	19.36	11.10 ^[Bor89]		14.49	9.46 ^[Gou03]
	19.35	15.40 ^[Bor88]		13.91	7.33 ^[Am87]

[Arn87] Arnett, E. M.; Harrelson, J. A., Jr. *J. Am. Chem. Soc.* **1987**, *109*, 809-812.

[Bor81] Bordwell, F. G.; Fried, H. E. *J. Org. Chem.* **1981**, *46*, 4327-4331.

[Bor86] Bordwell, F. G.; Bausch, M. J. *J. Am. Chem. Soc.* **1986**, *108*, 1979-1985.

[Bor88] Bordwell, F. G.; Cheng, J. P.; Bausch, M. J.; Bares, J. E. *J. Phys. Org. Chem.* **1988**, *1*, 209-223.

[Bor88a] Bordwell, F. G.; Bausch, M. J.; Branca, J. C.; Harrelson, J. A., Jr. *J. Phys. Org. Chem.* **1988**, *1*, 225-239.

[Bor88b] Bordwell, F. G.; Algrim, D. J. *J. Am. Chem. Soc.* **1988**, *110*, 2964-2968.

- [Bor88c] Bordwell, F. G.; Branca, J. C.; Bares, J. E.; Filler, R. *J. Org. Chem.* **1988**, *53*, 780-782.
- [Bor88d] Bordwell, F. G. *Acc. Chem. Res.* **1988**, *21*, 456-463.
- [Bor89] Bordwell, F. G.; Harrelson, J. A., Jr.; Satish, A. V. *J. Org. Chem.* **1989**, *54*, 3101-3105.
- [Bor94] Bordwell, F. G.; Satish, A. V. *J. Am. Chem. Soc.* **1994**, *116*, 8885-8889.
- [Gou03] Goumont, R.; Kizilian, E.; Buncel, E.; Terrier, F. *Org. Biomol. Chem.* **2003**, *1*, 1741-1748.
- [Kee79] Keeffe, J. R.; Morey, J.; Palmer, C. A.; Lee, J. C. *J. Am. Chem. Soc.* **1979**, *101*, 1295-1297.
- [Olm80] Olmstead, W. N.; Bordwell, F. G. *J. Org. Chem.* **1980**, *45*, 3299-3305.

Please note that the product studies carried out by Roland Appel have been omitted from this Experimental Section, as well as the kinetic experiments he performed. This data and the kinetic experiments carried out by Florian Seeliger for compound **2c** can be found in the Supporting Information of the published article.

Other contributions and those from Tadeusz Lemek are stated in *italics*.

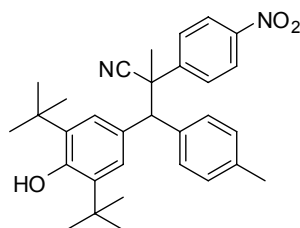
5.4. Product Studies

Products 5 from the reactions of the nucleophile 2c

3-(3,5-Di-*tert*.butyl-4-hydroxyphenyl)-2-methyl-2-(4-nitrophenyl)-3-*p*-tolylpropionitrile (5cc). After mixing **2c**-H (63.0 mg, 0.36 mmol) with KO*t*Bu (42.0 mg, 0.37 mmol) in DMSO (5 mL) and subsequent addition of **3c** (122 mg, 0.40 mmol), the reaction mixture was stirred for 30 min at ambient temperature. Then the reaction mixture was poured into cold aqueous acetic acid (1 %) and extracted with CH₂Cl₂. The combined organic layers were washed with water and dried (Na₂SO₄). Evaporation of the solvent under reduced pressure yielded the crude product, which was purified by chromatography (SiO₂, hexane/EtOAc 15:1, *R*_f = 0.5): 75 mg (0.15 mmol, 42 %; colorless solid (dr 1:1.1).

Major diastereomer: ¹H NMR (CDCl₃, 400 MHz): δ = 1.45 (s, 18 H, *t*butyl), 1.72 (s, 3 H, CH₃), 2.02 (s, 3 H, CH₃), 4.04 (s, 1 H, CH), 5.20 (s, 1 H, OH), 6.85 (s, 2 H, CH_{ar}), 6.93 (d, ³*J* = 8.0 H, 2 H, CH_{ar}), 7.10 (d, ³*J* = 8.0 H, 2 H, CH_{ar}), 7.55 (d, ³*J* = 8.8 H, 2 H, CH_{ar}), 8.10 ppm (d, ³*J* = 8.8 H, 2 H, CH_{ar}). ¹³C NMR (CDCl₃, 100 MHz): δ = 20.9 (q, CH₃), 26.8 (q, CH₃), 30.3 (s, C(CH₃)₃), 34.5 (s, C(CH₃)₃), 47.7 (s, CR₄), 61.9 (d, CH), 122.5 (s, CN), 123.6 (d, CH_{ar}), 125.6 (d, CH_{ar}), 127.5 (d, CH_{ar}), 128.5 (d, CH_{ar}), 129.1 (d, CH_{ar}), 135.9 (s, CH_{ar}), 136.4 (s), 136.7 (s), 147.0 (s), 147.6 (s), 152.8 ppm (s).

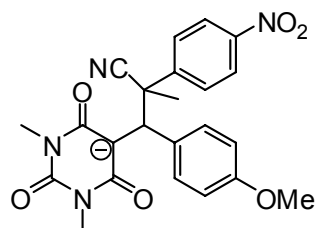
Minor diastereomer: ¹H-NMR (CDCl₃, 400 MHz): δ = 1.26 (s, 18 H, *t*butyl), 1.75 (s, 3 H, CH₃), 2.36 (s, 3 H, CH₃), 3.95 (s, 1 H, CH), 5.04 (s, 1 H, OH), 7.21 (d, ³*J* = 8.0 H, 2 H, CH_{ar}), 7.40 (s, 2 H, CH_{ar}), 7.43 (d, ³*J* = 8.8 H, 2 H, CH_{ar}), 7.58 (d, ³*J* = 8.0 H, 2 H, CH_{ar}), 8.11 ppm (d, ³*J* = 8.8 H, 2 H, CH_{ar}). ¹³C NMR (CDCl₃, 100 MHz): δ = 21.0 (q, CH₃), 28.1 (q, CH₃), 30.1 (s, C(CH₃)₃), 34.2 (s, C(CH₃)₃), 47.9 (s, CR₄), 62.6 (d, CH), 122.4 (s, CN), 123.3 (d, CH_{ar}), 125.9 (d, CH_{ar}), 127.4 (d, CH_{ar}), 128.5 (d, CH_{ar}), 129.6 (d, CH_{ar}), 136.3 (s, CH_{ar}), 137.4 (s), 137.4 (s), 147.0 (s), 147.9 (s), 153.3 ppm (s). HR-MS (EI) [M]⁺: calcd 484.2798; found 485.2928 [C₃₁H₃₇N₂O₃].



3-(1,3-Dimethyl-2,4,6-trioxohexahydropyrimidin-5-yl)-3-(4-methoxyphenyl)-2-methyl-2-(4-nitrophenyl)propionitrile anion (5ck). In an NMR tube **2c-K** (10.0 mg, 46.7 μmol) was dissolved in d_6 -DMSO (0.7 mL). After the addition of **3k** (10.6 mg, 38.6 μmol) the products were analyzed by NMR spectroscopy without further work up: **5ck** as a mixture of diastereomers (7:4).

^1H NMR (CDCl_3 , 200 MHz), major diastereomer: δ = 1.63 (s, 3 H, CH_3), 2.87 (s, 6 H, NCH_3), 3.72 (s, 3 H, OCH_3), 4.59 (s, 1 H, CH), 6.79 (d, 3J = 8.8 Hz, 2 H, Ar-H), 7.64 (d, 3J = 8.8 Hz, 2 H, Ar-H), 7.73 (d, 3J = 8.8 Hz, 2 H, Ar-H) 8.09 ppm (d, 3J = 8.8 Hz, 2 H, Ar-H).

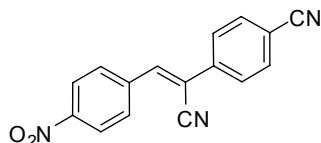
Minor diastereomer: δ = 1.70 (s, 3 H, CH_3), 3.02 (s, br., 3 H, NCH_3), 3.08 (s, br., 3 H, NCH_3), 3.64 (s, 3 H, OCH_3), 4.64 (s, 1 H, CH), 6.60 (d, 3J = 8.8 Hz, 2 H, Ar-H), 7.20 (d, 3J = 8.8 Hz, 2 H, Ar-H), 7.57 (d, 3J = 8.8 Hz, 2 H, Ar-H) 8.17 ppm (d, 3J = 8.8 Hz, 2 H, Ar-H).



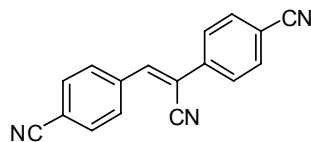
Products 6 from reactions of nucleophiles 1b,c with electrophile 3m–u

General. Equimolar amounts of NaOMe and CH-acids (**1b,c**)-H were dissolved in dry MeOH (5 mL). Subsequently electrophiles **3** (1 equiv.) were added. After stirring for 5–10 min at ambient temperature the resulting precipitates were isolated by filtration, washed with MeOH, and dried under reduced pressure to yield the products **6**. NMR signal assignments were based on additional DEPT, gHMBC and gHSQC experiments.

4-(1-Cyano-2-(4-nitrophenyl)-vinyl)benzotrile (6bm). From **1b**-H (114 mg, 0.80 mmol) and **3m** (234 mg, 0.80 mmol): 91 mg (0.33 mmol, 41 %); colorless solid; mp 212.9–213.7 °C (ref.^{S2}: mp 212 °C). ¹H NMR (d₆-DMSO, 400 MHz): δ = 7.99–8.05 (m, 4 H, CH_{ar}), 8.17 (d, ³J = 8.8 Hz, 2 H, CH_{ar}), 8.39–8.42 ppm (m, 3 H, CH_{ar} and C=CH). ¹³C NMR (d₆-DMSO, 100 MHz): δ = 112.1 (s), 112.6 (s), 116.5 (s), 118.2 (s), 124.0 (d, CH_{ar}), 126.9 (d, CH_{ar}), 130.4 (d, CH_{ar}), 132.1 (d, CH_{ar}), 133.1 (d, CH_{ar}), 137.4 (s), 139.4 (s), 143.3 (d, C=CH), 148.1 ppm (s). MS (EI) m/z (%) = 276 (16), 275 (100) [M⁺], 229 (28), 228 (26), 202 (14), 190 (20), 175 (10). HR-MS: calcd 275.0689; found 275.0692 [C₁₆H₉N₃O₂].



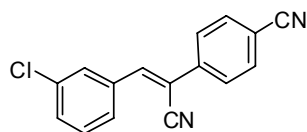
4,4'-(1-Cyanoethene-1,2-diyl)dibenzotrile (6bn). From **1b**-H (81 mg, 0.57 mmol) and **3n** (170 mg, 0.62 mmol): 109 mg (0.43 mmol, 75 %); colorless solid; mp 303–304 °C (dec.) (ref.^{S3}: mp 302–303 °C). ¹H NMR (d₆-DMSO, 400 MHz): δ = 7.98–8.06 (m, 6 H, CH_{ar}), 8.09–8.12 (m, 2 H, CH_{ar}), 8.35 ppm (s, 1 H, C=CH). ¹³C NMR (d₆-DMSO, 100 MHz): δ = 112.0 (s), 112.8 (s), 116.6 (s), 118.2 (s), 126.8 (d, CH_{ar}), 129.8 (d, CH_{ar}), 132.8 (d, CH_{ar}), 133.0 (d, CH_{ar}), 137.6 (s), 143.8 ppm (d, C=CH). MS (EI) m/z (%) = 256 (33), 255 (100) [M⁺], 254 (82), 228 (39), 215 (63), 200 (14). HR-MS: calcd 255.0796, found 255.0791 [C₁₇H₉N₃].



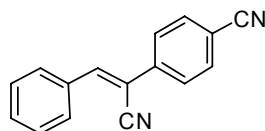
^{S2} Kroeger, D. J.; Stewart, R. *Can. J. Chem.* **1967**, *45*, 2163–2171.

^{S3} Bell, F.; Waring, D. H. *J. Chem. Soc.* **1948**, 1024–1026.

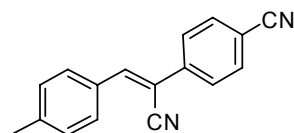
4-(2-(3-Chloro-phenyl)-1-cyanovinyl)benzonitrile (6bo). From **1b-H** (146 mg, 1.03 mmol) and **3o** (291 mg, 1.03 mmol): 121 mg (0.46 mmol, 45 %); colorless solid; mp 196.9-197.5 °C (Lit. ref.^{S2}: mp 195-195.5 °C). ¹H NMR (d₆-DMSO, 400 MHz): δ = 7.60-7.62 (m, 2 H, CH_{ar}), 7.95-8.02 (m, 6 H, CH_{ar}), 8.25 ppm (s, C=CH). ¹³C NMR (d₆-DMSO, 100 MHz): δ = 110.2 (s), 111.5 (s), 116.6 (s), 118.0 (s), 126.4 (d, CH_{ar}), 127.5 (d CH_{ar}), 128.8 (d, CH_{ar}), 130.6 (d, 2 × CH_{ar}), 132.8 (d, CH_{ar}), 133.3 (s), 135.0 (s), 137.5 (s), 143.8 ppm (d, C=CH). MS (EI), *m/z* (%): 266 (24), 264 (73) [M⁺], 229 (100), 202 (18), 201 (18), 100 (15). HR-MS: calcd 264.0448; found 264.0436 [C₁₆H₉³⁵CIN₂].



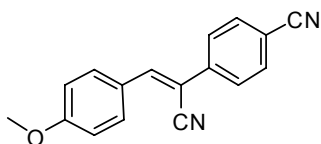
4-(1-Cyano-2-phenylvinyl)benzonitrile (6bp). From **1b-H** (99 mg, 0.70 mmol) and **3p** (172 mg, 0.69 mmol): 61 mg (0.26 mmol, 38 %); colorless solid; mp 146.0-146.5 °C (ref.^{S2}: mp 144.5-145.5 °C). ¹H NMR (d₆-DMSO, 400 MHz): δ = 7.56-7.58 (m, 3 H, CH_{ar}), 7.96-8.01 (m, 6 H, CH_{ar}), 8.26 ppm (s, 1 H, C=CH). ¹³C NMR (d₆-DMSO, 100 MHz): δ = 108.7 (s), 111.4 (s), 117.2 (s), 118.3 (s), 126.5 (d, CH_{ar}), 129.0 (d, CH_{ar}), 129.4 (d, CH_{ar}), 131.2 (s), 133.0 (d, CH_{ar}), 133.2 (d, CH_{ar}), 138.1 (s), 145.8 ppm (s, C=CH). MS (EI), *m/z* (%): 231 (15), 230 (100) [M⁺], 229 (55) [M - H⁺], 215 (18), 202 (11), 190 (16).



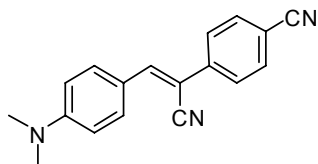
4-(1-Cyano-2-*p*-tolylvinyl)benzonitrile (6bq). From **1b-H** (98 mg, 0.69 mmol) and **3q** (182 mg, 0.69 mmol): 105 mg (0.43 mmol, 62 %); colorless solid; mp 172.8-173.8 °C. ¹H NMR (d₆-DMSO, 400 MHz): δ = 2.39 (s, CH₃), 7.38 (d, ³*J* = 8.2 Hz, 2 H, CH_{ar}), 7.89 (d, ³*J* = 8.2 Hz, 2 H, CH_{ar}), 7.93-7.99 (m, 4 H, CH_{ar}), 8.20 ppm (s, C=CH). ¹³C NMR (d₆-DMSO, 100 MHz): δ = 21.1 (q, CH₃), 107.4 (s), 111.1 (s), 117.4 (s), 118.3 (s), 126.3 (d, 2 × CH_{ar}), 129.5 (d, 2 × CH_{ar}), 130.5 (s), 132.9 (d, CH_{ar}), 138.3 (s), 141.7 (s), 145.7 ppm (d, C=CH). MS (EI), *m/z* (%): 245 (15), 244 (100) [M⁺], 229 (69). HR-MS: calcd 244.0995, found 244.0999 [C₁₇H₁₂N₂].



4-(1-Cyano-2-(4-methoxyphenyl)vinyl)benzotrile (6br). From **1b-H** (72 mg, 0.51 mmol) and **3r** (141 mg, 0.51 mmol): 60 mg (0.23 mmol, 45 %); yellow solid; mp 161.8-162.6 °C (ref.^{S4}: 161-162 °C). ¹H NMR (d₆-DMSO, 400 MHz): δ = 3.86 (OCH₃), 7.14 (d, ³J = 8.9 Hz, 2 H, CH_{ar}), 7.91-8.01 (m, 6 H, CH_{ar}), 8.17 ppm (s, C=CH). ¹³C NMR (d₆-DMSO, 100 MHz): δ = 55.4 (q, OCH₃), 105.2 (s), 110.6 (s), 114.6 (d, CH_{ar}), 117.7 (s), 118.4 (s), 125.7 (s), 126.1 (d, CH_{ar}), 131.6 (d, CH_{ar}), 132.9 (d, CH_{ar}), 138.6 (s), 145.2 (d, C=CH), 161.7 ppm (s). MS (EI), *m/z* (%): 261 (24), 260 (100) [M⁺], 215 (12), 190 (41). HR-MS: calcd 260.0945; found 260.0937 [C₁₇H₁₂N₂O].



4-(1-Cyano-2-(4-(dimethylamino)phenyl)vinyl)benzotrile (6bs). From **1b-H** (142 mg, 1.00 mmol) and **3s** (253 mg, 0.87 mmol): 191 mg (0.70 mmol, 80 %); yellow solid; mp 208.5-209.1 °C (ref.^{S5} 205 °C). ¹H NMR (d₆-DMSO, 400 MHz): δ = 3.05 (s, 6 H, N(CH₃)₂), 6.83 (d, ³J = 9.2 Hz, 2 H), 7.84-7.94 (m, 6 H, C-H_{ar}), 8.02 ppm (s, HC=C). ¹³C NMR (d₆-DMSO, 100 MHz): δ = 40.0 (t, N(CH₃)₂), 100.5 (s), 110.1 (s), 112.1 (d, CH_{ar}), 119.1 (s), 119.2 (s), 120.8 (s), 125.9 (d, CH_{ar}), 132.3 (d, CH_{ar}), 133.3 (d, CH_{ar}), 140.0 (s), 145.9 (d, CH_{ar}, HC=C), 152.7 ppm (s). MS (EI), *m/z* (%): 274 (15), 273 (100) [M⁺], 272 (61), 229 (9). HR-MS: calcd 273.1261; found 273.1254 [C₁₈H₁₅N₃].

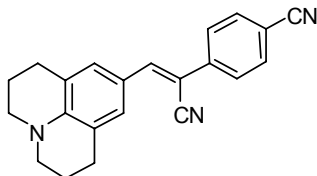


4-(1-Cyano-2-(1,2,3,5,6,7-hexahydropyrido[3,2,1-*ij*]quinolin-9-yl)vinyl)benzotrile (6bu). From **1b-H** (123 mg, 0.87 mmol) and **3u** (343 mg, 1.00 mmol): 255 mg (0.78 mmol, 90 %); orange solid; mp 164.0-164.5 °C. ¹H NMR (d₆-DMSO, 400 MHz): δ = 1.88 (quint, ³J = 6.0 Hz, 4 H, NCH₂CH₂CH₂), 2.69 (t, ³J = 6.0 Hz, 4 H, NCH₂CH₂CH₂), 3.29 (t, ³J = 6.0 Hz, 4 H, NCH₂CH₂CH₂), 7.50 (s, 2 H, C_{ar(jul)}), 7.79-7.90 ppm (m, 5 H, C_{ar}). ¹³C NMR (d₆-DMSO, 100 MHz): δ = 20.7 (t, NCH₂CH₂CH₂), 27.1 (t, NCH₂CH₂CH₂), 49.2 (t, NCH₂CH₂CH₂), 98.0 (s), 109.1 (s), 119.1 (s), 120.2 (s), 125.0 (d, CH_{ar}), 129.4 (d, CH_{ar}), 132.7 (d, CH_{ar}), 139.8 (s),

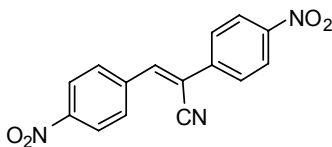
^{S4} Ichimura, K.; Watanabe, S. *Bull. Chem. Soc. Jpn.* **1976**, *49*, 2224-2229.

^{S5} Pfeiffer, P. *Justus Liebigs Annalen der Chemie* **1928**, 20-52.

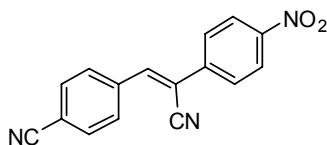
145.2 (d, HC=C), 145.6 ppm (s). MS (EI), m/z (%): 326 (22), 325 (100) [M^+], 322 (10). HR-MS: calcd 325.1574; found 325.1561 [$C_{22}H_{19}N_3$].



2,3-Bis-(4-nitrophenyl)acrylonitrile (6cm). From **1c-H** (144 mg, 0.89 mmol) and **3m** (260 mg, 0.89 mmol): 80 mg (0.27 mmol, 30 %); brown solid; mp 214.2-214.9 °C (ref.^{S2}: 214-215 °C). 1H NMR (d_6 -DMSO, 400 MHz): δ = 8.09 (d, 3J = 9.0 Hz, 2 H, CH_{ar}), 8.19 (d, 3J = 8.8 Hz, 2 H, CH_{ar}), 8.38 (d, 3J = 9.0 Hz, 2 H, CH_{ar}), 8.41 (d, 3J = 8.8 Hz, 2 H, CH_{ar}), 8.46 ppm (s, 1 H, C=CH). ^{13}C NMR (d_6 -DMSO, 100 MHz): δ = 112.2 (s), 116.6 (s), 124.0 (d, $2 \times CH_{ar}$), 124.3 d, $2 \times CH_{ar}$), 127.4 (d, $2 \times CH_{ar}$), 130.5 (d, $2 \times CH_{ar}$), 139.2, 139.3 ($2 \times$ s), 144.0 (d, C=CH), 147.8 (s), 148.2 ppm (s). MS (EI), m/z (%): 296 (18), 295 (100) [M^+], 203 (26), 190 (25); HR-MS: calcd 295.0588; found 295.0580 [$C_{15}H_9N_3O_4$].

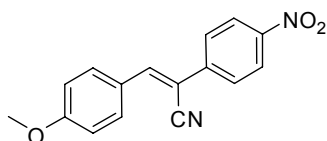


4-(2-Cyano-2-(4-nitrophenyl)vinyl)benzonitrile (6cn). From **1c-H** (124 mg, 0.76 mmol) and **3n** (204 mg, 0.75 mmol): 120 mg (0.44 mmol, 59 %); green solid; mp 134.0-135.1 °C. 1H NMR (d_6 -DMSO, 400 MHz): δ = 8.04-8.13 (m, 6 H, CH_{ar}), 8.37-8.40 ppm (m, 3 H, CH_{ar} , C=CH). ^{13}C NMR (d_6 -DMSO, 100 MHz): δ = 111.6 (s), 112.9 (s), 116.6 (s), 118.2 (s), 124.3 (d, CH_{ar}), 127.3 (d, CH_{ar}), 129.9 (d, CH_{ar}), 132.8 (d, CH_{ar}), 137.5 (s), 139.3 (s), 144.4 (d, C=CH), 147.7 ppm (s). MS (EI), m/z (%): 276 (15), 275 (100) [M^+], 228 (27), 201 (15). HR-MS: calcd 275.0689; found 275.0675 [$C_{16}H_9N_3O_2$].

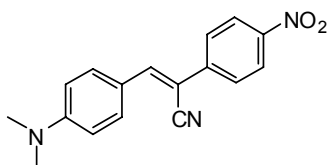


3-(4-Methoxyphenyl)-2-(4-nitrophenyl)acrylonitrile (6cr). From **1c-H** (150 mg, 0.93 mmol) and **3r** (257 mg, 0.92 mmol): 116 mg (0.41 mmol, 45 %); yellow solid; mp 160.8-161.4 °C (ref.^{S2}: 162-163 °C). 1H NMR (d_6 -DMSO, 400 MHz): δ = 3.86 (s, 3 H, OCH_3); 7.14 (d, 3J = 9.0 Hz, 2 H, CH_{ar}), 7.98-8.03 (m, 3 H, CH_{ar}), 8.22 (s, 1 H, HC=C), 8.33 ppm (d, 3J = 9.0 Hz, 2 H, CH_{ar}). ^{13}C NMR (d_6 -DMSO, 100 MHz): δ = 55.5 (q, OCH_3), 104.8 (s), 114.6 (d,

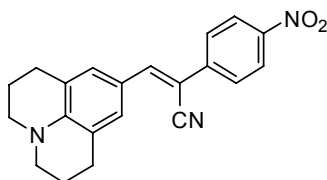
CH_{ar}), 117.7 (s), 124.2 (d, CH_{ar}), 125.7 (s), 126.4 (d, CH_{ar}), 131.8 (d, CH_{ar}), 140.5 (s), 145.9 (s), 146.9 (d, HC=C), 161.8 ppm (s). MS (EI), *m/z* (%): 281 (17), 280 (100) [M⁺], 189 (24). HR-MS: calcd 280.0843; found 280.0848 [C₁₆H₁₂N₂O₃].



3-(4-(Dimethylamino)phenyl)-2-(4-nitrophenyl)acrylonitrile (6cs). From **1c-H** (162 mg, 1.00 mmol) and **3s** (291 mg, 1.00 mmol): 200 mg (0.68 mmol, 68 %); dark red solid; mp 250.7-251.5 °C (ref.^{S6}: 245-246 °C). ¹H NMR (d₆-DMSO, 400 MHz): δ = 3.06 (s, 6 H, NMe₂), 6.85 (d, ³*J* = 9.0 Hz, 2 H, CH_{ar}), 7.94 (d, ³*J* = 7.2 Hz, 2 H, CH_{ar}), 7.96 (d, ³*J* = 7.2 Hz, 2 H, CH_{ar}), 8.09 (s, HC=C), 8.30 (d, ³*J* = 8.9 Hz, 2 H, CH_{ar}) (in agreement with ref.^{S7}). ¹³C NMR (d₆-DMSO, 100 MHz): δ = 39.8 (q, N(CH₃)₂), 99.5 (s), 111.6 (d, CH_{ar}), 118.7 (s), 120.2 (s), 124.2 (d, CH_{ar}), 125.6 (d, CH_{ar}), 132.0 (d, CH_{ar}), 141.6 (s), 146.1 (s), 146.1 (d, CH_{ar}, HC=C), 152.3 (s). HR-MS (EI): calcd 293.1159; found 293.1157 [C₁₇H₁₅N₃O₂].



3-(1,2,3,5,6,7-Hexahydropyrido[3,2,1-*ij*]quinolin-9-yl)-2-(4-nitrophenyl)acrylonitrile (6cu). From **1c-H** (108 mg, 0.67 mmol) and **3u** (228 mg, 0.66 mmol): 108 mg (0.41 mmol, 62 %); purple solid; mp 235.3 °C (dec). ¹H NMR (d₆-DMSO, 400 MHz): δ = 1.89 (quint, ³*J* = 6.2 Hz, 4 H, NCH₂CH₂CH₂), 2.70 (t, ³*J* = 6.2 Hz, 4 H, NCH₂CH₂CH₂), 3.31 (t, ³*J* = 6.2 Hz, 4 H, NCH₂CH₂CH₂), 7.54 (s, 2 H, CH_{ar(jul)}), 7.87-7.92 (m, 3 H, HC=C, 17-H, 21-H), 8.26 (d, ³*J* = 9.1 Hz, 2 H, 18-H, 20-H). ¹³C NMR (d₆-DMSO, 100 MHz): δ = 20.7 (t, NCH₂CH₂CH₂), 27.1 (t, NCH₂CH₂CH₂), 49.2 (t, NCH₂CH₂CH₂), 97.4 (s), 119.1 (s), 120.3 (d, C_{ar(jul)}), 124.2 (d, CH_{ar}), 125.1 (d, CH_{ar}), 129.6 (s), 142.0 (s), 145.6 (s), 145.9 (d, HC=C). HR-MS: calcd 345.1477; found 345.1472 [C₂₁H₁₉N₃O₂].



^{S6} Schwenker, G. *Arch. Pharm. Ber. Dtsch. Pharm. Ges.* **1966**, *299*, 131-139.

^{S7} Al-Shihry, S. S. *Molecules* **2004**, *9*, 658-665.

5.5. Deprotonation experiments

The formation of the carbanions **1a–c** and **2a** from their conjugate CH acids (**1a–c**)-H and **2a**-H, respectively, were recorded by using diode array UV-Vis spectrometers. The temperature during all experiments was kept constant by using a circulating bath (20.0 ± 0.02 °C). The CH acids (**1a–c**)-H and **2a**-H were dissolved in DMSO and subsequently treated with various amounts of KO*t*Bu or phosphazene base P₄-*t*Bu (dissolved in DMSO).

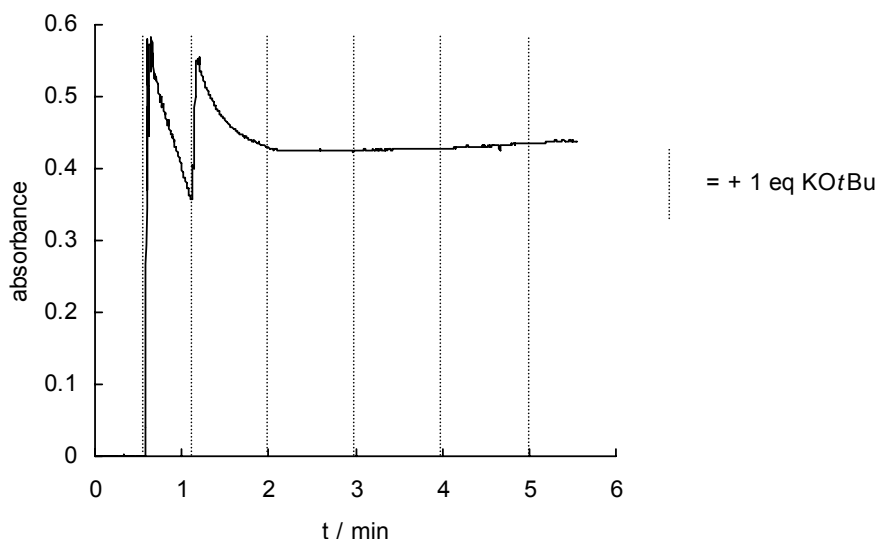


Figure S1: Deprotonation experiment with *p*-(trifluoromethyl)-phenyl-acetonitrile **1a**-H ($n = 1.35 \times 10^{-6}$ mol) in DMSO at 20 °C (deprotonated with KO*t*Bu, $\lambda = 360$ nm).

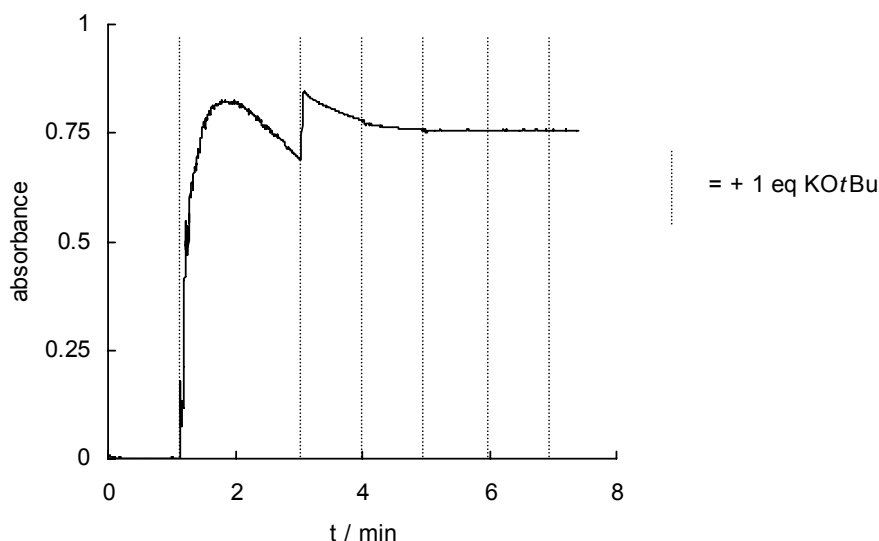


Figure S2: Deprotonation experiment with *p*-cyano-phenyl-acetonitrile **1b**-H ($n = 1.31 \times 10^{-6}$ mol) in DMSO at 20 °C (deprotonated with KO*t*Bu, $\lambda = 390$ nm).

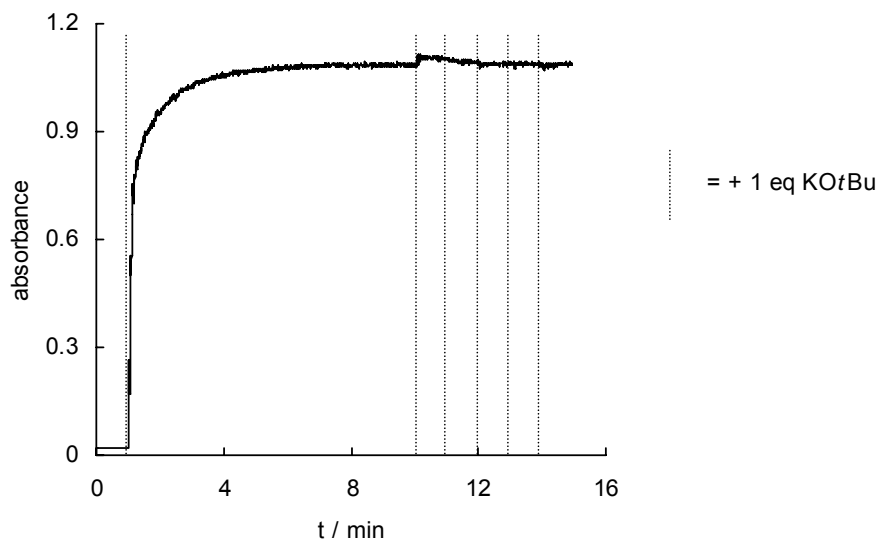


Figure S3: Deprotonation experiment with *p*-nitro-phenyl-acetonitrile **1c-H** ($n = 1.52 \times 10^{-6}$ mol) in DMSO at 20 °C (deprotonated with KO*t*Bu, $\lambda = 540$ nm).

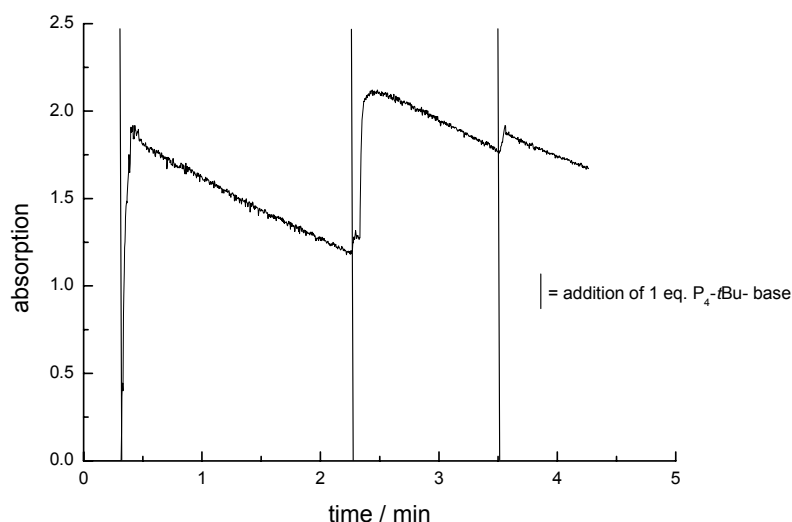


Figure S4: Deprotonation experiment of phenyl propionitrile **2a-H** in DMSO (with phosphazene base P₄-*t*Bu, $\lambda = 354$ nm, c_0 (**2a-H**) = 5.3×10^{-5} mol L⁻¹).

The influence of KO*t*Bu on the first order rate constant k_{obs} for the reactions of electrophiles **3e** with carbanion **2b** and of **3s** with **2a** was investigated in DMSO at 20 °C. The concentrations for the electrophiles **3e**, **3s**, and for the CH acids **2b-H** and **2a-H** were kept constant throughout the reactions. The influence of KO*t*Bu was investigated by changing the concentration of base, which is necessary for the generation of the carbanions **2a** and **2b**.

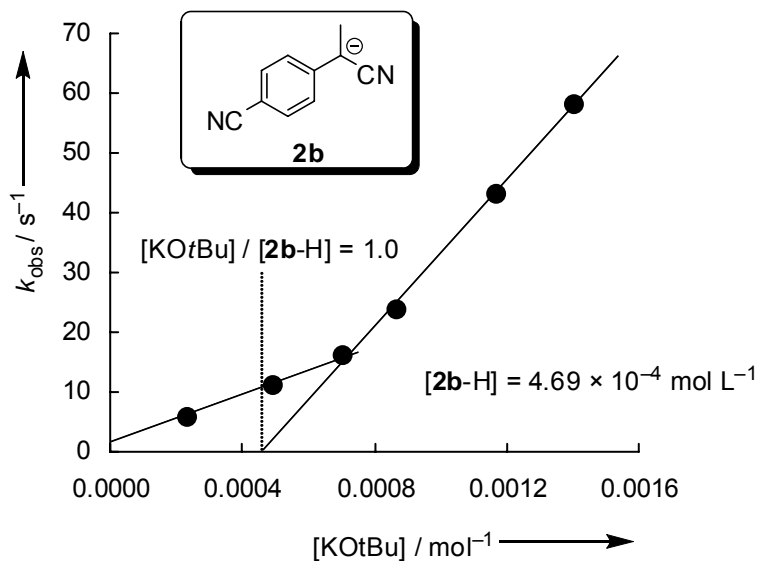


Figure S5: Plot of the first-order rate constants k_{obs} for the reactions of electrophile $\mathbf{3e}$ ($c_0 = 2.00 \times 10^{-5} \text{ mol L}^{-1}$) with the nucleophile $\mathbf{2b}$ against the concentration of KOtBu used for the deprotonation of $\mathbf{2b-H}$ ($c_0 = 4.69 \times 10^{-3} \text{ mol L}^{-1}$).

Table S2: First Order Rate Constants for the Reaction of the Electrophile $\mathbf{3s}$ ($c_0 = 2.00 \times 10^{-5} \text{ mol L}^{-1}$) with Carbanion $\mathbf{2b}$, Generated from $\mathbf{2b-H}$ ($c_0 = 4.69 \times 10^{-3} \text{ mol L}^{-1}$) with Various Amounts of KOtBu in DMSO at 20°C .

Entry	$[\text{KOtBu}] / \text{mol L}^{-1}$	Equivalents $[\text{KOtBu}]/[\mathbf{2b-H}]$	$k_{\text{obs}} / \text{s}^{-1}$ 1 s^a
1	2.35×10^{-4}	0.50	5.78
2	4.93×10^{-4}	1.05	11.00
3	7.04×10^{-4}	1.50	15.97
4	8.68×10^{-4}	1.85	23.70
5	1.17×10^{-3}	2.50	42.93
6	1.41×10^{-3}	3.00	58.10

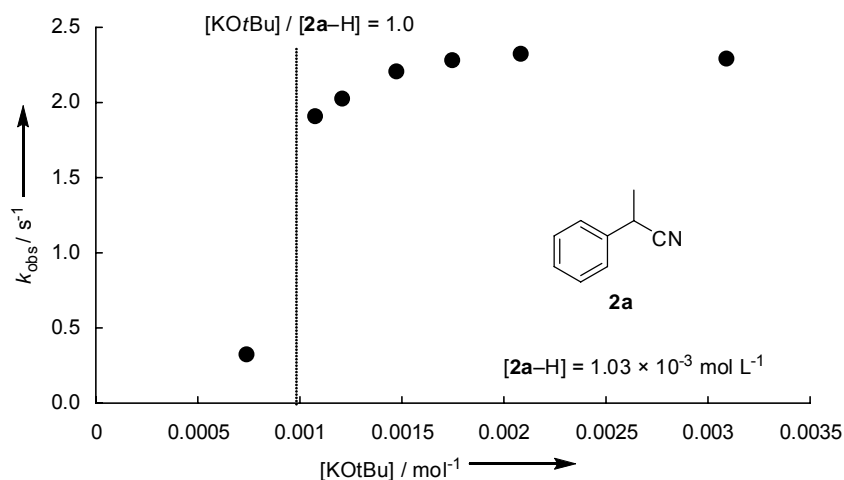


Figure S6: Plot of the first order rate constant k_{obs} for the reactions of electrophile $3\mathbf{s}$ ($c_0 = 3.23 \times 10^{-5} \text{ mol L}^{-1}$) with carbanion $2\mathbf{a}$ versus the concentration of KOtBu which has been used to generate $2\mathbf{a}$ from its corresponding CH acid $2\mathbf{a-H}$ ($c_0 = 1.03 \times 10^{-3} \text{ mol L}^{-1}$) in DMSO at 20°C .

Table S3: First Order Rate Constants for the Reaction of the Electrophile $3\mathbf{s}$ ($c_0 = 3.23 \times 10^{-5} \text{ mol L}^{-1}$) with Carbanion $2\mathbf{a}$, Generated from $2\mathbf{a-H}$ ($c_0 = 1.03 \times 10^{-3} \text{ mol L}^{-1}$) with Various Amounts of KOtBu in DMSO at 20°C .

Entry	$[\text{KOtBu}] / \text{mol L}^{-1}$	Equivalents $[\text{KOtBu}] / [2\mathbf{a-H}]$	$k_{\text{obs}} / \text{s}^{-1}$
1	7.39×10^{-4}	0.72	0.32
2	1.08×10^{-3}	1.05	1.90
3	1.21×10^{-3}	1.17	2.02
4	1.48×10^{-3}	1.43	2.02
5	1.75×10^{-3}	1.69	2.28
6	2.08×10^{-3}	2.02	2.32
7	3.09×10^{-3}	3.00	2.29

5.6. KINETICS

Table S4: Kinetics of the reaction of electrophile **3m** with the anion of (*p*-cyano-phenyl)acetonitrile (**1b**) in DMSO at 20 °C (deprotonated with 2 equiv. KO*t*Bu, stopped-flow UV-Vis spectrometer, $\lambda = 394$ nm).

Nr.	[Nu ⁻] ₀ / M	[E] ₀ / M	$k_{\text{obs}} / \text{s}^{-1}$
a313-1	4.08×10^{-5}	5.00×10^{-4}	7.60
a313-2	4.08×10^{-5}	1.00×10^{-3}	1.61×10^1
a313-3	4.08×10^{-5}	1.50×10^{-3}	2.53×10^1
a313-4	4.08×10^{-5}	2.00×10^{-3}	3.36×10^1
a313-5	4.08×10^{-5}	2.50×10^{-3}	4.13×10^1

$k_2 = 1.70 \times 10^4 \text{ L mol}^{-1} \text{ s}^{-1}$

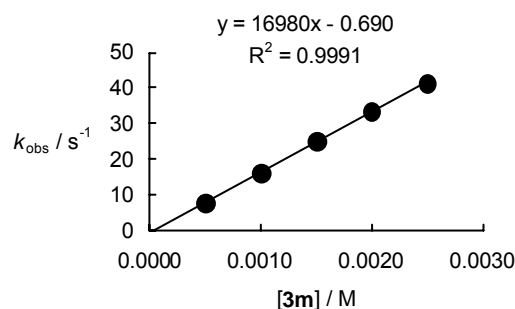


Table S5: Kinetics of the reaction of electrophile **3m** with the anion of (*p*-cyano-phenyl)acetonitrile (**1b**) in DMSO at 20 °C (deprotonated with 2 equiv. KO*t*Bu, in the presence of 18-crown-6, stopped-flow UV-Vis spectrometer, $\lambda = 398$ nm).

Nr.	[Nu ⁻] ₀ / M	[18-crown-6] / M	[E] ₀ / M	$k_{\text{obs}} / \text{s}^{-1}$
a325-1	4.18×10^{-5}	4.39×10^{-5}	7.21×10^{-4}	1.22×10^1
a325-2	4.18×10^{-5}	4.39×10^{-5}	1.44×10^{-3}	2.51×10^1
a325-3	4.18×10^{-5}	4.39×10^{-5}	2.16×10^{-3}	3.79×10^1
a325-4	4.18×10^{-5}	4.39×10^{-5}	2.88×10^{-3}	4.83×10^1
a325-5	4.18×10^{-5}	4.39×10^{-5}	3.60×10^{-3}	5.97×10^1

$k_2 = 1.64 \times 10^4 \text{ L mol}^{-1} \text{ s}^{-1}$

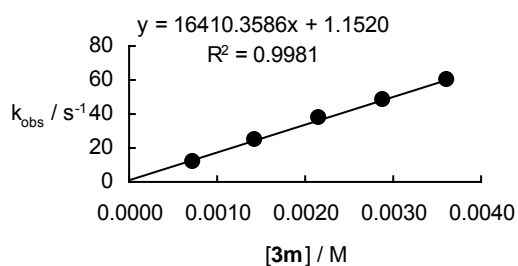


Table S6: Kinetics of the reaction of electrophile **3m** with the anion of (*p*-cyano-phenyl)acetonitrile (**1b**) in DMSO at 20 °C (deprotonated with 2 equiv. KO^tBu, addition 18-crown-6, addition of CH acid, stopped-flow UV-Vis spectrometer, $\lambda = 398$ nm).

Nr.	[Nu] ₀ / M	[18-crown-6] / M	[1b -H] / M	[E] ₀ / M	$k_{\text{obs}} / \text{s}^{-1}$
a325b-1	4.18×10^{-5}	4.39×10^{-5}	1.25×10^{-4}	7.21×10^{-4}	1.37×10^1
a325b-2	4.18×10^{-5}	4.39×10^{-5}	1.25×10^{-4}	1.44×10^{-3}	2.50×10^1
a325b-3	4.18×10^{-5}	4.39×10^{-5}	1.25×10^{-4}	2.16×10^{-3}	3.59×10^1
a325b-5	4.18×10^{-5}	4.39×10^{-5}	1.25×10^{-4}	2.88×10^{-3}	4.84×10^1

$$k_2 = 1.60 \times 10^4 \text{ L mol}^{-1} \text{ s}^{-1}$$

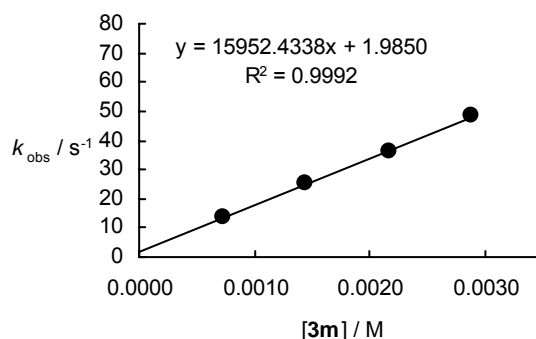


Table S7: Kinetics of the reaction of electrophile **3m** with the anion of (*p*-cyano-phenyl)acetonitrile (**1b**) in DMSO at 25 °C (deprotonated with 2 equiv. KO^tBu, addition of 18-crown-6, stopped-flow UV-Vis spectrometer, $\lambda = 398$ nm).

Nr.	[Nu] ⁻ ₀ / M	[18-crown-6] / M	[E] ₀ / M	$k_{\text{obs}} / \text{s}^{-1}$
a324-5	4.43×10^{-5}	4.65×10^{-5}	7.11×10^{-4}	1.72×10^1
a324-2	4.43×10^{-5}	4.65×10^{-5}	1.42×10^{-3}	3.03×10^1
a324-3	4.43×10^{-5}	4.65×10^{-5}	2.13×10^{-3}	4.35×10^1
a324-4	4.43×10^{-5}	4.65×10^{-5}	2.84×10^{-3}	5.75×10^1
a324-6	4.43×10^{-5}	4.65×10^{-5}	3.56×10^{-3}	6.97×10^1

$$k_2 = 1.86 \times 10^4 \text{ L mol}^{-1} \text{ s}^{-1}$$

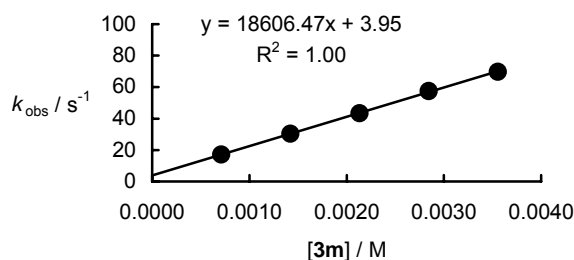


Table S8: Kinetics of the reaction of electrophile **3n** with the anion of (*p*-cyano-phenyl)acetonitrile (**1b**) in DMSO at 20 °C (deprotonated with 2 equiv. KO*t*Bu, stopped-flow UV-Vis spectrometer, $\lambda = 394$ nm).

Nr.	[Nu ⁻] ₀ / M	[E] ₀ / M	$k_{\text{obs}} / \text{s}^{-1}$
a312-5	4.08×10^{-5}	9.35×10^{-4}	7.89
a312-1	4.08×10^{-5}	1.40×10^{-3}	1.18×10^1
a312-2	4.08×10^{-5}	1.87×10^{-3}	1.61×10^1
a312-3	4.08×10^{-5}	2.34×10^{-3}	2.04×10^1
a312-4	4.08×10^{-5}	3.27×10^{-3}	2.85×10^1

$$k_2 = 8.87 \times 10^3 \text{ L mol}^{-1} \text{ s}^{-1}$$

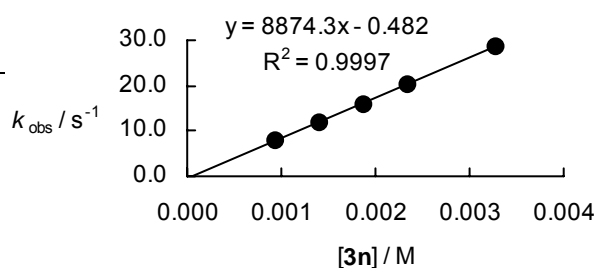


Table S9: Kinetics of the reaction of electrophile **3o** with the anion of (*p*-cyano-phenyl)acetonitrile (**1b**) in DMSO at 20 °C (deprotonated with KO*t*Bu, stopped-flow UV-Vis spectrometer, $\lambda = 397$ nm).

Nr.	[Nu ⁻] ₀ / M	[E] ₀ / M	$k_{\text{obs}} / \text{s}^{-1}$
a309-1	3.10×10^{-5}	6.59×10^{-4}	1.84
a309-3	3.10×10^{-5}	1.32×10^{-3}	3.55
a309-4	3.10×10^{-5}	1.98×10^{-3}	5.33
a309-4	3.10×10^{-5}	2.64×10^{-3}	7.24
a309-5	3.10×10^{-5}	3.30×10^{-3}	9.26

$$k_2 = 2.81 \times 10^3 \text{ L mol}^{-1} \text{ s}^{-1}$$

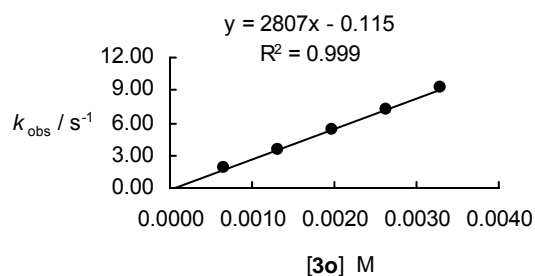


Table S10: Kinetics of the reaction of electrophile **3p** with the anion of (*p*-cyano-phenyl)acetonitrile (**1b**) in DMSO at 20 °C (deprotonated with KO*t*Bu, stopped-flow UV-Vis spectrometer, $\lambda = 397$ nm).

Nr.	[Nu ⁻] ₀ / M	[E] ₀ / M	$k_{\text{obs}} / \text{s}^{-1}$
a307b-1	2.12×10^{-5}	4.08×10^{-4}	1.07×10^{-1}
a307b-2	2.12×10^{-5}	8.16×10^{-4}	2.36×10^{-1}
a307b-3	2.12×10^{-5}	1.22×10^{-3}	3.42×10^{-1}
a307b-4	2.12×10^{-5}	1.63×10^{-3}	4.57×10^{-1}
a307b-5	2.12×10^{-5}	2.04×10^{-3}	5.68×10^{-1}

$k_2 = 2.80 \times 10^2 \text{ L mol}^{-1} \text{ s}^{-1}$

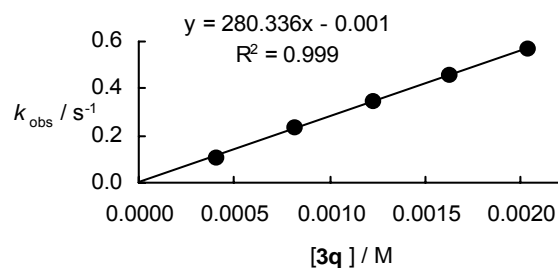


Table S11: Kinetics of the reaction of electrophile **3q** with the anion of (*p*-cyano-phenyl)acetonitrile (**1b**) in DMSO at 20 °C (deprotonated with KO*t*Bu, stopped-flow UV-Vis spectrometer, $\lambda = 394$ nm).

Nr.	[Nu ⁻] ₀ / M	[E] ₀ / M	$k_{\text{obs}} / \text{s}^{-1}$
a311-2	8.27×10^{-5}	1.43×10^{-3}	2.58×10^{-1}
a311-1	8.27×10^{-5}	2.86×10^{-3}	4.99×10^{-1}
a311-4	8.27×10^{-5}	4.29×10^{-3}	7.12×10^{-1}
a311-5	8.27×10^{-5}	5.72×10^{-3}	9.23×10^{-1}

$k_2 = 1.54 \times 10^2 \text{ L mol}^{-1} \text{ s}^{-1}$

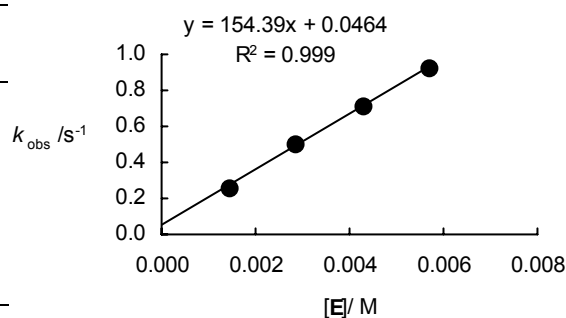
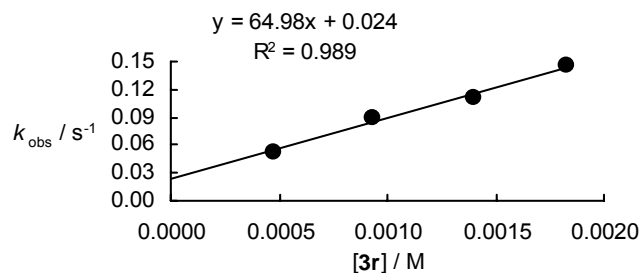


Table S12: Kinetics of the reaction of electrophile **3r** with the anion of (*p*-cyano-phenyl)acetonitrile (**1b**) in DMSO at 20 °C (deprotonated with KO*t*Bu, J&M UV-Vis spectrometer, $\lambda = 394$ nm).

Nr.	[E] ₀ / M	[Nu ⁻] ₀ / M	$k_{\text{obs}} / \text{s}^{-1}$
c310-1	4.33×10^{-5}	4.72×10^{-4}	5.26×10^{-2}
c310-2	4.33×10^{-5}	9.31×10^{-4}	8.83×10^{-2}
c310-3	4.33×10^{-5}	1.40×10^{-3}	1.10×10^{-1}
c310-4	4.33×10^{-5}	1.83×10^{-3}	1.45×10^{-1}

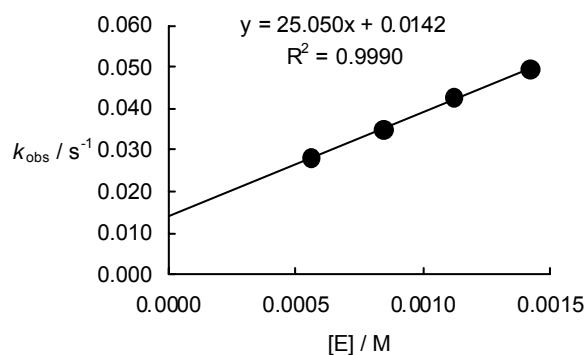
$k_2 = 6.50 \times 10^1 \text{ L mol}^{-1} \text{ s}^{-1}$



Kinetics for the anion of (*p*-nitro-phenyl)acetonitrile (1c**)****Table S13:** Kinetics of the reaction of electrophile **3m** with the anion of (*p*-nitro-phenyl)acetonitrile (**1c**) in DMSO at 20 °C (deprotonated with 1.05 equiv. KO*t*Bu, J&M UV-Vis spectrometer, $\lambda = 537$ nm).

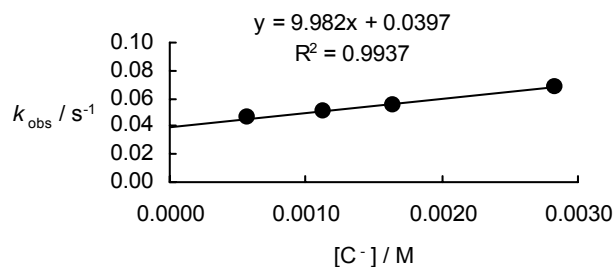
Nr.	[Nu ⁻] ₀ / M	[E] ₀ / M	$k_{\text{obs}} / \text{s}^{-1}$
c305-2	2.66×10^{-5}	5.57×10^{-4}	2.82×10^{-2}
c305-3	2.66×10^{-5}	8.44×10^{-4}	3.50×10^{-2}
c305-4	2.66×10^{-5}	1.12×10^{-3}	4.26×10^{-2}
c305-5	2.66×10^{-5}	1.42×10^{-3}	4.96×10^{-2}

$$k_2 = 2.51 \times 10^1 \text{ L mol}^{-1} \text{ s}^{-1}$$

**Table S14:** Kinetics of the reaction of electrophile **3n** with the anion of (*p*-nitro-phenyl)acetonitrile (**1c**) in DMSO at 20 °C (deprotonated with KO*t*Bu, J&M UV-Vis spectrometer, $\lambda = 537$ nm).

Nr.	[Nu ⁻] ₀ / M	[E] ₀ / M	$k_{\text{obs}} / \text{s}^{-1}$
c306-1	4.69×10^{-5}	5.70×10^{-4}	4.62×10^{-2}
c306-2	4.69×10^{-5}	1.13×10^{-3}	5.03×10^{-2}
c306-6	4.69×10^{-5}	1.65×10^{-3}	5.55×10^{-2}
c306-4	4.69×10^{-5}	2.83×10^{-3}	6.84×10^{-2}

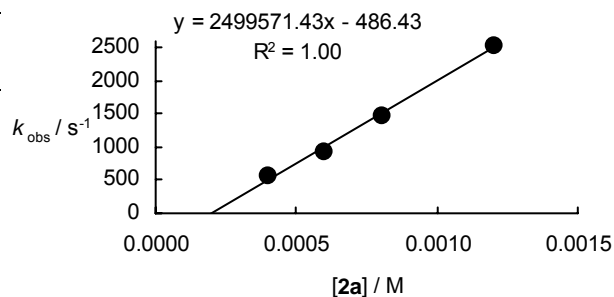
$$k_2 = 9.98 \text{ L mol}^{-1} \text{ s}^{-1}$$



Kinetics for the anion of 2-phenyl-propionitrile (2a)**Table S15:** Kinetics of the reaction of **3f** with the anion of 2-phenyl-propionitrile (**2a**) in DMSO at 20 °C (deprotonated with 1.05 eq. phosphazene base P₄-*t*Bu, stopped-flow UV-Vis spectrometer, $\lambda = 524$ nm).

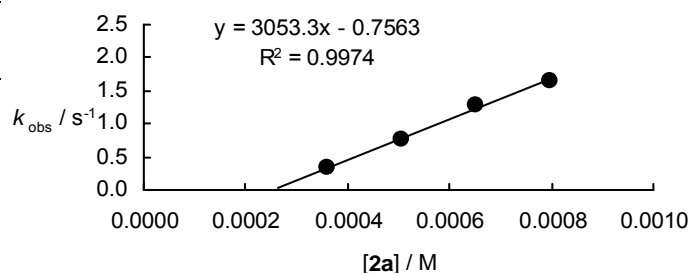
Nr.	[E] ₀ / M	[Nu ⁻] ₀ / M	<i>k</i> _{obs} / s ⁻¹
265-1	2.01 × 10 ⁻⁵	3.62 × 10 ⁻⁴	5.79 × 10 ²
265-2	2.01 × 10 ⁻⁵	5.07 × 10 ⁻⁴	9.40 × 10 ²
265-3	2.01 × 10 ⁻⁵	6.52 × 10 ⁻⁴	1.49 × 10 ³
265-4	2.01 × 10 ⁻⁵	7.97 × 10 ⁻⁴	2.54 × 10 ³

$$k_2 = 2.50 \times 10^6 \text{ L mol}^{-1} \text{ s}^{-1}$$

**Table S16:** Kinetics of the reaction of electrophile **3s** with the anion of 2-phenyl-propionitrile (**2a**) in DMSO at 20 °C (deprotonated with phosphazene base P₄-*t*Bu, stopped-flow UV-Vis spectrometer, $\lambda = 405$ nm).

Nr.	[E] ₀ / M	[Nu ⁻] ₀ / M	<i>k</i> _{obs} / s ⁻¹
a369-1	1.92 × 10 ⁻⁵	3.62 × 10 ⁻⁴	3.85 × 10 ⁻¹
a369-2	1.92 × 10 ⁻⁵	5.07 × 10 ⁻⁴	7.72
a369-3	1.92 × 10 ⁻⁵	6.52 × 10 ⁻⁴	1.28
a369-4	1.92 × 10 ⁻⁵	7.97 × 10 ⁻⁴	1.66

$$k_2 = 3.05 \times 10^3 \text{ L mol}^{-1} \text{ s}^{-1}$$

**Table S17:** Kinetics of the reaction of electrophile **3s** with the anion of 2-phenyl-propionitrile (**2a**) in DMSO at 20 °C (deprotonated with 1.05 eq. phosphazene base P₄-*t*Bu, stopped-flow UV-Vis spectrometer, $\lambda = 410$ nm).

Nr.	[E] ₀ / M	[Nu ⁻] ₀ / M	<i>k</i> _{obs} / s ⁻¹
a373-2	1.85 × 10 ⁻⁵	5.25 × 10 ⁻⁴	4.34 × 10 ⁻¹
a373-3	1.85 × 10 ⁻⁵	6.75 × 10 ⁻⁴	8.81 × 10 ⁻¹
a373-4	1.85 × 10 ⁻⁵	8.25 × 10 ⁻⁴	1.31
a373-5	1.85 × 10 ⁻⁵	9.75 × 10 ⁻⁴	1.73

$$k_2 = 2.87 \times 10^3 \text{ L mol}^{-1} \text{ s}^{-1}$$

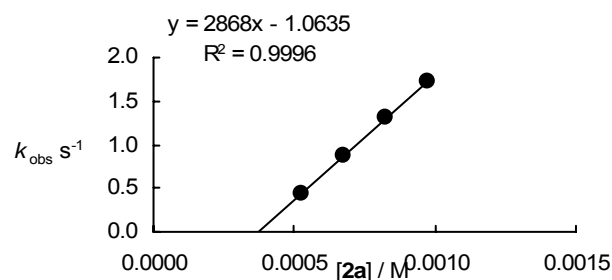


Table S18: Kinetics of the reaction of electrophile **3s** with the anion of 2-phenyl-propionitrile (**2a**) in DMSO at 20 °C (deprotonated with 1.05 equiv. KOtBu, stopped-flow UV-Vis spectrometer, $\lambda = 400$ nm).

Nr.	$[E]_0 / M$	$[Nu^-]_0 / M$	k_{obs} / s^{-1}
a368c-2	1.92×10^{-5}	5.75×10^{-4}	3.93×10^{-1}
a368c-3	1.92×10^{-5}	7.67×10^{-4}	9.47×10^{-1}
a368c-4	1.92×10^{-5}	9.58×10^{-4}	1.55
a368c-5	1.92×10^{-5}	1.12×10^{-3}	2.11

$k_2 = 3.12 \times 10^3 \text{ L mol}^{-1} \text{ s}^{-1}$

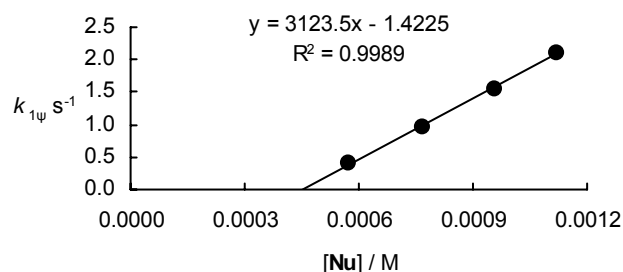


Table S19: Kinetics of the reaction of electrophile **3s** with the anion of 2-phenyl-propionitrile (**2a**) in DMSO at 20 °C (deprotonated with 2.00 equiv. KOtBu, stopped-flow UV-Vis spectrometer, $\lambda = 400$ nm).

Nr.	$[E]_0 / M$	$[Nu^-]_0 / M$	k_{obs} / s^{-1}
a368b-2	1.92×10^{-5}	4.38×10^{-4}	4.22×10^{-1}
a368b-3	1.92×10^{-5}	5.75×10^{-4}	7.72×10^{-1}
a368b-4	1.92×10^{-5}	7.67×10^{-4}	1.43
a368b-5	1.92×10^{-5}	9.31×10^{-3}	1.92

$k_2 = 3.09 \times 10^3 \text{ L mol}^{-1} \text{ s}^{-1}$

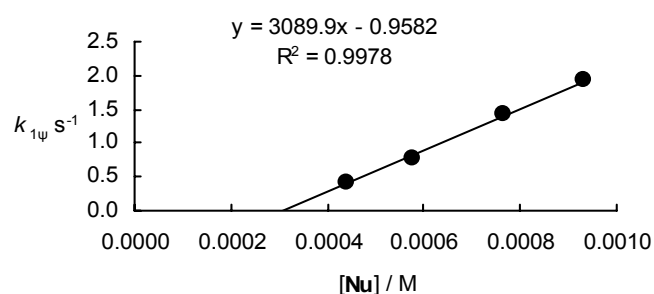


Table S20: Kinetics of the reaction of electrophile **3s** with the anion of 2-phenyl-propionitrile (**2a**) in DMSO at 20 °C (deprotonated with 3.00 equiv. KOtBu, stopped-flow UV-Vis spectrometer, $\lambda = 400$ nm).

Nr.	$[E]_0 / M$	$[Nu^-]_0 / M$	k_{obs} / s^{-1}
a368a-2	1.92×10^{-5}	4.38×10^{-4}	5.01×10^{-1}
a368a-3	1.92×10^{-5}	5.75×10^{-4}	9.29×10^{-1}
a368a-4	1.92×10^{-5}	7.67×10^{-4}	1.54
a368a-5	1.92×10^{-5}	9.58×10^{-3}	2.14

$k_2 = 3.15 \times 10^3 \text{ L mol}^{-1} \text{ s}^{-1}$

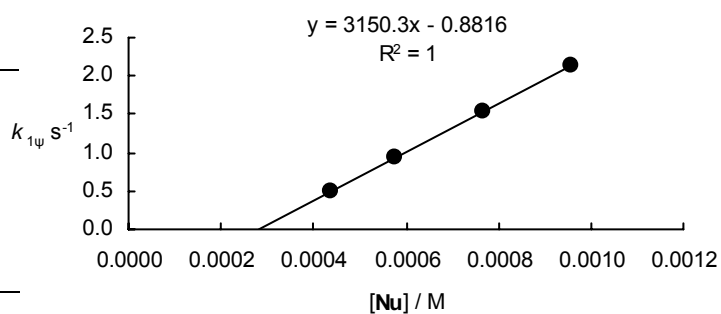


Table S21: Kinetics of the reaction of electrophile **3t** with the anion of 2-phenylpropionitrile (**2a**) in DMSO at 20 °C (deprotonated with P₄-*t*Bu phosphazene base, stopped-flow UV-Vis spectrometer, $\lambda = 405$ nm).

Nr.	[E] ₀ / M	[Nu ⁻] ₀ / M	$k_{\text{obs}} / \text{s}^{-1}$
a369b-1	1.66×10^{-5}	3.62×10^{-4}	3.50×10^{-1}
a369b-2	1.66×10^{-5}	5.07×10^{-4}	5.95×10^{-1}
a369b-3	1.66×10^{-5}	6.52×10^{-4}	8.86×10^{-1}
a369b-4	1.66×10^{-5}	7.97×10^{-4}	1.15

$$k_2 = 1.86 \times 10^3 \text{ L mol}^{-1} \text{ s}^{-1}$$

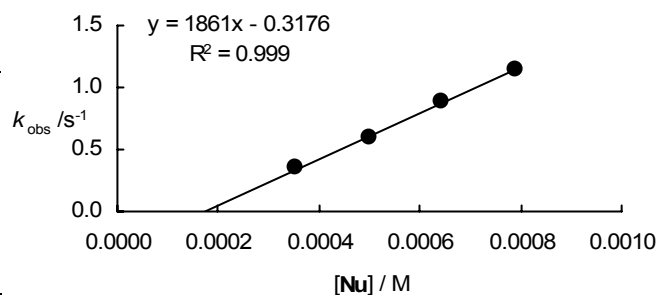


Table S22: Kinetics of the reaction of electrophile **3t** with the anion of 2-phenylpropionitrile (**2a**) in DMSO at 20 °C (deprotonated with 2.00 equiv. KO^{*t*}Bu, stopped-flow UV-Vis spectrometer, $\lambda = 405$ nm).

Nr.	[E] ₀ / M	[Nu ⁻] ₀ / M	$k_{\text{obs}} / \text{s}^{-1}$
a366-1	2.02×10^{-5}	3.18×10^{-4}	3.00×10^{-1}
a366-5	2.02×10^{-5}	3.98×10^{-4}	4.24×10^{-1}
a366-2	2.02×10^{-5}	6.36×10^{-4}	8.22×10^{-1}
a366-3	2.02×10^{-5}	8.35×10^{-4}	1.17
a366-4	2.02×10^{-5}	9.94×10^{-4}	1.44

$$k_2 = 1.69 \times 10^3 \text{ L mol}^{-1} \text{ s}^{-1}$$

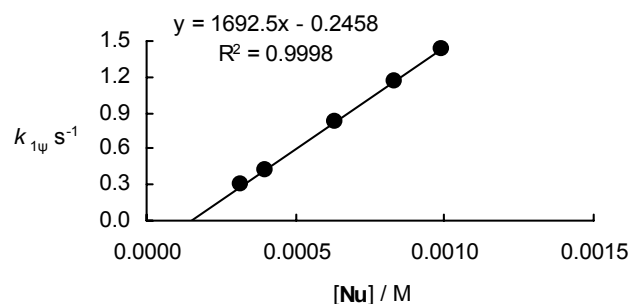


Table S23: Kinetics of the reaction of electrophile **3t** with the anion of 2-phenylpropionitrile (**2a**) in DMSO at 20 °C (deprotonated with 1.05 equiv. KO^{*t*}Bu, stopped-flow UV-Vis spectrometer, $\lambda = 405$ nm).

Nr.	[E] ₀ / M	[Nu ⁻] ₀ / M	$k_{\text{obs}} / \text{s}^{-1}$
a354-1	3.27×10^{-5}	6.04×10^{-4}	2.98×10^{-1}
a354-2	3.27×10^{-5}	9.05×10^{-4}	7.58×10^{-1}
a354-4	3.27×10^{-5}	1.21×10^{-3}	1.19
a354-5	3.27×10^{-5}	1.51×10^{-3}	1.67

$$k_2 = 1.50 \times 10^3 \text{ L mol}^{-1} \text{ s}^{-1}$$

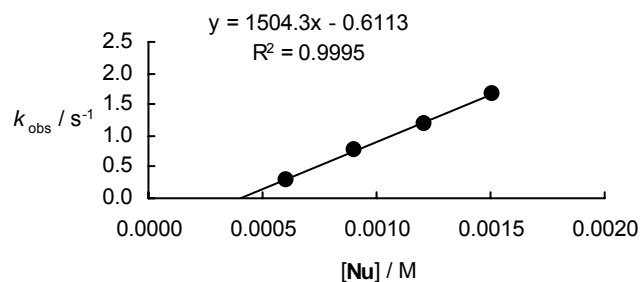


Table S24: Kinetics of the reaction of electrophile **3u** with the anion of 2-phenylpropionitrile (**2a**) in DMSO at 20 °C (deprotonated with P₄-tBu phosphazene base, stopped-flow UV-Vis spectrometer, $\lambda = 405$ nm).

Nr.	[E] ₀ / M	[Nu ⁻] ₀ / M	<i>k</i> _{obs} / s ⁻¹
a369c-1	1.63×10^{-5}	3.82×10^{-4}	2.86×10^{-1}
a369c-2	1.63×10^{-5}	5.35×10^{-4}	4.34×10^{-1}
a369c-3	1.63×10^{-5}	6.88×10^{-4}	5.88×10^{-1}
a369c-4	1.63×10^{-5}	8.41×10^{-3}	7.34×10^{-1}

$$k_2 = 9.90 \times 10^2 \text{ L mol}^{-1} \text{ s}^{-1}$$

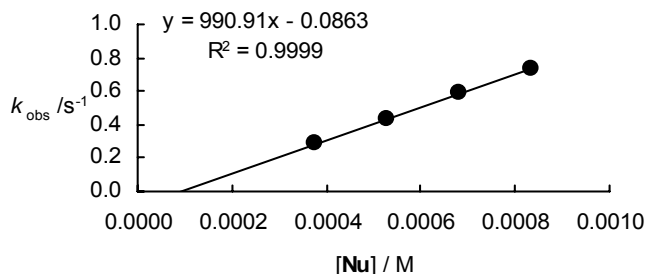


Table S25: Kinetics of the reaction of electrophile **3u** with the anion of 2-phenylpropionitrile (**2a**) in DMSO at 20 °C (deprotonated with 1.05 equiv. KOtBu, stopped-flow UV-Vis spectrometer, $\lambda = 405$ nm).

Nr.	[E] ₀ / M	[Nu ⁻] ₀ / M	<i>k</i> _{obs} / s ⁻¹
a352-2	2.88×10^{-5}	5.53×10^{-4}	1.58×10^{-1}
a352-3	2.88×10^{-5}	8.30×10^{-4}	4.29×10^{-1}
a352-4	2.88×10^{-5}	1.11×10^{-3}	6.37×10^{-1}
a352-5	2.88×10^{-5}	1.38×10^{-3}	8.77×10^{-1}

$$k_2 = 8.54 \times 10^2 \text{ L mol}^{-1} \text{ s}^{-1}$$

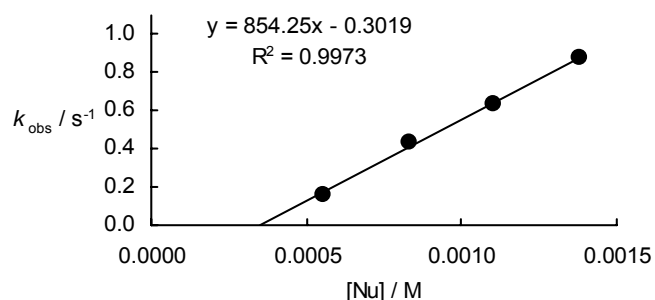
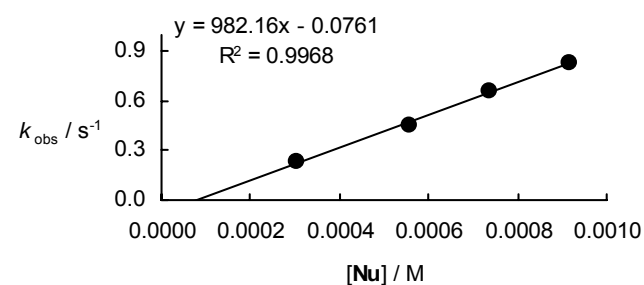


Table S26: Kinetics of the reaction of electrophile **3u** with the anion of 2-phenylpropionitrile (**2a**) in DMSO at 20 °C (deprotonated with 2.00 equiv. KOtBu, stopped-flow UV-Vis spectrometer, $\lambda = 405$ nm).

Nr.	[E] ₀ / M	[Nu ⁻] ₀ / M	<i>k</i> _{obs} / s ⁻¹
a365-1	1.96×10^{-5}	3.06×10^{-4}	2.34×10^{-1}
a365-6	1.96×10^{-5}	5.57×10^{-4}	4.50×10^{-1}
a365-5	1.96×10^{-5}	7.37×10^{-4}	6.57×10^{-1}
a365-3	1.96×10^{-5}	9.17×10^{-4}	8.27×10^{-1}

$$k_2 = 9.82 \times 10^2 \text{ L mol}^{-1} \text{ s}^{-1}$$



Kinetics for the anion of 2-(p-cyanophenyl)-propionitrile (2b)

Table S27: Kinetics of the reaction of **3b** with the anion of 2-(p-cyanophenyl)-propionitrile (**2b**) in DMSO at 20 °C (deprotonated with phosphazene base P₂-tBu, UV-Vis spectrometer, $\lambda = 533$ nm).

Nr.	[E] ₀ / M	[Nu ⁻] ₀ / M	$k_{\text{obs}} / \text{s}^{-1}$
270-1	8.00×10^{-6}	5.72×10^{-5}	4.04×10^2
270-2	8.00×10^{-6}	1.24×10^{-4}	9.22×10^2
270-3	8.00×10^{-6}	1.86×10^{-4}	1.42×10^3
270-4	8.00×10^{-6}	2.49×10^{-4}	1.87×10^3
270-5	8.00×10^{-6}	3.11×10^{-4}	2.37×10^3

$$k_2 = 7.73 \times 10^6 \text{ L mol}^{-1} \text{ s}^{-1}$$

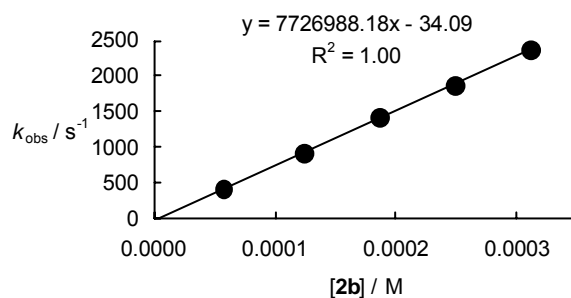


Table S28: Kinetics of the reaction of **3e** with the anion of 2-(p-cyanophenyl)-propionitrile (**2b**) in DMSO at 20 °C (deprotonated with phosphazene base P₂-tBu, stopped-flow UV-Vis spectrometer, $\lambda = 488$ nm).

Nr.	[E] ₀ / M	[Nu ⁻] ₀ / M	$k_{\text{obs}} / \text{s}^{-1}$
T-271-1	3.78×10^{-5}	2.49×10^{-4}	1.04×10^1
T-271-2	3.78×10^{-5}	3.73×10^{-4}	1.60×10^1
T-271-3	3.78×10^{-5}	4.97×10^{-4}	2.12×10^1
T-271-4	3.78×10^{-5}	7.46×10^{-4}	3.22×10^1
T-271-5	3.78×10^{-5}	9.94×10^{-4}	4.39×10^1
T-271-6	3.78×10^{-5}	1.24×10^{-3}	5.55×10^1

$$k_2 = 4.54 \times 10^4 \text{ L mol}^{-1} \text{ s}^{-1}$$

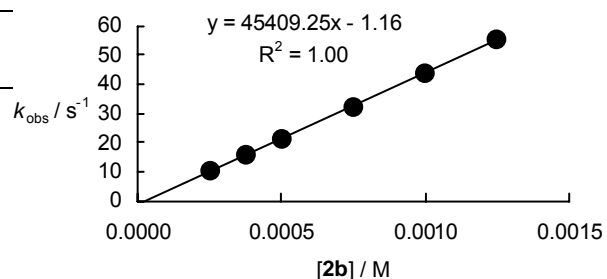


Table S29: Kinetics of the reaction of **3e** with the anion of 2-(*p*-cyanophenyl)-propionitrile (**2b**) in DMSO at 20 °C (deprotonated with 1.00 equiv. KO*t*Bu, stopped-flow UV-Vis spectrometer, $\lambda = 488$ nm).

Nr.	[E] ₀ / M	[Nu ⁻] ₀ / M	$k_{\text{obs}} / \text{s}^{-1}$
T-141-1	2.02×10^{-5}	2.61×10^{-4}	4.93
T-141-2	2.02×10^{-5}	5.00×10^{-4}	1.28×10^1
T-141-3	2.02×10^{-5}	7.51×10^{-4}	1.96×10^1
T-141-4	2.02×10^{-5}	1.00×10^{-3}	2.64×10^1
T-141-5	2.02×10^{-5}	1.25×10^{-3}	3.65×10^1
T-141-6	2.02×10^{-5}	1.50×10^{-3}	4.49×10^1

$$k_2 = 3.20 \times 10^4 \text{ L mol}^{-1} \text{ s}^{-1}$$

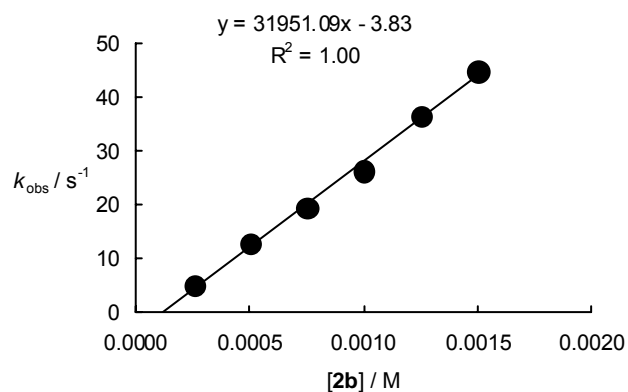


Table S30: Kinetics of the reaction of electrophile **3f** with the anion of 2-(*p*-cyanophenyl)-propionitrile (**2b**) in DMSO at 20 °C (deprotonated with phosphazene base P₂-*t*Bu, stopped-flow UV-Vis spectrometer, $\lambda = 524$ nm).

Nr.	[E] ₀ / M	[Nu ⁻] ₀ / M	$k_{\text{obs}} / \text{s}^{-1}$
272-1	2.48×10^{-5}	2.49×10^{-4}	9.71
272-2	2.48×10^{-5}	4.97×10^{-4}	1.51×10^1
272-3	2.48×10^{-5}	7.46×10^{-4}	2.15×10^1
272-4	2.48×10^{-5}	1.24×10^{-3}	3.30×10^1
272-5	2.48×10^{-5}	1.74×10^{-3}	4.72×10^1

$$k_2 = 2.51 \times 10^4 \text{ L mol}^{-1} \text{ s}^{-1}$$

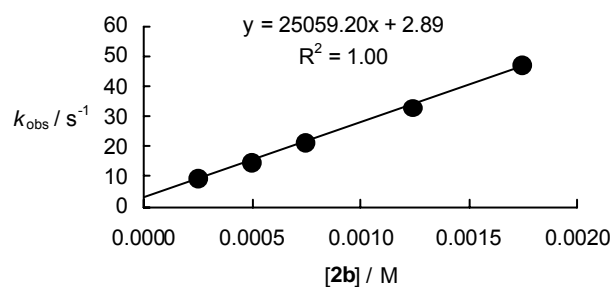


Table S31: Kinetics of the reaction of electrophile **3m** with the anion of 2-(*p*-cyanophenyl)propionitrile (**2b**) in DMSO at 20 °C (deprotonated with 2 eq. of KO^tBu, stopped-flow UV-Vis spectrometer, $\lambda = 403$ nm).

Nr.	[Nu ⁻] ₀ / M	[E] ₀ / M	$k_{\text{obs}} / \text{s}^{-1}$
a357-1	5.54×10^{-5}	5.29×10^{-4}	9.63
a357-2	5.54×10^{-5}	1.06×10^{-3}	1.52×10^1
a357-3	5.54×10^{-5}	1.59×10^{-3}	2.06×10^1
a357-4	5.54×10^{-5}	2.12×10^{-3}	2.65×10^1
a357-5	5.54×10^{-5}	2.29×10^{-3}	2.85×10^1
a357-6	5.54×10^{-5}	2.64×10^{-3}	3.26×10^1

$k_2 = 1.08 \times 10^4 \text{ L mol}^{-1} \text{ s}^{-1}$

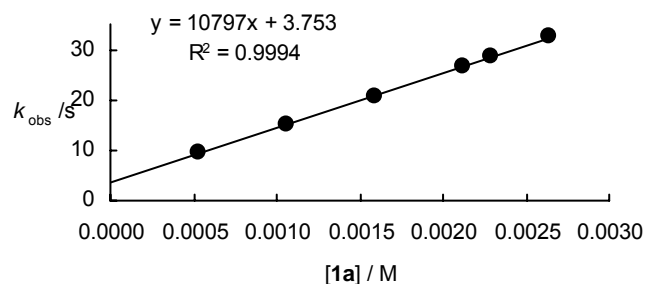


Table S32: Kinetics of the reaction of electrophile **3m** with the anion of 2-(*p*-cyanophenyl)propionitrile (**2b**) in DMSO at 20 °C under Ar atmosphere (deprotonated with 2 eq. of KO^tBu, stopped-flow UV-Vis spectrometer, $\lambda = 403$ nm).

Nr.	[Nu ⁻] ₀ / M	[E] ₀ / M	$k_{\text{obs}} / \text{s}^{-1}$
a357b-1	5.91×10^{-5}	4.06×10^{-4}	7.09
a357b-2	5.91×10^{-5}	8.12×10^{-4}	1.14×10^1
a357b-3	5.91×10^{-5}	1.22×10^{-3}	1.72×10^1
a357b-4	5.91×10^{-5}	1.62×10^{-3}	2.13×10^1
a357b-5	5.91×10^{-5}	2.03×10^{-3}	2.55×10^1

$k_2 = 1.15 \times 10^4 \text{ L mol}^{-1} \text{ s}^{-1}$

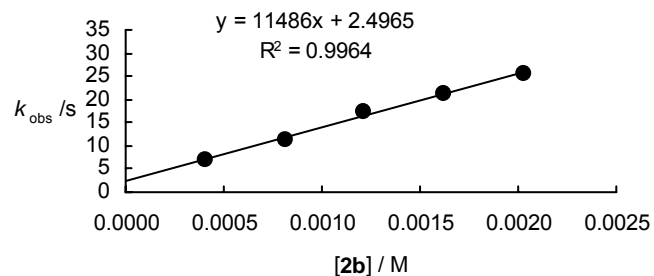


Table S33: Kinetics of the reaction of electrophile **3n** with the anion of 2-(*p*-cyanophenyl)propionitrile (**2b**) in DMSO at 20 °C (deprotonated with KO*t*Bu, stopped-flow UV-Vis spectrometer, $\lambda = 403$ nm).

Nr.	$[\text{Nu}^-]_0 / \text{M}$	$[\text{E}]_0 / \text{M}$	$k_{\text{obs}} / \text{s}^{-1}$
a355d-1	5.54×10^{-5}	1.95×10^{-3}	1.37×10^1
a355d-2	5.54×10^{-5}	3.89×10^{-3}	2.43×10^1
a355d-3	5.54×10^{-5}	5.84×10^{-3}	3.53×10^1
a355d-5	5.54×10^{-5}	9.73×10^{-3}	5.78×10^1

$$k_2 = 5.68 \times 10^3 \text{ L mol}^{-1} \text{ s}^{-1}$$

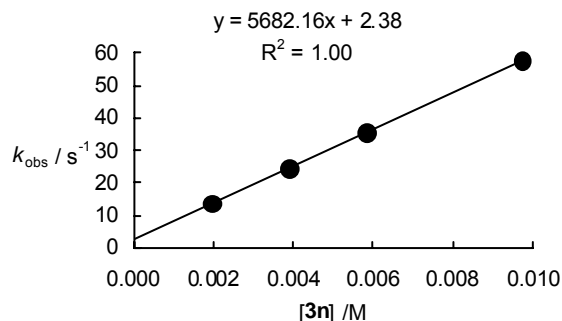


Table S34: Kinetics of the reaction of electrophile **3o** with the anion of 2-(*p*-cyanophenyl)propionitrile (**2b**) in DMSO at 20 °C (deprotonated with 2 eq. of KO*t*Bu, stopped-flow UV-Vis spectrometer, $\lambda = 403$ nm).

Nr.	$[\text{Nu}^-]_0 / \text{M}$	$[\text{E}]_0 / \text{M}$	$k_{\text{obs}} / \text{s}^{-1}$
a356-1	8.31×10^{-5}	8.30×10^{-4}	3.80
a356-2	8.31×10^{-5}	1.66×10^{-3}	5.59
a356-3	8.31×10^{-5}	2.49×10^{-3}	7.49
a356-4	8.31×10^{-5}	3.32×10^{-3}	9.34
a356-5	8.31×10^{-5}	4.98×10^{-3}	1.39×10^1

$$k_2 = 2.44 \times 10^3 \text{ L mol}^{-1} \text{ s}^{-1}$$

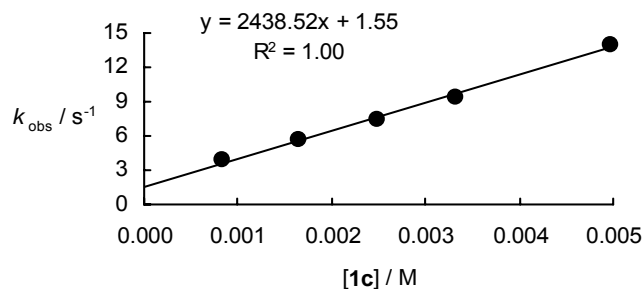
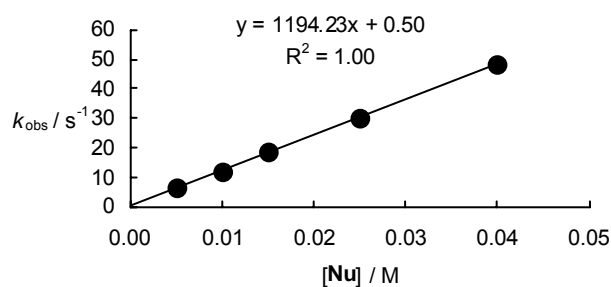


Table S35: Kinetics of the reaction of electrophile **3p** with the anion of 2-(*p*-cyanophenyl)propionitrile (**2b**) in DMSO at 20 °C (stopped-flow UV-Vis spectrometer, $\lambda = 403$ nm).

Nr.	$[\text{Nu}^-]_0 / \text{M}$	$[\text{E}]_0 / \text{M}$	$k_{\text{obs}} / \text{s}^{-1}$
148-1	1.00×10^{-4}	5.00×10^{-3}	6.86
148-2	1.00×10^{-4}	1.00×10^{-2}	1.20×10^1
148-3	1.00×10^{-4}	1.50×10^{-2}	1.85×10^1
148-4	1.00×10^{-4}	2.50×10^{-2}	3.05×10^1
148-5	1.00×10^{-4}	4.00×10^{-2}	4.84×10^1

$$k_2 = 1.19 \times 10^3 \text{ L mol}^{-1} \text{ s}^{-1}$$



Appendix

Figure A1 shows a correlation between the nucleophilicity parameter N of 30 carbanions from different classes versus their slope parameter s in dimethyl sulfoxide. Though the quality of the correlation is only of moderate quality ($R^2 = 0.82$), a clear trend is obvious: The correlation line depicted in Figure A1 reveals that the s parameter becomes smaller when the nucleophilicity of the carbanions increases. This effect becomes significant when the complete reactivity range of almost 16 orders of magnitude from $14 > N > 29$ is considered.

The slope parameters of the anion of Meldrum's acid, as well as the nitro substituted trifluoromethylsulfonyl stabilized benzyl anion, and the anion of phenylpropionitrile deviate positively from the correlation. On the other hand, the s parameters for the anions of nitromethane, and of some phenylsulfonyl stabilized carbanions are significantly smaller than expected from the correlation.

Typically, the absolute number of electrophile-nucleophile combinations used for the determination of the nucleophile-specific parameters N and s is large. However, for some carbanions, e.g., the anion of phenylpropionitrile, this deviation might be attributed to the small number of rate constants, which have been used to derive their nucleophilicity and slope parameters.

One reason for the decrease of the slope parameters for the carbanions with increasing N (Figure A1) could be attributed to the different sets of electrophiles which have been used to characterize the nucleophilicities of the carbanions. On one hand, benzhydrylium ions were used for the characterization of the less nucleophilic carbanions, whereas on the other hand, the quinone methides and Michael acceptors (benzylidene Meldrum's acids, benzylidene barbituric acids, benzylidene indandiones, and benzylidenemalonates) were employed to characterize some of the more reactive nucleophiles.

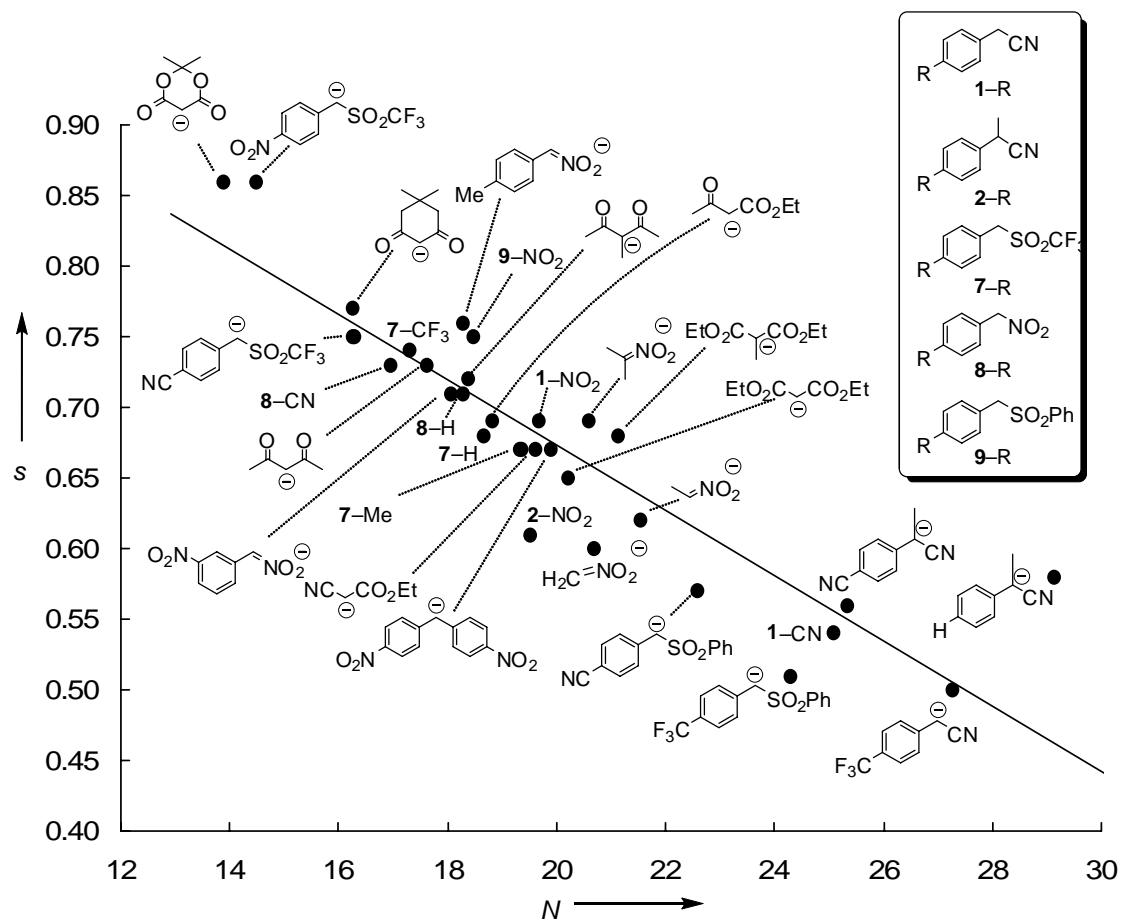


Figure A1. Plot of the slope parameters s of carbanions versus their nucleophilicity parameter N in DMSO. Overall correlation equation: $s = -0.023N + 1.134$, $R^2 = 0.818$.

Statistical errors due to the fact that more recently determined rate constants have not been used for reparametrizing the reactivity parameters E , N , and s of reference compounds may be responsible for the trend shown in Figure A1. A reparametrization of the full set of rate constants now available is necessary to examine whether this trend is real.

Chapter 6

Electrophilicities of Acceptor-Substituted Dienes

Introduction

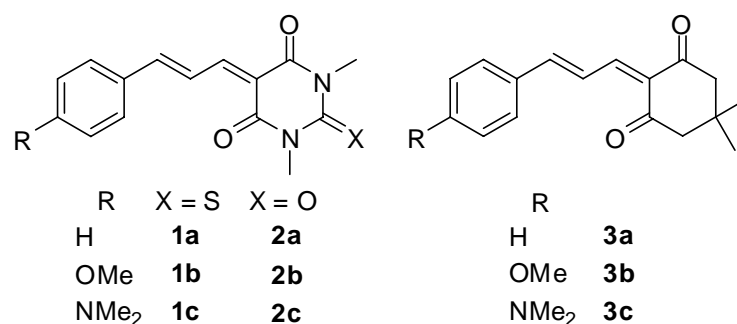
Numerous kinetic investigations showed that the rate constants for the reactions of benzhydrylium ions and structurally related quinone methides with carbanions can be described by Equation (6.1),¹⁻⁴ in which N and s are nucleophile-specific parameters, and E is an electrophile-specific parameter.

$$\log k_1 (20\text{ }^\circ\text{C}) = s(N + E) \quad (6.1)$$

Recently, we have shown that Equation (6.1) can also be employed for the determination of the electrophilicity parameters E of different types of Michael acceptors, such as benzylidene indandiones,⁵ benzylidene barbituric acids,⁶ benzylidene Meldrum's acids,⁷ and benzylidenemalonates.⁸

We have now studied the kinetics of the reactions of the acceptor-substituted dienes **1–3** (Scheme 6.1) with the carbanions **4a–h** in DMSO in order to derive the electrophilicity parameters E for the Michael acceptors **1–3**.

Recently, amines were reported to react significantly faster with Michael acceptors in DMSO and methanol than carbanions of similar N -values,⁵⁻⁷ which is in line with observations of Oh and Lee, who reported on reactions of Michael acceptors with amines in acetonitrile to profit from 4- or 6-membered cyclic transition states.⁹ We will therefore, report on the second-order rate constants for the reactions of amines and compounds **1–3** as well.

Scheme 6.1. Studied Acceptor-Substituted Michael Acceptors **1–3**.

We report that Equation (6.1) holds for the prediction of the second-order rate constants of the reactions of electrophiles **1–3** with the carbanions **4a–h** in dimethyl sulfoxide at 20 °C.

Table 6.1. *N*- and *s* Parameters of the Carbanions **4a–h** and the Amines **5a–d** in DMSO.

	Nucleophile	<i>N</i>	<i>s</i>
4a		21.54 ^a	0.62 ^a
4b		19.62 ^b	0.67 ^b
4c		19.36 ^b	0.67 ^b
4d		18.82 ^b	0.69 ^b
4e		18.38 ^c	0.72 ^c
4f		17.64 ^b	0.63 ^b
4g		16.27 ^b	0.77 ^b
4h		13.91 ^b	0.86 ^b
5a		17.19 ^c	0.71 ^c
5b		16.96 ^c	0.67 ^c
5c		16.07 ^c	0.61 ^c
5d		15.70 ^d	0.64 ^d

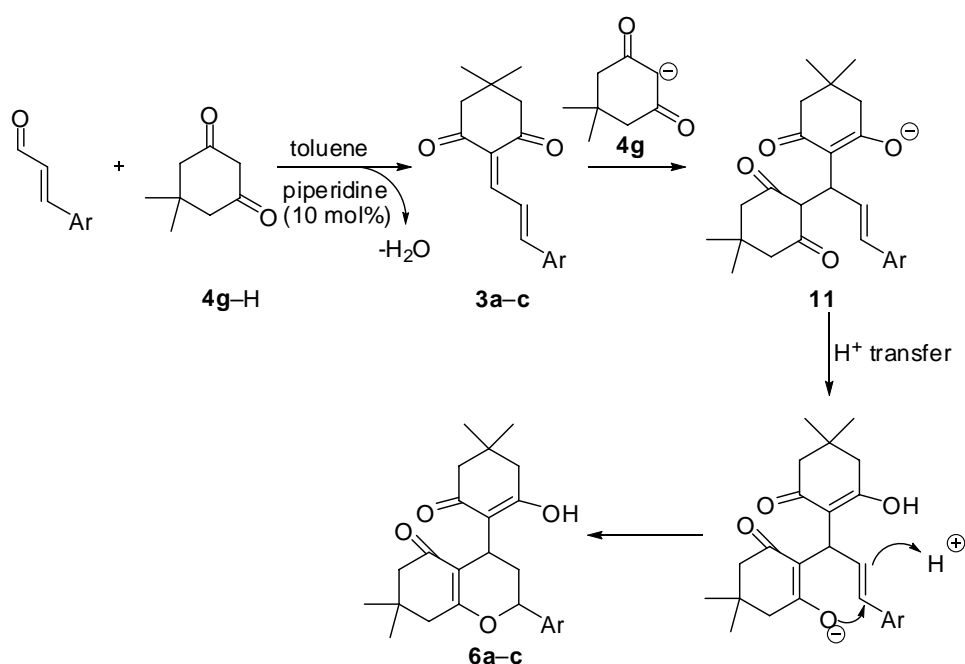
^a From ref. 3. ^b From ref. 1. ^c From ref. 10. ^d From ref. 11.

Results and Discussion

Synthesis. The Michael acceptors **1–3** were synthesized by Knoevenagel condensation from equimolar amounts of substituted cinnamaldehydes with 1,3-dimethylbarbituric- or 1,3-dimethyl-2-thiobarbituric acid in ethanol (compounds **1a–c** and **2a–c**),¹² and from reactions of substituted cinnamaldehydes with dimedone in the presence of catalytic amounts of piperidine, respectively (compounds **3a–c**).¹³

During their preparation, compounds **3a,b** were accompanied by small amounts (15 %) of perhydrochromanes **6a–c** (Scheme 6.2), which have previously been reported to be products from the reactions of substituted cinnamaldehydes with two equivalents of dimedone (**4g-H**) in the presence of catalytic amounts of piperidine.¹³ The formation of the perhydrochromanes has been attributed to the predominant enol structure of dimedone, facilitating the cyclization process. As the prevalent structure of 1,3-dimethyl(thio)barbituric acid is mainly based on its keto form, cyclization products were not encountered during the synthesis of compounds **1a–c** and **2a–c**.

Scheme 6.2. Formation of Perhydrochromanes **6a–c** via Cyclization of the Products **11**.

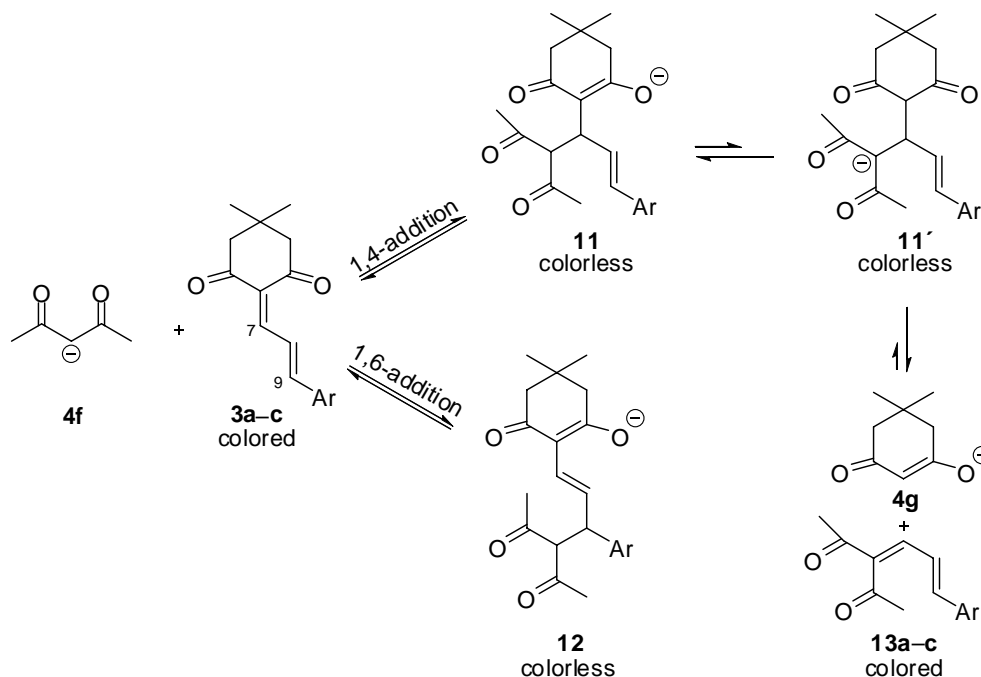


Analysis of the product mixtures after several hours indicated a slow subsequent further reaction or decomposition. Therefore, we cannot decide whether the 1,4-/1,6-adduct ratio reflects the result of kinetic or thermodynamic control.

The combinations of equimolar amounts of **4f**-**K** with **3a-c** in dimethoxyethane (DME) followed by acidification with diluted acetic acid yielded a \approx 1:1 mixture of **3a-c** and **13a-c** (Scheme 6.4). The mixtures were identified by GC-MS using the independently synthesized retro-Michael adducts **13a-c** as reference compounds.

The formation of the retro-Michael products in the studied electrophile-nucleophile combinations indicates an attack of the carbanions at C-7 of the electrophiles. However, a fast reversible attack of the nucleophile at C-9 cannot be excluded from these findings.

Scheme 6.4. Competing Pathways for the Reaction of the Anion of Acetylacetone **4f** with the Michael Acceptors **3a-c**.



Scheme 6.4 rationalizes the formation of **13a-c** from the reaction of Michael acceptor **3a-c** with the anion of acetylacetone (**4f**).

In a first reversible step, the carbanion **4f** can attack either at C-7 (1,4-addition) or at C-9 (1,6-addition) of the electrophile forming the colorless regioisomers **11** and **12**. Compound **11** may subsequently undergo a retro-Michael addition with formation of the colored diene **13** and the anion of dimedone (**4g**). The equilibrium of this reaction cascade can be expected to be on the side of the compounds **4g** and **13**, because **4g** ($pK_{\text{Ha}} = 11.16$) is considerably less basic than carbanion **4f** ($pK_{\text{Ha}} = 13.33$), and one can expect that the Lewis basicities of these carbanions mirror their Brønsted basicities.

Kinetics. Due to the large π -systems, the Michael acceptors **1–3** show strong absorption bands in the UV-Vis spectra. By nucleophilic attack at C-7 or C-9 (Scheme 6.4), the chromophore will be destroyed and the progress of the reaction can be followed by the decrease of the electrophile's absorbance. From the exponential decays of the UV-Vis absorbances of the electrophiles, the pseudo-first order rate constants k_{obs} were obtained.

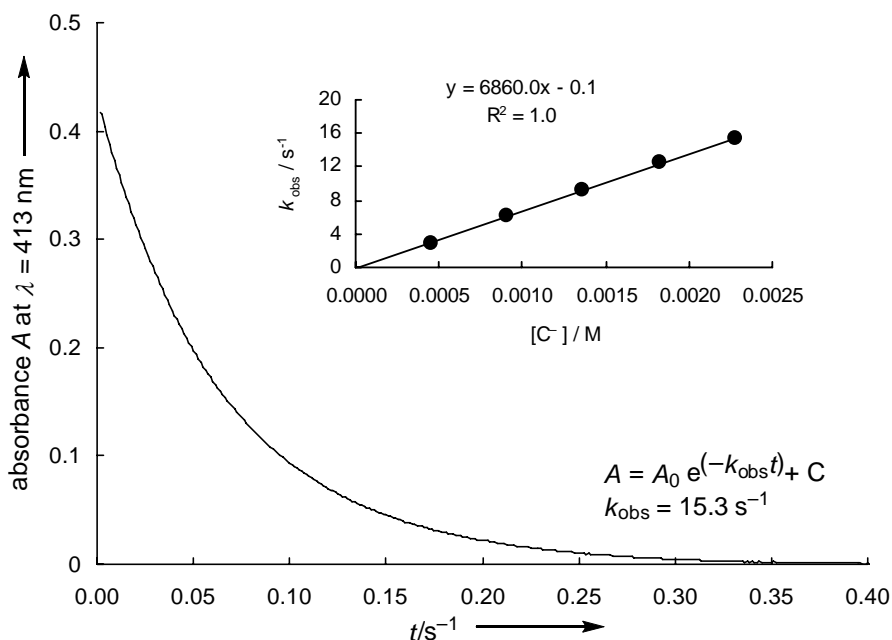


Figure 6.1. Exponential decay of the absorbance at $\lambda = 413 \text{ nm}$ for the reaction of **3b** ($c_0 = 2.64 \times 10^{-5} \text{ mol L}^{-1}$) with the carbanion **4f** ($c_0 = 2.28 \times 10^{-5} \text{ mol L}^{-1}$) in DMSO at $20 \text{ }^\circ\text{C}$.

All kinetic experiments were performed under pseudo-first order conditions using 10–100 equivalents of the nucleophiles. Generally, plots of k_{obs} versus the nucleophile concentration [Nu] resulted in straight lines (Figure 6.1) with the second-order rate constants k_1 (Table 6.2) as slopes. Previously, we have already demonstrated that ion pairing in dilute DMSO solutions is negligible under the conditions for our kinetic experiments;^{3,4,14} therefore the k_1 values can be considered to reflect the reactivities of the free carbanions.

In some of the reactions of compounds **1–3** with carbanions **4a–h** the subsequent formation of colored products has been observed, as exemplarily discussed for two cases.^{†2}

As depicted in Figure 6.2, the progress of the reaction of the Michael acceptor **1c** with the anion of Meldrum's acid **4h** in DMSO has been followed by UV-Vis spectroscopy at $\lambda = 583$ nm, whereas the formation of a colored product was followed at $\lambda \approx 530$ nm. The maximum wavelength of the formed colored product was found to be identical with λ_{max} of the retro-Michael product **16c** (assumed structure see Figure 6.2), which has been confirmed by independent synthesis of **16c**. The presence of two isosbestic points reveals that concentrations of the intermediate Michael adducts are negligible. Proton transfer reactions and retro-Michael addition are, therefore, not rate-determining.

^{†2} Please note that the formation of colored products can only be observed photometrically using the diode array mode of the stopped flow systems. As this has not generally been the case, the formation of colored products was not observed for all studied electrophile-nucleophile combinations.

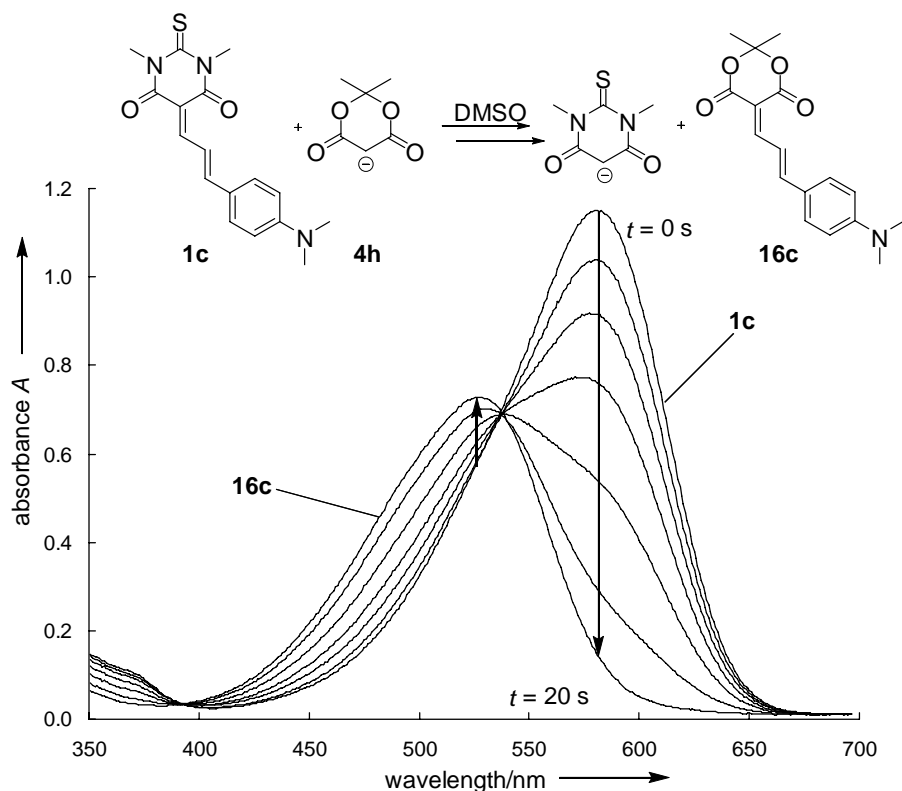


Figure 6.2. Reaction of **1c** ($c_0 = 1.89 \times 10^{-5} \text{ mol L}^{-1}$) with the anion of Meldrum's acid **4h** ($c_0 = 6.87 \times 10^{-4} \text{ mol L}^{-1}$) in dimethyl sulfoxide at 20 °C.

The reaction of the electrophile **1c** with the anion of dimedone (**4g**) was followed at $\lambda = 570 \text{ nm}$ (Figure 6.3). From the initial fast decrease of the absorbance of **1c** (insert in Figure 6.3) the second-order rate constant $k_1 = 6.4 \times 10^4 \text{ M}^{-1} \text{ s}^{-1}$ was determined. However, Figure 6.3 also reveals the slow subsequent formation of a colored product. From the absorbances A of the formed colored product after 40 s, one can conclude that its concentration is reciprocally dependent on the initial concentration of **4g**, i.e., A increases with smaller amounts of **4g**.

These findings can be explained by the proposed reaction mechanism depicted in Figure 6.4. The observed fast decolorization of the solution can be attributed to the addition of the carbanion **4g** to C-7 (1,4-addition) or C-9 (1,6-addition) of the electrophilic double bonds of the Michael acceptor **1c** with formation of the colorless products **7cg** or **8cg**. As **8cg** cannot undergo a retro-Michael addition, only **7cg** can react forward via proton transfer and retro-

Michael addition to yield the colored Michael acceptor **3c** and the anion of 1,3-dimethyl-2-thiobarbituric acid (SBA⁻).

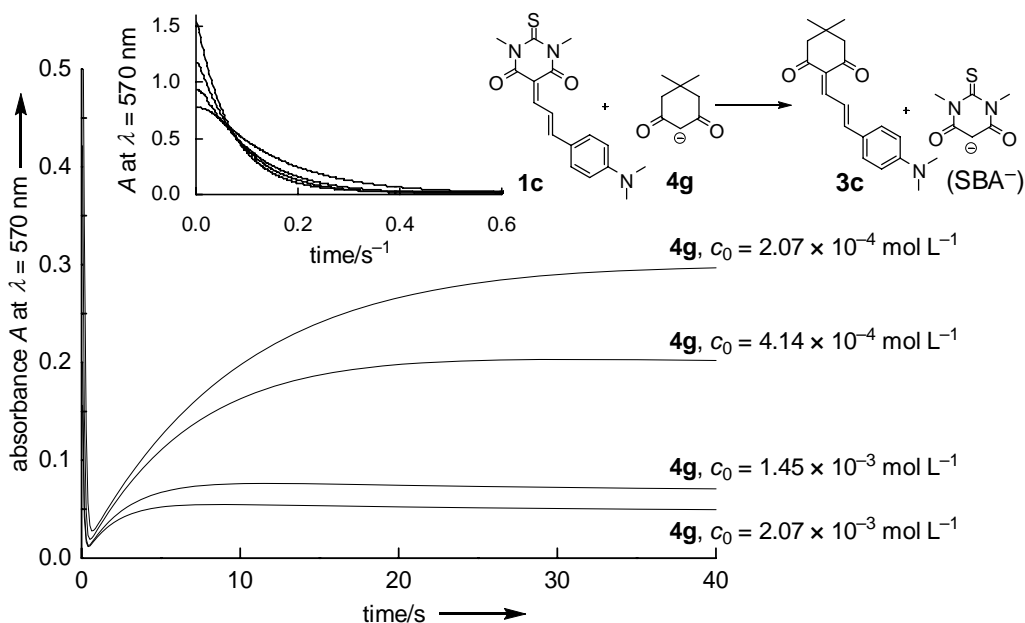


Figure 6.3. Reactions of **1c** ($c_0 = 1.89 \times 10^{-5}$ mol L⁻¹) with different amounts of the anion of dimedone **4g** in dimethyl sulfoxide at 20 °C.

3c subsequently reacts with the free carbanion **4g** (from the excess used for the kinetic experiments) to form the colorless products **11cg** or **12cg**. The reverse reaction of SBA⁻ with **3c** forming **7cg'** is less likely, because the concentration of SBA⁻ is small compared to the concentration of the dimedone anion **4g**, which was used in excess. Furthermore, SBA⁻ is expected to be less nucleophilic than **4g**, as thiobarbituric acid is known to be significantly more acidic than dimedone and therefore its conjugated anion should be less nucleophilic than **4g**, though deviations from nucleophilicity/basicity correlations have also been observed in this work.

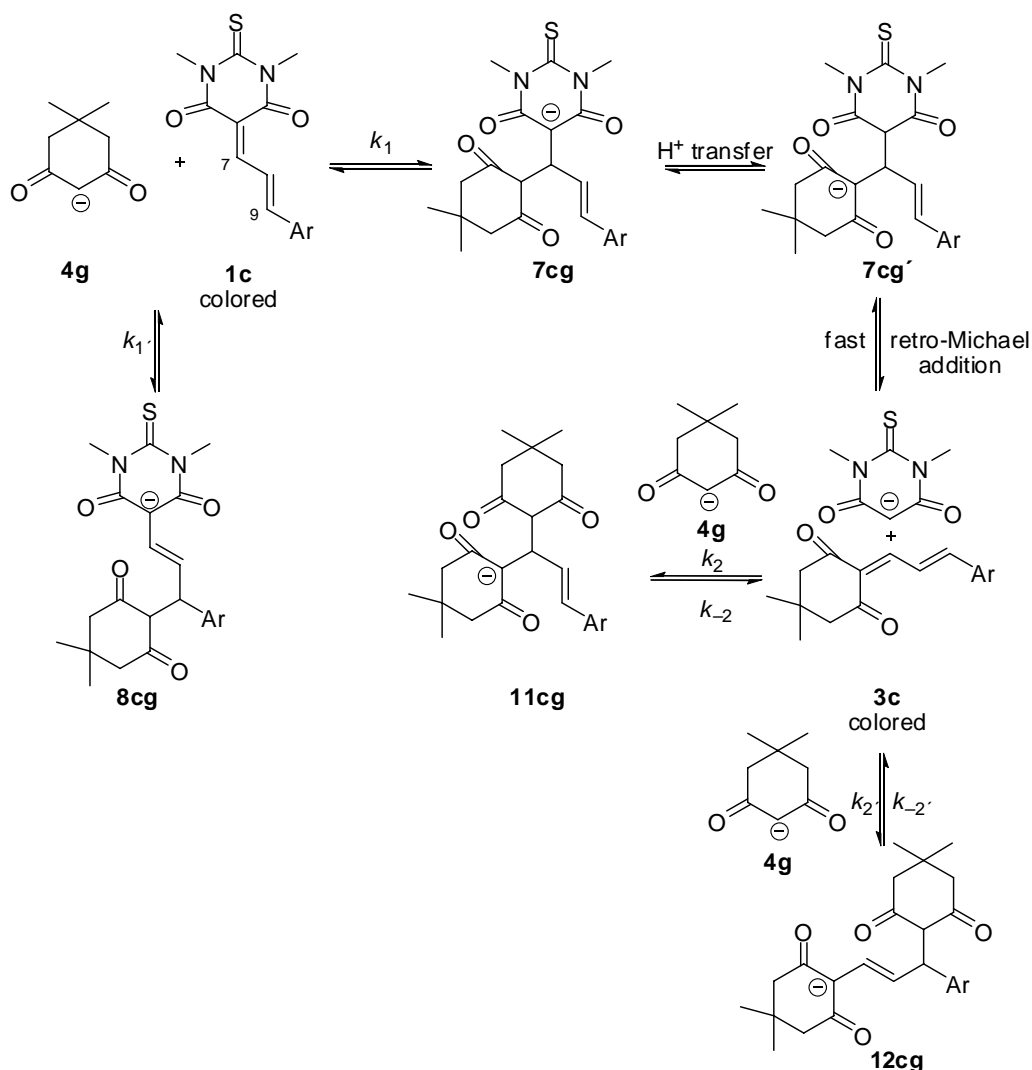


Figure 6.4. Possible reaction pathways for the addition of the anion of dimedone **4g** to Michael acceptor **1c** in dimethyl sulfoxide at 20 °C.

As already mentioned, the second-order rate constant $k_1 = 6.4 \times 10^4 \text{ M}^{-1}\text{s}^{-1}$ (Figure 6.4) has been determined from the decrease of the absorbance of **1c** (Figure 6.3). One can see that the end absorbance reached in the second stage of the reaction is reciprocally dependent on the carbanion concentration [**4g**] and that the maximum absorbances are reached earlier when larger concentrations of **4g** are present. As shown in (Figure 6.5), the plot of k_{obs} for the formation of **3c** versus the concentration of [**4g**] was linear.

How can one explain the fact that k_{obs} for the retro-Michael addition of **7cg** increases with the concentration of **4g**? Because the subsequent reaction of **4g** with **3c** is reversible, the observed

pseudo-first order rate constant equals the sum of the forward and the backwards reactions (Equation 6.2).¹⁵

$$k_{\text{obs}} = k_{-2} + (k_2 + k_{-2})[\mathbf{4g}] \quad (6.2)$$

Independent kinetic investigations of the reaction of electrophile **3c** with the carbanion **4g** (measuring the consumption of **3c**) resulted in a second-order rate constant $(k_2 + k_{-2}) = 1.9 \times 10^2 \text{ M}^{-1}\text{s}^{-1}$, which is comparable to $(k_2 + k_{-2})$ derived from the slope of Figure 6.5.

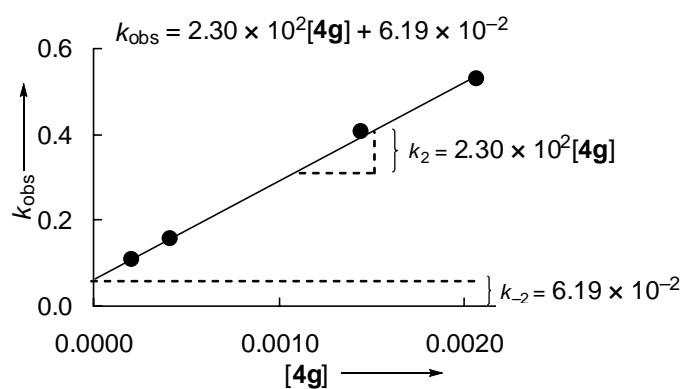


Figure 6.5. First-order rate constants for the reactions of **1c** with **4g** in DMSO at 20 °C.

Table 6.2. Second-Order Rate Constants k_1 for the Reactions of the Michael Acceptors **1–3** with the Carbanions **4a–f** and the Amines **5a–d** in DMSO at 20 °C.

Electrophile	E	Nucleophile	$k_1 / \text{M}^{-1} \text{s}^{-1}$
1a	-7.94 ^a	4h	3.35×10^4
		1b	-8.79
1c	-10.17	4g	7.02×10^5
		4h	6.99×10^3
		5c	2.73×10^4
		5d	3.56×10^4
		4f	2.19×10^5
		4g	6.87×10^4
		4g	6.38×10^{4b}
		4g	2.30×10^{2c}
		4h	3.59×10^2
		5a	1.09×10^5
		5c	4.04×10^3
2a	-10.19	5d	4.92×10^3
		4f	2.18×10^5
		4g	6.18×10^4
		4h	2.30×10^1
		5b	8.41×10^2
		5c	5.38×10^3
		5d	8.04×10^3
2b	-10.76	4d	3.72×10^5
		4f	8.57×10^4
		4g	2.17×10^4
		4h	1.01×10^1
		5b	8.30×10^2
		5c	2.85×10^3
		5d	3.42×10^3
		4b	6.38×10^4
2c	-12.17	4d	4.76×10^4
		4e	4.40×10^4
		4f	8.64×10^3
		4g	2.95×10^3
		5d	5.10×10^2
		4b	1.96×10^5
		4d	1.37×10^5
3a	-11.51	4f	2.35×10^4
		4g	6.97×10^3
		4b	6.58×10^4
		4c	5.48×10^4
		4d	3.77×10^4
		4f	6.86×10^3
		4g	1.96×10^3
3b	-12.26	5c	7.72×10^2
		5d	1.49×10^3

Table 6.2. *Continued.*

Electrophile	E	Nucleophile	$k_1 / \text{M}^{-1}\text{s}^{-1}$
3c	-13.61	4a	6.96×10^4
		4b	8.31×10^3
		4c	7.75×10^3
		4d	4.03×10^3
		4f	7.45×10^2
		4g	1.92×10^2

^a The calculated value -8.65 (from **1a** + **4h**) has been corrected by -0.7 , corresponding to the deviations of **4h** from the correlation lines in Figure 6.7. ^b From an independent experiment, decrease at $\lambda = 483$ nm, ^c increase at $\lambda = 570$ nm.

Equilibrium Constants. While most of the Michael additions of the electrophiles **1–3** with the carbanions **4** proceed quantitatively as indicated by negligible end absorptions of the solutions at the absorption maxima of the electrophiles, many reactions of the electrophiles **1–3** with the amines **5a–d** and with the anion of Meldrum's acid (**4h**) turned out to be reversible. As a consequence, the linear plots of k_{obs} versus $[\text{Nu}]$ had positive intercepts (see Experimental Section).

While the reactions of the electrophiles **1b,c** with primary amines, such as ethanolamine (**5c**) and *n*-propyl amine (**5d**), and of **2a** with **5d** were found to be irreversible, the reactions of the electrophile **2a** with **5c**, and the reactions of the weaker electrophiles **2b,c** and **3b** with ethanolamine (**5c**) and *n*-propyl amine (**5d**) turned out to be reversible. Furthermore, all reactions of the secondary amines piperidine (**5a**) and morpholine (**5b**) with electrophiles **1c**, **2a** and **2b** were reversible.

Table 6.3. Equilibrium Constants for the Reactions of the Electrophiles **1–3** with the Carbanions **4a–f** and the Amines **5a–d** in DMSO at 20 °C.

Electrophil e	Nucleophil e	k_- / s^{-1}	$K / \text{L mol}^{-1}$
1c	5a	8.0×10^1	1.4×10^3
2a	4h	1.5×10^{-2}	1.5×10^3
	5b	2.9	2.9×10^2
	5c	5.8	9.3×10^2
2b	4h	1.6×10^{-2}	6.5×10^2
	5b	3.6	2.5×10^2
	5c	8.3	3.4×10^2
	5d	5.0	6.9×10^2
2c	5d	6.0	8.4×10^1
3b	5c	6.0×10^{-2}	1.2×10^2
	5d	2.3	6.4×10^2

If no parallel reactions complicate the evaluation of the rate constants, it is possible to calculate the equilibrium constants K for these reversible reactions as the ratio of the forward (k_1) over the backward reaction¹⁶ (k_- , intercept of k_{obs} vs. [Nu] plot, Equation (6.3)), though we do not know the side of the nucleophilic attack of the carbanions. Because we have previously noted that equilibrium constants derived from the intercepts of k_{obs} versus [Nu] plots are not very reliable (see Chapter 5), we will not derive intrinsic barriers from these data. One can see, however, that the equilibrium constants for the additions of primary amines are generally larger than those for analogous additions of secondary amines (Table 6.3).

$$K = \frac{k_1}{k_-} \quad (6.3)$$

Correlation Analysis. By substituting the second-order rate constants k_1 (Table 6.2) and the previously published N - and s parameters for the carbanions **4a–g** (Table 6.1) into Equation (6.1), the electrophilicity parameters E of the Michael acceptors **1–3** were determined. Minimization of $\Delta^2 = \sum(\log k - s(N + E))^2$ with the non-linear solver

What's *Best!*, where k corresponds to the experimental rate constants for the reactions of **1–3** with the carbanions yields the optimized values for E . Please note, that the correlation lines are exclusively based on the reactions of the Michael acceptors **1–3** with the carbanions **4a–g** (filled symbols) and the slopes were fixed to 1.0, as required by Equation (6.1).

Due to their relatively high reactivities, electrophiles **1b** and **1c** could only be studied with three carbanions of which the anion of Meldrum's acid **4h** deviates strongly. As the correlation lines are based exclusively on the reactions of **1b,c** with carbanions (except **4h**) their experimental basis is poor. However, it is obvious that the second-order rates k_1 for the reactions of **1b,c** with the amines **5a**, **5c**, and **5d** beautifully match the correlation lines described by Equation (6.1). Acceleration of the amine additions by hydrogen bonding, as observed in the additions of amines to structurally related Michael acceptors⁷ is obviously absent in these reactions.

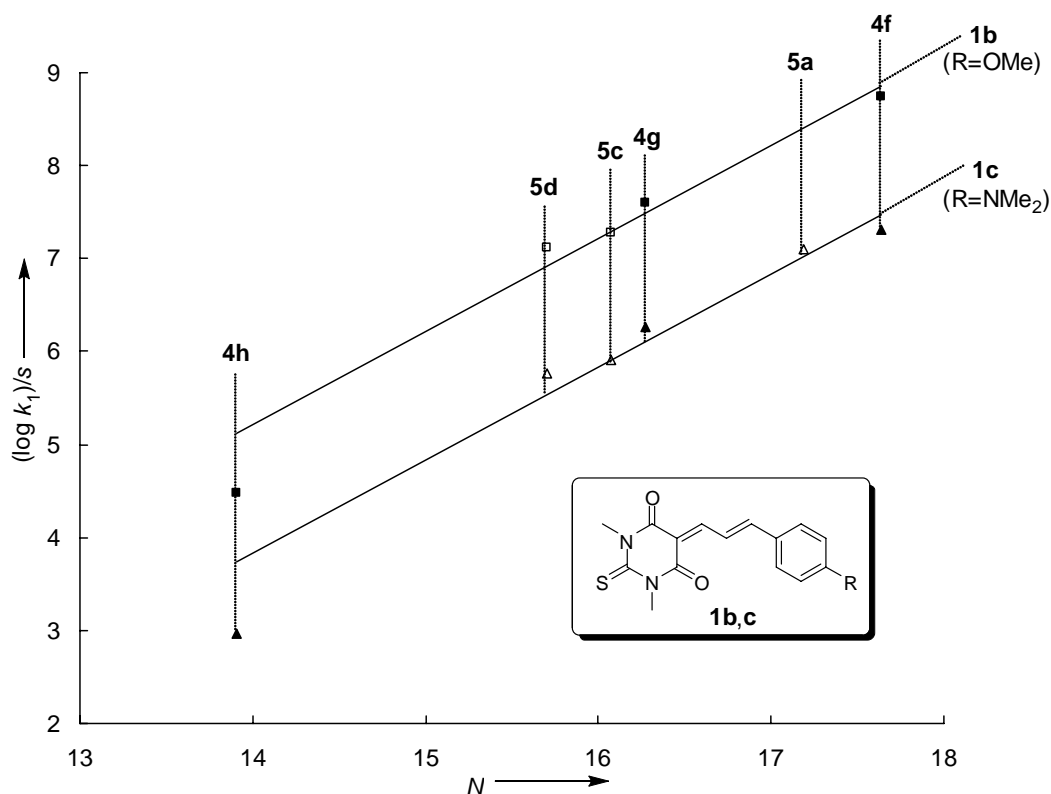


Figure 6.6. Plot of $(\log k_1)/s$ versus N for the reactions of **1a,b** with different carbanions (filled symbols) and amines (open symbols) in DMSO at 20 °C.

The correlations for the addition of carbanions and amines to the less reactive Michael acceptors **2a–c** (Figure 6.7) also show some deviations. On one hand, the anion of ethyl cyanoacetate **4b** reacts more slowly with **2c** than predicted by Equation (6.1), and on the other hand, **4g** reacts faster with Michael acceptors **2a–c** than expected. This is in line with previous findings for the reaction of **4g** with different Michael acceptors.⁷ The reactions of **2a,b** with **4h** are almost 70 times slower than calculated by Equation 6.1. As depicted in Figure 6.7, the reactions of **2a–c** with the amines **5c,d** were found to be up to five times faster than calculated from Equation (6.1) and their *N*- and *s* parameters in dimethyl sulfoxide. These deviations are smaller than those reported in Chapter 2 for the reactions of amines with benzylidene Meldrum's acids.

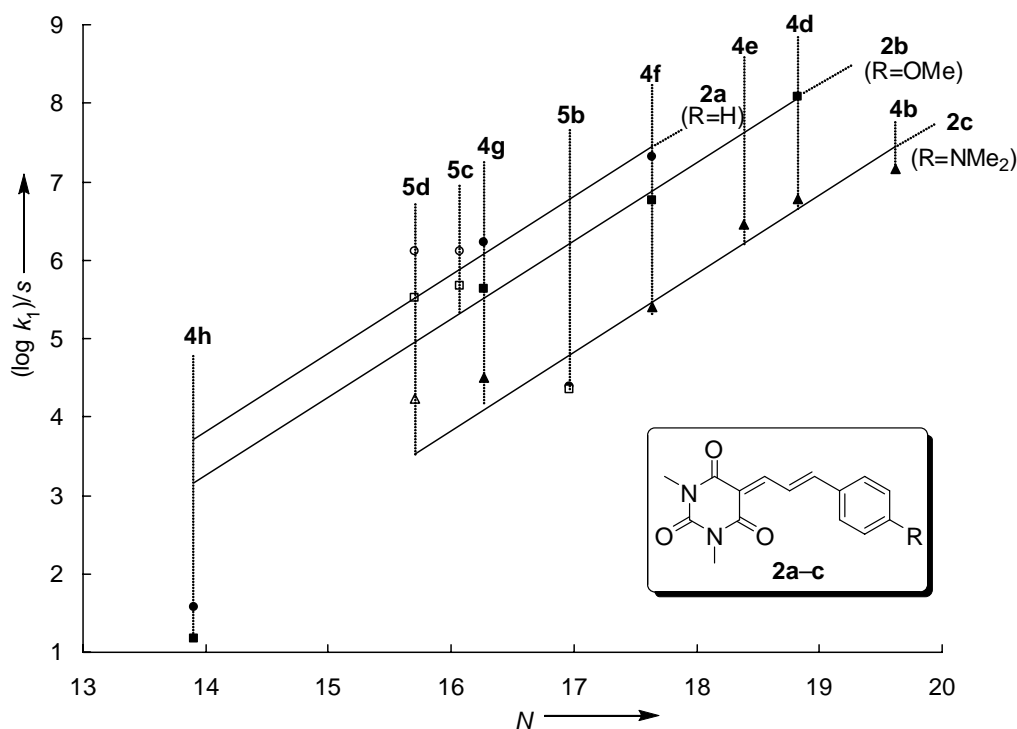


Figure 6.7. Plot of $(\log k_1)/s$ versus N for the reactions of **2a–c** with different carbanions (filled symbols) and amines (open symbols) in DMSO at 20 °C.

Due to a significantly larger number of investigated electrophile-nucleophile combinations, the basis of the correlation lines for compounds **3a–c** in Figure 6.8 is significantly better than those for **1a–c** and **2a–c**. Figure 6.8 reveals that the anion of dimedone **4g** is the only

carbanion, which deviates noticeable from the correlation lines for the reactions of **3a–c**. As discussed above for the reactions of **2a–c** with amines **5c,d**, the second-order rate constants k_1 for the reactions of Michael acceptor **3b** with amines **5c** and **5d** are significantly larger than calculated by Equation 6.1.

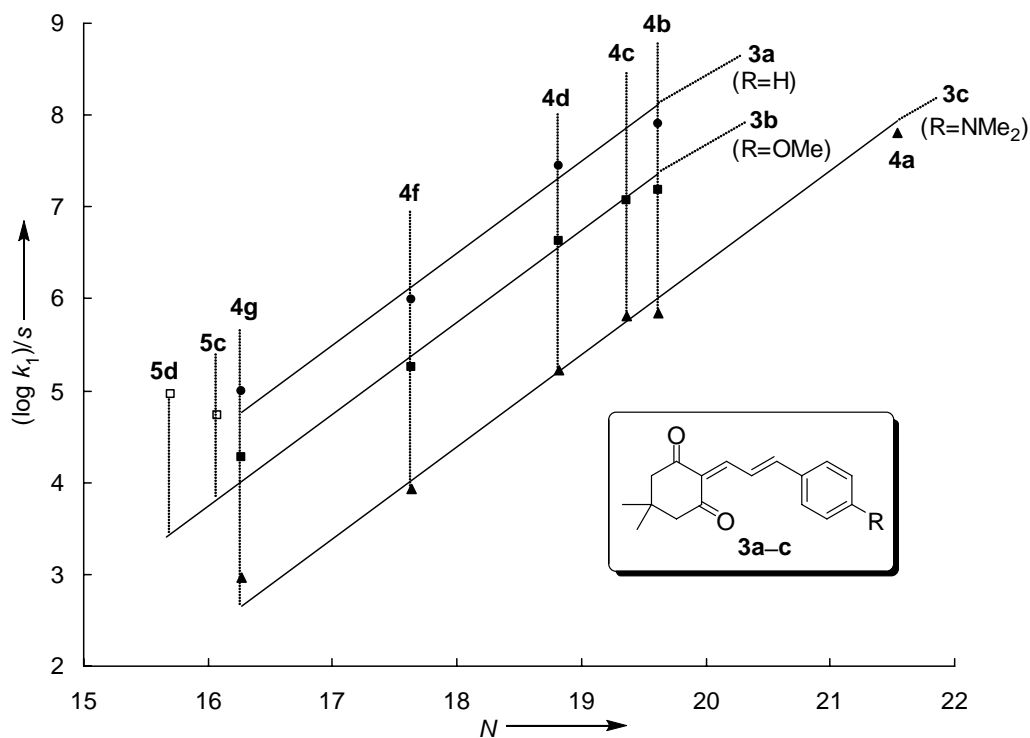
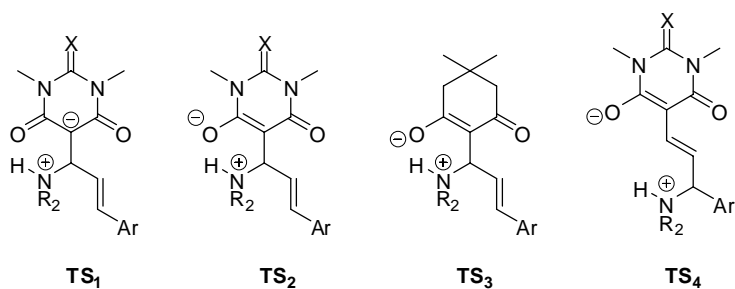


Figure 6.8. Plot of $(\log k_1)/s$ versus N for the reactions of **3a–c** with different carbanions (filled symbols) and amines (open symbols) in DMSO at 20 °C.

The different deviations of the rate constants for the reactions of amines with **1a–c**, **2a–c**, and **3a–c**, from the correlation lines defined by the reactions of **1a–c**, **2a–c**, and **3a–c** with carbanions, may be indicative of the influence of hydrogen bridges on the transition state depicted below. Obviously, hydrogen bridges do not play a significant role for the additions of amines to **1a–c** and **2a–c** (TS₁ and TS₂) in contrast to the analogous reactions with **3b** (TS₃).

If the rate constants for the reactions of the amines to **1** and **2** follow 1,6-additions, transition state TS₄ would be likely. The longer distance between the nitrogen and the negatively charged oxygen or carbon would then prevent a strong stabilizing hydrogen bridge.



Product studies, which would allow to decide whether this observation is due to 1,6-addition of the amines have not been performed.

From Equation (6.1) and the second-order rate constants k_1 in Table 6.2, electrophilicity parameters E have consequently been derived for all Michael acceptors **1–3**. However, the correlations are sometimes based only on a small number of measurements and some deviations from linearity are evident.

The comparison of the electrophilicity parameters E for different Michael acceptors (Figure 6.9) shows that the acceptor-substituted dienes **1–3** cover a range of almost 5 orders on our electrophilicity scale. Their reactivities are comparable to those of the benzylidene(thio)barbituric acids, published recently.⁶ Figure 6.9 also reveals that substitution of the oxygen in the barbituric acid by sulfur increases the reactivities of the Michael acceptors by almost 2 orders of magnitude. This observation is in line with the electrophilicities found for benzylidenebarbituric acids and benzylidene(thio)barbituric acids.⁶ This may be surprising because sulfur has an electronegativity comparable to carbon, but it has been reported that the dipole moments of thiocarbonyl compounds are larger than those for the corresponding carbonyl compounds, and that thiolactames possess larger dipole moments than lactames.¹⁷ Furthermore, the larger rotational barrier for amides have been attributed to the different resonance effects in amides and thioamides.¹⁸ In addition, quantum chemical calculations of rotational barriers by Wiberg showed that amide resonance is more important in thiolactames than in lactames.¹⁹

The electrophiles **3a–c** are roughly 2 orders of magnitude less reactive than the analogously substituted Michael acceptors **2a–c**. This is in line with the fact that dimedone ($pK_a(\text{H}_2\text{O}) = 5.2$)²⁰ is a weaker acid than barbituric- and thiobarbituric acids ($pK_a(\text{H}_2\text{O}) = 4.0$).²¹

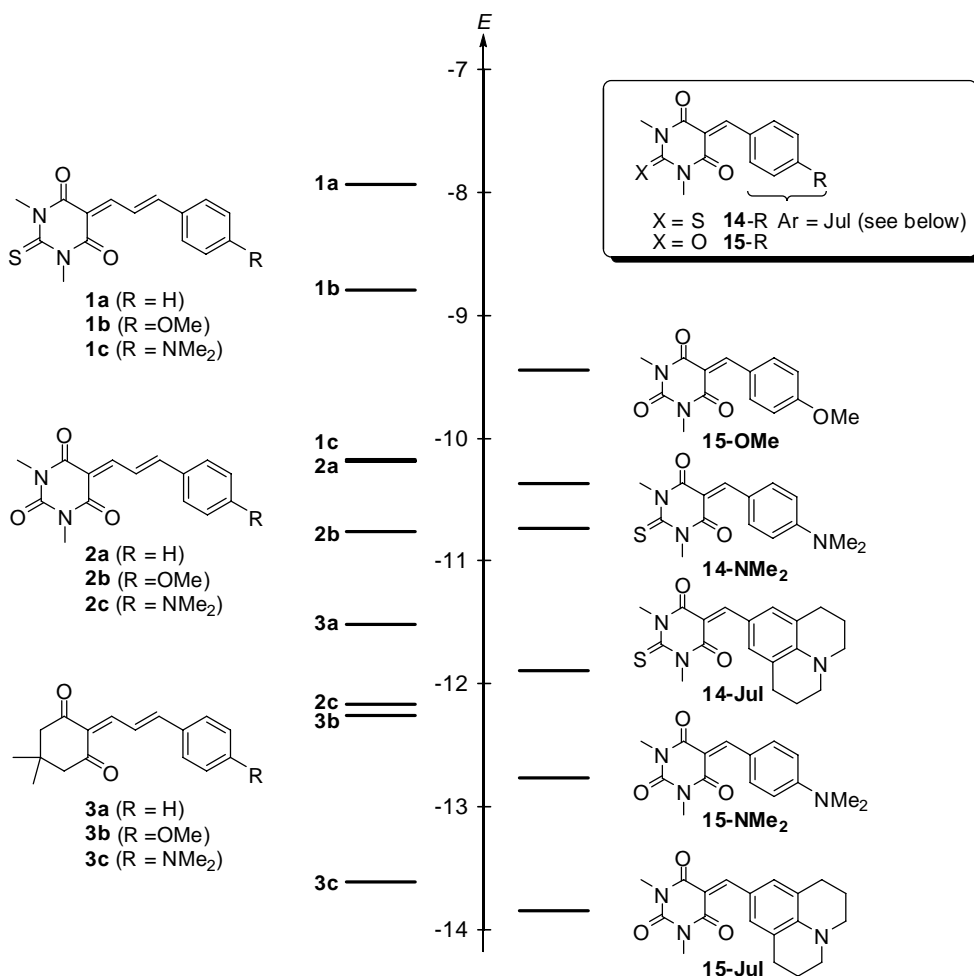


Figure 6.9. Comparison of the electrophilicity parameters E of Michael acceptors **1–3** with those of some benzylidene(thio)barbituric acids **14** and **15**.

Interestingly, the electrophilicity parameters of the dimethyl amino substituted dienes **1c** and **2c** are larger than those of their benzylidene counterparts **14-NMe₂** and **15-NMe₂**, respectively, whereas we find the opposite behavior for the methoxy substituted diene **2b** and its counterpart **15-OMe**. These findings reflect the different slopes of the correlation lines in the Hammett plot of Figure 6.10. Due to the larger slope for compounds **14** and **15** we find

higher electrophilicities for the methoxy substituted dienes and smaller values for the dimethyl amino substituted ones.

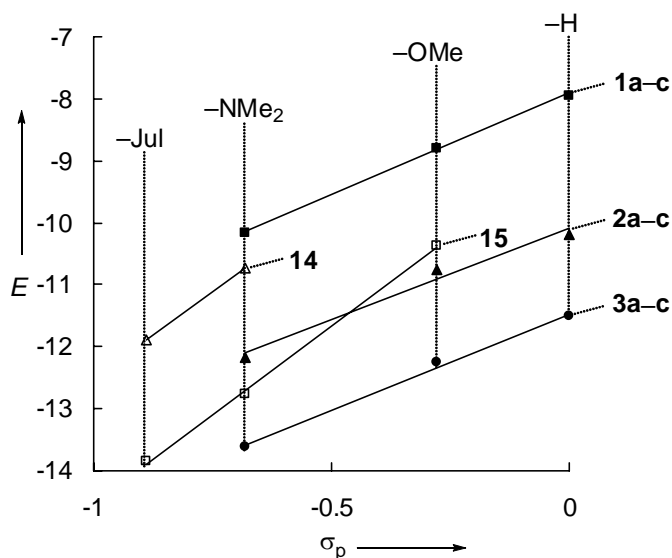


Figure 6.10. Correlations between the electrophilicity parameters E of Michael acceptors **1–3** (filled symbols) and of benzylidene (thio)barbituric acids **14** and **15** (open symbols) versus Hammett's σ_p values.^{7,22}

The slopes in the Hammett plots reflect the influence of the para substituent on the electrophilicity of the Michael acceptors **1–3** and **14** and **15**. From these slopes (5.52 – 5.73 for **14** and **15**; 2.95–3.30 for **1–3**) one can derive reaction constants of $\rho \approx 3.9$ and 2.2, respectively, for reactions with nucleophiles of $s = 0.7$ (Table 6.2), indicating that the substituent effects in the dienes **1–3** are considerably smaller than in the benzylidene(thio)barbituric acids **14** and **15**. The larger distance between the variable substituents and the reaction center in the dienes **1a–c**, **2a–c**, and **4a–c** than in **14** and **15** reduces the interactions between substituents and reactive site.

Conclusion

The linear free-energy relationship $\log k_1 (20\text{ }^\circ\text{C}) = s(N + E)$ (6.1) has been found to be applicable to the reactions of the Michael acceptors **1–3** with the carbanions **4a–h**. The rate constants for the reactions of **3a–c** with amines were 5–10 times larger than expected from

Equation (6.1), while the analogous reactions of **1** and **2** deviate much less. Compounds **1–3** cover almost 5 orders of magnitude on our electrophilicity scale ($-13.6 < E < -7.9$) and substitution of the oxygen in the 1,3-dimethylbarbituric acid by sulfur was found to increase the electrophilicity of the Michael acceptors by almost 2 orders of magnitude. It has also been found that the substituent effect for dienes **1–3** is considerably smaller than for benzylidene(thio)barbituric acids **14** and **15** indicated by reaction constants of $\rho \approx 2.2$

References

- (1) Lucius, R.; Loos, R.; Mayr, H. *Angew. Chem.* **2002**, *114*, 97–102; *Angew. Chem., Int. Ed.* **2002**, *41*, 91–95.
- (2) a) Minegishi, S.; Mayr, H. *J. Am. Chem. Soc.* **2003**, *125*, 286–295; b) Seeliger, F.; Mayr, H. *Org. Biomol. Chem.* **2008**, *6*, 3052–3058.
- (3) Bug, T.; Lemek, T.; Mayr, H. *J. Org. Chem.* **2004**, *69*, 7565–7576.
- (4) Berger, S. T. A.; Ofial, A. R.; Mayr, H. *J. Am. Chem. Soc.* **2007**, *129*, 9753–9761.
- (5) Berger, S. T. A.; Seeliger, F. H.; Hofbauer, F.; Mayr, H. *Org. Biomol. Chem.* **2007**, *5*, 3020–3026.
- (6) Seeliger, F.; Berger, S. T. A.; Remennikov, G. Y.; Polborn, K.; Mayr, H. *J. Org. Chem.* **2007**, *72*, 9170–9180.
- (7) Kaumanns, O.; Mayr, H. *J. Org. Chem.* **2008**, *73*, 2738–2745.
- (8) Kaumanns, O.; Lucius, R.; Mayr, H. *Chem. Eur. J.* **2008**, *14*, 9675–9682.
- (9) a) Oh, H. K.; Kim, I. K.; Lee, H. W.; Lee, I. *J. Org. Chem.* **2004**, *69*, 3806–3810; b) Oh, H. K.; Kim, T. S.; Lee, H. W.; Lee, I. *Bull. Korean Chem. Soc.* **2003**, *24*, 193–196.
- (10) Bug, T.; Mayr, H. *J. Am. Chem. Soc.* **2003**, *125*, 12980–12986.
- (11) Phan, T. B., unpublished results.

- (12) Jursic, B. S.; Stevens, E. D. *Tetrahedron Lett.* **2003**, *44*, 2203-2210.
- (13) Nagarajan, K.; Shenoy, S. J. *Indian J. Chem., Sect. B* **1992**, *31B*, 73-87.
- (14) Lemek, T.; Mayr, H. *J. Org. Chem.* **2003**, *68*, 6880-6886.
- (15) Maskill, H.; Editor *The Investigation of Organic Reactions and Their Mechanisms*; Blackwell Publishing: Oxford, 2006.
- (16) Schmid, R.; Sapunov, V. N. *Non-Formal Kinetics*; VCH: Weinheim, 1982.
- (17) Lee, C. M.; Kumler, W. D. *J. Org. Chem.* **1962**, *27*, 2052-2054.
- (18) Loewenstein, A.; Melera, A.; Rigny, P.; Walter, W. *J. Phys. Chem.* **1964**, *68*, 1597-1598.
- (19) Wiberg, K. B.; Rablen, P. R. *J. Am. Chem. Soc.* **1995**, *117*, 2201-2209.
- (20) Eistert, B.; Merkel, E.; Reiss, W. *Chem. Ber.* **1954**, *87*, 1513-1540.
- (21) Mautner, H. G.; Clayton, E. M. *J. Am. Chem. Soc.* **1959**, *81*, 6270-6273.
- (22) Exner, O. *Correlation Analysis of Chemical Data*; Plenum New York, 1988.

Experimental Section

Electrophilicities of Acceptor Substituted Dienes

6.1. Materials

General. Commercially available DMSO (content of H₂O < 50 ppm) was used without further purification. Stock solutions of KO^tBu in DMSO were prepared under nitrogen atmosphere. The carbanions were prepared as described previously.^{S1} The amines were distilled before use.

6.2. Instruments

NMR spectroscopy. In the ¹H and ¹³C NMR spectra chemical shifts are expressed in ppm and refer to CDCl₃ (δ_{H} 7.26, δ_{C} 77.0) as internal standard. The coupling constants are in Hz. Abbreviations used are s (singlet), d (doublet), t (triplet), q (quartet), quint (quintet), m (multiplet).

6.3. Determination of the Second-Order Rate Constants

The general method for the determination of the rate constants is described in the experimental part of the paper. The temperature of the solutions was kept constant (20 ± 0.1 °C) during all kinetic experiments by using a circulating bath thermostat. For evaluation of the kinetic experiments commercial stopped-flow UV-Vis spectrometer systems were used. Rate constants k_{obs} (s⁻¹) were obtained by fitting the single exponential function $A_t = A_0 \exp(-k_{1\psi}t) + C$ to the observed time-dependent absorbance of the minor component. Plotting k_{obs} against the concentrations of the nucleophiles resulted in linear correlations, the slopes, which correspond to the second-order rate constants k_1 (L mol⁻¹ s⁻¹). For stopped-flow experiments two stock solutions were used: A solution of electrophiles **1–3** in DMSO and a solution of the carbanions **4a–h** in DMSO generated by deprotonation of the corresponding CH acid with KO^tBu, or by dissolving the corresponding preformed potassium salt (**4a–h**)-K⁺ in DMSO.

^{S1} Lucius, R.; Mayr, H. *Angew. Chem., Int. Ed.* **2000**, *39*, 1995-1997.

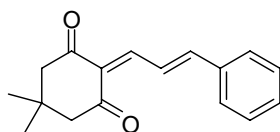
6.4. Synthesis of the Michael acceptors 1–3

General. Equimolar amounts of the CH acidic compounds (1,3-dimethylbarbituric acid or 1,3-dimethyl-2-thiobarbituric acid) and the cinnamaldehydes were refluxed in ethanol as described in ref. S2 to yield compounds **1a–c** and **2a–c**. Compounds **3a–c** were synthesized following a protocol of Nagarajan^{S3} by refluxing equimolar amounts of dimedone and cinnamaldehydes in the presence of 10 mol% piperidine in toluene for 90 min. After removing the solvent under reduced pressure, the crude reaction mixture was dissolved in methylene chloride and extracted from aqueous hydrochloric acid, saturated NaHCO₃ solution and NaCl solution. After drying of the organic phase over MgSO₄ the solvent was removed and the crude reaction mixture was recrystallized from *n*-hexane to yield compounds **3a–c**. Insoluble residue was washed with diethyl ether to yield compounds **6a–c**.

5,5-Dimethyl-2-(3-phenylallylidene)cyclohexane-1,3-dione (**3a**)

From cinnamaldehyde (2.53 g, 19.2 mmol), dimedone (2.74 g, 19.5 mmol), and piperidine (0.24 mg, 2.87 mmol) in toluene (40 mL). **3a** (1.87 g, 7.36 mmol, 38 %). Yellow solid; mp 90-92 °C (100-102 °C ref.^{S3})

¹H-NMR (CDCl₃, 300 MHz): δ = 1.08 (s, 6 H, 2 × CH₃), 2.55 (s, 4 H, 2 × CH₂), 7.35 (d, ³J = 15.6 Hz, 1 H, 9-H), 7.39 (m, 3 H, CH_{ar}), 7.62 (m, 2 H, CH_{ar}), 7.79 (d, ³J = 12.0 Hz, 1 H, 7-H), 8.37 ppm (dd, ³J = 15.6 Hz, 8-H). ¹³C-NMR (CDCl₃, 75.5 MHz): δ = 28.5 (q, 2 × CH₃), 30.1 (s, C(CH₃)₂), 52.4 (t, CH₂), 54.1 (t, CH₂), 125.6 (d, C-8), 128.7 (d, CH_{ar}), 129.0 (d, CH_{ar}), 130.9 (d, CH_{ar}), 135.7 (s), 151.2 (d, C-7), 153.3 (d, C-9), 197.8 (s), 198.9 ppm (s). MS (EI) m/z (%) = 255 (17), 254 (100) [M⁺], 253 (22), 239 (16), 198 (24), 177 (18), 179 (31), 142 (11), 141 (13), 128 (20), 127 (13).

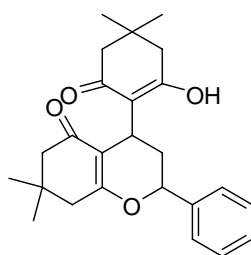


^{S2} Jursic, B. S.; Stevens, E. D. *Tetrahedron Lett.* **2003**, *44*, 2203-2210.

^{S3} Nagarajan, K.; Shenoy, S. J. *Indian J. Chem., Sect. B* **1992**, *31B*, 73-87.

4-(2-Hydroxy-4,4-dimethyl-6-oxocyclohex-1-enyl)-7,7-dimethyl-2-phenyl-3,4,7,8-tetrahydro-2H-chromen-5-(6H)-one (6a). (0.51 g, 1.27 mmol, 13 %). Yellow solid; mp 198-200 °C (220-222 °C ref.^{S3}).

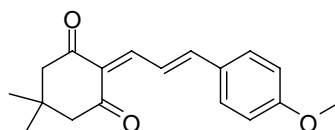
¹H-NMR (CDCl₃, 300 MHz): δ = 0.94 (s, 6 H, 2 × CH₃), 1.03, 1.09 (s, 6 H, 2 × CH₃), 1.54 (d, ³J = 13.6 Hz, 1 H, CH₂ (H-8)), 2.00-2.50 (m, 8 H, 4 × CH₂), 2.84 (td, ³J = 13.4 Hz, 5.6 Hz, 1 H, H-8), 3.90 (d, ³J = 4.8 Hz, 1 H, 7-H, CH), 5.02 (dd, ³J = 12.3 Hz, ³J = 2.0 Hz, 1 H, CH (9-H)), 7.15 (m, 3 H, CH_{ar}), 7.27 ppm (m, 2 H, CH_{ar}). ¹³C-NMR (CDCl₃, 100.5 MHz): δ = 27.7 (q, 2 × CH₃), 27.8, 28.2 (q, 2 × CH₃), 31.2 (s, C(CH₃)₃), 31.8 (s, C(CH₃)₃), 32.4 (t, CH₂), 33.8 (s, CH), 41.8 (t, 2 × CH₂), 50.2 (t, 2 × CH₂), 66.8 (d, CH), 109.6, 110.7 (s), 125.7 (d, CH_{ar}), 127.6 (d, 2 × CH_{ar}), 128.0 (d, 2 × CH_{ar}), 145.5, 171.3, 195.5 ppm (s). MS (EI) m/z (%) = 394 (18) [M⁺], 393 (100) [M-H⁺].



2-(3-(4-Methoxyphenyl)allylidene)-5,5-dimethylcyclohexane-1,3-dione (3b)

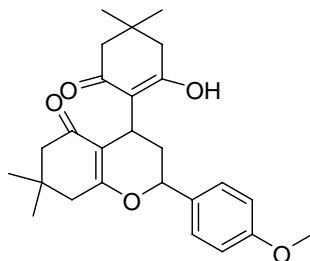
From methoxycinnamaldehyde (2.05 g, 12.7 mmol), dimedone (1.76 g, 12.6 mmol), and piperidine (0.18 mg, 2.06 mmol) in toluene (40 mL). **3b** (1.97 g, 6.93 mmol, 55 %). Red solid; mp 128-130 °C.

¹H-NMR: (CDCl₃, 400 MHz): δ = 1.08 (s, 6 H, 2 × CH₃), 2.52 (s, 4 H, 2 × CH₂), 3.84 (s, 3 H, OCH₃), 6.91 (d, ³J = 8.8 Hz, 2 H, CH_{ar}), 7.32 (d, ³J = 15.3 Hz, 1 H, 9-H), 7.59 (d, ³J = 8.8 Hz, 2 H, CH_{ar}), 7.80 (d, ³J = 12.1 Hz, 1 H, 7-H), 8.29 ppm (dd, ³J = 12.1 Hz, ³J = 15.3 Hz, 1 H, 8-H). ¹³C-NMR: (CDCl₃, 100.5 MHz): δ = 28.5 (q, 2 × CH₃), 30.1 (s, C(CH₃)₂), 52.3 (t, CH₂), 54.0 (t, CH₂), 55.4 (q, OCH₃), 114.5 (d, CH_{ar}), 123.6 (d, C-8), 127.7 (s), 128.6 (s), 130.8 (d, CH_{ar}), 152.1 (d, C-7), 153.9 (d, C-9), 162.2 (s), 197.9, 198.9 ppm (s). MS (EI) m/z (%) = 285 (15), 284 (100) [M⁺], 283 (19), 269 (16), 200 (14).



4-(2-Hydroxy-4,4-dimethyl-6-oxocyclohex-1-enyl)-2-4-(methoxyphenyl)-7,7-dimethyl-3,4,7,8-tetrahydro-2H-chromen-5-(6H)-one (6b). (0.49 g, 1.16 mmol, 18 %). Yellow solid; mp 171-173 °C (multipl. mp see ref. S3)

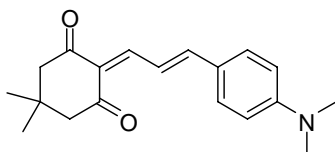
¹H-NMR (CDCl₃, 400 MHz): δ = 0.94 (s, 6 H, 2 × CH₃), 1.02, 1.08 (2 s, 6 H, 2 × CH₃), 1.50 (d, ³J = 13.5 Hz, 1 H, CH), 2.00 - 2.40 (m, 8 H, 4 × CH₂), 2.78 (td, ³J = 13.4 Hz, ³J = 5.5 Hz, 1 H, 8-H), 3.71 (s, 3 H, OCH₃), 3.84 (d, ³J = 4.9 Hz 1 H, CH), 5.02 (dd, ³J = 12.4 Hz, ³J = 2.2 Hz, 1 H, CH), 6.83 (d, ³J = 8.6 Hz 2 H, CH_{ar}), 7.02 ppm (d, ³J = 8.6 Hz 2 H, CH_{ar}). ¹³C-NMR (CDCl₃, 100.5 MHz): δ = 27.7 (2 C, q, 2 × CH₃), 27.8, 28.2 (2 q, 2 × CH₃), 31.3 (s, C(CH₃)₂), 31.7 (s), 32.6 (t, CH₂), 32.7 (d, CH), 41.8 (t, 2 × CH₂), 50.3 (2 C, t, 2 × CH₂), 54.9 (q, OCH₃), 66.8 (d, CH), 110.0, 110.9 (s), 113.4 (d, CH_{ar}), 128.5 (2 C, d, CH_{ar}), 137.3, 157.3, 171.1, 195.4 ppm (s). EI-MS: *m/z* (%) = 424 (26) [M⁺], 423 (100) [M-H⁺], 283 (7), 165 (12).



2-(3-(4-Dimethylamino)phenyl)allylidene)-5,5-dimethylcyclohexane-1,3-dione (3c).

From methoxycinnamaldehyde (2.58 g, 14.7 mmol), dimedone (2.06 g, 14.7 mmol), and piperidine (0.18 mg, 2.06 mmol) in toluene (40 mL). **3b** (2.87 g, 9.66 mmol, 66 %). purple crystals; mp 182-184 °C (174-176 °C ref.^{S3}).

¹H-NMR (CDCl₃, 400 MHz): δ = 1.07 (s, 6 H, 2 × CH₃), 2.49 (s, 4 H, × CH₂), 3.05 (s, 6 H, N(CH₃)₂), 6.65 (d, ³J = 8.9 Hz, 2 H, CH_{ar}), 7.33 (d, ³J = 14.9 Hz, 1 H, 9-H), 7.54 (d, ³J = 8.9 Hz, 2 H, CH_{ar}), 7.85 (d, ³J = 12.4 Hz, 1 H, 7-H), 8.29 ppm (dd, ³J = 12.4 Hz, ³J = 14.9 Hz, 1 H, 8-H). ¹³C-NMR (CDCl₃, 100.5 MHz): δ = 28.5 (2 C, q, 2 × CH₃), 30.2 (s, C(CH₃)₂), 40.0 (2 C, q, N(CH₃)₂), 52.2 (t, CH₂), 53.9 (t, CH₂), 111.7 (d, CH_{ar}), 121.1 (d, C-8), 123.7 (s), 125.3 (s), 131.5 (d, CH_{ar}), 152.6 (s), 153.4 (d, C-7), 156.5 (d, C-9), 197.9, 198.8 ppm (s). EI-MS: *m/z* (%) = 298 (19), 297 (100) [M⁺], 296 (31), 282 (13), 280 (11), 213 (16), 185 (13).

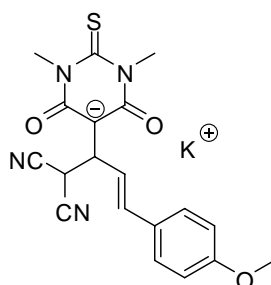


6.5. Product Studies (NMR)

The electrophile **1c** (20.1 mg, 6.35×10^{-5} mol) was allowed to react with the anion of malonitrile **4c** (7.0 mg, 6.72×10^{-5} mol) in d_6 -DMSO in an NMR tube. After 2 min of vigorous shaking, the solution was colorless and resulted in the formation of an almost equimolar mixture of two regioisomers.

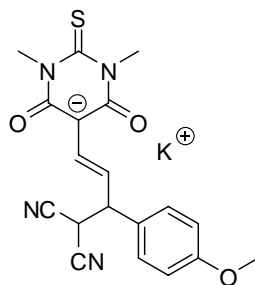
7bc: 1,4 addition product (**5-(1,1-dicyano-4-(4-methoxyphenyl)but-3-en-2-yl)-1,3-dimethyl-2,6-dioxo-2-thiohexahydropyrimidin-5-yl**)potassium

^1H NMR (d_6 -DMSO, 400 MHz) δ = 3.55 (s, 6 H, $2 \times \text{NCH}_3$), 3.75 (s, 3 H, OCH_3), 4.24 (dd, $^3J = 10.8, 9.2$ Hz, 1 H, CH), 5.52 (d, $^3J = 10.8$ Hz, 1H, $\text{CH}(\text{CN})_2$), 6.32 (dd, $^3J = 9.2, 15.8$ Hz, 1 H, $\text{C}=\text{CH}$), 6.50 (d, $^3J = 16.0$ Hz, 1 H, $\text{C}=\text{CH}$), 6.94 (d, $^3J = 8.8$ Hz, 2 H, CH_{ar}), 7.33 ppm (d, $^3J = 8.8$ Hz, 2 H, CH_{ar}). ^{13}C NMR (d_6 -DMSO, 100 MHz) δ = 25.6 (d, $\text{CH}(\text{CN})_2$), 34.4 (q, $2 \times \text{NCH}_3$), 50.0 (d, CH), 55.0 (q, OCH_3), 86.2 (C^-), 113.9 (d, CH_{ar}), 114.9 (s, CN), 124.0 (d, $\text{C}=\text{CH}$), 128.7 (d, CH_{ar}), 131.1 (d, $\text{C}=\text{CH}$), 132.0 (s, C_{ar}), 158.4 (s, $\text{C}=\text{O}$), 160.2 (s, $\text{C}=\text{S}$), 175.1 ppm ($\text{C}=\text{O}$).



8bc: 1,6 addition product (**5-(4,4-dicyano-3-(4-methoxyphenyl)but-1-enyl)-1,3-dimethyl-2,6-dioxo-2-thiohexahydropyrimidin-5-yl**)potassium

^1H NMR (d_6 -DMSO, 400 MHz) δ = 3.54 (s, 6 H, $2 \times \text{NCH}_3$), 3.74 (s, 3 H, OCH_3), 4.02 (m, 1 H, CH), 5.23 (m, 1H, $\text{CH}(\text{CN})_2$), 6.70 (d, $^3J = 15.2$ Hz, 1 H, $\text{C}=\text{CH}$), 6.77 (dd, $^3J = 8.4, 15.2$ Hz, 1 H, $\text{C}=\text{CH}$), 6.87 (d, $^3J = 8.8$ Hz, 2 H, CH_{ar}), 7.31 ppm (d, $^3J = 8.8$ Hz, 2 H, CH_{ar}). ^{13}C NMR (d_6 -DMSO, 100 MHz) δ = 30.0 (d, $\text{CH}(\text{CN})_2$), 34.3 (q, $2 \times \text{NCH}_3$), 42.7 (d, CH), 55.0 (q, OCH_3), 89.7 (C^-), 113.9 (d, CH_{ar}), 114.2 (s, CN), 116.7 (d, $\text{C}=\text{CH}$), 127.4 (d, CH_{ar}), 129.0 (d, $\text{C}=\text{CH}$), 131.9 (s, C_{ar}), 158.7 (s, $\text{C}=\text{O}$), 160.2 (s, $\text{C}=\text{S}$), 175.9 ppm ($\text{C}=\text{O}$).

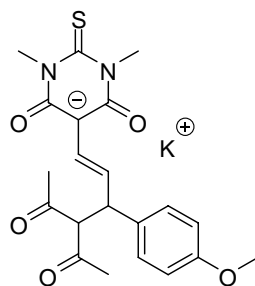


The electrophile **1b** (21.6 mg, 6.83×10^{-5} mol) was allowed to react with the anion of acetylacetone **4f** (11.0 mg, 7.96×10^{-5} mol) in d_6 -DMSO in an NMR tube. After 2 min of vigorous shaking, the solution was colorless and resulted in the formation of a 1:3 mixture of two regioisomers.

8bf: (major compound) **(5-(4-acetyl-3-(4-methoxyphenyl)-5-oxohex-1-enyl)-1,3-dimethyl-4,6-dioxo-2-thiohexahydropyrimidin-5-yl)potassium**

^1H NMR (d_6 -DMSO, 400 MHz) δ = 1.90 (s, 3 H, CH_3), 2.18 (s, 3 H, CH_3), 3.51 (s, 6 H, $2 \times \text{NCH}_3$), 3.70 (s, 3 H, OCH_3), 3.89 (dd, J = 8.8, 8.8 Hz, 1 H, CH), 4.43 (d, J = 11.6 Hz, 1 H, CH), 6.38 (d, J = 16 Hz, 1 H, $\text{C}=\text{CH}$), 6.50 (dd, J = 8.4, 15.4 Hz, 1 H, $\text{C}=\text{CH}$), 6.28 (d, J = 8.8 Hz, CH_{ar}), 7.14 ppm (d, J = 8.8 Hz, CH_{ar}). ^{13}C NMR (d_6 -DMSO, 100 MHz) δ = 30.3 (q, CH_3), 31.0 (q, CH_3), 34.4 (s, $\text{C}(\text{CH}_3)_2$), 50.5 (d, CH), 54.9 (q, OCH_3), 73.1 (d, CH), 89.8 (C^-), 113.7 (d, CH_{ar}), 121.8 (d, $\text{C}=\text{CH}$), 125.1 ($\text{C}=\text{CH}$), 128.5 (d, CH_{ar}), 135.0 (s, C_{ar}), 157.4 (s, $\text{C}=\text{O}$), 160.0 (s, $\text{C}=\text{O}$), 174.6 (s, $\text{C}=\text{S}$), 202.9 (s, COCH_3), 202.9 ppm (s, COCH_3).

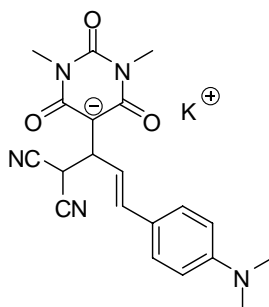
Due to some uncertainties in the ^{13}C NMR spectrum, assignments were only made for peaks of the major compound.



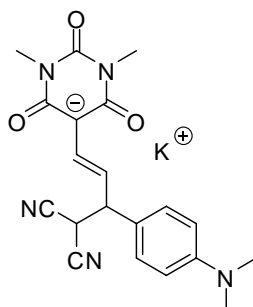
The electrophile **2c** (12.6 mg, 4.05×10^{-5} mol) was allowed to react with the anion of malonitrile **4c** (5.3 mg, 5.09×10^{-5} mol) in d_6 -DMSO in an NMR tube. After 2 min of vigorous shaking, the solution was colorless and resulted in the formation of almost equimolar amounts of two regioisomers.

9cc: 1,4 addition product (**5-(1,1-dicyano-4-(4-(dimethylamino)phenyl)but-3-en-2-yl)-1,3-dimethyl-2,4,6-trioxohexahydropyrimidin-5-yl**)potassium

^1H NMR (d_6 -DMSO, 400 MHz) δ = 2.88 (s, 6 H, $2 \times \text{NCH}_3$), 3.06 (s, 6 H, $\text{N}(\text{CH}_3)_2$), 4.17 (dd, $^3J = 10.4, 9.2$ Hz, 1 H, CH), 5.51 (d, $^3J = 11.2$ Hz, 1H, $\text{CH}(\text{CN})_2$), 6.20 (dd, $^3J = 9.2, 16$ Hz, 1 H, C=CH), 6.36 (d, $^3J = 15.6$ Hz, 1 H, C=CH), 6.70 (d, $^3J = 8.8$ Hz, 2 H, CH_{ar}), 7.19 ppm (d, $^3J = 8.8$ Hz, 2 H, CH_{ar}). ^{13}C NMR (d_6 -DMSO, 100 MHz) δ = 25.8 (d, $\text{CH}(\text{CN})_2$), 26.7 (q, $2 \times \text{NCH}_3$), 40.0 (q, $\text{N}(\text{CH}_3)_2$), 43.0 (d, CH), 81.4 (C^-), 112.1 (d, CH_{ar}), 114.5 (s, CN), 122.5 (d, C=CH), 124.5 (s, C_{ar}), 126.9 (d, CH_{ar}), 131.0 (d, C=CH), 149.7 (s, C_{ar}), 152.7 (s, C=O), 161.4, 161.6 ppm (C=O).

**10cc:** 1,6 addition product (**5-(4,4-dicyano-3-(4-(dimethylamino)phenyl)but-1-enyl)-1,3-dimethyl-2,4,6-trioxohexahydropyrimidin-5-yl**)potassium

^1H NMR (d_6 -DMSO, 400 MHz) δ = 2.88 (s, 6 H, $2 \times \text{NCH}_3$), 3.06 (s, 6 H, $\text{N}(\text{CH}_3)_2$), 3.84 (m, 1 H, CH), 5.08 (d, $^3J = 7.2$ Hz, 1H, $\text{CH}(\text{CN})_2$), 6.55-6.64 (m, 2 H, $2 \times \text{C}=\text{CH}$), 6.65 (d, $^3J = 9.2$ Hz, 2 H, CH_{ar}), 7.17 ppm (d, $^3J = 8.8$ Hz, 2 H, CH_{ar}). ^{13}C NMR (d_6 -DMSO, 100 MHz) δ = 26.7 (q, $2 \times \text{NCH}_3$), 30.4 (d, $\text{CH}(\text{CN})_2$), 40.0 (q, $\text{N}(\text{CH}_3)_2$), 50.4 (d, CH), 85.7 (C^-), 112.2 (d, CH_{ar}), 113.5 (d, C=CH), 115.2 (s, CN), 127.6 (s, C_{ar}), 128.1 (d, CH_{ar}), 129.5 (d, C=CH), 149.5 (s, C_{ar}), 152.2 (s, C=O), 161.4, 161.6 ppm (C=O).

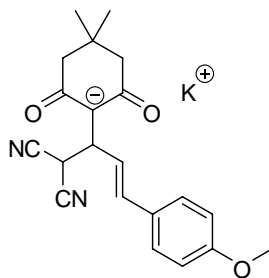


The electrophile **3a** (26.2 mg, 9.20×10^{-5} mol) was allowed to react with the anion of malonitrile **4c** (9.6 mg, 9.2×10^{-5} mol) in d_6 -DMSO in an NMR tube. After 2 min of vigorous shaking, the solution was colorless and resulted in the formation of compound **11bc**.

11bf: (1,1-dicyano-4-(4-methoxyphenyl)but-3-en-2-yl)-4,4-dimethyl-2,6-dioxocyclohexylpotassium

^1H NMR (d_6 -DMSO, 400 MHz) δ = 0.94 (s, 6 H, $2 \times \text{CH}_3$), 1.92 (s, 4 H, $2 \times \text{CH}_2$), 3.73 (s, 3 H, OMe), 4.27 (dd, 1 H, $^3J = 11.0$ Hz, 8.6 Hz, CH), 5.82 (d, $J = 11.0$ Hz, $\text{CH}(\text{CN})_2$), 6.30 (dd, $J = 8$ Hz, 1 H, $\text{C}=\text{CH}$), 6.35 (d, 1 H, $J = 16$ Hz, $\text{C}=\text{CH}$), 6.86 (d, $J = 8.8$ Hz, 1 H, CH_{ar}), 7.25 ppm (d, $J = 8.8$ Hz, 1 H, CH_{ar}).

^{13}C NMR (d_6 -DMSO, 100 MHz) δ = 24.9 (s, $\text{CH}(\text{CN})_2$), 28.8 (q, CH_3), 31.3 ($\text{C}(\text{CH}_3)_2$), 41.5 (d, CH), 50.6 (t, CH_2), 55.0 (q, OCH_3), 103.1 (s, C^-), 113.9 (d, CH_{ar}), 126.3 (d, $\text{C}=\text{CH}$), 127.0 (d, CH_{ar}), 129.6 (d, $\text{C}=\text{CH}$), 129.6 (s), 158.4 (s), 187.7 (s, $\text{C}=\text{O}$).



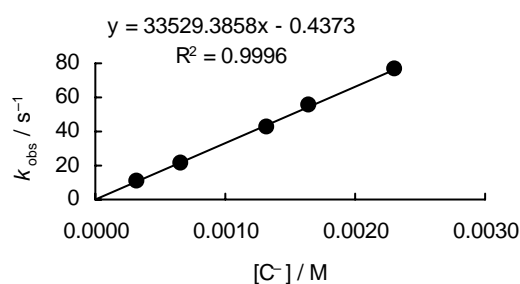
6.6. Reactivities of the Acceptor Substituted Dienes 1–3

Reactions of electrophile **1a**

Table S1: Kinetics of the reaction of **1a** with the anion of Meldrum's acid **4h** in DMSO at 20 °C (stopped-flow UV-Vis spectrometer, decrease at $\lambda = 412$ nm).

Nr.	[E] ₀ / M	[Nu ⁻] ₀ / M	<i>k</i> _{obs.} / s ⁻¹
241-1	1.84×10^{-5}	3.29×10^{-4}	1.08×10^1
241-2	1.84×10^{-5}	5.69×10^{-3}	2.16×10^1
241-3	1.84×10^{-5}	1.32×10^{-3}	4.29×10^1
241-4	1.84×10^{-5}	1.65×10^{-3}	5.54×10^1
241-5	1.84×10^{-5}	2.31×10^{-3}	7.68×10^1

$$k_1 = 3.35 \times 10^4 \text{ L mol}^{-1} \text{ s}^{-1}$$



Reactions of electrophile **1b**

Table S2: Kinetics of the reaction of **1b** with the anion of acetylacetone **4f** in DMSO at 20 °C (stopped-flow UV-Vis spectrometer, decrease at $\lambda = 445$ nm).

Nr.	[E] ₀ / M	[Nu ⁻] ₀ / M	<i>k</i> _{obs.} / s ⁻¹
225-1	5.22×10^{-6}	5.51×10^{-4}	1.36×10^1
225-2	5.22×10^{-6}	7.31×10^{-4}	1.80×10^1
225-3	5.22×10^{-6}	1.10×10^{-4}	2.67×10^1
225-5	5.22×10^{-6}	1.84×10^{-4}	4.43×10^1

$$k_1 = 2.39 \times 10^6 \text{ L mol}^{-1} \text{ s}^{-1}$$

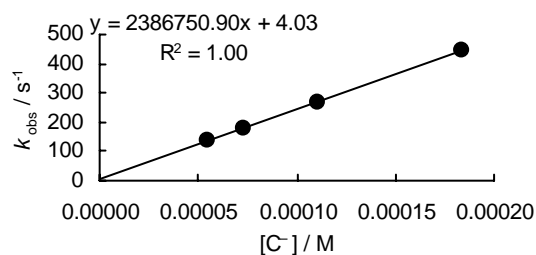


Table S3: Kinetics of the reaction of **1b** with the anion of dimedone **4g** in DMSO at 20 °C (stopped-flow UV-Vis spectrometer, decrease at $\lambda = 446$ nm).

Nr.	$[E]_0 / M$	$[Nu^-]_0 / M$	$k_{obs.} / s^{-1}$
227-3	9.80×10^{-6}	8.76×10^{-5}	8.46×10^1
227-4	9.80×10^{-6}	1.75×10^{-4}	1.56×10^2
227-1	9.80×10^{-6}	2.19×10^{-4}	1.83×10^2
227-5	9.80×10^{-6}	3.07×10^{-4}	2.50×10^2
227-2	9.80×10^{-6}	4.38×10^{-4}	3.33×10^2

$$k_1 = 7.02 \times 10^5 \text{ L mol}^{-1} \text{ s}^{-1}$$

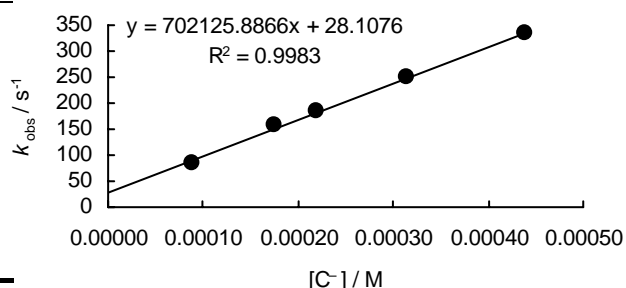


Table S4: Kinetics of the reaction of **1b** with the anion of Meldrum's acid **4h** in DMSO at 20 °C (stopped-flow UV-Vis spectrometer, decrease at $\lambda = 460$ nm).

Nr.	$[E]_0 / M$	$[Nu^-]_0 / M$	$k_{obs.} / s^{-1}$
238-1	1.98×10^{-5}	3.44×10^{-4}	3.41
238-2	1.98×10^{-5}	6.87×10^{-4}	6.05
238-3	1.98×10^{-5}	1.38×10^{-3}	1.01×10^1
238-4	1.98×10^{-5}	2.06×10^{-3}	1.44×10^1
238-5	1.98×10^{-5}	3.44×10^{-3}	2.54×10^1

$$k_1 = 6.99 \times 10^3 \text{ L mol}^{-1} \text{ s}^{-1}$$

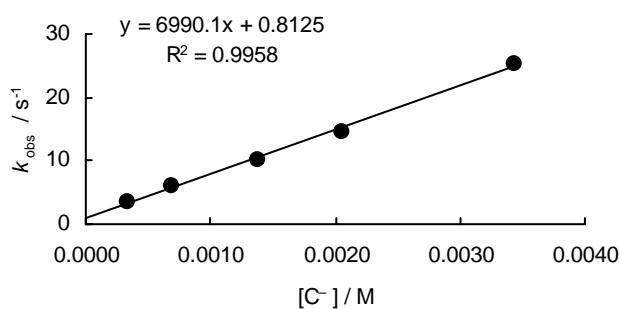


Table S5: Kinetics of the reaction of **1b** with ethanolamine **5c** in DMSO at 20 °C (stopped-flow UV-Vis spectrometer, decrease at $\lambda = 450$ nm).

Nr.	$[E]_0 / M$	$[Nu^-]_0 / M$	$k_{obs.} / s^{-1}$
261-1	2.78×10^{-5}	5.68×10^{-4}	1.59×10^1
261-2	2.78×10^{-5}	1.14×10^{-3}	3.30×10^1
261-3	2.78×10^{-5}	1.70×10^{-3}	4.70×10^1
261-4	2.78×10^{-5}	2.27×10^{-3}	6.29×10^1
261-5	2.78×10^{-5}	2.84×10^{-3}	7.84×10^1

$$k_1 = 2.73 \times 10^4 \text{ L mol}^{-1} \text{ s}^{-1}$$

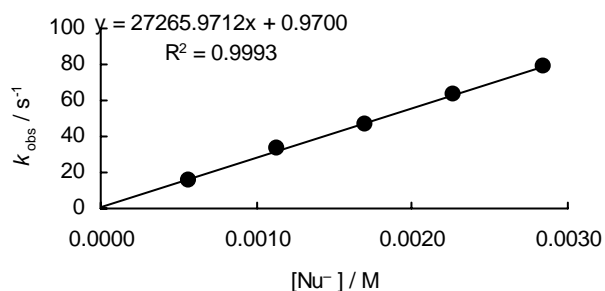
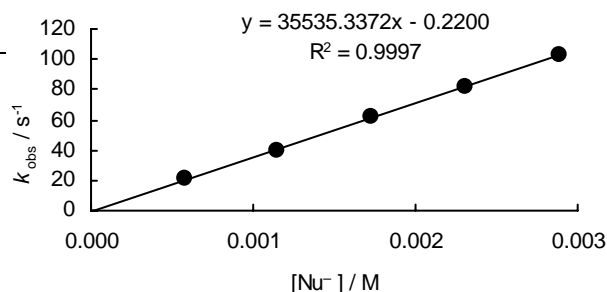


Table S6: Kinetics of the reaction of **1b** with n-propylamine **5d** in DMSO at 20 °C (stopped-flow UV-Vis spectrometer, decrease at $\lambda = 450$ nm).

Nr.	$[E]_0 / M$	$[Nu^-]_0 / M$	$k_{obs.} / s^{-1}$
254-1	2.30×10^{-5}	5.77×10^{-4}	2.08×10^1
254-2	2.30×10^{-5}	1.15×10^{-3}	3.99×10^1
254-3	2.30×10^{-5}	1.73×10^{-3}	6.14×10^1
254-4	2.30×10^{-5}	2.31×10^{-3}	8.21×10^1
254-5	2.30×10^{-5}	2.88×10^{-3}	1.02×10^2

$$k_1 = 3.55 \times 10^4 \text{ L mol}^{-1} \text{ s}^{-1}$$



Reactions of electrophile **1c**

Table S7: Kinetics of the reaction of **1c** with the anion of acetylacetone **4f** in DMSO at 20 °C (stopped-flow UV-Vis spectrometer, decrease at $\lambda = 593$ nm).

Nr.	$[E]_0 / M$	$[Nu^-]_0 / M$	$k_{obs.} / s^{-1}$
223-1	1.65×10^{-5}	1.84×10^{-4}	4.50×10^1
223-2	1.65×10^{-5}	4.04×10^{-4}	9.85×10^1
223-3	1.65×10^{-5}	6.62×10^{-4}	1.59×10^1
223-4	1.65×10^{-5}	1.10×10^{-3}	2.55×10^1
223-5	1.65×10^{-5}	1.65×10^{-3}	3.68×10^2

$$k_1 = 2.19 \times 10^5 \text{ L mol}^{-1} \text{ s}^{-1}$$

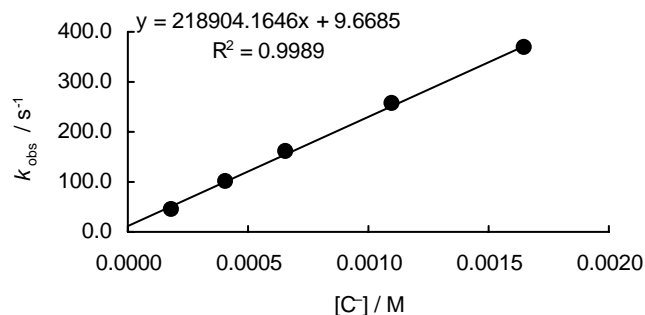


Table S8: Kinetics of the reaction of **1c** with the anion of dimedone **4g** in DMSO at 20 °C (stopped-flow UV-Vis spectrometer, decrease at $\lambda = 470$ nm).

Nr.	$[E]_0 / M$	$[Nu^-]_0 / M$	$k_{obs.} / s^{-1}$
233-1	1.57×10^{-5}	1.52×10^{-4}	1.18×10^1
233-2	1.57×10^{-5}	3.04×10^{-4}	2.36×10^1
233-3	1.57×10^{-5}	6.07×10^{-4}	4.50×10^1
233-4	1.57×10^{-5}	1.21×10^{-3}	8.64×10^1
233-5	1.57×10^{-5}	1.52×10^{-3}	1.06×10^2

$$k_1 = 6.87 \times 10^4 \text{ L mol}^{-1} \text{ s}^{-1}$$

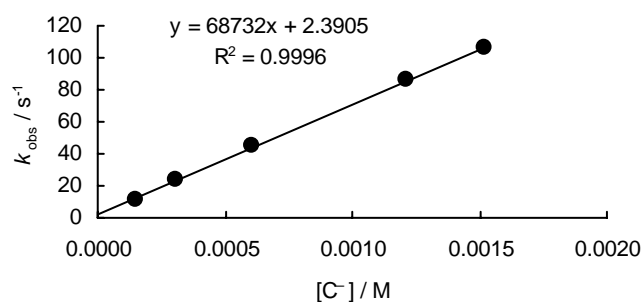


Table S9a: Kinetics of the reaction of **1c** with the anion of dimedone **4g** in DMSO at 20 °C (stopped-flow UV-Vis spectrometer, decrease at $\lambda = 483$ nm).

Nr.	[E] ₀ / M	[Nu ⁻] ₀ / M	<i>k</i> _{obs.} / s ⁻¹
229-1	1.88×10^{-5}	2.07×10^{-4}	1.49×10^1
229-2	1.88×10^{-5}	4.14×10^{-4}	2.92×10^1
229-3	1.88×10^{-5}	8.27×10^{-4}	5.69×10^1
229-4	1.88×10^{-5}	1.45×10^{-3}	9.55×10^1
229-5	1.88×10^{-5}	2.07×10^{-3}	1.34×10^2

$$k_1 = 6.38 \times 10^4 \text{ L mol}^{-1} \text{ s}^{-1}$$

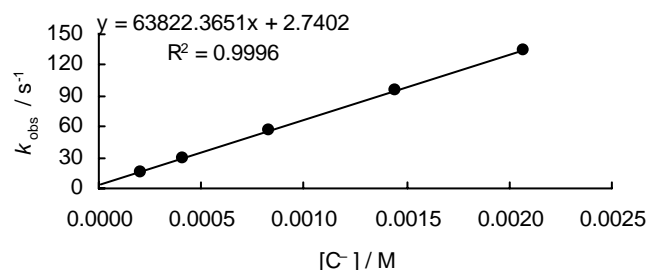


Table S9b: Kinetics of the reaction of **1c** with the anion of dimedone **4g** in DMSO at 20 °C (stopped-flow UV-Vis spectrometer, increase at $\lambda = 570$ nm).

Nr.	[E] ₀ / M	[Nu ⁻] ₀ / M	<i>k</i> _{obs.} / s ⁻¹
229-1	1.88×10^{-5}	2.07×10^{-4}	1.07×10^{-1}
229-2	1.88×10^{-5}	4.14×10^{-4}	1.56×10^{-1}
229-4	1.88×10^{-5}	1.45×10^{-3}	4.07×10^{-1}
229-5	1.88×10^{-5}	2.07×10^{-3}	5.29×10^{-1}

$$k_1 = 2.30 \times 10^2 \text{ L mol}^{-1} \text{ s}^{-1}$$

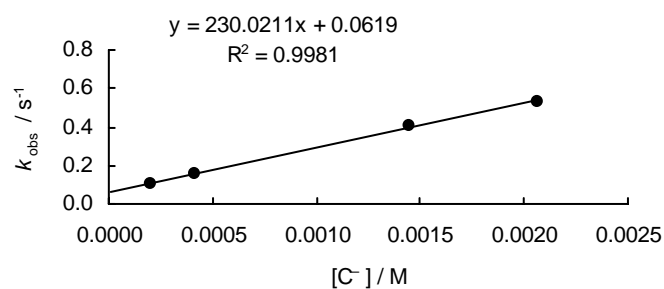


Table S10: Kinetics of the reaction of **1c** with the anion of Meldrum's acid **4h** in DMSO at 20 °C (stopped-flow UV-Vis spectrometer, decrease at $\lambda = 582$ nm).

Nr.	[E] ₀ / M	[Nu ⁻] ₀ / M	<i>k</i> _{obs.} / s ⁻¹
239-1	1.89×10^{-5}	3.44×10^{-4}	1.25×10^{-1}
239-2	1.89×10^{-5}	6.87×10^{-4}	2.44×10^{-1}
239-3	1.89×10^{-5}	1.38×10^{-3}	4.78×10^{-1}
239-4	1.89×10^{-5}	2.06×10^{-3}	7.30×10^{-1}
239-5	1.89×10^{-5}	3.44×10^{-3}	1.24

$$k_1 = 3.59 \times 10^2 \text{ L mol}^{-1} \text{ s}^{-1}$$

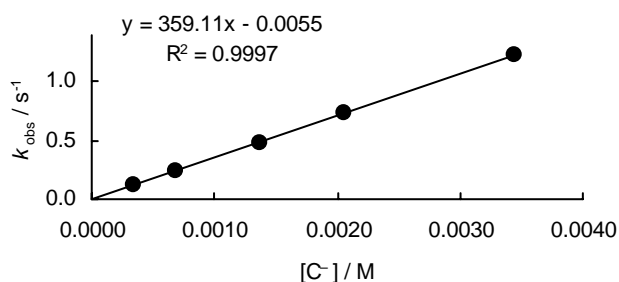
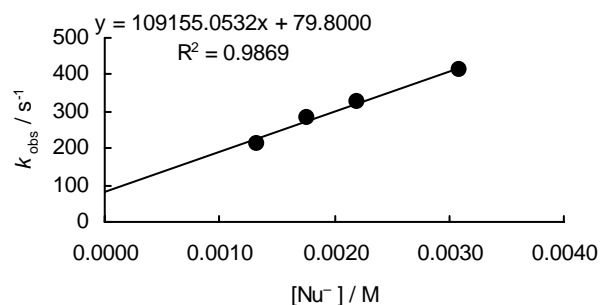


Table S11: Kinetics of the reaction of **1c** with piperidine **5a** in DMSO at 20 °C (stopped-flow UV-Vis spectrometer, decrease at $\lambda = 583$ nm).

Nr.	$[E]_0 / M$	$[Nu^-]_0 / M$	$k_{obs.} / s^{-1}$
259-1	2.34×10^{-5}	3.09×10^{-4}	2.14×10^2
259-3	2.34×10^{-5}	1.33×10^{-4}	2.83×10^2
259-4	2.34×10^{-5}	1.77×10^{-3}	3.12×10^2
239-5	2.34×10^{-5}	2.21×10^{-3}	4.12×10^2

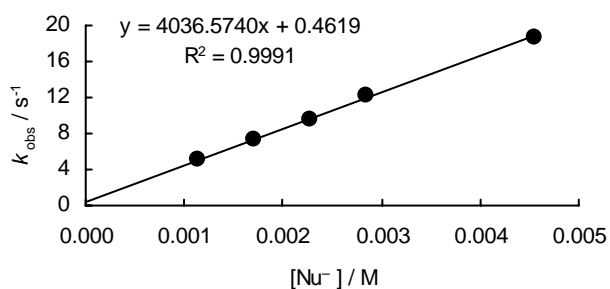
$$k_1 = 1.09 \times 10^5 \text{ L mol}^{-1} \text{ s}^{-1}$$

$$k_- = 8.0 \times 10^1 \text{ s}^{-1}, K = 1.4 \times 10^3 \text{ L mol}^{-1}$$

**Table S12:** Kinetics of the reaction of **1c** with ethanolamine **5c** in DMSO at 20 °C (stopped-flow UV-Vis spectrometer, decrease at $\lambda = 583$ nm).

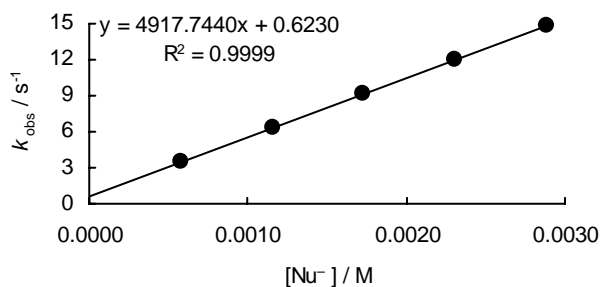
Nr.	$[E]_0 / M$	$[Nu^-]_0 / M$	$k_{obs.} / s^{-1}$
262-2	1.55×10^{-5}	1.14×10^{-3}	5.03
262-3	1.55×10^{-5}	1.70×10^{-3}	7.30
262-4	1.55×10^{-5}	2.27×10^{-3}	9.51
262-5	1.55×10^{-5}	2.84×10^{-3}	1.22×10^1
262-1	1.55×10^{-5}	4.55×10^{-3}	1.87×10^1

$$k_1 = 4.04 \times 10^3 \text{ L mol}^{-1} \text{ s}^{-1}$$

**Table S13:** Kinetics of the reaction of **1c** with n-propylamine **5d** in DMSO at 20 °C (stopped-flow UV-Vis spectrometer, decrease at $\lambda = 583$ nm).

Nr.	$[E]_0 / M$	$[Nu^-]_0 / M$	$k_{obs.} / s^{-1}$
253-1	2.34×10^{-5}	5.77×10^{-4}	3.45
253-2	2.34×10^{-5}	1.15×10^{-3}	6.33
253-3	2.34×10^{-5}	1.73×10^{-3}	9.09
253-4	2.34×10^{-5}	2.31×10^{-3}	1.20×10^1
253-5	2.34×10^{-5}	2.88×10^{-3}	1.48×10^1

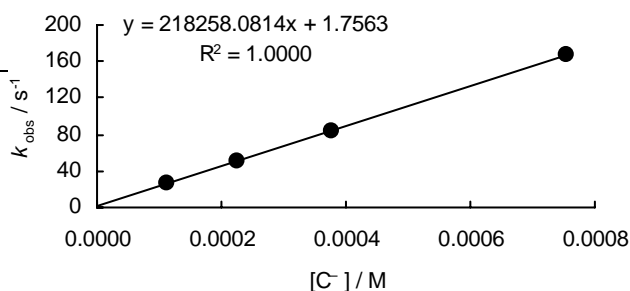
$$k_1 = 4.92 \times 10^3 \text{ L mol}^{-1} \text{ s}^{-1}$$



Reactions of electrophile **2a****Table S14:** Kinetics of the reaction of **2a** with the anion of acetylacetone **4f** in DMSO at 20 °C (stopped-flow UV-Vis spectrometer, decrease at $\lambda = 375$ nm).

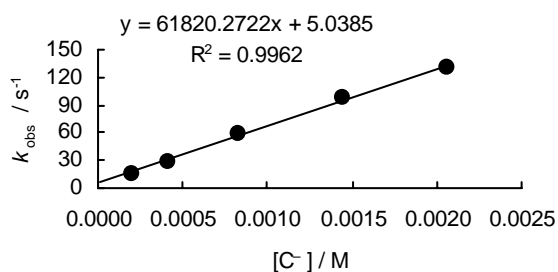
Nr.	[E] ₀ / M	[Nu ⁻] ₀ / M	<i>k</i> _{obs.} / s ⁻¹
237-1	1.04×10^{-5}	1.13×10^{-4}	2.67×10^1
237-2	1.04×10^{-5}	2.27×10^{-4}	5.10×10^1
237-3	1.04×10^{-5}	3.78×10^{-4}	8.41×10^1
237-5	1.04×10^{-5}	7.55×10^{-4}	1.67×10^2

$$k_1 = 2.18 \times 10^5 \text{ L mol}^{-1} \text{ s}^{-1}$$

**Table S15:** Kinetics of the reaction of **2a** with the anion of dimedone **4g** in DMSO at 20 °C (stopped-flow UV-Vis spectrometer, decrease at $\lambda = 375$ nm).

Nr.	[E] ₀ / M	[Nu ⁻] ₀ / M	<i>k</i> _{obs.} / s ⁻¹
231-1	1.84×10^{-5}	2.07×10^{-4}	1.62×10^1
231-2	1.84×10^{-5}	4.14×10^{-4}	2.93×10^1
231-3	1.84×10^{-5}	8.27×10^{-4}	5.84×10^1
231-4	1.84×10^{-5}	1.45×10^{-3}	9.84×10^1
231-5	1.84×10^{-5}	2.07×10^{-3}	1.30×10^2

$$k_2 = 6.18 \times 10^4 \text{ L mol}^{-1} \text{ s}^{-1}$$

**Table S16:** Kinetics of the reaction of **2a** with the anion of Meldrum's acid **4h** in DMSO at 20 °C (J&M, decrease at $\lambda = 375$ nm).

Nr.	[E] ₀ / M	[Nu ⁻] ₀ / M	<i>k</i> _{obs.} / s ⁻¹
240-1	3.73×10^{-5}	3.95×10^{-4}	2.48×10^{-2}
240-2	3.73×10^{-5}	1.07×10^{-3}	3.95×10^{-2}
240-3	3.73×10^{-5}	1.87×10^{-3}	5.87×10^{-2}
240-4	3.73×10^{-5}	2.50×10^{-3}	7.29×10^{-2}

$$k_1 = 2.3 \times 10^1 \text{ L mol}^{-1} \text{ s}^{-1}$$

$$k_- = 1.5 \times 10^{-2} \text{ s}^{-1}, K = 1.5 \times 10^3 \text{ L mol}^{-1}$$

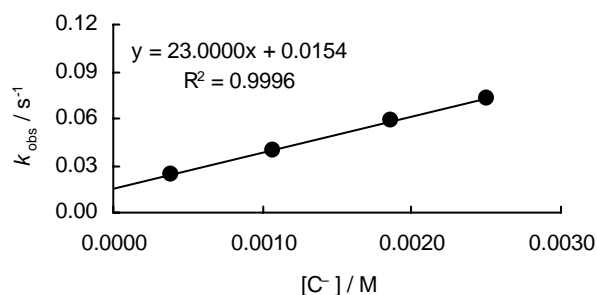
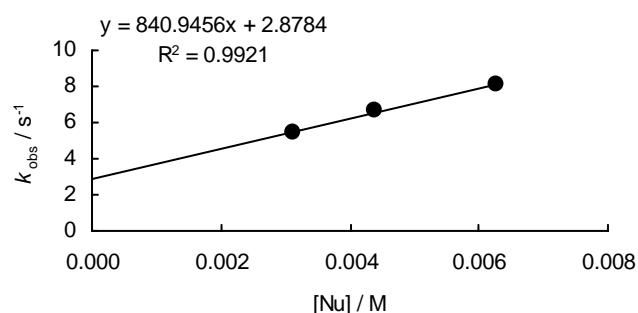


Table S17: Kinetics of the reaction of **2a** with morpholine **5b** in DMSO at 20 °C (stopped-flow UV-Vis spectrometer, decrease at $\lambda = 375$ nm).

Nr.	[E] ₀ / M	[Nu ⁻] ₀ / M	<i>k</i> _{obs.} / s ⁻¹
252-3	3.04×10^{-5}	3.13×10^{-4}	5.43
252-4	3.04×10^{-5}	4.38×10^{-3}	6.70
252-5	3.04×10^{-5}	6.26×10^{-3}	8.09

$$k_1 = 8.41 \times 10^2 \text{ L mol}^{-1} \text{ s}^{-1}$$

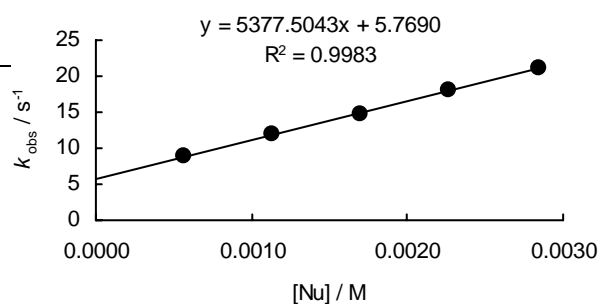
$$k_- = 2.9 \text{ s}^{-1}, K = 2.9 \times 10^2 \text{ L mol}^{-1}$$

**Table S18:** Kinetics of the reaction of **2a** with ethanolamine **5c** in DMSO at 20 °C (stopped-flow UV-Vis spectrometer, decrease at $\lambda = 374$ nm).

Nr.	[E] ₀ / M	[Nu ⁻] ₀ / M	<i>k</i> _{obs.} / s ⁻¹
265-1	1.89×10^{-5}	5.68×10^{-4}	9.00
265-2	1.89×10^{-5}	1.14×10^{-3}	1.19×10^1
265-3	1.89×10^{-5}	1.70×10^{-3}	1.46×10^1
265-4	1.89×10^{-5}	2.27×10^{-3}	1.80×10^1
265-5	1.89×10^{-5}	2.84×10^{-3}	2.12×10^1

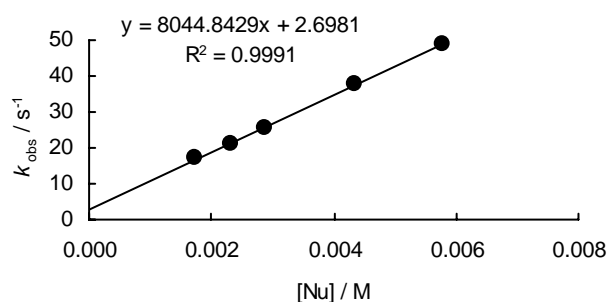
$$k_1 = 5.38 \times 10^3 \text{ L mol}^{-1} \text{ s}^{-1}$$

$$k_- = 5.8 \text{ s}^{-1}, K = 9.3 \times 10^2 \text{ L mol}^{-1}$$

**Table S19:** Kinetics of the reaction of **2a** with n-propylamine **5d** in DMSO at 20 °C (stopped-flow UV-Vis spectrometer, decrease at $\lambda = 375$ nm).

Nr.	[E] ₀ / M	[Nu ⁻] ₀ / M	<i>k</i> _{obs.} / s ⁻¹
256-3	3.40×10^{-5}	1.73×10^{-3}	1.70×10^1
256-2	3.40×10^{-5}	2.31×10^{-3}	2.12×10^1
256-1	3.40×10^{-5}	2.88×10^{-3}	2.53×10^1
256-4	3.40×10^{-5}	4.33×10^{-3}	3.78×10^1
256-5	3.40×10^{-5}	4.91×10^{-3}	4.91×10^1

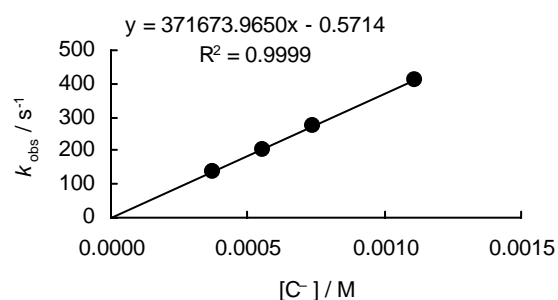
$$k_1 = 8.04 \times 10^3 \text{ L mol}^{-1} \text{ s}^{-1}$$



Reactions of electrophile **2b****Table S20:** Kinetics of the reaction of **2b** with the anion of ethyl aceto acetate **4d** in DMSO at 20 °C (stopped-flow UV-Vis spectrometer, decrease at $\lambda = 416$ nm).

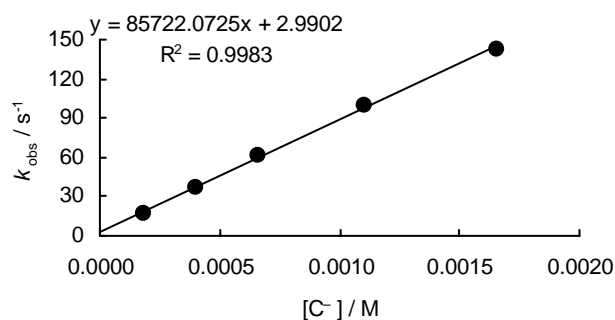
Nr.	[E] ₀ / M	[Nu ⁻] ₀ / M	<i>k</i> _{obs.} / s ⁻¹
250-1	3.60×10^{-5}	3.70×10^{-4}	1.37×10^2
250-4	3.60×10^{-5}	5.54×10^{-4}	2.04×10^2
250-3	3.60×10^{-5}	7.39×10^{-4}	2.76×10^2
250-2	3.60×10^{-5}	1.11×10^{-3}	4.11×10^2

$$k_1 = 3.72 \times 10^5 \text{ L mol}^{-1} \text{ s}^{-1}$$

**Table S21:** Kinetics of the reaction of **2b** with the anion of acetylacetone **4f** in DMSO at 20 °C (stopped-flow UV-Vis spectrometer, decrease at $\lambda = 412$ nm).

Nr.	[E] ₀ / M	[Nu ⁻] ₀ / M	<i>k</i> _{obs.} / s ⁻¹
224-1	1.55×10^{-5}	1.84×10^{-4}	1.68×10^1
224-2	1.55×10^{-5}	4.04×10^{-4}	3.72×10^1
224-3	1.55×10^{-5}	6.62×10^{-4}	6.19×10^1
224-4	1.55×10^{-5}	1.10×10^{-3}	9.97×10^1
224-5	1.55×10^{-5}	1.65×10^{-3}	1.43×10^2

$$k_1 = 8.57 \times 10^4 \text{ L mol}^{-1} \text{ s}^{-1}$$

**Table S22:** Kinetics of the reaction of **2b** with the anion of dimedone **4g** in DMSO at 20 °C (stopped-flow UV-Vis spectrometer, decrease at $\lambda = 418$ nm).

Nr.	[E] ₀ / M	[Nu ⁻] ₀ / M	<i>k</i> _{obs.} / s ⁻¹
235-1	2.00×10^{-5}	2.99×10^{-4}	7.53
235-2	2.00×10^{-5}	5.98×10^{-4}	1.36×10^1
235-3	2.00×10^{-5}	1.20×10^{-4}	2.70×10^1
235-4	2.00×10^{-5}	1.79×10^{-3}	4.02×10^1
235-5	2.00×10^{-5}	2.39×10^{-3}	5.27×10^2

$$k_1 = 2.17 \times 10^4 \text{ L mol}^{-1} \text{ s}^{-1}$$

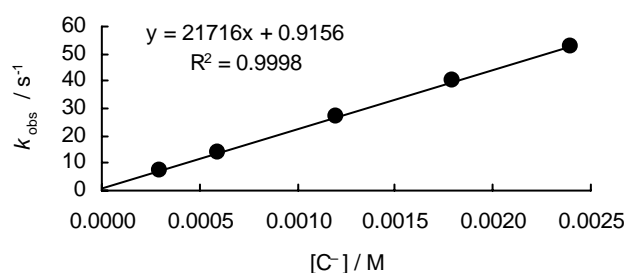


Table S23: Kinetics of the reaction of **2b** with the anion of Meldrum's acid **4h** in DMSO at 20 °C (J&M, decrease at $\lambda = 418$ nm).

Nr.	$[E]_0 / M$	$[Nu^-]_0 / M$	$k_{obs.} / s^{-1}$
243-1	3.66×10^{-5}	5.59×10^{-4}	2.14×10^{-2}
243-2	3.66×10^{-5}	1.06×10^{-3}	2.57×10^{-2}
243-3	3.66×10^{-5}	1.86×10^{-3}	3.57×10^{-2}
243-4	3.66×10^{-5}	2.54×10^{-3}	4.01×10^{-2}
243-5	3.66×10^{-5}	3.31×10^{-3}	4.94×10^{-2}

$$k_1 = 1.01 \times 10^1 L mol^{-1} s^{-1}$$

$$k_- = 1.6 \times 10^{-2} s^{-1}, K = 6.5 \times 10^2 L mol^{-1}$$

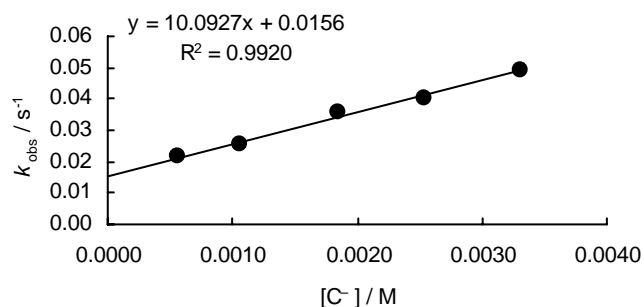


Table S24: Kinetics of the reaction of **2b** with morpholine **5b** in DMSO at 20 °C (stopped-flow UV-Vis spectrometer, decrease at $\lambda = 416$ nm).

Nr.	$[E]_0 / M$	$[Nu^-]_0 / M$	$k_{obs.} / s^{-1}$
251-2	3.60×10^{-5}	1.57×10^{-3}	4.65
251-3	3.60×10^{-5}	3.13×10^{-3}	5.93
251-4	3.60×10^{-5}	4.70×10^{-3}	7.31
251-5	3.60×10^{-5}	6.26×10^{-3}	8.52

$$k_1 = 8.30 \times 10^2 L mol^{-1} s^{-1}$$

$$k_- = 3.6 s^{-1}, K = 2.5 \times 10^2 L mol^{-1}$$

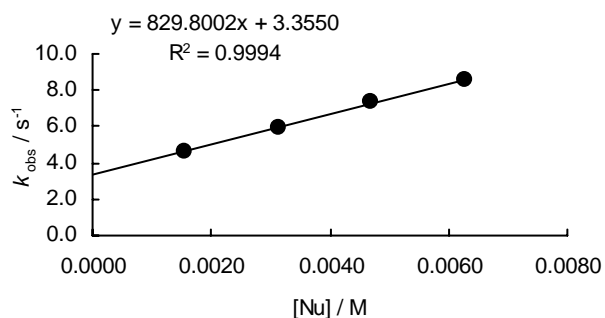


Table S25: Kinetics of the reaction of **2b** with ethanolamine **5c** in DMSO at 20 °C
(stopped-flow UV-Vis spectrometer, decrease at $\lambda = 416$ nm).

Nr.	$[E]_0 / M$	$[Nu^-]_0 / M$	$k_{obs.} / s^{-1}$
262-3	3.13×10^{-5}	1.70×10^{-3}	1.33×10^1
262-4	3.13×10^{-5}	2.27×10^{-3}	1.44×10^1
262-5	3.13×10^{-5}	2.84×10^{-3}	1.65×10^1
262-7	3.13×10^{-5}	3.41×10^{-3}	1.80×10^1
262-6	3.13×10^{-5}	3.98×10^{-3}	1.96×10^1

$$k_1 = 2.85 \times 10^3 \text{ L mol}^{-1} \text{ s}^{-1}$$

$$k_- = 8.3 \text{ s}^{-1}, K = 3.4 \times 10^2 \text{ L mol}^{-1}$$

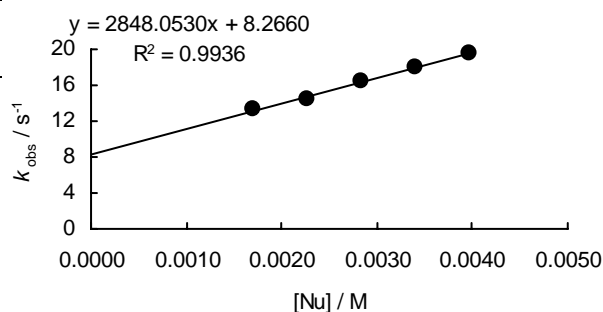
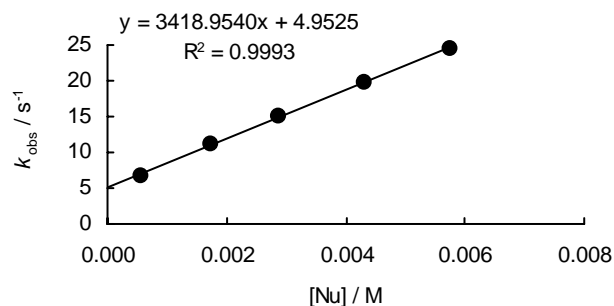


Table S26: Kinetics of the reaction of **2b** with n-propylamine **5d** in DMSO at 20 °C
(stopped-flow UV-Vis spectrometer, decrease at $\lambda = 416$ nm).

Nr.	$[E]_0 / M$	$[Nu^-]_0 / M$	$k_{obs.} / s^{-1}$
255-3	3.60×10^{-5}	5.77×10^{-4}	6.68
255-4	3.60×10^{-5}	1.73×10^{-3}	1.11×10^1
255-5	3.60×10^{-5}	2.88×10^{-3}	1.49×10^1
255-7	3.60×10^{-5}	4.33×10^{-3}	1.98×10^1
255-6	3.60×10^{-5}	5.77×10^{-3}	2.54×10^1

$$k_1 = 3.42 \times 10^3 \text{ L mol}^{-1} \text{ s}^{-1}$$

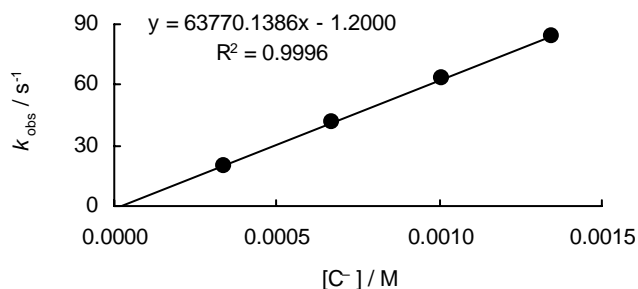
$$k_- = 5.0 \text{ s}^{-1}, K = 6.9 \times 10^2 \text{ L mol}^{-1}$$



Reactions of electrophile **2c****Table S27:** Kinetics of the reaction of **2c** with the anion of ethyl cyano acetate **4b** in DMSO at 20 °C (stopped-flow UV-Vis spectrometer, decrease at $\lambda = 535$ nm).

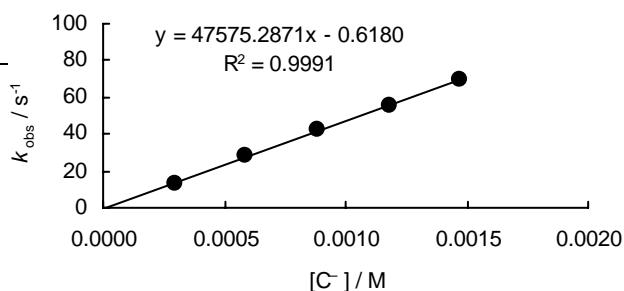
Nr.	[E] ₀ / M	[Nu ⁻] ₀ / M	<i>k</i> _{obs.} / s ⁻¹
247-1	1.44×10^{-5}	3.36×10^{-4}	1.98×10^1
247-2	1.44×10^{-5}	6.72×10^{-3}	4.20×10^1
247-3	1.44×10^{-5}	1.01×10^{-3}	6.50×10^1
247-4	1.44×10^{-5}	1.34×10^{-3}	8.40×10^1

$$k_1 = 6.38 \times 10^4 \text{ L mol}^{-1} \text{ s}^{-1}$$

**Table S28:** Kinetics of the reaction of **2c** with the anion of ethyl aceto acetate **4d** in DMSO at 20 °C (stopped-flow UV-Vis spectrometer, decrease at $\lambda = 535$ nm).

Nr.	[E] ₀ / M	[Nu ⁻] ₀ / M	<i>k</i> _{obs.} / s ⁻¹
248-1	1.44×10^{-5}	2.95×10^{-4}	1.26×10^1
248-2	1.44×10^{-5}	5.90×10^{-4}	2.82×10^1
248-3	1.44×10^{-5}	8.84×10^{-4}	4.21×10^1
248-4	1.44×10^{-5}	1.18×10^{-3}	5.52×10^1
248-5	1.44×10^{-5}	1.47×10^{-3}	6.92×10^1

$$k_1 = 4.76 \times 10^4 \text{ L mol}^{-1} \text{ s}^{-1}$$

**Table S29:** Kinetics of the reaction of **2c** with the anion of 2-methyl acetylacetone **4e** in DMSO at 20 °C (stopped-flow UV-Vis spectrometer, decrease at $\lambda = 535$ nm).

Nr.	[E] ₀ / M	[Nu ⁻] ₀ / M	<i>k</i> _{obs.} / s ⁻¹
249-1	1.44×10^{-5}	3.26×10^{-4}	9.65
249-2	1.44×10^{-5}	6.53×10^{-4}	2.59×10^1
249-3	1.44×10^{-5}	9.79×10^{-4}	4.02×10^1
249-4	1.44×10^{-5}	1.47×10^{-3}	6.12×10^1
249-5	1.44×10^{-5}	1.80×10^{-3}	7.47×10^1

$$k_1 = 4.40 \times 10^4 \text{ L mol}^{-1} \text{ s}^{-1}$$

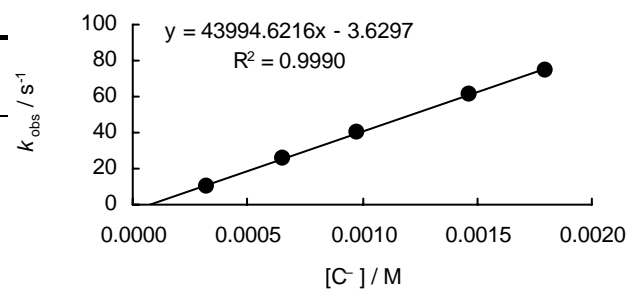
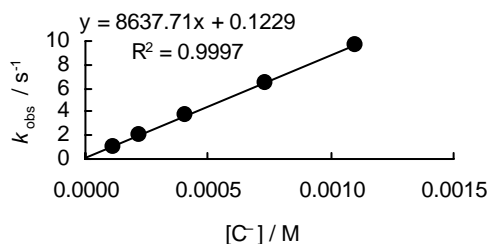


Table S30: Kinetics of the reaction of **2c** with the anion of acetylacetonate **4f** in DMSO at 20 °C (stopped-flow UV-Vis spectrometer, decrease at $\lambda = 535$ nm).

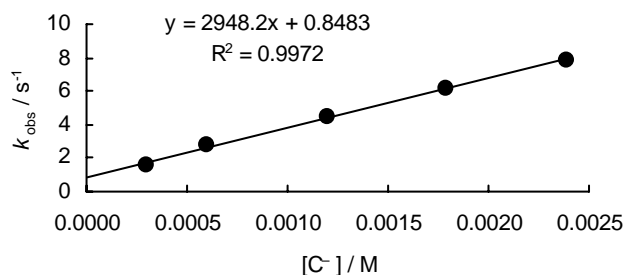
Nr.	$[E]_0 / M$	$[Nu^-]_0 / M$	$k_{obs.} / s^{-1}$
222-1	1.37×10^{-5}	1.10×10^{-4}	1.01
222-2	1.37×10^{-5}	2.21×10^{-4}	2.02
222-3	1.37×10^{-5}	4.04×10^{-4}	3.70
222-4	1.37×10^{-5}	7.35×10^{-4}	6.51
222-5	1.37×10^{-5}	1.10×10^{-3}	9.60

$$k_1 = 8.64 \times 10^3 \text{ L mol}^{-1} \text{ s}^{-1}$$

**Table S31:** Kinetics of the reaction of **2c** with the anion of dimedone **4g** in DMSO at 20 °C (stopped-flow UV-Vis spectrometer, decrease at $\lambda = 535$ nm).

Nr.	$[E]_0 / M$	$[Nu^-]_0 / M$	$k_{obs.} / s^{-1}$
235-1	1.58×10^{-5}	2.99×10^{-4}	1.54
235-2	1.58×10^{-5}	5.98×10^{-4}	2.77
235-3	1.58×10^{-5}	1.20×10^{-3}	4.45
235-4	1.58×10^{-5}	1.79×10^{-4}	6.16
235-5	1.58×10^{-5}	2.39×10^{-3}	7.83

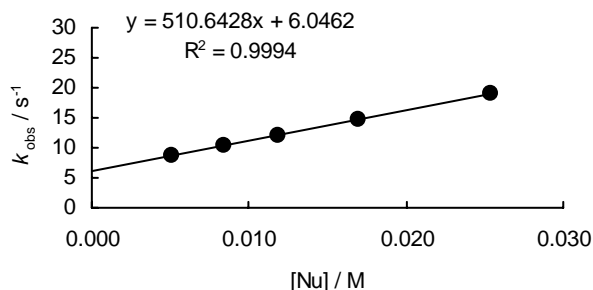
$$k_1 = 2.95 \times 10^3 \text{ L mol}^{-1} \text{ s}^{-1}$$

**Table S32:** Kinetics of the reaction of **2c** with n-propylamine **5d** in DMSO at 20 °C (stopped-flow UV-Vis spectrometer, decrease at $\lambda = 535$ nm).

Nr.	$[E]_0 / M$	$[Nu^-]_0 / M$	$k_{obs.} / s^{-1}$
257-1	2.94×10^{-5}	5.09×10^{-3}	8.79
257-2	2.94×10^{-5}	8.48×10^{-3}	1.03×10^1
257-3	2.94×10^{-5}	1.19×10^{-2}	1.20×10^1
257-4	2.94×10^{-5}	1.70×10^{-2}	1.47×10^1
257-5	2.94×10^{-5}	2.54×10^{-2}	1.91×10^1

$$k_1 = 5.10 \times 10^2 \text{ L mol}^{-1} \text{ s}^{-1}$$

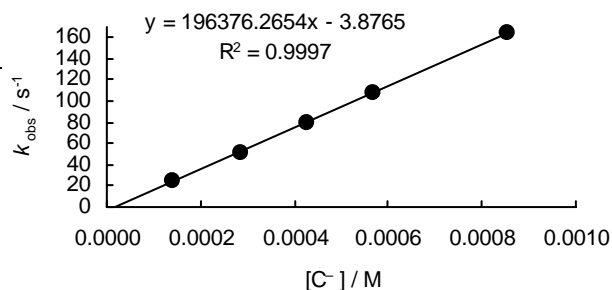
$$k_- = 6.0 \text{ s}^{-1}, K = 8.4 \times 10^1 \text{ L mol}^{-1}$$



Reactions of electrophile **3a****Table S33:** Kinetics of the reaction of **3a** with the anion of ethyl cyano acetate **4b** in DMSO at 20 °C (stopped-flow UV-Vis spectrometer, decrease at $\lambda = 374$ nm).

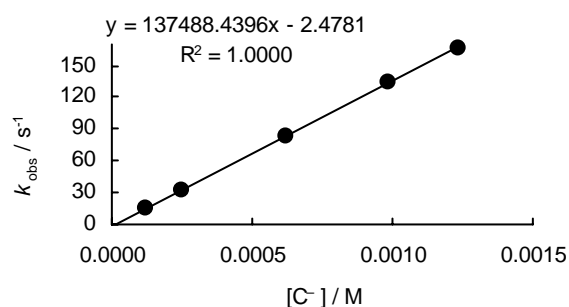
Nr.	$[E]_0 / M$	$[Nu^-]_0 / M$	$k_{obs.} / s^{-1}$
M03-04-4	2.97×10^{-5}	1.42×10^{-4}	2.53×10^1
M03-04-2	2.97×10^{-5}	2.84×10^{-4}	5.07×10^1
M03-04-5	2.97×10^{-5}	4.27×10^{-4}	7.94×10^1
M03-04-1	2.97×10^{-5}	5.69×10^{-4}	1.08×10^2
M03-04-3	2.97×10^{-5}	8.53×10^{-4}	1.64×10^2

$$k_1 = 1.96 \times 10^5 \text{ L mol}^{-1} \text{ s}^{-1}$$

**Table S34:** Kinetics of the reaction of **3a** with the anion of ethyl aceto acetate **4d** in DMSO at 20 °C (stopped-flow UV-Vis spectrometer, decrease at $\lambda = 374$ nm).

Nr.	$[E]_0 / M$	$[Nu^-]_0 / M$	$k_{obs.} / s^{-1}$
M03-03-4	2.83×10^{-5}	1.24×10^{-4}	1.42×10^1
M03-03-3	2.83×10^{-5}	2.47×10^{-4}	3.16×10^1
M03-03-5	2.83×10^{-5}	6.18×10^{-4}	8.28×10^1
M03-03-2	2.83×10^{-5}	9.89×10^{-4}	1.34×10^2
M03-03-1	2.83×10^{-5}	1.24×10^{-3}	1.67×10^2

$$k_1 = 1.37 \times 10^5 \text{ L mol}^{-1} \text{ s}^{-1}$$

**Table S35:** Kinetics of the reaction of **3a** with the anion of acetylacetone **4f** in DMSO at 20 °C (stopped-flow UV-Vis spectrometer, decrease at $\lambda = 374$ nm).

Nr.	$[E]_0 / M$	$[Nu^-]_0 / M$	$k_{obs.} / s^{-1}$
M03-02-1	1.91×10^{-5}	3.15×10^{-4}	7.18
M03-02-2	1.91×10^{-5}	6.31×10^{-4}	1.48×10^1
M03-02-3	1.91×10^{-5}	9.46×10^{-4}	2.20×10^1
M03-03-4	1.91×10^{-5}	1.26×10^{-4}	2.91×10^2
M03-03-5	1.91×10^{-5}	1.58×10^{-3}	3.71×10^2

$$k_1 = 2.35 \times 10^4 \text{ L mol}^{-1} \text{ s}^{-1}$$

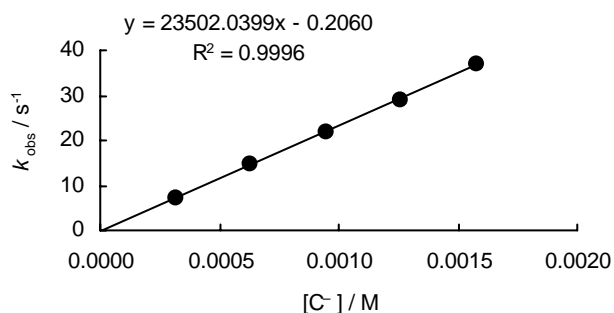
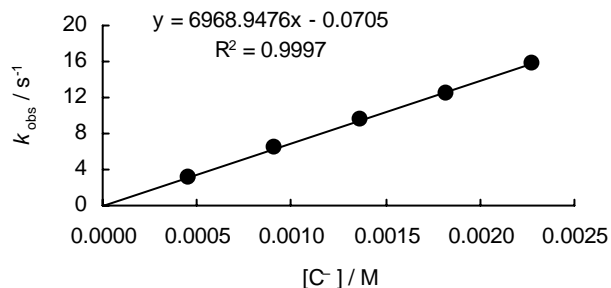


Table S36: Kinetics of the reaction of **3a** with the anion of dimedone **4g** in DMSO at 20 °C (stopped-flow UV-Vis spectrometer, decrease at $\lambda = 374$ nm).

Nr.	$[E]_0 / M$	$[Nu^-]_0 / M$	$k_{obs.} / s^{-1}$
M03-01-1	1.91×10^{-5}	4.55×10^{-4}	3.05
M03-01-2	1.91×10^{-5}	9.11×10^{-4}	6.36
M03-01-3	1.91×10^{-5}	1.37×10^{-3}	9.50
M03-01-4	1.91×10^{-5}	1.82×10^{-3}	1.25×10^1
M03-01-5	1.91×10^{-5}	2.28×10^{-3}	1.59×10^1

$k_1 = 6.97 \times 10^3 \text{ L mol}^{-1} \text{ s}^{-1}$



Reactions of electrophile **3b**

Table S37: Kinetics of the reaction of **3b** with the anion of ethyl cyano acetate **4b** in DMSO at 20 °C (stopped-flow UV-Vis spectrometer, decrease at $\lambda = 413$ nm).

Nr.	$[E]_0 / M$	$[Nu^-]_0 / M$	$k_{obs.} / s^{-1}$
M02-06-1	1.76×10^{-5}	3.00×10^{-4}	1.80×10^1
M02-06-2	1.76×10^{-5}	5.99×10^{-4}	3.77×10^1
M02-06-3	1.76×10^{-5}	8.99×10^{-4}	5.78×10^1
M02-06-4	1.76×10^{-5}	1.20×10^{-3}	7.80×10^1
M02-06-5	1.76×10^{-5}	1.45×10^{-3}	9.64×10^1

$k_1 = 6.58 \times 10^4 \text{ L mol}^{-1} \text{ s}^{-1}$

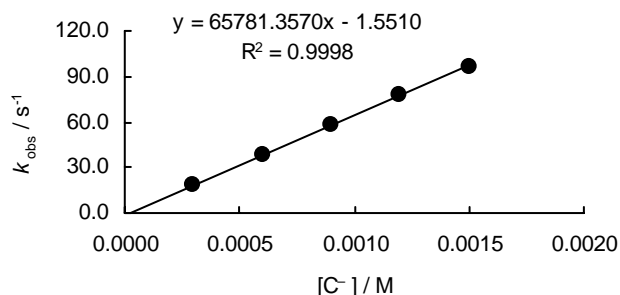


Table S38: Kinetics of the reaction of **3b** with the anion of malononitrile **4c** in DMSO at 20 °C (stopped-flow UV-Vis spectrometer, decrease at $\lambda = 413$ nm).

Nr.	$[E]_0 / M$	$[Nu^-]_0 / M$	$k_{obs.} / s^{-1}$
M02-05-1	1.76×10^{-5}	2.14×10^{-4}	1.09×10^1
M02-05-2	1.76×10^{-5}	4.28×10^{-4}	2.33×10^1
M02-05-3	1.76×10^{-5}	6.42×10^{-4}	3.48×10^1
M02-05-4	1.76×10^{-5}	4.56×10^{-4}	4.63×10^1
M02-05-5	1.76×10^{-5}	1.07×10^{-3}	5.81×10^1

$k_1 = 5.48 \times 10^4 \text{ L mol}^{-1} \text{ s}^{-1}$

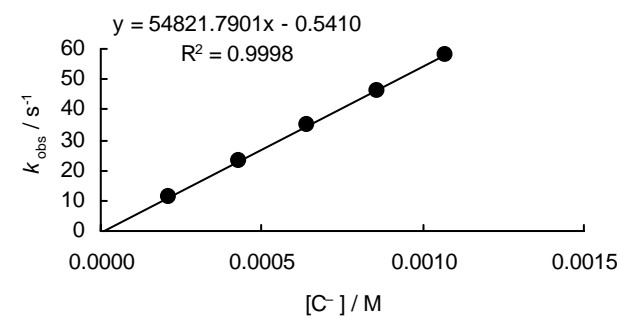
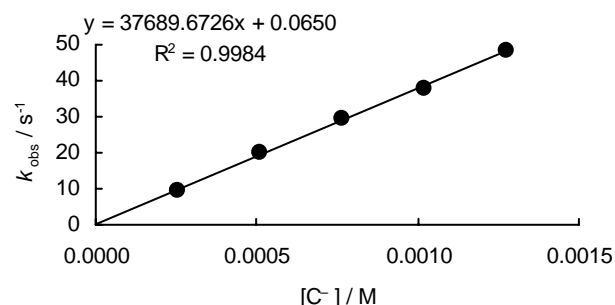


Table S39: Kinetics of the reaction of **3b** with the anion of ethyl aceto acetate **4d** in DMSO at 20 °C (stopped-flow UV-Vis spectrometer, decrease at $\lambda = 413$ nm).

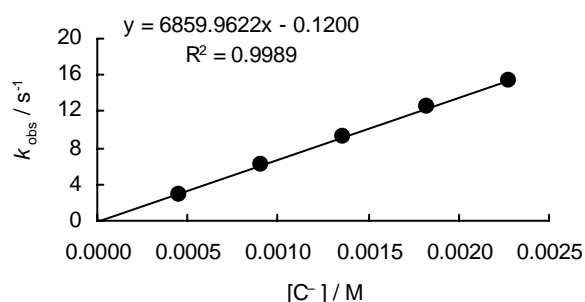
Nr.	$[E]_0 / M$	$[Nu^-]_0 / M$	$k_{obs.} / s^{-1}$
M02-03-1	2.64×10^{-5}	2.56×10^{-4}	9.35
M02-03-2	2.64×10^{-5}	5.11×10^{-4}	1.99×10^1
M02-03-3	2.64×10^{-5}	7.67×10^{-4}	2.93×10^1
M02-03-4	2.64×10^{-5}	1.02×10^{-3}	3.77×10^1
M02-03-5	2.64×10^{-5}	1.28×10^{-3}	4.86×10^1

$k_1 = 3.77 \times 10^4 \text{ L mol}^{-1} \text{ s}^{-1}$

**Table S40:** Kinetics of the reaction of **3b** with the anion of acetylacetone **4f** in DMSO at 20 °C (stopped-flow UV-Vis spectrometer, decrease at $\lambda = 413$ nm).

Nr.	$[E]_0 / M$	$[Nu^-]_0 / M$	$k_{obs.} / s^{-1}$
M02-01-1	2.64×10^{-5}	4.55×10^{-4}	2.86
M02-01-2	2.64×10^{-5}	9.10×10^{-4}	6.22
M02-01-3	2.64×10^{-5}	1.37×10^{-3}	9.29
M02-01-4	2.64×10^{-5}	1.82×10^{-3}	1.26×10^1
M02-01-5	2.64×10^{-5}	2.28×10^{-3}	1.50×10^1

$k_1 = 6.86 \times 10^3 \text{ L mol}^{-1} \text{ s}^{-1}$

**Table S41:** Kinetics of the reaction of **3b** with the anion of dimedone **4g** in DMSO at 20 °C (stopped-flow UV-Vis spectrometer, decrease at $\lambda = 413$ nm).

Nr.	$[E]_0 / M$	$[Nu^-]_0 / M$	$k_{obs.} / s^{-1}$
M02-02-1	2.64×10^{-5}	4.82×10^{-4}	8.75×10^{-1}
M02-02-2	2.64×10^{-5}	9.65×10^{-4}	1.82
M02-02-3	2.64×10^{-5}	1.45×10^{-3}	2.81
M02-02-4	2.64×10^{-5}	1.93×10^{-3}	3.66
M02-02-5	2.64×10^{-5}	2.41×10^{-3}	4.69

$k_1 = 1.96 \times 10^3 \text{ L mol}^{-1} \text{ s}^{-1}$

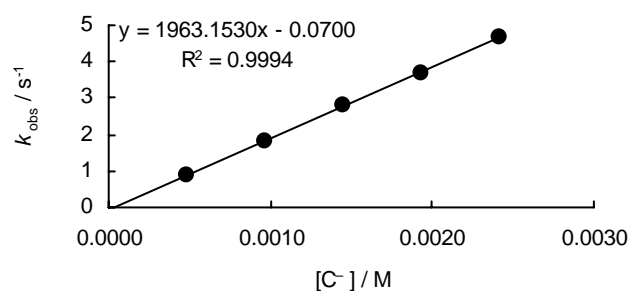
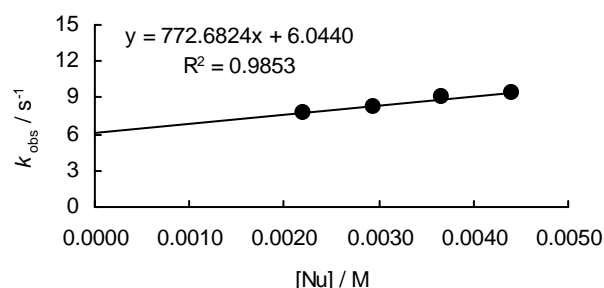


Table S42: Kinetics of the reaction of **3b** with ethanolamine **5c** in DMSO at 20 °C (stopped-flow UV-Vis spectrometer, decrease at $\lambda = 413$ nm).

Nr.	$[E]_0 / M$	$[Nu^-]_0 / M$	$k_{obs.} / s^{-1}$
M02-07-1	2.64×10^{-5}	2.21×10^{-4}	7.75
M02-07-2	2.64×10^{-5}	2.94×10^{-4}	8.25
M02-07-3	2.64×10^{-5}	3.68×10^{-3}	9.01
M02-07-4	2.64×10^{-5}	4.41×10^{-3}	9.39

$$k_1 = 7.72 \times 10^2 \text{ L mol}^{-1} \text{ s}^{-1}$$

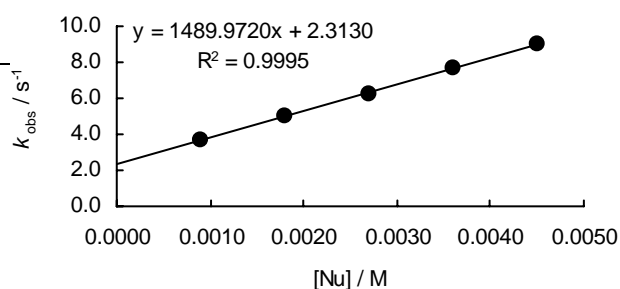
$$k_- = 6.0 \times 10^{-2} \text{ s}^{-1}, K = 1.3 \times 10^2 \text{ L mol}^{-1}$$

**Table S43:** Kinetics of the reaction of **3b** with n-propylamine **5d** in DMSO at 20 °C (stopped-flow UV-Vis spectrometer, decrease at $\lambda = 413$ nm).

Nr.	$[E]_0 / M$	$[Nu^-]_0 / M$	$k_{obs.} / s^{-1}$
M02-07-1	2.64×10^{-5}	9.00×10^{-4}	3.66
M02-07-2	2.64×10^{-5}	1.80×10^{-4}	5.04
M02-07-3	2.64×10^{-5}	2.70×10^{-4}	6.26
M02-07-4	2.64×10^{-5}	3.60×10^{-3}	7.67
M02-07-5	2.64×10^{-5}	4.50×10^{-3}	9.05

$$k_1 = 1.49 \times 10^3 \text{ L mol}^{-1} \text{ s}^{-1}$$

$$k_- = 2.3 \text{ s}^{-1}, K = 6.4 \times 10^2 \text{ L mol}^{-1}$$



Reactions of electrophile **3c**

Table S44: Kinetics of the reaction of **3c** with the anion of nitro ethane **4a** in DMSO at 20 °C (stopped-flow UV-Vis spectrometer, decrease at $\lambda = 521$ nm).

Nr.	$[E]_0 / M$	$[Nu^-]_0 / M$	$k_{obs.} / s^{-1}$
M01-06-1	1.14×10^{-5}	1.65×10^{-4}	1.00×10^1
M01-06-2	1.14×10^{-5}	3.30×10^{-4}	2.06×10^1
M01-06-3	1.14×10^{-5}	6.61×10^{-4}	4.44×10^1
M01-06-4	1.14×10^{-5}	9.91×10^{-4}	6.76×10^1
M01-06-5	1.14×10^{-5}	1.32×10^{-3}	8.99×10^1

$$k_1 = 6.96 \times 10^4 \text{ L mol}^{-1} \text{ s}^{-1}$$

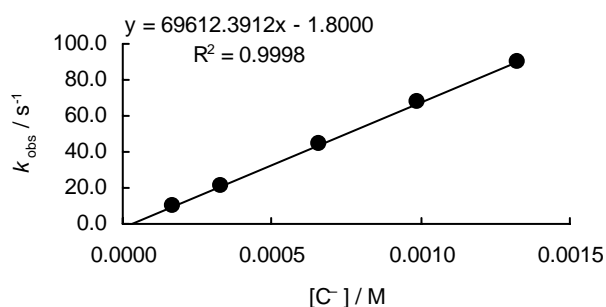
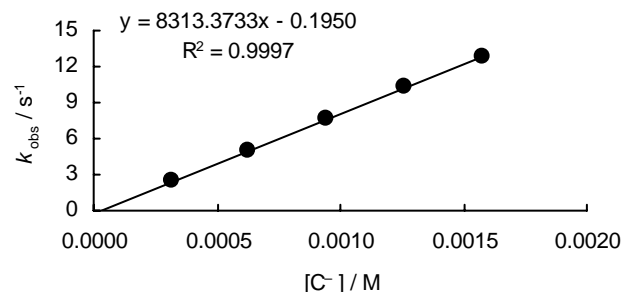


Table S45: Kinetics of the reaction of **3c** with the anion of ethyl cyano acetate **4b** in DMSO at 20 °C (stopped-flow UV-Vis spectrometer, decrease at $\lambda = 521$ nm).

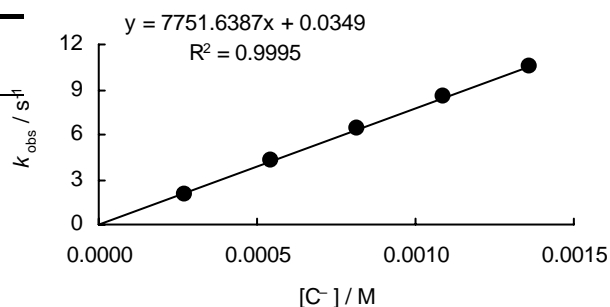
Nr.	$[E]_0 / M$	$[Nu^-]_0 / M$	$k_{obs.} / s^{-1}$
M01-04-1	1.14×10^{-5}	3.15×10^{-4}	2.45
M01-04-2	1.14×10^{-5}	6.30×10^{-4}	4.99
M01-04-3	1.14×10^{-5}	9.44×10^{-4}	7.63
M01-04-4	1.14×10^{-5}	1.26×10^{-3}	1.04×10^1
M01-04-5	1.14×10^{-5}	1.57×10^{-3}	1.28×10^1

$$k_1 = 8.31 \times 10^3 \text{ L mol}^{-1} \text{ s}^{-1}$$

**Table S46:** Kinetics of the reaction of **3c** with the anion of malononitrile **4c** in DMSO at 20 °C (stopped-flow UV-Vis spectrometer, decrease at $\lambda = 521$ nm).

Nr.	$[E]_0 / M$	$[Nu^-]_0 / M$	$k_{obs.} / s^{-1}$
M01-03-1	1.68×10^{-5}	2.72×10^{-4}	2.05
M01-03-2	1.68×10^{-5}	5.43×10^{-4}	4.32
M01-03-3	1.68×10^{-5}	8.15×10^{-4}	6.43
M01-03-4	1.68×10^{-5}	1.09×10^{-3}	8.47
M01-03-5	1.68×10^{-5}	1.36×10^{-3}	1.05×10^1

$$k_1 = 7.75 \times 10^3 \text{ L mol}^{-1} \text{ s}^{-1}$$

**Table S47:** Kinetics of the reaction of **3c** with the anion of ethyl aceto acetate **4d** in DMSO at 20 °C (stopped-flow UV-Vis spectrometer, decrease at $\lambda = 521$ nm).

Nr.	$[E]_0 / M$	$[Nu^-]_0 / M$	$k_{obs.} / s^{-1}$
M01-05-1	1.14×10^{-5}	3.39×10^{-4}	1.30
M01-05-2	1.14×10^{-5}	6.78×10^{-4}	2.72
M01-05-3	1.14×10^{-5}	1.02×10^{-3}	4.11
M01-05-4	1.14×10^{-5}	1.36×10^{-3}	5.46
M01-05-5	1.14×10^{-5}	1.69×10^{-3}	6.76

$$k_1 = 4.03 \times 10^3 \text{ L mol}^{-1} \text{ s}^{-1}$$

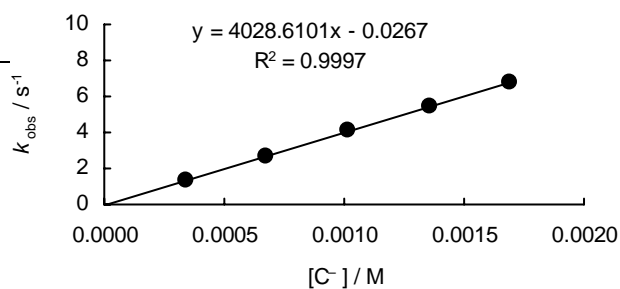


Table S48: Kinetics of the reaction of **3c** with the anion of acetylacetonone **4f** in DMSO at 20 °C (stopped-flow UV-Vis spectrometer, decrease at $\lambda = 521$ nm).

Nr.	$[E]_0 / M$	$[Nu^-]_0 / M$	$k_{obs.} / s^{-1}$
M01-02-2	1.68×10^{-5}	1.35×10^{-4}	1.20
M01-02-1	1.68×10^{-5}	1.69×10^{-4}	1.45
M01-02-3	1.68×10^{-5}	2.02×10^{-3}	1.74
M01-02-4	1.68×10^{-5}	2.70×10^{-3}	2.23
M01-02-5	1.68×10^{-5}	3.37×10^{-3}	2.71

$$k_1 = 7.45 \times 10^2 \text{ L mol}^{-1} \text{ s}^{-1}$$

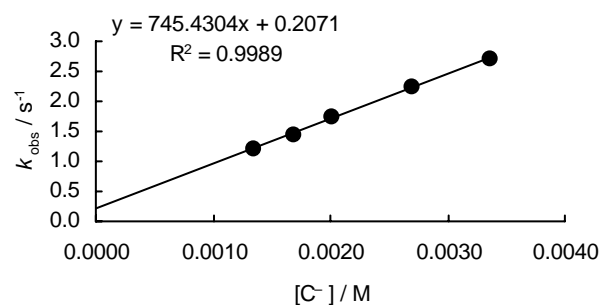
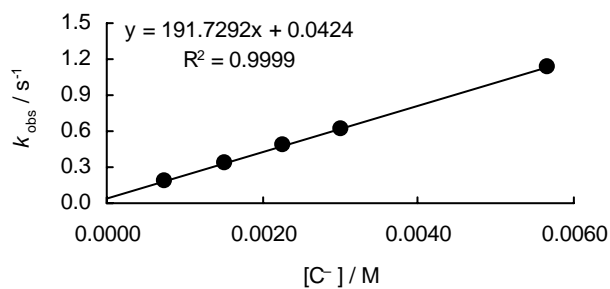


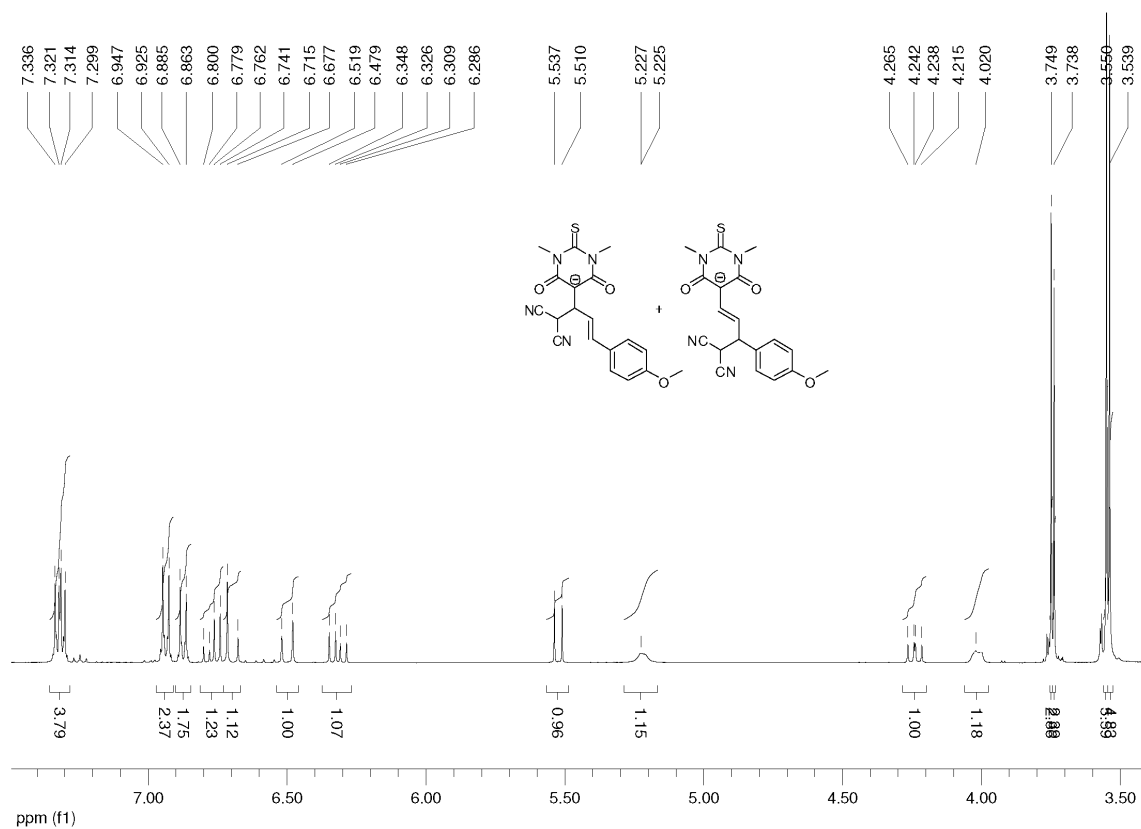
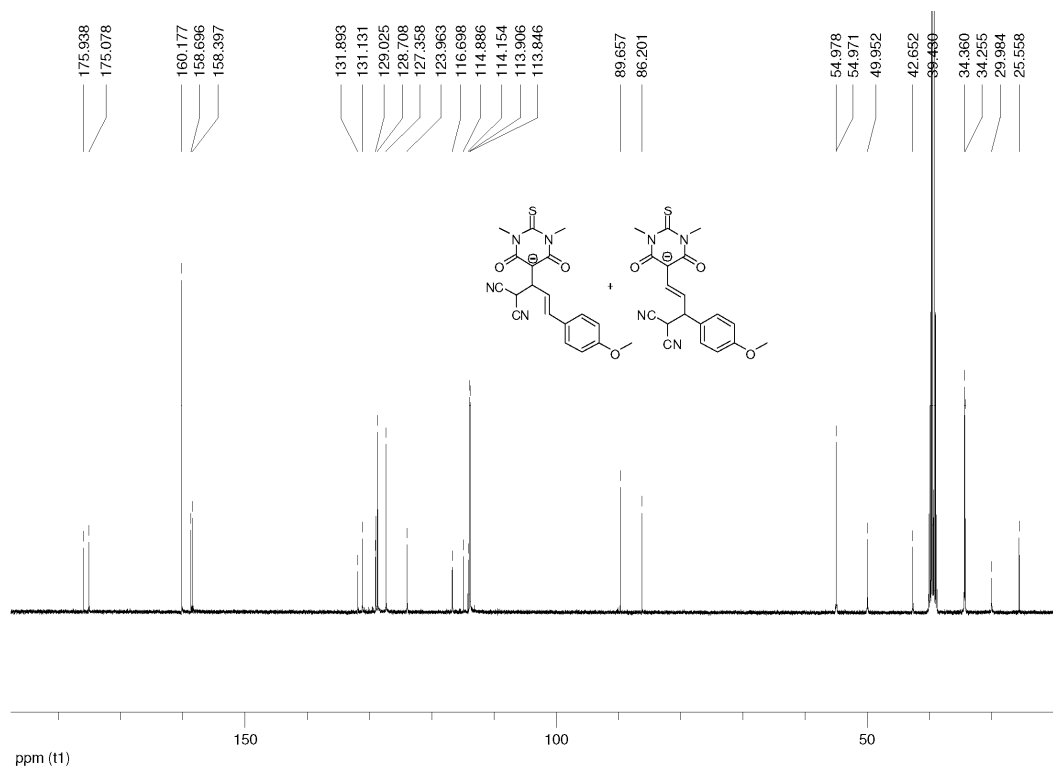
Table S49: Kinetics of the reaction of **3c** with the anion of dimedone **4g** in DMSO at 20 °C (stopped-flow UV-Vis spectrometer, decrease at $\lambda = 528$ nm).

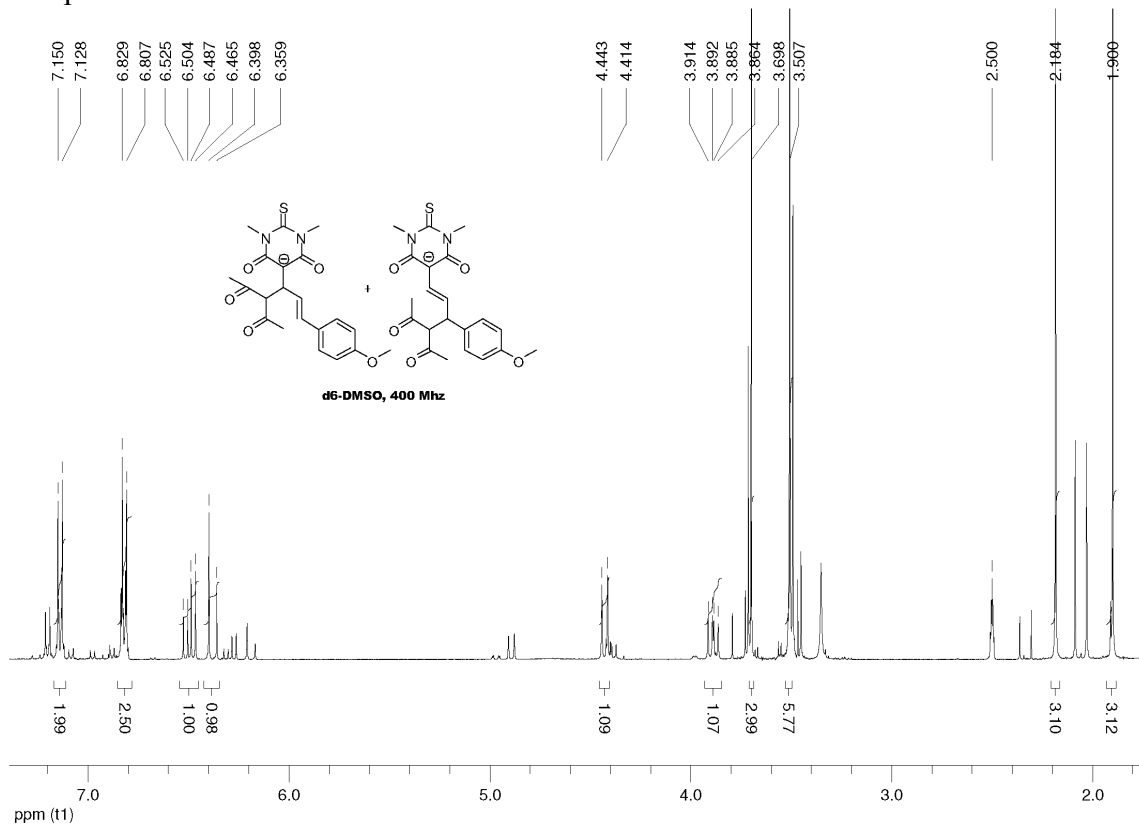
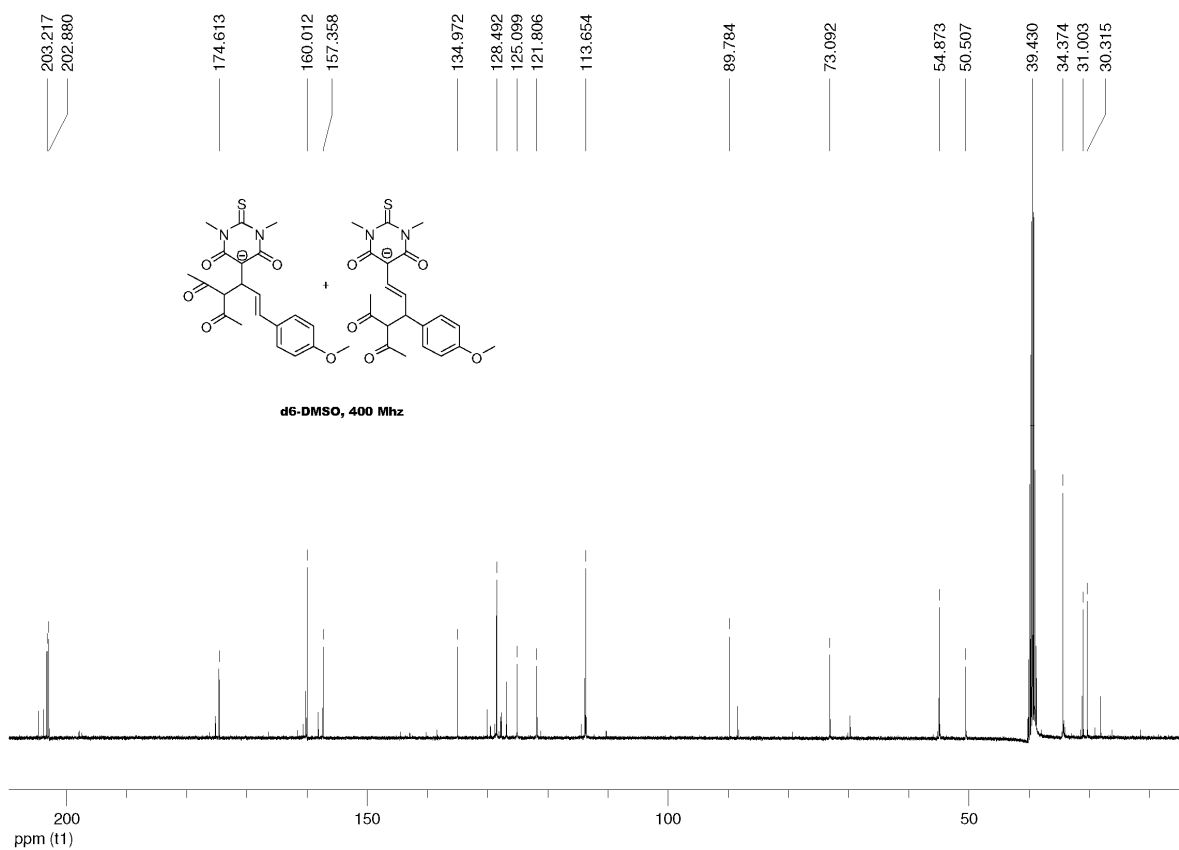
Nr.	$[E]_0 / M$	$[Nu^-]_0 / M$	$k_{obs.} / s^{-1}$
a267-1	2.82×10^{-5}	7.56×10^{-4}	1.91×10^{-1}
a267-2	2.82×10^{-5}	1.51×10^{-4}	3.27×10^{-1}
a267-3	2.82×10^{-5}	2.27×10^{-3}	4.77×10^{-1}
a267-4	2.82×10^{-5}	3.03×10^{-3}	6.24×10^{-1}
a267-5	2.82×10^{-5}	5.67×10^{-3}	1.13

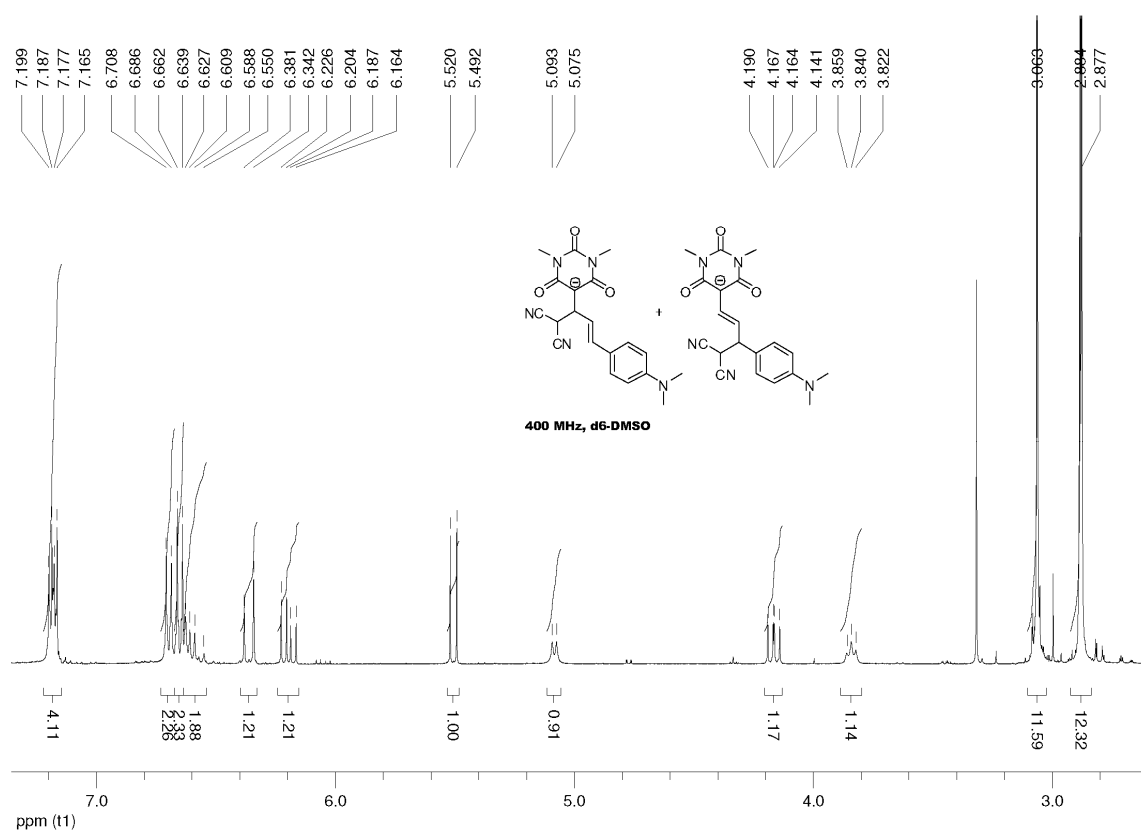
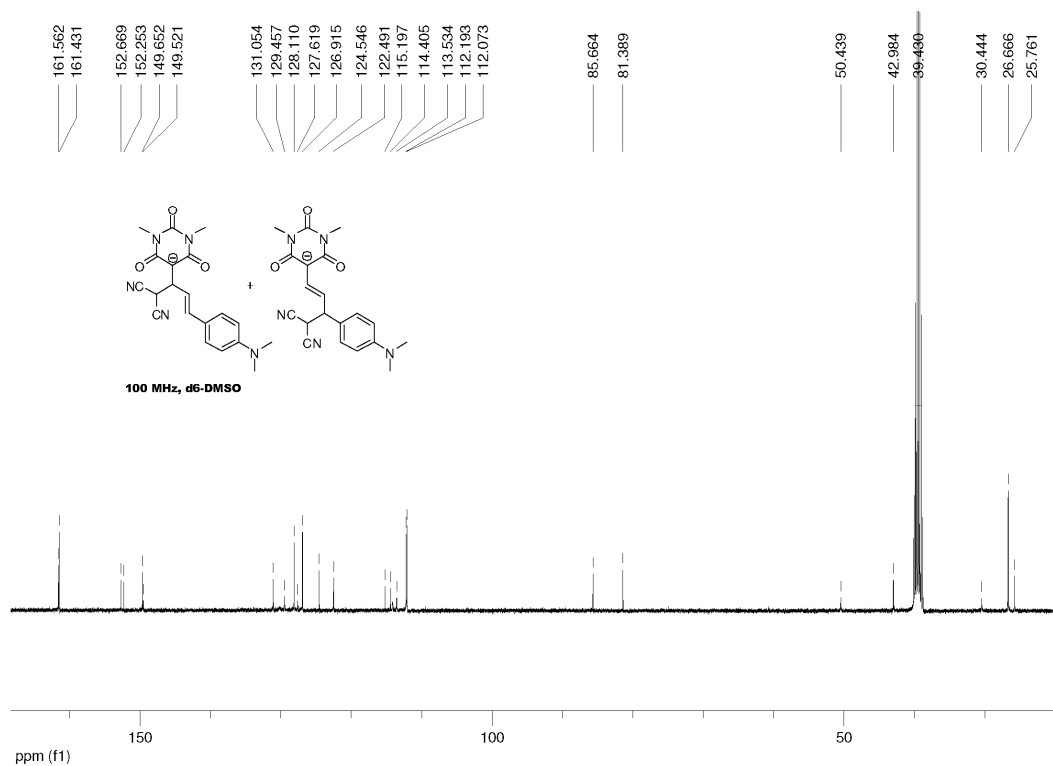
$$k_1 = 1.92 \times 10^2 \text{ L mol}^{-1} \text{ s}^{-1}$$

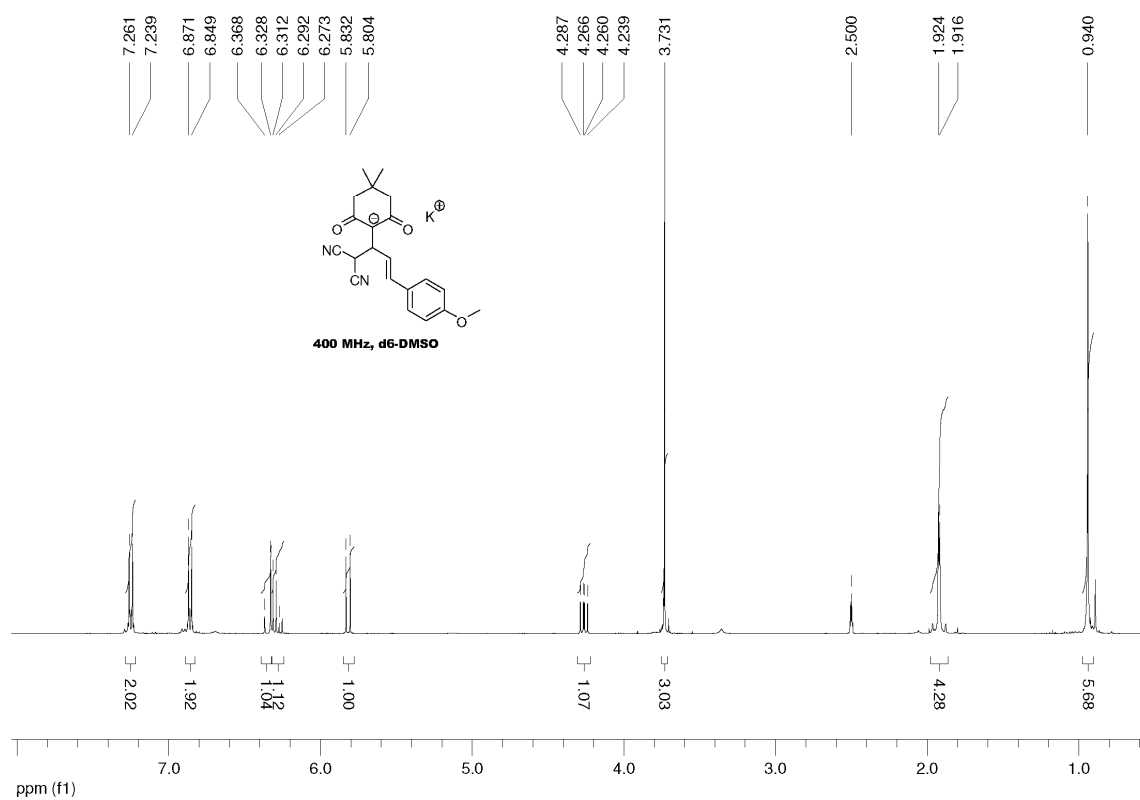
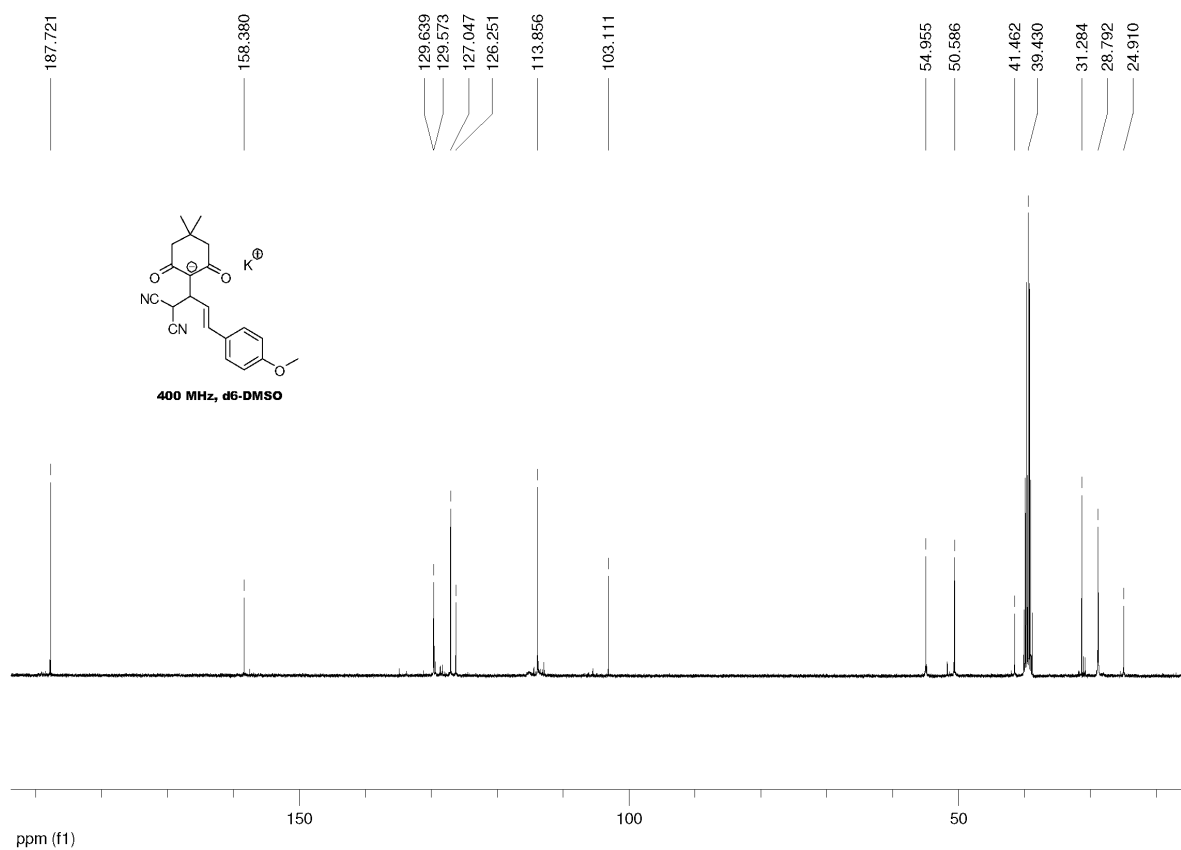


6.7. Copies of NMR Spectra

Compounds **7bc** and **8bc** ^1H NMR ^{13}C NMR

Compounds **7bf** and **8bf** ^1H NMR ^{13}C NMR

Compounds **9cc** and **10cc** ^1H NMR ^{13}C NMR

Compound **11bc** ^1H NMR ^{13}C NMR:

Chapter 7

Hydride Affinities of Michael Acceptors in Acetonitrile

Introduction

Hydride transfer reactions play a significant role in living organisms. The reduced form of nicotinamide adenine dinucleotide coenzyme (NAD(P)H), which bears a 1,4-dihydropyridine ring as the reactive center, is known to transfer a hydride ion or an electron to the surrounding substrates. In analogy to NADH, hydride abstractions from various types of dihydropyridines have found numerous applications in organic synthesis, most recently also in organocatalytic reductions of α,β -unsaturated compounds.¹ Hence, recent investigations in our group focused on the determination of the hydride donating abilities of 1,4-dihydropyridines and their comparison to borohydrides.^{2,3}

Our nucleophilicity scales could be extended significantly by integration of the borohydrides and 1,4-dihydropyridines as hydride donors. The linear-free energy relationship (7.1), which has previously been employed to compare the π -nucleophilicities of alkenes, allyl silanes, and enol ethers can also be employed for a comparison with the σ -nucleophilicities of hydride donors, such as organosilanes and organostannanes.^{4,5}

$$\log k_2 (20\text{ }^\circ\text{C}) = s(N + E) \quad (7.1)$$

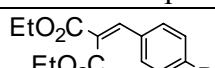
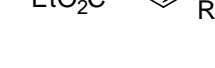
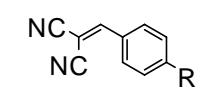
E = electrophilicity parameter, N = nucleophilicity parameter, s = nucleophile-specific slope parameter

Recently, quantum chemical calculations of the methyl anion- and the hydride affinities of benzhydrylium ions showed, that these thermodynamic terms correlate linearly with the electrophilicity parameters E of benzhydrylium ions and can therefore be employed for the prediction of E parameters of benzhydrylium ions.⁶

In contrast, the rate constants $\log k_{\text{rel}}$ of the reactions of nitro(hetero)arenes with the anion of chloromethyl phenyl sulfone correlate poorly with their methyl anion affinities. Therefore, it was concluded that the methyl anion affinities of heteroarenes are not suitable for the prediction of the relative electrophilicities of the studied arenes.⁷

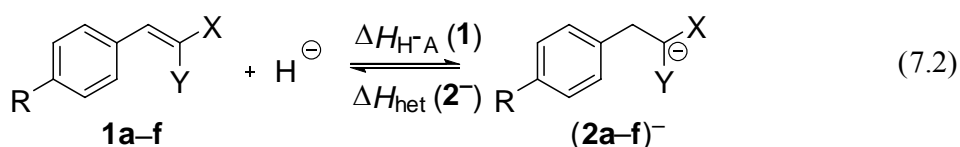
Recently, Zhu et al. reported about a new method for the determination of hydride affinities of the polarized olefins **1a–f** (Table 7.1) in acetonitrile.⁸

Table 7.1. Electrophilicity Parameters E of the Michael Acceptors **1a–q**.

	Michael acceptors	R	E
1a		OMe	-21.47 ^a
1b		Me	-21.11 ^a
1c		H	-20.55 ^a
1d		NO ₂	-17.67 ^a
1e		OMe	-10.80 ^b
1f		H	-9.42 ^b

^a See ref. 9, ^b see ref. 10

As discussed by Zhu, the hydride affinity of olefins can be expressed as the change of enthalpy during the reaction of an olefin with a free hydride ion under formation of the corresponding carbanion (Equation 7.2).



Due to the unknown enthalpy of the hydride ion in solution, the direct determination of the hydride affinities $\Delta H_{\text{H}^- \text{A}}$ is problematic (Equation (7.3)).

$$\Delta H_{\text{H}^- \text{A}}(\mathbf{1}) = H(\mathbf{2}^-) - [H(\text{H}^-) + H(\mathbf{1})] \quad (7.3)$$

Equation (7.2) shows, that the hydride affinities of olefins **1** equal the negative values of the reverse reactions, i.e., the enthalpies of the heterolytic cleavage of the C-H σ -bond of compounds **2⁻**.

By using this relationship, the relative hydride affinities of the olefins **1** can be determined by measuring the enthalpy change ΔH_r of the reaction of the carbanion **2⁻** and a hydride acceptor (exemplarily depicted in Figure 7.1 for the reaction of **2⁻** with the *N*-methylacridinium ion (**3a⁺**)) under formation of the corresponding olefin **1** and the reduced compound **3a**.

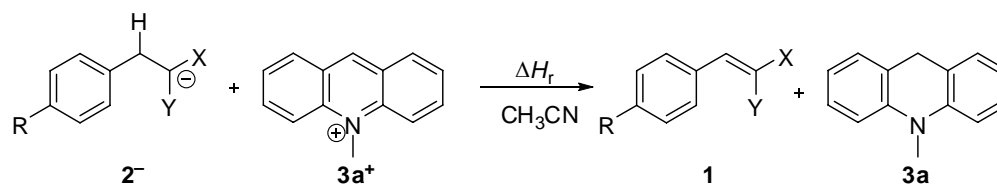


Figure 7.1. Reaction of a carbanion **2⁻** with the hydride acceptor **3a⁺** under formation of the olefin **1** and the reduced hydride acceptor **3a**.

In Equation (7.4), ΔH_r is the enthalpy change of the reaction in Figure 7.1, which can be obtained by titration calorimetry. By using Equation (7.5), the hydride affinity ΔH_{H-A} can be calculated from ΔH_r and $\Delta H_{het}(\mathbf{3a})$, which is the previously reported heterolytic C9-H bond dissociation energy of the 9,10-dihydroacridine (**3a**) in solution.¹¹

$$\Delta H_r = \Delta H_{het}(\mathbf{2}^-) - \Delta H_{het}(\mathbf{3a}) \quad (7.4)$$

$$\Delta H_{H-A}(\mathbf{1}) = -\Delta H_{het}(\mathbf{2}^-) = -[\Delta H_r + \Delta H_{het}(\mathbf{3a})] \quad (7.5)$$

In analogy to this new approach, it is now possible to systematically investigate the hydride affinities of further Michael acceptors **1g–q** (benzylidene Meldrum's acids, benzylidene indandiones, benzylidene barbituric acids, and quinone methides, Table 7.2).

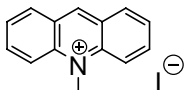
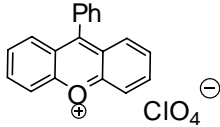
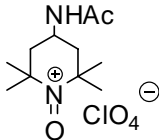
Table 7.2. Electrophilicity Parameters E of the Michael Acceptors **1g–q**.

	Michael acceptors	R	E
1g		Jul ^a	-13.79 ^b
1h		NMe ₂	-12.76 ^b
1i		OMe	-10.28 ^b
1j		Jul ^a	-13.84 ^c
1k		NMe ₂	-12.76 ^c
1l		OMe	-10.37 ^c
1m		OMe	-11.32 ^d
1n		Jul ^a	-17.90 ^e
1o		NMe ₂	-17.29 ^e
1p		OMe	-16.11 ^e
1q		Me	-15.86 ^e

^a For the structure of the julolidyl substituent see Figure 7.2.; ^b see ref.¹², ^c see ref. 13, ^d see ref. 14, ^e see ref. 15

Table 7.3 gives the bond dissociation energies ΔH_{het} of the hydride donors yielding the cations (**3a–c**)⁺. Due to the large differences of the hydride affinities of **1g–q**, three different hydride acceptors had to be employed: the *N*-methylacridinium ion (**3a**⁺), the 9-phenylxanthylum ion (**3b**⁺), and the 4-acetamido-2,2,6,6-tetramethyl-1-oxopiperidinium ion (**3c**⁺). The hydride affinity of **3b**⁺ had been confirmed independently by studying the enthalpy of its reaction with *N*-benzyl-1,4-dihyronicotinamide (BNAH) as reference using ITC experiments (second entry for **3b**⁺ $-\Delta H_{\text{het}} = 96.4$ kcal/mol in Table 7.3).

Table 7.3. Bond Dissociation Energies ΔH_{het} of the Hydride Donors Yielding the Hydride Acceptors (**3a–c**)⁺ in Acetonitrile.

	Hydride acceptors	$-\Delta H_{\text{het}}$ [kcal/mol]
3a⁺		81.1 ^a
3b⁺		96.8 ^b 96.4 ^c
3c⁺		99.2 ^d

^a From ref. 11, ^b from ref. 16, ^c differences result from an independent determination of ΔH_{het} for **3b⁺** by four ITC measurements with BNAH and the published value, ^d unpublished results from Zhu et al.

Results and Discussion

Preparation of the Carbanions (2g–m)[−] and of the Phenolates (2n–q)[−]. The Michael acceptors **1g–m** (Table 7.2) and the quinone methides **1n–q** (Table 7.2) were prepared by condensation of the corresponding aldehydes with Meldrum's acid, dimethylbarbituric acid, indandione, and 2,6-di-*tert*-butylphenol respectively, as described earlier.^{9,10,12-15} Subsequent reduction of **1g–q** with sodium borohydride in MeOH/EtOH¹⁷ (Figure 7.2) or with zinc in acetic acid¹⁸ yielded compounds **2g–q**. The carbanions (**2g–m**)[−] and the phenolates (**2n–q**)[−] were obtained by treating the compounds **2g–q** with potassium hydride in dry acetonitrile directly before the ITC measurements (Figure 7.2).

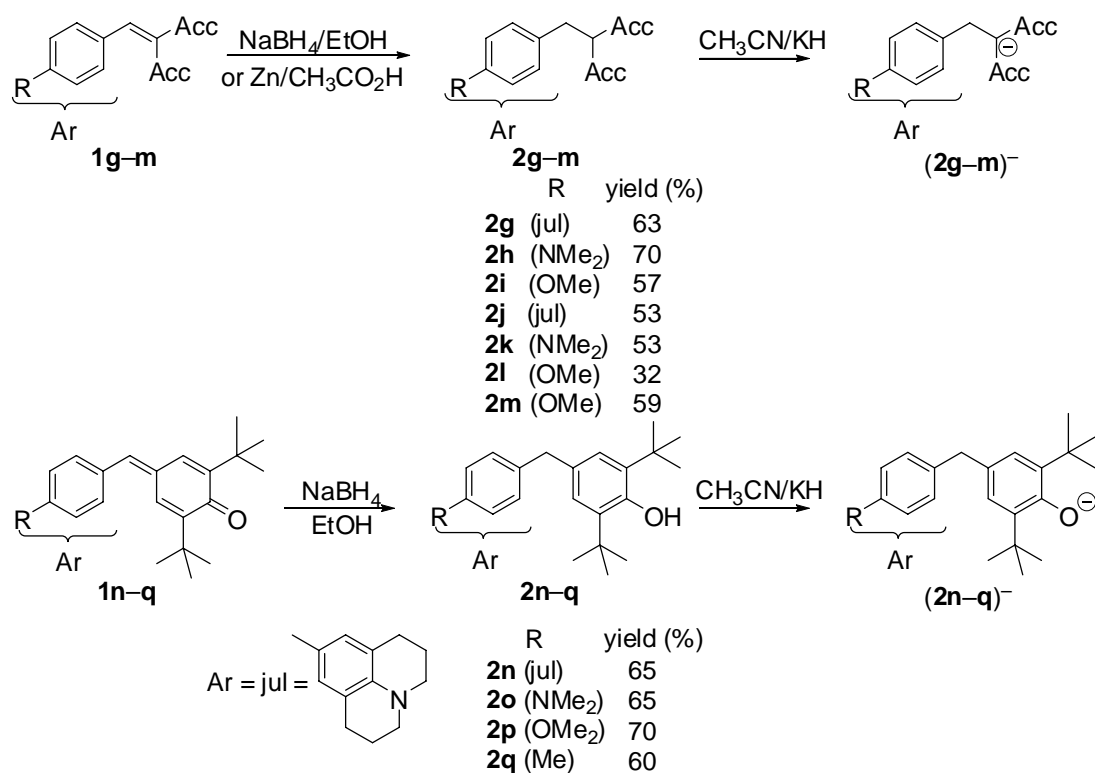


Figure 7.2. Reduction of the Michael acceptors **1g–m** and the quinone methides **1n–q** with $\text{NaBH}_4/\text{EtOH}$ or $\text{Zn}/\text{CH}_3\text{CO}_2\text{H}$ under formation of the corresponding reduced compounds **2n–q**, and subsequent treatment with KH under formation of the anions $(\mathbf{2a-q})^-$.

Isothermal Titration Calorimeter Experiments. Isothermal titration calorimeter experiments were performed in dry acetonitrile solutions at 25 °C on a CSC 4200 isothermal titration calorimeter. Prior to use, the instrument was calibrated against an internal heat pulse. Data points were collected every 2 s. The heats of the reactions of the anions $(\mathbf{2g-q})^-$ with the hydride acceptors $(\mathbf{3a-c})^+$ were determined by injecting 5–15 μL of the hydride acceptors $(\mathbf{3a-c})^+$ (~2.5 mM) into the reaction cell (1.00 mL) containing the compounds $(\mathbf{2g-q})^-$ (~75 mM) and measuring the heat flow. As illustrated in Figure 7.3, this injection was repeated nine to twelve times after delay times of 300–500 s, and the heats of reactions were obtained by averaging the integrals of the areas of the peaks except the first one or two.

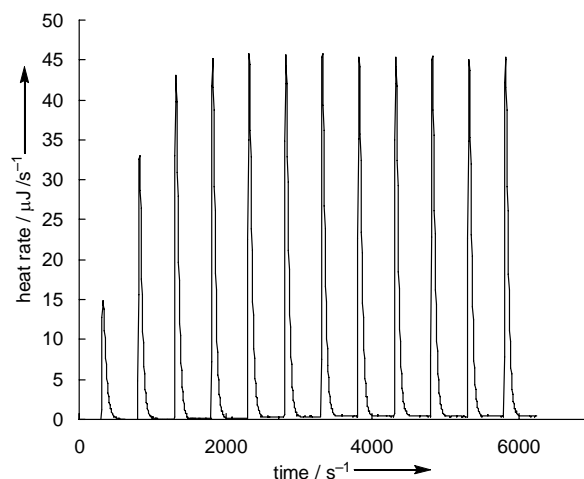


Figure 7.3. Isothermal titration calorimetry (ITC) for the reaction heat of the phenolate $2q^-$ with the hydride acceptor $3c^+$ in acetonitrile at 25 °C. The heat of reaction was conducted by adding 10 μL of $3c^+$ (2.16 mM) every 300 s into the acetonitrile solution containing the carbanion $2q^-$ (~75 mM).

Product Studies. Product studies for the reactions of the benzhydrylium tetrafluoroborates ($4a-j$) $^+$ (structures see Table 7.5) with borohydrides and dihydropyridines showed the exclusive formation of the corresponding diarylmethanes $4a-j$.² When the phenolate ion $2q^-$ and the strong hydride acceptor $3c^+$ were combined in dry acetonitrile and stirred for 10 min, 45 % of the quinone methide $1q$ was isolated after chromatographic workup (Figure 7.4).

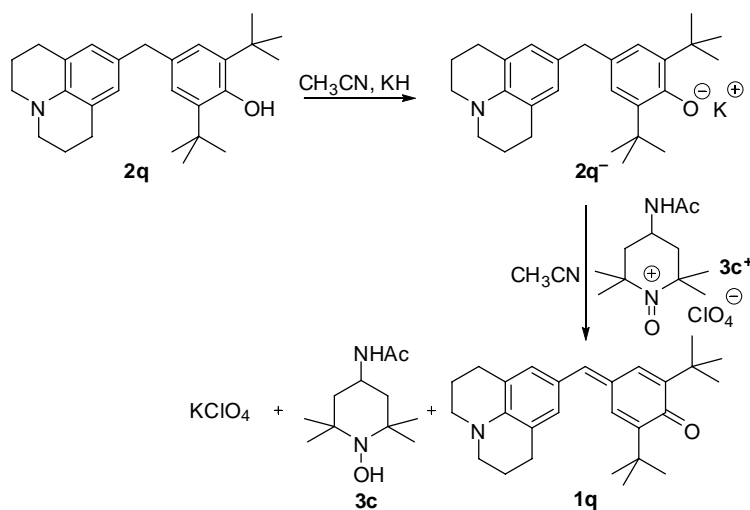


Figure 7.4. Reaction of the phenolate $2q^-$ with the hydride acceptor $3c^+$ in dry acetonitrile.

Analogous results were obtained for the reaction of the phenolate ion $2p^-$ with $3c^+$. TLC indicated the formation of a mixture of $1p$ and $3c$, along with the starting material $2p$. The incomplete conversions may be due to the fact that equimolar amounts of the hydride acceptor $3c^+$ were not sufficient for a complete oxidation of the phenolate ion $2p^-$. This is unlike the conditions used for the ITC experiments, in which typically large excesses of carbanions were used. In contrast, Zhu reported that reactions of $(2a-f)^-$ with the weaker hydride acceptor $3a^+$ resulted in quantitative formation of the corresponding olefins $1a-f$ and of $3a$ (Figure 7.5).⁸

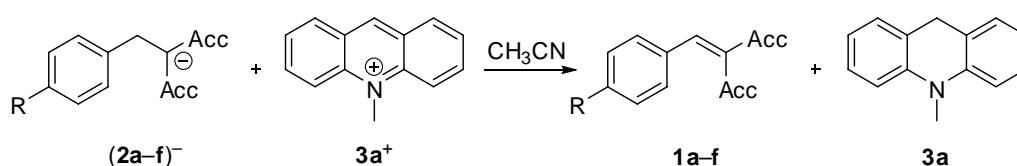
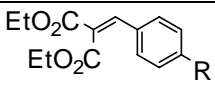
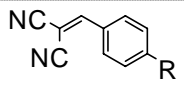
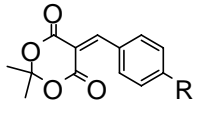
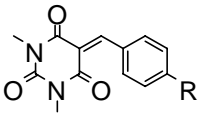
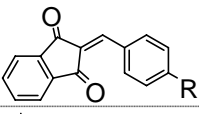
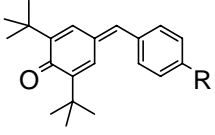


Figure 7.5. Reaction of the carbanions $(2a-f)^-$ with the hydride acceptor $3a^+$ in dry acetonitrile.

The hydride affinities ΔH_{H-A} of the Michael acceptors $1a-q$ derived from reactions with different hydride acceptors are listed in Table 7.4. Please note that the hydride affinities of compounds $1a-f$ have previously been reported by Zhu,⁸ whereas the hydride affinities of compounds $1g-q$ were determined in this work from more than 60 single experimental ITC measurements.

Table 7.4. Hydride Affinities ΔH_{H^-A} of the Michael Acceptors **1a–q** in Acetonitrile at 25 °C.

	R		ΔH_{H^-A} [kcal/mol] ^a	Hydride acceptor
	OMe	1a	-52.8 ^b	3a⁺
	Me	1b	-53.1 ^b	3a⁺
	H	1c	-53.7 ^b	3a⁺
	NO ₂	1d	-55.7 ^b	3a⁺
	OMe	1e	-60.4 ^b	3a⁺
	H	1f	-61.0 ^b	3a⁺
	Jul	1g	-72.4	3c⁺
	NMe ₂	1h	-76.0	3b⁺
	OMe	1i	-77.5	3b⁺
	Jul ^a	1j	-69.1	3c⁺
	NMe ₂	1k	-67.4	3a⁺
	OMe	1l	-68.7	3a⁺
	OMe	1m	-75.0	3b⁺
	Jul ^a	1n	-70.1	3c⁺
	NMe ₂	1o	-69.7	3c⁺
	OMe	1p	-70.2	3c⁺
	Me	1q	-70.2	3c⁺

^a Calculated from Equation 7.5 by using the averages of at least three individually determined heats of reactions ΔH_r (see Experimental Section), ^b from ref. 8

The hydride affinities ΔH_{H^-A} for **1g–q** (Table 7.4) result from at least three individual ITC measurements (for further details please see Experimental Section) of the compounds (**2g–q**)⁻ with the hydride acceptors listed in the last column of Table 7.4. Please note that a direct comparison of the hydride affinities of compounds **1a–q** is problematic because they were determined from reactions with a single hydride acceptor only, and no cross-checks have been carried out to verify the internal consistency of the results. The hydride acceptor **3c⁺** was used because the carbanions of the julolidyl-substituted Michael acceptors **2g⁻** and **2j⁻**, as well as

the phenolates (**2n–q**)[–] did not show quantitative reactions with the less reactive hydride acceptors **3a**⁺ and **3b**⁺.

However, from the results listed in Table 7.4, one can conclude that the hydride affinities ΔH_{H-A} of the olefins **1a–q** are much smaller than those of primary benzyl cations ions in acetonitrile (compare $\Delta G_{H-A} = -106$ to -123 kcal/mol for 4-MeOC₆H₄CH₂⁺ and 4-NCC₆H₄CH₂⁺, respectively)¹⁹ and also considerably smaller than ΔH_{H-A} of most of the benzhydrylium ions listed in Table 7.5. The hydride affinities of compounds **1g–q** are comparable to those of NAD⁺ models (NADH = nicotinamide adenine dinucleotide) in acetonitrile, e.g. $\Delta H_{H-A} = -64.2$ kcal/mol for BNA⁺,¹¹ which indicates that the olefins are no strong hydride acceptors of Table 7.4. Among the Michael acceptors, the methoxy substituted benzylidene Meldrum's acid **1i** ($\Delta H_{H-A} = -77.5$ kcal/mol) is the strongest oxidant and easiest to reduce, whereas the donor substituted benzylidene malonate **1a** ($\Delta H_{H-A} = -52.8$ kcal/mol) is the weakest oxidant and the most difficult to reduce. Furthermore, Table 7.4 indicates that the para-substituent of the quinone methides **1n–q** ($\Delta H_{H-A} = -69.7$ to -70.2 kcal/mol) does not have a large influence on the thermodynamic stability of the phenolate ions, as the hydride affinities of compounds **1n–q** are almost constant. Thus, if the Michael acceptors **1a–f** are to be reduced efficiently, relatively strong hydride donors such as NaBH₃(CN) ($\Delta H_{het}(\text{B–H}) = 45.0$ kcal/mol)²⁰ should be chosen. Weaker reducing agents, such as *N*-benzyl-1,4-dihydronicotinamide can only be used for the reduction of the stronger oxidants **1g–q**.

The reduction of the olefins **1a–q** by a hydride donor involves the formation of a new C–H σ -bond to and the breaking of a C=C π -bond to consume energy. It has, therefore, been concluded that the hydride affinities of olefins **1a–q** equal the heterolytic dissociation energy of the newly formed C–H σ -bond minus the heterolytic dissociation energy of the broken C=C π -bond.⁸

Unpublished results from Zhu and co-workers revealed a linear correlation of the hydride affinities $\Delta H_{\text{H-A}}$ of ten benzhydrylium ions $\mathbf{4}^+$ with their electrophilicity parameters E (Table 7.5, Figure 7.6). As the quinone methides $\mathbf{1n-q}$ are structurally closely related to the benzhydrylium ions, it is of interest to know whether their electrophilicities and those of other Michael acceptors also correlate linearly with their hydride affinities in acetonitrile.

Table 7.5. Electrophilicity Parameters E and Hydride Affinities $\Delta H_{\text{H-A}}$ of the Benzhydrylium Ions ($\mathbf{4a-j}^+$) in Acetonitrile.

	Benzhydrylium Ion	$\Delta H_{\text{H-A}}/[\text{kcal/mol}]^a$	E^b
$\mathbf{4a}^+$		-103.4	0.00
$\mathbf{4b}^+$		-102.1	-1.36
$\mathbf{4c}^+$		-94.0	-4.72
$\mathbf{4d}^+$		-90.1	-5.53
$\mathbf{4e}^+$		-91.3	-7.02
$\mathbf{4f}^+$		-87.1	-7.69
$\mathbf{4g}^+$		-86.3	-8.22
$\mathbf{4h}^+$		-86.0	-8.76
$\mathbf{4i}^+$		-81.8	-9.45
$\mathbf{4j}^+$		-79.0	-10.04

^a Hydride affinities determined from the reactions of $\mathbf{4}^+$ with *N*-benzyl-1,4-dihydronicotinic amide in CH_3CN (unpublished results from Zhu). ^b Electrophilicity parameters E from ref. 4

Except for the dimethylamino substituted benzhydrylium ion (**4e**⁺) no significant deviations from linearity for the ΔH_{H-A} vs. E plot are observed (Figure 7.6).

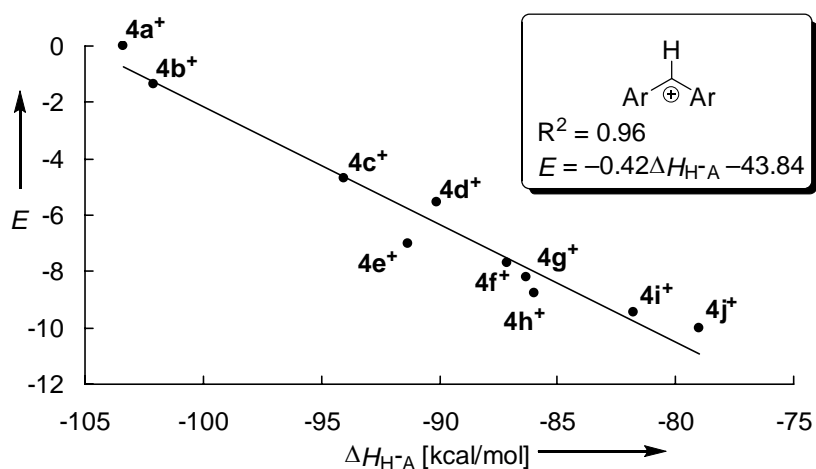


Figure 7.6. Plot of the electrophilicity parameters E of the benzhydrylium ions (**4a–j**)⁺ versus their hydride affinities ΔH_{H-A} [kcal/mol] in acetonitrile at 25 °C.

Figure 7.7 shows a plot of the electrophilicity parameters E of the benzhydrylium ions (**4a–j**)⁺ and the Michael acceptors **1a–q** versus their hydride affinities ΔH_{H-A} . The correlation line is based exclusively on the hydride affinities of the benzhydrylium ions (**4a–j**)⁺ in acetonitrile. Figure 7.7 shows that the hydride affinities of the Michael acceptors **1a–q** in acetonitrile do not correlate well with their electrophilicity parameters E . The benzylidene barbituric acids **1k,l** (\diamond) for example, show electrophilicities which are larger than expected from their hydride affinities, whereas the quinone methides **1n–q** (\circ) are less electrophilic than expected from their hydride affinities. The strongest deviation from the E vs. ΔH_{H-A} correlation are found for the benzylidenemalonates and the benzylidene malonodinitriles, which react faster than expected from ΔH_{H-A} as reported by Zhu et al.⁸

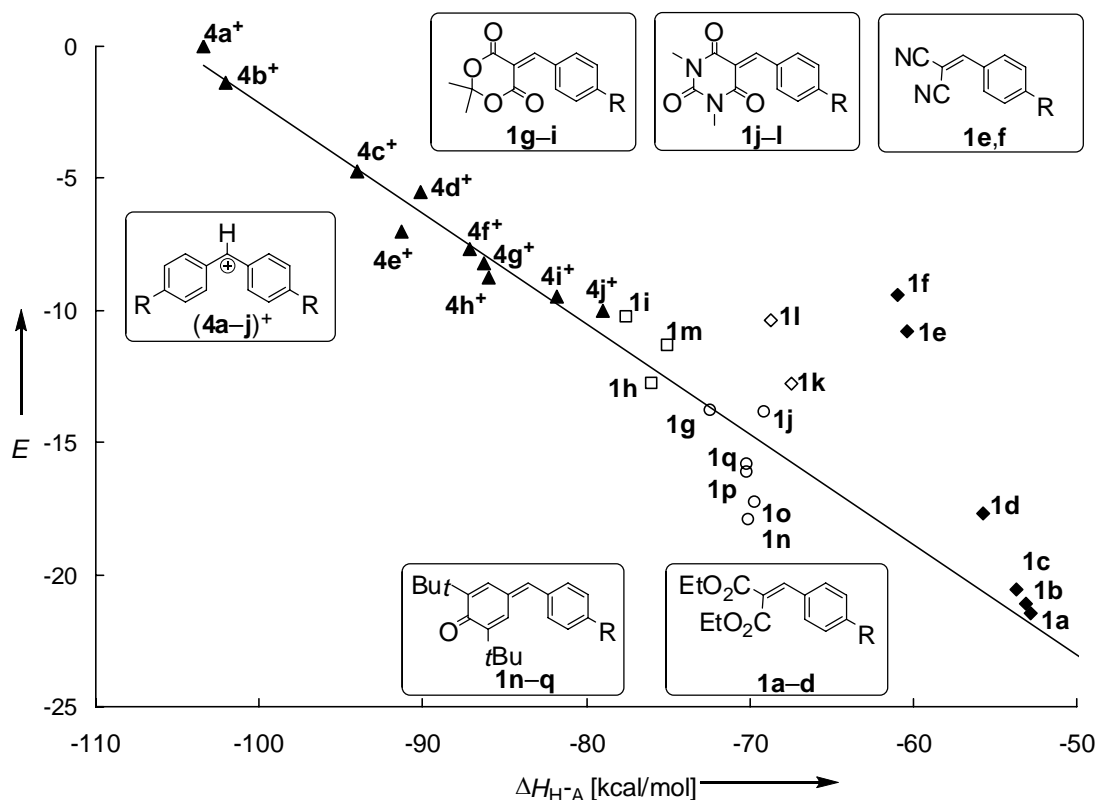


Figure 7.7. Plot of the electrophilicity parameters E of the benzhydrylium ions $(4a-j)^+$ and the Michael acceptors $1a-q$ versus their hydride affinities ΔH_{H-A} [kcal/mol] in acetonitrile at 25 °C. The symbols correspond to the different hydride acceptors used for the determinations of ΔH_{H-A} : $3a^+$ (\diamond), $3b^+$ (\square), $3c^+$ (\circ), *N*-benzyl-1,4-dihydropyridin-2(1*H*)-one (Δ), filled symbols: unpublished results from Zhu et al. or from ref. 8, open symbols: determined in this work.

Figure 7.7 reveals that the hydride affinities of the benzylidene Meldrum's acids **1h** and **1i** were determined using the hydride acceptor $3b^+$ (symbol \square), whereas the hydride affinity of the julolidyl-substituted benzylidene Meldrum's acid **1g** has been determined using the stronger hydride acceptor $3c^+$ (\circ). According to Table 7.4 the hydride affinities of compounds **1i-l** increase in the series $1k < 1l < 1j$, i.e., a different order than expected from Hammett's substituent constants σ or σ^+ . This inconsistency may be due to systematic errors caused by the fact that the hydride affinities of **1j** was derived from reactions with the hydride acceptor $3c^+$ while the other hydride affinities of **1k** and **1l** were derived from reactions with $3a^+$.

However, it has to be emphasized that the error limit of the determined hydride affinities ΔH_{H-A} for **1g–q** is ± 1.7 kcal/mol. This is much less accurate than the error limit reported by Zhu for the determination of hydride affinities of the olefins **1a–f** (± 0.5 kcal/mol).

However, in order to exclude systematic errors for certain hydride acceptors the hydride affinities ΔH_{H-A} of the Michael acceptors **1g–q**, have to be confirmed by additional ITC measurements with more than only one of the hydride acceptors (**3a–c**)⁺.

The reproducibility for the reactions of the neutral BNAH with the hydride acceptor **3b**⁺ was significantly better (± 0.4 kcal/mol). It also has to be mentioned that the hydride affinity of **3c**⁺ is still preliminary and has so far not been published.

Conclusion

The hydride affinities of typical Michael acceptors **1g–q** were found to be slightly larger than those previously reported by Zhu et. al for benzylidenemalonates and benzylidene malononitriles **1a–f** but they are considerably smaller than the hydride affinities of primary benzyl cations. The strongest oxidant, the methoxy substituted benzylidene Meldrum's acid (**1i**) shows a hydride affinity which is comparable to that of the weakest benzhydrylium ion **4j**⁺. Furthermore, several of the Michael acceptors **1a–q** deviate significantly from the linear correlation between electrophilicity and hydride affinity of benzhydrylium ions.

References

- (1) Zhu, X.-Q.; Wang, H.-Y.; Wang, J.-S.; Liu, Y.-C. *J. Org. Chem.* **2001**, *66*, 344-347.
- (2) Richter, D; Mayr, H.. *Angew. Chem.* **2008**, submitted.
- (3) a) Lelais, G.; MacMillan, D. W. C. *Aldrichimica Acta* **2006**, *39*, 79-87; b) Connon, S. J. *Org. Biomol. Chem.* **2007**, *5*, 3407-3417; c) Erkkilae, A.; Majander, I.; Pihko, P. M. *Chem. Rev. (Washington, DC, U. S.)* **2007**, *107*, 5416-5470; d) Pellissier, H. *Tetrahedron* **2007**, *63*, 9267-9331; e) Ouellet, S. G.; Walji, A. M.; Macmillan, D. W. C. *Acc. Chem. Res.* **2007**, *40*, 1327-1339; f) Denmark, S. E.; Beutner, G. L. *Angew. Chem., Int. Ed.* **2008**, *47*, 1560-1638.
- (4) Mayr, H.; Bug, T.; Gotta, M. F.; Hering, N.; Irrgang, B.; Janker, B.; Kempf, B.; Loos, R.; Ofial, A. R.; Remennikov, G.; Schimmel, H. *J. Am. Chem. Soc.* **2001**, *123*, 9500-9512.
- (5) a) Mayr, H.; Patz, M. *Angew. Chem.* **1994**, *106*, 990-1010; *Angew. Chem. Int. Ed.* **1994**, *33*, 938-957; b) Mayr, H.; Kempf, B.; Ofial, A. R. *Acc. Chem. Res.* **2003**, *36*, 66-77; c) Mayr, H.; Ofial, A. R. *Pure Appl. Chem.* **2005**, *77*, 1807-1821; d) Mayr, H.; Ofial, A. R. *J. Phys. Org. Chem.* **2008**, *21*, 584-595.
- (6) Singer, T., *Thesis*, Ludwig-Maximilians Universität München, 2008.
- (7) Seeliger, F., *Thesis*, Ludwig-Maximilians Universität München, 2008.
- (8) Zhu, X.-Q.; Zhang, M.; Liu, Q.-Y.; Wang, X.-X.; Zhang, J.-Y.; Cheng, J.-P. *Angew. Chem. Int. Ed.* **2006**, *45*, 3954-3957.
- (9) Kaumanns, O.; Lucius, R.; Mayr, H. *Chem. Eur. J.* **2008**, *14*, 9675-9682.
- (10) Lemek, T.; Mayr, H. *J. Org. Chem.* **2003**, *68*, 6880-6886.
- (11) Zhu, X.-Q.; Li, H.-R.; Li, Q.; Ai, T.; Lu, J.-Y.; Yang, Y.; Cheng, J.-P. *Chem. Eur. J.* **2003**, *9*, 871-880.
- (12) Kaumanns, O.; Mayr, H. *J. Org. Chem.* **2008**, *73*, 2738-2745.

- (13) Seeliger, F.; Berger, S. T. A.; Remennikov, G. Y.; Polborn, K.; Mayr, H. *J. Org. Chem.* **2007**, *72*, 9170-9180.
- (14) Berger, S. T. A.; Seeliger, F. H.; Hofbauer, F.; Mayr, H. *Org. Biomol. Chem.* **2007**, *5*, 3020-3026.
- (15) Lucius, R.; Loos, R.; Mayr, H. *Angew. Chem.* **2002**, *114*, 97-102; *Angew. Chem., Int. Ed.* **2002**, *41*, 91-95.
- (16) Zhu, X.-Q., unpublished results.
- (17) a) Tanaka, K.; Chen, X.; Kimura, T.; Yoneda, F. *Tetrahedron Lett.* **1987**, *28*, 4173-4176; b) Desai, U. V.; Pore, D. M.; Mane, R. B.; Solabannavar, S. B.; Wadgaonkar, P. P. *Synth. Commun.* **2004**, *34*, 25-32.
- (18) Jursic, B. S.; Stevens, E. D. *Tetrahedron Lett.* **2003**, *44*, 2203-2210.
- (19) Cheng, J.; Handoo, K. L.; Parker, V. D. *J. Am. Chem. Soc.* **1993**, *115*, 2655-2660.
- (20) Ellis, W. W.; Ciancanelli, R.; Miller, S. M.; Raebiger, J. W.; DuBois, M. R.; DuBois, D. L. *J. Am. Chem. Soc.* **2003**, *125*, 12230-12236.

Experimental Section

Hydride Affinities of Michael Acceptors in Acetonitrile

7. 1. Materials

Reagent grade acetonitrile was distilled twice over $\text{KMnO}_4/\text{K}_2\text{CO}_3$ and twice over P_2O_5 , in order to remove water and impurities. All other solvents were treated according to standard procedures.

Preparation of the compounds 1g–q. The Michael acceptors **1g–q** were already available from previous studies and can typically be synthesized by Knoevenagel condensation from the corresponding substituted aldehydes with Meldrum's acid, indandione, and N,N-dimethyl barbituric acid, respectively. The quinone methides **1g–m** can analogously be obtained from reactions of the substituted aldehydes with di-*tert*-butylphenol.

Preparation of the compounds 2g–m. The corresponding saturated compounds **2g–m** were obtained from the reduction of compounds **1g–m** with NaBH_4 in ethanol, or with Zn in acetic acid as described in ref. S1

Preparation of the compounds 2n–q. General. The quinone methides **1n–q** were dissolved in EtOH (20 mL), and NaBH_4 was added subsequently in small portions. After complete decolorization of the solution (indicating the complete reduction of **1n–q**), dilute aqueous hydrochloric acid was added to adjust a pH value of 7. The crude reaction mixtures were extracted with methylene chloride (2×20 mL), and dried over MgSO_4 . The solvent was

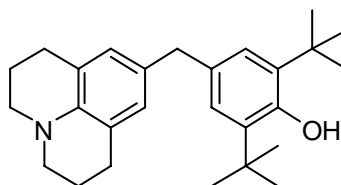
^{S1} a) Desai, U. V.; Pore, D. M.; Mane, R. B.; Solabannavar, S. B.; Wadgaonkar, P. P. *Synth. Commun.* **2004**, *34*, 25-32; b) Jursic, B. S.; Stevens, E. D. *Tetrahedron Lett.* **2003**, *44*, 2203-2210.

removed under reduced pressure and the crude product was recrystallized from *n*-hexane to yield the solid products.

2,6-di-*tert*-butyl-4-((1,2,3,5,6,7-hexahydropyrido[3,2,1-*ij*]quinolin-9-yl)methyl)phenol (2n).

1n (350 mg, 0.89 mmol) was dissolved in ethanol when NaBH₄ (300 mg, 7.89 mmol, 11 eq.) was added subsequently. **2n** (240 mg, 0.61 mmol, 65 %) was obtained as colorless needles.

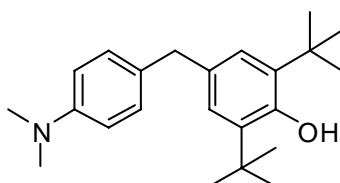
¹H-NMR (CDCl₃, 300 MHz), δ = 1.42 (s, 18 H, *tert*.-butyl), 1.98 (m, 4 H, CH₂), 2.73 (m, 4 H, CH₂), 3.10 (m, 4 H, CH₂), 3.71 (s, 2 H, CH₂), 5.02 (s, 1 H, OH), 6.65 (s, 2 H, CH_{ar}), 7.01 ppm (s, 2 H, CH_{ar}).



2,6-di-*tert*-butyl-4-(4-dimethylaminobenzyl)phenol (2o).

1o (320 mg, 0.95 mmol) was dissolved in ethanol when NaBH₄ (240 mg, 6.31 mmol, 6.6 eq.) was added subsequently. **2o** (210 mg, 0.62 mmol, 65 %) was obtained as pale yellow needles.

¹H NMR (CDCl₃, 300 MHz), δ = 1.42 (s, 18 H, *tert*.-butyl), 2.92 (s, 6 H, N(CH₃)₂), 3.82 (s, 2 H, CH₂), 5.04 (s, 1 H, OH), 6.73 (d, *J* = 8.0 Hz, 2 H, CH_{ar}), 7.00 (s, 2 H, CH_{ar}), 7.09 ppm (d, *J* = 8.0 Hz, 2 H, CH_{ar}). In agreement with ref. S2

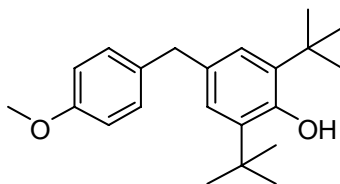


2,6-di-*tert*-butyl-4-(4-methoxybenzyl)phenol (2p).

1p (510 mg, 1.57 mmol) was dissolved in ethanol when NaBH₄ (290 mg, 7.63 mmol, 5 eq.) was added subsequently. **2p** (360 mg, 1.10 mmol, 70 %) was obtained as colorless crystals.

^{S2} Baik, W.; Lee, H. J.; Yoo, C. H.; Jung, J. W.; Kim, B. H. *J. Chem. Soc., Perkin Trans. 1* **1997**, 587-589.

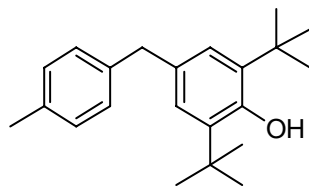
^1H NMR (CDCl_3 , 300 MHz), δ = 1.42 (s, 18 H, *tert.*-butyl), 3.78 (s, 3 H, OCH_3), 3.84 (s, 2 H, CH_2), 5.06 (s, 1 H, OH), 6.83 (d, J = 8.4 Hz, 2 H, CH_{ar}), 6.98 (s, 2 H, CH_{ar}), 7.13 ppm (d, J = 8.4 Hz, 2 H, CH_{ar}). In agreement with ref. S2



2,6-di-*tert*-butyl-4-(4-methylbenzyl)phenol (2q).

1q (500 mg, 1.61 mmol) was dissolved in ethanol when NaBH_4 (190 mg, 5.03 mmol, 3 eq.) was added subsequently. **2q** (300 mg, (0.97 mmol, 60 %) was obtained as a pale yellow solid.

^1H NMR (CDCl_3 , 300 MHz), δ = 1.42 (s, 18 H, *tert.*-butyl), 2.33 (s, 3 H, CH_3), 3.87 (s, 2 H, CH_2), 5.06 (s, 1 H, OH), 7.00 (s, 2 H, CH_{ar}), 7.10 ppm (m, 4 H, CH_{ar}). In agreement with ref. S2



The hydride acceptors (**3a–c**)⁺ were already available from previous studies. 10-methyl-acridinium iodide (**3a**⁺) can be obtained from acridine by treatment with methyl iodide.^{S3} 9-phenylxanthylium chlorate (**3b**⁺) can be obtained as precipitate from an aqueous solution of 9-phenylxanthylium iodide and NaClO_4 in water.

^{S3} Joseph, J.; Kuruvilla, E.; Achuthan, A. T.; Ramaiah, D.; Schuster, G. B. *Bioconjugate Chem.* **2004**, *15*, 1230-1235.

7.2. Heat of reactions

Table S1. Heat of Reactions $-\Delta H_r$ and Hydride Affinities ΔH_{H-A} for the Reactions of the Michael Acceptors **1g–q** with the Hydride Acceptors (**3a–c**)⁺ in Acetonitrile at 25 °C.

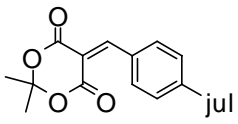
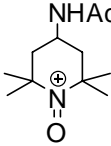
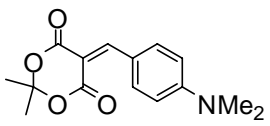
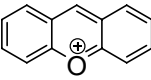
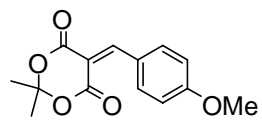
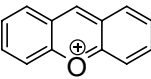
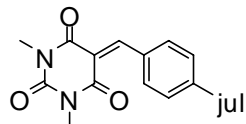
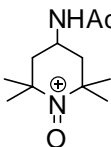
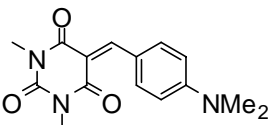
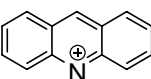
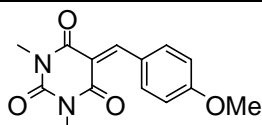
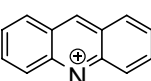
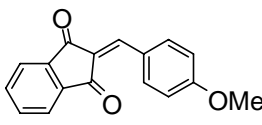
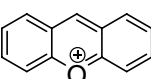
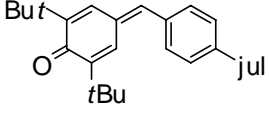
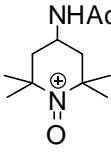
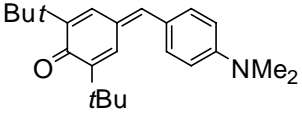
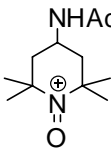
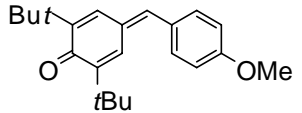
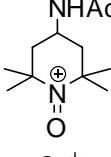
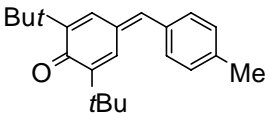
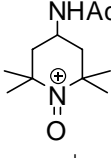
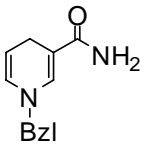
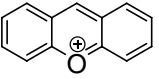
number	Michael acceptor	Hydride acceptor	$-\Delta H_r$ [kcal/mol]	average	ΔH_{H-A} [kcal/mol]
35-1	 1g	NHAc	25.7	26.8±1.1	-72.4
35-2		 3c ⁺	26.9		
35-4			27.9		
11-1	 1h	 3b ⁺	20.3	20.4±0.6	-76.0
11-2			20.7		
11-3			19.9		
11-5			20.5		
17-1	 1i	 3b ⁺	17.6	18.9±1.3	-77.5
17-2			18.7		
19-1			19.6		
19-2			19.5		
48-1	 1j	 3c ⁺	28.5	30.1±1.5	-69.1
48-2			30.7		
48-4			31.1		
8-1	 1k	 3a ⁺	13.5	13.7±0.9	-67.4
8-2			14.6		
8-3			13.5		
8-4			13.7		
8-5			13.9		
8-6			13.0		
6-1	 1l	 3a ⁺	12.9	12.4±1.0	-68.7
6-2			12.0		
6-4			11.4		
6-6			12.7		
6-7			12.8		
17-5	 1m	 3b ⁺	20.6	21.4±1.3	75.0
17-6			22.1		
18-5			21.4		
18-6			21.1		
18-7			21.0		
18-8			22.0		

Table S1. Continued.

number	Michael acceptor	Hydride acceptor	$-\Delta H_r$ [kcal/mol]	average	ΔH_{H-A} [kcal/mol]		
28-1			31.4	29.1±1.7	-70.1		
28-2			31.1				
28-3			28.2				
28-4			28.4				
43-1			1n			3c⁺	28.2
43-2			27.3				
29-1			28.0	29.5±1.0	-69.7		
29-2			28.5				
29-3			29.7				
39-1			30.0				
39-4			1o			3c⁺	31.0
27-1			28.2	29.0±1.7	-70.2		
27-2			28.5				
27-3			29.5				
27-4			1p			3c⁺	29.9
25-3							28.5
25-4	28.4						
25-6	28.7						
25-7	29.4						
28-8	29.4						
28-9	30.5						
42-1	28.3						
42-2	28.7						
15-1			32.5	32.2±0.4	-96.4		
15-2			31.8				
15-3			32.5				
15-4			BNAH			3b⁺	31.8

Lebenslauf

Oliver Kaumanns
14.06.1978 in Bremen
deutsch
ledig

Hochschulstudium

Chemie 08/2004 – 11/2008	(Ludwig-Maximilians-Universität München) Promotion, <i>Physikalisch-Organische Chemie</i> : „Reactions of Michael Acceptors with Carbanions–Novel References for the Construction of Comprehensive Reactivity Scales“ Betreuung durch Prof. Dr. Herbert Mayr
Chemie 10/1999 – 05/2004	(Universität Bremen) Diplom Diplomarbeit, <i>Organische Chemie</i> : „Studien zur Synthese eines Chlorophyllbausteins aus Hagemann-Ester“ Betreuung durch Prof. Dr. Franz-Peter Montforts
Wirtschaftswissenschaften 04/2005 – 09/2006	(FernUniversität in Hagen) Vordiplom

Schulausbildung

06/1998 Gymnasium Lilienthal, Allgemeine Hochschulreife

Zivildienst

08/1998 – 09/1999 Deutsches Rotes Kreuz Osterholz-Scharmbeck, Sozialstation Lilienthal

Auslandsaufenthalt

03/2008 – 05/2008 Forschungsaufenthalt im Rahmen der Promotion an der Nankai University
Tianjin, VR China im Arbeitskreis von Prof. Dr. Zhū Xiǎo-Qíng

Stipendium

03/2008 – 05/2008 Stipendium des Bayerischen Hochschulzentrums für China

Berufstätigkeit

10/2001 – 04/2002 Studentische Hilfskraft im Praktikum „Quantitative Analytik“ für
Studierende der Chemie im Arbeitskreis von Prof. Dr. Rüdiger
Mews an der Universität Bremen